

# **Cellular and molecular mechanisms of action of UV sunscreens in the regulation of growth and motility of human breast cancer cells**

Thesis submitted for the degree of Doctor of Philosophy (PhD)  
**School of Biological Sciences**

**Maha Alamer**

September 2016

## **Declaration**

I confirm that this thesis is my own work and the use of all materials from other sources has been properly and fully acknowledged.

Signed: Maha Mohammed Alamer

September, 2016

## Acknowledgments

I would like to show my gratitude to my country, The Kingdom of Saudi Arabia represented by my previous and current sponsors; University of Dammam and University of Hafer albatin for financing my studies.

My sincere thanks go to my supervisor Professor Philippa Darbre, for the opportunity to join her laboratory and for continues encouragement and advice through the challenges that faced me during the laboratory work and the writing stage of this thesis.

I thank my colleagues Abdullah Farasani, Ayse Bakir and Graeme Williams for their friendship. Thanks are also extended to my friends in the Hopkins building who have created a multinational scientific community that enriched my experience.

I must express my appreciation and gratitude to my parents. I thank them for believing in me since I was a child, for letting me follow my dreams and for supporting me through all of my life. Without that I would never have become the person that I am today.

I would also like to thank my grandmother, my brothers, my sisters, my family in-law and all the members of my family back home for the continued prayers, for remembering us and keeping in touch.

I thank my husband for his continued support words cannot describe my appreciation. Also, I thank my children, my lovely angels (Reem and Mishael), for taking care of mummy through this rough trip

Last but not least, I would like to acknowledge the ladies who participate in our knowledge of breast cancer, who died of breast cancer and were the source of the breast cancer cell lines that I have used in my work. To Catherine Frances (MCF-7 cells source) and to the ladies how provided us with MDA-MB-231 cells and T-47-D cells. You might have been gone but this part of you has lived to serve science, you will always be remembered.

## List of abbreviations

<b>4MBC</b>	4-Methylbenzylidene camphor
<b>AF1</b>	Activating function 1
<b>AF2</b>	Activating function 2
<b>AhR</b>	Aryl hydrocarbon receptor
<b>AP1</b>	Activator protein 1
<b>BMP7</b>	Bone morphogenetic protein 7
<b>Bp1</b>	Benzophenone-1
<b>Bp2</b>	Benzophenone-2
<b>Bp3</b>	Benzophenone-3
<b>DBD</b>	DNA binding domain
<b>DCFCS</b>	Dextran-charcoal stripped FCS
<b>DCIS</b>	Ductal carcinoma in situ
<b>ddH<sub>2</sub>O</b>	Double distilled water
<b>DMEM</b>	Dulbecco's modified Eagle's medium
<b>ECM</b>	Extracellular matrix
<b>EGF</b>	Epidermal growth factor
<b>EMT</b>	Epithelial to mesenchymal transition
<b>ER</b>	Oestrogen receptor
<b>ERE</b>	Oestrogen response element

<b>ERE-LUC</b>	ERE–luciferase assay
<b>ERM</b>	Actin-binding protein family ezrin/radixin/moesin
<b>ER<math>\alpha</math></b>	Oestrogen receptor $\alpha$
<b>ER<math>\beta</math></b>	Oestrogen receptor $\beta$
<b>FCS</b>	Foetal calf serum
<b>GP<math>\alpha</math></b>	G-protein-coupled estrogen receptor 1
<b>HBSS</b>	Hanks' balanced salt solution
<b>HER2</b>	Epidermal growth factor receptor 2
<b>HRT</b>	Hormone replacement therapy
<b>HS</b>	Homosalate
<b>IC</b>	Invasive carcinoma
<b>IDC</b>	Invasive ductal carcinoma
<b>LBD</b>	Ligand binding domain
<b>LCIS</b>	Lobular carcinoma in situ
<b>LEF/TEF</b>	Lymphoid enhancer factor-1/T-cell factor transcription factors
<b>LOEC</b>	Lowest observed effect concentrations
<b>LUC</b>	Luciferase assay
<b>MAPK</b>	Mitogen-activated protein kinase
<b>MMPs</b>	Matrix metalloproteinases
<b>OCs</b>	Organochlorines

<b>OMC</b>	Octyl methoxycinnamate
<b>PI3K</b>	Phosphatidyl-inositol 3-kinase
<b>PIK3R1</b>	Phosphoinositide-3-kinase regulatory subunit 1
<b>POPs</b>	Persistent organochlorine pollutants
<b>PR</b>	Progesterone receptor
<b>RAPs</b>	Receptor associated proteins
<b>RT-PCR</b>	Reverse Transcriptase Polymerase Chain Reaction
<b>SE</b>	Standard error
<b>TFF1</b>	Trefoil factor 1 (known previously as pS2)
<b>TGF-<math>\alpha</math></b>	Transforming growth factor $\alpha$
<b>TGF-<math>\beta</math></b>	Transforming growth factor $\beta$
<b>TIMP</b>	Tissue inhibitors of matrix metalloproteinases
<b>Twist-1</b>	Basic helix-loop-helix transcription factor
<b>UV</b>	Ultra violet
<b>UVR</b>	Ultraviolet rays
<b>ZEB</b>	Zinc-finger-E-box-binding

## Abstract

Breast cancer is a major health problem and exposure to oestrogen is a main risk factor. Many environmental chemicals with oestrogenic activity are known to enter the human breast from exposure through diet, the domestic environment and personal care products. In this study, six chemicals, used to absorb ultraviolet light (UV screens) in consumer products and known to be detectable in human milk, have been studied for their effects on proliferation and migration of MCF-7, T-47-D and MDA-MB-231 human breast cancer cells. The six chemicals were benzophenone-1 (Bp1), benzophenone-2 (Bp2), benzophenone-3 (Bp3), octylmethoxycinnamate (OMC), 3-(4-methylbenzilidene) camphor (4MBC) and homosalate (HS). All six of these UV screens at  $10^{-5}$ M could induce luciferase activity from an ERE-LUC reporter gene stably transfected into MCF-7 cells. Dose-response experiments on proliferation of oestrogen-responsive MCF-7 and T-47-D cells showed increased proliferation following the exposure to the UV screens but not OMC, which had no effect on proliferation of MCF-7 cells except when cells are seeded on a laminin matrix. No effect on MDA-MB-231 cell proliferation was recorded. Although the oestrogenic activity of these chemicals has been shown to influence proliferation, this is only one of the hallmarks of cancer cells. Another important hallmark is activation of invasion and metastasis which is relevant for breast cancer where mortality arises not from growth of the primary tumour but from metastatic tumour spread. Effects of these UV screens have therefore been studied on migration and invasion of MCF-7, T-47-D and MDA-MB-231 cells following prior (2 weeks) or (up to 30 weeks) exposure using a wound healing assay, time-lapse microscopy or xCELLigence technology. 2 weeks of exposure to  $10^{-5}$ M OMC, 4MBC and HS increased the motility of MCF-7 cells as determined by xCELLigence technology or time-lapse microscopy. 21 weeks of exposure to  $10^{-5}$  M Bp1, Bp3, to  $10^{-7}$ M concentrations of OMC, 4MBC and HS increased the motility of MCF-7 cells. Results using western immunoblotting suggest a decrease in E-cadherin mRNA levels by  $10^{-5}$  M Bp1, Bp3, OMC, 4MBS and HS and protein levels of cells exposed to  $10^{-5}$  M Bp1 and HS.  $10^{-5}$ M Bp1 also increased the secretion of MMP-9 as measured by zymography and the protein levels of pro-MMP-14 as measured by western immunoblotting.  $\beta$ -catenin protein was reduced in MCF-7 cells following the exposure to  $10^{-5}$ M OMC, which also reduced the mRNA levels of other two molecular markers of motility (PIK3R1 and BMP7). T-47-D cells exposed to  $10^{-5}$ M of the UV screens have shown an increase in motility as determined by xCELLigence but only Bp1 increased the migration as determined by wound healing. MDA-MB-231 cells showed no increase in motility following 2 weeks of exposure to the UV screens. However, 8 weeks of exposure to  $10^{-7}$  M Bp2, Bp3, 4MBC and HS increased the cells motility as determined by the xCELLigence and 15 weeks of exposure to  $10^{-7}$  M of the UV screens increased the motility of MDA-MB-231 cell as measured by the time-lapse microscopy. OMC and 4MBC increased the secretion of MMP-2 by MDA-MB-231 cells. Overall, these results demonstrate for the first time that these six UV screens can influence not only proliferation but also migration of human breast cancer cells.

# Table of Contents

Acknowledgments .....	II
List of abbreviations .....	III
Abstract.....	VI
<b>Chapter 1 Introduction.....</b>	<b>1</b>
<b>1.1 Introduction .....</b>	<b>1</b>
<b>1.2 Introduction to breast cancer .....</b>	<b>2</b>
1.2.1 The biology of normal breast .....	2
1.2.2 The hallmarks of cancer .....	3
1.2.3 Classification of breast cancer .....	4
1.2.4 Risk factors for breast cancer.....	5
<b>1.3 The role of oestrogens in the development of breast cancer.....</b>	<b>10</b>
1.3.1 Molecular action of oestrogen.....	12
1.3.2 Oestrogen and breast epithelial cell proliferation .....	17
1.3.3 Oestrogen and breast cancer cell metastasis .....	18
<b>1.4 Breast cancer and UV screens.....</b>	<b>25</b>
1.4.1 Introduction to UV screens .....	25
1.4.2 Human exposure and tissue levels.....	28
1.4.3 The oestrogenic action of UV screens <i>in vitro</i> and <i>in vivo</i> .....	31
<b>1.5 Underlying hypothesis.....</b>	<b>35</b>
<b>1.6 Aims of project.....</b>	<b>35</b>
<b>Chapter 2 Materials and Methods.....</b>	<b>37</b>
<b>2.1 Culture of human breast cancer cells .....</b>	<b>37</b>

2.1.1	Culture of stock MCF-7 human breast cancer cells.....	37
2.1.2	Culture of stock T-47-D human breast cancer cells.....	37
2.1.3	Culture of stock MDA-MB-231 human breast cancer cells .....	37
2.1.4	Sub culturing of stock human breast cancer cells .....	38
2.1.5	Maintenance of human breast cancer cells with UV screens .....	38
2.1.6	Sub culturing of human breast cancer cells exposed to UV screens .....	39
<b>2.2</b>	<b>Measurement of cell proliferation.....</b>	<b>39</b>
2.2.1	Measurement of cell proliferation using a ZBI Coulter counter .....	40
2.2.2	Measurement of cell proliferation using xCELLigence technology .....	41
<b>2.3</b>	<b>Ligand ability to increase expression of ERE-LUC reporter gene in MCF-7 cells..</b>	<b>43</b>
<b>2.4</b>	<b>Cell migration and motility assays.....</b>	<b>44</b>
2.4.1	Wound healing assay .....	44
2.4.2	Cell motility assay as measured by time-lapse microscopy .....	45
2.4.3	Cell migration using xCELLigence technology.....	45
<b>2.5</b>	<b>Cell invasion using xCELLigence technology.....</b>	<b>47</b>
<b>2.6</b>	<b>Real-Time Reverse Transcriptase Polymerase Chain Reaction (RT-PCR).....</b>	<b>47</b>
2.6.1	Preparation of total cellular RNA.....	47
2.6.2	Total cellular RNA extraction after 1 week of exposure to the UV screens.	47
2.6.3	Total cellular RNA extraction after 24-25 weeks of exposure to UV screens	48
2.6.4	Total cellular RNA extraction.....	49
2.6.5	cDNA synthesis .....	49
2.6.6	PCR assay .....	50
2.6.7	RT-PCR analysis.....	50
<b>2.7</b>	<b>Western immunoblotting.....</b>	<b>52</b>
2.7.1	Preparation of whole cell lysates.....	52

2.7.2	Protein assay using the Pierce BCA reagent.....	52
2.7.3	Sodium Dodecyl Sulphate-polyacrylamide gel electrophoresis (SDS-PAGE) 53	
2.7.4	Protein transfer .....	53
2.7.5	Immunostaining of protein .....	54
2.7.6	Quantitation of protein and data analysis .....	55
<b>2.8</b>	<b>Gelatin zymography .....</b>	<b>56</b>
2.8.1	Conditioned media collection.....	56
2.8.2	Loading and running zymography SDS gelatin gels .....	57
2.8.3	Developing the zymogram.....	57
2.8.4	Staining and destaining of zymography SDS gelatin gel .....	57
2.8.5	Quantifying the proteinases activity and data analysis .....	57
<b>2.9</b>	<b>Data Analysis .....</b>	<b>58</b>
<b>Chapter 3 The oestrogenic activity of UV screens in oestrogen responsive MCF-7</b>		
<b>human breast cancer cells .....</b>		
		<b>59</b>
<b>3.1</b>	<b>Introduction .....</b>	<b>59</b>
<b>3.2</b>	<b>Experimental aims.....</b>	<b>60</b>
<b>3.3</b>	<b>Results .....</b>	<b>61</b>
3.3.1	Effects on ERE-LUC reporter gene expression .....	61
3.3.2	Effects of exposure to UV screens on ER $\alpha$ protein levels .....	72
3.3.3	Effects of exposure to UV screens on TFF1 mRNA levels.....	72
3.3.4	Effects of UV screens on proliferation of MCF-7 human breast cancer cells 76	
3.3.5	Comparisons between the effects of different UV screens on MCF-7 human breast cancer cells .....	97
<b>3.4</b>	<b>Discussion .....</b>	<b>101</b>

<b>Chapter 4</b>	<b>Effects of the UV screens on migration and invasion of MCF-7 human breast cancer cells</b>	<b>110</b>
<b>4.1</b>	<b>Introduction</b>	<b>110</b>
<b>4.2</b>	<b>Experimental aims</b>	<b>112</b>
<b>4.3</b>	<b>Results</b>	<b>113</b>
4.3.1	Effects of Bp1 on migration of MCF-7 human breast cancer cells	113
4.3.2	Effects of Bp2 on migration of MCF-7 human breast cancer cells	124
4.3.3	Effects of Bp3 on migration of MCF-7 human breast cancer cells	131
4.3.4	Effects of OMC on migration of MCF-7 human breast cancer cells	143
4.3.5	Effects of 4MBC on migration of MCF-7 human breast cancer cells	156
4.3.6	Effects of HS on migration of MCF-7 human breast cancer cells	169
4.3.7	Comparisons of effects among different UV screen and different exposure time points:	180
4.3.8	Effects of the UV screens on molecular markers related to motility and invasion of MCF-7 human breast cancer cells	187
<b>4.4</b>	<b>Discussion</b>	<b>208</b>
<b>Chapter 5</b>	<b>Effect of UV screens on T-47-D human breast cancer cells</b>	<b>219</b>
<b>5.1</b>	<b>Introduction</b>	<b>219</b>
<b>5.2</b>	<b>Experimental aim</b>	<b>220</b>
<b>5.3</b>	<b>Results</b>	<b>220</b>
5.3.1	Effects of UV screens on proliferation of T-47-D human breast cancer cells	220
5.3.2	Effects of UV screens on motility of T-47-D human breast cancer cells	229
<b>5.4</b>	<b>Discussion</b>	<b>243</b>
<b>Chapter 6</b>	<b>Effects of UV screens on MDA-MB-231 human breast cancer cells</b>	<b>246</b>
<b>6.1</b>	<b>Introduction</b>	<b>246</b>

<b>6.2 Experimental aims</b> .....	<b>247</b>
<b>6.3 Results</b> .....	<b>247</b>
6.3.1 Effects of UV screens on proliferation of MDA-MB-231 human breast cancer cells	247
6.3.2 Effect of UV screens on motility of MDA-MB-231 human breast cancer cells	249
6.3.3 Effect of UV screens on invasion of MDA-MB-231 human breast cancer cells as determined by xCELLigence technology.....	256
6.3.4 Effect of UV screens on matrix metalloproteinase activity of MDA-MB-231 human breast cancer cells as measured by zymography.....	256
<b>6.4 Discussion</b> .....	<b>260</b>
<b>Chapter 7 General discussion</b> .....	<b>262</b>
<b>References</b> .....	<b>268</b>

## List of Figures

<b>Figure 1.1</b> Human female breast biology.....	<b>2</b>
<b>Figure 1.2</b> The hallmarks of cancer. ....	<b>3</b>
<b>Figure 1.3</b> Types and examples of environmental oestrogens.....	<b>8</b>
<b>Figure 1.4</b> The structure of oestradiol, oestrone and oestriol.....	<b>11</b>
<b>Figure 1.5</b> Biosynthesis of oestrogens in the ovary and the liver.....	<b>11</b>
<b>Figure 1.6</b> Schematic representation of the functional domains of the human oestrogen receptors ER $\alpha$ and ER $\beta$ .....	<b>13</b>
<b>Figure 1.7</b> Crystal structure of the ligand binding of 17 $\beta$ -oestradiol to oestrogen receptor alpha.....	<b>14</b>
<b>Figure 1.8</b> Molecular mechanisms of action of oestrogen.....	<b>16</b>
<b>Figure 1.9</b> Schematic representation of epithelial cell-cell adhesion mediated by E-cadherin.....	<b>21</b>
<b>Figure 2.1</b> xCELLigence real-time cell analysis (RCTA) instrument.....	<b>42</b>
<b>Figure 2.2</b> The E-plate 16.....	<b>42</b>
<b>Figure 2.3</b> The CIM-plate16.....	<b>46</b>
<b>Figure 2.4</b> Bio-Rad Gel Doc EZ imager and the turbo transfer system.....	<b>54</b>
<b>Figure 2.5</b> Bio-Rad Gel Doc imager trays.....	<b>58</b>
<b>Figure 3.1</b> Regulation of a stably transfected oestrogen-inducible ERE-LUC reporter gene in MCF-7 human breast cancer cells following exposure to 17 $\beta$ -oestradiol or ethanol..	<b>63</b>
<b>Figure 3.2</b> Regulation of a stably transfected oestrogen-inducible ERE-LUC reporter gene in MCF-7 human breast cancer cells following exposure to 10 <sup>-5</sup> M of UV screens, 10 <sup>-8</sup> M of 17 $\beta$ -oestradiol or ethanol.....	<b>64</b>
<b>Figure 3.3</b> Regulation of a stably transfected oestrogen-inducible ERE-LUC reporter gene in MCF-7 human breast cancer cells following exposure to increasing doses of Bp1.....	<b>65</b>

<b>Figure 3.4</b> Regulation of a stably transfected oestrogen-inducible ERE-LUC reporter gene in MCF-7 human breast cancer cells following exposure to increasing doses of Bp2. ....	<b>66</b>
<b>Figure 3.5</b> Regulation of a stably transfected oestrogen-inducible ERE-LUC reporter gene in MCF-7 human breast cancer cells following exposure to increasing doses of Bp3. ....	<b>67</b>
<b>Figure 3.6</b> Regulation of a stably transfected oestrogen-inducible ERE-LUC reporter gene in MCF-7 human breast cancer cells following exposure to increasing doses of OMC.....	<b>68</b>
<b>Figure 3.7</b> Regulation of a stably transfected oestrogen-inducible ERE-LUC reporter gene in MCF-7 human breast cancer cells following exposure to increasing doses of 4MBC.....	<b>69</b>
<b>Figure 3.8</b> Regulation of a stably transfected oestrogen-inducible ERE-LUC reporter gene in MCF-7 human breast cancer cells following exposure to increasing doses of HS.....	<b>70</b>
<b>Figure 3.9</b> Effect of fulvestrant on induction of ERE-LUC reporter gene by exposure to Bp1, Bp2, 17 $\beta$ -oestradiol or ethanol control. ....	<b>71</b>
<b>Figure 3.10</b> Effect of 1 week of exposure to oestradiol or benzophenones on the expression level of oestrogen receptor $\alpha$ .....	<b>73</b>
<b>Figure 3.11</b> Effect of 1 week of exposure to oestradiol, OMC, 4MBC or homosalate on the expression level of oestrogen receptor $\alpha$ . ....	<b>74</b>
<b>Figure 3.12</b> Effect of UV screens on the relative levels of TFF1 mRNA in MCF-7 cells after 7 days and 24 weeks of exposure.....	<b>75</b>
<b>Figure 3.13</b> Effect of 17 $\beta$ -oestradiol on proliferation of MCF-7 human breast cancer cells in monolayer culture. ....	<b>76</b>
<b>Figure 3.14</b> Effect of Bp1 on proliferation of MCF-7 human breast cancer cells in monolayer culture. ....	<b>78</b>
<b>Figure 3.15</b> Effect of Bp2 on proliferation of MCF-7 human breast cancer cells in monolayer culture. ....	<b>79</b>
<b>Figure 3.16</b> Effect of Bp3 on proliferation of MCF-7 human breast cancer cells in monolayer culture. ....	<b>80</b>
<b>Figure 3.17</b> Effect of OMC on proliferation of MCF-7 human breast cancer cells in monolayer culture. ....	<b>81</b>

<b>Figure 3.18</b> Effect of 4MBC on proliferation of MCF-7 human breast cancer cells in monolayer culture. ....	<b>82</b>
<b>Figure 3.19</b> Effect of HS on proliferation of MCF-7 human breast cancer cells in monolayer culture. ....	<b>83</b>
<b>Figure 3.20</b> Effect of fulvestrant on the proliferation of MCF-7 human breast cancer cells proliferation following exposure to Bp1, Bp2, 17 $\beta$ -oestradiol or ethanol control. ....	<b>84</b>
<b>Figure 3.21</b> Effect of Bp1, Bp2, Bp3 or 4MBC on the proliferation of MCF-7 human breast cancer cells in the presence and absence of 17 $\beta$ -oestradiol in monolayer culture. ....	<b>86</b>
<b>Figure 3.22</b> Effect of different coated surfaces on adhesion (A), proliferation (B) and morphology (C-E) of MCF-7 human breast cancer cells. ....	<b>89</b>
<b>Figure 3.23</b> Effect of different coated surfaces on MCF-7 human breast cancer cell proliferation after treatment with 17 $\beta$ -oestradiol.....	<b>90</b>
<b>Figure 3.24</b> Effect of Bp1 on proliferation of MCF-7 human breast cancer cells on different coated surfaces.....	<b>91</b>
<b>Figure 3.25</b> Effect of Bp2 on proliferation of MCF-7 human breast cancer cells on different coated surfaces.....	<b>92</b>
<b>Figure 3.26</b> Effect of Bp3 on proliferation of MCF-7 human breast cancer cells on different coated surfaces.....	<b>93</b>
<b>Figure 3.27</b> Effect of OMC on proliferation of MCF-7 human breast cancer cells on different coated surfaces.....	<b>94</b>
<b>Figure 3.28</b> Effect of 4MBC on proliferation of MCF-7 human breast cancer cells on different coated surfaces. ....	<b>95</b>
<b>Figure 3.29</b> Effect of HS on proliferation of MCF-7 human breast cancer cells on different coated surfaces.....	<b>96</b>
<b>Figure 3.30</b> Statistical comparison and summary of the varying effect of the UV screens on oestrogen-inducible ERE-LUC reporter gene in stably transfected MCF-7 human breast cancer cells (A) and proliferation of MCF-7 human breast cancer cells in monolayer culture (B).....	<b>100</b>

<b>Figure 4.1</b> Effect of exposure to Bp1 or 17 $\beta$ -oestradiol on collective motility of MCF-7 human breast cancer cells as measured by wound healing assay. ....	<b>115</b>
<b>Figure 4.2</b> Representative images of the effect of Bp1 on motility of MCF-7 human breast cancer cells as determined by wound healing assay. ....	<b>116</b>
<b>Figure 4.3</b> Effect of exposure to Bp1 on motility of individual MCF-7 human breast cancer cells as determined by time-lapse microscopy. ....	<b>117</b>
<b>Figure 4.4</b> Short-term effect of Bp1 or 17 $\beta$ -oestradiol on migration of MCF-7 human breast cancer cells using chemotaxis stimulus as determined by xCELLigence technology.....	<b>118</b>
<b>Figure 4.5</b> Long-term effect of Bp1 or 17 $\beta$ -oestradiol on migration of MCF-7 human breast cancer cells using chemotaxis stimulus as determined by xCELLigence technology.....	<b>119</b>
<b>Figure 4.6</b> Long-term effect of Bp1 or 17 $\beta$ -oestradiol on migration of MCF-7 human breast cancer cells using chemotaxis stimulus as determined by xCELLigence technology.....	<b>120</b>
<b>Figure 4.7</b> Effect of 31 weeks of exposure to Bp1 or 17 $\beta$ -oestradiol on invasion of MCF-7 human breast cancer cells through matrigel using chemotaxis stimulus as determined by xCELLigence technology. ....	<b>122</b>
<b>Figure 4.8</b> Effect of exposure to Bp2 or 17 $\beta$ -oestradiol on collective motility of MCF-7 human breast cancer cells as measured by wound healing assay. ....	<b>126</b>
<b>Figure 4.9</b> Effect of exposure to Bp2 on motility of individual MCF-7 human breast cancer cells as determined by time-lapse microscopy. ....	<b>127</b>
<b>Figure 4.10</b> Short-term effect of Bp2 or 17 $\beta$ -oestradiol on migration of MCF-7 human breast cancer cells using chemotaxis stimulus as determined by xCELLigence technology.....	<b>128</b>
<b>Figure 4.11</b> Long-term effect of Bp2 or 17 $\beta$ -oestradiol on migration of MCF-7 human breast cancer cells using chemotaxis stimulus as determined by xCELLigence technology.....	<b>129</b>
<b>Figure 4.12</b> Effect of exposure to Bp3 or 17 $\beta$ -oestradiol on collective motility of MCF-7 human breast cancer cells as measured by wound healing assay. ....	<b>133</b>
<b>Figure 4.13</b> Effect of exposure to Bp3 on motility of individual MCF-7 human breast cancer cells as determined by time-lapse microscopy. ....	<b>134</b>
<b>Figure 4.14</b> Short-term effect of Bp3 or 17 $\beta$ -oestradiol on migration of MCF-7 human breast cancer cells using chemotaxis stimulus as determined by xCELLigence technology.....	<b>135</b>

<b>Figure 4.15</b> Long-term effect of Bp3 or 17 $\beta$ -oestradiol on migration of MCF-7 human breast cancer cells using chemotaxis stimulus as determined by xCELLigence technology.....	<b>136</b>
<b>Figure 4.16</b> Long-term effect of Bp3 or 17 $\beta$ -oestradiol on migration of MCF-7 human breast cancer cells using chemotaxis stimulus as determined by xCELLigence technology.....	<b>137</b>
<b>Figure 4.17</b> Long-term effect of Bp3 or 17 $\beta$ -oestradiol on migration of MCF-7 human breast cancer cells using chemotaxis stimulus as determined by xCELLigence technology.....	<b>138</b>
<b>Figure 4.18</b> Short-term effect of Bp3 or 17 $\beta$ -oestradiol on invasion of MCF-7 human breast cancer cells through matrigel using chemotaxis stimulus as determined by xCELLigence technology.....	<b>140</b>
<b>Figure 4.19</b> Long-term effect of Bp3 or 17 $\beta$ -oestradiol on invasion of MCF-7 human breast cancer cells through matrigel using chemotaxis stimulus as determined by xCELLigence technology.....	<b>141</b>
<b>Figure 4.20</b> Effect of exposure to OMC or 17 $\beta$ -oestradiol on collective motility of MCF-7 human breast cancer cells as measured by wound healing assay. ....	<b>145</b>
<b>Figure 4.21</b> Effect of exposure to OMC on motility of individual MCF-7 human breast cancer cells as determined by time-lapse microscopy. ....	<b>146</b>
<b>Figure 4.22</b> Short-term effect of OMC or 17 $\beta$ -oestradiol on migration of MCF-7 human breast cancer cells using chemotaxis stimulus as determined by xCELLigence technology.	<b>147</b>
<b>Figure 4.23</b> Long-term effect of OMC or 17 $\beta$ -oestradiol on migration of MCF-7 human breast cancer cells using chemotaxis stimulus as determined by xCELLigence technology.	<b>148</b>
<b>Figure 4.24</b> Long-term effect of OMC or 17 $\beta$ -oestradiol on migration of MCF-7 human breast cancer cells using chemotaxis stimulus as determined by xCELLigence technology.	<b>149</b>
<b>Figure 4.25</b> Long-term effect of OMC or 17 $\beta$ -oestradiol on migration of MCF-7 human breast cancer cells using chemotaxis stimulus as determined by xCELLigence technology.	<b>150</b>
<b>Figure 4.26</b> Short-term effect of OMC or 17 $\beta$ -oestradiol on invasion of MCF-7 human breast cancer cells through matrigel using chemotaxis stimulus as determined by xCELLigence technology.....	<b>152</b>
<b>Figure 4.27</b> Long-term effect of OMC or 17 $\beta$ -oestradiol on invasion of MCF-7 human breast cancer cells through matrigel using chemotaxis stimulus as determined by xCELLigence technology.....	<b>153</b>

<b>Figure 4.28</b> Long-term effect of OMC or 17 $\beta$ -oestradiol on invasion of MCF-7 human breast cancer cells through matrigel using chemotaxis stimulus as determined by xCELLigence technology.....	<b>154</b>
<b>Figure 4.29</b> Effect of exposure to 4MBC or 17 $\beta$ -oestradiol on collective motility of MCF-7 human breast cancer cells as measured by wound healing assay. ....	<b>158</b>
<b>Figure 4.30</b> Effect of exposure to 4MBC on motility of individual MCF-7 human breast cancer cells as determined by time-lapse microscopy. ....	<b>159</b>
<b>Figure 4.31</b> Short-term effect of 4MBC or 17 $\beta$ -oestradiol on migration of MCF-7 human breast cancer cells using chemotaxis stimulus as determined by xCELLigence technology.	<b>160</b>
<b>Figure 4.32</b> Long-term effect of 4MBC or 17 $\beta$ -oestradiol on migration of MCF-7 human breast cancer cells using chemotaxis stimulus as determined by xCELLigence technology.	<b>161</b>
<b>Figure 4.33</b> Long-term effect of 4MBC or 17 $\beta$ -oestradiol on migration of MCF-7 human breast cancer cells using chemotaxis stimulus as determined by xCELLigence technology.	<b>162</b>
<b>Figure 4.34</b> Long-term effect of 4MBC or 17 $\beta$ -oestradiol on migration of MCF-7 human breast cancer cells using chemotaxis stimulus as determined by xCELLigence technology.	<b>163</b>
<b>Figure 4.35</b> Short-term effect of 4MBC or 17 $\beta$ -oestradiol on invasion of MCF-7 human breast cancer cells through matrigel using chemotaxis stimulus as determined by xCELLigence technology. ....	<b>165</b>
<b>Figure 4.36</b> Long-term effect of 4MBC or 17 $\beta$ -oestradiol on invasion of MCF-7 human breast cancer cells through matrigel using chemotaxis stimulus as determined by xCELLigence technology. ....	<b>166</b>
<b>Figure 4.37</b> Long-term effect of 4MBC or 17 $\beta$ -oestradiol on invasion of MCF-7 human breast cancer cells through matrigel using chemotaxis stimulus as determined by xCELLigence technology. ....	<b>167</b>
<b>Figure 4.38</b> Effect of exposure to HS or 17 $\beta$ -oestradiol on collective motility of MCF-7 human breast cancer cells as measured by wound healing assay. ....	<b>171</b>
<b>Figure 4.39</b> Effect of exposure to HS on motility of individual MCF-7 human breast cancer cells as determined by time-lapse microscopy. ....	<b>172</b>
<b>Figure 4.40</b> Short-term effect of HS or 17 $\beta$ -oestradiol on migration of MCF-7 human breast cancer cells using chemotaxis stimulus as determined by xCELLigence technology.....	<b>173</b>

<b>Figure 4.41</b> Long-term effect of HS or 17 $\beta$ -oestradiol on migration of MCF-7 human breast cancer cells using chemotaxis stimulus as determined by xCELLigence technology.....	<b>174</b>
<b>Figure 4.42</b> Long-term effect of HS or 17 $\beta$ -oestradiol on migration of MCF-7 human breast cancer cells using chemotaxis stimulus as determined by xCELLigence technology.....	<b>175</b>
<b>Figure 4.43</b> Long-term effect of HS or 17 $\beta$ -oestradiol on migration of MCF-7 human breast cancer cells using chemotaxis stimulus as determined by xCELLigence technology.....	<b>176</b>
<b>Figure 4.44</b> Short-term effect of HS or 17 $\beta$ -oestradiol on invasion of MCF-7 human breast cancer cells through matrigel using chemotaxis stimulus as determined by xCELLigence technology.....	<b>177</b>
<b>Figure 4.45</b> Long-term effect of HS or 17 $\beta$ -oestradiol on invasion of MCF-7 human breast cancer cells through matrigel using chemotaxis stimulus as determined by xCELLigence technology.....	<b>178</b>
<b>Figure 4.46</b> Statistical comparison of the varying effect of the UV screens on MCF-7 human breast cancer cells collective motility as indicated by the wound healing assay.....	<b>182</b>
<b>Figure 4.47</b> Statistical comparison of the effects of different times of exposure of MCF-7 human breast cancer cells to the UV screens as indicated by the wound healing assay. ....	<b>183</b>
<b>Figure 4.48</b> Effect of different exposure times to Bp3 or 17 $\beta$ -oestradiol on migration of MCF-7 human breast cancer cells using chemotaxis stimulus as determined by xCELLigence technology.....	<b>184</b>
<b>Figure 4.49</b> Effect of different exposure times to OMC or 17 $\beta$ -oestradiol on migration of MCF-7 human breast cancer cells using chemotaxis stimulus as determined by xCELLigence technology.....	<b>185</b>
<b>Figure 4.50</b> Effect of different exposure times to 4MBC or 17 $\beta$ -oestradiol on migration of MCF-7 human breast cancer cells using chemotaxis stimulus as determined by xCELLigence technology.....	<b>186</b>
<b>Figure 4.51</b> Representative images of the long-term effect of UV screens on morphology of MCF-7 human breast cancer cells. ....	<b>188</b>
<b>Figure 4.52</b> Representative images of the long-term effect of UV screens on morphology of MCF-7 human breast cancer cells. ....	<b>189</b>

<b>Figure 4.53</b> Effect of exposure to the UV screens on levels of E-cadherin mRNA in MCF-7 cells as determined using real-time RT-PCR.....	<b>190</b>
<b>Figure 4.54</b> Effect of long-term exposure to UV screens on the level of E-cadherin.....	<b>191</b>
<b>Figure 4.55</b> Effect of long-term exposure to UV screens on the level of E-cadherin.....	<b>192</b>
<b>Figure 4.56</b> Effect of exposure to the UV screens on levels of $\beta$ -catenin mRNA in MCF-7 cells as determined using real-time RT-PCR.....	<b>194</b>
<b>Figure 4.57</b> Effect of short-term exposure to UV screens on the level of $\beta$ -catenin. ....	<b>195</b>
<b>Figure 4.58</b> Effect of short-term exposure to UV screens on the level of $\beta$ -catenin. ....	<b>196</b>
<b>Figure 4.59</b> Effect of long-term exposure to UV screens on the level of $\beta$ -catenin. ....	<b>197</b>
<b>Figure 4.60</b> Effect of benzophenones on secreted MMP-9 activity of MCF-7 human breast cancer cells as measured by gelatin zymography. ....	<b>199</b>
<b>Figure 4.61</b> Effect of long-term exposure to UV screens on the intracellular level of MMP-14 in MCF-7 cells. ....	<b>200</b>
<b>Figure 4.62</b> Effect of exposure to the UV screens on levels of Snail mRNA in MCF-7 cells as determined using real-time RT-PCR. ....	<b>203</b>
<b>Figure 4.63</b> Effect of exposure to the UV screens on levels of Twist-1 mRNA in MCF-7 cells as determined using real-time RT-PCR.....	<b>204</b>
<b>Figure 4.64</b> Effect of exposure to the UV screens on levels of PIK3R1 mRNA in MCF-7 cells as determined using real-time RT-PCR.....	<b>205</b>
<b>Figure 4.65</b> Effect of exposure to the UV screens on levels of BMP7 mRNA in MCF-7 cells as determined using real-time RT-PCR.....	<b>206</b>
<b>Figure 4.66</b> The effect of $17\beta$ -oestradiol on MCF-7 human breast cells as determined by the xCELLigence technology. ....	<b>217</b>
<b>Figure 4.67</b> The effect of $17\beta$ -oestradiol on MCF-7 human breast cells as determined by the wound healing assay. ....	<b>218</b>
<b>Figure 5.1</b> Effect of $17\beta$ -oestradiol on proliferation of T-47-D human breast cancer cells in monolayer culture. ....	<b>221</b>

<b>Figure 5.2</b> Effect of Bp1 on proliferation of T-47-D human breast cancer cells in monolayer culture. ....	<b>222</b>
<b>Figure 5.3</b> Effect of Bp2 on proliferation of T-47-D human breast cancer cells in monolayer culture. ....	<b>223</b>
<b>Figure 5.4</b> Effect of Bp3 on proliferation of T-47-D human breast cancer cells in monolayer culture. ....	<b>224</b>
<b>Figure 5.5</b> Effect of OMC on proliferation of T-47-D human breast cancer cells in monolayer culture. ....	<b>225</b>
<b>Figure 5.6</b> Effect of 4MBC on proliferation of T-47-D human breast cancer cells in monolayer culture. ....	<b>226</b>
<b>Figure 5.7</b> Effect of HS on proliferation of T-47-D human breast cancer cells in monolayer culture. ....	<b>227</b>
<b>Figure 5.8</b> Comparison and summary of the varying effect of the UV screens on proliferation of T-47-D human breast cancer cells in monolayer culture (B). ....	<b>228</b>
<b>Figure 5.9</b> Effect of 3 weeks of exposure to UV screens on motility of T-47-D human breast cancer cells as determined by wound healing assay. ....	<b>230</b>
<b>Figure 5.10</b> Representative images of the effect of 3 weeks of exposure to UV screens on motility of T-47-D human breast cancer cells as determined by wound healing assay. ....	<b>231</b>
<b>Figure 5.11</b> Representative images of the effect of 3 weeks of exposure to UV screens on motility of T-47-D human breast cancer cells as determined by wound healing assay. ....	<b>232</b>
<b>Figure 5.12</b> Effect of 13 weeks of exposure to UV screens on motility of T-47-D human breast cancer cells as determined by wound healing assay. ....	<b>233</b>
<b>Figure 5.13</b> Effect of 30 weeks of exposure to UV screens on motility of T-47-D human breast cancer cells as determined by wound healing assay. ....	<b>234</b>
<b>Figure 5.14</b> Representative images of the effect of UV screens after 30 weeks on motility of T-47-D human breast cancer cells as determined by wound healing assay. ....	<b>235</b>
<b>Figure 5.15</b> Effect of 2 weeks of exposure to UV screens on T-47-D breast cancer cell migration towards chemotaxis stimulus on an uncoated surface. ....	<b>237</b>

<b>Figure 5.16</b> Effect of 2 weeks of exposure to UV screens on T-47-D breast cancer cell migration towards chemotaxis stimulus on an uncoated surface.....	<b>238</b>
<b>Figure 5.17</b> Effect of 7 weeks of exposure to UV screens on T-47-D breast cancer cell migration towards chemotaxis stimulus on an uncoated surface.....	<b>239</b>
<b>Figure 5.18</b> Effect of 7 weeks of exposure to UV screens on T-47-D breast cancer cell migration towards chemotaxis stimulus on an uncoated surface.....	<b>240</b>
<b>Figure 5.19</b> Effect of 13 weeks of exposure to UV screens on T-47-D breast cancer cell migration towards chemotaxis stimulus on an uncoated surface.....	<b>241</b>
<b>Figure 5.20</b> Effect of 21 weeks of exposure to UV screens on T-47-D breast cancer cell migration towards chemotaxis stimulus on an uncoated surface.....	<b>242</b>
<b>Figure 6.1</b> Effect of UV screens on MDA-MB-231 breast cancer cell proliferation as determined by xCELLigence technology. ....	<b>248</b>
<b>Figure 6.2</b> Effect of 2 weeks of exposure to $10^{-5}$ M of UV screens on MDA-MB-231 breast cancer cell migration towards chemotaxis on an uncoated surface. ....	<b>250</b>
<b>Figure 6.3</b> Effect of 8 weeks of exposure to $10^{-5}$ M concentrations of UV screens on MDA-MB-231 breast cancer cell migration towards chemotaxis on an uncoated surface. ....	<b>251</b>
<b>Figure 6.4</b> Effect of 8 weeks of exposure to $10^{-7}$ M concentrations of UV screens on MDA-MB-231 breast cancer cell migration towards chemotaxis on an uncoated surface. ....	<b>252</b>
<b>Figure 6.5</b> Effect of 2 weeks of exposure to UV screens on MDA-MB-231 breast cancer cell motility as measured by time-lapse microscopy.....	<b>254</b>
<b>Figure 6.6</b> Effect of 15 week of exposure to UV screens on MDA-MB-231 breast cancer cell motility as measured by time-lapse microscopy.....	<b>255</b>
<b>Figure 6.7</b> Effects of UV screens on MDA-MB-231 human breast cancer cells invasion through matrigel coated surfaces. ....	<b>257</b>
<b>Figure 6.8</b> Effects of UV screens on secreted MMP-2 of MDA-MB-231 breast cancer cells as measured by gelatin zymography. ....	<b>258</b>
<b>Figure 6.9</b> Effect of long-term exposure to UV screens on the protein level of MMP-14 in MDA-MB-231 breast cancer cells as determined by western immunoblotting. ....	<b>259</b>

## List of Tables

<b>Table 1.1</b> Breast cancer classification based on variation in molecular features and related examples of commonly used human breast cancer cell lines <i>in vitro</i> .....	<b>5</b>
<b>Table 1.2</b> Chemical components of cosmetics which possess oestrogenic activity.....	<b>9</b>
<b>Table 1.3</b> Selected benzophenones used in this study.....	<b>26</b>
<b>Table 1.4</b> Other selected UV screens used in this study. ....	<b>27</b>
<b>Table 1.5</b> Measurement of UV screens in human samples and the recommended maximal amount in cosmetics in The European Union (EU).....	<b>30</b>
<b>Table 2.1</b> Final concentration of UV screens in media for short and long-term exposure experiments.....	<b>39</b>
<b>Table 2.2</b> Densities of MCF-7 cells seeded in relation to the proliferation rate. ....	<b>48</b>
<b>Table 2.3</b> The QuantiTect primers (Qiagen) and their GeneGlobe specifications.....	<b>51</b>
<b>Table 2.4</b> List of antibodies used for immunoblotting.....	<b>55</b>
<b>Table 3.1</b> Summary table of the oestrogenic action of $10^{-5}$ M UV screens on MCF-7 human breast cancer cells in comparison to $10^{-8}$ M $17\beta$ -oestradiol. ....	<b>98</b>
<b>Table 3.2</b> Summary table showing the comparative effects of different coating materials on proliferation of $10^{-5}$ M UV screens on MCF-7 human breast cancer cells in comparison to $10^{-8}$ M $17\beta$ -oestradiol. ....	<b>99</b>
<b>Table 4.1</b> Effects of Bp1 on motility and invasion of MCF-7 human breast cancer cells ....	<b>123</b>
<b>Table 4.2</b> Effects of Bp2 on motility and invasion of MCF-7 human breast cancer cells ....	<b>130</b>
<b>Table 4.3</b> Effects of Bp3 on motility and invasion of MCF-7 human breast cancer cells ...	<b>142</b>
<b>Table 4.4</b> Effects of OMC on motility and invasion of MCF-7 human breast cancer cells..	<b>155</b>
<b>Table 4.5</b> Effects of 4MBC on motility and invasion of MCF-7 human breast cancer cells	<b>168</b>
<b>Table 4.6</b> Effects of HS on motility and invasion of MCF-7 human breast cancer cells.....	<b>179</b>
<b>Table 4.7</b> Summary table of the effects of UV screens on selected molecular markers. ....	<b>207</b>

# Chapter 1 Introduction

## 1.1 Introduction

Breast cancer is the leading cancer of women and causes the death of 517,000 women worldwide annually (World Health Organization, 2008). It is worth noting that incidence of breast cancer is higher in developed countries than in developing countries (Key et al., 2001). The UK's Office for National Statistics published that the incidence rate per 100,000 of female breast cancer in England was 163.6 in 2005 (Office for National Statistics, 2016), while in Saudi Arabia the documented incidence rate in the same year was 21.6 (Al-Kuraya et al., 2005). However, even if the incidence rate of breast cancer is relatively lower than in the UK, breast cancer represents the highest type of cancer among Saudi females. Interestingly, the eastern region of Saudi Arabia has the highest rate of the disease along with a high incidence rate in other neighbouring Arabian Gulf countries including Bahrain, Kuwait and Oman (Al-Eid et al., 2004). The reasons for the increasing incidence of breast cancer in the eastern region of Saudi Arabia are not published, but this part of the country is distinguished by oil industry activities (Price, 1993), which might correlate with the incidence of the disease.

Oestrogen is a main risk factor for breast cancer (Key et al., 2001) and therefore exposure to environmental pollutants, which mimic the action of oestrogen, may play a role in breast cancer development (Byford et al., 2002; Darbre and Charles, 2010) by mirroring the role of oestrogen in initiating (Russo and Russo, 2006) or influencing some of the hallmarks of breast cancer including proliferation (Darbre and Daly, 1989) or metastasis (Planas-Silva and Waltz, 2007; Chakravarty et al., 2010; Li et al., 2010; Chaudhri et al., 2012; Ganapathy et al., 2012; Ogba et al., 2014; Zhou et al., 2016; Saha Roy and Vadlamudi, 2012).

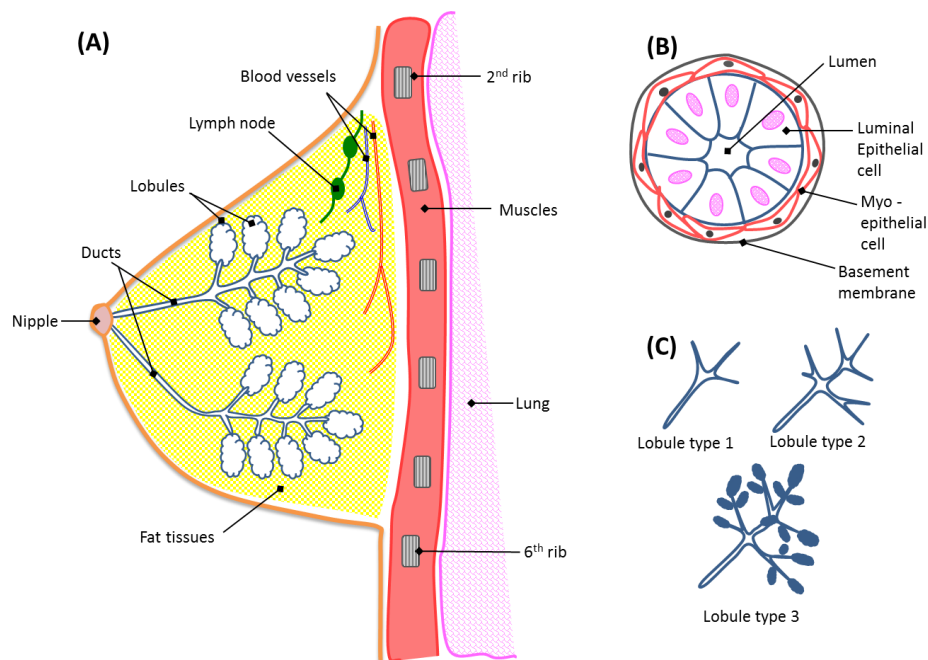
UV screens are widely used in cosmetics and other household products (Shaath, 2010; Darbre and Charles, 2010). The oestrogenicity of some of these chemicals has been reported through evidence of their influence on endocrine disruption of fish (Weisbrod et al., 2007), uterotrophic activity in rodents and proliferation of oestrogen responsive breast cancer cells *in vitro* (Schlumpf et al., 2001). A number of the UV screens have been measured in human

milk (Schlumpf et al., 2010), so they are presented in human breast and their effect on breast cancer development is plausible. Since mortality from breast cancer mainly results when the cancer cells metastasise (Solomayer et al., 2000; Schairer et al., 2004; Manders et al., 2006; Saha Roy and Vadlamudi, 2012), this study has focused on the potential effect for UV screens to increase migration and invasion of breast cancer cells *in vitro*.

## 1.2 Introduction to breast cancer

### 1.2.1 The biology of normal breast

A typical mature female breast contains milk-producing glands (lobules), which are connected to ducts that end in the nipple (Figure 1 (A)). These lobules consist of acini, formed of two cell types, the luminal epithelial cells and the myoepithelial cells (Figure 1 (B)) which are separated by the basement membrane from the surrounding connective and fatty tissues (Cichon et al., 2010; Zhu and Nelson, 2013; Liu and Gartner, 2012). The breast is supplied with blood vessels and surrounded by the lymphatic system (Russo and Russo, 2014).



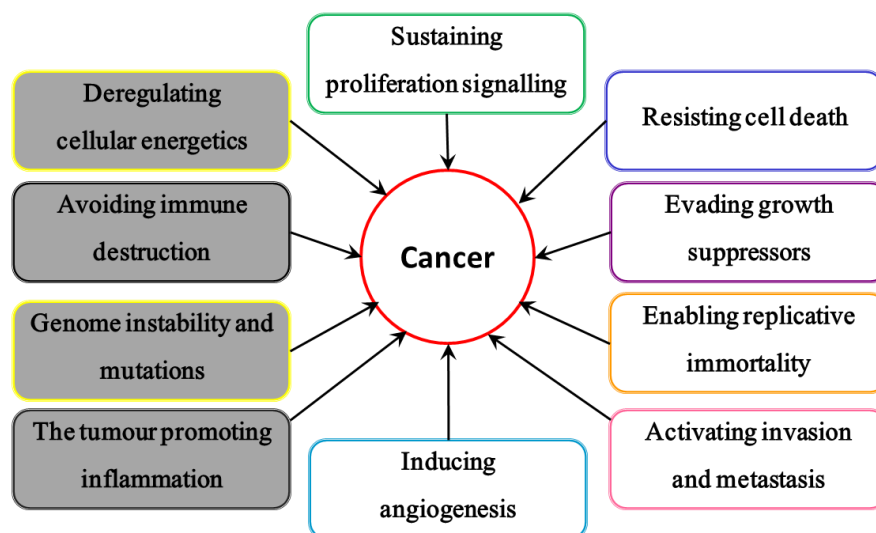
**Figure 1.1 Human female breast biology.**

Figure 1.1 represents (A) Cross section of human female breast, adapted from (Zhu and Nelson, 2013). (B) Diagram showing cross-section of an acini of a lobule, adapted from (Liu and Gartner, 2012) . (C) Lobule types (Russo and Russo, 1994).

The human breast is a hormone-responsive organ which is mainly controlled by ovarian hormones. These regulate development of the lobules through puberty, pregnancy and lactation. The undifferentiated lobule type 1 is found in childhood but the influence of oestrogen and progesterone enables a more branched and differentiated lobule type 2/3 during puberty. In pregnancy and lactation, lobule type 4 is present, a more branched and larger lobule. Following cessation of lactation, lobules regress into type 3 (Russo et al., 2000) (Figure 1.1 (C)).

### 1.2.2 The hallmarks of cancer

For cancer to develop, cell processes undergo multiple physiological alterations which transform normal cells to malignant ones. The proposal of the hallmarks of cancer defines the malignancy as exhibiting 8 hallmarks which are shared in diverse cancers as illustrated in (Figure 1.2) (Hanahan and Weinberg, 2011) and driven by 2 underlying characteristics; genome instability and mutations and the tumour promoting inflammation (Hanahan and Weinberg, 2011). Breast cancer starts when normal breast cells develop the hallmarks of cancer, especially sustained uncontrolled cell proliferation and/or the ability for cell migration and invasion (Allred et al., 2001; Hanahan and Weinberg, 2011), both hallmarks will be studied in this work.



**Figure 1.2 The hallmarks of cancer.**

This scheme represents the original six hallmarks of cancer proposed by Hanahan and Weinberg in 2000 (unshaded boxes)(Hanahan and Weinberg, 2000) and the new emerged markers proposed in 2011 (shaded boxes). Adapted from (Hanahan and Weinberg, 2011).

### 1.2.3 Classification of breast cancer

Breast cancer starts with an excessive uncontrolled proliferation of cells in the lobules or ducts which results in the production of atypical hyperplasia, a form of benign tumour which can progress into carcinoma. Based on the location of the disrupted epithelial cells, breast cancer is classified into ductal carcinoma in situ (DCIS), lobular carcinoma in situ (LCIS) or invasive ductal carcinoma (IDC). In DCIS and LCIS, the cells over-proliferate and lose typical characteristics but remain within the breast ducts (DCIS) or lobules (LCIS). In an advanced stage, a large number of the cancer cells will start to infiltrate into the local environment resulting in invasive carcinoma (IC). IC is classified into different types according to architectural features and origin of the cancer (Allred et al., 2001; Malhotra et al., 2010). In addition, breast cancer is divided into different sub-types based on the gene expression profile and some of the molecular features. Perou and his colleagues have initially classified breast cancer cells into 4 types including luminal, basal-like, enriched epidermal growth factor receptor 2 (HER2) and normal breast-like (Perou et al., 2000). Based on the expression of oestrogen receptor (ER), the luminal cells were later classified into luminal A and luminal B (Sorlie et al., 2001). More recently, specific mutations and signalling pathways were found to be subtype associated and that suggested heterogeneity within the major 4 types of breast cancer (Perou and Network, 2012). Other molecular features including Claudin-3/4/7 (Herschkowitz et al., 2007), progesterone receptor (PR), E-cadherin and vimentin were used to classify breast cancer (Andre and Pusztai, 2006; Malhotra et al., 2010; Holliday and Speirs, 2011) (Table 1.1). In addition to the 4 types which were suggested by Perou and colleagues in 2000, other groups have suggested the addition of interferon-regulated (Hu et al., 2006) or apocrine androgen receptor enriched subtype, which is ER and PR negative (Farmer et al., 2005). This heterogeneity categorization has also been used to classify the existing *in vitro* models of human breast cancer cell lines (Perou et al., 2000; Holliday and Speirs, 2011) as illustrated in Table 1.1.

**Table 1.1 Breast cancer classification based on variation in molecular features and related examples of commonly used human breast cancer cell lines *in vitro*** (Adapted from (Peruo et al., 2000; Sorlie et al., 2001; Herschkowitz et al., 2007; Malhotra et al., 2010; Holliday and Speirs, 2011; Eroles et al., 2012))

Breast cancer type	Molecular characteristics	Cell line
Luminal A	ER $\alpha$ <sup>high</sup> and Her2 <sup>low</sup>	MCF-7 and T-47-D
Luminal B	ER $\alpha$ <sup>low</sup> and Her2 <sup>low</sup>	ZR-75-1
Claudin low	ER $\alpha$ <sup>-</sup> , Claudin-3/4/7 <sup>low</sup> , E-cadherin <sup>low</sup> and vimentin <sup>+</sup>	MDA-MB-231
Basal	ER $\alpha$ <sup>-</sup> , PR <sup>-</sup> , Her2 <sup>-</sup> and EGFR <sup>+</sup>	MDA-MB-468
HER2 enriched	HER2 <sup>+</sup> and ER $\alpha$ <sup>-</sup>	SKBR3

#### 1.2.4 Risk factors for breast cancer

Several risk factors have been related to the development of breast cancer. In addition to the inherited susceptibility through loss of tumour suppressor genes, several epidemiological studies have shown that a westernized lifestyle has a major impact on the development of the disease. Hormone disruption and environmental pollution are also crucial players in the development of the breast cancer (Key et al., 2001; Hulka and Moorman, 2001).

##### 1.2.4.1 Family history

Inheritance of genetic factors increase the susceptibility in up to 10% of breast cancer (McPherson et al., 2000). Familial risk of breast cancer has been reported to increase the risk of having the disease 2-fold when a first-degree relative is affected (Pharoah et al., 1997). The loss of function of BRCA1 (Hall et al., 1990) or BRCA2 (Wooster et al., 1994) are the main links between breast cancer incidence and inherited risk factors (Claus et al., 1998). Loss of

these genes is associated with defects in several crucial biological functions of the cell including loss of DNA repair and cell cycle check points regulation (Venkitaraman, 2002).

#### **1.2.4.2 The influence of lifestyle**

There is a noticeable relation between lifestyle and becoming a breast cancer patient. An interesting point of view has emerged from different epidemiological studies in linking breast cancer and westernized lifestyle (Hortobagyi et al., 2005; Youlten et al., 2012). Migrating into high risk countries such as the USA can increase the risk of breast cancer within the migrants who come from low risk countries such as Japan (Ziegler et al., 1993). Different lifestyle choices and practices can add to the risk of breast cancer, including bearing children at a late age, avoiding breast feeding and having high alcohol consumption (Snedeker and Diaugustine, 1996; McPherson et al., 2000; Key et al., 2001; Boyle, 2005; Anand et al., 2008).

#### **1.2.4.3 Hormones and breast cancer**

An elevation of the main female sex hormones (oestrogens) have been found to correlate with the development of breast cancer, especially in postmenopausal women (Missmer et al., 2004; Trehan et al., 2012).

Oestrogen levels naturally change in the female body throughout different life stages, notably through the menstrual cycle, during pregnancy and after menopause (Wright et al., 1999; Darbre, 2015). Perturbations to the balanced hormone system through use of hormone replacement therapy (HRT) has been linked to an increased risk of development of invasive breast cancer within 1.7 % of HRT users after 2.6 years (Beral, 2003), and use of oral contraceptives has also been found to cause an increase in breast cancer incidence (Collaborative Group on Hormonal Factors in Breast Cancer, 1996).

#### **1.2.4.4 Environmental pollution and environmental oestrogens**

The environment is now thought to play a crucial role in carcinogenesis and cancer progression in the breast through the exposure to either radiation and/or chemical pollutants caused by different human activities (McPherson et al., 2000; Key et al., 2001; Darbre, 2006). A study conducted in the United States of America to measure the effect of radiation on women who worked as radiological technologists before 1940 found a high mortality of

breast cancer among participants and these deaths were believed to be connected to the high dosage of radiation (Mohan et al., 2002). Furthermore, high radiation exposure was found to be correlated with increased breast cancer incidence from the Japan atomic bomb survivors (Tokunaga et al., 1979).

In addition, other studies have demonstrated the effect of chemical pollutants on human health and on cancer incidence. In 2009, Landau-Ossondo and his colleagues found a linear relationship between the usage of organochlorine (OCs) pesticides and an increase of both prostate and breast cancer among the people who live on the island of Martinique (Landau-Ossondo et al., 2009). In another study, OCs were measured in the adipose tissue of females from Long Island, New York, where it is a high risk region for breast cancer (Stellman et al., 2000) and a correlation between high concentration of OCs and breast cancer has been reported (Muscat et al., 2003).

Among the various chemical pollutants in the environment, multiple chemicals of natural or artificial origins can manipulate the human hormonal system by mimicking specific natural hormones and interfering with their natural signalling pathways (Olea and Fernandez, 2007); compounds which interfere in oestrogen action are called “environmental oestrogens” (Darbre, 2006).

Organic or inorganic environmental oestrogens can enter the human body from activities of daily life. It can enter through diet and water, through consumption of phytoestrogens (plant-derived xenoestrogens) and through exposure to different domestic and cosmetic products including lotions, hair sprays, shampoos, underarm deodorant/ antiperspirant see Figure 1.3 below (Darbre, 2006; Darbre and Charles, 2010; Darbre, 2015).

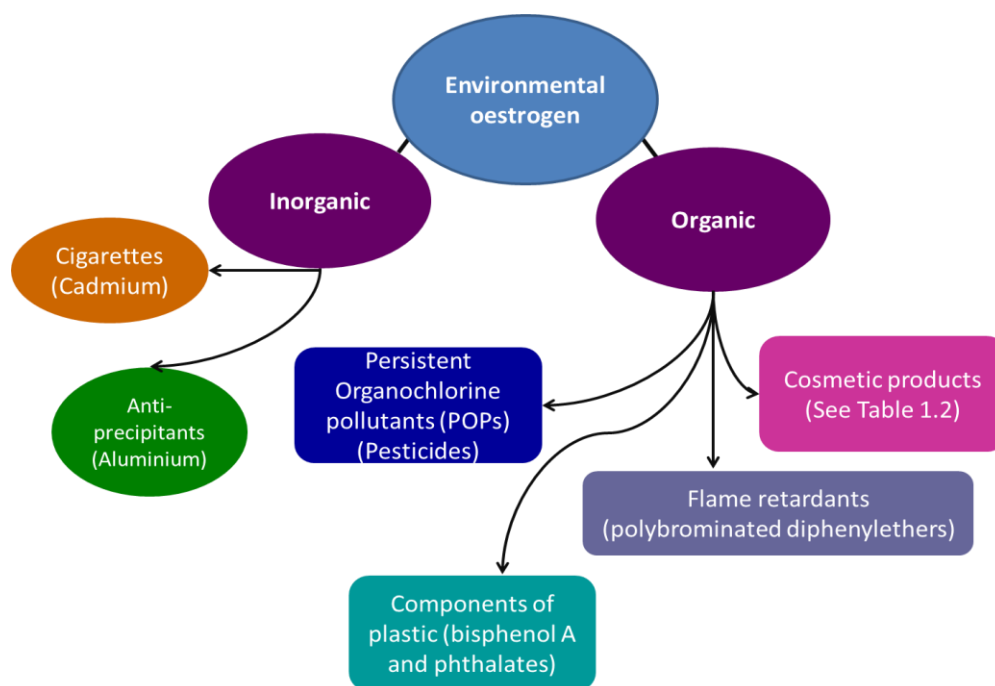


**Figure 1.3 Types and examples of environmental oestrogens.**

Adapted from (Payne et al., 2001; Darbre, 2006)

Although the sources of these chemicals might vary between different individual lifestyles, entry of these chemicals into the human body has been confirmed by several studies that measured their existence either in human breast tissue (Darbre et al., 2004; Waliszewski et al., 2005; Barr et al., 2012; Exley et al., 2007), in human milk samples (Chao et al., 2007; Schlumpf et al., 2010; Toms et al., 2011) (Table 1.2) or in human blood within hours of dermal application (Janjua et al., 2004; Janjua et al., 2007). This has led to taking into consideration the influence of several factors on the action of these chemicals including the concentration of these chemicals, the additive effect of their mixtures, the exposure route and time (Olea and Fernandez, 2007; Kortenkamp, 2007; Darbre and Charles, 2010).

Even if some of these chemicals have a very weak oestrogenic activity or might be detected in low concentrations, they might cause an oestrogenic effect after exposure as mixtures (Charles and Darbre, 2013), and disrupt the natural state and elevate the level of oestrogen related activities, which might be correlated to breast cancer progression (Darbre and Fernandez, 2013; Darbre, 2015).

**Table 1.2 Chemical components of cosmetics which possess oestrogenic activity.**

(Adapted from Darbre, 2006)

<b>Chemical component</b>	<b>Function in cosmetics</b>	<b>Evidence indicating entry to human breast</b>
<b>Parabens</b>	Preservative	Measured in human breast tissue (85.5 ng/g tissue) (Barr et al., 2012).
<b>Sunscreens</b>	Absorb or reflect UV light	Measured in human milk (19- 117 ng/g lipid) (Schlumpf et al., 2010).
<b>Phthalates</b>	Plasticizer	Measured in human milk (1.12-34.06 ng/g lipid) (Schlumpf et al., 2010).
<b>Aluminium salts</b>	Antiperspirant	Measured in human breast tissue (4-437 nmol/g dry wt.)(Exley et al., 2007).
<b>Triclosan</b>	Antimicrobial	Measured in human milk (<20-300 µg/kg lipid weight) (Adolfsson-Erici et al., 2002).
<b>Musks</b>	Fragrance chemicals	Measured in human milk (2.93-6.17 ng/g lipid) (Schlumpf et al., 2010).

### 1.3 The role of oestrogens in the development of breast cancer

Oestrogens are the main endogenous female hormones that regulate multiple important physiological processes related to the function of the reproductive system and the development of the secondary sex characteristics (Delemarre et al., 2008). There are three types of oestrogens: oestrone, oestradiol and oestriol and the most potent physiological type is  $17\beta$ -oestradiol (Alonso and Rosenfield, 2002), as illustrated in Figure 1.4 below. Oestrogen is secreted mainly by the ovaries in premenopausal women and this change after menopause to lower secretion from adipose tissue and the adrenal cortex. The precursor of oestrone is androstenedione, which is converted to oestradiol and then oestriol by aromatase (Nelson and Bulun, 2001). The enzyme aromatase also converts testosterone to oestradiol (Thomas and Potter, 2013), as shown in Figure 1.5.

The relationship between breast cancer and oestrogen was first recorded in 1896 by Beatson. He showed that breast tumour growth was reduced by surgical removal of the ovaries in premenopausal breast cancer patients (Beatson, 1896). In addition to the increasing risk of breast cancer which has been observed following the use of oral contraceptives and HRT (Key et al., 2001) as described in 1.2.4.3, further evidence for the role of oestrogen in affecting breast cancer cell proliferation was found from *in vitro* and *in vivo* models (Nandi et al., 1995; Harvell et al., 2000; Mense et al., 2008). In Darbre *et al.*'s study in 1983, oestrogen was shown to increase proliferation of the human breast cancer cell line ZR-75-1 in a dose dependent manner (Darbre et al., 1983). Based on the involvement of oestrogen in breast cancer development, therapeutic strategies against hormone-dependent breast cancer target the effect of oestrogen on breast cancer cells either by inhibiting oestrogen from binding to its cellular receptors using anti-oestrogenic drugs such as tamoxifen (Jordan, 2006), by down-regulating the oestrogen receptor protein levels using fulvestrant (Wakeling, 1995) or by preventing oestrogen synthesis using aromatase inhibitors (Manders and Gradishar, 2005).

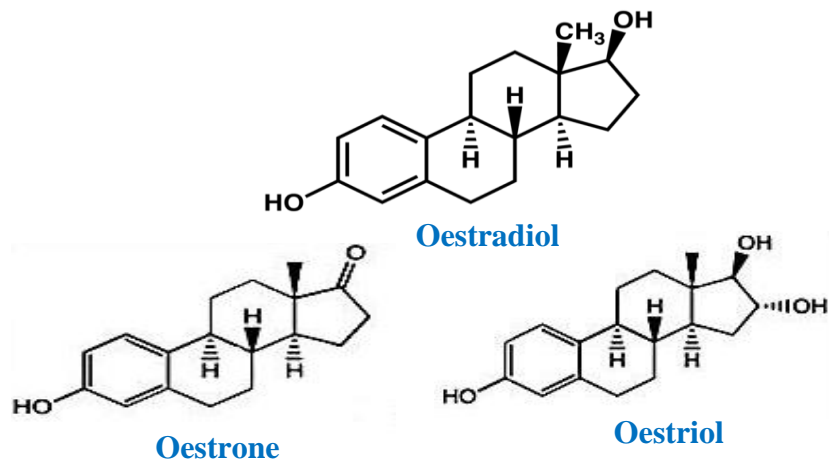


**Figure 1.4** The structure of oestradiol, oestrone and oestriol.

Adapted from (Thomas and Potter, 2013).

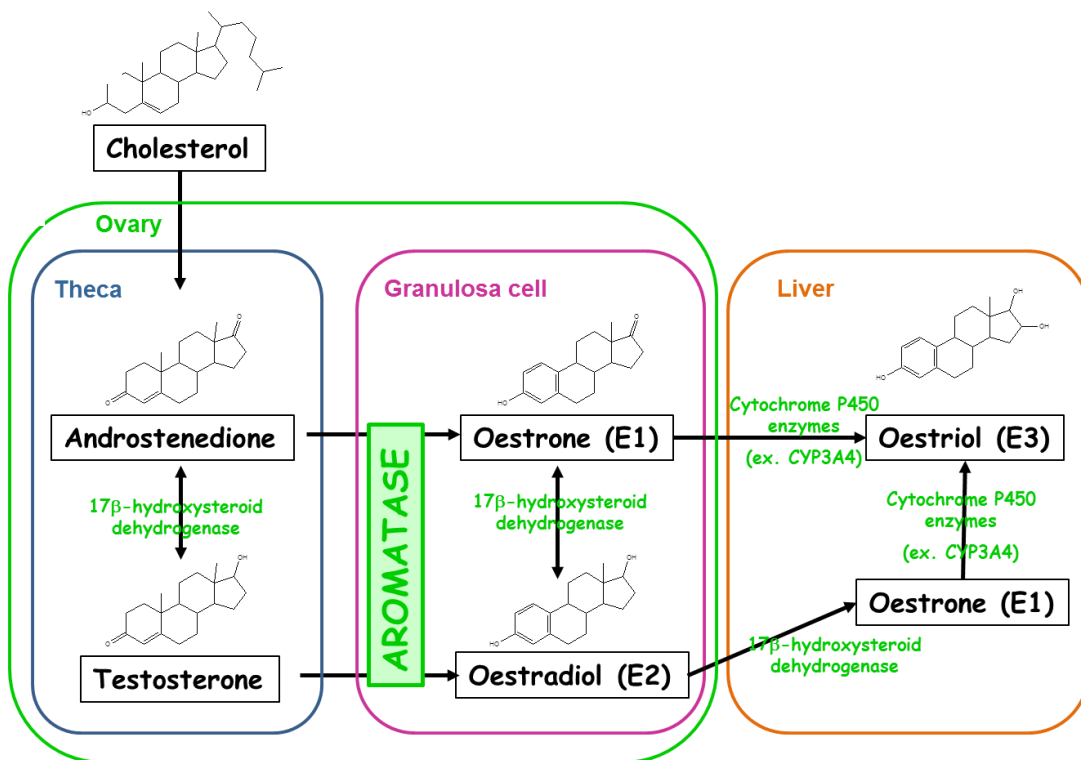


**Figure 1.5** Biosynthesis of oestrogens in the ovary and the liver.

The precursors of oestrogens (androstenedione and testosterone) are biosynthesised in the theca interna and converted in the granulosa cells to oestrogens by the enzyme aromatase. (Adapted from (Cheng et al., 2001; Thomas and Potter, 2013; Darbre, 2015)).

### **1.3.1 Molecular action of oestrogen**

Although the lipophilic nature of oestrogens allow them to diffuse passively through the cell membrane (Beato and Klug, 2000), their biological functions require the presence of intracellular oestrogen receptor proteins ER $\alpha$  and ER $\beta$  (Nelson and Bulun, 2001). After the binding of oestrogen to ER, molecular mechanisms of action may be genomic or non-genomic (Katzenellenbogen et al., 2000; Cheskis et al., 2007; McDevitt et al., 2008; Darbre, 2012).

#### **1.3.1.1 Oestrogen receptors**

In the late 1960s the mechanism of action of oestrogen was confirmed to be dependent on its interaction with cellular receptor proteins (Toft and Gorski, 1966). The cDNA for oestrogen receptor  $\alpha$  (ER $\alpha$ ) was first cloned in 1985 (Walter et al., 1985). Eleven years later the oestrogen receptor  $\beta$  (ER $\beta$ ) was cloned (Mosselman et al., 1996). ER $\alpha$  and ER $\beta$  share a close structural homology although they are produced from two separate genes. ER $\alpha$  is localized on the human chromosome 6q24-q27 (Gosden et al., 1986), while ER $\beta$  is localized on chromosome 14q22-q24 (Enmark et al., 1997). Both proteins are composed of 5 functional domains (A-F). The first is located at the N-terminal (A/B) region and encodes the hormonal independent transcriptional activation function 1 (AF1). The second domain is region C, called the DNA binding domain (DBD). DBD is responsible for the specific binding of oestrogen-ER dimers to enhancer elements termed oestrogen response elements (ERE) in the region of the target genes through zinc finger motifs. The third domain (the hinge) in region D facilitates the receptor conformational changes and dimerization. The fourth domain is the region E, known as the ligand binding domain (LBD) and is where the oestrogen binds into a specific binding pocket to the ER. The final domain is region F and contains the hormone-dependent transcriptional activation function 2 (AF2) (Figure 1.6) (Nilsson et al., 2001; Osborne et al., 2001; Ascenzi et al., 2006; Darbre, 2012).

Although 17 $\beta$ -oestradiol has the highest binding affinity to the ER in comparison with other oestrogens (Zhu et al., 2006) (Figure 1.7), oestrogen receptors binding affinity is known for its high plasticity. Along with oestrogens, these receptors can accommodate phyto-oestrogens or synthetic chemicals (environmental oestrogens) of quite different sizes and structures (Kiyama and Wada-Kiyama, 2015) and activate subsequent oestrogenic responses (Jordan et al., 1985; Katzenellenbogen, 1995; Oostenbrink et al., 2000). One key binding requirement

seems to be a *p*-hydroxy phenyl ring group together with a hydrophobic region, which can then bind into LBD in an analogous manner to 17 $\beta$ -oestradiol (Katzenellenbogen, 1995; Fang et al., 2001) (Figure 1.7).

Oestrogen receptors are present not only in the breast but also in other tissues such as the ovaries, uterus, bones, and brain. These tissues vary in the levels of ER $\alpha$  and ER $\beta$  (Nilsson et al., 2001; Gustafsson, 2003; Heldring et al., 2007; Pearce and Jordan, 2004) and together with varied levels of coactivators or corepressors this leads to a tissue specific response to oestrogens (Katzenellenbogen et al., 1996; Nilsson et al., 2001; Heldring et al., 2007). In breast cancer cells both ER $\alpha$  and ER $\beta$  are present (Jarvinen et al., 2000; Pearce and Jordan, 2004; Hartman et al., 2009) with higher levels of ER $\alpha$  in ER-positive breast cancer tumours (Miyoshi et al., 2010). It has been shown that induced expression of ER $\beta$  works as a negative modulator of ER $\alpha$  in cells that express both receptors and reduces the 17 $\beta$ -oestradiol proliferative response of MCF-7 cells (Paruthiyil et al., 2004) and T-47-D cells (Strom et al., 2004).

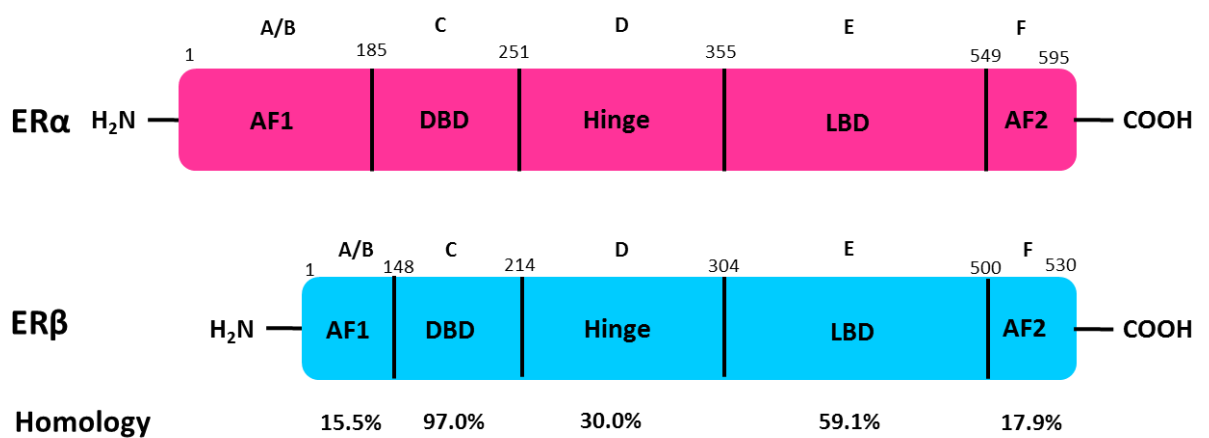


**Figure 1.6 Schematic representation of the functional domains of the human oestrogen receptors ER $\alpha$  and ER $\beta$ .**

AF1= activating function 1; AF2= activating function 2; DBD= DNA binding domain; LBD= ligand binding domain. The relative amino acid homology between corresponding domains is shown. Adapted from (Osborne et al., 2001; Darbre, 2012).

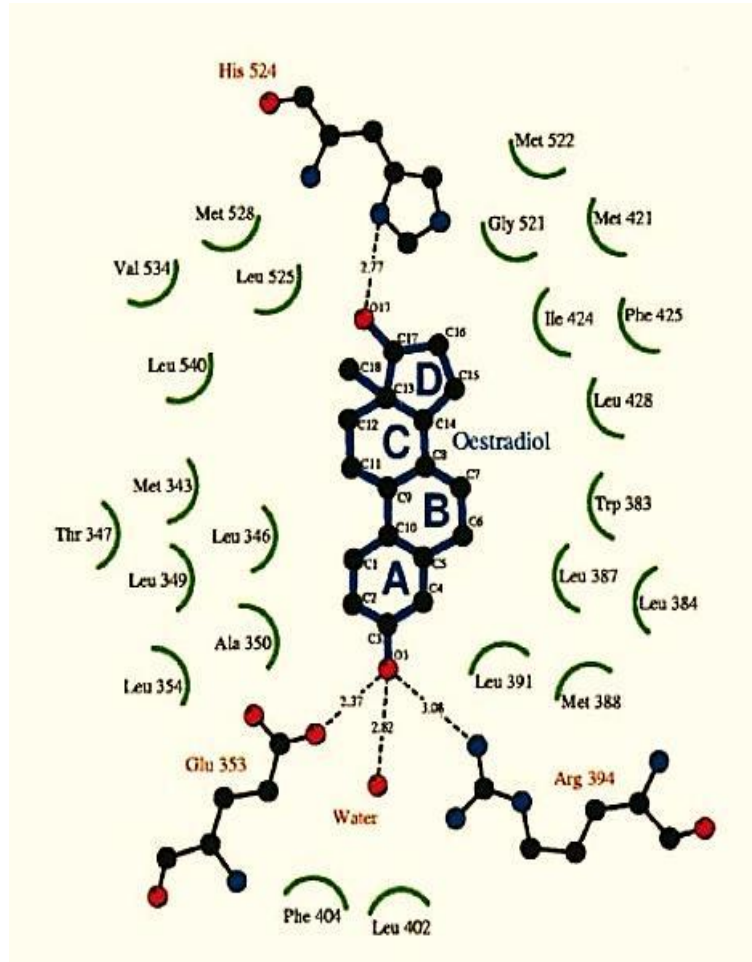


**Figure 1.7 Crystal structure of the ligand binding of 17 $\beta$ -oestradiol to oestrogen receptor alpha.**

Figure 1.7 illustrates the hydrogen bonding (dotted lines) between 17- $\beta$  oestradiol and specific amino acids of the ligand binding domain of the oestrogen receptor and water molecules. Glu 353, Arg 394 and His 524 (histidine 542) are the key polar amino acids in the ER pocket (coloured in red) (from (Brzozowski et al., 1997)).

### **1.3.1.2 Genomic action of oestrogen**

In the absence of ligand, oestrogen receptors remain inactive as a result of binding to receptor associated proteins (RAPs). However, binding of ER to oestrogen in a 1:1 ratio causes the phosphorylation of ER and the dissociation of RAPs (Pratt, 1992; Klinge et al., 1997). Oestrogen binds to the LBD of the ER, which results in a change of conformation of the ER and dimerization of the oestrogen-ER complexes. Dimers translocate to the nucleus and bind to specific nucleotide sequences in the DNA, a sequence called oestrogen response elements (ERE). Coactivators or corepressors will then be recruited and transactivation results in modulation of cellular gene expression (as reviewed by (Nilsson et al., 2001; Darbre, 2015)). Many genes are known to be regulated through the direct genomic action of oestrogen. One early oestrogen-regulated gene was the Trefoil factor 1 (TFF1) isolated as pS2 (Masiakowski et al., 1982; Brown et al., 1984; Jakowlew et al., 1984) (Figure 1.8 (1)). TFF1 protein is predominantly expressed in the gastrointestinal tract (Rio et al., 1988), where it stimulates epithelial cells restitution and migration (Marchbank et al., 1998). The biological role of TFF1 protein in breast cancer was unknown (May and Westley, 1997) until the stimulation of MCF-7 and MDA-MB-231 breast cancer cells migration by TFF1 protein was documented (Prest et al., 2002). Many hundreds of other genes are regulated by oestrogen, more of which are downregulated than upregulated (Frasor et al., 2003). Among the molecular actions of oestrogen, the genomic action is the most considered in the context of breast cancer tumorigenicity and progression and as consequence was targeted therapeutically using tamoxifen (Jordan, 2006) and fulvestrant (Wakeling, 1995).

### **1.3.1.3 Indirect genomic action of oestrogen**

Molecular action of the dimerized oestrogen-ER complexes is not always through binding directly to DNA. The complex can act also as a coactivator by interacting with other specific transcription factors, such as Fos/Jun AP-1 complex (Webb et al., 1999), leading to modifications of gene expression which are not mediated by the ERE (Umayahara et al., 1994; Darbre, 2012) (Figure 1.8 (2)).

### **1.3.1.4 Non-genomic action of oestrogen**

Non-genomic mechanisms of action occur when the oestrogen binds to oestrogen receptors in the cellular membrane which can generate cytosolic signalling cascades (Razandi et al., 2002; Darbre, 2012; Kow and Pfaff, 2016). One mode of action involves the modulation of ion

channels (Picotto et al., 1999; Kow and Pfaff, 2016). Another mode of  $17\beta$ -oestradiol action is to mediate signalling pathways through the binding of E-ER complexes to tyrosine kinase receptors (Filardo et al., 2002) or through binding of oestrogen to G-protein-coupled estrogen receptor 1 (GPER) (Filardo et al., 2000). The interaction of  $17\beta$ -oestradiol with the cell membrane receptors resulting in activation of mitogen-activated protein kinase (MAPK) (Filardo et al., 2002; Song et al., 2002b) and phosphatidylinositol 3-kinase (PI3K)/Akt signalling pathways (Haynes et al., 2000) in oestrogen responsive cells and therefore regulates cell proliferation and migration (Figure 1.8 (3)).

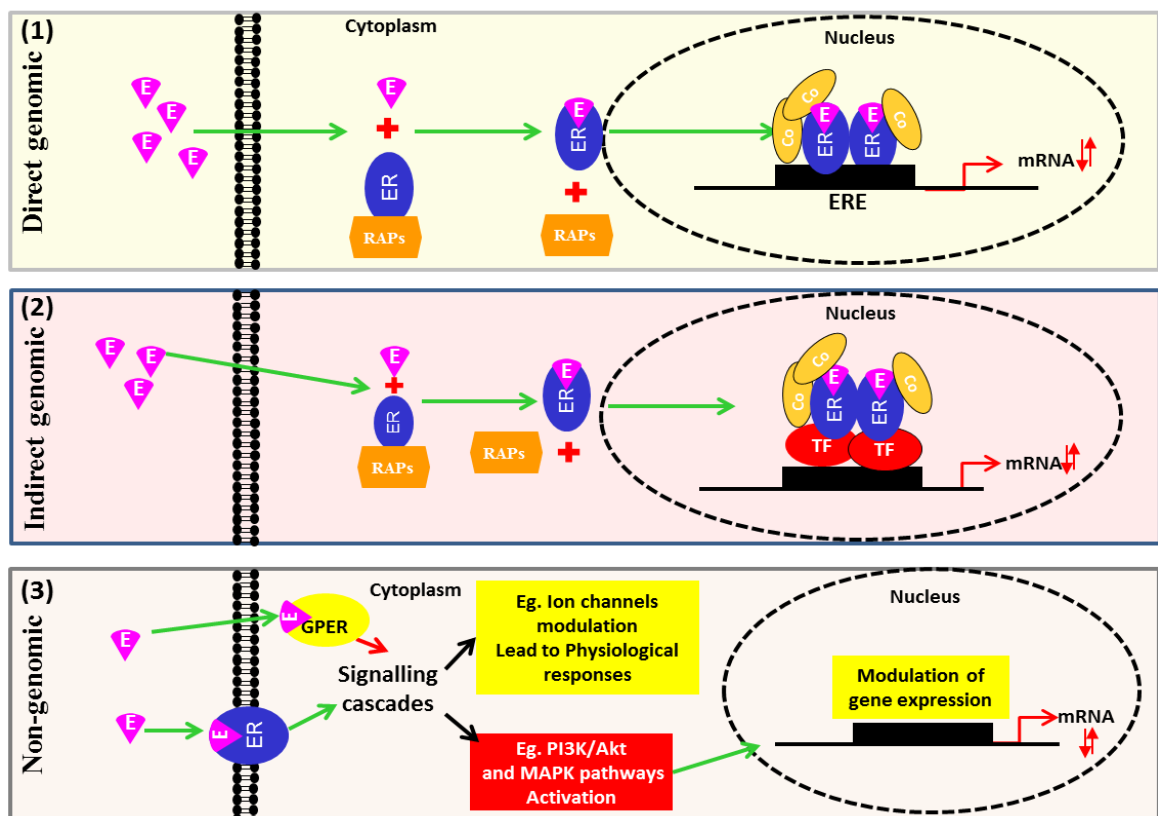


**Figure 1.8 Molecular mechanisms of action of oestrogen.**

(1) Direct genomic action via the interaction between oestrogen (E), oestrogen receptor (ER) and the oestrogen responsive element (ERE) (DNA-protein interaction). (2) Indirect genomic action by interacting of E-ER complex with transcription factors (TF) (protein-protein interaction). (3) Non-genomic interaction, E binds to membrane ER or transmembrane GPER and initiates signalling cascades which activates different cellular pathways and physiological responses. Adapted from (Heldring et al., 2007; Darbre, 2012; Arevalo et al., 2015; Contrò et al., 2015).

### 1.3.2 Oestrogen and breast epithelial cell proliferation

One of the hallmarks of cancer is the ability of malignant cells to keep sustained uncontrolled proliferation, which can result in changing of the normal tissue structure and losing the physiological functions of the organ (Hanahan and Weinberg, 2011). As described in section 1.2.1 above, oestrogen has an important role in normal breast development and growth (Russo et al., 2000). However, evidence has now been gathered to show it can also stimulates the proliferation of oestrogen responsive breast cancer cells (Lippman and Dickson, 1989). The profound effect of oestrogen on cell proliferation can occur through alteration to growth factor signalling pathways (Lippman and Dickson, 1989) and cell cycle-regulated proteins (Sutherland et al., 1998; Darbre, 2012).

Growth factors act by binding to specific growth factor receptors which act through signal transduction pathways to influence cellular processes such as proliferation and differentiation (Bafico and Aaronson, 2003). In breast cancer, oestrogen can cross talk with several growth factor signalling pathways such as the transforming growth factor  $\alpha$  (TGF- $\alpha$ ), epidermal growth factor (EGF), insulin- like growth factors (IGF) and platelet derived growth factor (PDGF) (Lippman and Dickson, 1989). Oestrogen can cross-talk with growth factor signalling pathways either by influencing the levels of the growth factors (Lippman et al., 1987), their receptors (Lee et al., 1999; Maor et al., 2006), their binding proteins (Matsuda et al., 2001) or by increasing the sensitivity of breast cancer cells towards their regulation (Stewart et al., 1990). Moreover, some of the growth factors can phosphorylate and activate the oestrogen receptors in the absence of ligand (Bunone et al., 1996).

Oestrogen and the growth factors have been found to increase oestrogen responsive cell proliferation through influencing cell cycle regulation (Dufourny et al., 1997; Mawson et al., 2005). To achieve this effect, oestrogen regulates c-myc, a nuclear transcriptional factor that is known to enhance oestrogen responsive cell proliferation via the alteration of cell cycle proteins (Dubik et al., 1987; Watson et al., 1991; Sutherland et al., 1998; Doisneau-Sixou et al., 2003). Oestrogen can increase cyclin D1 expression (Altucci et al., 1996) and activate cyclin E as well as increasing its expression (Planas-Silva and Weinberg, 1997; Niu et al., 2015). Both of those cell cycle proteins mediate G1/S progression (Musgrove et al., 1994; Prall et al., 1998; Doisneau-Sixou et al., 2003). Oestrogen can also reduce the recruitment of

cell cycle kinase inhibitors and their ability to bind to the cyclin proteins (Sutherland et al., 1998).

### **1.3.3 Oestrogen and breast cancer cell metastasis**

Breast cancer motility arises mainly when the breast cancer cells migrate from the primary tumour site, invade and localize in other distant organs in a process known as breast cancer metastasis (Weigelt et al., 2003; Redig and McAllister, 2013). The main distant organs affected by breast cancer metastasis are the bone, liver, lung and brain (Nguyen et al., 2009).

Cancer cell metastasis is a complex process which involves modulating interaction of cells with their extracellular matrix (ECM) and with other surrounding cells (Timar et al., 2001; Martin et al., 2013). In order to achieve metastasis, cancer cells have to undergo multiple changes in their morphology and adhesion properties to enable their mobility (Ridley et al., 2003). Then cancer cells have to invade surrounding barriers including the basement membrane and ECM components in order to reach the lymph nodes and the blood stream (intravasation) to be carried to the new site. Finally, they invade the new tissue (extravasation) and return to their non-motile form and start colonizing and proliferating in the new site (Nguyen et al., 2009; Hanahan and Weinberg, 2011).

Breast cancer cells migrate both individually (van Zijl et al., 2011; Y.-C. Chen et al., 2015) or collectively (Planas-Silva and Waltz, 2007; van Zijl et al., 2011; Cheung et al., 2013). Both migration types include similar mechanisms but the process of migration that is found in single cell migration will extend across the entire cell sheet with maintenance of cell-cell adhesion (Friedl and Gilmour, 2009; Friedl et al., 2012).

The role of oestrogen and its receptors in breast cancer metastasis remains to be fully understood. While several studies have documented the negative effect of oestrogen and its receptors on breast cancer cell metastasis (Rocheffort et al., 1998; Sisci et al., 2004; Ma and Gollahon, 2016), other studies have recorded a positive effect (Planas-Silva and Waltz, 2007; Chakravarty et al., 2010; Li et al., 2010; Chaudhri et al., 2012; Ganapathy et al., 2012; Ogba et al., 2014; Zhou et al., 2016). The following sections focus on some of the biological characteristics and molecular markers influenced by oestrogen in breast cancer cell metastasis.

### **1.3.3.1 Mechanisms of breast cells; polarity, adhesion, motility and epithelial to mesenchymal transition (EMT)**

The architecture of breast epithelial cells is disrupted in malignancy (Bazzoun et al., 2013). Normal epithelial cells have an apical-basal polarity where the apical part is directed toward the lumen and the opposite edge (the base) is adhered to the basement membrane or the ECM. This architecture is achieved by the presence of tight junctions that separate the apical area from the lateral sides between the cells, by the sufficient cohesive intracellular adhesion on the lateral sides, by the maintenance of base adhesion to the ECM and by the preservation of the polarized distribution of the cytoskeleton (Rodriguez-Boulan and Nelson, 1989).

Intracellular adhesion (cell-cell adhesion) is mediated by tight junctions in the apical domain, adherens junctions, desmosomes and gap junctions on the lateral sides of the cells (Bazzoun et al., 2013; Martin et al., 2013). Many proteins are involved in cell-cell adherens junctions including E-cadherin,  $\beta$ -catenin and  $\alpha$ -catenin of which E-cadherin binds directly to the cytoskeletal actin (Ratheesh and Yap, 2012; Martin et al., 2013) (Figure 1.9).

E-cadherin (135 kDa) (Vestweber and Kemler, 1984) is a transmembrane protein (Takeichi, 1991) encoded by the CDH1 gene (Berx et al., 1995). The N-terminal portion of E-cadherin extends into the extracellular environment of the cells. This N-terminal region of the protein is formed of 5 domains of cadherin sequence repeats of 110 amino acids separated by  $\text{Ca}^{++}$  binding sites (Patel et al., 2003; Parisini et al., 2007), which facilitate the homophilic binding with E-cadherin from neighbouring cells (Takeichi, 1991). The intracellular part of E-cadherin is linked to the actin cytoskeleton (Ozawa et al., 1989) via the catenin proteins (Kemler, 1993)( $\beta$ -catenin,  $\gamma$ -catenin,  $\alpha$ -catenin and P120-catenin) to strengthen cell-cell adhesion, and mediates signalling through catenins (Vestweber, 2015).

$\beta$ -catenin and  $\gamma$ -catenin serve as anchor between the E-cadherin intracellular domain (Nagafuchi and Takeichi, 1989; Kemler, 1993; Zhurinsky et al., 2000) and  $\alpha$ -catenin which binds to the actin filaments (Rimm et al., 1995; Yonemura, 2011; C.-S. Chen et al., 2015). P120-catenin binds to the intracellular domain of E-cadherin including the juxtamembrane region and is believed to have a role in E-cadherin clustering at the adherens junctions (Yap et al., 1998).

$\beta$ -catenin (92 kDa) (Ozawa et al., 1989) is encoded by the CTNNB1 gene (van Hengel et al., 1995). Alongside localization in adherens junctions, this protein was also found to serve as a nuclear transcriptional coactivator when unengaged with E-cadherin. Initially the free  $\beta$ -catenin cytoplasmic pool increases when  $\beta$ -catenin is stabilized by activation of the Wnt signalling pathway (Papkoff et al., 1996; Novak and Dedhar, 1999). Then  $\beta$ -catenin re-localizes to the nucleus where it complexes with lymphoid enhancer factor-1/T-cell factor transcription factors (LEF/TEF) (Behrens et al., 1996; Hsu et al., 1998) and trans-activates LEF/TEF targeted genes (Eastman and Grosschedl, 1999). It is worth noting that the  $\beta$ -catenin/Wnt pathway also increases cancer cell proliferation (Tan et al., 2016). One of the possible explanations is that  $\beta$ -catenin transactivates LEF/TEF to increase the expression of c-myc (He et al., 1998) and cyclin D1 (Shtutman et al., 1999; Lin et al., 2000) which are both regulators of cancer cell proliferation (see section 1.3.2 above). In addition, some of the downstream targets of the  $\beta$ -catenin/Wnt signalling pathway are also involved in cancer cell metastasis through inducing activators of epithelial-mesenchymal (EMT) transition (Prasad et al., 2008) such as Twist and Snail (Yook et al., 2006; Kahlert et al., 2012). Knock down of  $\beta$ -catenin (Xu et al., 2015) or suppressing the  $\beta$ -catenin/Wnt signalling pathway (Tsai et al., 2013; Fan and Guo, 2015; Hu and Xie, 2015) also impairs breast cancer cell metastasis capability.

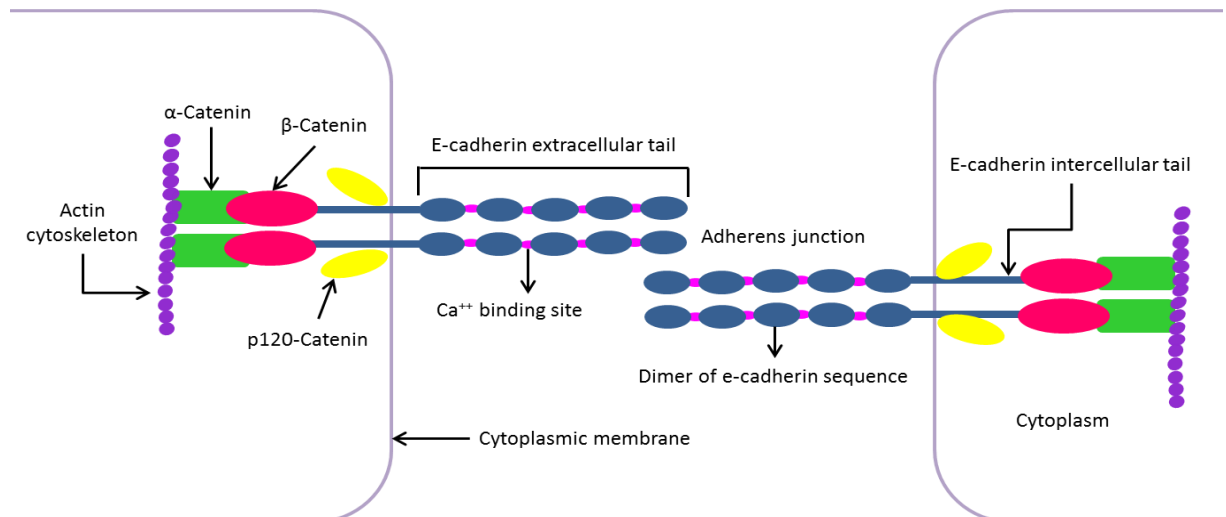


**Figure 1.9 Schematic representation of epithelial cell-cell adhesion mediated by E-cadherin.**

The adherens junction is formed by homophilic binding of the extracellular tail of E-cadherin from neighbouring cells. The intracellular part of E-cadherin is linked to the actin cytoskeleton through binding to  $\beta$ -catenin and  $\alpha$ -catenin. P120-catenin binds E-cadherin to the juxtamembrane sites. Adapted from (Pecina-Slaus, 2003; Wheelock et al., 2008; Vestweber, 2015).

In order to maintain the apical-basal polarity, epithelial cells maintain cell-ECM adhesion. The extracellular matrix or the basement membrane consists of different macromolecules including laminin, collagen and fibronectin (Yurchenco et al., 2004). Epithelial cell-ECM adhesion can be achieved mechanically through focal adhesion (BurrIDGE et al., 1988). Part of the focal adhesion is the integrin family, which are transmembrane adhesion receptors (Calderwood et al., 2000) that directly affect cell polarization through coupling to the actin cytoskeleton (BurrIDGE and Chrzanowska-Wodnicka, 1996; Ciobanasu et al., 2013). The interaction between the ECM and focal adhesion molecules can fire a cascade of signalling pathways (BurrIDGE and Chrzanowska-Wodnicka, 1996) and influence cell proliferation and metastasis (Larsen et al., 2006; Tilghman and Parsons, 2008).

The initial step in epithelial cell migration is the loss of the apical-basal polarity (Drasin et al., 2011). In a subsequent step, there is an alteration of adhesion between cells and/or between cells and the ECM (Ridley et al., 2003). Cells then show front-back end polarity by being

directed towards a leading edge, where protrusions are formed to reach a new site and new adhesions occur. On the opposite side of the cell is a trailer edge where detachment of adhesion occurs (Ridley et al., 2003; Steeg, 2006). The cell will cause an actin-myosin fibre contraction within the cytoskeleton, which will move the cell forwards (Morton and Parsons, 2011).

Breast cancer cells exhibit morphological changes during metastasis which are associated with the acquisition of mesenchymal or fibroblast spindle-like morphology in a process called epithelial-mesenchymal transition (EMT)(Drasin et al., 2011). At a molecular level, multiple transcription factors are involved in EMT such as Twist, Snail and zinc-finger-E-box-binding (ZEB) (Lamouille et al., 2014). During EMT, epithelial cells lose cell-cell adhesion through suppression of the expression of E-cadherin and cytokeratins, and obtain mesenchymal properties such as overexpression of N-cadherin and vimentin which together results in more motile and invasive cell behaviour (Christiansen and Rajasekaran, 2006; Kalluri and Weinberg, 2009; Sanchez-Tillo et al., 2012). When arriving at the new site, cancer cells regain the epithelial characteristics (Bukholm et al., 2000) in a process known as mesenchymal-epithelial transition (Yao et al., 2011; Heerboth et al., 2015).

The mode of tumour motility varies between different cancer cell types (Friedl and Wolf, 2003; Clark and Vignjevic, 2015) from individual amoeboid or mesenchymal cell motility to collective cell migration (Friedl and Alexander, 2011). Although EMT was reported to play a crucial role in cancer metastasis (Thiery, 2002; Xue et al., 2003; de Herreros et al., 2010; May et al., 2011), some reports suggest that some of the epithelial cells can gain motility in a manner independent of EMT (Pinkas and Leder, 2002) or partially acquire some of the mesenchymal cell markers besides retaining epithelial cell morphology and markers such as the expression of E-cadherin (Boyer et al., 1992; Klymkowsky and Savagner, 2009; de Herreros et al., 2010; Uchino et al., 2010; Gao et al., 2014), producing a transit status known as metastable phenotype (Lee et al., 2006; Klymkowsky and Savagner, 2009). In addition, in collective migration the expression of E-cadherin remains essential for motility of cell sheets (Hwang et al., 2012). The plasticity of cancer cells contributes to the varied routes of cancer cell metastasis and invasion (Friedl and Alexander, 2011).

### **1.3.3.2 Oestrogen regulation of breast cancer cell morphology and EMT**

Oestrogen was found to enhance breast cancer cell migration through influencing several morphological and molecular characteristics of the epithelial breast cancer cells. One of the earliest studies was conducted by Sapino *et.al* in 1986 in which they noted that exposure to oestrogen caused rearrangement of the cytoskeleton of MCF-7 cells and increased the pseudopodial protrusions where adhesion areas were mostly localized (Sapino et al., 1986). Also, the F-actin cytoskeleton of MCF-7 cells was found to be rearranged after exposure to oestrogen. This change in the cytoskeleton was marked by the presence of active lamellipodial structures beneath the cell clusters with the presence of E-cadherin cell-cell adhesion (DePasquale, 1999). Later, Song and his colleagues reported that oestrogen increases the ruffling and pseudopodia formation in the membrane of MCF-7 cells, both of which are characteristic features of migratory cells (Song et al., 2002b). In another study oestrogen was found to enhance a spindle-like elongated cell morphology in both MCF-7 and ZR-75-1 human breast cancer cells and enhance collective migration of a subset of MCF-7 cell clusters which retained the expression of E-cadherin (Planas-Silva and Waltz, 2007). Since E-cadherin was not lost entirely in the presence of oestradiol, EMT and subsequent motility caused by oestrogen in MCF-7 cells is suggested to be through the down-regulation of E-cadherin expression (Oesterreich et al., 2003), the alteration of localization of associated proteins such as  $\beta$ -catenin (Planas-Silva and Waltz, 2007) or alteration of localization of E-cadherin (DePasquale, 1999).

However, oestrogen was also found to influence other signalling pathways during the observed increase in breast cancer cell motility. It has been documented that oestrogen increases the motility of T-47-D cells via interacting with PI3K and MAPK signalling pathways, which activate focal adhesion kinase, paxillin and c-Src (Li et al., 2010). Recently Ho and his colleagues have reported that oestrogen influences the phosphorylation of the PI3K/Akt signalling pathway in MCF-7 cells via the interaction of ER $\alpha$  and integrin  $\beta$ 4 resulting in enhanced cell motility (Ho et al., 2016).

### **1.3.3.3 Oestrogen regulation of matrix metalloproteinases (MMPs) in breast cancer cell migration and invasion**

Degradation of the ECM components and surrounding tissue is an essential process in cancer cell metastasis. This process is influenced mainly by the secretion of matrix metalloproteinases (MMPs) (Stamenkovic, 2000) which results in targeting and releasing several growth factors from the surrounding microenvironment (Song et al., 2007; Kessenbrock et al., 2010; Sbardella et al., 2012) and disrupting the ECM structure (Stamenkovic, 2000).

MMPs are a family of endopeptidases expressed in both normal and cancer cells and controlled by the tissue inhibitors of matrix metalloproteinases (TIMP) (Gomez et al., 1997; Nagase and Woessner, 1999). MMPs are either secreted extracellularly (Stamenkovic, 2000) or remained anchored to the cells as transmembrane proteins (Sato et al., 1994; Takino et al., 1995). They are subdivided into different subclasses depending on their ability to degrade different substrates such as gelatin and collagen (Stamenkovic, 2000). The activation of the latent form of the MMPs can be initiated by interaction with several modulators and by auto activation between the family members (Stamenkovic, 2000). For example, the regulation of MMP-2 was found to be activated via the interaction with the membrane anchored MMP-14 (Atkinson et al., 1995). Several members of the MMPs family were found to be highly expressed in primary human breast cancers in comparison to non-cancerous controls (Kohrmann et al., 2009). MMP-2 and MMP-9 were found to be expressed in human breast cancer tissue in a greater amount than normal breast tissue (Garbett et al., 2000), and have also been reported in breast cancer cells *in vitro* (Kohrmann et al., 2009) and the membrane attached MMP-14 (Devy et al., 2009). The ability of MMPs to induce EMT in breast cancer cells enables them to move through the breast stroma in the process of metastasis (Radisky and Radisky, 2010).

In breast cancer patients, the high expression of MMP-9 and MMP-11 was found to correlate with distant metastasis (Vizoso et al., 2007) which supports the findings from the *in vitro* studies showing a correlation of MMPs activity and the metastatic ability of breast cancer cells. In MDA-MB-231 cells, MMP-14 was found to be a key enzyme in the formation of functional invadopodia that degrade the gelatin matrix (Artym et al., 2006). Moreover, it was found that TIMP-4 transfection can inhibit the MMPs activity and impair invasion activity of

the MDA-MB-435 cells (Wang et al., 1997). *In vivo* the survival rate of nude mice which were injected with TIMP-2 transfected MDA-MB-231 cells was higher than the mice injected with the wild type of non-transfected MDA-MB-231 cells (Yoneda et al., 1997).

The non-genomic action of oestradiol in MCF-7 cells was found to activate the MAPK signalling pathway by activating a linear sequences of events including MMP-2 and MMP-9 (Song et al., 2007). Furthermore, oestradiol was found to increase the expression of MMP-9 mRNA expression in MCF-7, MDA-MB-231 and ZR-75-1 cell lines (Kousidou et al., 2008). In contrast, others reported a reducing effect of oestradiol on the activity of MMP-2/MMP-9 in MCF-7 cells (Nilsson et al., 2007).

## **1.4 Breast cancer and UV screens**

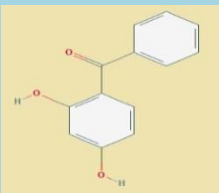
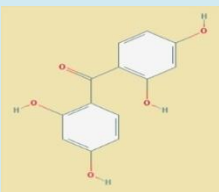
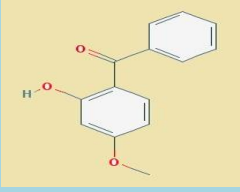
### **1.4.1 Introduction to UV screens**

Ultraviolet rays (UVR) are a component of the solar radiation waves that reach the earth (Rai et al., 2012). Different sub-types of these UVR negatively affect the integrity of industrial products (Yousif and Hasan, 2015). Further, they are able to cause skin damage to humans. For these reasons, use of sunscreen products which absorb, scatter or reflect the UVR has increased over recent decades (Rai et al., 2012). UV screens are either organic compounds (used to absorb UVR) or inorganic agents (used to scatter or reflect UVR) (Shaath, 2010; Latha et al., 2013), and due to their different mechanisms of action a mixture from each group is usually used to achieve full sun protection of both user and product (Serpone et al., 2007; Rai et al., 2012; Latha et al., 2013). A wide range of products contain various UV screens including adhesives, plastics (Wypych, 2015), furnishing, clothes (Hoffmann et al., 2001) and cosmetics (Serpone et al., 2007; Darbre, 2006; Manová et al., 2013; Yousif and Hasan, 2015). Extensive use of the UV screens in consumer products has resulted in the wash out of these chemicals into waste water systems (Poiger et al., 2004; Brooke et al., 2008) and due to their stability, they are accumulating in the environment with measurable levels in water and in soil (Poiger et al., 2004; Brooke et al., 2008; Zhang et al., 2011; Jurado et al., 2014; Careghini et al., 2015) and in tissues of aquatic species (Balmer et al., 2005; Buser et al., 2006; Gago-Ferrero et al., 2015). Furthermore, UV screens can now be measured in human tissue as discussed in the section 1.4.2 below.

Among the different UV screens, fifty five chemicals are approved for use in various different countries but only 10 of them are approved for global use (Shaath, 2010). For this thesis, 6 organic UV screens (detailed in tables 1.3-1.4) known to be used in cosmetics were chosen for investigation based on the current knowledge of their levels and stable presence in the environment and the aquatic species (Poiger et al., 2004; Balmer et al., 2005; Buser et al., 2006; Brooke et al., 2008; Zhang et al., 2011; Jurado et al., 2014; Careghini et al., 2015; Gago-Ferrero et al., 2015), their absorbance by the human skin, their existence in human samples (section 1.4.2) and their reported oestrogenicity (section 1.4.3). Other reflective compounds were not selected due to time and physical limitations.

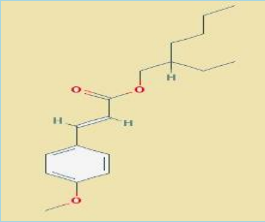
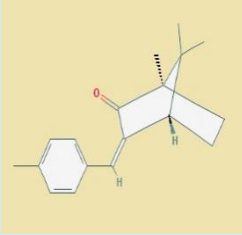
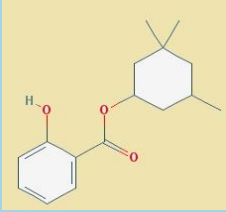
**Table 1.3 Selected benzophenones used in this study.**

Benzophenones absorb two sub-types of the UVR (UVA and UVB). Information from Shaath, 2010; Krause et al., 2012 and the structures from <http://pubchem.ncbi.nlm.nih.gov>.

UV screen	Chemical name (CAS number)	Chemical structure and Relative binding affinity to ER (RBA)	Approval for use
Benzophenone-1 (Bp1)	2,4-dihydroxy-benzophenone (CAS 131-56-6)	 <p>RBA to ER = 0.002 % (IC<sub>50</sub> 3.65 X 10<sup>-5</sup> M ± 0.45 x 10<sup>-5</sup> M) (Blair et al., 2000)</p>	Japan And South Africa
Benzophenone-2 (Bp2)	2,2',4,4'-tetrahydroxy-benzophenone (CAS 131-55-5)	 <p>RBA to ER = information not available</p>	Australia/ New Zealand- Japan-South Africa
Benzophenone-3 (Bp3)	2-Hydroxy-4-methoxybenzophenone (CAS 131-57-7)	 <p>RMA to ER = low (IC<sub>50</sub> &gt; 1.00 X 10<sup>-4</sup> M) (Blair et al., 2000)</p>	Worldwide

**Table 1.4 Other selected UV screens used in this study.**

Both octyl methoxycinnamate (OMC) and homosalate (HS) absorb UVB, while 4-methylbenzylidene camphor (4MBC) absorbs UVA. Information from Shaath, 2010; Krause et al., 2012 and the structures from <http://pubchem.ncbi.nlm.nih.gov>.

UV screen	Chemical name (CAS number)	Chemical structure and (RBA)	Approval for use
Octyl methoxycinnamate (OMC)	2-Ethylhexyl-p-methoxycinnamate (CAS 5466-77-3)	 <p>RBA to ER = information not available</p>	Worldwide
4-Methylbenzylidene camphor (4MBC)	3-(4-Methylbenzylidene)camphor (CAS 36861-47-9)	 <p>RBA to ER = 0.006 % ER<math>\beta</math> binding IC<sub>50</sub> = <math>3.53 \times 10^{-5} \pm 2.04 \times 10^{-5}</math> M (Schlumpf et al., 2004a)</p>	EU- Australia/ New Zealand- Japan- South Africa
Homosalate (HS)	3,3,5-Trimethyl-cyclohexyl- salicylate (CAS 118-56-9)	 <p>RBA to ER = information not available</p>	Worldwide

Limited published work has documented the binding affinity of some of the 6- UV screens under investigation and the ER. Blair and co-workers have documented Bp1, Bp2 and Bp3 binding affinity to ER by using the rat uterus ER binding competitive assay of 3H-oestradiol with the benzophenones (Blair et al., 2000), while among the other UV screens only 4-MBC binding affinity to human ER $\beta$  was documented by Schlumpf and her

colleagues (Schlumpf et al., 2004a). Further Kerdivel and colleagues have conducted a docking analysis of the interaction between benzophenone compounds including Bp1, Bp2 and Bp3 and the ER. Results have showed that benzophenones phenolic A-ring with a hydroxyl group interacts with Arg-394, Glu-353 or Phe-404 of the ligand-binding pocket of ER $\alpha$  (Kerdivel et al., 2013). The oestrogenic effects of the 6 selected UV screens are further detailed in section 1.4.3.

### **1.4.2 Human exposure and tissue levels**

Humans are exposed to UV screens through the dermal application of cosmetic products that contain these chemicals. Penetration of these chemicals into the human body has been demonstrated (Hayden et al., 1997; Jiang et al., 1999; Janjua et al., 2004; Schlumpf et al., 2010), and varies according to the lipophilic characteristics of the UV screen and the product formulation (Chatelain et al., 2003; Kim et al., 2014). Dermal application of a commercial sunscreen lotion containing Bp3 6% (w/v), OMC 7.5% (w/v), octyl salicylate 5% (w/v) and octocrylene 7% (w/v), resulted in the detection of Bp3 in the urine samples of nine human volunteers after 48 hours (Hayden et al., 1997). Janjua and his colleagues detected three of the commonly used UV screens (4MBC, OMC or Bp3) in human plasma and urine after two weeks of daily dermal application on males and post-menopausal women (Janjua et al., 2004). In a following study, similar findings were obtained but after only 4 days of repetitive whole body application of 4MBC, OMC and Bp3; these three chemicals were detected in plasma after 2 hours of application and in the urine with higher concentrations after 96 hour of the application than after 24 hours (Janjua et al., 2008). Some of the UV screens have been detected in animal blood/plasma following topical application such as HS (Kim et al., 2014) and Bp2 in rat plasma (Schlecht et al., 2008).

Evidence of human exposure to the UV screens in the general population was obtained from several reports, which measured these chemicals in human urine, blood/serum, milk and placenta. This is documented in Table 1.5 below. A large scale study was conducted to test urine and blood samples of Chinese participants who were not known to have a work-related exposure to Bp1, Bp2 and Bp3. In that study, 101 urine samples were tested and Bp1, Bp2 and Bp3 were detected in 57%, 5% and 25% of the samples respectively. Moreover, Bp3 was detected in 83% of the analysed adult blood samples. However, Bp1 was only detected in two blood samples and Bp2 was never observed in the blood (Zhang et al., 2013). In Korea, the

linear association between the use of different cosmetic products and the high concentration of Bp3 in the urine samples was recently documented (Ko et al., 2016).

The presence of HS, 3-benzylidene camphor (3-BC) and 4MBC in the human placenta was reported in 2013 (Jimenez-Diaz et al., 2013). In a more recent study, Valle-Sistac and his colleagues have measured Bp1, Bp2, Bp3 and benzophenone-4 (Bp4) in 12 human placenta samples. However, Bp3 could not be observed in the tissue while its largest metabolite (Bp1) was observed in all of the samples. In the same study, Bp2 was measured in only one sample but Bp4 was measured in all of the samples (Valle-Sistac et al., 2016).

#### **1.4.2.1 UV screens in human milk**

Concentrations of the UV screens in human breast tissue have not yet been measured but levels have been measured in human milk and measurement in milk is reflective of levels in the breast. A significant correlation with the use of dermally applied cosmetics that contain UV screens and the presence of these chemicals in human milk was reported by Schlumpf and her colleagues in 2010. Eight of the UV screens (Bp2, Bp3, OMC, 4MBC, HS, octocrylene, 3-BC and octyl-dimethyle PABA (OD-PABA)) were chosen to be investigated, and 54 milk samples were collected along with detailed questionnaires regarding the use of cosmetics from every participant. Notably, 85.2% of the milk samples contained one of the eight UV screens included in this study except for Bp2 which was not detected in the milk samples. Moreover, 4MBC and octocrylene were found to be correlate significantly with the use of cosmetic products (Schlumpf et al., 2010). In addition, Bp1 was recently detected in nine of ten samples collected from lactating women from Spain, and Bp3 was found in a higher concentration than Bp1 in the same study (Rodriguez-Gomez et al., 2015). However, it is noteworthy that Bp1 is a metabolite of BP3 that was measured in rats (Jeon et al., 2008), after *in vitro* incubation of Bp3 with isolated rat hepatocytes (Nakagawa and Suzuki, 2002), and in human urine after 4 hours of topical application of Bp3 (Felix et al., 1998). Thus even if Bp1 is not used in cosmetics in the EU, it might be generated from the metabolism of the world-wide approved Bp3. Concentrations of UV screens in human milk are documented in Table 1.5 below.

The evidence of the presence of UV screens in human tissues is important in the context that these chemicals are considered to be endocrine disruptors with an ability to mimic the action of oestrogen. This is discussed in more detail in the next section.

**Table 1.5 Measurement of UV screens in human samples and the recommended maximal amount in cosmetics in The European Union (EU).**

UV Sunscreen	Concentration (Range) in				Amount in cosmetics (EU Directive 76/768/EEC from Brook et.al, 2008)
	Human urine	Human plasma/ blood	Human milk	Human tissue (placenta)	
<b>Bp1</b>	<b>0.07 - 14.6 ng/ml</b> ( $2.8 \times 10^{-10}$ M - $6.8 \times 10^{-8}$ M) (Zhang et al., 2013)	<b>0.06 - 0.15 ng/ml</b> ( $2.8 \times 10^{-10}$ M - $7 \times 10^{-10}$ M) (Zhang et al., 2013)	<b>0.61 ng/ml</b> ( $2.8 \times 10^{-9}$ M) (Rodriguez-Gomez et al., 2015)	* <b>0.02-0.07 ng/g fw</b> ( $9.3 \times 10^{-11}$ M - $2.8 \times 10^{-10}$ M ) (Valle-Sistac et al., 2016) * <b>0.5-9.8 ng/g</b> ( $2.3 \times 10^{-9}$ M - $4.6 \times 10^{-8}$ M ) (Vela-Soria et al., 2011)	Not listed in the EU Directive 76/768/EEC
<b>Bp2</b>	--	--	<b>Not detected. Participants reported no usage of Bp2</b> (Schlumpf et al., 2010)	* <b>0.05 ng/g fw</b> ( $2 \times 10^{-10}$ M) (Valle-Sistac et al., 2016) * <b>0 - 8.9 ng/g</b> ( $0$ M - $3.6 \times 10^{-8}$ M ) (Vela-Soria et al., 2011)	Not listed in the EU Directive 76/768/EEC
<b>Bp3</b>	* <b>0 - 468 ng/ml</b> ( $0$ M - $2.8 \times 10^{-6}$ M) (Janjua et al., 2008) * <b>0.11 - 46.1 ng/ml</b> ( $4.8 \times 10^{-10}$ M - $2 \times 10^{-7}$ M) (Zhang et al., 2013)	* <b>28 - 392 ng/ml</b> ( $1.2 \times 10^{-7}$ M - $1.7 \times 10^{-6}$ M) (Janjua et al., 2008) * <b>0.41 - 3.38 ng/ml</b> ( $1.7 \times 10^{-9}$ M - $1.4 \times 10^{-10}$ M ) (Zhang et al., 2013)	* <b>7.3 - 121.4 ng/g Lipid</b> ( $1.14 \times 10^{-9}$ M - $2 \times 10^{-8}$ M) (Schlumpf et al., 2010) * <b>4.5-15.7 ng/ml</b> ( $7.8 \times 10^{-10}$ M - $2.95 \times 10^{-9}$ M) (Rodriguez-Gomez et al., 2015)	* <b>Not detected</b> (Valle-Sistac et al., 2016) * <b>Not detected</b> (Vela-Soria et al., 2011)	<b>10%</b>
<b>OMC</b>	<b>1 - 39 ng/ml</b> ( $3.4 \times 10^{-9}$ M - $1.3 \times 10^{-7}$ M ) (Janjua et al., 2008)	<b>0 - 40 ng/ml</b> ( $0$ M - $1.4 \times 10^{-7}$ M ) (Janjua et al., 2008)	<b>2.1 - 79.85 ng/g Lipid</b> ( $3 \times 10^{-10}$ M to $1 \times 10^{-8}$ M) (Schlumpf et al., 2010)	--	<b>10%</b>
<b>4MBC</b>	<b>0 - 32 ng/ml</b> ( $0$ M - $1.25 \times 10^{-7}$ M ) (Janjua et al., 2008)	<b>0 - 39 ng/ml</b> ( $0$ M - $1.5 \times 10^{-7}$ M ) (Janjua et al., 2008)	<b>6.7 - 48.37 ng/g Lipid</b> ( $1 \times 10^{-9}$ M - $7.6 \times 10^{-9}$ M) (Schlumpf et al., 2010)	<b>2 - 73 ng/g</b> ( $7.8 \times 10^{-9}$ M - $2.8 \times 10^{-7}$ M ) (Jimenez-Diaz et al., 2013)	<b>4%</b>
<b>HS</b>	--	--	<b>11.4 - 61.2 ng/g Lipid</b> ( $1.7 \times 10^{-9}$ M - $9.33 \times 10^{-9}$ M) (Schlumpf et al., 2010)	<b>2.1- 73 ng/g</b> ( $8 \times 10^{-9}$ M - $2.8 \times 10^{-7}$ M ) (Jimenez-Diaz et al., 2013)	<b>10%</b>

(--) No information available

### **1.4.3 The oestrogenic action of UV screens *in vitro* and *in vivo***

#### **1.4.3.1 *In vitro* oestrogenic activity of UV screens**

*In vitro* oestrogenic activity of these chemicals can be measured in terms of their ability to bind to oestrogen receptor and to regulate oestrogen responsive gene expression. It can also be measured in terms of the ability to stimulate proliferation of oestrogen responsive human breast cancer cells (Darbre, 2015).

##### **1.4.3.1.1 Reporter gene assays**

The oestrogenic activity of OMC, 4MBC, HS and Bp3 was studied *in vitro* using reporter gene assays. The ERE–luciferase assay (ERE-LUC) was conducted on either ER $\alpha$  or ER $\beta$  stably transfected HEK293 kidney cells after exposure to UV screens for 24 hours. All tested chemicals activated ER $\alpha$  transcription, although to different extents. The EC<sub>50</sub> (the concentration which caused 50 % of the maximal effect of the chemical) of hER $\alpha$  transcriptional activity for each UV screen was 2.8 X 10<sup>-5</sup> M Bp3, 6.2 X 10<sup>-6</sup> M 4MBC and 1.6 X 10<sup>-6</sup> M HS while the transcriptional activity for OMC dose-response was beyond 42 %. OMC was the only tested chemical not to activate ER $\beta$  mediated transcriptional activity (Schreurs et al., 2005). Gomez and co-workers confirmed Schreurs work. In their study they used transfected HeLa cervical cells and reported an oestrogenic ER $\alpha$  transcriptional activity in the presence of 10<sup>-5</sup> M OMC, 3 X 10<sup>-6</sup> M 4MBC and 10<sup>-6</sup> M HS (Gomez et al., 2005). Using a reporter gene assay, Kerdivel and his colleagues measured the effect of Bp1, Bp2 and Bp3 (in concentrations from 10<sup>-8</sup> M to 10<sup>-6</sup> M) on the luciferase activity of oestrogen responsive targets in MCF-7 cells transfected with ERE-LUC. Both 10<sup>-6</sup> M Bp1 and 10<sup>-7</sup> M Bp2 significantly increased the transactivation activity of ERE and the effect was decreased using the antioestrogen fulvestrant at 10<sup>-7</sup> M concentration. However, no significant change in the transactivation activity was observed following the exposure to Bp3 (Kerdivel et al., 2013).

##### **1.4.3.1.2 Endogenous oestrogen regulated genes**

The oestrogen mimicking activity of the UV screens has also been investigated using endogenous oestrogen-regulated genes in MCF-7 cells. The radioimmunoassay for TFF1 protein was performed to measure the secretion of TFF1 by MCF-7 cells in the culture media following 3 days of exposure to 5 X 10<sup>-5</sup> M of OMC, 4MBC, HS and Bp3, which resulted in

significant elevation of TFF1 protein expression when compared to the control. The highest levels were measured following exposure to 4MBC, HS and Bp3 respectively but no effect of OMC was found (Schlumpf et al., 2001). A further effect of the UV screens on TFF1 mRNA transcription levels was reported by Heneweer and his colleagues who found a dose response increase in TFF1 gene transcription in MCF-7 cells after 24 hours exposure to Bp1, Bp3, OMC or 4MBC, at concentrations ranging from  $10^{-8}$  M to  $10^{-5}$  M. In the same study, a mixture of equipotent components, which individually showed no significant effect in comparison to  $17\beta$ -oestradiol at C50 (the concentration of which the UV screen increased 50% of the basal TFF1 gene transcription), induced TFF1 gene expression to a similar levels of that of  $17\beta$ -oestradiol (Heneweer et al., 2005).

More oestrogen regulated genes were studied by Kerdivel and his colleagues. The effect on TFF1 gene expression was documented following MCF-7 cell exposure, Bp1, Bp2 and Bp3 at concentrations of  $10^{-8}$  M to  $10^{-6}$  M or  $10^{-8}$  M  $17\beta$ -oestradiol. The cells were deprived of serum for 24 hours and then incubated with oestradiol, Bp1, Bp2 and Bp3 in the presence of 2.5% dextran-charcoal treated serum for 48 hours. Among the treatments, oestradiol induced the highest effect on TFF1 mRNA expression followed by  $10^{-6}$  M Bp2 and  $10^{-6}$  M Bp3 respectively. The effect on the TFF1 gene by oestradiol and these chemicals was decreased by using the antioestrogen fulvestrant. While  $10^{-6}$  M Bp1 did not increase the expression of TFF1 gene in MCF-7 cells, it increased the expression of progesterone receptor (PR) mRNA which is another oestrogen regulated gene, and a similar effect was found after exposure to  $10^{-6}$  M Bp2. The induction of CXCL12 and amphiregulin expressions were achieved after exposure to  $10^{-6}$  M Bp2 (Kerdivel et al., 2013).

#### **1.4.3.1.3 The recombinant yeast assay**

The recombinant yeast assay was used to measure the ability of UV screens to activate ERE *in vitro*. This technique is performed with transfecting two different plasmids in yeast, the first is the expression plasmid which is integrated with human cDNA that produces ER and the second is the reporter plasmid which is consisted of ERE reporter gene upstream of  $\beta$ -galactosidase structural gene. Once the compounds binds to ER and activated the receptors, the dimerized ERs consequently activates the ERE reporter gene, which activate the release of  $\beta$ -galactosidase in the medium (Coldham et al., 1997). Kunz and colleagues measured the effect of Bp1, Bp2, Bp3, OMC, 4MBC or HS on recombinant yeast carrying human ER $\alpha$ . In their study a high potency was detected following incubation with  $2.59 \times 10^{-10}$  M  $17\beta$ -

oestradiol,  $1.15 \times 10^{-6}$  M Bp1 and  $1.09 \times 10^{-5}$  M Bp2. Mild potency was achieved by the presence of  $1.86 \times 10^{-5}$  M Bp3 and no oestrogenic effect was detected after the exposure to OMC, 4MBC or HS (Kunz et al., 2006). Miller and his colleagues studied 73 different compounds used in cosmetics of which 18 were UV screens. Using yeast transfected with human ER $\alpha$  gene, the oestrogenic potency relative to 17 $\beta$ -oestradiol of Bp1 was (1/3,000) and of Bp2 was (1/7,000) while Bp3 showed even weaker potency (1/100,000). Furthermore, they have suggested that the UV screens with oestrogenic activity (Bp1 and Bp2) have an unhindered phenolic ring with OH in a para configuration and an appropriate molecular size (140 - 250 kDa) which allows the chemical to fit and bind in the ER $\alpha$  site (Miller et al., 2001) (see section 1.3.1.1 and see Table 1.3).

#### **1.4.3.1.4 Proliferation of oestrogen responsive human breast cancer cells**

Several studies have shown the oestrogenic activity of UV sunscreens on cell proliferation *in vitro*. In 2001, Schlumpf and her colleagues reported an increase in MCF-7 cell proliferation after 6 days of exposure to different concentrations of Bp3, OMC, 4MBC and HS. Significant increase in MCF-7 cell proliferation was reported following the exposure to  $5 \times 10^{-6}$  M Bp3,  $5 \times 10^{-6}$  M OMC,  $5 \times 10^{-5}$  M 4MBC and  $1 \times 10^{-6}$  M HS (Schlumpf et al., 2001). Further studies reported an increase in MCF-7 cell proliferation after exposure to  $10^{-6}$  M Bp2 (Kerdivel et al., 2013) and  $10^{-8}$  M Bp1 (Nakagawa and Suzuki, 2002). Similar positive effects on MCF-7 cell proliferation after exposure to 4MBC or HS were reported by Jimenez-Diaz et al., (2013). In contrast with the reported positive effect of Bp1 or Bp3 on MCF-7 cell proliferation, Kerdivel and his colleagues did not observe similar results and neither Bp3 nor Bp1 at concentrations from  $10^{-8}$  M to  $10^{-6}$  M increased MCF-7 cell proliferation in their studies (Kerdivel et al., 2013). The most likely explanation for the differences lies in the variation of the oestrogen responsiveness of MCF-7 cells between different laboratories, and the diverse experimental conditions (Osborne et al., 1987; Shaw et al., 2006).

#### **1.4.3.2 *In vivo* oestrogenic activity of UV screens**

In addition to the *in vitro* oestrogenic activity of UV screens, multiple *in vivo* studies have been conducted which demonstrate oestrogenic activity in rodents. One of the first experiments to measure the oestrogenic effect of the UV screens using the uterotrophic assay in immature rats was conducted by Schlumpf and her colleagues in 2001. The dermal

application of olive oil containing 5 % and 7.5 % 4MBC on immature rats caused an increased uterine weight after 6 days of applying the chemical twice a day (Schlumpf et al., 2001). This effect on immature rat uterus was confirmed by another research group who administered 4MBC as either a subcutaneous injection or oral inoculation (Tinwell et al., 2002). However, Mueller and co-workers have suggested that the increase in the uterine weight in rat after exposure to 4MBC might not be mediated through an oestrogenic pathway because of the weak transcriptional activity of ER $\alpha$  and ER $\beta$  after the exposure to 4MBC in transiently transfected human endometrial Ishikawa cells (Mueller et al., 2003). The uterotrophic assay was also used to measure the effect of orally introduced UV screens including OMC, HS, Bp1, Bp2 or Bp3, and a positive increase in the uterine weight was detected following the treatment for all but HS (Schlumpf et al., 2004).

The endocrine disruption in fish after exposure for 14 days to Bp1 and Bp2 was found by measuring the endocrine disruptor marker Vitellogenin (VGA) using ELISA, and no effect was found after exposure to Bp3, OMC, 4MBC or HS (Kunz et al., 2006). On the other hand, VGA mRNA expression was induced following the exposure to OMC or 4MBC in another fish species (Inui et al., 2003). However, different *in vivo* results might be caused by different species (Kunz et al., 2006).

The endocrine disruption of some of these chemicals was further demonstrated *in vivo* in the literature. Disruption has been recorded on the endocrine system in rats including effects on the pituitary gland (Klammer et al., 2005), measured by the reduction of luteinising hormone synthesis (Jarry et al., 2004), by interference with thyroid hormone production (Seidlová-Wuttke et al., 2006; Klammer et al., 2007; Schmutzler et al., 2007), and by interference with lipid metabolism (Jarry et al., 2004; Seidlová-Wuttke et al., 2006). Moreover, some UV screens were associated with a delay in puberty in male rats due to their androgenic effects (Schlumpf et al., 2004), and disturbance to the reproductive ability of fish species (Fathead Minnows) (Weisbrod et al., 2007).

Since UV screens possess oestrogen mimicking properties and their entry to the human body is documented, further investigation should be carried out in order to explore their probable influence through endocrine disruption to related human health concerns.

## 1.5 Underlying hypothesis

The evidence of the UV screens entry to the human body along with their oestrogen mimicking properties as indicated in both *in vitro* and *in vivo* models as well as the previously elaborated evidence of the role of oestrogen on breast cancer progression, make the hypothesis of the possible effect of the UV screens on breast cancer progression biologically plausible and applicable to this research. For this reason, the hypothesis was tested that UV screens might enable multiple hallmarks of cancer and might increase not only proliferation but also migration/invasion of human breast cancer cells.

## 1.6 Aims of project

The overall aims of this research were to investigate the effects of six UV screens on the proliferation, migration and invasion of human breast cancer cells, using different times of exposure.

The first aim was to study the oestrogenic effect of six UV screen (Bp1, Bp2, Bp3, OMC, 4MBC and HS) on MCF-7 human breast cancer cells by:

- 1- The ERE-LUC reporter gene assay in stably transfected MCF-7 human breast cancer cells.
- 2- Evaluate the effect of exposure to the six UV screens on TFF1 mRNA levels using RT-PCR.
- 3- Evaluate the effect of exposure to the six UV screens on ER $\alpha$  protein levels in MCF-7 cells.
- 4- MCF-7 human breast cancer cell proliferation in monolayer culture using plastic culture dishes and in 3D culture using plates coated with fibronectin or laminin.

A second aim was to investigate the effect of the exposure to the benzophenones (Bp1, Bp2 or Bp3) and the other group of the selected UV screens (OMC, 4MBC or HS) on migration of MCF-7 human breast cancer cells after different times of exposure, using time-lapse microscopy, wound healing assays and xCELLigence technology, and on invasion of MCF-7 human breast cancer cells using xCELLigence technology plates coated with matrigel. Further research investigated some potential molecular mechanisms underlying any changes in the migration and invasion of MCF-7 cells using western immunoblotting, zymography and on Reverse Transcriptase Polymerase Chain Reaction (RT-PCR). The focus was mainly

directed toward the markers of EMT (E-cadherin,  $\beta$ -catenin, Twist-1 and snail), and other markers of motility including bone morphogenetic protein 7 (BMP7), phosphoinositide-3-kinase regulatory subunit 1 (PIK3R1), MMP-2, MMP-9 and MMP-14.

The third aim was to validate the findings obtained using the MCF-7 cell line by using a second oestrogen responsive (ER+) human breast cancer cell line, the T-47-D human breast cell line.

Finally, the fourth aim was to investigate the effect of the UV screens on the proliferation, migration and invasion of oestrogen unresponsive human breast cancer cells using the MDA-MB-231 cell line. The effect of the UV screens on the molecular level of this cell line was carried on by investigating the effects on MMPs using western immunoblotting and zymography.

## **Chapter 2 Materials and Methods**

### **2.1 Culture of human breast cancer cells**

#### **2.1.1 Culture of stock MCF-7 human breast cancer cells**

MCF-7 McGrath human breast cancer cells were provided by C.K. Osborne in 1987 at passage number 390 (Osborne et al., 1987). Cells were maintained as monolayer cultures in 9-cm tissue culture dishes (63.6 cm<sup>2</sup> culture area per dish) (Nunc, Denmark) in a humidified atmosphere of 10% carbon dioxide in air at 37°C. Stock culture medium consisted of Dulbecco's modified Eagle's medium (DMEM) (containing phenol red) (Invitrogen, Paisley, UK), 5% (v/v) foetal calf serum (FCS) (Invitrogen), 10<sup>-8</sup> M 17β-oestradiol (Steraloids, Croydon, UK), streptomycin (100µg/ml), penicillin (100U/ml) (Invitrogen) and insulin (10µg/ml) (Sigma, Poole, UK) (Darbre and Daly, 1989). Oestradiol was dissolved in ethanol as a 10<sup>-4</sup> M stock solution and diluted 1/10,000 in culture medium. Insulin (bovine pancreas) was purchased at 10mg/ml from Sigma (10516-5ml) and diluted 1/1000 in culture medium.

#### **2.1.2 Culture of stock T-47-D human breast cancer cells**

T-47-D human breast cancer cells were provided by the originator (Keydar et al., 1979). These cells were grown as a monolayer cultures in 9-cm tissue culture dishes (63.6 cm<sup>2</sup> culture area per dish) (Nunc, Denmark) in a humidified atmosphere of 10% carbon dioxide in air at 37°C. Stock culture medium consisted of Dulbecco's modified Eagle's medium (DMEM) (containing phenol red) (Invitrogen, Paisley, UK), 5% (v/v) foetal calf serum (FCS) (Invitrogen), 10<sup>-8</sup> M 17β-oestradiol (Steraloids, Croydon, UK), streptomycin (100µg/ml) and penicillin (100U/ml) (Invitrogen).

#### **2.1.3 Culture of stock MDA-MB-231 human breast cancer cells**

MDA-MB-231 human breast cancer cells were obtained from The American Tissue Culture Collection at passage 28. Cells were maintained as monolayer cultures in 9-cm tissue culture dishes (63.6 cm<sup>2</sup> culture area per dish) (Nunc, Denmark) in a humidified atmosphere of 10% carbon dioxide in air at 37°C. Stock culture medium consisted of Dulbecco's modified Eagle's medium (DMEM) (containing phenol red) (Invitrogen, Paisley, UK), 10% (v/v) foetal calf serum (FCS) (Invitrogen), streptomycin (100µg/ml) and penicillin (100U/ml) (Invitrogen).

### **2.1.4 Sub culturing of stock human breast cancer cells**

Stock cells were sub-cultured at weekly intervals. The cells in monolayer were washed twice with 2 ml of Hanks' balanced salt solution (HBSS) (Invitrogen). Then cells were incubated in 2ml of HBSS containing 0.06% trypsin (w/v), 0.02% EDTA, pH7.3 (Invitrogen) in a humidified atmosphere of 10% carbon dioxide in air at 37°C for 2 minutes. The cells were suspended and then added to relevant culture medium and re-plated at 1/10th dilution into 9-cm tissue culture dishes (Nunc, Denmark).

### **2.1.5 Maintenance of human breast cancer cells with UV screens**

MCF-7 and T-47-D human breast cancer cells were maintained as separate stock cultures in phenol red-free DMEM (Invitrogen) containing 5% (v/v) dextran-charcoal stripped FCS (DCFCS) (Darbre et al., 1983), 2 mM L-glutamine, 100 µg/ml streptomycin and 100 U/ml penicillin (Invitrogen, Paisley, UK) with no further addition or with the relevant concentration of UV screens in a humidified atmosphere of 10% carbon dioxide in air at 37°C. DC treatment of sera was carried out by incubating FCS (Invitrogen) with 1 % charcoal (Sigma) and 0.1 % dextran T-70 (Pharmacia, Sweden) with rotation for 35 minutes at 55°C (Darbre et al., 1983). Then DCFS was filter sterilized and aliquots were stored at -20°C. 2,4-dihydroxybenzophenone (Bp1) (CAS 131-56-6) with purity of 99% , 2,2',4,4'-tetrahydroxybenzophenone (Bp2) (CAS 131-55-5) with purity of 97%, 2-Hydroxy-4-methoxybenzophenone (Bp3) (CAS 131-57-7) with purity of 98%, 2-Ethylhexyl-p-methoxycinnamate (OMC) (CAS 5466-77-3) with purity of 98%, 3-(4-Methylbenzylidene)camphor (4MBC) (CAS 36861-47-9) with purity of 98% and 3,3,5-Trimethyl-cyclohexyl- salicylate (HS) (CAS 118-56-9) with purity of 99.9% were purchased from Sigma-Aldrich (UK). Stock concentrations of the UV screens were made in ethanol and diluted 1/10,000 in cell culture media. Controls contained the same volume of ethanol. Experiments contained final concentrations of each UV screen at concentrations of  $10^{-8}$  M to  $10^{-5}$  M (Table 2.1). Media were changed routinely every 3-4 days.

The same methodology was used for maintaining MDA-MB-231 human breast cancer cells except that the DMEM contained phenol red and 10% FCS (Invitrogen, Paisley, UK).

Experiments were conducted on cells exposed to different treatments for 1-2 weeks, while longer-term exposure experiments were carried out on the cells treated for 7-40 weeks.

**Table 2.1 Final concentration of UV screens in media for short and long-term exposure experiments**

Human breast cancer cells	Proliferation experiments	Migration and motility experiments	
	1 week	Short-term exposure	Long-term exposure
MCF-7 cells	$10^{-8}$ M, $10^{-7}$ M, $10^{-6}$ M and $10^{-5}$ M	$10^{-7}$ M, $10^{-6}$ M and $10^{-5}$ M (2 weeks)	$10^{-7}$ M, $10^{-6}$ M and $10^{-5}$ M (7 - 13 - 31 weeks)
T-47-D cells	$10^{-8}$ M, $10^{-7}$ M, $10^{-6}$ M and $10^{-5}$ M	$10^{-5}$ M (2 - 3 weeks)	$10^{-5}$ M (7- 13 - 20 - 40 weeks)
MDA-MB-231 cells	$10^{-5}$ M	$10^{-7}$ M and $10^{-5}$ M (2 weeks)	$10^{-7}$ M and $10^{-5}$ M (8 - 15 weeks)

### 2.1.6 Sub culturing of human breast cancer cells exposed to UV screens

Long-term exposed human breast cancer cells were maintained in 6-well plates. Cells were sub cultured at weekly intervals. 0.8ml of HBSS was used to wash the cell monolayer twice. And cells were incubated in in a humidified atmosphere of 10% carbon dioxide in air at 37°C for 2 minutes in 0.8 ml of HBSS containing 0.06% trypsin (w/v) and 0.02% EDTA pH 7.3. After that cells were re-plated at 1/5<sup>th</sup> dilution in relevant media into 6-well plates.

### 2.2 Measurement of cell proliferation

Cell proliferation was determined by either using the Coulter counter in order to count the number of nuclei released from adherent cells in a monolayer or by monitoring the change in electrical impedance, which is correlated with the increase of proliferation as determined by the xCELLigence technology.

## **2.2.1 Measurement of cell proliferation using a ZBI Coulter counter**

### **2.2.1.1 Measurement of cell proliferation on non-coated plates using a Coulter counter**

Cells were suspended from stock dishes by treatment with trypsin-EDTA solution as described above and seeded at  $0.2 \times 10^5$  cells per ml in phenol-red-free-DMEM containing 5% DCFCS in 0.5 ml aliquots into 4-well ( $2.01 \text{ cm}^2$  culture area per well (1.6 cm diameter)) and 24-well ( $2.01 \text{ cm}^2$  culture area per well) plastic tissue culture dishes (Nunc). The medium was replenished after 24h to contain the required concentration of UV screen, an ethanol vehicle control or  $10^{-8}$  M  $17\beta$ -oestradiol as a positive control. Medium was changed routinely every 3-4 days.

Cell number was measured by counting cell nuclei on a ZBI Coulter counter. Cells in a 4-well plate were lysed on day zero and cells in monolayer in 24-well plates were lysed after 7 or 14 days of incubation. To achieve nuclei release, cells were washed with 0.9% (w/v) NaCl in water and lysed in 0.01 M HEPES/ 1.5 mM  $\text{MgCl}_2$  plus two drops of Zap-oglobin II (lytic reagent used to lyse the cells and release the nuclei) (Beckman Coulter) for 20 minutes. According to the manufacturer, Zap-oglobin II active ingredients include organic quaternary ammonium salt, potassium cyanide, sodium Nitrate and sodium nitroferricyanide. Released nuclei were counted in isoton (Beckman Coulter) in triplicate on a ZBI Coulter counter (Beckman Coulter). Cell counts were done in triplicate and cell numbers are the average of triplicate wells for each treatment  $\pm$  standard error (SE). The results were calculated using Microsoft Excel 2010 package and plotted using GraphPad Prism software version-6.01 (GraphPad Software Inc.).

### **2.2.1.2 Measurement of cell proliferation on coated plates using a Coulter counter**

In order to study the effect of the UV screens on cells seeded on coated plates, ( $2.01 \text{ cm}^2$  culture area per well) and 24-well ( $2.01 \text{ cm}^2$  culture area per well) tissue culture plates (Nunc) were used uncoated or coated with  $6.5 \mu\text{g}/\text{cm}^2$  laminin or with  $6.5 \mu\text{g}/\text{cm}^2$  fibronectin. Laminin (Engelbreth-holm-swarm murine sarcoma basement membrane Sigma, Poole, UK) [1mg/ml in Tris buffered NaCl] was received suitable for tissue culture and was diluted in HBSS in sterilized conditions.

Wells were coated with  $6.5 \mu\text{g}/\text{cm}^2$  laminin for each well. Then the tissue culture plates were incubated 2 hours at  $37^\circ\text{C}$  in the incubator and 1 hour at room temperature. Excess laminin was removed and the wells were washed 3X with HBSS. Plates were kept at  $4^\circ\text{C}$  for 24 hours prior to the seeding experiment.

Fibronectin from human plasma (Sigma, Poole, UK) was received dry and was dissolved in sterilized ddH<sub>2</sub>O by incubating the mixture at  $37^\circ\text{C}$  using the water bath. Wells were coated with  $6.5 \mu\text{g}/\text{cm}^2$  of fibronectin diluted in HBSS and then left at room temperature in the hood to dry for 1 hour. Excess fibronectin was removed and the wells were washed 3X with HBSS. Plates were kept at  $4^\circ\text{C}$  for 24 hours prior to the seeding experiment.

The coated plates were washed with phenol-red-free-DMEM containing 5% DCFCS in 0.5 ml aliquots prior to seeding of MCF-7 cells. Cells were suspended from stock dishes by treatment with trypsin-EDTA solution as described above (section 2.1.4) and seeded at  $0.2 \times 10^5$  cells per ml in phenol-red-free-DMEM containing 5% DCFCS in 0.5 ml aliquots into the coated and uncoated plates. The medium was replenished after 24h to contain the required concentration of UV screen, an ethanol vehicle control or  $10^{-8}$  M  $17\beta$ -oestradiol as a positive control. Medium was changed routinely every 3-4 days and the cell counting experiment was carried out on day 7 using the ZBI Coulter counter as previously described (in section 2.2.1.1).

## **2.2.2 Measurement of cell proliferation using xCELLigence technology**

For measurement of MDA-MB-231 cell proliferation, aliquots of 100  $\mu\text{l}$  of phenol-red-DMEM containing 10% FCS were added to each of 16 wells in an E-plate (ACEA Biosciences, USA), incubated for one hour and then assembled into the cradle of the xCELLigence machine (Figure 2.1 and Figure 2.2) according to manufacturer's instructions (ACEA Biosciences, USA). Stock cells were added to the required volume of phenol-red-DMEM containing 10% FCS at a concentration of  $0.2 \times 10^5$  cells per ml and 100  $\mu\text{l}$  aliquots added to each of the 16 wells of the E-plate. After 24 hours, the medium was replaced to contain the required concentration of UV screen or ethanol control. The culture medium was changed routinely every 3-4 days and the electrical impedance (cell index) monitored every hour for one week. Cell index after 7 days of exposure was determined by RTCA-DP software 1.2.1 (ACEA Biosciences, USA) and results were plotted using GraphPad Prism software version-6.01 (GraphPad Software Inc.).

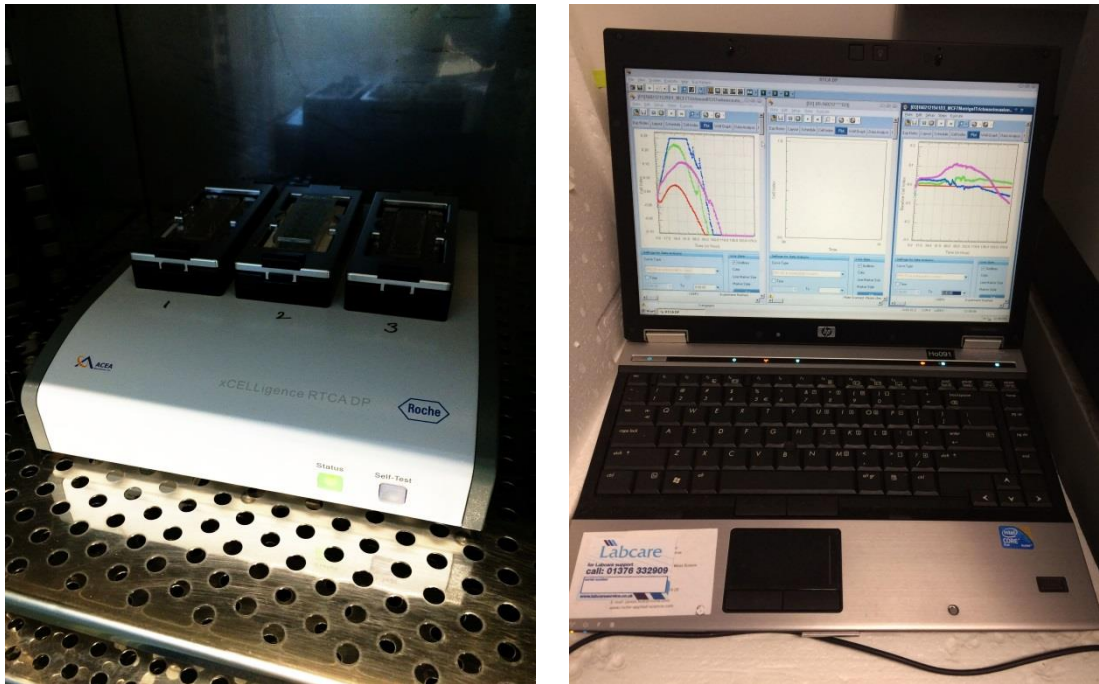


**Figure 2.1 xCELLigence real-time cell analysis (RCTA) instrument.**

The instrument is placed inside the incubator and was externally controlled via a cable connection to the RCTA system on a laptop computer.



**Figure 2.2 The E-plate 16.**

E-Plate 16 was used to measure cell proliferation by monitoring the live change in the electrical impedance of the microelectrode in the bottom of wells using the xCELLigence technology.

### 2.3 Ligand ability to increase expression of ERE-LUC reporter gene in MCF-7 cells

The ability of each chemical to regulate an oestrogen-responsive gene was tested using a stably transfected oestrogen regulated ERE-LUC reporter gene in MCF-7 cells. The oestrogen-inducible ERE-LUC vector consisted of the oestrogen response element (ERE)-containing nucleotide sequence from the vitellogenin A2 gene from -331 to -295 bp (5'-CTAGAAAGTCAGGTCACAGTGACCTGATCAAT -3') (Klein-Hitpass et al., 1986) cloned into the multiple cloning site of the pGL3promoter vector containing the coding sequence for firefly luciferase (Promega). Oestrogen regulation of transiently transfected oestrogen-inducible ERE-LUC reporter gene in MCF-7 cells was published in 2006 (Shaw et al., 2006). However, a line of MCF-7 cells stably transfected with the same ERE-LUC reporter gene has been produced but not validated by prior publication.

Transfected MCF-7 stocks were maintained in the same stock medium as MCF-7 cells (section 2.1.1) plus G418 sulphate (100 µg/ml) (Invitrogen). For reporter assays cells were seeded at  $0.2 \times 10^5$  cells per ml in phenol-red-free-DMEM containing 5% DCFCs in 0.5 ml aliquots into 24-well (2.01 cm<sup>2</sup> culture area per well) plastic tissue culture dishes (Nunc) and grown for 6 days with a change of medium after 3 days. After 6 days, the medium was changed again but to contain the required concentration of the relevant UV screen, an ethanol vehicle control or  $10^{-8}$  M 17β-oestradiol and cells grown for a further 24 hours. Six wells were used for each treatment. Three wells were used for cell counts and three wells were used for luciferase assays. For cell counts, each well was washed twice with isotonic saline and cell counts were performed using a ZBI Coulter counter as described (in section 2.2.1). Luciferase assays were performed using a commercial assay kit (Promega). For this, each well was washed twice with isotonic saline, cells were lysed using 50 µl of Promega passive lysis buffer and assays were performed without delay according to the manufacturer's instructions (Promega). Cell extracts from each well were assayed in triplicate by mixing 4 µl of cell extract and 20 µl of luciferase reagent (Promega) in a 96-well white luminometer plate (Nunc) and measuring the luminescence within 10 minutes using an Anthos Lucy 1 microplate luminometer. Results were calculated as average units of luminescence per 24 hours for the triplicate assays. Results are presented as average luminescence units per 10,000 cells ± standard error for the triplicate wells.

## **2.4 Cell migration and motility assays**

Three different techniques were used to study the effect of short-term and long-term exposure to UV screens on motility or migration of human breast cancer cells in this study. In order to detect the effect on the collective migration of MCF-7 and T-47-D human breast cancer cells, wound healing assays were performed. To observe a live change in cell motility, time-lapse microscopy was carried out for both MCF-7 and MDA-MB-231 cell lines. To achieve a live monitoring of the effect of UV screens on chemotaxis driven migration of human breast cancer cells, the xCELLigence technology was used.

### **2.4.1 Wound healing assay**

MCF-7 and T-47-D cells were seeded in phenol-red-free DMEM supplemented with 5% DCFCS, penicillin (100 U/ml), streptomycin (100 µg/ml) in 2.5 ml aliquots into 12-well (3.14 cm<sup>2</sup> culture area per well) plastic tissue culture dishes (Nunc) with the required concentrations of the UV screen, 10<sup>-8</sup> M 17β-oestradiol or ethanol control. Triplicate wells were prepared for each treatment. Cells were grown to confluence and wounds were made down the centre of each well using a sterile 200µl plastic pipette tip (Liang et al., 2007). The cells were washed with HBSS (Invitrogen) to remove detached cells. Medium was replenished with the same test media plus mitomycin-C (Calbiochem, Merck Biosciences, Nottingham, UK) to inhibit cell proliferation. Mitomycin-c is an anticancer drug (Bradner, 2001), which stops the proliferation of cells by acting as DNA cross-linker and impairs DNA replication (Szybalski and Iyer, 1964). Mitomycin-C was dissolved in autoclaved distilled water to make a stock solution of 0.5 mg/ml and further diluted 1/1000 into cell culture media to give a concentration of 0.5 µg/ml. A minimum of five images (×4 objective) per well were taken along the length of the wound at 0 hour and 24 hours using an Axion inverted microscope attached to a Nikon-Ds-Fi2 camera and running NIS-elements AR4.10 software and equipped with a digital camera. The area of the wound at 0 hour was taken as 100% to assess cellular migration at 24 hours.

#### **2.4.1.1 Analysis of cell migration from wound healing assay**

Analysis of wound closure was conducted using Image J (version 1.47) open source software, obtained from the National Institutes of Health (NIH, USA). Wound area was selected using the freehand selection tool for 0 and 24 hour pictures and the measurements were exported to Excel sheets to calculate the percentage of the closure of the wound area of three replicates ±

SE. The percentage values of wound closure were plotted using GraphPad Prism version-6.01 software (GraphPad Software, La Jolla, CA).

## **2.4.2 Cell motility assay as measured by time-lapse microscopy**

Cells were incubated in phenol-red-free DMEM supplemented with 5% DCFCS (for MCF-7 cells) or phenol-red DMEM supplemented with 10% FCS (for MDA-MB-231 cells), penicillin (100 U/ml), streptomycin (100 µg/ml) and the required concentration of UV screen,  $10^{-8}$  M  $17\beta$ -oestradiol or ethanol alone for 2, 13 or 22 weeks prior to the experiment. 48 hours prior to microscopy, cells were trypsinised and seeded at  $0.2 \times 10^5$  cells/ml in relevant media containing the required concentration of treatment in 0.5ml aliquots into 12-well (3.14 cm<sup>2</sup> culture area per well) plastic tissue culture dishes (Nunc). After 48 hours, the medium was changed to contain mitomycin-C (0.5 µg/ml) and the dishes were placed on a microscope stage in a chamber heated to 37°C in an atmosphere of 5% carbon dioxide in air. Cell migration was observed over 24 hours by using a Nikon Eclipse TiE inverted microscope running NIS-elements AR4.10 software and equipped with a digital camera.

### **2.4.2.1 Analysis of cell motility as measured by time-lapse microscopy**

Time-lapse videos were generated by capturing specific points of the 12-well (3.14 cm<sup>2</sup> culture area per well) plates every 15 minutes for 24 hours. Ten cells per field of view (three fields per well) were tracked for the entire period by using Image J software and MTrackJ plugin to calculate the total length of travel of each cell (cumulative length) and the percentage of motile cells. Results were calculated from the average value for 10 cells per field of view and then the average of three fields per well. Results are shown as mean  $\pm$  SE for three wells. Results were plotted using GraphPad Prism version-6.01 software (GraphPad Software, La Jolla, CA).

### **2.4.3 Cell migration using xCELLigence technology**

Cells were incubated in either phenol-red-free DMEM supplemented with 5% DCFCS (for MCF-7 and T-47-D) or phenol-red DMEM supplemented with 10% FCS (For MDA-MB-231 cells), penicillin (100 U/ml), streptomycin (100 µg/ml) with the required concentration of UV screen,  $10^{-8}$  M  $17\beta$ -oestradiol or ethanol alone as vehicle control for 2 weeks and beyond prior to the experiment. Experiments were set up in an uncoated CIM-plate16 according to the manufacturer's instructions (ACEA Biosciences, USA). The CIM-plate16 consists of two

chambers separated by a polyethylene terephthalate membrane with 8  $\mu$  pore size. The motility of cells from the upper to the lower chambers induces change in the electrical impedance of integrated gold microelectrodes on the underside of the membrane (Figure 2.3).

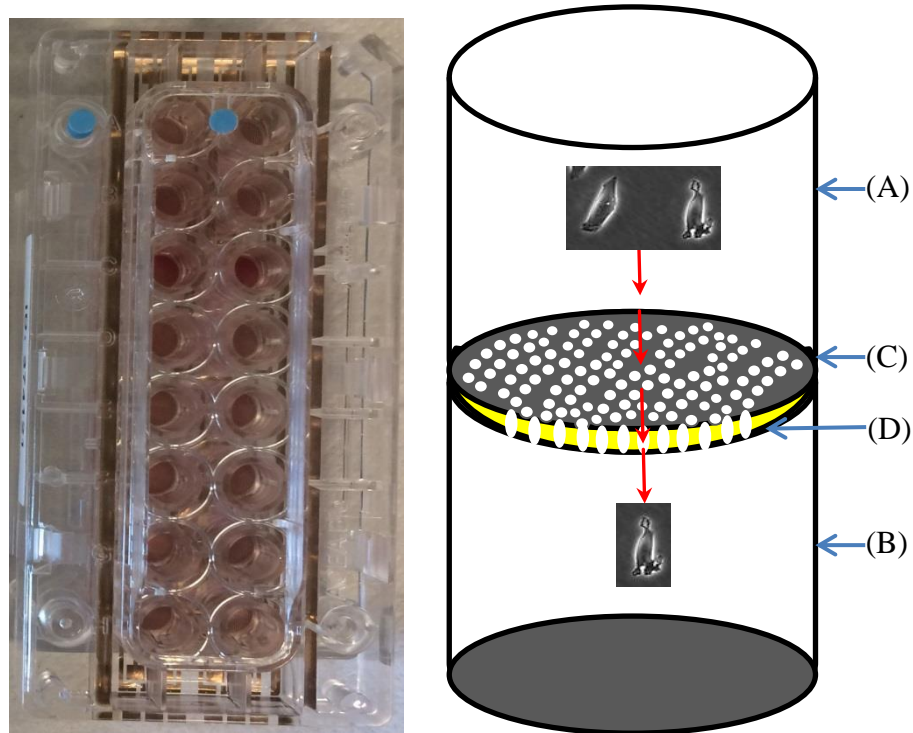


**Figure 2.3 The CIM-plate16.**

The CIM-plate16 consists of upper chamber (A), lower chamber (B) separated by a polyethylene terephthalate membrane with 8  $\mu$  pore size (C) and integrated with gold microelectrodes (D). Red arrows demonstrate the cell migration from top chamber to the lower chamber through the membrane and onto the electrodes.

According to the manufacturer's instructions, 160 $\mu$ l of phenol-red-free DMEM with 5% DCFCS and the relevant concentration of 17 $\beta$ -oestradiol, UV compounds or ethanol control was added to fill lower chamber completely. In the upper chamber 30  $\mu$ l of relevant medium lacking serum was added and the plate was incubated for 1 hour in the incubator and the background was set before seeding the cells.

Cells were trypsinized as described above and counted by using a haemocytometer. After that the cells were pelleted by centrifugation for 2 minutes at 800 rpm (87xg) (Eppendorf centrifuge 5810) and re-suspended at the required density in relevant media lacking serum in order to generate a chemotactic signal towards the lower chamber. In each well the cell

density was 40,000 cells / 100  $\mu$ l. The real time change of the electrical impedance (cell index) was then determined by the xCELLigence analyser system (RTCA-DP, ACEA Biosciences, USA) every 5 minutes for 24 hours.

#### **2.4.3.1 Analysis of cell migration using xCELLigence technology**

Results were obtained as curves that represent the average of cell index values for each time point for independent duplicate/triplicate wells as indicated for each experiment using RTCA software 1.2.1 (RTCA-DP, ACEA Biosciences, USA). Traces are the average of duplicate or triplicate wells. Cell index at 24 hours was plotted using GraphPad Prism version-6.01 software (GraphPad Software, La Jolla, CA). Error bars represent mean average  $\pm$ SE of triplicate wells.

### **2.5 Cell invasion using xCELLigence technology**

Wells of CIM-16 plates (ACEA Biosciences, USA) were coated with a solution of growth-factor-reduced-matrigel (BD Biosciences) in serum-free DMEM (lacking phenol red) (20 $\mu$ l 1:40-diluted matrigel per well on the upper surface only). The CIM-plate16 was incubated in a humidified atmosphere of 10% carbon dioxide in air at 37°C for 4 hours prior to the experiment. Experimental steps were carried on as described above (section 2.4.3. and 2.4.3.1) but the real time change of the electrical impedance (cell index) was determined by the xCELLigence analyser system (RTCA-DP, ACEA Biosciences, USA) every 5 minutes for 48 hours.

## **2.6 Real-Time Reverse Transcriptase Polymerase Chain Reaction (RT-PCR)**

### **2.6.1 Preparation of total cellular RNA**

### **2.6.2 Total cellular RNA extraction after 1 week of exposure to the UV screens**

In order to obtain the same cell density at collection time after short term exposure to UV screens, MCF-7 human breast cancer cells were trypsinized from stock dishes and were plated in 9-cm (63.6 cm<sup>2</sup> culture area per well) and 4-well (2.01 cm<sup>2</sup> culture area per well) tissue culture dishes (Nunc) at different densities based on different effects of UV screens on

the proliferation rate of MCF-7 human breast cancer cells (Table 2.2). Cells were seeded in phenol-red-free DMEM (Invitrogen) containing 5% DCFCS, 2mM L-glutamine, 100 µg/ml streptomycin and 100 U/ml penicillin (Invitrogen). After 24 hours, the medium was replenished with fresh medium containing  $10^{-5}$  M of the UV screens,  $10^{-8}$  M 17β-oestradiol or ethanol. After 7 days, 4-well (2.01 cm<sup>2</sup> culture area per well) tissue culture dishes were counted as described (in section 2.2.1) to provide the cell density at the time of harvest. From the 9-cm dishes, MCF-7 cells were collected after washing twice with 2 ml of 0.9% (w/v) NaCl in water and scraped off the dish using a rubber scraper. Cells were pelleted by centrifugation at 1000 rpm (113 xg) (Eppendorf centrifuge 5810) for 2 minutes and cell pellets were stored at -80°C.

**Table 2.2 Densities of MCF-7 cells seeded in relation to the proliferation rate.**

Cell proliferation rate	UV screen	Seeding density
Low	$10^{-5}$ M Bp3, $10^{-7}$ M Bp3, $10^{-5}$ M OMC, $10^{-7}$ M OMC, $10^{-7}$ M 4MBC and $10^{-7}$ M HS or ethanol control	$5 \times 10^5$ cells/ml
Medium	$10^{-7}$ M Bp1, $10^{-7}$ M Bp2, $10^{-5}$ M 4MBC or $10^{-5}$ M HS	$2.5 \times 10^5$ cells/ml
High	$10^{-8}$ M 17β-oestradiol and $10^{-5}$ M Bp1 or $10^{-5}$ M Bp2.	$0.8 \times 10^5$ cells/ml

### 2.6.3 Total cellular RNA extraction after 24-25 weeks of exposure to UV screens

Prior to the RNA extraction MCF-7 human breast cancer cells were long-term exposed (24-25 weeks) to  $10^{-5}$  M of each of the six UV screens,  $10^{-8}$  M 17β-oestradiol or ethanol control. Cells were maintained in phenol red-free DMEM (Invitrogen) containing 5% DCFCS, 2mM L-glutamine, 100 µg/ml streptomycin, 100 U/ml penicillin (Invitrogen) and the relevant treatment or ethanol control. MCF-7 human breast cancer cells were trypsinized from stock dishes and 16 ml of suspended cells were plated in 9-cm dishes (63.6 cm<sup>2</sup> culture area per

dish) at  $0.8 \times 10^5$  cells/ml in relevant media. After 7 days, cells were collected after washing twice with 2 ml of 0.9% (w/v) NaCl in water and scraped off the dish using a rubber scraper. In 15ml tubes, cells were pelleted by centrifugation at 1000 rpm (113 xg) (Eppendorf centrifuge 5810) for 2 minutes. The pellets were kept at  $-80^\circ\text{C}$  until the RNA extraction procedure.

#### **2.6.4 Total cellular RNA extraction**

MCF-7 whole cell RNA was produced using the Qiagen RNeasy® kit with on-column DNase treatment. According to the manufacturer, 600  $\mu\text{l}$  RLT buffer and 6  $\mu\text{l}$   $\beta$ -mercaptoethanol were added to each cell pellet and mixed by vortexing. The lysate was then passed through a QIA shredder spin column (Qiagen) by centrifuging for 2 minutes at maximum speed. The flow-through represents the homogenized cell lysate. To precipitate the DNA, 1 volume (600  $\mu\text{l}$ ) of 70% ethanol [prepared in RNase-free water (Qiagen)] was added to the cell lysate and mixed by pipetting. Then 700  $\mu\text{l}$  of that mix was transferred onto an RNeasy spin column placed in a 2 ml collection tube and spun for 15 seconds at 8000 xg. The flow-through was discarded and the same step was repeated for the remaining ethanol-cell lysate mix. Subsequently, 700  $\mu\text{l}$  of buffer RW1 was added to the column and then centrifuged for 15 seconds at 8000 xg. The flow-through was discarded. Then 500  $\mu\text{l}$  of buffer RPE was added to the column and spun for 15 seconds at 8000 xg. This step was repeated another time using an increased centrifugation time of 2 minutes. The column was placed in a new 2 ml collection tube and spun on full speed (13000 xg) for 1 minute. To elute the RNA, the column was placed into a 1.5 ml collection tube and 50  $\mu\text{l}$  of RNase-free water was added to the column. Finally, the column was spun for 1 minute at 8000 xg, and the eluate containing the RNA was collected and stored at  $-80^\circ\text{C}$ . The concentration of RNA was assessed from the OD at 260 nm and the purity of the sample was revealed using the ratio of OD values 260/280 nm using a NanoDrop 2000 spectrophotometer (Thermo Scientific, USA).

#### **2.6.5 cDNA synthesis**

First strand cDNA was synthesised using the QuantiTect® Reverse Transcription Kit (Qiagen). Before starting the procedure, RNA samples and the kit components were thawed on ice. In order to eliminate the genomic DNA, 2  $\mu\text{l}$  of gDNA buffer was added to 1  $\mu\text{g}$  of RNA sample in a 0.5 ml microcentrifuge and RNase-free water was added to complete the final reaction volume to 14  $\mu\text{l}$ . According to Qiagen technical support, gDNA buffer contains

a double strand specific endonuclease and the buffer conditions are optimised to allow the removal of residual DNA without the removal of ssDNA or RNA. The tubes were incubated for 2 minutes at 45°C and then placed immediately on ice. Next the reverse transcription reaction mixture was prepared by mixing 1 µl of Quantiscript Reverse Transcriptase, 4 µl of Quantiscript RT buffer, 1 µl RT Primer mix and 14 µl of the RNA template, which was prepared in the previous step. The reaction components were mixed by pipetting and then incubated for 15 minutes at 45°C and then 3 minutes at 95°C to inactivate the Quantiscript Reverse Transcriptase. cDNA samples were diluted (1 in 20) in RNase-free water and stored in -80°C.

### **2.6.6 PCR assay**

QuantiTect primers (Table 2.3) were supplied as bioinformatically validated by Qiagen. Each primer was supplied dry and reconstituted in 1.1 ml TE buffer [1M Tris pH 8.0 and 0.05 M EDTA in RNase-free water] and then were stored at -20°C. The PCR reaction mix was prepared by mixing 7 µl of QuantiTect SYBR Green PCR Master Mix (Qiagen, UK), 1.4 µl of QuantiTect primer and 0.6 µl RNase-free water. The PCR assay was carried out in a volume of 14 µl including 9 µl of the reaction mix –described above- and 5 µl of cDNA (1/20 dilution) or 5 µl RNase-free water (negative control) in 96-well optical reaction plate (1900 High speed low profile PCR plate, Thermo Scientific, UK). Then the plates were sealed using optical adhesive cover (MicroAmp, Applied Biosystems). Subsequently, the 96-well plate was vortexed and spun to remove bubbles using Perfect Spin-P (PEQLAB, USA) before loading the PCR plates into the StepOne™ Plus real-time PCR instrument (Applied Biosystems, Life Technologies Ltd.). The thermal profile for all reactions was 95°C for 15 minutes, followed by 94°C for 15 seconds and 60°C for 1 minute (50 cycles). All reactions were performed in triplicate and β-actin was used as an endogenous housekeeping gene.

### **2.6.7 RT-PCR analysis**

The relative gene expression quantification method was used to compare the gene expression of the control sample with the gene expression of 17β-oestradiol or UV screen exposed samples. Ct values of the endogenous control β-actin and from different targeted genes were used to calculate the fold change in relative gene expression using the  $2^{-\Delta\Delta C_T}$  method (Livak and Schmittgen, 2001). Each reaction was all carried out in triplicate and results are shown as

the average  $\pm$  SE of biological replicates from separate cell cultures. The results were plotted using Graph Pad Prism version-6.01 software (GraphPad Software, La Jolla, CA).

**Table 2.3 The QuantiTect primers (Qiagen) and their GeneGlobe specifications**

QuantiTect Primer (product number)	Species	Gene ID	Amplicon length	Detected transcript
TFF1 (QT00209608)	Homo sapiens	7031	75 bp	NM_003225 (508 bp)
E-cadherin (CDH1) (QT00080143)	Homo sapiens	999	84 bp	NM_004360 (4815 bp)
$\beta$ -catenin (CTNNB1) (QT00077882)	Homo sapiens	1499	130 bp	NM_001098209 (3415bp)
TWIST1(QT00011956)	Homo sapiens	7291	127 bp	NM_000474 (1669 bp)
Snail 1 (QT00010010)	Homo sapiens	6615	131 bp	NM_005985 (1722 bp)
PIK3R1(QT00023100)	Homo sapiens	5295	117 bp	NM_001242466 (5554 bp)
BMP7 (QT00068936)	Homo sapiens	655	128 bp	NM_001719 (4049 bp)
$\beta$ -actin (ACTB) (QT-01680476)	Homo sapiens	60 bp	104 bp	NM_001101 (1852 bp)

## **2.7 Western immunoblotting**

### **2.7.1 Preparation of whole cell lysates**

#### **2.7.1.1 Preparation of MCF-7 whole cell lysates after exposure to the UV screens**

In order to prepare MCF-7 whole cell lysates, the same procedures (in sections 2.6.2 and 2.6.3) were performed to collect the appropriate number of MCF-7 cells after 1 week and 21-23 weeks of exposure to  $10^{-5}$  M of the UV screens,  $10^{-8}$  M  $17\beta$ -oestradiol or ethanol control.

#### **2.7.1.2 Protein extraction**

Lysis buffer was prepared freshly [50 mM Tris-HCl pH7.4, 250 mM NaCl, 5 mM EDTA, 0.3% Triton X-100, 0.3 mM AEBSF (4-2 aminoethylbenzenesulfonyl fluoride), 10  $\mu$ g/ml leupeptin and 2  $\mu$ g/ml aprotinin] and the required amount for each cell pellet (prepared in section 2.7.1) was calculated based on the cell count for each stock to obtain a final concentration of  $1 \times 10^5$  cells/ $\mu$ l. The cell pellet was mixed with the lysis buffer and kept on ice for 30 minutes. The cell lysate was moved to an autoclaved 1.5 ml microcentrifuge tube then the lysate was passed through needles of decreasing size from 19G (7 times) to 25G (7 times). The tubes were centrifuged at 13,000 rpm (MSE, Jencons-Pls, UK) for 2 minutes and the supernatant was collected and aliquoted into labelled 0.5 ml microcentrifuge tubes and kept at  $-80^{\circ}\text{C}$  until required.

### **2.7.2 Protein assay using the Pierce BCA reagent**

Protein assays were performed using the Pierce BCA reagent kit (Pierce, USA). In 0.5 ml microcentrifuge tubes, standards of bovine serum albumin (BSA) (Sigma) were prepared over a range of concentrations from 0-16  $\mu$ g/ $\mu$ l and 2  $\mu$ l of the lysis buffer was added to each tube. The final volume of each microcentrifuge tube was made to 10  $\mu$ l by adding double distilled water. 2  $\mu$ l of cell lysate samples were added to 8 $\mu$ l of double distilled water in 0.5 ml microcentrifuge tubes in triplicates. According to the manufacturer instructions, 5ml of Reagent A was mixed with 0.1 ml of reagent B and 200  $\mu$ l of the reagent mixture was added to each microcentrifuge tube. The tubes were incubated in the oven (hybridization/shaker oven, Amersham Life Science) at  $60^{\circ}\text{C}$  for 30 minutes. 150  $\mu$ l aliquots of the standards and

samples were then transferred into the wells of a 96-well plate (Falcon, USA). The absorbance was then read at a wavelength of 540 nm using an EMax precision microplate reader (Molecular Devices, USA). The concentrations of the cell lysate were then calculated from the standard curve of the BSA samples of known concentration.

### **2.7.3 Sodium Dodecyl Sulphate-polyacrylamide gel electrophoresis (SDS-PAGE)**

Prior to the SDS-PAGE, protein samples were denatured and reduced by mixing the sample 1:1 with 2x Laemmli buffer (Bio-Rad) supplemented with 2-mercaptoethanol (50  $\mu$ l in 950  $\mu$ l) (Sigma-Aldrich) and incubated for 3 minutes at 100°C. Gradient (4-15%) or 10% precast TGX stain-free mini PAGE gels (Bio-Rad, Hertfordshire, UK) were used to separate the protein samples according to their molecular weight. After removing the comb, the gel was placed into the electrophoresis tank and washed with running buffer [25 mM Tris pH 8.3, 0.1% (w/v) SDS, 192 mM glycine]. 6  $\mu$ l of Precision plus protein unstained protein standard (marker) in the range of 10-250 kDa (Bio-Rad) was loaded as a marker in each gel and 25  $\mu$ g of protein samples were loaded per gel track. The gel was run at 200 volts for 30 minutes. Stain-free gels are designed to facilitate obtaining the volume of total protein in each gel track after blotting the protein onto the membrane. In order to estimate the amount of total protein the gel was activated by using the Gel Doc EZ imager (Bio-Rad) on the stain-free tray for five minutes.

### **2.7.4 Protein transfer**

Proteins were transferred from the gels onto 0.2  $\mu$ m PVDF by semi-dry western blotting using Trans-Blot turbo transfer pack (Bio-Rad), which contains 0.2  $\mu$ m PVDF membrane and the Whatman papers soaked with transfer buffer and ready to use (Trans-Blot turbo transfer pack, Bio-Rad). The membrane and the gel were set up into the Trans-Blot Turbo transfer system (Bio-Rad) and the transfer was set up at 2.5 A constant current for 3 minutes. The Gel Doc EZ imager was then used to scan the membrane and image the total protein in each track on the PVDF membrane. Later the total protein level was determined using Image Lab software (version 5.0, Bio-Rad) (Figure 2.4). This total protein was used as a loading control.

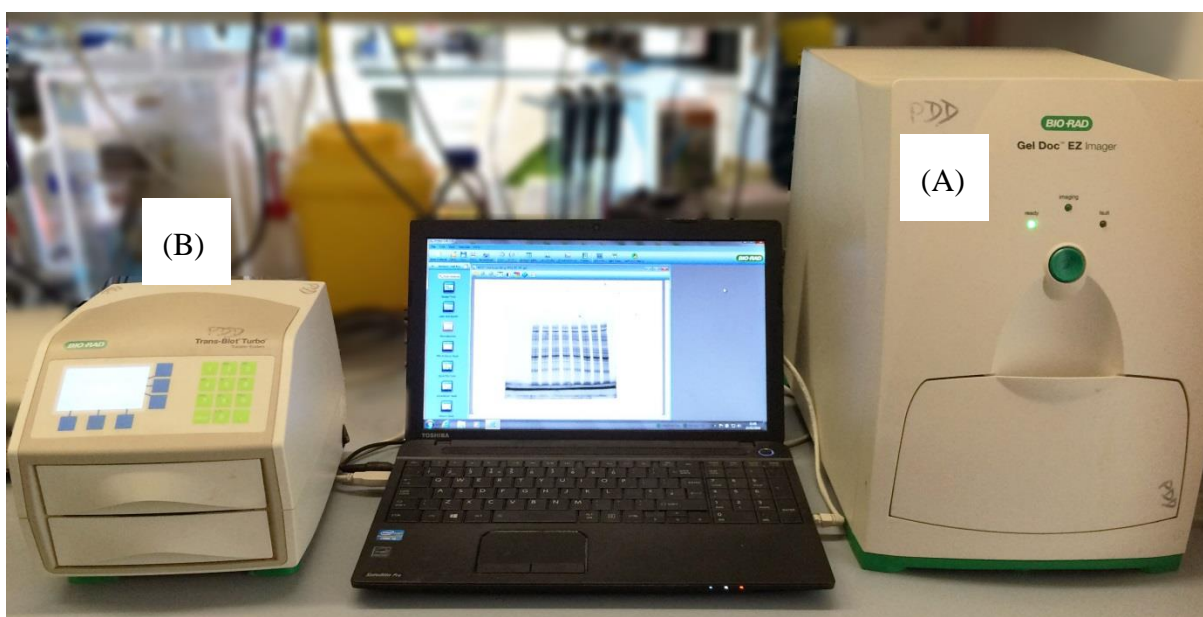


**Figure 2.4 Bio-Rad Gel Doc EZ imager and the turbo transfer system.**

This image illustrates Bio-Rad Gel Doc EZ imager (A) and the Trans-Blot Turbo transfer system (B).

### **2.7.5 Immunostaining of protein**

The membrane was blocked with 5% (w/v) dried milk in TBS-T [0.1 % Tween-20, 150 mM NaCl, 2 mM KCl and 50 mM Tris pH 7.4] at room temperature for one hour with gentle rocking. The membrane was then washed three times for 5 minutes each with 15 ml of TBS-T. In order to avoid stripping the membrane, the membrane was cut to have the loading control (actin) immunostained separately from targets of interest. Membranes were incubated in a heat sealable bag with appropriate primary antibody at the required concentration (Table 2.4) diluted in 5% w/v BSA (Sigma) in TBS-T at 4°C overnight on a rotating drum. The following day, the membrane was washed three times with TBS-T for 5 minutes each and then incubated with appropriate HRP-linked secondary antibody (Table 2.4) at a dilution of 1:2000 and the marker conjugate (Precision Plus protein StrepTactin-HRP conjugate) at a dilution of 1:5000 both diluted in TBS-T and 5% w/v dried milk for 1 hour at room temperature. The membrane was washed again 3 times for 5 minutes each in TBS-T.

The ECL-Prime western blotting detection reagent (GE Healthcare) was prepared according to the manufacturer's instructions and the membrane was incubated in the reagent for 3 minutes. The membrane was covered with Saranwrap and imaged on a luminescent image analyser (Image Quant LAS4000mini, GE Healthcare). Exposure time was optimized for band detection.

**Table 2.4 List of antibodies used for immunoblotting**

Primary Antibody	Manufacturer - Product number	Source	Dilution
Oestrogen receptor $\alpha$	Cell Signalling - 6844	Rabbit	1:1000
E-cadherin	Cell Signalling - 3195	Rabbit	1:1000
$\beta$ -catenin	Cell Signalling - 9582	Rabbit	1:1000
MMP14	Cell Signalling - 13130	Rabbit	1:1000
$\beta$ -actin	Cell Signalling - 8457	Rabbit	1:1000
Secondary Antibody	Manufacturer	Source	Dilution
HRP-linked, anti-rabbit	Cell Signalling - 7074	Goat	1:2000
Precision Plus protein StrepTactin-HRP conjugate	Bio-Rad	-	1:5000

### 2.7.6 Quantitation of protein and data analysis

Quantification of each protein band was performed by quantitating the relative intensity of each band present on the digital image acquired by Image Quant LAS4000min (GE Healthcare). The Image was analysed using Image J software and gel analyser plugin. The intensity of each band was obtained in numerical form. Results were expressed as a ratio to the relevant loading control ( $\beta$ -actin or total protein). The results were expressed as mean  $\pm$  standard error (SE) from at least three independent cell cultures.

## 2.8 Gelatin zymography

Zymography is a semi-quantitative technique used to detect the activity of matrix metalloproteinases (MMPs). Different substrates can be used in this technique and the selection of the substrate depends on the group of MMPs under investigation. In order to detect MMP-2 and MMP-9 activity, SDS gelatin gels were chosen (Hu and Beeton, 2010).

### 2.8.1 Conditioned media collection

MMP-2 and MMP-9 are secreted by human breast cancer cells and were therefore assayed by collection of serum free media (Das et al., 2008). Prior to the collection, MCF-7 cells were exposed to  $10^{-5}$  M UV screens in the presence of 5% DFCS for 35-37 weeks and MDA-MB-231 cells were exposed to  $10^{-7}$  M UV in the presence of 10% FCS for 15 weeks.

After 35 weeks of exposure with  $10^{-5}$  M of UV screens,  $10^{-8}$  M  $17\beta$ -oestradiol or ethanol control, MCF-7 human breast cancer cells were trypsinized from long-term maintained dishes and were plated at  $0.8 \times 10^5$  cells/ml (16 ml/dish) in 9-cm ( $63.6 \text{ cm}^2$  culture area per dish) and 4-well ( $2.01 \text{ cm}^2$  culture area per well) tissue culture dishes (Nunc) (0.5 ml/well). Cells were seeded in phenol red-free DMEM (Invitrogen) containing 5% DCFCS, 2mM L-glutamine, 100  $\mu\text{g/ml}$  streptomycin, 100 U/ml penicillin (Invitrogen) and the  $10^{-5}$  M of UV screen,  $10^{-8}$  M  $17\beta$ -oestradiol or ethanol.

On day 7, dishes were washed two times. Firstly, with 2 ml of HBSS (Invitrogen) and secondly with 2 ml of serum free media [phenol red-free DMEM (Invitrogen), 2 mM L-glutamine, 100  $\mu\text{g/ml}$  streptomycin and 100 U/ml penicillin (Invitrogen)] in the presence of different treatments or control. After the washing steps, 4 ml of serum free media were added to each 9-cm dish and 0.25  $\mu\text{l}$  volume in the 4-well plates. The plates were incubated in a humidified atmosphere of 10% carbon dioxide in air at  $37^\circ\text{C}$  for 24 hours.

Then, the 4 ml conditioned media samples were collected and concentrated using ultra-4 centrifugal-filter units (10,000 NMWL) (Milipore, USA). The units were spun at 3000 xg for 20 minutes and the yield of samples was between 250-400  $\mu\text{l}$ . simultaneously, cells in 4-well tissue culture dishes were counted as described in section 2.2.1 to provide the cell density at the time of conditioned media collection.

The same procedure was carried out in order to collect conditioned media from MDA-MB-231 cell lines exposed to  $10^{-7}$  M UV screens or control for 15 weeks. However, the media

used for long-term maintenance of MDA-MB-231 was phenol-red DMEM supplemented with 10% FCS 100 µg/ml streptomycin and 100U/ml penicillin with relative UV screen or ethanol, and the conditioned media consisted of [phenol-red DMEM, 100 µg/ml streptomycin and 100 U/ml penicillin] with the relative UV screen or ethanol, and the MDA-MB-231 cells were collected to prepare protein lysate as described (in section 2.7.1.2).

### **2.8.2 Loading and running zymography SDS gelatin gels**

The volume of concentrated conditioned media from  $10^5$  cells was mixed with an equal amount of zymogram loading buffer (Bio-Rad). Then the samples were kept at room temperature for 10 minutes and vortexed prior to loading in each gel track.

Precast 10% polyacrylamide-SDS gels with gelatin (Bio-Rad) were used to run the prepared samples at 125 V for 1 hour 20 minutes. Before loading the samples, the gels were washed with the running buffer [25 mM Tris pH 8.3, 0.1% (w/v) SDS, 192 mM glycine].

### **2.8.3 Developing the zymogram**

After running the samples, the proteases were renatured by incubating the gel in renaturation buffer [2.5% Triton-X-100]. Then the protease activity was developed by initially incubating the gels with 100 ml developing buffer [100 mM Tris-Base, 399 mM Tris-HCL, 2 M NaCl, 66.6 mM CaCl<sub>2</sub> and 0.2% Brij35] for 30 minutes at room temperature with gentle shaking. After discarding the buffer, another fresh 100 ml of the developing buffer was added and the gels were incubated at 37°C in an oven for 24 hours.

### **2.8.4 Staining and destaining of zymography SDS gelatin gel**

Prior to the staining step, the developed gels were washed 3 times with ddH<sub>2</sub>O with gentle shaking. Later the gels were stained with 50 ml of 0.5% Coomassie blue R-250 (Bio-Rad) for 30 minutes with gentle shaking. After that, the stained gels were destained using 20 ml of destaining solution [40% methanol, 10% glacial acetic acid] for 15 minutes and replacing the destaining solution every 30 minutes for 1 and 1/2 hour.

### **2.8.5 Quantifying the proteinases activity and data analysis**

The MMP-2 and MMP-9 activities showed as white bands (representing the gelatinase activity) against a blue background. By using the BioRad Gel Doc imager (white light tray), images of the gels were obtained, and then Image J software, was used to convert the image

into grayscale and to quantify the band area (Hu and Beeton, 2010). Results were normalized against the negative control. All results show the average  $\pm$  SE of three biological replicates (n=3). The results were plotted using Graph Pad Prism version-6.01 software (GraphPad Software, La Jolla, CA).

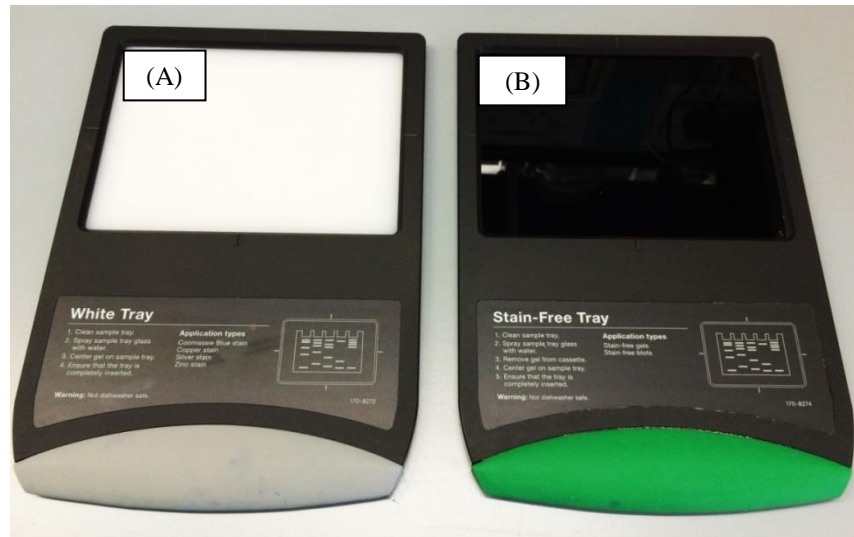


**Figure 2.5 Bio-Rad Gel Doc imager trays**

This figure shows the white tray used for zymogram gel imaging (A) and the stain-free tray used to activate the stain-free western blot gels and to obtain the total protein image from the PVDF membrane (B).

## 2.9 Data Analysis

Statistical differences involving 2 groups were subjected to t-Test assuming unequal variance, but those involving more than 2 groups were analysed by one-way analysis of variance (ANOVA) with Dunnett's post-hoc test to compare the result of each treatment to a single control or Tukey's post-hoc test to compare pairs of means within the tested group. In an experiment where cells were subjected to two variances, data were analysed by two-way analysis of variance (Two-way-ANOVA) with Bonferroni post-hoc test. Statistics were conducted using Minitab 17 statistics package or GraphPad Prism version-6.01 software (GraphPad Software, La Jolla, CA). A value of  $p$ -value  $\leq 0.05$  was considered statistically significant and the results were plotted using GraphPad Prism version-6.01 software (GraphPad Software, La Jolla, CA).

## Chapter 3 The oestrogenic activity of UV screens in oestrogen responsive MCF-7 human breast cancer cells

### 3.1 Introduction

17 $\beta$ -oestradiol, the endogenous female hormone responsible for reproductive processes including the growth of female breasts (Russo and Russo, 2014), has been linked to breast cancer development due to its positive influence on breast epithelial cell proliferation (Russo and Russo, 2006; Yue et al., 2010). In order to investigate the mechanistic processes related to the role of oestrogen in breast cancer, *in vitro* model systems have been developed.

The MCF-7 human breast cancer cell line has been the most widely used cell line in the field of breast cancer research (Lippman et al., 1977; Burdall et al., 2003). Among the *in vitro* models, MCF-7 cells have been used to study the effects of oestrogen on breast cancer cells because it is oestrogen responsive in culture when phenol red is removed from the culture medium (Berthois et al., 1986). Oestrogens bind to oestrogen receptor in MCF-7 cells (Brooks et al., 1973). Both ER $\alpha$  and ER $\beta$  are expressed in this cell line with high predominance of ER $\alpha$  (Shaw et al., 2006; Nadal-Serrano et al., 2012). Once ER is activated by oestrogen, the proliferation of MCF-7 cells increases (Darbre and Daly, 1989; Dupont and Le Roith, 2001; Lai et al., 2001; Liao et al., 2014) and the use of the pure antioestrogen fulvestrant decreases the proliferative response of MCF-7 cells towards 17 $\beta$ -oestradiol (Shaw et al., 2006). Exposure to 17 $\beta$ -oestradiol not only increases the proliferation of MCF-7 cells but it also influences oestrogen-regulated gene expression such as the TFF1 (pS2) gene, which increases following MCF-7 cell exposure to 17 $\beta$ -oestradiol (Masiakowski et al., 1982; Brown et al., 1984; Jakowlew et al., 1984; May and Westley, 1986; Kida et al., 1989).

These properties of the MCF-7 cell line have made it a useful starting point to evaluate the endocrine disruptive capabilities of the environmental chemicals *in vitro* (Soto et al., 1995). Among the many of the endocrine disruptors that have entered human tissues, are the UV screens (Hayden et al., 1997; Jiang et al., 1999; Janjua et al., 2004; Schlumpf et al., 2010; Valle-Sistac et al., 2016). Although human use of UV screens is very high, only few studies have explored their effect on breast cancer cell proliferation, TFF1 gene expression and reporter gene assays (see section 1.4.3.1.). In this chapter, 6 UV screens benzophenone-1 (Bp1), benzophenone-2 (Bp2), benzophenone-3 (Bp3), octyl-methoxycinnamate (OMC), 4-

methylbenzylidene camphor (4MBC) and homosalate (HS) have been investigated for their comparative oestrogenic activity.

Previous studies have examined the effect of some of these UV screens on the proliferation of MCF-7 cells (Schlumpf et al., 2001; Nakagawa and Suzuki, 2002; Jimenez-Diaz et al., 2013; Kerdivel et al., 2013). Among different laboratories the MCF-7 human breast cancer cell line has been found to exhibit variation in some biological properties including the proliferation rate (Osborne et al., 1987) and the sensitivity towards oestrogen (Darbre and Daly, 1989; Villalobos et al., 1995; Hamelers et al., 2003). For these reasons, this work investigated the effects of these 6 UV screens on proliferation using MCF-7 cells from our laboratory, prior to investigating their potential influence on other hallmarks of cancer.

Moreover, previous *in vitro* proliferation studies have only considered the effect of these chemicals on MCF-7 cells growing on plastic. However, breast cancer cells seeded on coated plates with extracellular matrix (ECM) components have shown different responses towards different treatments (Sonohara et al., 1998; Woodward et al., 2000; Korah et al., 2004; Ohbayashi et al., 2008; Pontiggia et al., 2012), which offers a more realistic model of cancer cell growth *in vivo* in the human body. The changes caused by cell-extracellular matrix interactions via the integrins (a family of transmembrane heterodimeric glycoproteins) initiate several signalling pathways and subsequently affect several biological processes such as cell proliferation and differentiation (Schwartz et al., 1995; Longhurst and Jennings, 1998). It is noteworthy that the sensitivity of MCF-7 cells towards  $17\beta$ -oestradiol was found to be different in the presence of different coating materials. In contrast to the increase in sensitivity toward  $17\beta$ -oestradiol by cells seeded on a fibronectin coating, the sensitivity was found to be reduced by laminin (Woodward et al., 2000). To date, no studies have shown the effect of the dual presence of extracellular matrix proteins and the UV screens on the proliferation of MCF-7 cells.

## **3.2 Experimental aims**

The overall aims of this chapter were to compare the oestrogenic effect of six UV screens (benzophenone-1 (Bp1), benzophenone-2 (Bp2), benzophenone-3 (Bp3), octyl-methoxycinnamate (OMC), 4-methylbenzylidene camphor (4MBC) and homosalate (HS)) using the MCF-7 human breast cancer cell line in our laboratory by measuring ERE-LUC reporter gene expression, ER $\alpha$  protein levels, TFF1 gene expression and stimulation of cell

proliferation. Since oestrogen is present *in vivo* in the female body in the range of  $10^{-11}$  M to  $10^{-10}$  M (Wright et al., 1999), the influence of different concentrations of  $17\beta$ -oestradiol with the UV screens was studied on the proliferation of MCF-7 cells.

Another aim of this chapter was to compare the influence of fibronectin or laminin coating on the proliferation of MCF-7 cells following the exposure to  $17\beta$ -oestradiol or UV screens.

### **3.3 Results**

#### **3.3.1 Effects on ERE-LUC reporter gene expression**

To assess the oestrogenic effect of UV screens on MCF-7 cells, an oestrogen responsive reporter gene assay was performed (as described in section 2.3). Oestrogen regulation of a transiently transfected oestrogen-inducible ERE-LUC reporter gene in MCF-7 cells was published in 2006 (Shaw et al., 2006). However, a line of MCF-7 cells stably transfected with the same ERE-LUC reporter gene has been produced but not validated by publication. Before assessing the effect of UV screens on the ERE-LUC reporter gene in these cells, validation of the assay was needed.

##### **3.3.1.1 Validation of the stably transfected ERE-LUC reporter gene in MCF-7 cells**

MCF-7 cells stably transfected with the ERE-LUC reporter gene were kept in stock media supplemented with G418 sulphate (100  $\mu\text{g}/\text{ml}$ ) for two weeks. Cells were re-plated in 24 well plates into experimental medium lacking any treatments for 6 days prior to the experiment. Cells were then exposed to  $10^{-8}$  M  $17\beta$ -oestradiol or ethanol control for 24 hours prior to the luciferase assay.  $10^{-8}$  M  $17\beta$ -oestradiol induced luciferase gene expression from a control value of  $0.77 \pm 0.12$  to a value of  $2.89 \pm 0.56$  (Figure 3.1) ( $p$ -value  $\leq 0.01$ ). This experiment is the result of 3 independent biological replicates.

##### **3.3.1.2 Effects of UV screens on ERE-LUC reporter gene expression**

MCF-7 cells stably transfected with the ERE-LUC reporter gene were used to evaluate the ability of UV screens to induce luciferase activity.  $10^{-5}$  M Bp1 was found to induce luciferase activity significantly from a control value of  $0.63 \pm 0.04$  to a value of  $2.14 \pm 0.15$  (Figure 3.2 (A)) ( $p$ -value  $\leq 0.0001$ ) and comparison with  $10^{-8}$  M  $17\beta$ -oestradiol (Figure 3.2 (G)) revealed that  $10^{-5}$  M Bp1 caused a greater induction of luciferase activity than  $10^{-8}$  M  $17\beta$ -oestradiol

(Figure 3.2 (H)) ( $p$ -value  $\leq 0.05$ ). Among the UV screens under the study,  $10^{-5}$  M Bp2 was found to induce the highest luciferase activity from a control value of  $0.63 \pm 0.04$  to a value of  $3.42 \pm 0.32$ . It is also noteworthy that the luciferase activity induced by  $10^{-5}$  M Bp2 (Figure 3.2(B)) ( $p$ -value  $\leq 0.0001$ ) was greater than that by  $10^{-8}$  M  $17\beta$ -oestradiol (Figure 3.2 (H)) ( $p$ -value  $\leq 0.0001$ ). A lower induction of the luciferase activity from a control value of  $0.63 \pm 0.04$  was detected following the exposure to  $10^{-5}$  M Bp3 to a value of  $1.57 \pm 0.12$  (Figure 3.2 (C)) ( $p$ -value  $\leq 0.0001$ ),  $10^{-5}$  M OMC to a value of  $1.07 \pm 0.11$  (Figure 3.2 (D)) ( $p$ -value  $\leq 0.05$ ),  $10^{-5}$  M 4MBC to a value of  $0.79 \pm 0.06$  (Figure 3.2 (E)) ( $p$ -value  $\leq 0.01$ ) and  $10^{-5}$  M HS to a value of  $0.793 \pm 0.06$  (Figure 3.2 (F)) ( $p$ -value  $\leq 0.01$ ). No significant difference in Luciferase activity was found between  $10^{-5}$  M Bp3 and  $10^{-8}$  M  $17\beta$ -oestradiol. However, effects of  $10^{-5}$  M OMC,  $10^{-5}$  M 4MBC and  $10^{-5}$  M HS were significantly lower than the effect caused by  $10^{-8}$  M  $17\beta$ -oestradiol (Figure 3.2 (H)).

Dose response experiments were then carried using a range of concentrations for each of the UV screens. Increased luciferase activities were observed in line with the increase in molar concentration (Figures 3.3-3.8). Although some effects on the luciferase activity were detected following exposure to  $10^{-5}$  M of OMC, 4MBC or HS, lower concentrations of these chemicals were not found to show more effect than the activities following exposure to  $10^{-5}$  M. The dose response curve of luciferase activities following exposure to either OMC (Figure 3.6) or HS (Figure 3.8) showed an increase in luciferase activities with increasing molar concentrations. However,  $10^{-7}$  M,  $10^{-6}$  M and  $10^{-5}$  M 4MBC concentrations were found to induce similar luciferase activity from a control value of  $0.54 \pm 0.02$  to a value of  $0.77 \pm 0.04$ ,  $0.77 \pm 0.03$  and  $0.79 \pm 0.09$ , suggesting lower molar concentrations need to be studied (Figure 3.7).

### **3.3.1.3 Effect of fulvestrant on induction of ERE-LUC reporter gene by UV screens**

Fulvestrant (ICI 182,780) (AstraZeneca, Macclesfield, UK) is an oestrogen receptor antagonist, which reduces oestrogen action through the ER (Wakeling et al., 1991). In order to investigate whether Bp1 and Bp2 induce ERE-LUC reporter gene expression via an ER-mediated pathway, cells were incubated with  $10^{-7}$  M fulvestrant and  $10^{-5}$  M Bp1 or  $10^{-5}$  M Bp2.

The effect of  $10^{-8}$  M  $17\beta$ -oestradiol on the luciferase activity was decreased from a value of  $4.052 \pm 1.31$  to a value of  $0.685 \pm 0.42$  using  $10^{-7}$  M fulvestrant ( $p$ -value  $\leq 0.01$ ). In the same experiment,  $10^{-7}$  M fulvestrant decreased the luciferase activity following the exposure to  $10^{-5}$  M Bp1 from a value of  $3.15 \pm 0.21$  to a value of  $1.01 \pm 0.07$  ( $p$ -value  $\leq 0.001$ ) and to  $10^{-5}$  M Bp2 from a value of  $4.39 \pm 0.52$  to a value of  $1.96 \pm 0.16$  ( $p$ -value  $\leq 0.001$ ) (Figure 3.9).

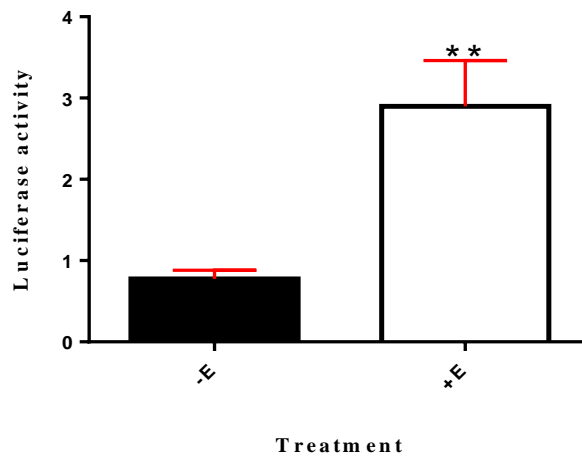


**Figure 3.1 Regulation of a stably transfected oestrogen-inducible ERE-LUC reporter gene in MCF-7 human breast cancer cells following exposure to  $17\beta$ -oestradiol or ethanol control.**

MCF-7 cells were plated at  $0.2 \times 10^5$  cells/well in 24 well plates and grown in phenol-red-free-DMEM containing 5% DCFCS for 6 days prior to the experiment. Media were replenished on day 1 and day 4. On day 7 media was replenished with fresh media plus  $10^{-8}$  M  $17\beta$ -oestradiol (+E) or ethanol control (-E). Luciferase assay was conducted after 24 hours of exposure. Results were calculated as the average luciferase activity per 10,000 cells. Each experiment was conducted in triplicate. Values are the average  $\pm$ SE of 3 independent experiments (n=3). \*\*  $p$ -value  $\leq 0.01$  versus no addition by t-Test.

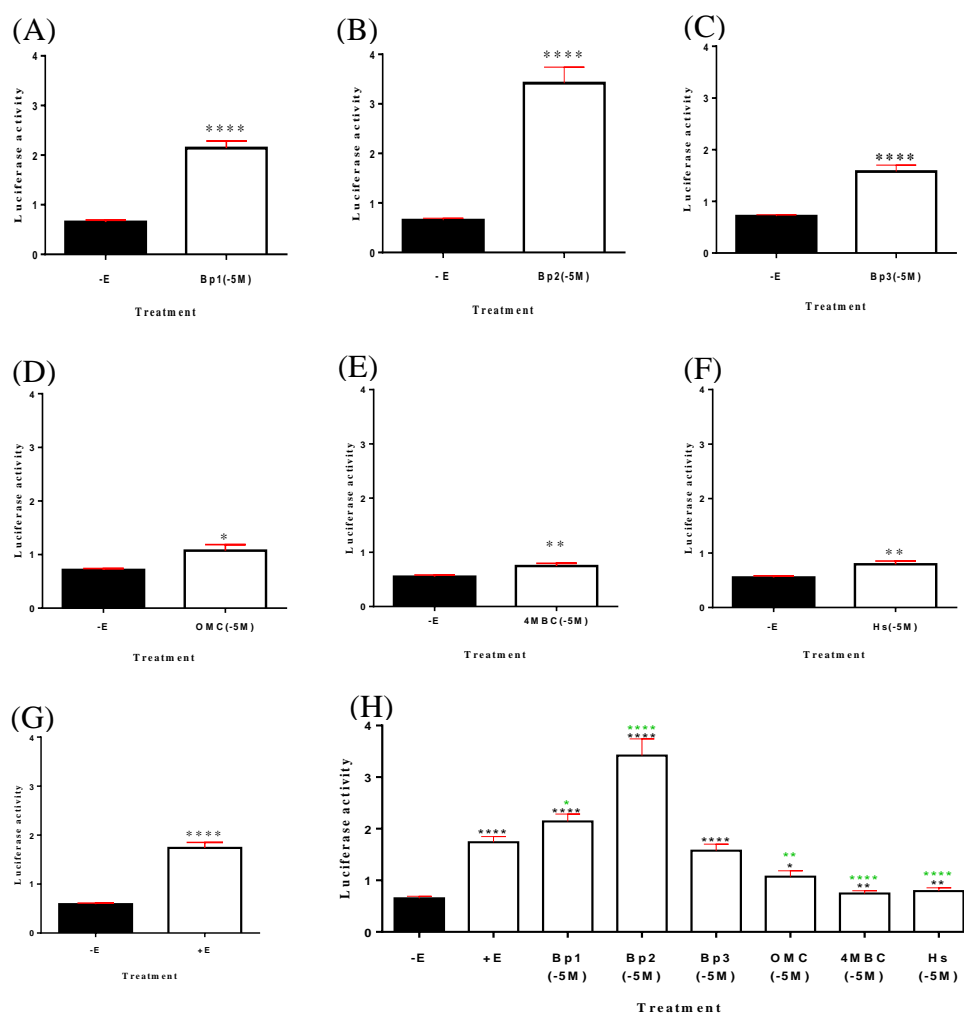


**Figure 3.2 Regulation of a stably transfected oestrogen-inducible ERE-LUC reporter gene in MCF-7 human breast cancer cells following exposure to  $10^{-5}$ M of UV screens,  $10^{-8}$ M of  $17\beta$ -oestradiol or ethanol.**

Stably transfected MCF-7 cells were plated at  $0.2 \times 10^5$  cells/well in 24 well plates and grown in phenol-red-free-DMEM containing 5% DCFCS for 6 days prior to the experiment. Media were replenished on day 1 and day 4. On day 7 media was replenished with fresh media plus  $10^{-5}$  M Bp1 (Bp1 (-5M)) (A),  $10^{-5}$  M Bp2 (Bp2 (-5M)) (B),  $10^{-5}$  M Bp3 (Bp3 (-5M)) (C),  $10^{-5}$  M OMC (OMC (-5M)) (D),  $10^{-5}$  M 4MBC (4MBC (-5M)) (E),  $10^{-5}$  M HS (Hs (-5M)) (F),  $10^{-8}$  M  $17\beta$ -oestradiol (+E) (G) or ethanol control (-E). Comparisons between the UV screens and +E (green asterisk) is present in (H). Luciferase assay was conducted after 24 hours of exposure. Results were calculated as the average luciferase activity per 10,000 cells. Values are the average  $\pm$ SE of three wells from three independent experiments for Bp1 and Bp2 (n=3) and two independent experiments for Bp3, OMC, 4MBC and HS (n=2). \* *p*-value  $\leq 0.01$ , \*\* *p*-value  $\leq 0.001$  and \*\*\*\* *p*-value  $\leq 0.0001$  versus no addition (black asterisks) or +E (green asterisks) by t-Test.

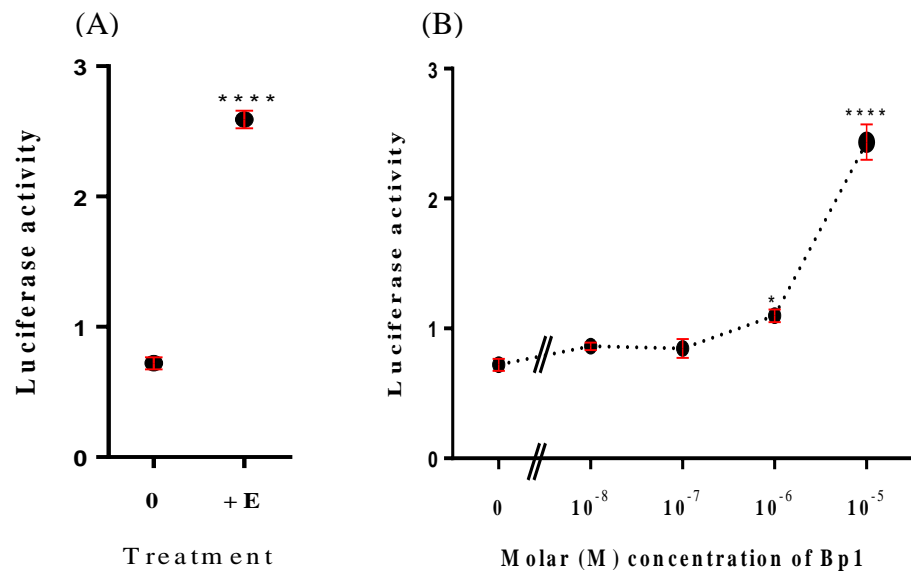


**Figure 3.3 Regulation of a stably transfected oestrogen-inducible ERE-LUC reporter gene in MCF-7 human breast cancer cells following exposure to increasing doses of Bp1.**

MCF-7 cells were plated at  $0.2 \times 10^5$  cells/well in 24 well plates and grown in phenol-red-free-DMEM containing 5% DCFCS for 6 days prior to the experiment. Media were replenished on day 1 and day 4. On day 7 media was replenished with fresh media without or with  $10^{-8}$  M  $17\beta$ -oestradiol (+E) (A) or with indicated concentrations of Bp1 (B). Luciferase assay was conducted after 24 h of exposure. Results were calculated as average luciferase activity per 10,000 cells. Values are the average  $\pm$ SE of 3 independent wells. \* *p-value*  $\leq 0.05$  and \*\*\*\* *p-value*  $\leq 0.0001$  versus no addition by t-Test (A) or by one-way ANOVA Dunnett's test (B).

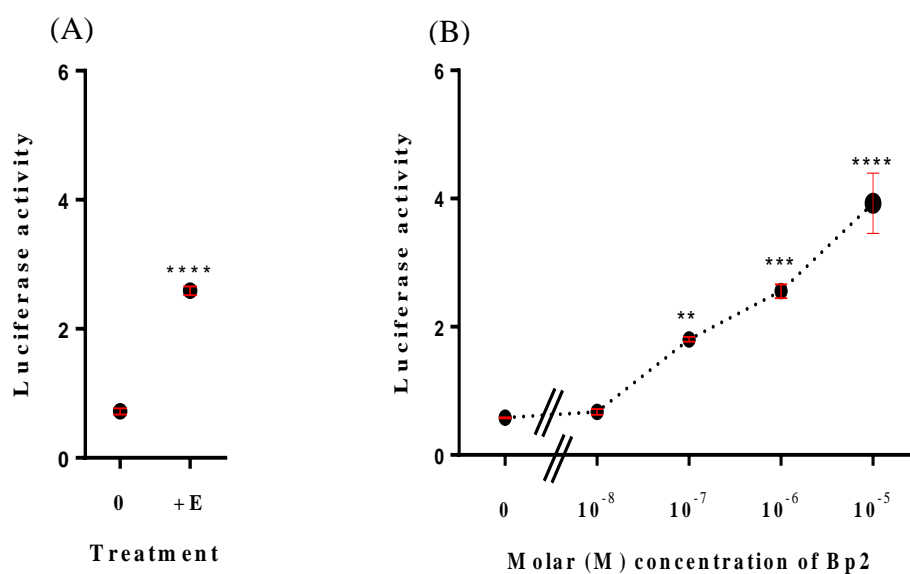


**Figure 3.4 Regulation of a stably transfected oestrogen-inducible ERE-LUC reporter gene in MCF-7 human breast cancer cells following exposure to increasing doses of Bp2.**

MCF-7 cells were plated at  $0.2 \times 10^5$  cells/well in 24 well plates and grown in phenol-red-free-DMEM containing 5% DCFCS for 6 days prior to the experiment. Media were replenished on day 1 and day 4. On day 7 media was replenished with fresh media without or with  $10^{-8}$  M  $17\beta$ -oestradiol (+E) (A) or with indicated concentrations of Bp2 (B). Luciferase assay was conducted after 24 hours of exposure. Results were calculated as average luciferase activity per 10,000 cells. Values are the average  $\pm$ SE of 3 independent wells. \*\*  $p$ -value  $\leq 0.01$ , \*\*\*  $p$ -value  $\leq 0.001$  and \*\*\*\*  $p$ -value  $\leq 0.0001$  versus no addition by t-Test (A) or by one-way ANOVA Dunnett's test (B).

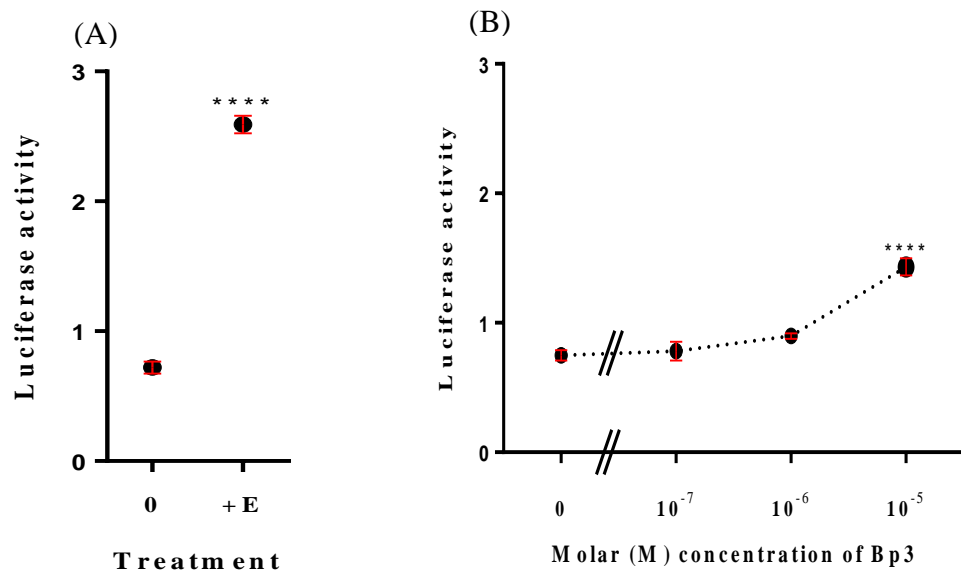


**Figure 3.5 Regulation of a stably transfected oestrogen-inducible ERE-LUC reporter gene in MCF-7 human breast cancer cells following exposure to increasing doses of Bp3.**

MCF-7 cells were plated at  $0.2 \times 10^5$  cells/well in 24 well plates and grown in phenol-red-free-DMEM containing 5% DCFCS for 6 days prior to the experiment. Media were replenished on day 1 and day 4. On day 7 media was replenished with fresh media without or with  $10^{-8}$  M  $17\beta$ -oestradiol (+E) (A) or with indicated concentrations of Bp3 (B). Luciferase assay was conducted after 24 hours of exposure. Results were calculated as average luciferase activity per 10,000 cells. Values are the average  $\pm$ SE of 3 independent wells. \*\*\*\*  $p$ -value  $\leq 0.0001$  versus no addition by t-Test (A) or by one-way ANOVA Dunnett's test (B).

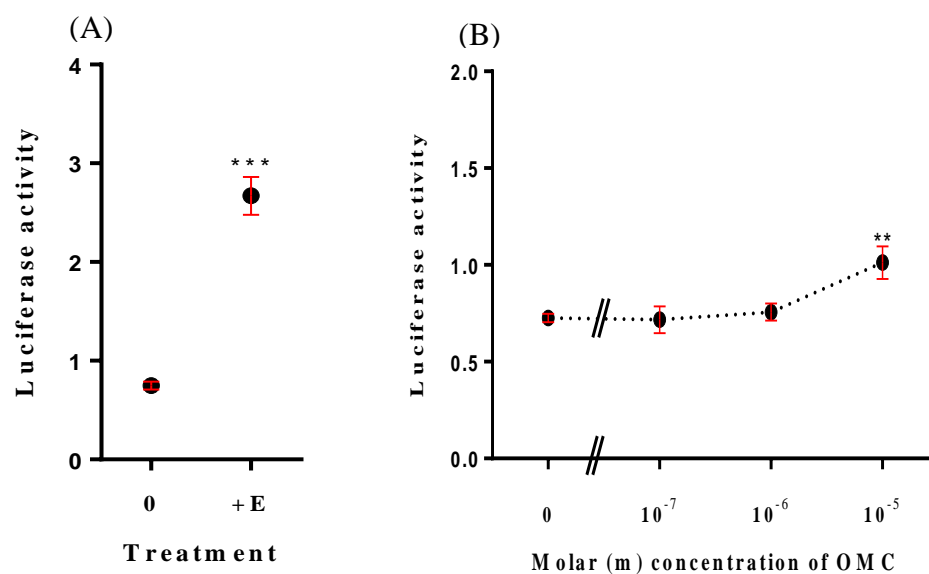


**Figure 3.6 Regulation of a stably transfected oestrogen-inducible ERE-LUC reporter gene in MCF-7 human breast cancer cells following exposure to increasing doses of OMC.**

MCF-7 cells were plated at  $0.2 \times 10^5$  cells/well in 24 well plates and grown in phenol-red-free-DMEM containing 5% DCFCS for 6 days prior to the experiment. Media were replenished on day 1 and day 4. On day 7 media was replenished with fresh media without or with  $10^{-8}$  M  $17\beta$ -oestradiol (+E) (A) or with indicated concentrations of OMC (B). Luciferase assay was conducted after 24 hours of exposure. Results were calculated as average luciferase activity per 10,000 cells. Values are the average  $\pm$ SE of 3 independent wells. \*\* *p-value*  $\leq 0.01$  and \*\*\* *p-value*  $\leq 0.001$  versus no addition by t-Test (A) or by one-way ANOVA Dunnett's test (B).

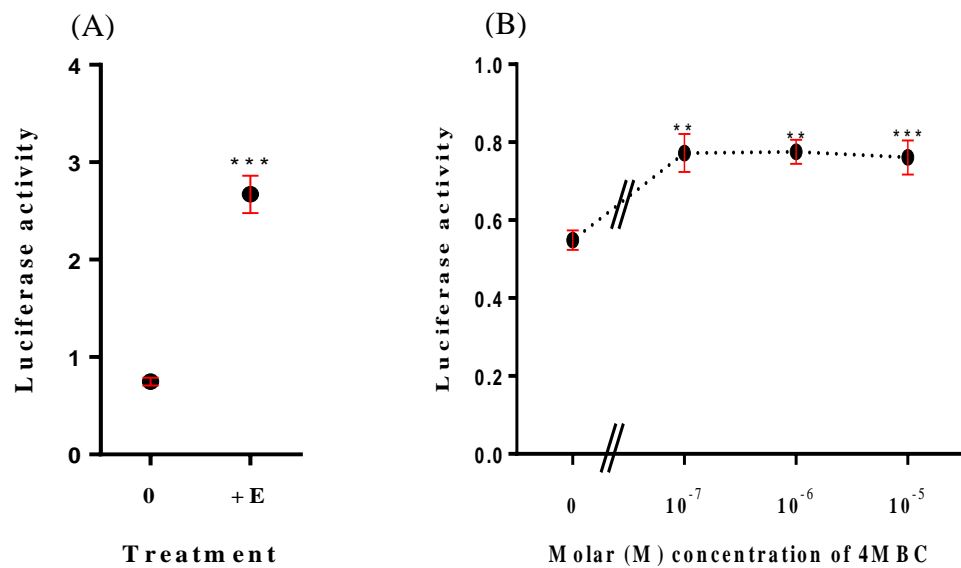


**Figure 3.7 Regulation of a stably transfected oestrogen-inducible ERE-LUC reporter gene in MCF-7 human breast cancer cells following exposure to increasing doses of 4MBC.**

MCF-7 cells were plated at  $0.2 \times 10^5$  cells/well in 24 well plates and grown in phenol-red-free-DMEM containing 5% DCFCS for 6 days prior to the experiment. Media were replenished on day 1 and day 4. On day 7 media was replenished with fresh media without or with  $10^{-8}$  M  $17\beta$ -oestradiol (+E) (A) or with indicated concentrations of 4MBC (B). Luciferase assay was conducted after 24 hours of exposure. Results were calculated as average luciferase activity per 10,000 cells. Values are the average  $\pm$ SE of 3 independent wells. \*\* *p*-value  $\leq 0.01$  and \*\*\* *p*-value  $\leq 0.001$  versus no addition by t-Test (A) or by one-way ANOVA Dunnett's test (B).

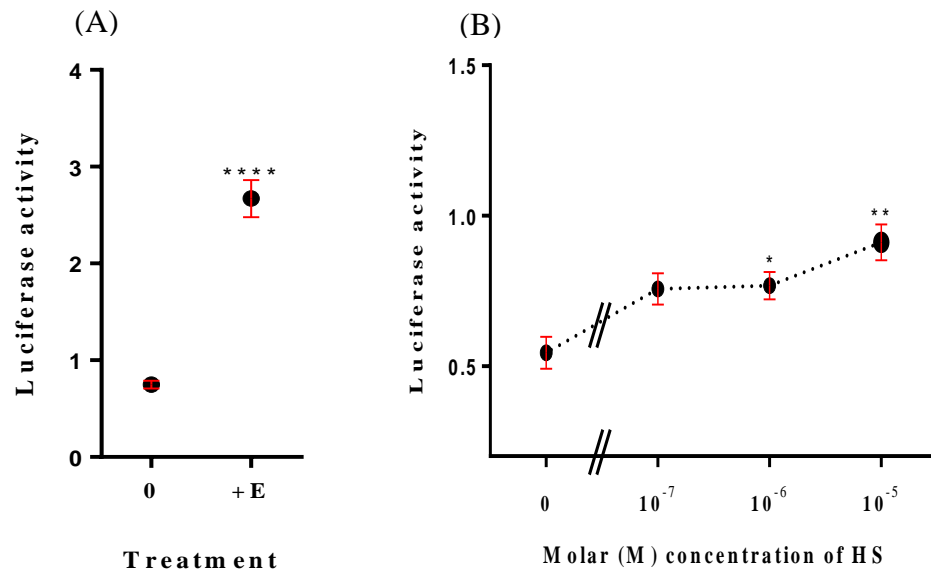


**Figure 3.8 Regulation of a stably transfected oestrogen-inducible ERE-LUC reporter gene in MCF-7 human breast cancer cells following exposure to increasing doses of HS.**

MCF-7 cells were plated at  $0.2 \times 10^5$  cells/well in 24 well plates and grown in phenol-red-free-DMEM containing 5% DCFCS for 6 days prior to the experiment. Media were replenished on day 1 and day 4. On day 7 media was replenished with fresh media without or with  $10^{-8}$  M  $17\beta$ -oestradiol (+E) (A) or with indicated concentrations of HS (B). Luciferase assay was conducted after 24 hours of exposure. Results were calculated as average luciferase activity per 10,000 cells. Values are the average  $\pm$ SE of 3 independent wells. \*  $p$ -value  $\leq 0.05$ , \*\*  $p$ -value  $\leq 0.01$  and \*\*\*\*  $p$ -value  $\leq 0.0001$  versus no addition by t-Test (A) or by one-way ANOVA Dunnett's test (B).

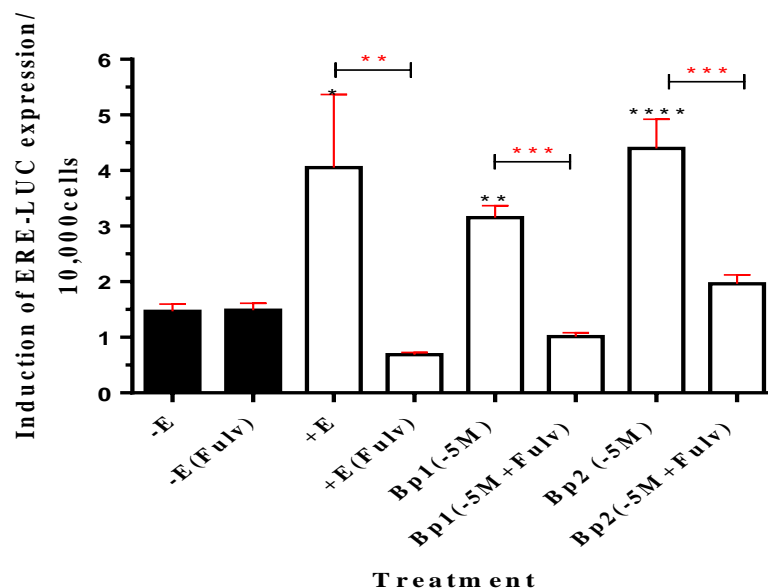


**Figure 3.9 Effect of fulvestrant on induction of ERE-LUC reporter gene by exposure to Bp1, Bp2, 17 $\beta$ -oestradiol or ethanol control.**

MCF-7 cells were plated at  $0.2 \times 10^5$  cells/well in 24 well plates and grown in phenol-red-free-DMEM containing 5% DCFCS for 6 days prior to the experiment. Media were replenished on day 1 and day 4. On day 7 media was replenished with fresh media plus  $10^{-5}$  M Bp1 (Bp1(-5M)),  $10^{-5}$  M Bp1 and  $10^{-7}$  M fulvestrant (Bp1(-5M+Fulv)),  $10^{-5}$  M Bp2 (Bp2(-5M)),  $10^{-5}$  M Bp2 and  $10^{-7}$  M fulvestrant (Bp2(-5M+Fulv)),  $10^{-10}$  M 17 $\beta$ -oestradiol (+E),  $10^{-10}$  M 17 $\beta$ -oestradiol and  $10^{-7}$  M fulvestrant (+E(Fulv)), ethanol control (-E) or ethanol control and  $10^{-7}$  M fulvestrant (-E(Fulv)). Luciferase assay was conducted after 24 hours of exposure. Results were calculated as the average luciferase activity per 10,000 cells. Values are the average  $\pm$ SE of three independent wells. \* *p*-value  $\leq$  0.05, \*\* *p*-value  $\leq$  0.01, \*\*\* *p*-value  $\leq$  0.001 and \*\*\*\* *p*-value  $\leq$  0.0001 versus no addition (-E) (black asterisks) or to compare the effect of fulvestrant on the treatment (red asterisk) by one-way ANOVA Tukey's test.

### **3.3.2 Effects of exposure to UV screens on ER $\alpha$ protein levels**

Levels of ER $\alpha$  protein were measured using western immunoblotting (as described in section 2.7). MCF-7 cells were grown in phenol-red-free-DMEM containing 5% DCFCS with  $10^{-8}$  M  $17\beta$ -oestradiol,  $10^{-5}$  M of UV screens,  $10^{-7}$  M of UV screens or ethanol control for 7 days and three biological replicate cell lysates were prepared. Calculated averages of replicates normalized to total protein showed that relative levels of ER $\alpha$  protein were reduced by  $0.62 \pm 0.05$  following 1 week of exposure to  $10^{-8}$  M  $17\beta$ -oestradiol (Figure 3.10). Levels of ER $\alpha$  protein were also reduced by  $10^{-7}$  M Bp1,  $10^{-5}$  M Bp2,  $10^{-7}$  M Bp2 (Figure 3.10),  $10^{-5}$  M 4MBC and  $10^{-5}$  M HS (Figure 3.11).

### **3.3.3 Effects of exposure to UV screens on TFF1 mRNA levels**

Effects of short and long-term exposure to UV screens were investigated on levels of TFF1 mRNA by RT-PCR (as described in 2.6). MCF-7 cells were grown in phenol-red-free-DMEM containing 5% DCFCS with  $10^{-8}$  M  $17\beta$ -oestradiol,  $10^{-5}$  M of UV screens, or ethanol control for 7 days and 24-25 weeks and three biological replicate cell lysates were prepared for each treatment. Using real time RT-PCR, increased levels of TFF1 mRNA were observed after the 1 week and 24-25 weeks of exposure to  $10^{-8}$  M  $17\beta$ -oestradiol ( $p$ -value  $\leq 0.01$ ) and ( $p$ -value  $\leq 0.0001$ ) respectively (Figure 3.12). Although an increased level of TFF1 mRNA was observed following one week of exposure to  $10^{-5}$  M Bp1 ( $5.26 \pm 2.43$ ) and  $10^{-5}$  M Bp2 ( $4.34 \pm 1.98$ ), statistics showed no significant difference compared to the control. In addition, no significant effect on TFF1 mRNA level was recorded following the exposure to  $10^{-5}$  M of the other UV screens after one week of exposure (Figure 3.12 (A)). However, increased levels of TFF1 mRNA were observed after 24-25 weeks of exposure to  $10^{-5}$  M 4MBC ( $p$ -value  $\leq 0.05$ ) and  $10^{-5}$  M HS ( $p$ -value  $\leq 0.01$ ) (Figure 3.12 (B)).

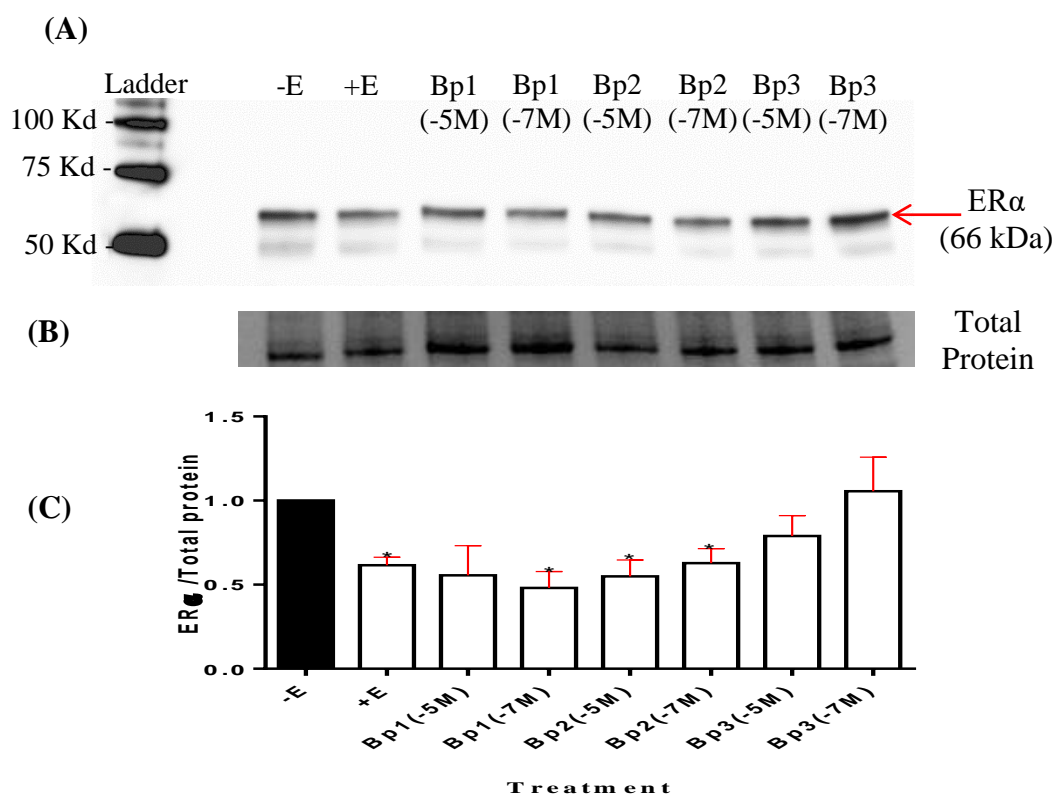


**Figure 3.10 Effect of 1 week of exposure to oestradiol or benzophenones on the expression level of oestrogen receptor  $\alpha$ .**

MCF-7 human breast cancer cells were grown for the 1 week in phenol-red-free DMEM with 5% DCFCS, without (-E) or with  $10^{-8}$  M  $17\beta$ -oestradiol (+E),  $10^{-5}$  M Bp1 (Bp1 (-5M)),  $10^{-7}$  M Bp1 (Bp1 (-7M)),  $10^{-5}$  M Bp2 (Bp2 (-5M)),  $10^{-7}$  M Bp2 (Bp2 (-7M)),  $10^{-5}$  M Bp3 (Bp3 (-5M)) or  $10^{-7}$  M Bp3 (Bp3(-7M)). Media were replenished on day 1 and day 4. Total cellular protein was loaded at  $25\mu\text{g}$  per track and immunoblotted with an antibody against ER $\alpha$  (A). The same membrane was imaged prior to the immunoblotting using BioRad stain-free technology on the Gel Doc EZ imager to obtain the total protein as a control for loading (B). The bar diagram shows levels of ER $\alpha$  relative to total protein (C) and expressed as a fold change from control (-E). Error bars are the SE $\pm$  of three independent experiments (n=3). \* *p*-value  $\leq 0.05$  versus no addition by t-Test.

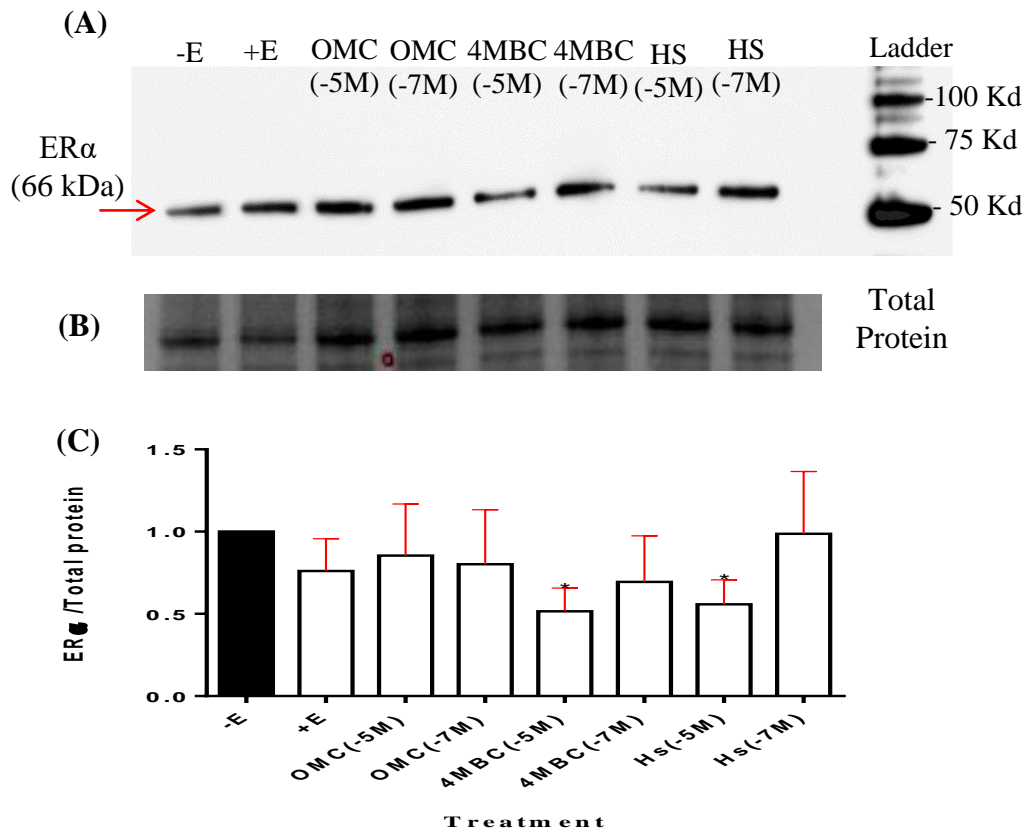


**Figure 3.11 Effect of 1 week of exposure to oestradiol, OMC, 4MBC or homosalate on the expression level of oestrogen receptor  $\alpha$ .**

MCF-7 human breast cancer cells were grown for 1 week in phenol-red-free DMEM with 5% DCFCS, without (-E) or with  $10^{-8}$  M  $17\beta$ -oestradiol (+E),  $10^{-5}$  M OMC (OMC (-5M)),  $10^{-7}$  M OMC (OMC (-7M)),  $10^{-5}$  M 4MBC (4MBC (-5M)),  $10^{-7}$  M 4MBC (4MBC (-7M)),  $10^{-5}$  M homosalate (HS (-5M)) or  $10^{-7}$  M homosalate (HS (-7M)). Media were replenished on day 1 and day 4. Total cellular protein was loaded at 25 $\mu$ g per track and immunoblotted with an antibody against ER $\alpha$  (A). The same membrane was imaged prior to the immunoblotting using BioRad stain-free technology on the Gel Doc EZ imager to obtain the total protein as a control for loading (B). The bar diagram shows levels of ER $\alpha$  relative to total protein (C) and expressed as a fold change from control (-E). Error bars are the SE $\pm$  of three independent experiments (n=3). \* *p*-value  $\leq 0.05$  versus no addition by t-Test.

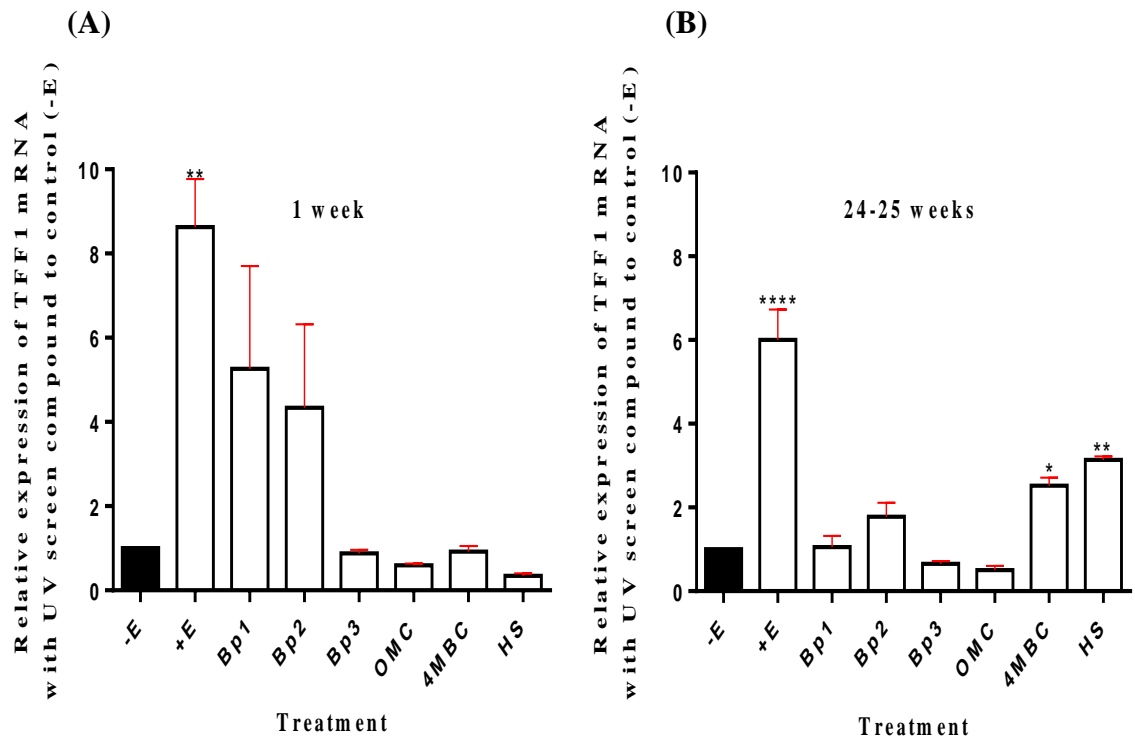


**Figure 3.12 Effect of UV screens on the relative levels of TFF1 mRNA in MCF-7 cells after 7 days and 24 weeks of exposure.**

MCF-7 cells were plated at  $0.2 \times 10^5$  cells/well in 24 well plates and grown in phenol-red-free-DMEM containing 5% DCFCS with  $10^{-8}$  M 17 $\beta$ -oestradiol (+E),  $10^{-5}$  M Bp1 (Bp1),  $10^{-5}$  M Bp2 (Bp2),  $10^{-5}$  M Bp3 (Bp3),  $10^{-5}$  M OMC (OMC),  $10^{-5}$  M 4MBC (4MBC) or homosalate (HS) for 7 days (media were replenished on day 1 and day 4.) (A) Or 24-25 weeks (media was replenished every 3-4 days) (B) prior to RNA isolation. For each RT-PCR assay, TFF1 values were normalised to  $\beta$ -actin values, expressed as fold change from control cells grown without the UV screens by  $2^{-\Delta\Delta C_T}$  method and the average SE of three independent experiments (n=3) taken from cells grown for 1 week or 24-25 weeks of culture. Fold change for cell grown with 17 $\beta$ -oestradiol or UV screens are shown in the bar graph compared to the negative control. \* *p*-value  $\leq 0.05$  and \*\* *p*-value  $\leq 0.01$  and \*\*\*\* *p*-value  $\leq 0.0001$  versus no addition (-E) by t-Test.

### 3.3.4 Effects of UV screens on proliferation of MCF-7 human breast cancer cells

17 $\beta$ -oestradiol induces the proliferation of MCF-7 human breast cancer cells in a dose response manner. Doses of 10<sup>-12</sup> M 17 $\beta$ -oestradiol and above simulated the proliferation of MCF-7 cells with maximum simulation between 10<sup>-10</sup> M and 10<sup>-6</sup> M after 14 days (Figure 3.13). In this section, the effect of UV screens (materials and methods Table 2.1) on the proliferation of MCF-7 human breast cancer cells was investigated after 14 days of exposure.

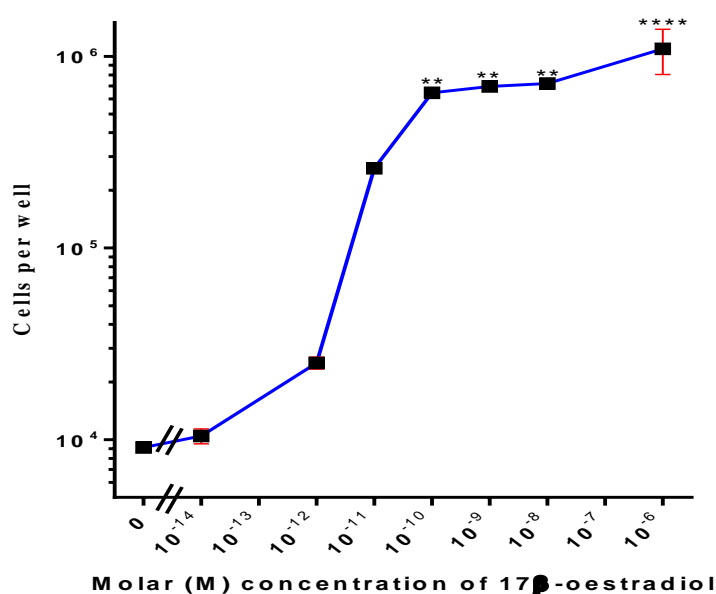


**Figure 3.13 Effect of 17 $\beta$ -oestradiol on proliferation of MCF-7 human breast cancer cells in monolayer culture.**

Cells were grown for 14 days in phenol-red-free-DMEM containing 5% DCFCS with ethanol control only (0) or with indicated molar concentrations of 17 $\beta$ -oestradiol. Media were replenished every 3-4 days. Values are the average  $\pm$ SE of triplicate independent wells. \*\* *p*-value  $\leq$  0.01 and \*\*\*\* *p*-value  $\leq$  0.0001 versus no addition by one-way ANOVA Dunnett's test.

#### **3.3.4.1 Effects of UV screens on MCF-7 human breast cancer cell proliferation in a monolayer culture on an uncoated surface**

MCF-7 human breast cancer cells were grown in phenol-red-free-DMEM containing 5% DCFCS with  $10^{-8}$  M  $17\beta$ -oestradiol or with increasing concentrations of UV screens (from  $10^{-8}$  M to  $10^{-5}$  M for 7 days and the cell count measured by counting cell nuclei on a ZBI Coulter counter (as described in 2.2.1.1). Cell growth experiments showed that among the tested UV screens,  $10^{-5}$  M Bp1 and  $10^{-5}$  M Bp2 had the highest stimulation effect on the proliferation of MCF-7 cells and the proliferation was stimulated significantly by  $10^{-6}$  M Bp1 (Figure 3.14) and  $10^{-6}$  M Bp2 (Figure 3.15). Concentrations of  $10^{-8}$  M to  $10^{-5}$  M Bp3 and OMC did not stimulate the proliferation of MCF-7 cells (Figures 3.16 and 3.17). Proliferation of MCF-7 cells was stimulated by 4MBC at  $10^{-7}$  M and the maximal effect was found at  $10^{-6}$  M (Figure 3.18). A similar pattern in proliferation was found on MCF-7 cells after exposure to HS and maximal effect was observed at  $10^{-5}$  M (Figure 3.19).

#### **3.3.4.2 Effects of fulvestrant on proliferation of MCF-7 human breast cancer cells after exposure to $17\beta$ -oestradiol or UV screens**

In order to verify that  $10^{-5}$  M Bp1 and  $10^{-5}$  M Bp2 were inducing MCF-7 cell proliferation via interaction with oestrogen receptors,  $10^{-7}$  M fulvestrant was used. Fulvestrant (ICI 182,780) (AstraZeneca, Macclesfield, UK) is an oestrogen receptor antagonist, which reduces oestrogen action through the ER (Wakeling et al., 1991).

MCF-7 cells were grown in phenol-red-free-DMEM containing 5% DCFCS with no addition or with  $10^{-8}$  M  $17\beta$ -oestradiol,  $10^{-5}$  M Bp1,  $10^{-5}$  M Bp2 with or without  $10^{-7}$  M fulvestrant for 7 days. The addition of  $10^{-7}$  M fulvestrant to  $10^{-5}$  M Bp1 or  $10^{-5}$  M Bp2 reduced the stimulation of MCF-7 cell proliferation caused by both chemicals without the addition of fulvestrant and the cell numbers were close to the negative control (Figure 3.20).

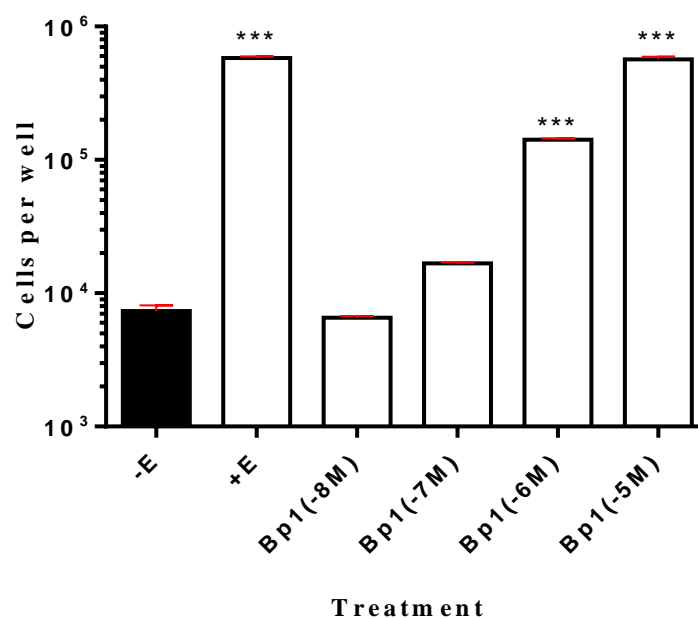


**Figure 3.14 Effect of Bp1 on proliferation of MCF-7 human breast cancer cells in monolayer culture.**

Cells were grown in phenol-red-free-DMEM containing 5% DCFCS with ethanol control only (-E),  $10^{-8}$  M  $17\beta$ -oestradiol (+E), with  $10^{-8}$  M Bp1 (Bp1 (-8M)),  $10^{-7}$  M Bp1 (Bp1 (-7M)),  $10^{-6}$  M Bp1 (Bp1 (-6M)) or  $10^{-5}$  M Bp1 (Bp1 (-5M)) for 14 days. Media were replenished every 3-4 days. Values are the average  $\pm$ SE of triplicate independent wells. Where no bars are seen, error was too small to be visualized. \*\*\*  $p$ -value  $\leq$  0.001 versus no addition by one-way ANOVA Dunnett's test. Three replicate experiments showed similar results (n=3).

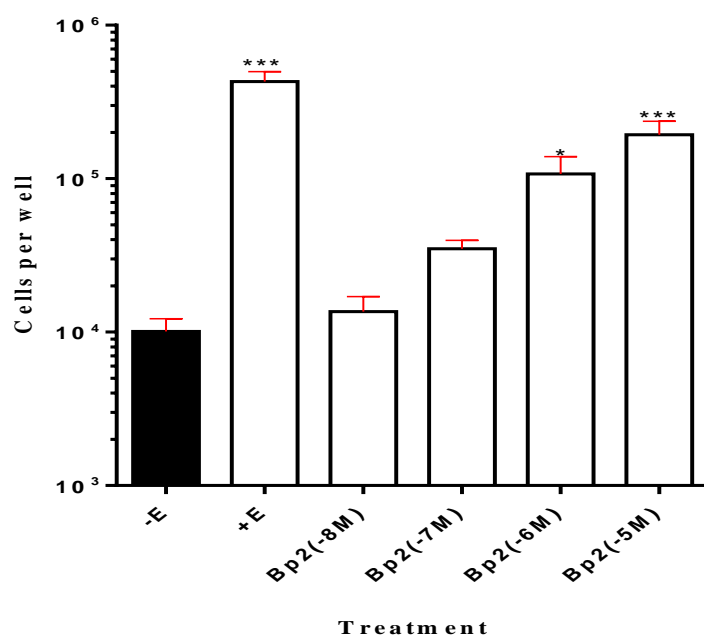


**Figure 3.15 Effect of Bp2 on proliferation of MCF-7 human breast cancer cells in monolayer culture.**

Cells were grown in phenol-red-free-DMEM containing 5% DCFCS with ethanol control only (-E),  $10^{-8}$  M  $17\beta$ -oestradiol (+E), with  $10^{-8}$  M Bp2 (Bp2 (-8M)),  $10^{-7}$  M Bp2 (Bp2 (-7M)),  $10^{-6}$  M Bp2 (Bp2 (-6M)) or  $10^{-5}$  M Bp2 (Bp2 (-5M)) for 14 days. Media were replenished every 3-4 days. Values are the average  $\pm$ SE of triplicate independent wells. Where no bars are seen, error was too small to be visualized. \* *p*-value  $\leq 0.05$  and \*\*\* *p*-value  $\leq 0.001$  versus no addition by one-way ANOVA Dunnett's test. Three replicate experiments showed similar results (n=3).

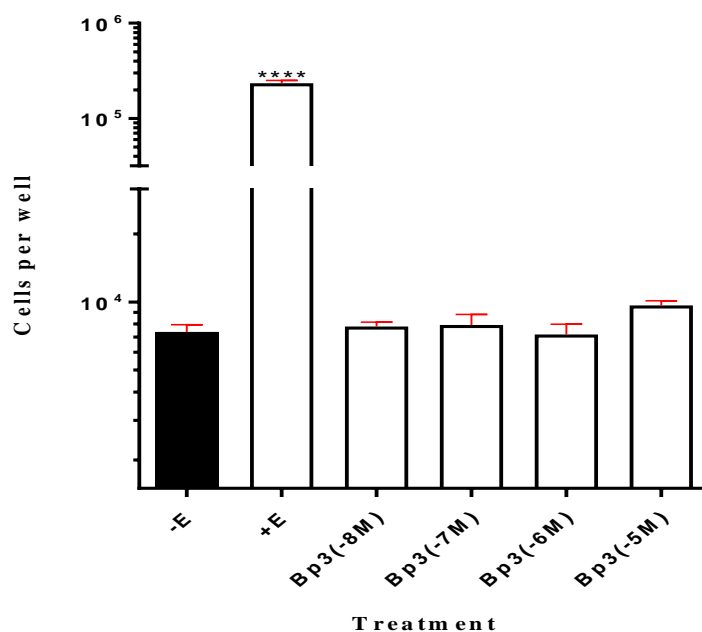


**Figure 3.16 Effect of Bp3 on proliferation of MCF-7 human breast cancer cells in monolayer culture.**

Cells were grown in phenol-red-free-DMEM containing 5% DCFCS with ethanol control only (-E),  $10^{-8}$  M  $17\beta$ -oestradiol (+E), with  $10^{-8}$  M Bp3 (Bp3 (-8M)),  $10^{-7}$  M Bp3 (Bp3 (-7M)),  $10^{-6}$  M Bp3 (Bp3 (-6M)) or  $10^{-5}$  M Bp3 (Bp3 (-5M)) for 14 days. Media were replenished every 3-4 days. Values are the average  $\pm$ SE of triplicate wells. Where no bars are seen, error was too small to be visualized. \*\*\*\*  $p$ -value  $\leq 0.0001$  versus no addition by one-way ANOVA Dunnett's test. Three replicate experiments showed similar results (n=3).

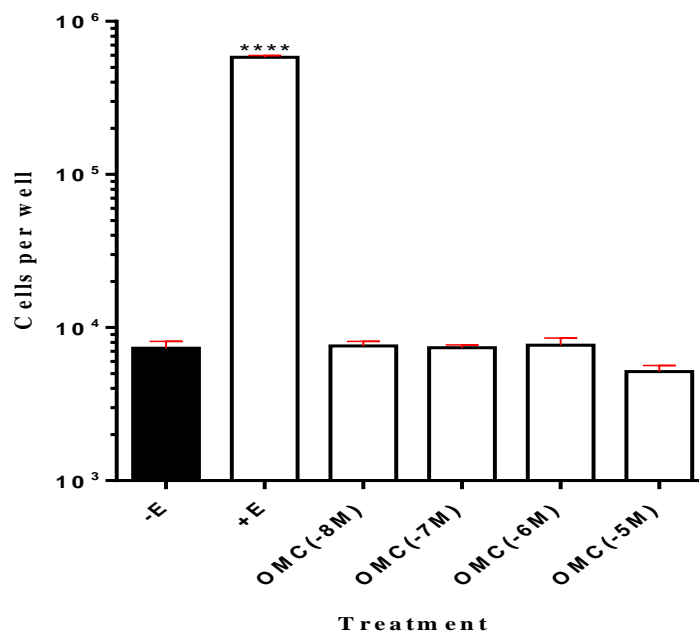


**Figure 3.17 Effect of OMC on proliferation of MCF-7 human breast cancer cells in monolayer culture.**

Cells were grown in phenol-red-free-DMEM containing 5% DCFCS with ethanol control only (-E),  $10^{-8}$  M  $17\beta$ -oestradiol (+E), with  $10^{-8}$  M OMC (OMC (-8M)),  $10^{-7}$  M OMC (OMC (-7M)),  $10^{-6}$  M OMC (OMC (-6M)) or  $10^{-5}$  M OMC (OMC (-5M)) for 14 days. Media were replenished every 3-4 days. Values are the average  $\pm$ SE of triplicate wells. Where no bars are seen, error was too small to be visualized. \*\*\*\*  $p$ -value  $\leq 0.0001$  versus no addition by one-way ANOVA Dunnett's test. Three replicate experiments showed similar results (n=3).

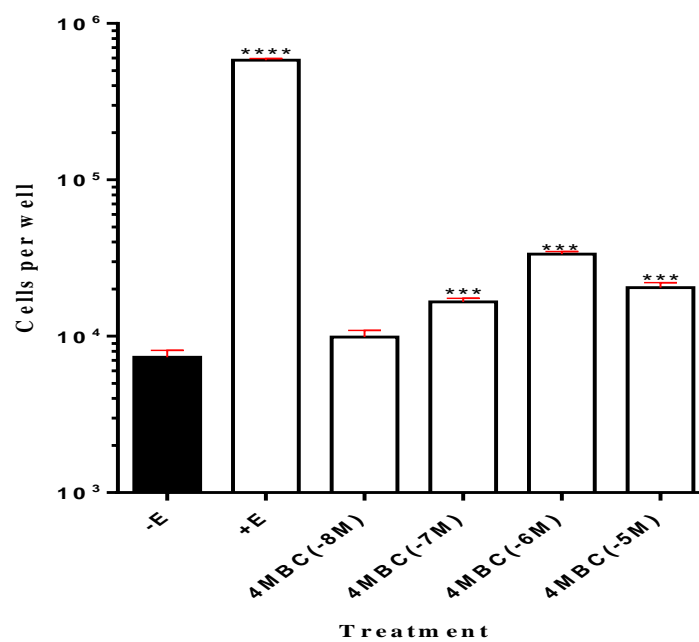


**Figure 3.18 Effect of 4MBC on proliferation of MCF-7 human breast cancer cells in monolayer culture.**

Cells were grown in phenol-red-free-DMEM containing 5% DCFCS with ethanol control only (-E),  $10^{-8}$  M  $17\beta$ -oestradiol (+E), with  $10^{-8}$  M 4MBC (4MBC (-8M)),  $10^{-7}$  M 4MBC (4MBC (-7M)),  $10^{-6}$  M 4MBC (4MBC (-6M)) or  $10^{-5}$  M 4MBC (4MBC (-5M)) for 14 days. Media were replenished every 3-4 days. Values are the average  $\pm$ SE of triplicate wells. Where no bars are seen, error was too small to be visualized. \*\*\*  $p$ -value  $\leq 0.001$  and \*\*\*\*  $p$ -value  $\leq 0.0001$  versus no addition by one-way ANOVA Dunnett's test. Three replicate experiments showed similar results (n=3).

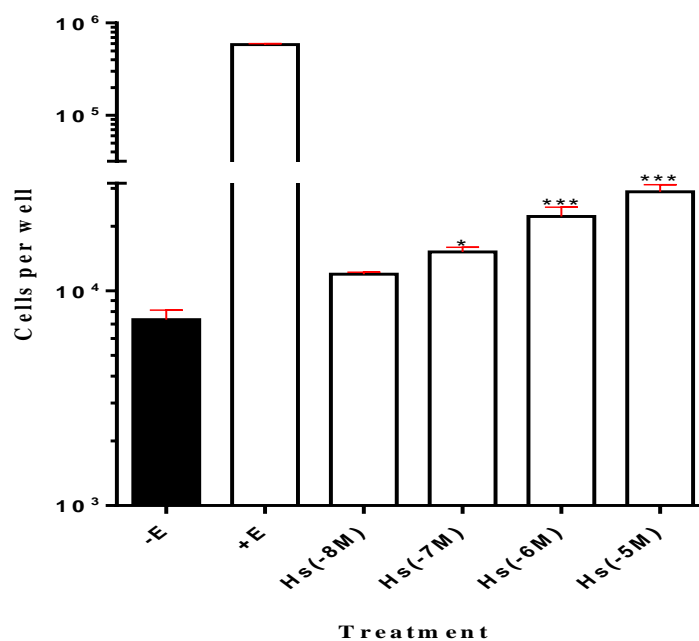


**Figure 3.19 Effect of HS on proliferation of MCF-7 human breast cancer cells in monolayer culture.**

Cells were grown in phenol-red-free-DMEM containing 5% DCFCS with ethanol control only (-E),  $10^{-8}$  M  $17\beta$ -oestradiol (+E), with  $10^{-8}$  M homosalate (HS (-8M)),  $10^{-7}$  M homosalate (HS (-7M)),  $10^{-6}$  M homosalate (HS (-6M)) or  $10^{-5}$  M homosalate (HS (-5M)) for 14 days. Media were replenished every 3-4 days. Values are the average  $\pm$ SE of triplicate wells. Where no bars are seen, error was too small to be visualized. \*  $p$ -value  $\leq 0.05$  and \*\*\*  $p$ -value  $\leq 0.001$  versus no addition by one-way ANOVA Dunnett's test. Three replicate experiments showed similar results (n=3).

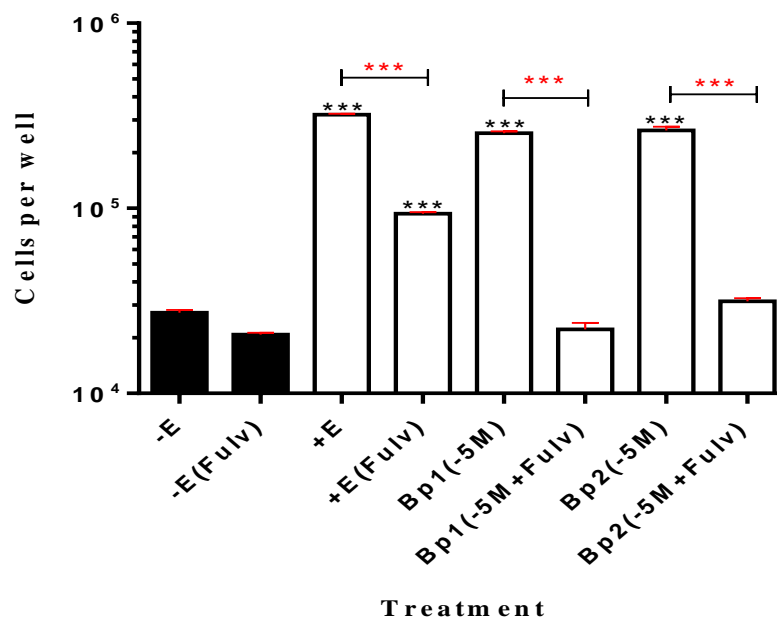


**Figure 3.20 Effect of fulvestrant on the proliferation of MCF-7 human breast cancer cells proliferation following exposure to Bp1, Bp2, 17 $\beta$ -oestradiol or ethanol control.**

MCF-7 cells were plated at  $0.2 \times 10^5$  cells/well in 24 well plates and grown in phenol-red-free-DMEM containing 5% DCFCS for 7 days with  $10^{-5}$  M Bp1 (Bp1 (-5M)),  $10^{-5}$  M Bp1 and  $10^{-7}$  M fulvestrant (Bp1 (-5M+Fulv)),  $10^{-5}$  M Bp2 (Bp2 (-5M)),  $10^{-5}$  M Bp2 and  $10^{-7}$  M fulvestrant (Bp2 (-5M+Fulv)),  $10^{-8}$  M 17 $\beta$ -oestradiol (+E),  $10^{-8}$  M 17 $\beta$ -oestradiol and  $10^{-7}$  M fulvestrant (+E (Fulv)), ethanol control (-E) or ethanol control and  $10^{-7}$  M fulvestrant (-E (Fulv)). Media were replenished on day 1 and day 4. Values are the average  $\pm$ SE of triplicates independent wells. Where no bars are seen, error was too small to be visualized. \*\*\*  $p$ -value  $\leq 0.001$  versus no addition (-E) (black asterisks) or to compare the effect of fulvestrant on the treatment (red asterisks) by one-way ANOVA Tukey's test.

### **3.3.4.3 Effects of UV screens on MCF-7 human breast cancer cell proliferation in the presence of 17 $\beta$ -oestradiol**

Oestrogens are physiologically present in premenopausal female in a range of  $10^{-11}$  M to  $10^{-10}$  M (Wright et al., 1999). Thus, the effect of UV screens on proliferation of MCF-7 cells in the presence of different concentrations of 17 $\beta$ -oestradiol was investigated. MCF-7 cells were grown in phenol-red-free-DMEM containing 5% DCFCS with different concentrations of 17 $\beta$ -oestradiol alone or mixed with  $10^{-5}$  M of UV screens for 7 days. Increase in MCF-7 cells proliferation with  $10^{-5}$  M Bp1 and  $10^{-5}$  M Bp2 was not affected by the presence of different concentrations of 17 $\beta$ -oestradiol (Figure 21 (A and B)).

Among the other tested UV screens  $10^{-5}$  M Bp3 and  $10^{-5}$  M 4MBC have a small yet significant antagonist effect on cells exposed to higher doses of 17 $\beta$ -oestradiol ( $10^{-11}$  M and  $10^{-10}$  M) (Figure 21 (C and D)). In contrast,  $10^{-5}$  M OMC and  $10^{-5}$  M HS seemed to have no effect on the proliferation of MCF-7 cells in a mixture with different concentrations of 17 $\beta$ -oestradiol (data not shown).

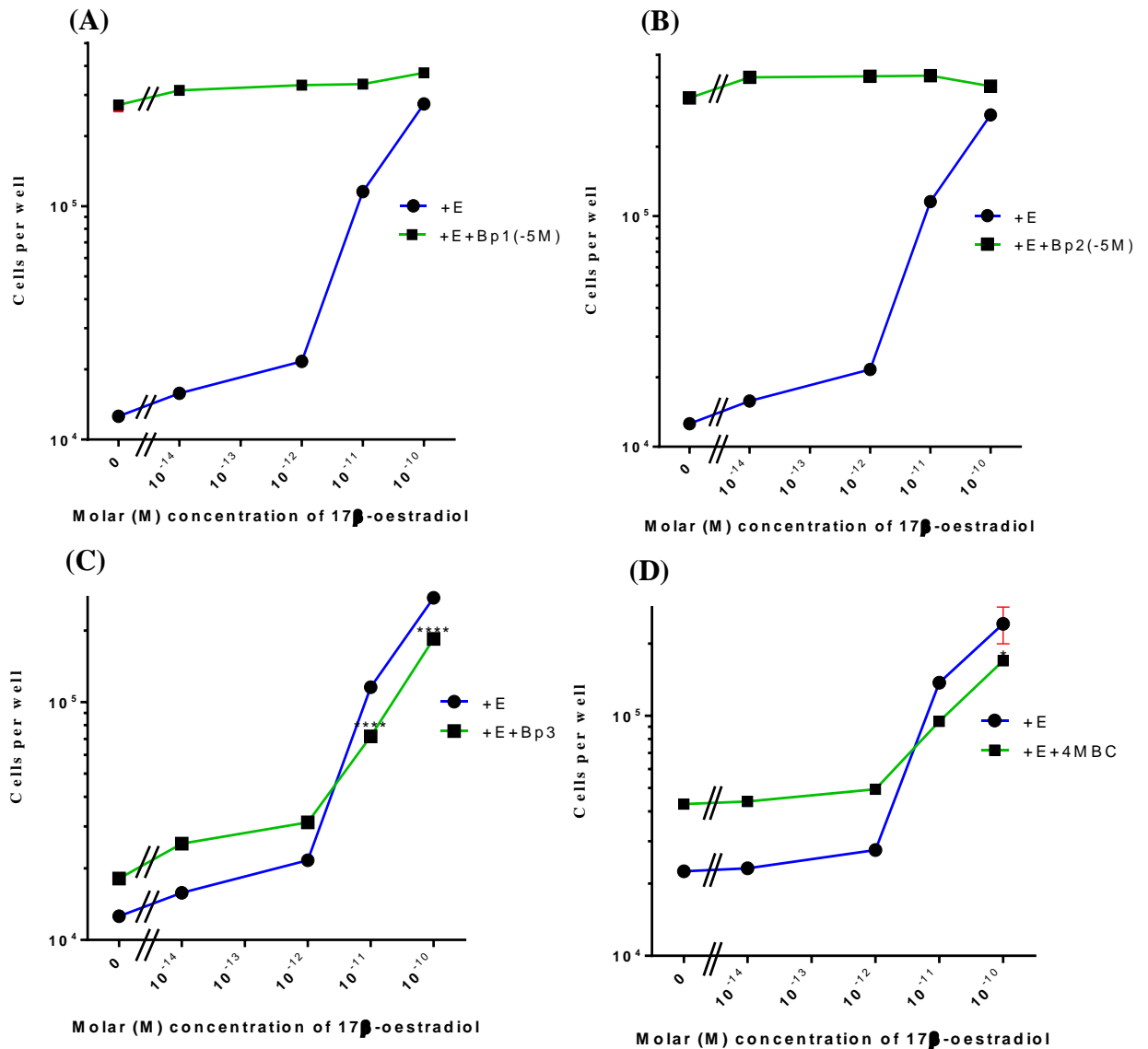


**Figure 3.21 Effect of Bp1, Bp2, Bp3 or 4MBC on the proliferation of MCF-7 human breast cancer cells in the presence and absence of 17β-oestradiol in monolayer culture.**

Cells were grown in phenol-red-free-DMEM containing 5% DCFCS with 17β-oestradiol only (control, blue curves) at the indicated concentrations or with 10<sup>-5</sup> M Bp1 (A, green curve), 10<sup>-5</sup> M Bp2 (B, green curve), 10<sup>-5</sup> M Bp3 (C, green curve) or 10<sup>-5</sup> M 4MBC (D, green curve) for 7 days. Media were replenished on day 1 and day 4. Values are the average ±SE of triplicate independent wells. Where no bars are seen, error was too small to be visualized. \* *p*-value ≤ 0.05 and \*\*\*\* *p*-value ≤ 0.0001 versus relative 17β-oestradiol concentration by one-way ANOVA Tukey's test.

### **3.3.4.4 Effect of UV screens on the proliferation of MCF-7 human breast cancer cells on laminin or fibronectin coated plates**

MCF-7 cells were grown in phenol-red-free-DMEM containing 5% DCFCS on uncoated plates or plates coated with 6.5  $\mu\text{g}/\text{cm}^2$  fibronectin or 6.5  $\mu\text{g}/\text{cm}^2$  laminin (as described in 2.2.1.2.) in the presence of  $10^{-8}\text{M}$   $17\beta$ -oestradiol or increasing concentrations of UV screens (from  $10^{-8}\text{M}$  to  $10^{-5}\text{M}$ ) for 7 days. Initially, the effect of different coating materials was investigated on adhesion, proliferation and morphology of MCF-7 cells.

No significant difference was recorded in the number of cells adhered to fibronectin compared to the number of cells adhered to plastic after 24 hours of seeding as indicated by counting the adhered cells using a ZBI Coulter counter (Figure 3.22 (A)). Nor was any change observed on MCF-7 cell monolayer islands morphology when seeded on fibronectin (Figure 3.22 (C and D)). By contrast, MCF-7 cells showed significantly lower adhesion on laminin ( $p$ -value  $\leq 0.0001$ ) in comparison with adhesion on plastic or fibronectin, and exhibited colony formation (Figure 3.22 (A and E)). After 7 days of incubating MCF-7 cells on 6.5  $\mu\text{g}/\text{cm}^2$  fibronectin or 6.5  $\mu\text{g}/\text{cm}^2$  laminin, cells were counted to estimate the proliferation using the ZBI Coulter counter. Both fibronectin and laminin significantly increased the proliferation of MCF-7 cells ( $p$ -value  $\leq 0.01$ ) in comparison with cells seeded on plastic (Figure 3.22 (B)).

The effect of coating with fibronectin or laminin on the proliferative response of MCF-7 cells to  $10^{-8}\text{M}$   $17\beta$ -oestradiol was then studied.  $10^{-8}\text{M}$   $17\beta$ -oestradiol significantly increased MCF-7 cell proliferation on all surfaces. However, the presence of 6.5  $\mu\text{g}/\text{cm}^2$  fibronectin caused a significantly greater increase in MCF-7 cell proliferation in comparison with plastic. On the other hand, coating with 6.5  $\mu\text{g}/\text{cm}^2$  laminin significantly reduced the proliferative response of MCF-7 cells compared to both plastic and fibronectin coating ( $p$ -value  $\leq 0.0001$ ) (Figure 3.23).

A similar pattern was observed following cell exposure to  $10^{-5}\text{M}$  Bp1 (Figure 3.24). Likewise, laminin coating reduced the proliferative effect of  $10^{-5}\text{M}$  Bp2 on MCF-7 cells but no significant increase was recorded in the presence of fibronectin coating with this chemical (Figure 3.25).

Interestingly,  $10^{-5}$  M OMC significantly increased the proliferation of MCF-7 cells on  $6.5 \mu\text{g}/\text{cm}^2$  laminin coated 24 well plates (Figure 3.26). Moreover, laminin and fibronectin both significantly increased the proliferation of MCF-7 cells following one week of exposure to  $10^{-5}$  4MBC (Figure 3.27). However, no effect of different coating materials were recorded on the proliferation of MCF-7 cells following one week exposure to lower concentrations of Bp1, Bp2, OMC, 4MBC, Bp3 (Figure 3.28) or HS (Figure 3.39).

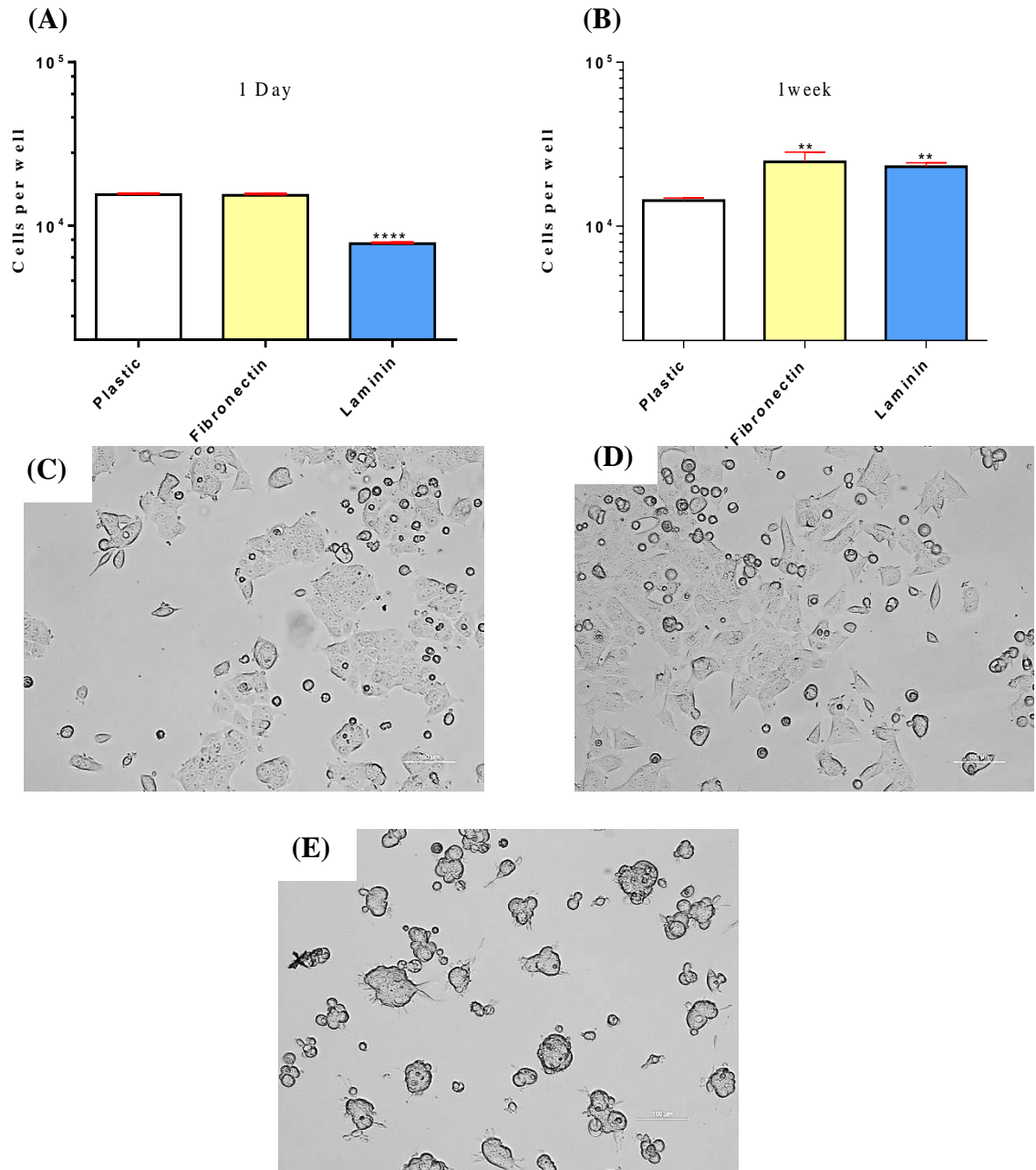


**Figure 3.22 Effect of different coated surfaces on adhesion (A), proliferation (B) and morphology (C-E) of MCF-7 human breast cancer cells.**

MCF-7 cells were plated at  $0.2 \times 10^5$  cells/well in 24 well plates. The wells were either uncoated (plastic), coated with  $6.5 \mu\text{g}$  fibronectin or coated with  $6.5 \mu\text{g}$  laminin. Cells were grown in phenol-red-free-DMEM containing 5% DCFCS for 24 hours or 1 week. Bar-graph represents the cell count per well as measured by a ZBI Coulter counter after 24 hours of incubation (A) or after 1 week of incubation (media replenished on day 1 and day 4) (B). Values are the average  $\pm$ SE of three independent wells. Where no bars are seen, error was too small to be visualized. \*\*  $p$ -value  $\leq 0.01$  and \*\*\*\*  $p$ -value  $\leq 0.0001$  versus plastic by one-way ANOVA Dunnett's test. Images are representative phase contrast microscopy images of the appearance of MCF-7 cells grown for 24 hours on plastic (C), fibronectin (D) or laminin (E).

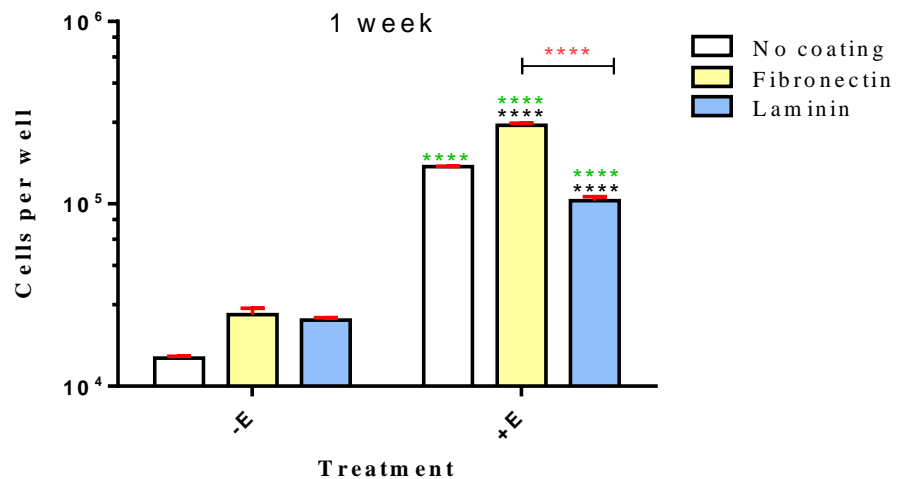


**Figure 3.23 Effect of different coated surfaces on MCF-7 human breast cancer cell proliferation after treatment with 17β-oestradiol.**

MCF-7 cells were plated at  $0.2 \times 10^5$  cells/well in 24 well plates. The wells were either uncoated (plastic), coated with  $6.5 \mu\text{g}$  fibronectin or coated with  $6.5 \mu\text{g}$  laminin. Cells were grown in phenol-red-free-DMEM containing 5% DCFCS for 7 days with  $10^{-8}$  M 17β-oestradiol (+E) or with ethanol vehicle (-E). Media were replenished on day 1 and day 4. Bar-graph represents the cell count per well as measured by the Coulter counter. Values are the average  $\pm$ SE of three independent experiments. Where no bars are seen, error was too small to be visualized. \*\*\*\*  $p$ -value  $\leq 0.0001$  versus plastic (black asterisks), compared between different coating material for the same treatment (red asterisks) or compared to no addition (-E) with relative coating material (green asterisks) by two-way ANOVA Bonferroni test.

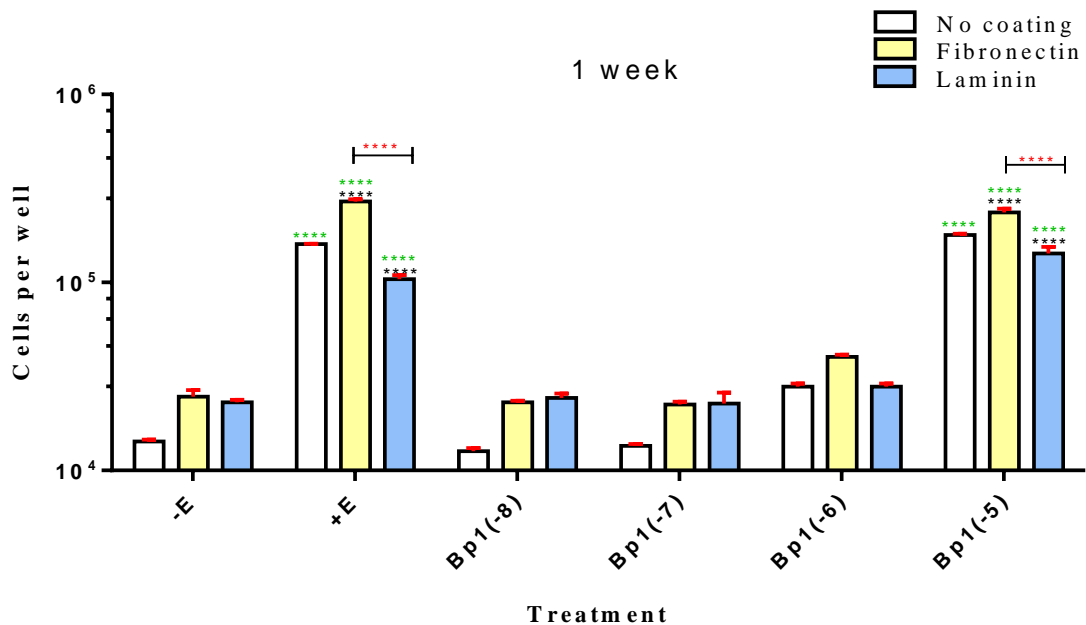


**Figure 3.24 Effect of Bp1 on proliferation of MCF-7 human breast cancer cells on different coated surfaces.**

Cells were grown in phenol-red-free-DMEM containing 5% DCFCS with ethanol control only (-E),  $10^{-8}$  M  $17\beta$ -oestradiol (+E), with  $10^{-8}$  M Bp1 (Bp1 (-8M)),  $10^{-7}$  M Bp1 (Bp1 (-7M)),  $10^{-6}$  M Bp1 (Bp1 (-6M)) or  $10^{-5}$  M Bp1 (Bp1 (-5M)) for 7 days. Media were replenished on day 1 and day 4. Prior to the experiment, the wells were either uncoated (plastic), coated with 6.5  $\mu$ g fibronectin or coated with 6.5  $\mu$ g laminin. Values are the average  $\pm$ SE of triplicate independent wells. Where no bars are seen, error was too small to be visualized. \*\*\*\*  $p$ -value  $\leq 0.0001$  compared to plastic (black asterisks), compared between different coating material for the same treatment (red asterisks) or compared to no addition (-E) with relative coating material (green asterisks) by two-way ANOVA Bonferroni test.

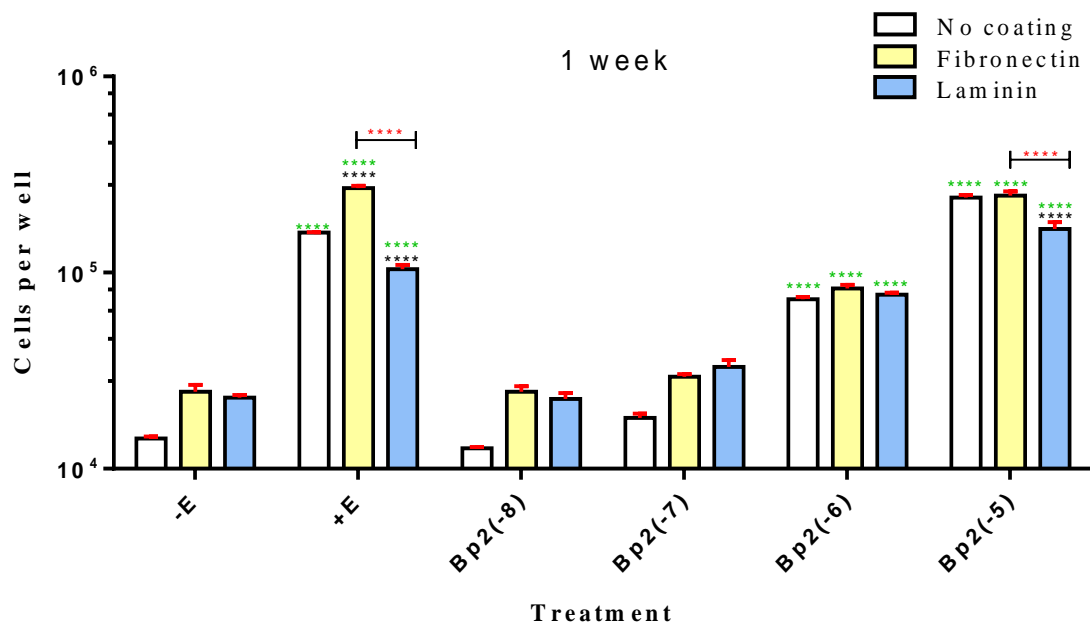


**Figure 3.25 Effect of Bp2 on proliferation of MCF-7 human breast cancer cells on different coated surfaces.**

Cells were grown in phenol-red-free-DMEM containing 5% DCFCS with ethanol control only (-E),  $10^{-8}$  M  $17\beta$ -oestradiol (+E), with  $10^{-8}$  M Bp2 (Bp2 (-8M)),  $10^{-7}$  M Bp2 (Bp2 (-7M)),  $10^{-6}$  M Bp2 (Bp2 (-6M)) or  $10^{-5}$  M Bp2 (Bp2 (-5M)) for 7 days. Media were replenished on day 1 and day 4. Prior to the experiment, the wells were either uncoated (plastic), coated with 6.5  $\mu$ g fibronectin or coated with 6.5  $\mu$ g laminin. Values are the average  $\pm$ SE of triplicate independent wells. Where no bars are seen, error was too small to be visualized. \*\*\*\*  $p$ -value  $\leq 0.0001$  compared to plastic (black asterisks), compared between different coating material for the same treatment (red asterisks) or compared to no addition (-E) with relative coating material (green asterisks) by two-way ANOVA Bonferroni test.

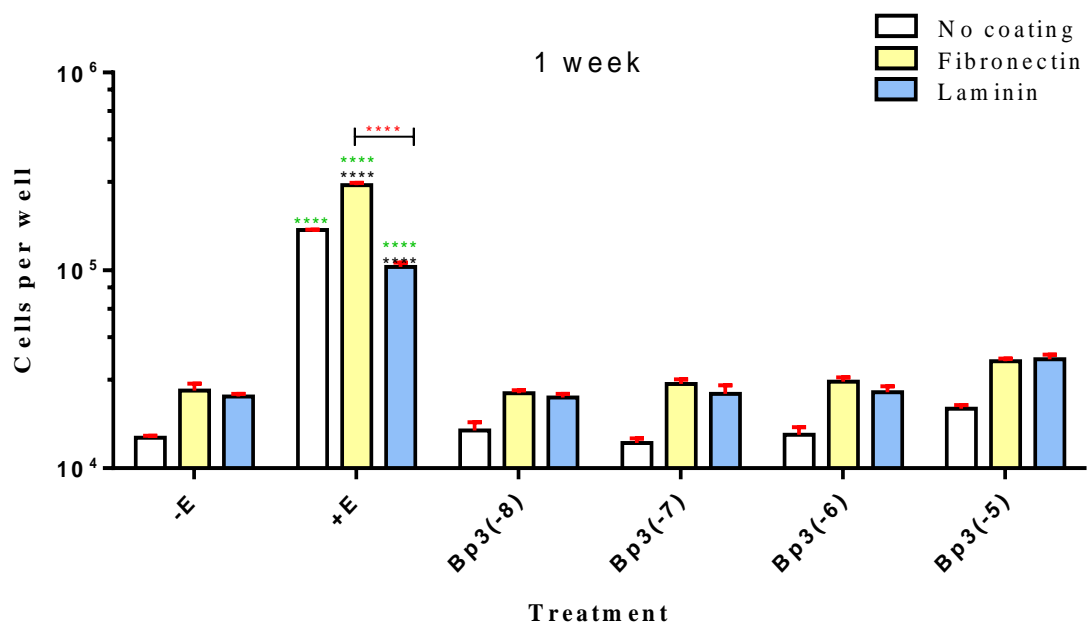


**Figure 3.26 Effect of Bp3 on proliferation of MCF-7 human breast cancer cells on different coated surfaces.**

Cells were grown in phenol-red-free-DMEM containing 5% DCFCS with ethanol control only (-E),  $10^{-8}$  M  $17\beta$ -oestradiol (+E), with  $10^{-8}$  M Bp3 (Bp3 (-8M)),  $10^{-7}$  M Bp3 (Bp3 (-7M)),  $10^{-6}$  M Bp3 (Bp3 (-6M)) or  $10^{-5}$  M Bp3 (Bp3 (-5M)) for 7 days. Media were replenished on day 1 and day 4. Prior to the experiment, the wells were either uncoated (plastic), coated with 6.5  $\mu$ g fibronectin or coated with 6.5  $\mu$ g laminin. Values are the average  $\pm$ SE of triplicate independent wells. Where no bars are seen, error was too small to be visualized. \* *p*-value  $\leq$  0.05, \*\* *p*-value  $\leq$  0.01, \*\*\* *p*-value  $\leq$  0.001 and \*\*\*\* *p*-value  $\leq$  0.0001 compared to plastic (black asterisks), compared between different coating material for the same treatment (red asterisks) or compared to no addition (-E) with relative coating material (green asterisks) by two-way ANOVA Bonferroni test.

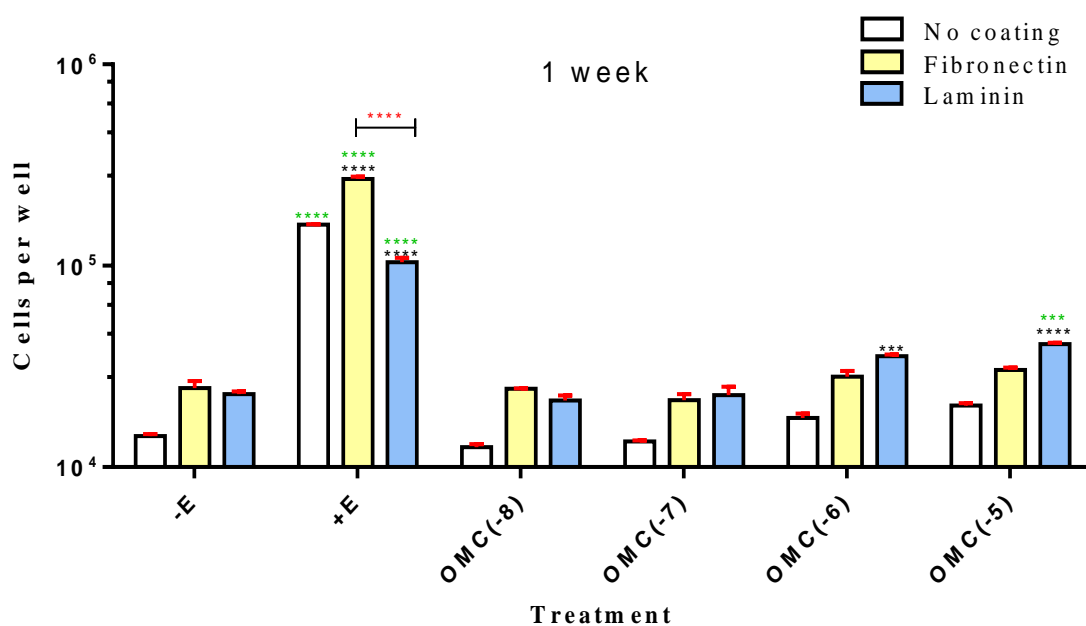


**Figure 3.27 Effect of OMC on proliferation of MCF-7 human breast cancer cells on different coated surfaces.**

Cells were grown in phenol-red-free-DMEM containing 5% DCFCS with ethanol control only (-E),  $10^{-8}$  M  $17\beta$ -oestradiol (+E), with  $10^{-8}$  M OMC (OMC (-8M)),  $10^{-7}$  M OMC (OMC (-7M)),  $10^{-6}$  M OMC (OMC (-6M)) or  $10^{-5}$  M OMC (OMC (-5M)) for 7 days. Media were replenished on day 1 and day 4. Prior to the experiment, the wells were either uncoated (plastic), coated with  $6.5 \mu\text{g}$  fibronectin or coated with  $6.5 \mu\text{g}$  laminin. Values are the average  $\pm$ SE of triplicate independent wells. Where no bars are seen, error was too small to be visualized. \*\*\*  $p$ -value  $\leq 0.001$  and \*\*\*\*  $p$ -value  $\leq 0.0001$  compared to plastic (black asterisks), compared between different coating material for the same treatment (red asterisks) or compared to no addition (-E) with relative coating material (green asterisks) by two-way ANOVA Bonferroni test.

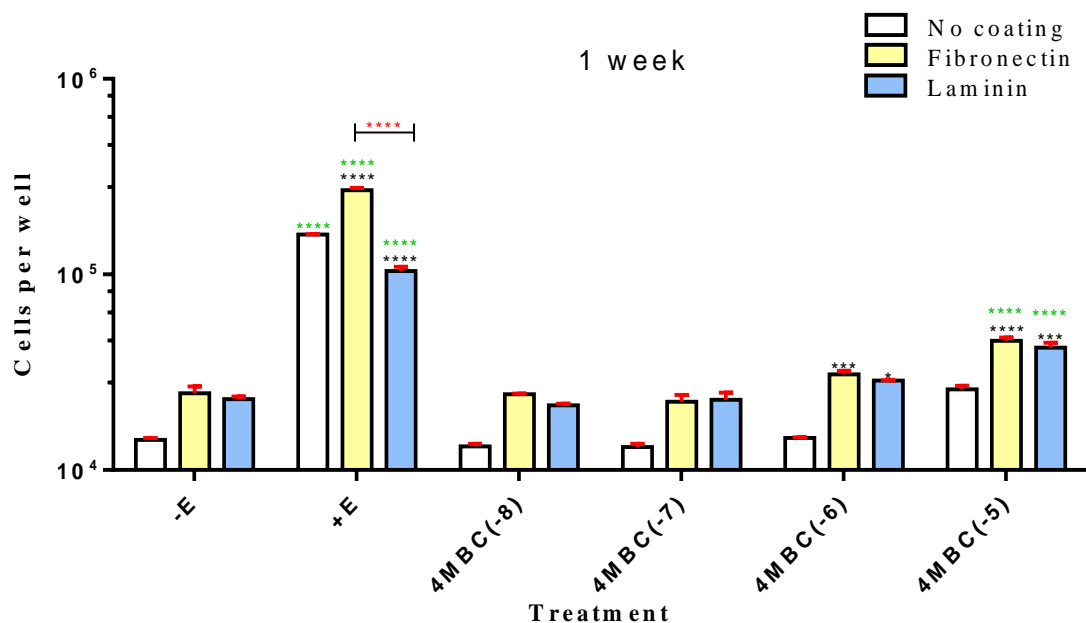


**Figure 3.28 Effect of 4MBC on proliferation of MCF-7 human breast cancer cells on different coated surfaces.**

Cells were grown in phenol-red-free-DMEM containing 5% DCFCs with ethanol control only (-E),  $10^{-8}$  M  $17\beta$ -oestradiol (+E), with  $10^{-8}$  M 4MBC (4MBC (-8M)),  $10^{-7}$  M OMC (4MBC (-7M)),  $10^{-6}$  M 4MBC (4MBC (-6M)) or  $10^{-5}$  M 4MBC (4MBC (-5M)) for 7 days. Media were replenished on day 1 and day 4. Prior to the experiment, the wells were either uncoated (plastic), coated with  $6.5 \mu\text{g}$  fibronectin or coated with  $6.5 \mu\text{g}$  laminin. Values are the average  $\pm$ SE of triplicate independent wells. Where no bars are seen, error was too small to be visualized. \* *p-value*  $\leq 0.05$ , \*\*\* *p-value*  $\leq 0.001$  and \*\*\*\* *p-value*  $\leq 0.0001$  compared to plastic (black asterisks), compared between different coating influence on the same treatment (red asterisks) or compared to no addition (-E) with relative coating material (green asterisks) by two-way ANOVA Bonferroni test.

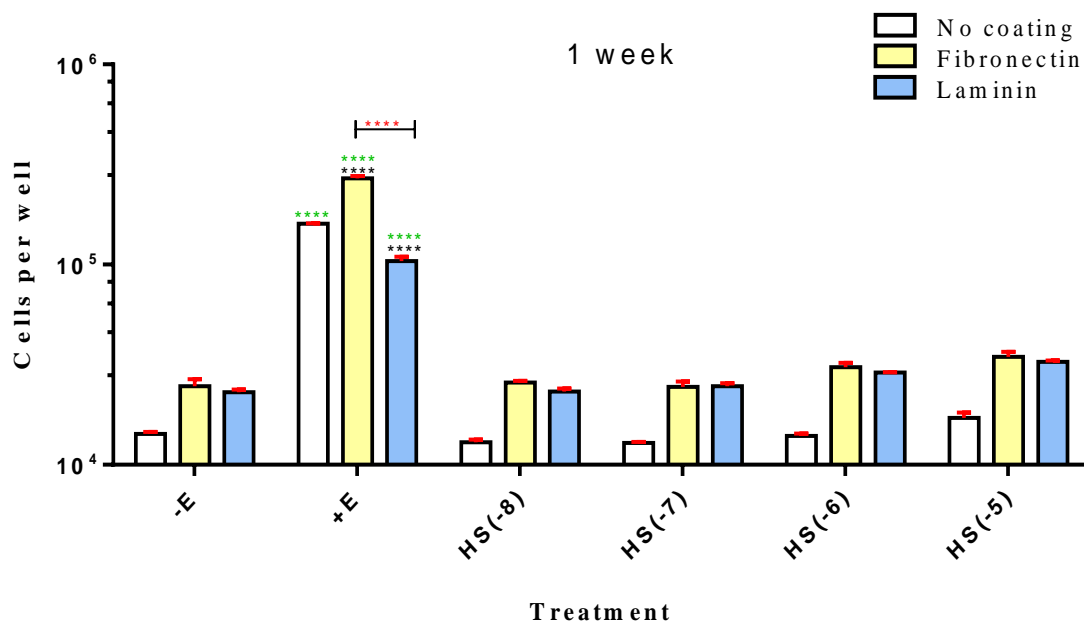


**Figure 3.29 Effect of HS on proliferation of MCF-7 human breast cancer cells on different coated surfaces.**

Cells were grown in phenol-red-free-DMEM containing 5% DCFCS with ethanol control only (-E),  $10^{-8}$  M  $17\beta$ -oestradiol (+E), with  $10^{-8}$  M HS (HS (-8M)),  $10^{-7}$  M HS (HS (-7M)),  $10^{-6}$  M HS (HS (-6M)) or  $10^{-5}$  M HS (HS (-5M)) for 7 days. Media were replenished on day 1 and day 4. Prior to the experiment, the wells were either uncoated (plastic), coated with 6.5  $\mu$ g fibronectin or coated with 6.5  $\mu$ g laminin. Values are the average  $\pm$ SE of triplicate independent wells. Where no bars are seen, error was too small to be visualized. \* *p*-value  $\leq 0.05$ , \*\*\* *p*-value  $\leq 0.001$  and \*\*\*\* *p*-value  $\leq 0.0001$  compared to plastic (black asterisks), compared between different coating influence on the same treatment (red asterisks) or compared to no addition (-E) with relative coating material (green asterisks) by two-way ANOVA Bonferroni test.

### 3.3.5 Comparisons between the effects of different UV screens on MCF-7 human breast cancer cells

Comparisons between the effects on MCF-7 human breast cancer cells produced by the exposure to the UV screens or 17 $\beta$ -oestradiol using the different end points are summarized in Tables 3.1 and 3.2.

To enable the statistical comparison between the different UV screens and their effects on ERE luciferase activity or MCF-7 proliferation, a summary figure was produced (Figure 3.30). In comparison with the six UV screens, the highest ERE-Luciferase activity was caused by the exposure to 10<sup>-5</sup> M Bp2. 10<sup>-5</sup> M Bp2 increased the luciferase activity to a greater extent than 10<sup>-5</sup> M Bp1 (*p-value*  $\leq$  0.0001), greater than 10<sup>-5</sup> M Bp3 (*p-value*  $\leq$  0.0001), greater than 10<sup>-5</sup> M OMC, 4MBC and HS (*p-value*  $\leq$  0.0001) (Figure 3.30 (A)). No significant difference was found by comparing the effects of 10<sup>-5</sup> M Bp1 and 10<sup>-5</sup> M Bp3 or 10<sup>-5</sup> M Bp3 and 10<sup>-5</sup> M OMC. In addition, differences of luciferase activity of 10<sup>-5</sup> M OMC, 10<sup>-5</sup> M 4MBC and 10<sup>-5</sup> M HS was not found statistically significant. However, the ERE-luciferase activity increased by 10<sup>-5</sup> M Bp3 was found greater than 10<sup>-5</sup> M 4MBC (*p-value*  $\leq$  0.01) and 10<sup>-5</sup> M HS (*p-value*  $\leq$  0.05).

The proliferation experiments revealed that 10<sup>-5</sup> M Bp1 caused the highest proliferation among the 6 UV screens. It increased MCF-7 cell proliferation to a greater extent than 10<sup>-5</sup> M Bp2 (*p-value*  $\leq$  0.05), 10<sup>-5</sup> M Bp3, 10<sup>-5</sup> M OMC, 10<sup>-5</sup> M 4MBC and 10<sup>-5</sup> M HS (*p-value*  $\leq$  0.0001). Bp2 was found to increase the proliferation of MCF-7 cells statistically significant in comparisons with 10<sup>-5</sup> M Bp3, 10<sup>-5</sup> M OMC and 10<sup>-5</sup> M 4MBC (*p-values*  $\leq$  0.05) but not HS. No statistical significant difference was recorded in comparing the effects of 10<sup>-5</sup> M Bp1, 10<sup>-5</sup> M Bp2 and 10<sup>-8</sup> M 17 $\beta$ -oestradiol on MCF-7 cells proliferation (Figure 3.30 (B)).

**Table 3.1 Summary table of the oestrogenic action of  $10^{-5}$ M UV screens on MCF-7 human breast cancer cells in comparison to  $10^{-8}$ M  $17\beta$ -oestradiol.**

Treatments	The evaluation tools used to determine the oestrogenic activity			
	ERE-LUC reporter assay	TFF1 gene expression	ER $\alpha$ protein levels	Proliferation experiments on plastic
<b>17<math>\beta</math>-oestradiol</b>	↑ ****	↑ **	↓ *	↑ ***
<b>Bp1</b>	↑ ****	n.s.	↓ *	↑ ***
<b>Bp2</b>	↑ ****	n.s.	↓ *	↑ ***
<b>Bp3</b>	↑ ****	n.s.	n.s.	n.s.
<b>OMC</b>	↑ *	n.s.	n.s.	n.s.
<b>4MBC</b>	↑ **	↑ * After 24-25 weeks of exposure	↓ *	↑ ***
<b>HS</b>	↑ **	↑ ** After 24-25 weeks of exposure	↓ *	↑ ***

Arrows indicate increase (↑) or decrease (↓). \* *p-value* ≤ 0.05, \*\* *p-value* ≤ 0.01, \*\*\* *p-value* ≤ 0.001 and \*\*\*\* *p-value* ≤ 0.0001 versus negative control and (n.s.) indicates no significant effect.

**Table 3.2 Summary table showing the comparative effects of different coating materials on proliferation of  $10^{-5}$ M UV screens on MCF-7 human breast cancer cells in comparison to  $10^{-8}$ M  $17\beta$ -oestradiol.**

Treatments	Proliferation experiments		
	On plastic	Laminin coating	Fibronectin coating
<b>17<math>\beta</math>-oestradiol</b>	↑ *** versus no addition	↓ **** versus growth on plastic	↑ **** versus growth on plastic
<b>Bp1</b>	↑ *** versus no addition	↓ **** versus growth on plastic	↑ **** versus growth on plastic
<b>Bp2</b>	↑ *** versus no addition	↓ **** versus growth on plastic	n.s. versus growth on plastic
<b>Bp3</b>	n.s. versus no addition	n.s. versus growth on plastic	n.s. versus growth on plastic
<b>OMC</b>	n.s. versus no addition	↑ **** versus growth on plastic	n.s. versus growth on plastic
<b>4MBC</b>	↑ *** versus no addition	↑ **** versus growth on plastic	↑ *** versus growth on plastic
<b>HS</b>	↑ *** versus no addition	n.s. versus growth on plastic	n.s. versus growth on plastic

Arrows indicates increase (↑) or decrease (↓). \* *p-value* ≤ 0.05, \*\* *p-value* ≤ 0.01, \*\*\* *p-value* ≤ 0.001 and \*\*\*\* *p-value* ≤ 0.0001 versus negative control (no addition) or versus growth on plastic and (n.s.) indicates no significant effect.

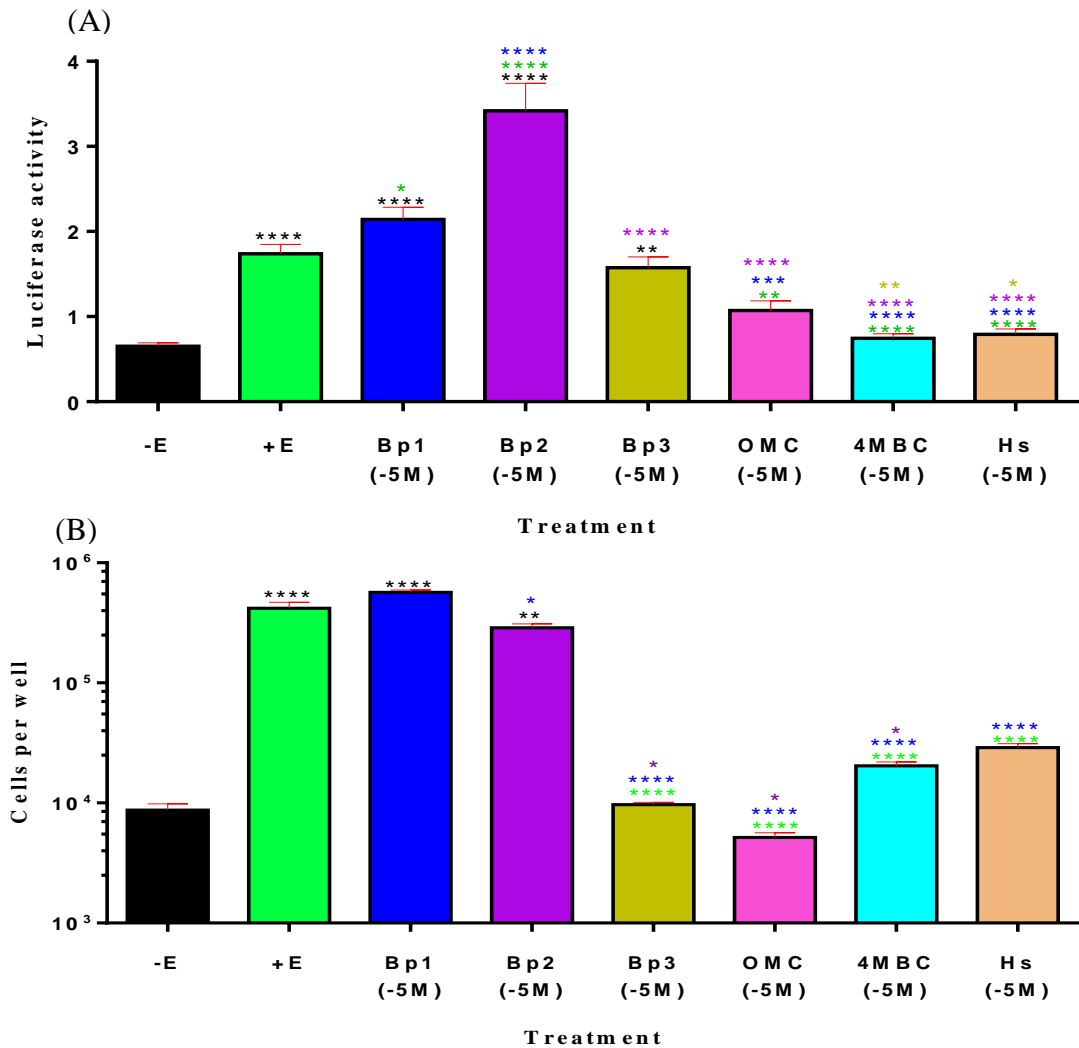


**Figure 3.30** Statistical comparison and summary of the varying effect of the UV screens on oestrogen-inducible ERE-LUC reporter gene in stably transfected MCF-7 human breast cancer cells (A) and proliferation of MCF-7 human breast cancer cells in monolayer culture (B). Stably ERE-LUC transfected MCF-7 cells ( $0.2 \times 10^5$  cells/well) were exposed to  $10^{-8}$  M  $17\beta$ -oestradiol (+E),  $10^{-5}$  M Bp1 (Bp1 (-5M)),  $10^{-5}$  M Bp2 (Bp2 (-5M)),  $10^{-5}$  M Bp3 (Bp3 (-5M)),  $10^{-5}$  M OMC (OMC (-5M)),  $10^{-5}$  M 4MBC (4MBC (-5M)) or  $10^{-5}$  M HS (HS (-5M)) or ethanol control (-E) in phenol-red-free DMEM and 5% DCFS for 24 hours prior to the measurement (A). Monolayers of MCF-7 cells ( $0.2 \times 10^5$  cells/well) were exposed to the same treatments and media for 14 days (B). (A) Values are the average  $\pm$ SE of 3 independent experiments for Bp1 and Bp2 ( $n=3$ ) and 2 independent experiments for Bp3, OMC and HS. (B) Values are the average  $\pm$ SE of 3 independent wells ( $n=3$ ). \*  $p$ -value  $\leq 0.05$ , \*\*  $p$ -value  $\leq 0.01$  and \*\*\*\*  $p$ -value  $\leq 0.0001$  versus no addition (black asterisks),  $17\beta$ -oestradiol (green asterisks), Bp1 (blue asterisks), Bp2 (purple asterisks), Bp3 (lime asterisks) by one-way ANOVA Tukey's test.

### 3.4 Discussion

Overall six UV screens have been found to have effects on gene expression and proliferation of oestrogen responsive MCF-7 human breast cancer cells. The six chemicals were, benzophenone-1(Bp1), benzophenone-2 (Bp2), benzophenone-3(Bp3), octyl-methoxycinnamate (OMC), 4-methylbenzylidene camphor (4MBC) and homosalate (HS). In order to evaluate the oestrogenic potency of these chemicals, 4 methods were conducted; ERE-LUC reporter gene assay, measuring the levels of ER $\alpha$  protein by western immunoblotting, TFF1 gene expression by RT-PCR and effects on cell proliferation. The results are summarized in Table 3.1.

***UV screens increases the ERE-LUC activity.*** The ERE-LUC reporter gene assay results have shown a significant increase in the luciferase activity following the exposure of the stably transfected MCF-7 cells to all of the UV screens albeit to different extents.  $10^{-5}$ M Bp2 induced the highest luciferase activity followed by  $10^{-5}$ M Bp1 and then  $10^{-5}$  M Bp3. Three of the six UV screens ( $10^{-5}$  M OMC,  $10^{-5}$  M 4MBC and  $10^{-5}$  M HS) have shown positive effects compared to the control but their effects on the ERE-LUC activity were statistically lower than the benzophenones. Dose response curves for each of the chemicals has shown that the lowest observed effect concentrations (LOEC) were  $10^{-7}$  M Bp2,  $10^{-6}$  M Bp1,  $10^{-7}$  M 4MBC,  $10^{-6}$  M HS,  $10^{-5}$  M Bp3 and  $10^{-5}$  M OMC. These findings are consistent with three published studies using ER $\alpha$  or ER $\beta$  stably transfected HEK293 kidney cells, the ERE activity following exposure to Bp3, OMC, 4MBC and HS were similar to our findings (Schreurs et al., 2002). Gomez and colleagues showed similar results of oestrogenic activity obtained from ER $\alpha$  transfected HeLa cervical cells following exposure to OMC, 4MBC and HS (Gomez et al., 2005). Induction of ERE-LUC activity in transiently transfected MCF-7 cells following exposure to Bp1 and Bp2 has been reported by Kerdivel and colleagues but they did not find any significant effect of Bp3 (Kerdivel et al., 2013). The Kerdivel group used  $10^{-6}$  M as the highest concentration of Bp3 which is in line with our finding using the same concentration. However, the results here reported a significant effect of  $10^{-5}$  M. The Kerdivel group has also investigated the effects on non-oestrogen responsive promoters and found a significant increase in transactivation activity of stimulating protein 1-luciferase (SP1-LUC) and complement 3-luciferase (C3-LUC) caused by  $10^{-6}$  M Bp1 and  $10^{-7}$  M Bp2, suggesting a possible effects on MCF-7 cells via other pathways besides the ER mediated ones (Kerdivel et al., 2013).

The ERE-luciferase activity induced by Bp1 and Bp2 was decreased using  $10^{-7}$  M fulvestrant in our study and in the Kerdivel work (Kerdivel et al., 2013), which suggests the dependency on ER as a mechanism of action of these chemicals in activating the ERE-reporter gene. In this work,  $10^{-7}$  M fulvestrant have been found to successfully reduce the effects of  $10^{-5}$  M Bp1 and Bp2 in increasing ERE-LUC activity. Further work is to be conducted to confirm if the other UV screens have increased ERE-LUC activity via ER mediated pathway.

Other supporting evidence for the *in vitro* oestrogenic potency of these chemicals on gene expression have been published using ER-ELISA and yeast two-hybrid assay (Morohoshi et al., 2005), recombinant yeast assay carrying human ER (Miller et al., 2001; Kunz and Fent, 2006) and ER binding assay (Schlumpf et al., 2004). Whereas some of the reports report high oestrogenic potency of Bp1 and Bp2, the partial potency of Bp3 has also been described (Miller et al., 2001; Kunz and Fent, 2006). Some reports have shown no oestrogenic potency of OMC, 4MBC (Morohoshi et al., 2005; Kunz and Fent, 2006) and HS (Kunz and Fent, 2006).

***ER $\alpha$  protein levels in MCF-7 cells are reduced following one week exposure to the UV screens.*** Levels of ER $\alpha$  protein are known to be reduced by the addition of oestradiol (Saceda et al., 1988; Borrás et al., 1994). The change of ER $\alpha$  protein level as determined by western blot was carried out therefore to verify the extent of the oestrogenic profile of the UV screens. MCF-7 cells were exposed to  $10^{-7}$  M and  $10^{-5}$  M of the UV screens for 1 week prior to the lysate preparations.  $10^{-7}$  M Bp1,  $10^{-7}$  M Bp2,  $10^{-5}$  M Bp2,  $10^{-5}$  M 4MBC and  $10^{-5}$  M HS all gave a reduction in ER $\alpha$  levels but Bp3 and OMC did not. Kerdivel and his colleagues have not found an effect on ER $\alpha$  levels following exposure to  $10^{-6}$  M Bp1,  $10^{-6}$  M Bp2 and  $10^{-6}$  M Bp3 but it is noteworthy that they also have not recorded a reduced level of ER $\alpha$  after exposure to 17 $\beta$ -oestradiol (Kerdivel et al., 2013). The investigation of the effect of these UV screens on the protein levels of ER $\beta$  was not carried out in this research. This will be interesting future research because others documented the ability of Bp3, HS (Schreurs et al., 2002) and 4MBC (Schlumpf et al., 2004) to interact with ER $\beta$ . However, the endogenous levels of ER $\beta$  in MCF-7 cells are much lower than ER $\alpha$  protein levels (Shaw et al., 2006; Holbeck et al., 2010; AL-Bader et al., 2011; Ford et al., 2011; Nadal-Serrano et al., 2012; Ma and Gollahon, 2016). Thus the effects of the UV screens on ER $\beta$  levels have not been carried out in this work.

***TFF1 mRNA levels are increased after 24 weeks of exposure to 4MBC and HS.*** The induction of TFF1(pS2)-mRNA by  $17\beta$ -oestradiol (Jakowlew et al., 1984) makes it a suitable biomarker for the oestrogenic activity in MCF-7 cells (Jørgensen et al., 2000; Jung et al., 2012). Therefore, it has been used to confirm the oestrogenicity of many endocrine disruptors such as bisphenol A (Olsen et al., 2003), triclosan (Huang et al., 2014) and parabens (Byford et al., 2002). Schlumpf and co-workers have recorded an induction in TFF1 protein secretion following exposure of MCF-7 cells to Bp3, 4MBC and HS but not OMC (Schlumpf et al., 2001). Moreover, Heneweer and co-workers have described the induction of the TFF1 gene in MCF-7 cells after 24 hours of exposure to Bp1, Bp3, OMC and HS (Heneweer et al., 2005). In another recent study, TFF1-mRNA was significantly increased by the exposure to Bp2 and Bp3 but not by Bp1 (Kerdivel et al., 2013). Results in this study were not similar after 1 week of exposure to the same chemicals. The main reason is the variation in the experimental designs, mRNA samples of this work was collected after one week of exposure, without prior hormone deprivation (or in this case UV screen deprivation), while the other groups collected the mRNA samples following 1 day of hormone deprivation and 24 hours (Heneweer et al., 2005) or 48 hours (Kerdivel et al., 2013) of exposure to the UV screens.

After 23-24 weeks of exposure TFF1-mRNA was found to be increased significantly by  $10^{-5}$  M 4MBC and  $10^{-5}$  M HS. In comparison with previous studies, Schlumpf had measured the secreted TFF1 protein after 6 days of exposure and not the mRNA expression while the other two studies measured the TFF1-mRNA after 24 and 48 hours of exposure respectively (Heneweer et al., 2005; Kerdivel et al., 2013). Such differences in the experiments might explain these contradictory findings.

However, lack of the induction of TFF1 gene expression by the six UV screens despite their ability to induce the ERE-luciferase reporter gene expression might be explained by the difference in experimental design. While the ERE-LUC reporter gene assay was conducted using stably transfected MCF-7 cells after 24 hours of exposure, measuring the TFF1-mRNA was carried out by collecting the RNA of MCF-7 cells after 7 days or longer (23-24 weeks) exposure. Although the oestrogenicity results obtained from the ERE-LUC activity after exposure to Bp1, Bp2, Bp3 and OMC have not been confirmed by the induction of the TFF1 gene, the possible effect of these chemicals on other oestrogen responsive genes should now be studied because the activation of ER generates alteration to hundreds of oestrogen target genes (Frasor et al., 2003; Gruber et al., 2004). The variation of the ability of Bp1, Bp2 and

Bp3 to induce the expression of the TFF1 gene and other oestrogen responsive genes was published by Kerdivel and his colleagues and their investigation included PR, CXCL12 and amphiregulin (Kerdivel et al., 2013). Only Bp2 induced the expression of all of these oestrogen responsive genes and the TFF1 gene. In contrast, neither Bp1 nor Bp3 were able to induce the expression of all of the other 3 genes collectively whereas they have both induced the TFF1 gene and only Bp1 induced PR (Kerdivel et al., 2013). It is noteworthy that our positive control (17 $\beta$ -oestradiol) has significantly increased the luciferase activity as well as induced the TFF1-mRNA expression.

***UV screens increase MCF-7 cell proliferation.*** As is well known, the oestrogen responsive proliferation of MCF-7 cells (Berthois et al., 1986) enables the use of this cell line as a tool to estimate the oestrogenic potency of endocrine disruptors (Soto et al., 1995). This application of MCF-7 cells helped in revealing many of the oestrogenic compounds (Soto et al., 1994; Jones et al., 1998; Olsen et al., 2003; Charles and Darbre, 2013). Among the tested UV screens, Bp2 gave the greatest effect on proliferation of MCF-7 cells, with Bp1 a close second and less increase in MCF-7 cell proliferation was achieved by 4MBC and HS. These findings are in agreement with previous studies (Schlumpf et al., 2001; Nakagawa and Suzuki, 2002; Jimenez-Diaz et al., 2013). However, in contrast to Schlumpf's work, our data showed no significant effect following the exposure to Bp3 or OMC. Similar findings of no effect of Bp3 on MCF-7 cell proliferation was published by Kerdivel and his colleagues, who also disagreed with the effect of Bp1 on MCF-7 cell proliferation (Kerdivel et al., 2013). Such differences could be explained by differences in experimental methods and in experimental conditions such as the concentration of DCFCS, the time of exposure, the concentrations of the UV screens and the source of MCF-7 cells (Osborne et al., 1987). Since Bp1 and Bp2 were the most potent compounds on MCF-7 cell growth the addition of the antioestrogen fulvestrant was tested on the compounds and the proliferative response was significantly downregulated by 10<sup>-7</sup> M fulvestrant, which suggests that the proliferation caused by Bp1 and Bp2 was ER mediated. Whether the effect of 4MBC and HS on the proliferation of MCF-7 cells is ER mediated is yet to be confirmed by the same assay in future work.

***Variation of the oestrogenic effects of the UV screens in relation to their molecular structure and their binding affinity to ER.*** Throughout this chapter, the six UV screens have shown different effects on the points under investigation. Miller and colleagues have studied the effect of 73 oestrogenic chemicals on the recombinant yeast assay and documented that

oestrogenic chemicals with a phenolic ring with para-hydroxyl group and with a molecular weight of 140-250 are able to activate ER (Miller et al., 2001). Among the tested UV screens, Bp2 induced the highest luciferase activity and second highest increase in proliferation after Bp1. The molecular structure of Bp2 (246.218 MW) has 4 hydroxyl groups of which two are para-hydroxy phenolic groupings (see structure table 1.3), which is consistent with Millers suggestions of the requirements of oestrogenic chemicals to activate ER. Further, Kerdivel and co-workers have conducted a docking analysis to study Bp2 and other benzophenones binding to the ER ligand binding pocket. In their study, the hydroxyl groups of Bp2 formed hydrogen bonds with Arg-394 and Glu-353 but with no interaction with His-524 (Kerdivel et al., 2013). These interactions are important in the conformation of ER after binding with 17 $\beta$ -oestradiol as shown by the crystal structure of the ligand binding of 17 $\beta$ -oestradiol and ER $\alpha$  (Brzozowski et al., 1997) (see Figure 1.7).

Bp1 (214.22 MW) had the highest effect in increasing the proliferation of MCF-7 cells and the second in increasing the luciferase activity with a molecular structure that consists of 1 phenolic ring with ortho- and para- hydroxyl groups (see structure Table 1.3), which also is consistent with Millers suggestions and is related to the documented binding affinity of Bp1 to ER $\alpha$  (Blair et al., 2000). Among the benzophenones, Bp3 came in third place in increasing the luciferase activity and did not have any effect on MCF-7 cell proliferation. The low binding affinity of Bp3 to ER may explain the lower potency of Bp3 (Blair et al., 2000). Although the molecular weight of Bp3 (228.274 MW) is within the range suggested by Miller et al., (2001), the chemical structure of Bp3 has one ortho-hydroxyl group on the phenolic ring and no interaction of Bp3 with Arg-394, Glu-353 or His-524 was found in docking analysis, instead this chemical activates ER through the hydrophobic bounding (Kerdivel et al., 2013).

No docking data was found for OMC, 4MBC and HS. The luciferase activity caused by these chemicals was lower than the ones caused by the benzophenones and only 4MBC and HS increased the proliferation of MCF-7. The molecular structures of these three chemicals (see Table 1.4) show that OMC and 4MBC do not have a phenolic ring. HS has one phenolic ring but the hydroxyl group is in the ortho position. It is worth noting that the molecular weights of OMC (290.403 MW), 4MBC (254.373 MW) and HS (262.349 MW) are larger than the range proposed by Miller et al. (2001) and that might be related also to the lower potency of these chemicals.

***UV screens in combination with 17 $\beta$ -oestradiol influence MCF-7 cell proliferative response.*** Since 17 $\beta$ -oestradiol is an endogenous hormone in the human body, the interaction of 17 $\beta$ -oestradiol with the UV screens was considered. The influence of UV screens on the proliferation of MCF-7 cells was investigated in combination with different concentrations of 17 $\beta$ -oestradiol. No significant difference was obtained by combining 10<sup>-12</sup> M of 17 $\beta$ -oestradiol with the no-observed-effect concentration (NOEC) of the UV screens on MCF-7 cell proliferation in comparison with the effect of 10<sup>-12</sup> M 17 $\beta$ -oestradiol alone (data are not shown). Thus, we investigated the effect of combining 17 $\beta$ -oestradiol at different doses (from 10<sup>-14</sup> M to 10<sup>-10</sup> M) with Bp1, Bp2, 4MBC and HS in the range causing maximum proliferative effect (10<sup>-5</sup> M). The use of 10<sup>-5</sup> M concentration of these chemicals might be necessary to provoke their effect *in vitro*. One example is the requirement of using 10<sup>-4</sup>M parabens to induce the proliferation of MCF-7 cells (Byford et al., 2002). A down side of using the high concentration of the chemicals in a binary mixture model is the possibility of producing saturable effects. At the same time, further investigation was also conducted to observe the effect of Bp3 and OMC regardless of their failure to induce MCF-7 cell proliferation. The combinations of 10<sup>-5</sup> M Bp1 or 10<sup>-5</sup> M Bp2 with 17 $\beta$ -oestradiol enhanced cell proliferation, while Bp3 and 4MBC showed an antagonist effect in combination with higher concentrations of 17 $\beta$ -oestradiol (10<sup>-11</sup> M and 10<sup>-10</sup> M). Similar experiments using the same UV screens were not found in literature. Although, the effect of binary mixtures of 17 $\beta$ -oestradiol and other environmental oestrogens including bisphenol A and butylbenzyl phthalate on MCF-7 cell proliferation was previously studied (Suzuki et al., 2001). Mixtures of Bp1, Bp2, Bp3 and other UV screens in combination with 17 $\beta$ -oestradiol showed a synergistic effect on the recombinant yeast assay carrying hER $\alpha$  (Kunz and Fent, 2006). The ability of these chemicals to interact with the effect of 17 $\beta$ -oestradiol on MCF-7 cell proliferation might point out of other possible actions within the human body.

***Proliferative response of MCF-7 cells to UV screens is affected by the use of laminin and fibronectin coating.*** Using another approach, we have studied the effects of UV screens on the proliferative response of MCF-7 cells on laminin or fibronectin coated surfaces in order to recapitulate in culture the responses to these chemicals *in vivo*. Studies on interactions of MCF-7 cells with extracellular matrix components (ECM) showed influence on their morphology (Kenny et al., 2007), proliferation (Nista et al., 1997; Li et al., 2014) and variation in their responses to 17 $\beta$ -oestradiol (Woodward et al., 2000). The decision to use laminin in this research was based on laminin being one of the major components of the

basement membrane (reviewed in (Colognato and Yurchenco, 2000)) which reduced the sensitivity of oestrogen responsive cells toward  $17\beta$ -oestradiol (Woodward et al., 2000). The decision to use fibronectin was based on its increased levels during the progression of breast cancer (Ioachim et al., 1997; Oskarsson, 2013) and its opposite action to those of laminin on MCF-7 cell growth response to  $17\beta$ -oestradiol where it increases the proliferative response (Woodward et al., 2000; Xie and Haslam, 2008). To our knowledge, this was the first study that investigated the effect of coating with ECM components on the UV screen action on MCF-7 cell proliferation. Results of this work showed that both fibronectin and laminin increased the proliferation of MCF-7 cells after one week of exposure without the addition of  $17\beta$ -oestradiol and that is in line with previous studies (Nista et al., 1997; Li et al., 2014). After the addition of  $17\beta$ -oestradiol, MCF-7 cells showed a significant increase in cell proliferation on fibronectin and reduced proliferation on laminin coated plates and these results have confirmed the published work by Woodwork and co-workers (Woodward et al., 2000). In order to address the oestrogen mimicking properties' of the six UV screens, the proliferative responses to the UV screens of MCF-7 cells on the same coating components was conducted. Among the tested chemicals,  $10^{-5}$  M Bp1 was the only UV screen which showed a similar effect to  $10^{-8}$  M  $17\beta$ -oestradiol on MCF-7 cells seeded on the coating material and Bp2 had similar decrease in cell proliferation on laminin coated plates with no notable increase in the proliferation on fibronectin coated plates. Interestingly, in contrast to the non-significant effect of  $10^{-5}$  M OMC on MCF-7 cell proliferation on plastic,  $10^{-5}$  M OMC significantly increased the proliferation of MCF-7 cell proliferation on laminin. Further,  $10^{-5}$  M 4MBC exhibited an increase in the proliferation on both fibronectin and laminin coated plates. However, Bp3 and HS did not exhibit any increase in proliferation on coated plates. Further investigations using this methodology might provide new insights into the effect of other environmental oestrogens *in vitro*. Whether the molecular mechanisms for the UV screens are similar to those of oestrogen on coated plates remains to be clarified for each UV screen individually in future work.

***In summary***, using a combination of different techniques to estimate the possible oestrogen mimicking ability of these UV screens served in overcoming any technical limitations, which might be caused by the weak oestrogenic effect of these UV screens. Indeed, the oestrogenic activities of these chemicals were far less than the effects observed by the exposure to the endogenous hormone  $17\beta$ -oestradiol. However, Bp1 and Bp2 have been found to mimic  $17\beta$ -oestradiol in most of the endpoints tested. Both chemicals were considered to possess more

oestrogenic potency as measured by the ERE-LUC reporter gene assay and proliferation in comparison to the other chemicals in this study. These activities are ER mediated, which were confirmed by knocking down the effects by the oestrogen receptor antagonist fulvestrant. However, lack of the induction of TFF1 gene expression by these two chemicals presents a missing gap in confirming the oestrogenic activity for Bp1 and Bp2, which can be explained by the different experimental design that was conducted in this research and was different than the one used to address the change in the levels of TFF1 mRNA (Heneweer et al., 2005 ; Kerdivel et al., 2013). Also, more biological replicates might reveal different findings on this matter and the interaction of these chemicals with other oestrogen-related genes should be investigated. 4MBC and HS gave significant differences in all of the endpoints except for the induction of TFF1 gene expression, which was only found after 24 weeks of exposure (see Table 3.1).

In contrast to the reducing effect of laminin on MCF-7 cell proliferative response toward 17 $\beta$ -oestradiol, 4MBC increased MCF-7 cell proliferation on laminin and proliferative response to HS was not influenced by the use of coating materials (Table 3.2). This variation in comparison with 17 $\beta$ -oestradiol suggests that 4MBC and HS might trigger other signalling pathways beside the ER-mediated mechanism. In comparison between 4MBC and HS, Schlumpf had found HS to induce higher *in vitro* oestrogenic activity than the one induced by 4MBC. However, this was reversed in the *in vivo* model and 4MBC showed higher effect in increasing the uterine weight in immature rats (Schlumpf et al., 2001). The complexity of the interactions of these chemicals or their metabolites *in vivo* must be further investigated to provide a full profile of their oestrogenic abilities.

Despite the ability of Bp3 and OMC to induce the ERE-LUC reporter gene activity, no other oestrogenic action on the other endpoints was documented. In contrast, OMC has induced the proliferation on laminin coated plates (see Table 3.2). Although Bp3 and OMC are considered to be partial agonists, they need further investigation because they are among the most detected UV screens in human samples and widely used in cosmetics (Janjua et al., 2008; Schlumpf et al., 2010; Zhang et al., 2013). Furthermore, since Bp1 is one of the metabolites of Bp3 (Jeon et al., 2008), which has shown high oestrogenic activity, further investigation of the effect of Bp3 and its metabolites remains important.

While our model focused on the individual action of these chemicals, the additive effect of compound mixtures is another approach that can resemble their daily intake into the human

body and should be carried out in future studies. Mixtures of UV screens (Bp1, Bp3, OMC and 4MBC) (at IC50 concentrations) were found to induce TFF1 gene expression to similar levels caused by 17 $\beta$ -oestradiol (Heneweer et al., 2005). Thus, the possible effect of combinations of weaker environmental oestrogens should not be neglected. The effect of mixtures of other environmental oestrogens on MCF-7 cell proliferation was documented (Payne et al., 2001; Charles and Darbre, 2013) but further effects of UV screens in combination remains to be explored at the same concentration found in human milk or in human tissue.

Although the oestrogenic activity of some of these chemicals has been shown to influence proliferation, this is only one of the hallmarks of cancer cells. Another important hallmark is activation of invasion and metastasis (Hanahan and Weinberg, 2011), which is relevant for breast cancer where mortality arises not from growth of the primary tumour but from metastatic tumour spread (Solomayer et al., 2000; Schairer et al., 2004; Manders et al., 2006). This hallmark is further investigated in the next chapters.

## Chapter 4 Effects of the UV screens on migration and invasion of MCF-7 human breast cancer cells

### 4.1 Introduction

Proliferation of MCF-7 human breast cancer cells has been used as an *in vitro* model to demonstrate oestrogenicity of environmental chemicals (Soto et al., 1995) and their potential influence on breast cancer growth. However, mortality of breast cancer is mediated by the metastasis of cancer cells to distant organs (Solomayer et al., 2000; Schairer et al., 2004; Manders et al., 2006) and several reports document a supporting role of oestrogen on breast cancer cell migration *in vitro* (Saji et al., 2005; Malek et al., 2006; Planas-Silva and Waltz, 2007; Giretti et al., 2008; Chakravarty et al., 2010; Li et al., 2010; Jimenez-Salazar et al., 2014) and *in vivo* (Ganapathy et al., 2012; Ogba et al., 2014). It is therefore possible that environmental chemicals with oestrogenic activity might also influence motility and invasion of breast cancer cells through an ER-mediated mechanism.

In 2012, Yao and his colleagues reported an increase in migration and invasion of human testicular embryonal carcinoma cells (NT2/D1) after being exposed to phthalate esters (Yao et al., 2012). In another study Khanna and colleagues (2014) have recorded an increase of MCF-7 and T-47-D human breast cancer cell migration and invasion after long-term exposure to parabens (Khanna et al., 2014). In view of the effect of the UV screens on MCF-7 cell proliferation described in the previous chapter, studies are described here of the ability of these chemicals to influence motility and invasion in MCF-7 cells and possible underlying molecular mechanisms have been investigated.

The process of metastasis involves many alterations to cell morphology and metastasis-related markers that facilitate the transition of non-motile epithelial MCF-7 cells into more motile cells. It was suggested that epithelial to mesenchymal transition (EMT) could be one of the possible mechanisms that underly the metastasis of epithelial cells (Guarino et al., 2007). The morphological and cytoskeletal changes of the epithelial cells undergoing EMT is underlaid by several EMT-related molecular markers including loss of E-cadherin and  $\beta$ -catenin and induced N-cadherin and vimentin (Micalizzi et al., 2010). It is noteworthy that loss of E-cadherin in breast cancer tissues was found to be correlated with poor prognosis in clinical studies (Gamallo et al., 1993; Oka et al., 1993; Siitonen et al., 1996; Jeschke et al.,

2007). E-cadherin expression can be repressed by several regulators including elevated expression of the zinc-finger proteins (Snail) (Batlle et al., 2000) and the basic helix-loop-helix transcription factor (Twist-1) (Yang et al., 2004; Vesuna et al., 2008), both of which were described as promoters of cancer metastasis (Nguyen et al., 2009).

Other genes have also been linked to the promotion of cancer metastasis through EMT such as Phosphoinositide-3-Kinase Regulatory Subunit 1 (PIK3R1) and Bone morphogenetic protein 7 (BMP7). A correlation between EMT induction and down-regulation of BMP7 and PIK3R1 was described *in vitro* (Yang et al., 2005; Buijs et al., 2007; Lin et al., 2015). Furthermore, the depletion of PIK3R1 expression was correlated with poor breast cancer patient survival (Cizkova et al., 2013). Bone morphogenetic proteins are a sub-family of the transforming growth factor  $\beta$  (TGF- $\beta$ ) family, which are correlated with cell proliferation and differentiation (Ye and Jiang, 2015). BMP7 is detected in human breast cancer tissue (Schwalbe et al., 2003; Alarmo et al., 2006) and BMP7 mRNA expression was found to be elevated in MCF-7 cells and not expressed in the invasive motile MDA-MB-231 human breast cancer cells (Alarmo et al., 2007). Uchino and his colleagues have shown a link between the decrease in mRNA expression of BMP7 and PIK3R1 and the increase in motility and invasive activity of matrigel-selected MCF-7 cells (MCF-7-14). Moreover, they have shown similar down-regulated expression of both BMP7 and PIK3R1 in MCF-7-14 cells and MDA-MB-231 cells by microarray analysis. The same group has suggested that MCF-7-14 cells have turned into a metastable phenotype due to the retained E-cadherin expression and elevated cell motility in comparison with parental MCF-7 cells (Uchino et al., 2010).

Metastasis of cancer cells has also been reported to be influenced by the activity of matrix metalloproteases (MMPs). MMPs play a crucial role in degrading the ECM components in order to facilitate cancer invasion (Woodhouse et al., 1997; Roy et al., 2009). In the context of breast cancer, several MMPs have been linked to the induced metastasis of breast cancer cells including MMP-1, MMP-2, MMP-9 and the membrane-type MMP-14 (Deryugina et al., 1997; Gupta et al., 2007; Kohrmann et al., 2009; Zarrabi et al., 2011). MMP-14 is an intracellular MMP, which is involved in the activation of pro-MMP-2 (Deryugina et al., 2001). 17 $\beta$ -oestradiol was found to modulate MMP-2/MMP-9 activity in MCF-7 cells (Nilsson et al., 2007; Song et al., 2007). The effect of UV screens on MMP activities in MCF-7 cells has therefore been investigated.

## 4.2 Experimental aims

The MCF-7 human breast cancer cell line was found to give a proliferative response to some of the UV screens (see chapter 3). The overall aims of this chapter are to investigate the effect of six UV screens (Bp1, Bp2, Bp3, OMC, 4MBC and HS) on motility and invasion of MCF-7 cells after short-term (2 weeks) and long-term (24-31 weeks) exposure to these compounds and then to study molecular mechanisms that might underly any change in MCF-7 cell behaviour. These time points were suggested based on previous publications that have documented an increase in MCF-7 cell motility after long term exposure to environmental oestrogens. MCF-7 cell showed an increased motility after  $20 \pm 2$  weeks exposure to parabens (Khanna et al., 2014), while exposure to aluminium increased MCF-7 cells motility after 32 weeks (Darbre et. al, 2013).

In order to achieve these aims the motility of MCF-7 cells was assessed using a wound healing assay, using live cell imaging by time-lapse microscopy and using the xCELLigence technology (see materials and methods chapter 2).

Assessment of changes in MCF-7 cell invasive activity after exposure to the UV screens was carried out by monitoring cell migration through matrigel coated plates using the xCELLigence technology (see section 2.5). Investigation of the ability of these chemicals to alter MCF-7 cell invasive properties through alteration to MMPs was done by measuring changes in MMP-2 and MMP-9 secretion into the media using gelatin zymography (see section 2.8) and by measuring the levels of the intracellular MMP-14 using western immunoblotting (see section 2.7).

Since motility of epithelial cells can be induced by EMT (Guarino et al., 2007), the work of this chapter examined the effect of short and long-term exposure of MCF-7 cells to the UV screens on two of EMT related markers; E-cadherin and  $\beta$ -catenin. mRNA levels were investigated by RT-PCR (see section 2.6) and protein levels by western immunoblotting (see section 2.7). mRNA levels of two of the upstream transcriptional regulators (Snail and Twist-1) of E-cadherin were investigated using RT-PCR. Moreover, mRNA levels of BMP7 and PIK3R1 were measured as they are considered as molecular markers of cell motility (Yang et al., 2005; Buijs et al., 2007; Uchino et al., 2010; Lin et al., 2015).

## **4.3 Results**

### **4.3.1 Effects of Bp1 on migration of MCF-7 human breast cancer cells**

#### **4.3.1.1 Effects of Bp1 on collective migration of MCF-7 human breast cancer cells as measured by wound healing**

The wound healing assay (as described in 2.4.1) was used to determine the effect of long term exposure to Bp1 on motility of MCF-7 human breast cancer cells. Results showed that after 7 weeks of exposure to  $10^{-5}$  M Bp1 the wound healing was higher than the negative control.  $10^{-5}$  M Bp1 closed  $47.63 \pm 5.36$  % of the wound, while the closure percentage was  $14.25 \pm 1.77$  % in the negative control wells (Figure 4.1 (A)) ( $p$ -value  $\leq 0.05$ ). Longer exposure time of 13 weeks showed that neither  $10^{-5}$  M Bp1 nor  $10^{-7}$  M Bp1 altered MCF-7 cell motility compared to the negative control (Figure 4.1 (B)). However, after 21 weeks of exposure to  $10^{-7}$  M Bp1 the wound healing activities of MCF-7 cells were found up-regulated to  $68.11 \pm 15.49$  % in comparison to  $24.75 \pm 0.69$  % in the negative control (Figure 4.1 (C)) ( $p$ -value  $\leq 0.05$ ). Represented images are illustrated in (Figure 4.2).

#### **4.3.1.2 Effects of Bp1 on migration of individual MCF-7 human breast cancer cells as measured by time-lapse microscopy**

MCF-7 human breast cancer cells were exposed for 2 weeks and 21 weeks to  $10^{-5}$  M Bp1 or  $10^{-7}$  M Bp1. 48 hours prior to the experiment, cells were re-seeded in 12-well plates and cell migration was analysed using live cell imaging (time-lapse microscopy) (as described in section 2.4.2). 10 cells were tracked in 5 fields per well for 24 hours and the number of motile cells and cumulative length moved (total travelled length of cell) were measured for each treatment.

A statistically significant % increase of motile cells ( $10.67 \pm 2.40$  %) was indicated in MCF-7 cells exposed to  $10^{-5}$  M Bp1 after 2 weeks (Figure 4.3 (A)) ( $p$ -value  $\leq 0.05$ ) compared to the control ( $4.00 \pm 1.37$  %). After the same period of exposure, MCF-7 cells exposed to  $10^{-7}$  M Bp1 did not show any increase in % motile cells or cumulative length moved (Figure 4.3 (A and B)). However, the % increase of motile cells of MCF-7 cells exposed to  $10^{-7}$  M Bp1 and  $10^{-5}$  M Bp1 were elevated after 21 weeks of exposure to  $18.67 \pm 1.764$  % and  $18.67 \pm 6.360$  % respectively (Figure 4.3 (C)), although cumulative length was not significantly increased (Figure 4.3 (D)).

### **4.3.1.3 Effects of Bp1 on migration of MCF-7 human breast cancer cells as determined by xCELLigence technology**

Movement of cells through 8µm pores of a membrane towards a chemotaxis stimulus of FCS has also been investigated by using the xCELLigence technology. Cells were exposed to  $10^{-5}$  M Bp1,  $10^{-6}$  M Bp1,  $10^{-7}$  M Bp1,  $10^{-8}$  M  $17\beta$ -oestradiol or no addition for 2, 10 or 21 weeks prior to the experiment. Then the experiment was carried out according to the manufacturer's instruction (as described in section 2.4.3). Results of short and long-term exposure to Bp1 at  $10^{-7}$  M and  $10^{-5}$  M, suggested that Bp1 at  $10^{-5}$  M triggered the migratory activity of MCF-7 cells after 2 weeks of exposure with 0.22 cell index compared to 0.033 increase in cell index by the cells of the control (Figure 4.4) with a lower but similar pattern after 20 weeks of exposure (Figure 4.6). However, the effect of  $10^{-6}$  M Bp1 on the migratory cells index was increasing throughout the different time points of the experiments. After 2, 10 and 20 weeks of exposure,  $10^{-6}$  M Bp1 increased the cell index to 0.11, 0.14 and 0.22 respectively in comparison with no addition (with cell index 0.034, 0.084 and 0.044) (Figures 4.4-4.6). Whereas Bp1 at  $10^{-7}$  M gave an increase in the cell motility after 2 weeks of exposure (cell index 0.18 compared to 0.03 of cells of no addition) (Figure 4.4), which shows similar pattern after 20 weeks of exposure (cell index 0.22 compared to 0.04 of cells of no addition) (Figure 4.6).

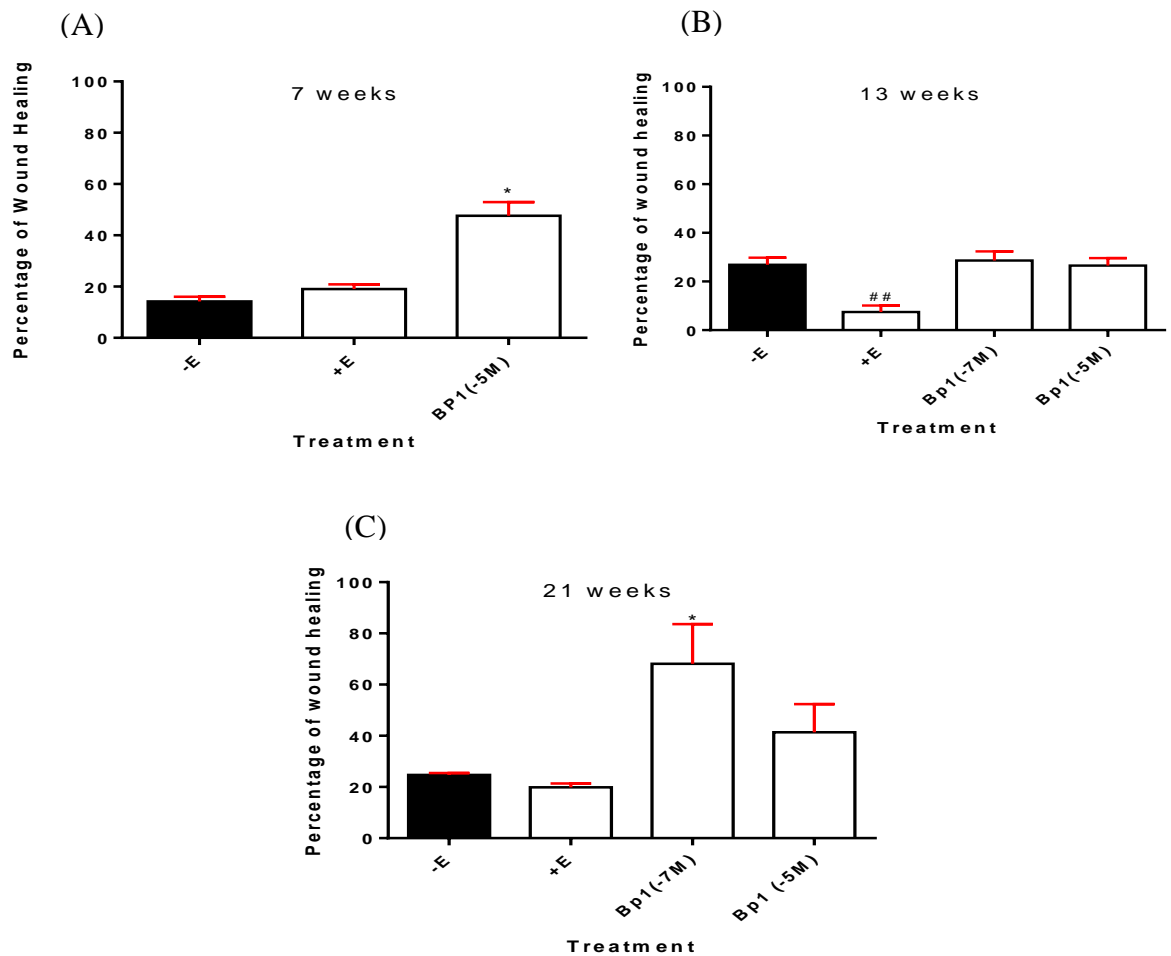


**Figure 4.1 Effect of exposure to Bp1 or 17 $\beta$ -oestradiol on collective motility of MCF-7 human breast cancer cells as measured by wound healing assay.**

Cells were grown in phenol-red-free-DMEM containing 5% DCFCS with ethanol control (-E) only, 10<sup>-8</sup> M 17 $\beta$ -oestradiol (+E), with 10<sup>-7</sup> M Bp1 (Bp1 (-7M)) or with 10<sup>-5</sup> M Bp-1 (Bp1 (-5M)) for 7 weeks (A), 13 weeks (B) and 21 weeks (C) respectively. Media were replenished and cells were split every 3-4 days. Cells were then reseeded in 12-well plates and once the cells became  $\geq 95\%$  confluent, wound was made and mitomycin c (0.5 $\mu$ g/ml) was added. Images were captured at 0 hour and 24 hours. Cell migration was quantified by analysing 5 images from each well by using Image J software. (A) Values are the average  $\pm$  SE of triplicate wells of three independent experiments (n=3). (B and C) Values are the average  $\pm$  SE of triplicate independent wells. Where no bars are seen, error was too small to be visualized. \* *p*-value  $\leq 0.05$  increase versus no addition. ## *p*-value  $\leq 0.01$  decrease versus no addition by one-way ANOVA Dunnett's test.

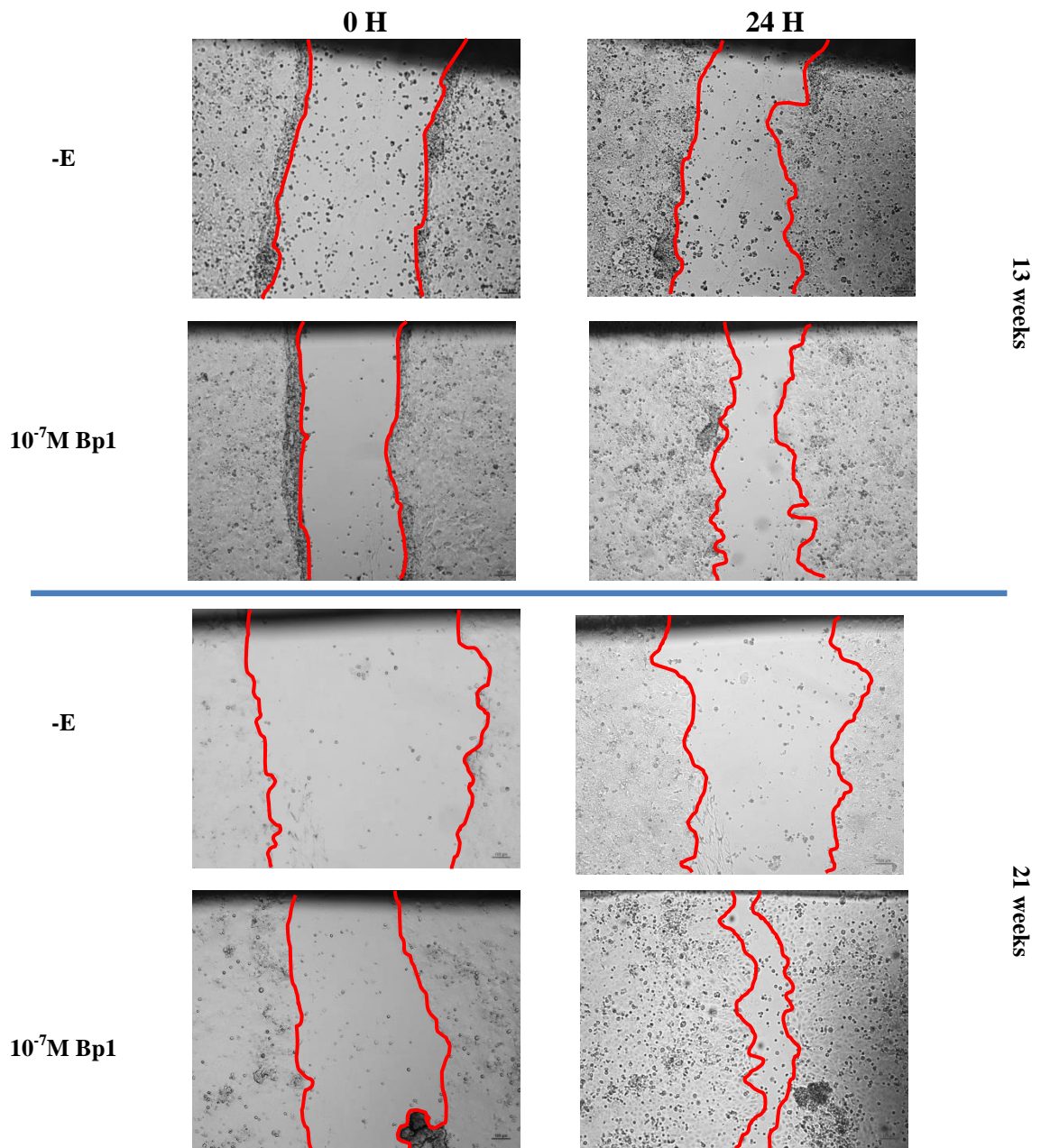


**Figure 4.2 Representative images of the effect of Bp1 on motility of MCF-7 human breast cancer cells as determined by wound healing assay.**

Cells were grown in phenol-red-free-DMEM containing 5% DCFCS with ethanol control (-E) only or with  $10^{-7}$ M Bp1 for 13 and 21 weeks. Cells were then reseeded in 12-well plates and once the cells became  $\geq 95\%$  confluent, wound was made and mitomycin c ( $0.5 \mu\text{g/ml}$ ) was added. Images were captured at 0 hour and 24 hours.

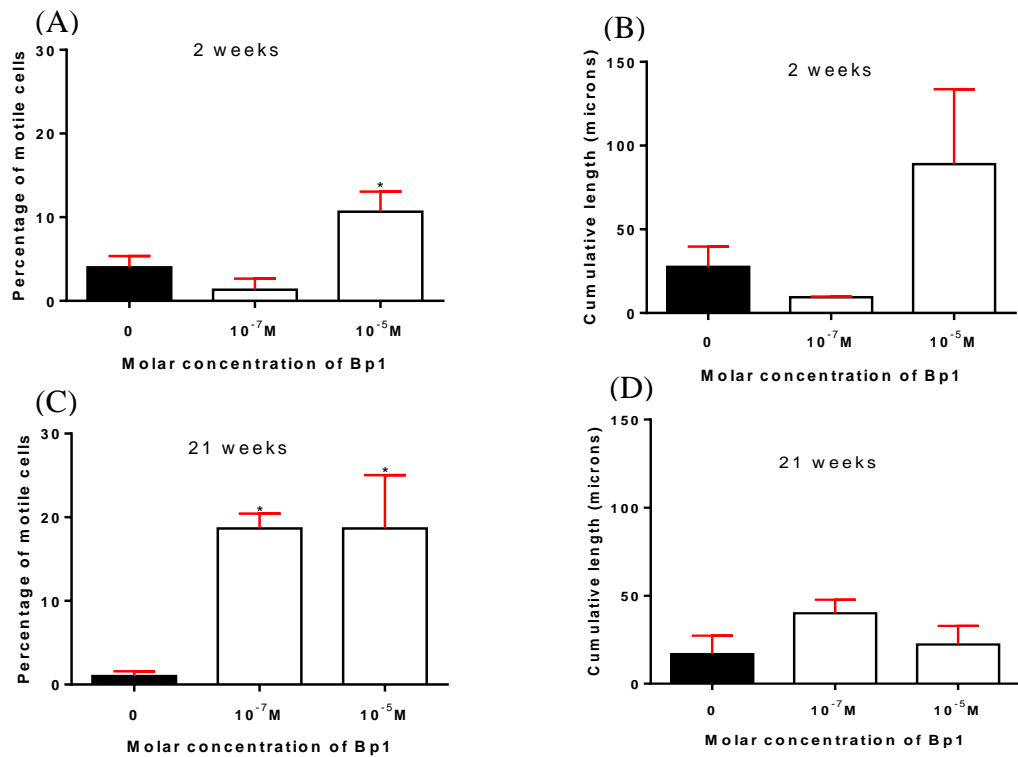


**Figure 4.3 Effect of exposure to Bp1 on motility of individual MCF-7 human breast cancer cells as determined by time-lapse microscopy.**

Cells were grown in phenol-red-free-DMEM containing 5% DCFCS with ethanol control (0) only or with Bp1 at indicated concentrations for 2 (A, B) and 21 (C, D) weeks. Media were replenished and cells were split every 3-4 days. 2 days prior to the experiment, cells were reseeded in 12-well plates at  $0.2 \times 10^5$  cells/well. Time-lapse images of 5 fields per well were recorded. Results represent the percentage of motile cells (A, C) and cumulative length moved (B, D). Values are the average  $\pm$ SE of triplicate independent wells. \*  $p$ -value  $\leq 0.05$  versus no addition by one-way ANOVA Dunnett's test.

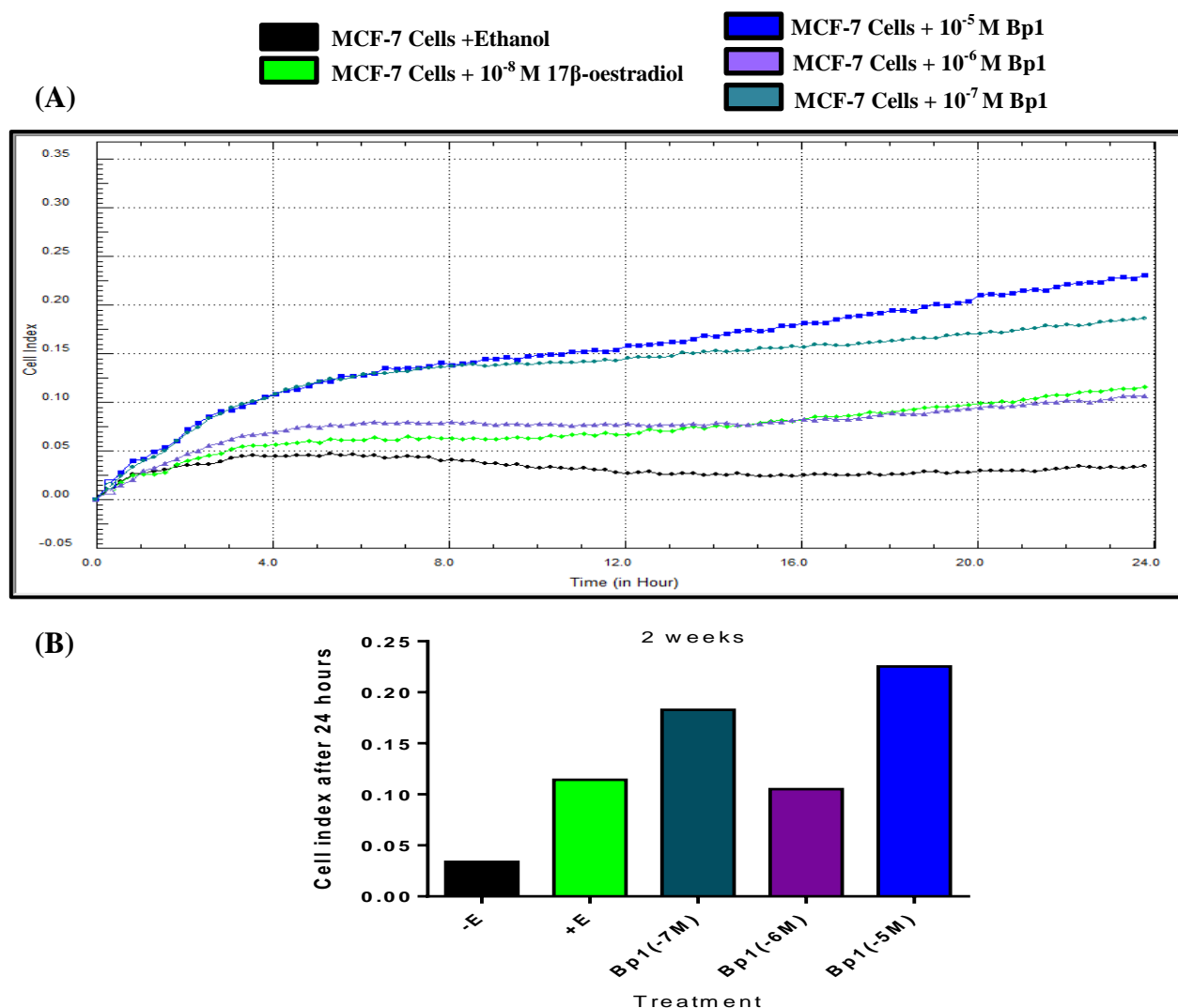


**Figure 4.4 Short-term effect of Bp1 or 17 $\beta$ -oestradiol on migration of MCF-7 human breast cancer cells using chemotaxis stimulus as determined by xCELLigence technology.**

Cells were grown in phenol-red-free-DMEM containing 5% DCFCS with ethanol control only (-E), 10<sup>-8</sup> M 17 $\beta$ -oestradiol (+E), 10<sup>-7</sup> M Bp1 (Bp1 (-7M)), 10<sup>-6</sup> M Bp1 (Bp1 (-6M)) or 10<sup>-5</sup> M Bp1 (Bp1 (-5M)) for 2 weeks. Media were replenished and cells were split every 3-4 days. (A) The relative change in cell index of duplicate wells as indicated by the changes in impedance caused by cell migration from upper chambers to lower ones through the pores of the polycarbonate membrane. Cell index was recorded every 5 minutes and monitored for 24 hours. (B) Bar graph represents the average of the end point measurements (Cell index) of cell migration of duplicate independent wells at 24 hours.

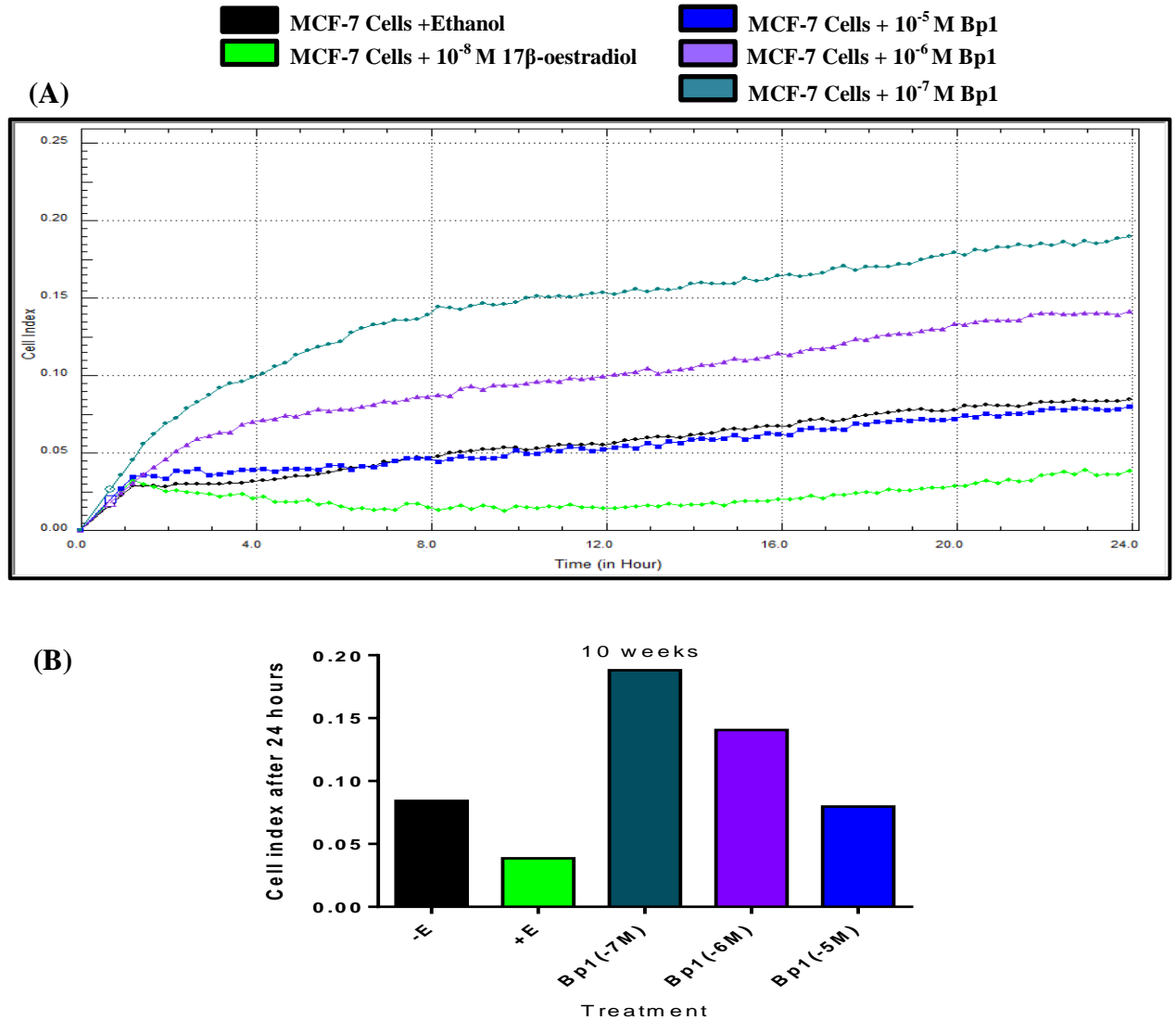


**Figure 4.5 Long-term effect of Bp1 or 17β-oestradiol on migration of MCF-7 human breast cancer cells using chemotaxis stimulus as determined by xCELLigence technology.**

Cells were grown in phenol-red-free-DMEM containing 5% DCFCS with ethanol control only (-E), 10<sup>-8</sup> M 17β-oestradiol (+E), 10<sup>-7</sup> M Bp1 (Bp1 (-7M)), 10<sup>-6</sup> M Bp1 (Bp1 (-6M)) or 10<sup>-5</sup> M Bp1 (Bp1 (-5M)) for 10 weeks. Media were replenished and cells were split every 3-4 days. (A) The relative change in cell index of duplicate wells as indicated by the changes in impedance caused by cell migration from upper chambers to lower ones through the pores of the polycarbonate membrane. Cell index was recorded every 5 minutes and monitored for 24 hours. (B) Bar graph represents the average of the end point measurements (Cell index) of cell migration of duplicate independent wells at 24 hours.

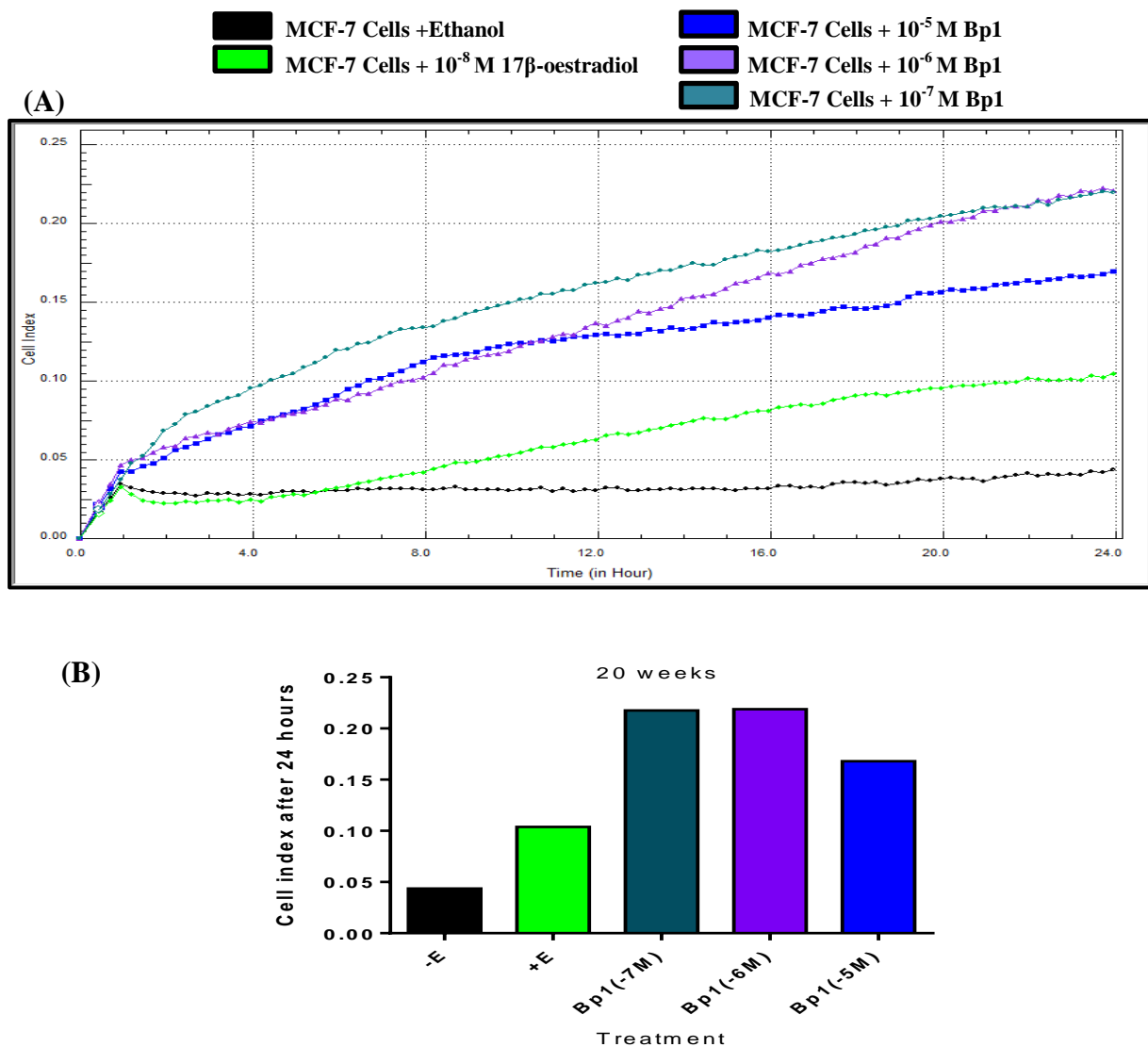


**Figure 4.6 Long-term effect of Bp1 or 17β-oestradiol on migration of MCF-7 human breast cancer cells using chemotaxis stimulus as determined by xCELLigence technology.**

Cells were grown in phenol-red-free-DMEM containing 5% DCFCS with ethanol control only (-E), 10<sup>-8</sup> M 17β-oestradiol (+E), 10<sup>-7</sup> M Bp1 (Bp1 (-7M)), 10<sup>-6</sup> M Bp1 (Bp1 (-6M)) or 10<sup>-5</sup> M Bp1 (Bp1 (-5M)) for 20 weeks. Media were replenished and cells were split every 3-4 days. (A) The relative change in cell index of duplicate wells as indicated by the changes in impedance caused by cell migration from upper chambers to lower ones through the pores of the polycarbonate membrane. Cell index was recorded every 5 minutes and monitored for 24 hours. (B) Bar graph represents the average of the end point measurements (Cell index) of cell migration of duplicate independent wells at 24 hours.

#### **4.3.1.4 Effects of Bp1 on invasion of MCF-7 human breast cancer cells as determined by xCELLigence technology**

MCF-7 cells exposed to Bp1 for 2 weeks, 11 weeks and 21 weeks were monitored for their invasive activity in real time using xCELLigence technology. According to the manufacturer's instructions (ACEA Biosciences, USA), cells were seeded on matrigel (1:40 dilution) in the upper chamber of a CIM-plate 16 (as described in section 2.5). The lower chamber of the plate was filled with phenol-red-free-DMEM without or with  $10^{-8}$  M  $17\beta$ -oestradiol,  $10^{-7}$  M Bp1,  $10^{-6}$  M Bp1 or  $10^{-5}$  M Bp1 supplemented with 5% DCFCS, while the upper chamber was filled with the same media without the serum. Invasion was monitored every 15 minutes for 48 hours as cells moved through the matrigel coated membrane onto the gold electrodes in lower chamber by chemotaxis stimulus of FCS.

No effect on the invasive activities was observed after 2 weeks and 11 weeks of exposure to  $10^{-7}$  M Bp1,  $10^{-6}$  M Bp1 or  $10^{-5}$  M Bp1 (data not shown). However, longer exposure time (31 weeks) to  $10^{-5}$  M Bp1 showed an increase in invasion (cell index 0.01) compared to cells with no addition (cell index -0.08) (Figure 4.7) ( $p$ -value  $\leq 0.05$ ).

#### **4.3.1.5 Summary of effects with Bp1**

Table 4.1 summarises all the results in section 4.3.1. The results are shown as determined by wound healing, time-lapse microscopy and the xCELLigence technology after 2 weeks and longer time points of exposure to concentrations of  $10^{-7}$  M and  $10^{-5}$  M Bp1.

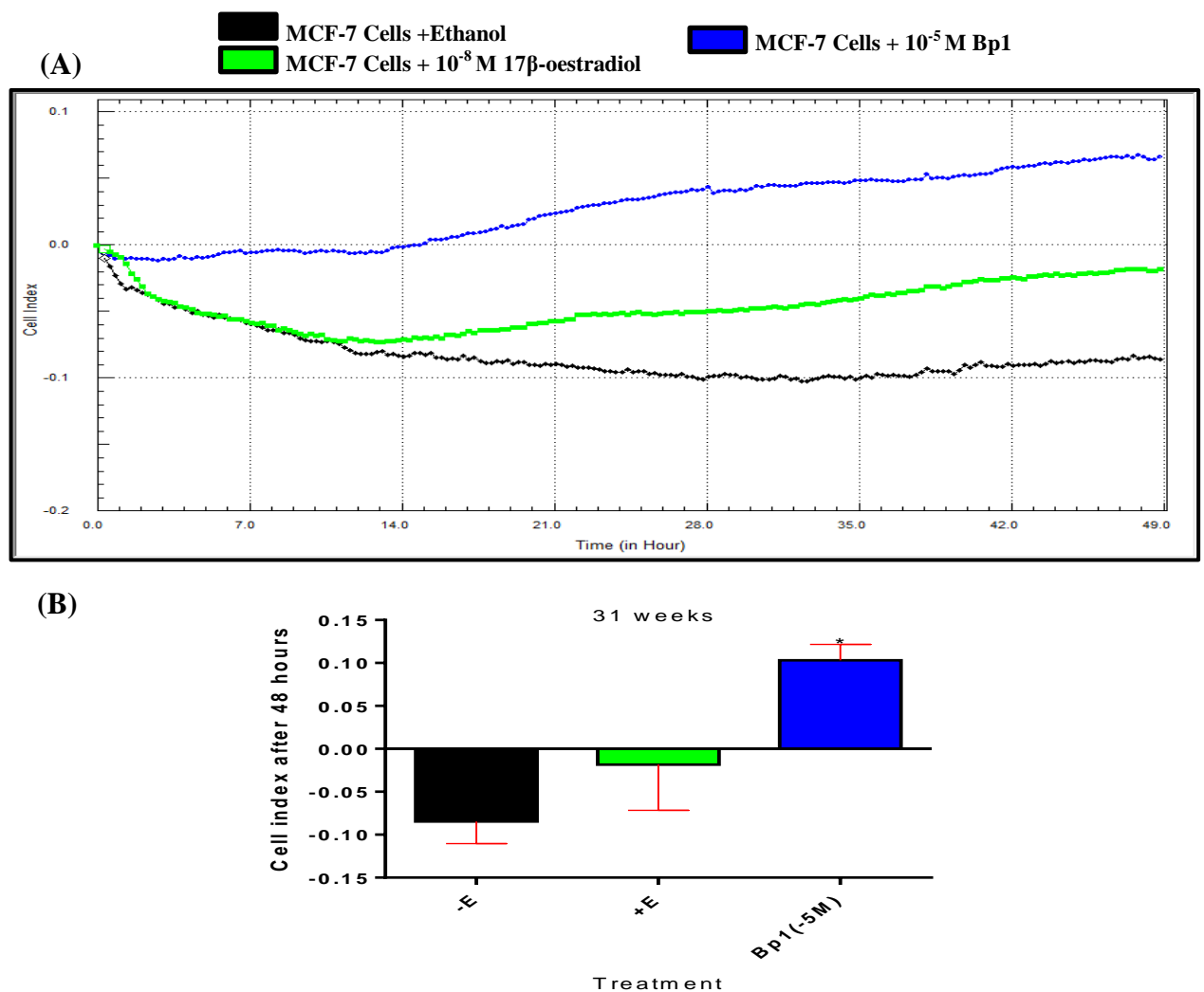


**Figure 4.7 Effect of 31 weeks of exposure to Bp1 or  $17\beta$ -oestradiol on invasion of MCF-7 human breast cancer cells through matrigel using chemotaxis stimulus as determined by xCELLigence technology.**

Cells were grown in phenol-red-free-DMEM containing 5% DCFCS with ethanol control only (-E),  $10^{-8}$  M  $17\beta$ -oestradiol (+E) or  $10^{-5}$  M Bp1 (Bp1 (-5M)) for 31 weeks. Media were replenished and cells were split every 3-4 days. Cells were analysed for their invasive activity through matrigel (1:40) coated CIM-plate 16 in a real time invasion assay (xCELLigence RTCA device) (A) The relative change in cell index of triplicate wells as indicated by the changes in impedance caused by cell migration from upper chambers to lower ones through the pores of the polycarbonate membrane through matrigel. Cell index was recorded every 5 minutes and monitored for 48 hours. (B) Bar graph represents the cell index at 48 hours as calculated by the xCELLigence RTCA software. Values are the average  $\pm$ SE of triplicate independent wells. \*  $p$ -value  $\leq 0.05$  versus no addition (-E) by one-way ANOVA Dunnett's test.

**Table 4.1 Effects of Bp1 on motility and invasion of MCF-7 human breast cancer cells**

Experiment	Molar concentration		Incubation time prior to the experiment
	10 <sup>-7</sup> M	10 <sup>-5</sup> M	
Wound healing	--	*	7 weeks
	n.s.	n.s.	13 weeks
	*	n.s.	21 weeks
Time-lapse	n.s.	(*) in percentage of motile cells	2 weeks
	(*) in percentage of motile cells	(*) in percentage of motile cells	21 weeks
Real-time monitoring of cell motility (xCELLigence)	O.	O.	2 weeks
	O.	n.o.	10 weeks
	O.	O.	21 weeks
Real-time monitoring of cell invasion through matrigel (xCELLigence)	n.s.	n.s.	2 weeks and 11 weeks
	--	(*)	31 weeks

(--) experiment was not conducted; \*  $p$ -value  $\leq 0.05$  versus no addition; (n.s.)  $p$ -value  $> 0.05$  not significant; (O.) effect observed using duplicates only-no statistical analysis possible for duplicates; (n.o.) no effects observed using duplicates.

### **4.3.2 Effects of Bp2 on migration of MCF-7 human breast cancer cells**

#### **4.3.2.1 Effects of Bp2 on collective migration of MCF-7 human breast cancer cells as measured by wound healing**

The wound healing assay was used to determine the effect of long term exposure to Bp2 on motility of MCF-7 human breast cancer cells. Results showed that after 7 weeks of exposure to  $10^{-5}$  M Bp2 the wound healing was higher than the negative control.  $10^{-5}$  M Bp2 closed  $39.28 \pm 5.80$  % of the wound, while the closure percentage was  $14.64 \pm 2.10$  % in the negative control wells (Figure 4.8 (A)) ( $p$ -value  $\leq 0.01$ ). Longer exposure times have shown that after 13 weeks of exposure to  $10^{-5}$  M Bp2, no statistically significant effect was observed at any of the concentrations tested. However, it is noteworthy that at  $10^{-5}$  M Bp2 almost the same effect on wound closure ( $31.99 \pm 2.21$  %) was noted as after 7 weeks of exposure but the motility of the untreated cells (-E) ( $26.88 \pm 2.27$  %) had risen (Figure 4.8 (B)). However, after 21 weeks of exposure to  $10^{-7}$  M Bp2 MCF-7 cells have shown significant increase in the wound healing activities. Percentage of the wound closure in MCF-7 cells exposed to  $10^{-7}$  M Bp2 was  $78.95 \pm 2.22$  % in comparison to  $24.75 \pm 0.68$  % closure in the negative control (Figure 4.8 (C)) ( $p$ -value  $\leq 0.001$ ).

#### **4.3.2.2 Effects of Bp2 on migration of individual MCF-7 human breast cancer cells as measured by time-lapse microscopy**

MCF-7 human breast cancer cells were exposed for 2 weeks and 13 weeks to  $10^{-5}$  M Bp2,  $10^{-7}$  M Bp2 or no addition. 48 hours prior the experiment, cells were re-seeded in 12-well plates and cell migration was analysed using time-lapse microscopy. 10 cells were tracked in 5 fields per well for 24 hours and the number of motile cells and cumulative length moved were measured for each treatment. Results showed no increase in percentage of motile cells (Figure 4.9 (A)) but a statistically significant increase in cumulative length moved in MCF-7 cells exposed to  $10^{-7}$  M Bp2 for 2 weeks (Figure 4.9 (B)) ( $p$ -value  $\leq 0.01$ ). Longer exposure time (13 weeks) to  $10^{-7}$  M Bp2 did increase the percentage of motile cells significantly to  $34.76 \pm 5.21$  % in comparison to the negative control ( $5.33 \pm 1.33$  %) (Figure 4.9 (C)) ( $p$ -value  $\leq 0.01$ ) and increased the cumulative length moved by MCF-7 cells to  $87.57 \pm 16.05$  microns in comparison to the control ( $27.92 \pm 3.60$  microns) (Figure 4.9 (D)) ( $p$ -value  $\leq 0.01$ ). The apparent difference in percentage of motile cells and cumulative length for cells exposed to  $10^{-5}$  M Bp2 were not significant (Figure 4.9 (C and D)). Due to technical problems the

collection of time-lapse videos to assess the effect of Bp2 on MCF-7 cells motility at 21 weeks was not conducted.

#### **4.3.2.3 Effects of Bp2 on migration of MCF-7 human breast cancer cells as determined by xCELLigence technology**

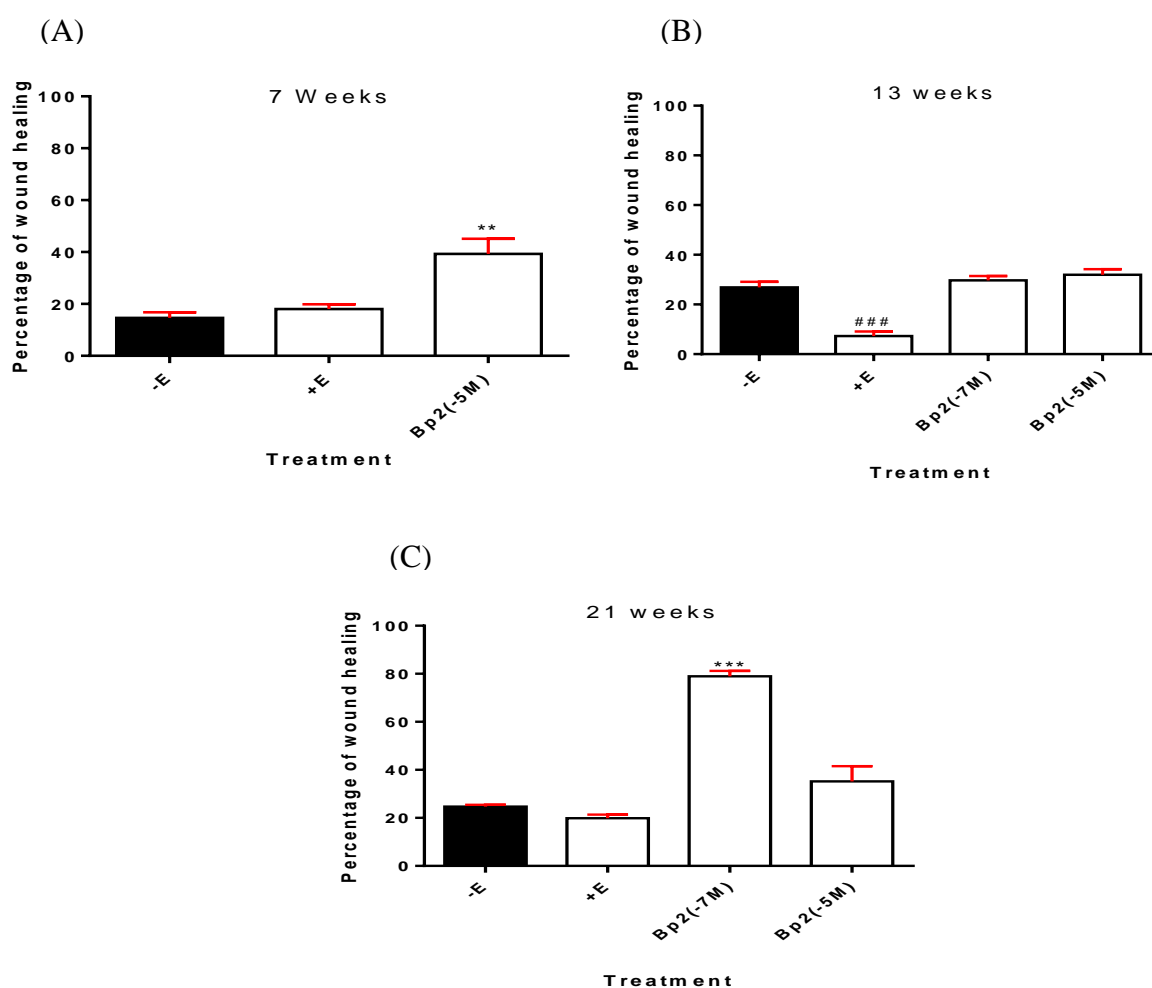
MCF-7 cells were exposed to  $10^{-7}$  M Bp2,  $10^{-6}$  M Bp2,  $10^{-5}$  M Bp2,  $10^{-8}$  M  $17\beta$ -oestradiol or no addition for 2 weeks, 10 weeks or 21 weeks prior to the migration experiments. Minor increase was observed in the cell index of cells exposed to  $10^{-5}$  M Bp2 for 2 weeks (cell index 0.15) in comparison with the control cells (cell index 0.11) (Figure 4.10). Further increase in cell index was observed in cells exposed to  $10^{-7}$  M Bp2 for 10 weeks (cell index 0.14) compared to cells of no addition (cell index 0.08) (Figure 4.11). No effect on MCF-7 motility was determined after 21 weeks of exposure to Bp2 (data not shown).

#### **4.3.2.4 Effects of Bp2 on invasion of MCF-7 human breast cancer cells as determined by xCELLigence technology**

The invasive activities of MCF-7 cells exposed to  $10^{-7}$  M Bp2,  $10^{-6}$  M Bp2 and  $10^{-5}$  M Bp2 were further investigated using the xCELLigence real-time as previously described (in section 2.5). However, no observed effect on MCF-7 cells invasive activity was noted after 2, 10 and 31 weeks of exposure (data not shown).

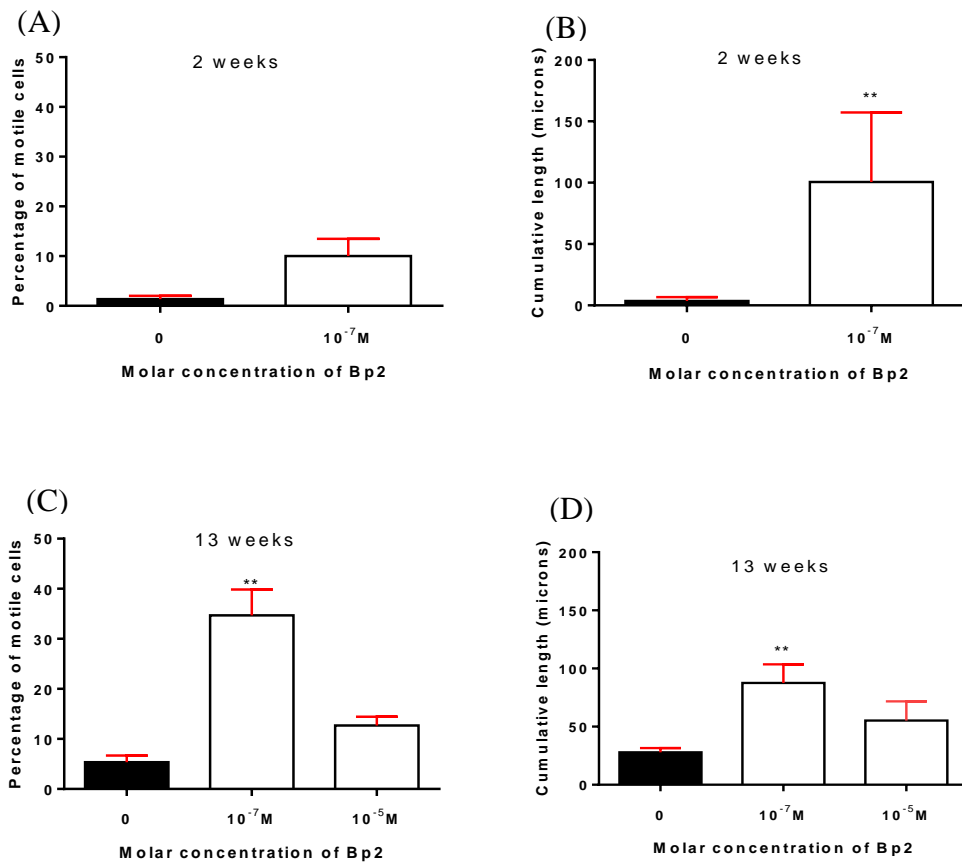
#### **4.3.2.5 Summary of effects with Bp2**

Table 4.2 summarises all the results in section 4.3.2. The results are shown as determined by wound healing, time-lapse microscopy and the xCELLigence technology after 2 weeks and longer time points of exposure to concentrations of  $10^{-7}$  M and  $10^{-5}$  M Bp2.



**Figure 4.8 Effect of exposure to Bp2 or 17 $\beta$ -oestradiol on collective motility of MCF-7 human breast cancer cells as measured by wound healing assay.**

Cells were grown in phenol-red-free-DMEM containing 5% DCFCS with ethanol control (-E) only,  $10^{-8}$  M 17 $\beta$ -oestradiol (+E), with  $10^{-7}$  M Bp2 (Bp2 (-7M) or with  $10^{-5}$  M Bp2 (Bp2 (-5M)) for 7 weeks (A), 13 weeks (B) and 21 weeks (C). Media were replenished and cells were split every 3-4 days. Cells were then reseeded in 12-well plates and once the cells became  $\geq 95\%$  confluent, wound was made and mitomycin c (0.5  $\mu\text{g/ml}$ ) was added. Images were captured at 0 hour and 24 hours. Cell migration was quantified by analysing minimum 5 images from each well. (A) Values are the average  $\pm$  SE of triplicate wells of three independent experiments (n=3). (B and C) Values are the average  $\pm$  SE of triplicate independent wells. \*\* *p-value*  $\leq 0.01$  and \*\*\* *p-value*  $\leq 0.001$  increase versus no addition. ### *p-value*  $\leq 0.001$  decrease versus no addition by one-way ANOVA Dunnett's test.



**Figure 4.9 Effect of exposure to Bp2 on motility of individual MCF-7 human breast cancer cells as determined by time-lapse microscopy.**

Cells were grown in phenol-red-free-DMEM containing 5% DCFCS with ethanol control (0) only or with Bp2 at indicated concentrations for 2 (A, B) and 13 weeks (C, D). Media were replenished and cells were split every 3-4 days. 2 days prior to the experiment, cells were reseeded in 12-well plate at  $0.2 \times 10^5$  cells/well. Time-lapse images of 5 fields per well were recorded. Results represent the percentage of motile cells (A, C) and cumulative length moved (B, D). Values are the average  $\pm$ SE of triplicate independent wells. \*\* *p*-value  $\leq 0.01$  versus no addition (0) by t-Test (A and B) and one-way ANOVA Dunnett's test (C and D).

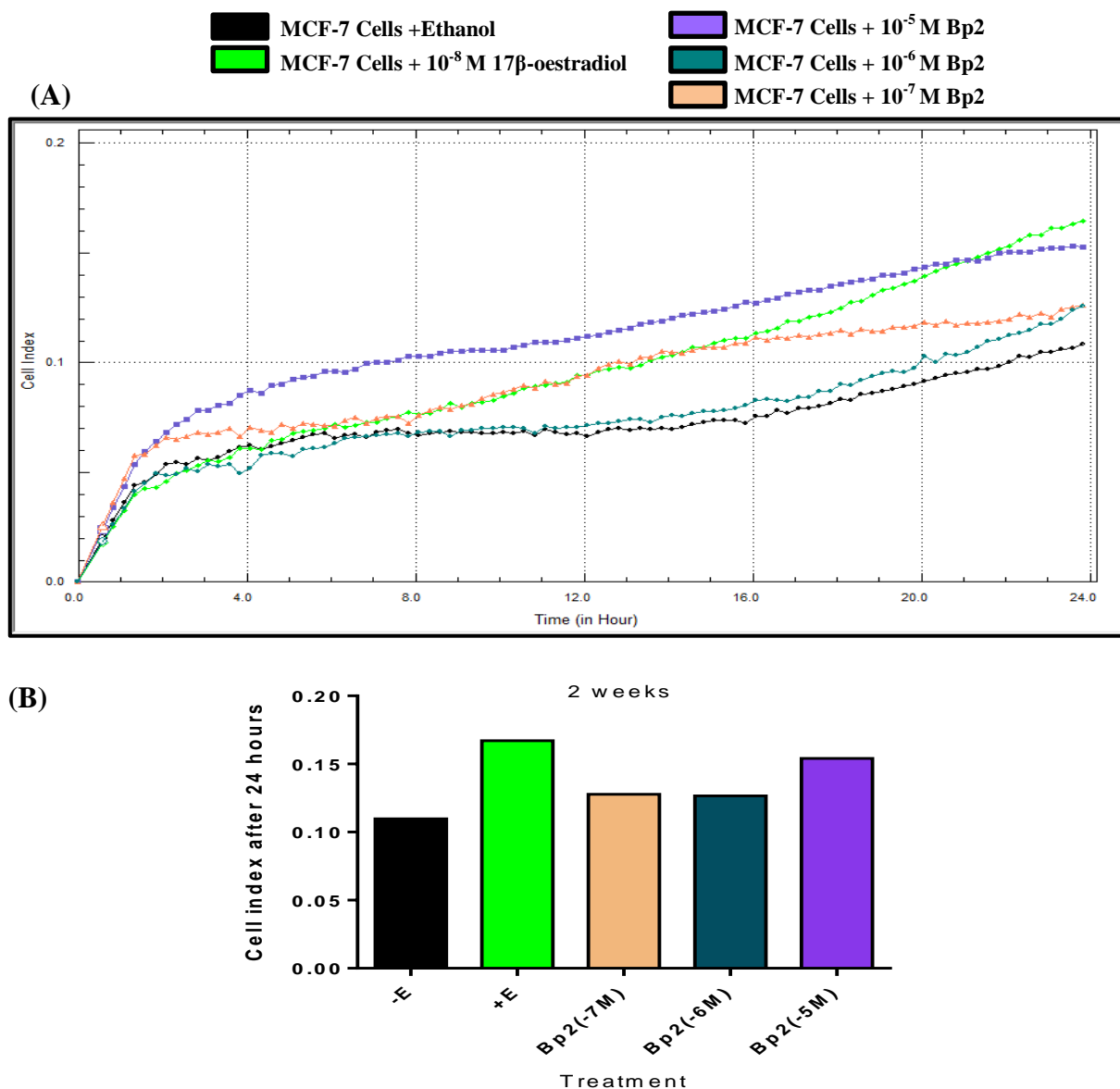


**Figure 4.10 Short-term effect of Bp2 or 17β-oestradiol on migration of MCF-7 human breast cancer cells using chemotaxis stimulus as determined by xCELLigence technology.**

Cells were grown in phenol-red-free-DMEM containing 5% DCFCS with ethanol control only (-E), 10<sup>-8</sup> M 17β-oestradiol (+E), 10<sup>-7</sup> M Bp2 (Bp2 (-7M)), 10<sup>-6</sup> M Bp2 (Bp2 (-6M)) or 10<sup>-5</sup> M Bp2 (Bp2 (-5M)) for 2 weeks. Media were replenished and cells were split every 3-4 days. (A) The relative change in cell index of duplicate wells as indicated by the changes in impedance caused by cell migration from upper chambers to lower ones through the pores of the polycarbonate membrane. Cell index was recorded every 5 minutes and monitored for 24 hours. (B) Bar graph represents the average of the end point measurements (Cell index) of cell migration of duplicate independent wells at 24 hours.

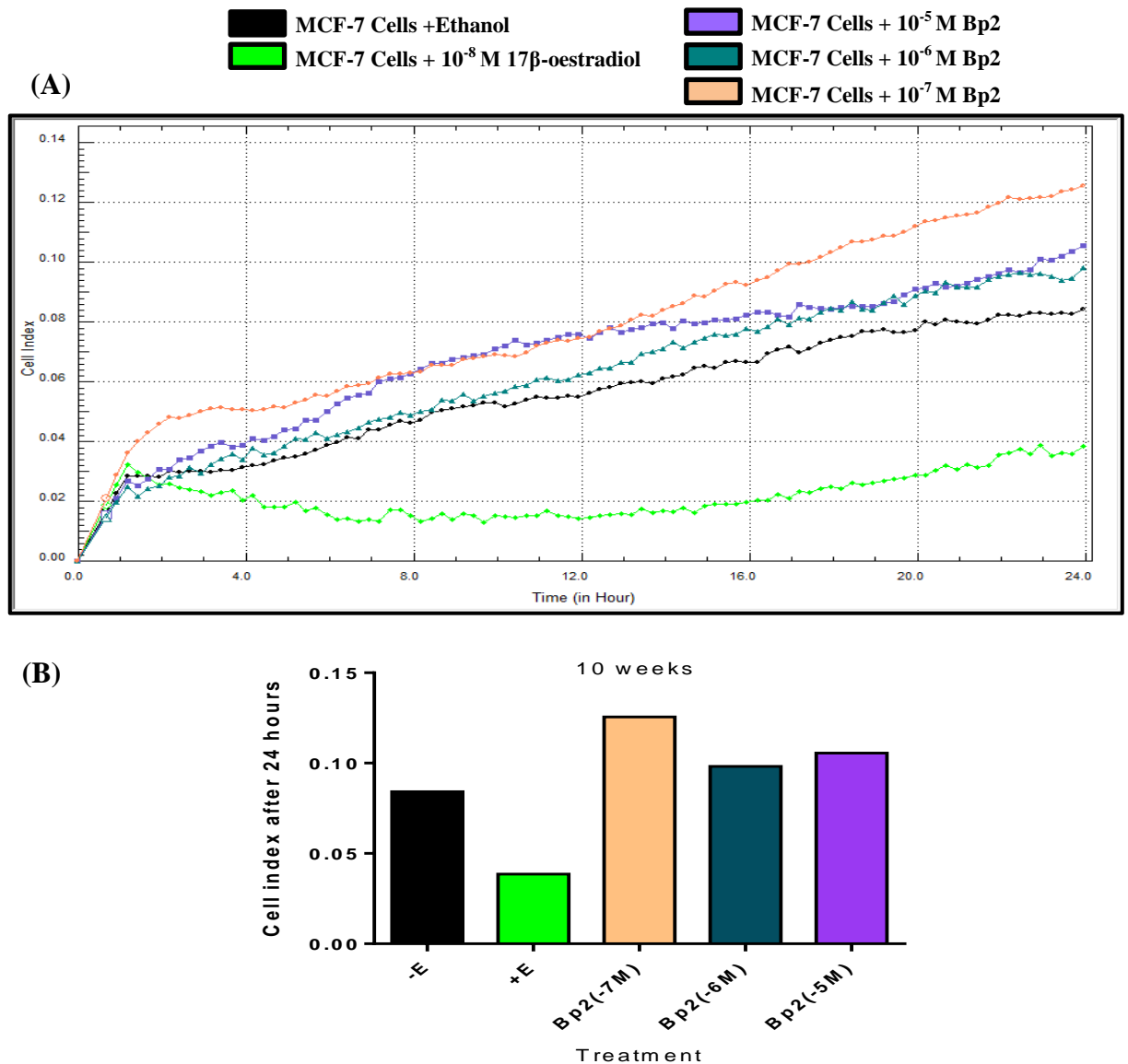


**Figure 4.11 Long-term effect of Bp2 or  $17\beta$ -oestradiol on migration of MCF-7 human breast cancer cells using chemotaxis stimulus as determined by xCELLigence technology.**

Cells were grown in phenol-red-free-DMEM containing 5% DCFCS with ethanol control only (-E),  $10^{-8}$  M  $17\beta$ -oestradiol (+E),  $10^{-7}$  M Bp2 (Bp2 (-7M)),  $10^{-6}$  M Bp2 (Bp2 (-6M)) or  $10^{-5}$  M Bp2 (Bp2 (-5M)) for 10 weeks. Media were replenished and cells were split every 3-4 days. (A) The relative change in cell index of duplicate wells as indicated by the changes in impedance caused by cell migration from upper chambers to lower ones through the pores of the polycarbonate membrane. Cell index was recorded every 5 minutes and monitored for 24 hours. (B) Bar graph represents the average of the end point measurements (Cell index) of cell migration of duplicate independent wells at 24 hours.

**Table 4.2 Effects of Bp2 on motility and invasion of MCF-7 human breast cancer cells**

Experiment	Molar concentration		Incubation time prior to the experiment
	10 <sup>-7</sup> M	10 <sup>-5</sup> M	
Wound healing	--	(**)	7 weeks
	n.s.	n.s.	13 weeks
	(***)	n.s.	21 weeks
Time-lapse	(*) in cumulative length moved	--	2 weeks
	(**) in cumulative length moved and in percentage of motile cells	n.s.	21 weeks
Real-time monitoring of cell motility (xCELLigence)	n.o.	O.	2 weeks
	O.	n.o.	10 weeks
	n.o.	n.o.	21 weeks
Real-time monitoring of cell invasion through matrigel ( xCELLigence)	n.s.	n.s.	2 weeks and 11 weeks
	--	n.s.	31 weeks

(--) experiment was not conducted; \*  $p$ -value  $\leq 0.05$  versus no addition; \*\*  $p$ -value  $\leq 0.01$  versus no addition; \*\*\*  $p$ -value  $\leq 0.001$  versus no addition; (n.s.)  $p$ -value  $> 0.05$  not significant; (O.) effect observed using duplicates only-no statistical analysis possible for duplicates; (n.o.) no effects observed using duplicates.

### **4.3.3 Effects of Bp3 on migration of MCF-7 human breast cancer cells**

#### **4.3.3.1 Effects of Bp3 on collective migration of MCF-7 human breast cancer cells as measured by wound healing**

The wound healing assay was used to determine the effect of long term exposure to Bp3 on motility of MCF-7 human breast cancer cells. Results showed that after 8 and 13 weeks of exposure to Bp3 no increase in the percentage of wound closure in comparison to the negative control was indicated. After 8 weeks of exposure,  $10^{-5}$  M Bp3 gave  $20.38 \pm 1.33$  % closure of the wound compared to  $19.80 \pm 0.66$  % in the negative control (Figure 4.12 (A)). After 13 weeks of exposure to  $10^{-5}$  M Bp3,  $26.03 \pm 2.78$  % closure of the wound was recorded, while the closure percentage was  $24.75 \pm 2.10$  % in the negative control (Figure 4.12 (B)). However, longer exposure time has shown that after 21 weeks of exposure to  $10^{-5}$  M Bp3 an increase in the wound healing activities ( $59.28 \pm 5.39$  %) in comparison to the negative control ( $24.75 \pm 0.68$  %) was recorded (Figure 4.12 (C)) ( $p$ -value  $\leq 0.01$ ). Similarly after 21 weeks of exposure,  $10^{-7}$  M Bp3 increased the wound closure to  $35.26 \pm 2.35$  % (Figure 4.12 (C)) ( $p$ -value  $\leq 0.01$ ) and that effect was not shown after 13 weeks of exposure.

#### **4.3.3.2 Effects of Bp3 on migration of individual MCF-7 human breast cancer cells as measured by time-lapse microscopy**

MCF-7 human breast cancer cells were exposed for 2 weeks and 21 weeks to  $10^{-5}$  M Bp3,  $10^{-7}$  M Bp3 or no addition. 48 hours prior the experiment, cells were re-seeded in 12-well plates and cell migration was analysed using time-lapse microscopy. 10 cells were tracked in 5 fields per well for 24 hours and the number of motile cells and cumulative length moved were measured for each treatment. MCF-7 cells exposed to  $10^{-7}$  M and  $10^{-5}$  M Bp3 for 2 weeks did not show significant increase in motile cell number or in the cumulative length moved by cells (Figure 4.13 (A and B)). While longer exposure to  $10^{-7}$  M Bp3 increased the number of motile cells statistically significantly up to  $14.67 \pm 0.33$  % in comparison to the negative control ( $6.00 \pm 2.08\%$ ) (Figure 4.13 (B)) ( $p$ -value  $< 0.05$ ), although the average of cumulative length moved was not different from the control (Figure 4.13 (C and D)).

#### **4.3.3.3 Effects of Bp3 on migration and invasion of MCF-7 human breast cancer cells as determined by xCELLigence technology**

MCF-7 cells were exposed to  $10^{-7}$  M Bp3,  $10^{-6}$  M Bp3,  $10^{-5}$  M Bp3,  $10^{-8}$  M  $17\beta$ -oestradiol or no addition for 3, 11, 21 and 23 weeks prior to the experiment. Results of 3 weeks of exposure to  $10^{-5}$  M Bp3 showed an increase in the motility of MCF-7 cells (cell index 0.11) in comparison to the negative control (cell index 0.05) (Figure 4.14) and longer exposure times to  $10^{-5}$  M Bp3 had a greater observed effect in increasing MCF-7 cells motility in comparison to the effect of 3 weeks of exposure (Figure 4.17). Similar increase in cell motility was observed after 11 and 21 weeks of exposure to  $10^{-7}$  M Bp3 and  $10^{-6}$  M Bp3 (Figures 4.15-4.16). MCF-7 cells exposed to  $10^{-5}$  M Bp3 showed an increase in cell motility (cell index  $0.20 \pm 0.03$ ) in comparison to the negative control (cell index  $0.09 \pm 0.02$ ) (Figure 4.17) ( $p$ -value  $\leq 0.05$ ).

According to ACEA application note no.6 (2013) and Roach technical support, lower cell index (negative signals) refers to lower dynamic range of cell behaviour (motility or cell adhesion). In figure 4.14, negative chemotactic cell index of  $17\beta$ -oestradiol reflects the lower activity in migration.

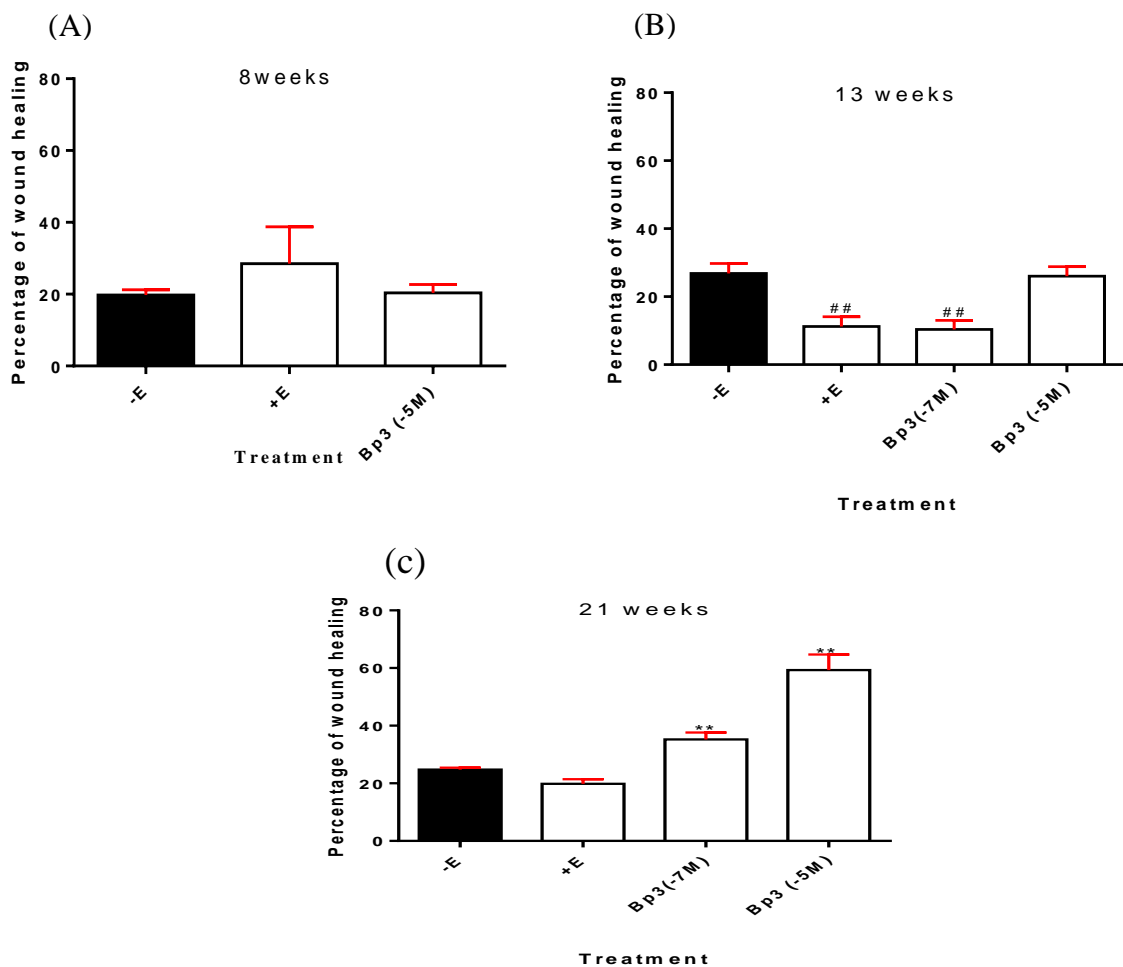


**Figure 4.12 Effect of exposure to Bp3 or 17 $\beta$ -oestradiol on collective motility of MCF-7 human breast cancer cells as measured by wound healing assay.**

Cells were grown in phenol-red-free-DMEM containing 5% DCFCS with ethanol control (-E) only,  $10^{-8}$  M 17 $\beta$ -oestradiol (+E), with  $10^{-7}$  M Bp3 (Bp3 (-7M)), or with  $10^{-5}$  M Bp3 (Bp3 (-5M)) for 8 (A), 13 weeks (B) and 21 weeks (C). Media were replenished and cells were split every 3-4 days. Cells were then reseeded in 12-well plates and once the cells became  $\geq 95\%$  confluent, wound was made and mitomycin c (0.5  $\mu$ g/ml) was added. Images were captured at 0 hour and 24 hours. Cell migration was quantified by analysing minimum 5 images from each well. (A) Values are the average  $\pm$  SE of triplicate wells of three independent experiments (n=3). (B and C) Values are the average  $\pm$  SE of triplicate independent wells. \*\* *p*-value  $\leq 0.01$  increase versus no addition. ## *p*-value  $\leq 0.01$  decrease versus no addition by one-way ANOVA Dunnett's test.

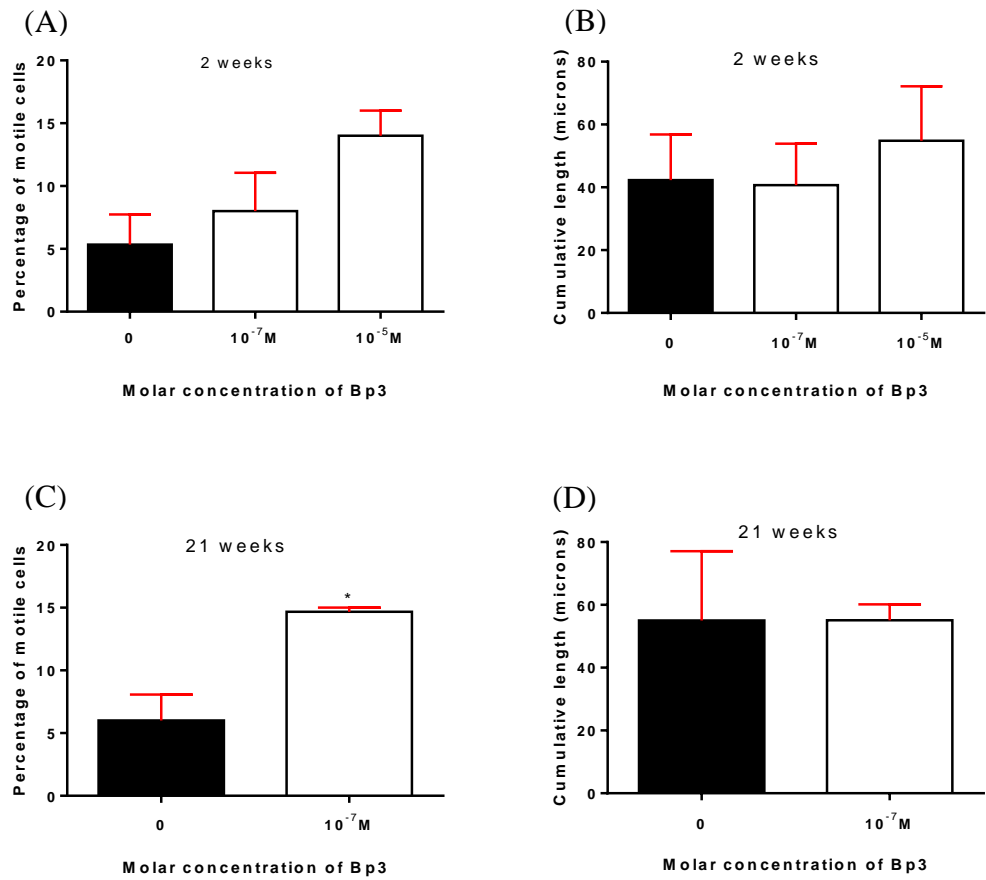


**Figure 4.13 Effect of exposure to Bp3 on motility of individual MCF-7 human breast cancer cells as determined by time-lapse microscopy.**

Cells were grown in phenol-red-free-DMEM containing 5% DCFCS with ethanol control (0) only or with Bp3 at indicated concentrations for 2 (A, B) and 21 weeks (C, D). Media were replenished and cells were split every 3-4 days. 2 days prior to the experiment, cells were reseeded in 12-well plate at  $0.2 \times 10^5$  cells/well. Time-lapse images of 5 fields per well were recorded. Results represent the percentage of motile cells (A, C) and cumulative length moved (B, D). Values are the average  $\pm$ SE of triplicate wells. \* *p-value*  $\leq 0.05$  versus no addition by t-Test (C and D).

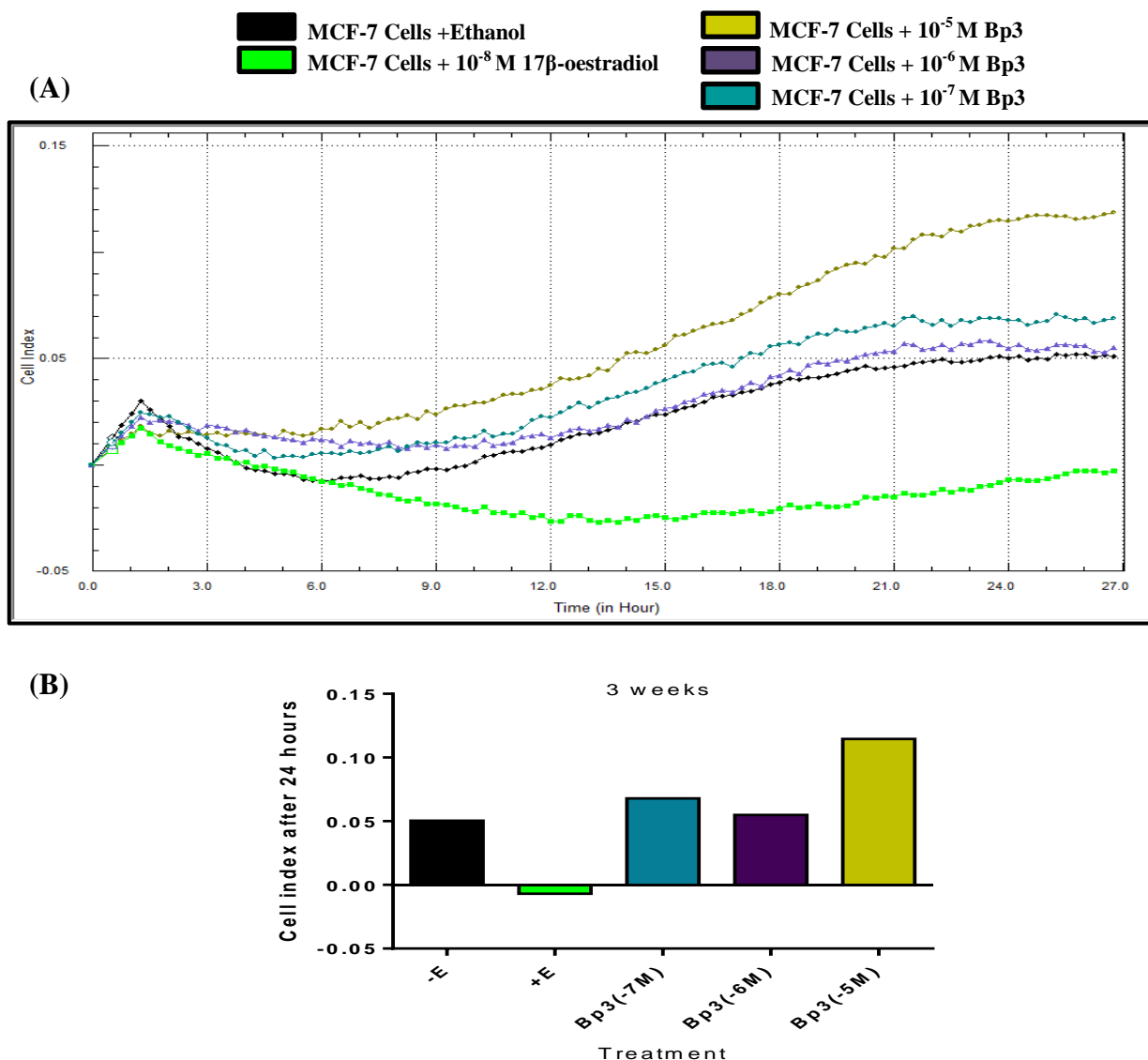


**Figure 4.14 Short-term effect of Bp3 or  $17\beta$ -oestradiol on migration of MCF-7 human breast cancer cells using chemotaxis stimulus as determined by xCELLigence technology.**

Cells were grown in phenol-red-free-DMEM containing 5% DCFCS with ethanol control only (-E),  $10^{-8}$  M  $17\beta$ -oestradiol (+E),  $10^{-7}$  M Bp3 (Bp3 (-7M)),  $10^{-6}$  M Bp3 (Bp3 (-6M)) or  $10^{-5}$  M Bp3 (Bp3 (-5M)) for 3 weeks. Media were replenished and cells were split every 3-4 days. (A) The relative change in cell index of duplicate wells as indicated by the changes in impedance caused by cell migration from upper chambers to lower ones through the pores of the polycarbonate membrane. Cell index was recorded every 5 minutes and monitored for 24 hours. (B) Bar graph represents the average of the end point measurements (Cell index) of cell migration of duplicate independent wells at 24 hours.

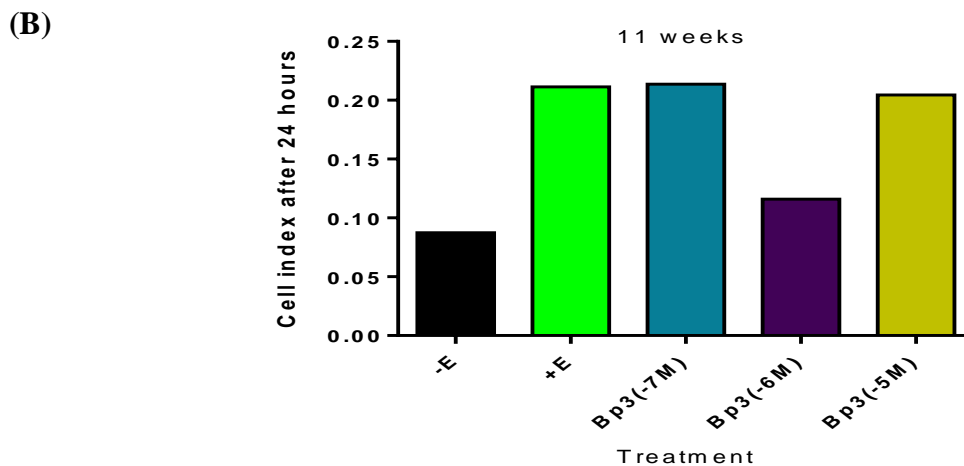
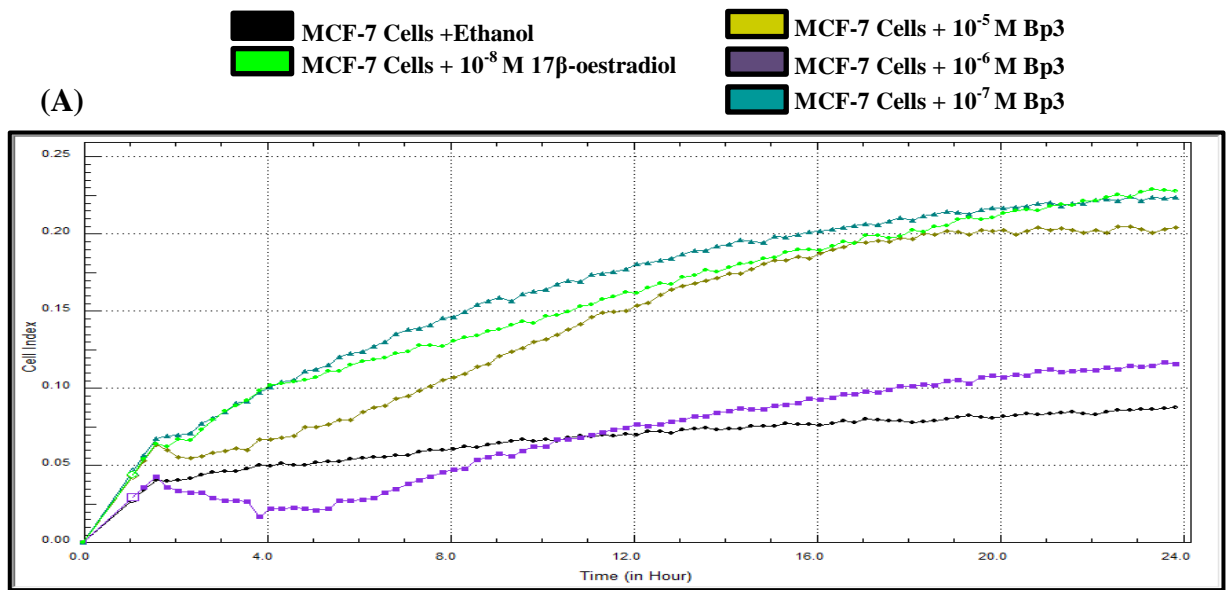


**Figure 4.15 Long-term effect of Bp3 or  $17\beta$ -oestradiol on migration of MCF-7 human breast cancer cells using chemotaxis stimulus as determined by xCELLigence technology.**

Cells were grown in phenol-red-free-DMEM containing 5% DCFCS with ethanol control only (-E),  $10^{-8}$  M  $17\beta$ -oestradiol (+E),  $10^{-7}$  M Bp3 (Bp3 (-7M)),  $10^{-6}$  M Bp3 (Bp2 (-6M)) or  $10^{-5}$  M Bp3 (Bp3 (-5M)) for 11 weeks. Media were replenished and cells were split every 3-4 days. (A) The relative change in cell index of duplicate wells as indicated by the changes in impedance caused by cell migration from upper chambers to lower ones through the pores of the polycarbonate membrane. Cell index was recorded every 5 minutes and monitored for 24 hours. (B) Bar graph represents the average of the end point measurements (Cell index) of cell migration of duplicate wells at 24 hours.

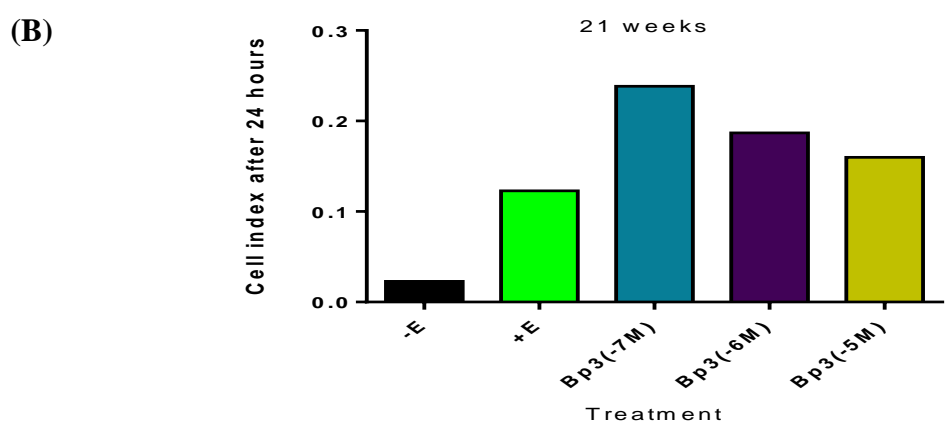
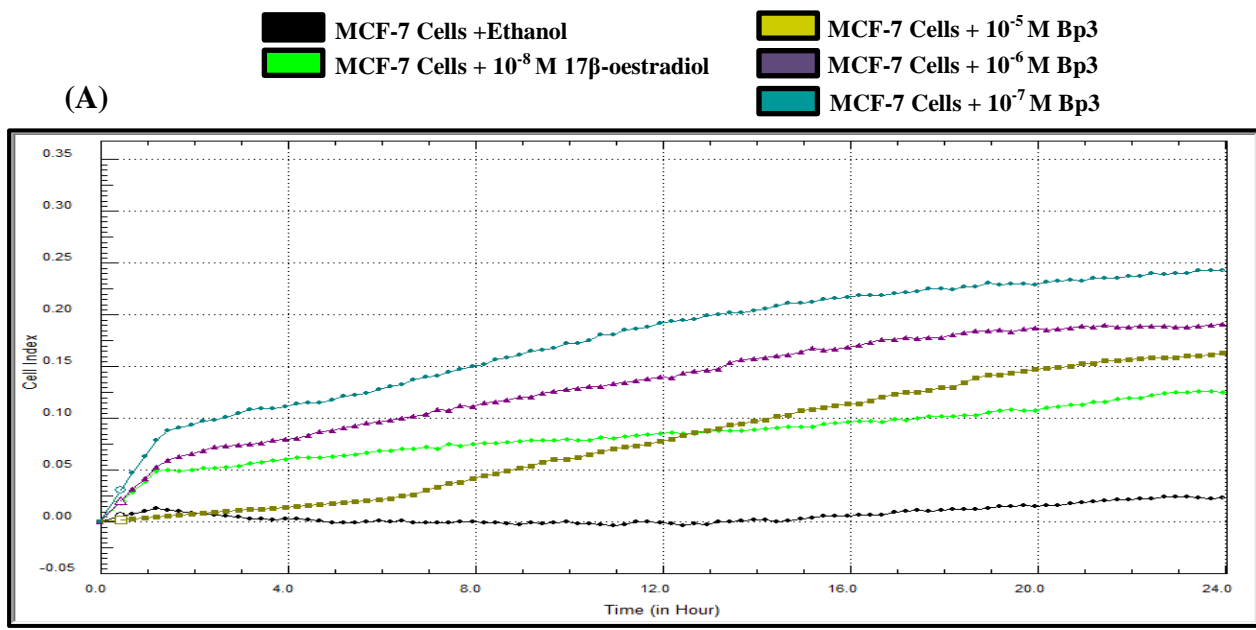


**Figure 4.16 Long-term effect of Bp3 or 17β-oestradiol on migration of MCF-7 human breast cancer cells using chemotaxis stimulus as determined by xCELLigence technology.**

Cells were grown in phenol-red-free-DMEM containing 5% DCFCS with ethanol control only (-E), 10<sup>-8</sup> M 17β-oestradiol (+E), 10<sup>-7</sup> M Bp3 (Bp3 (-7M)), 10<sup>-6</sup> M Bp3 (Bp3 (-6M)) or 10<sup>-5</sup> M Bp3 (Bp3 (-5M)) for 21weeks. Media were replenished and cells were split every 3-4 days. (A) The relative change in cell index of duplicate wells as indicated by the changes in impedance caused by cell migration from upper chambers to lower ones through the pores of the polycarbonate membrane. Cell index was recorded every 5 minutes and monitored for 24 hours. (B) Bar graph represents the average of the end point measurements (Cell index) of cell migration of duplicate independent wells at 24 hours.

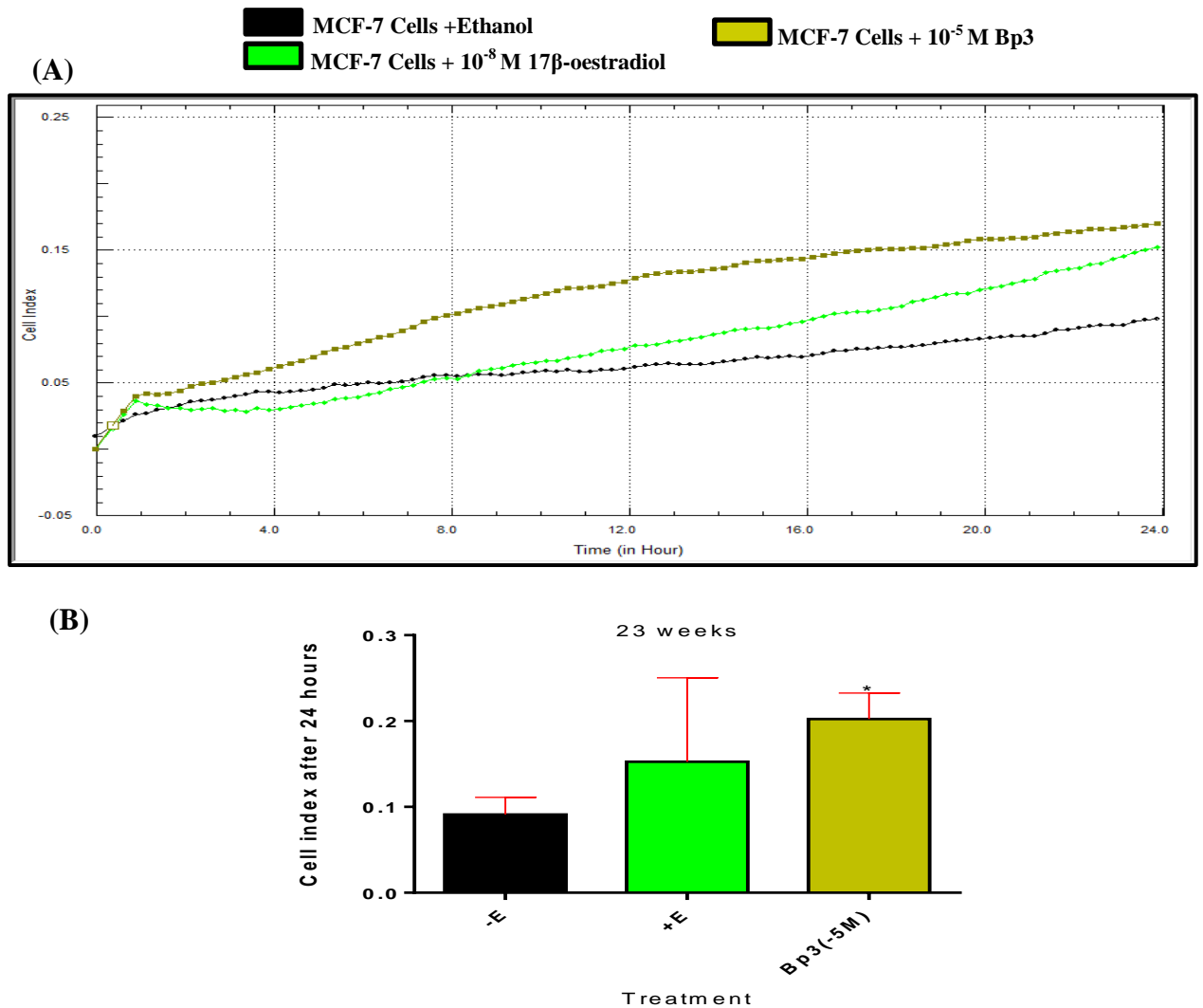


**Figure 4.17 Long-term effect of Bp3 or  $17\beta$ -oestradiol on migration of MCF-7 human breast cancer cells using chemotaxis stimulus as determined by xCELLigence technology.**

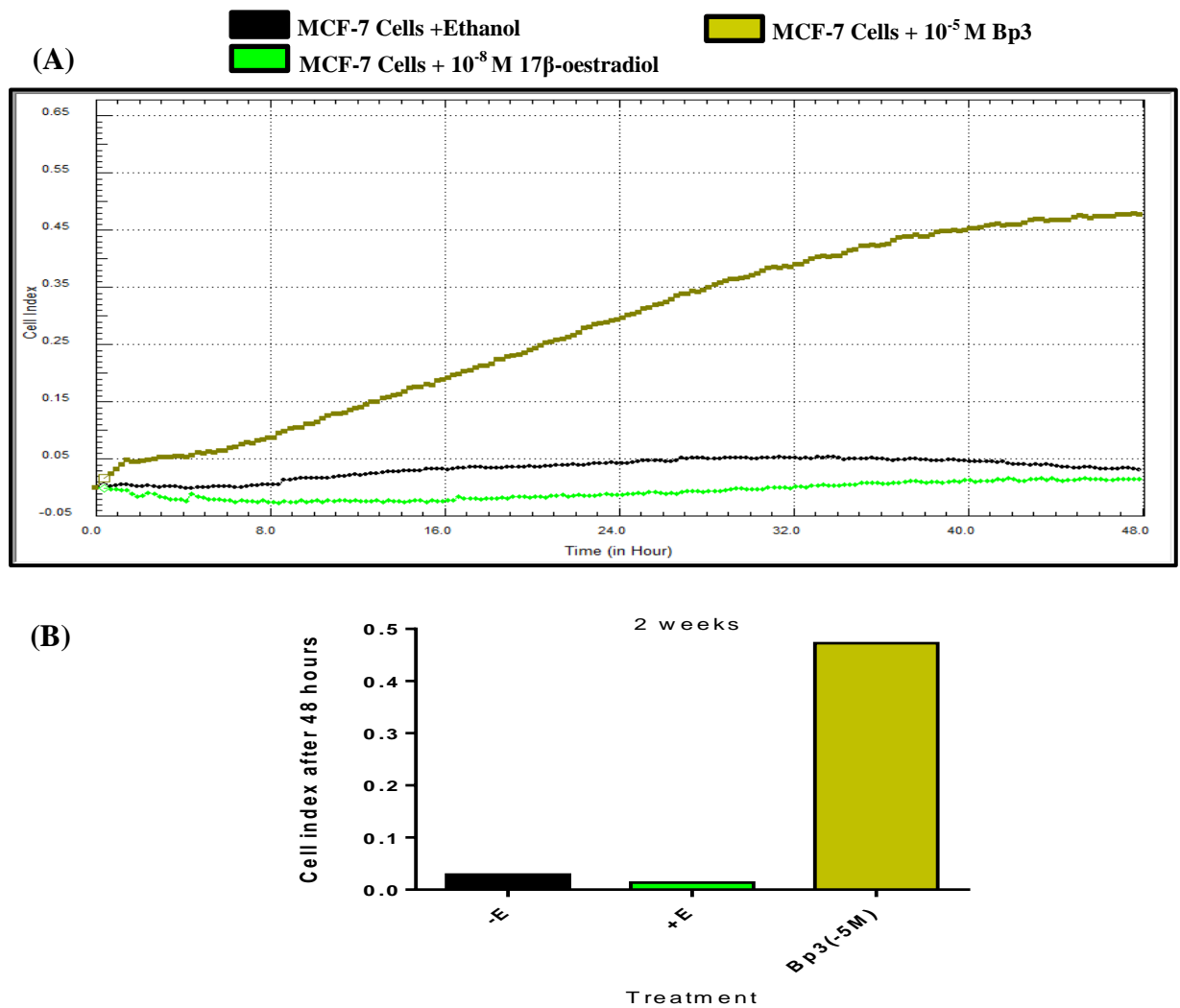
Cells were grown in phenol-red-free-DMEM containing 5% DCFCS with ethanol control only (-E),  $10^{-8}$  M  $17\beta$ -oestradiol (+E) or  $10^{-5}$  M Bp3 (Bp3 (-5M)) for 23 weeks. Media were replenished and cells were split every 3-4 days. (A) The relative change in cell index of triplicate wells as indicated by the changes in impedance caused by cell migration from upper chambers to lower ones through the pores of the polycarbonate membrane. Cell index was recorded every 5 minutes and monitored for 24 hours. (B) Bar graph represents the average of the end point measurements (Cell index) of cell migration of triplicate wells at 24 hours. Values are the average  $\pm$ SE of triplicate independent wells. \*  $p$ -value  $\leq$  0.05 versus no addition (-E) by one-way ANOVA Dunnett's test.

#### **4.3.3.4 Effects of Bp3 on invasion of MCF-7 human breast cancer cells as determined by xCELLigence technology**

Monitoring MCF-7 cell invasive activity in real-time using xCELLigence technology (as described previously in section 2.5) did show a clear increase in invasive activity of cells exposed to  $10^{-5}$  M Bp3 after 2 weeks of exposure (cell index 0.47) in comparison to the control cells (cell index 0.028) (Figure 4.18), which continued in a similar pattern after 11 weeks of exposure to  $10^{-7}$  M,  $10^{-6}$  M and  $10^{-5}$  M Bp3 (Figure 4.19). However, MCF-7 cells exposed to  $10^{-5}$  M Bp3 for 31 weeks showed no significant increase in invasive activity (data not shown).

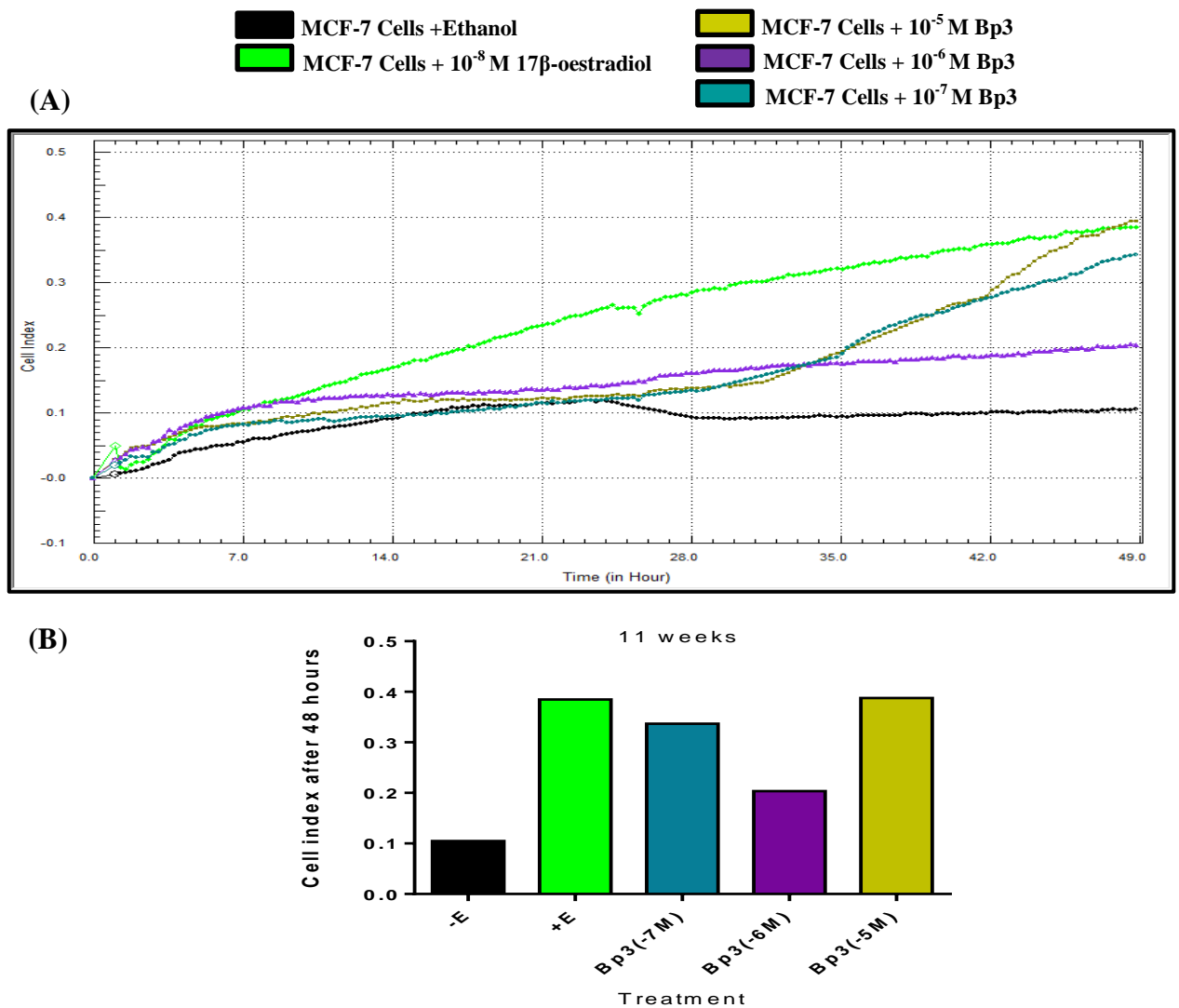
#### **4.3.3.5 Summary of effects with Bp3**

Table 4.2 summarises all the results in section 4.3.3. The results are shown as determined by wound healing, time-lapse microscopy and the xCELLigence technology after 2 weeks and longer time points of exposure to concentrations of  $10^{-7}$  M and  $10^{-5}$  M Bp3.



**Figure 4.18 Short-term effect of Bp3 or  $17\beta$ -oestradiol on invasion of MCF-7 human breast cancer cells through matrigel using chemotaxis stimulus as determined by xCELLigence technology.**

Cells were grown in phenol-red-free-DMEM containing 5% DCFCS with ethanol control only (-E),  $10^{-8}$  M  $17\beta$ -oestradiol (+E) or  $10^{-5}$  M Bp3 (Bp3 (-5M)) for 2 weeks. Media were replenished and cells were split every 3-4 days. Cells were analysed for their invasive activity through matrigel (1:40) coated CIM-plate 16 in a real time invasion assay (xCELLigence RTCA device) (A) The relative change in cell index of duplicate wells as indicated by the changes in impedance caused by cell migration from upper chambers to lower ones through the pores of the polycarbonate membrane coated with matrigel. Cell index was recorded every 5 minutes and monitored for 48 hours. (B) Bar graph represents the average of the end point measurements (Cell index) of cell invasion of duplicate independent wells at 48 hours.



**Figure 4.19 Long-term effect of Bp3 or 17 $\beta$ -oestradiol on invasion of MCF-7 human breast cancer cells through matrigel using chemotaxis stimulus as determined by xCELLigence technology.**

Cells were grown in phenol-red-free-DMEM containing 5% DCFCS with ethanol control only (-E), 10<sup>-8</sup> M 17 $\beta$ -oestradiol (+E), 10<sup>-7</sup> M Bp3 (Bp3 (-7M)), 10<sup>-6</sup> M Bp3 (Bp3 (-6M)) or 10<sup>-5</sup> M Bp3 (Bp3 (-5M)) for 11 weeks. Media were replenished and cells were split every 3-4 days. Cells were analysed for their invasive activity through matrigel (1:40) coated CIM-plate 16 in a real time invasion assay (xCELLigence RTCA device) (A) The relative change in cell index of duplicate wells as indicated by the changes in impedance caused by cell migration from upper chambers to lower ones through the pores of the polycarbonate membrane coated with matrigel. Cell index was recorded every 5 minutes and monitored for 48 hours. (B) Bar graph represents the average of the end point measurements (Cell index) of cell invasion of duplicate independent wells at 48 hours.

**Table 4.3 Effects of Bp3 on motility and invasion of MCF-7 human breast cancer cells**

Experiment	Molar concentration		Incubation time prior to the experiment
	10 <sup>-7</sup> M	10 <sup>-5</sup> M	
Wound healing	--	n.s.	7 weeks
	n.s.	n.s.	13 weeks
	(**)	(**)	21 weeks
Time-lapse	n.s.	n.s.	2 weeks
	(*) in cumulative length moved	--	21 weeks
Real-time monitoring of cell motility (xCELLigence)	n.o.	O.	2 weeks
	O.	O.	11 weeks
	O.	O.	21 weeks
	--	*	23 weeks
Real-time monitoring of cell invasion through matrigel (xCELLigence)	O.	O.	11 weeks
	--	n.s.	31 weeks

(--)  
experiment was not conducted; \*  $p$ -value  $\leq 0.05$  versus no addition; \*\*  $p$ -value  $\leq 0.01$  versus no addition; (n.s.)  $p$ -value  $> 0.05$  not significant; (O.) effect observed using duplicates only-no statistical analysis possible for duplicates; (n.o.) no effects observed using duplicates.

#### **4.3.4 Effects of OMC on migration of MCF-7 human breast cancer cells**

##### **4.3.4.1 Effects of OMC on collective migration of MCF-7 human breast cancer cells as measured by wound healing**

The wound healing assay was used to determine the effect of long term exposure to OMC on motility of MCF-7 human breast cancer cells. Results showed that after 7 weeks of exposure to  $10^{-5}$  M OMC the wound healing was higher than in the negative control.  $10^{-5}$  M OMC closed  $30.16 \pm 2.57$  % of the wound, while the closure percentage was  $14.64 \pm 2.10$  % in the negative control (Figure 4.20 (A)) ( $p$ -value  $\leq 0.001$ ). Longer exposure times after 13 weeks of exposure to  $10^{-5}$  M OMC and  $10^{-7}$  M OMC had shown reduced wound closure in comparison with the negative control (Figure 4.20 (B)). However, after 21 weeks of exposure to  $10^{-5}$  M OMC or  $10^{-7}$  M OMC, MCF-7 cells have shown an increase in the wound healing activities. Closure percentage of the wound in MCF-7 cells exposed to  $10^{-7}$  M OMC was  $35.13 \pm 0.79$  % and to  $10^{-5}$  M OMC was  $37.42 \pm 5.47$  % in comparison to  $24.75 \pm 0.68$  % closure in the negative control (Figure 4.20 (C)) ( $p$ -value  $\leq 0.001$ ).

##### **4.3.4.2 Effects of OMC on migration of individual MCF-7 human breast cancer cells as measured by time-lapse microscopy**

MCF-7 human breast cancer cells were exposed for 2 weeks and 21 weeks to  $10^{-5}$  M OMC,  $10^{-7}$  M OMC or no addition. 48 hours prior the experiment, cells were re-seeded in 12-well plates and cell migration was analysed using time-lapse microscopy. 10 cells were tracked in 5 fields per well for 24 hours and the number of motile cells and cumulative length moved were measured for each treatment. Results indicated a  $14.00 \pm 2.00$  % increase in % motile cells (Figure 4.21 (A)) ( $p$ -value  $\leq 0.05$ ) but no difference in cumulative length moved in MCF-7 cells exposed to  $10^{-5}$  M OMC or  $10^{-7}$  M OMC after 2 weeks (Figure 4.21 (B)). 21 weeks of exposure to  $10^{-7}$  M OMC showed no difference in the percentage of motile cells or in cumulative length moved by MCF-7 cells (Figure 4.21 (C and B)).

#### **4.3.4.3 Effects of OMC on migration of MCF-7 human breast cancer cells as determined by xCELLigence technology**

MCF-7 cells were exposed to  $10^{-5}$  M OMC,  $10^{-6}$  M OMC,  $10^{-7}$  M OMC,  $10^{-8}$  M  $17\beta$ -oestradiol or no addition for 2 weeks (Figure 4.22), 10 weeks (Figure 4.23), 21 weeks (Figure 4.24) or 23 weeks (Figure 4.25) prior to the experiment. Results of 2 weeks of exposure to OMC suggested that  $10^{-6}$  M OMC and  $10^{-5}$  M OMC increased the motility of MCF-7 cells (with cell index 0.15 and 0.25 respectively) in comparison to the negative control (cell index 0.03), while no difference in cell motility was indicated for cells exposed to the lowest concentration used  $10^{-7}$  M OMC (cell index 0.03) (Figure 4.22). However, results of 21 weeks of exposure to  $10^{-7}$  M OMC increased MCF-7 cells motility in comparison to the control (Figure 4.24). Although longer exposure (23 weeks) to  $10^{-5}$  M OMC showed significant increase in cell motility (cell index  $0.23 \pm 0.01$ ) in comparison to the control cells (cell index  $0.09 \pm 0.02$ ) (Figure 4.25) ( $p$ -value  $\leq 0.01$ ), the increase in cell index was similar to that of the cells exposed for 2 weeks to the same concentration of OMC (Figure 4.22).

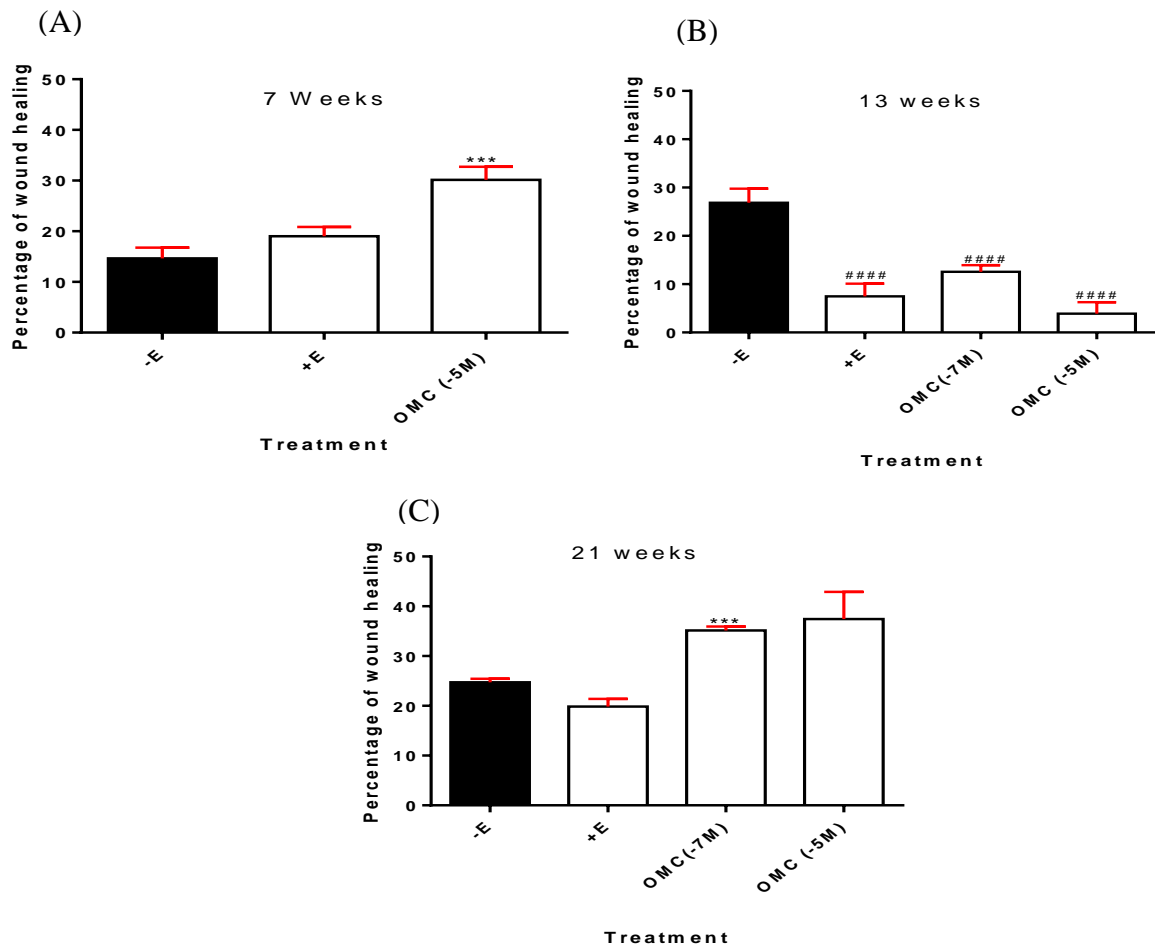


**Figure 4.20 Effect of exposure to OMC or 17 $\beta$ -oestradiol on collective motility of MCF-7 human breast cancer cells as measured by wound healing assay.**

Cells were grown in phenol-red-free-DMEM containing 5% DCFCS with ethanol control (-E) only, 10<sup>-8</sup> M 17 $\beta$ -oestradiol (+E), with 10<sup>-7</sup> M OMC (OMC (-7M)) or with 10<sup>-5</sup> M OMC (OMC (-5M)) for 7 weeks (A), 13 weeks (B) and 21 weeks (C). Media were replenished and cells were split every 3-4 days. Cells were then reseeded in 12-well plates and once the cells became  $\geq 95\%$  confluent, wound was made and mitomycin c (0.5  $\mu\text{g/ml}$ ) was added. Images were captured at 0 hour and 24 hours. Cell migration was quantified by analysing minimum 5 images from each well. (A) Values are the average  $\pm$  SE of triplicate wells of three independent experiments (n=3). (B and C) Values are the average  $\pm$  SE of triplicate independent wells. \*\*\* *p*-value  $\leq 0.001$  increase versus no addition and #### *p*-value  $\leq 0.0001$  decrease versus no addition by one-way ANOVA Dunnett's test.

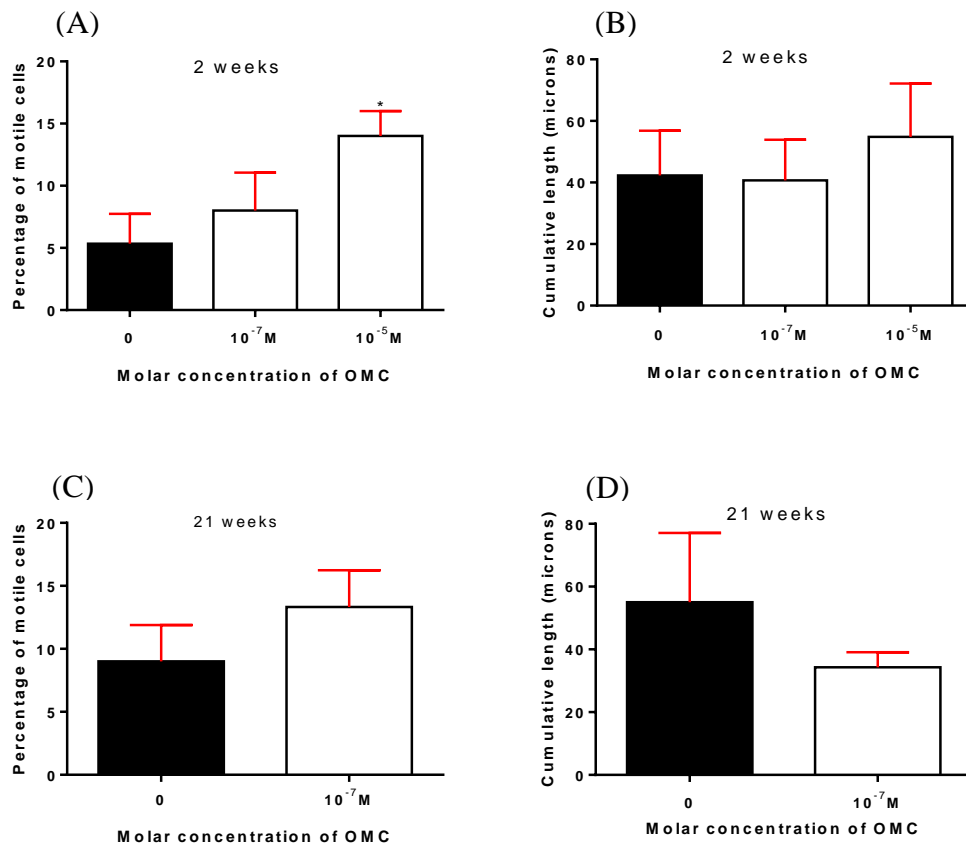


**Figure 4.21 Effect of exposure to OMC on motility of individual MCF-7 human breast cancer cells as determined by time-lapse microscopy.**

Cells were grown in phenol-red-free-DMEM containing 5% DCFCS with ethanol control (0) only or with OMC at indicated concentrations for 2 (A, B) and 21 weeks (C, D). Media were replenished and cells were split every 3-4 days. 2 days prior to the experiment, cells were reseeded in 12-well plates at  $0.2 \times 10^5$  cells/well. Time-lapse images of 5 fields per well were recorded. Results represent the percentage of motile cells (A, C) and cumulative length moved (B, D). Values are the average  $\pm$ SE of triplicate independent wells. \*  $p$ -value  $\leq 0.05$  versus no addition by one-way ANOVA Dunnett's test (A).

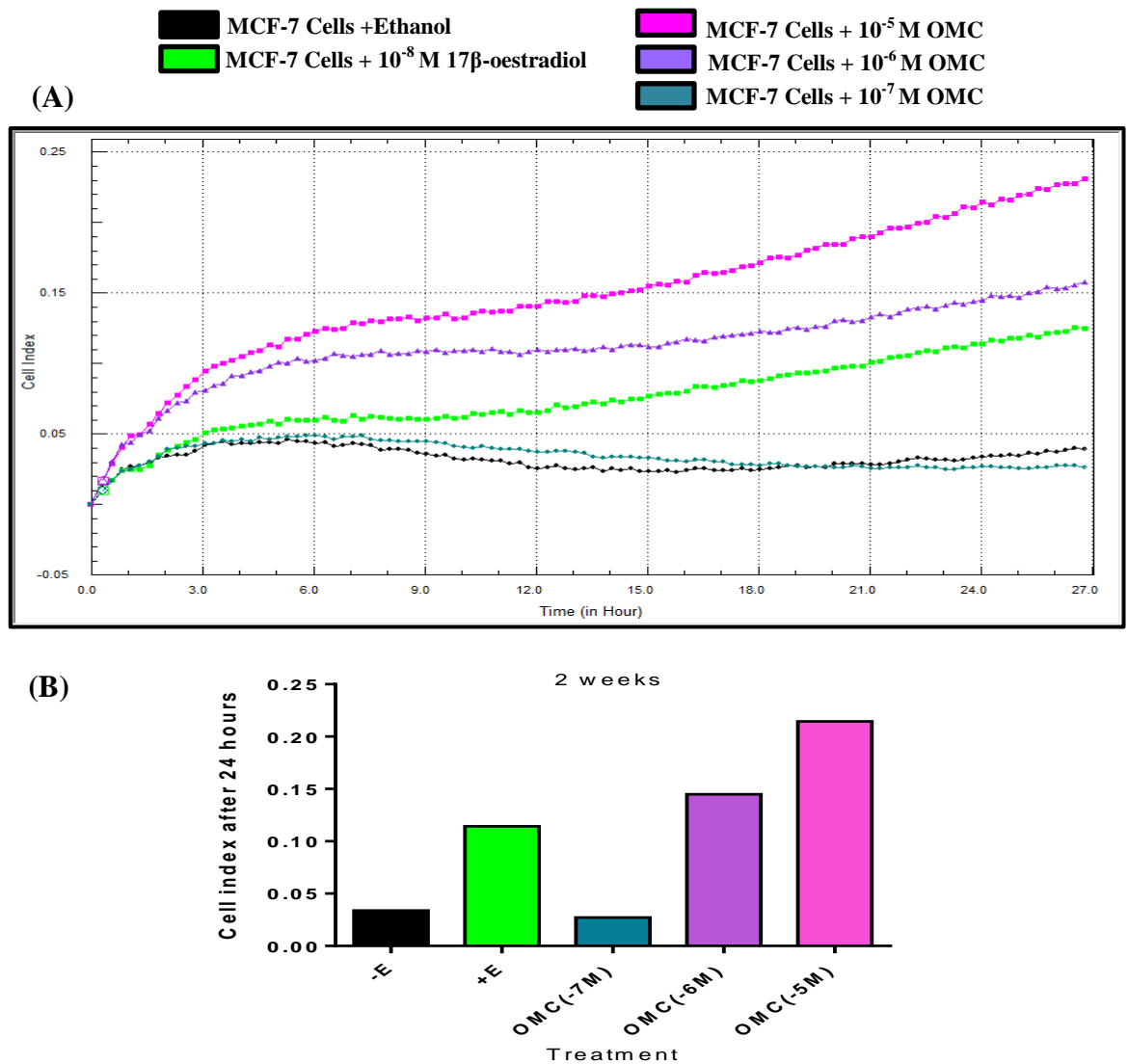


**Figure 4.22 Short-term effect of OMC or  $17\beta$ -oestradiol on migration of MCF-7 human breast cancer cells using chemotaxis stimulus as determined by xCELLigence technology.**

Cells were grown in phenol-red-free-DMEM containing 5% DCFCs with ethanol control only (-E),  $10^{-8}$  M  $17\beta$ -oestradiol (+E),  $10^{-7}$  M OMC (OMC (-7M)),  $10^{-6}$  M OMC (OMC (-6M)) or  $10^{-5}$  M OMC (OMC (-5M)) for 2 weeks. Media were replenished every 3-4 days. (A) The relative change in cell index of duplicate wells as indicated by the changes in impedance caused by cell migration from upper chambers to lower ones through the pores of the polycarbonate membrane. Cell index was recorded every 5 minutes and monitored for 24 hours. (B) Bar graph represents the average of the end point measurements (Cell index) of cell migration of duplicate independent wells at 24 hours.

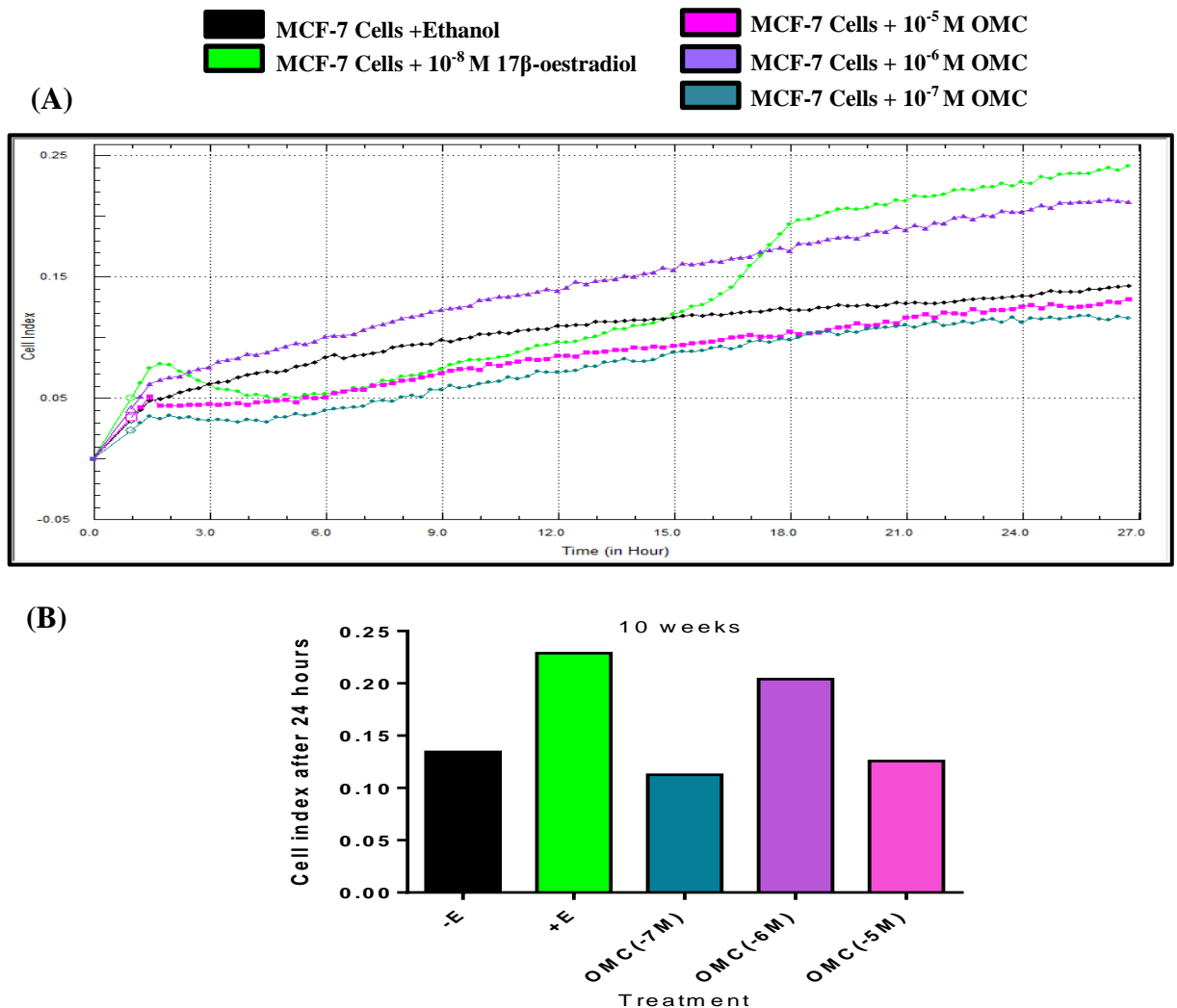


**Figure 4.23 Long-term effect of OMC or 17 $\beta$ -oestradiol on migration of MCF-7 human breast cancer cells using chemotaxis stimulus as determined by xCELLigence technology.**

Cells were grown in phenol-red-free-DMEM containing 5% DCFCS with ethanol control only (-E), 10<sup>-8</sup> M 17 $\beta$ -oestradiol (+E), 10<sup>-7</sup> M OMC (OMC (-7M)), 10<sup>-6</sup> M OMC (OMC (-6M)) or 10<sup>-5</sup> M OMC (OMC (-5M)) for 10 weeks. Media were replenished and cells were split every 3-4 days. (A) The relative change in cell index of duplicate wells as indicated by the changes in impedance caused by cell migration from upper chambers to lower ones through the pores of the polycarbonate membrane. Cell index was recorded every 5 minutes and monitored for 24 hours. (B) Bar graph represents the average of the end point measurements (Cell index) of cell migration of duplicate independent wells at 24 hours.

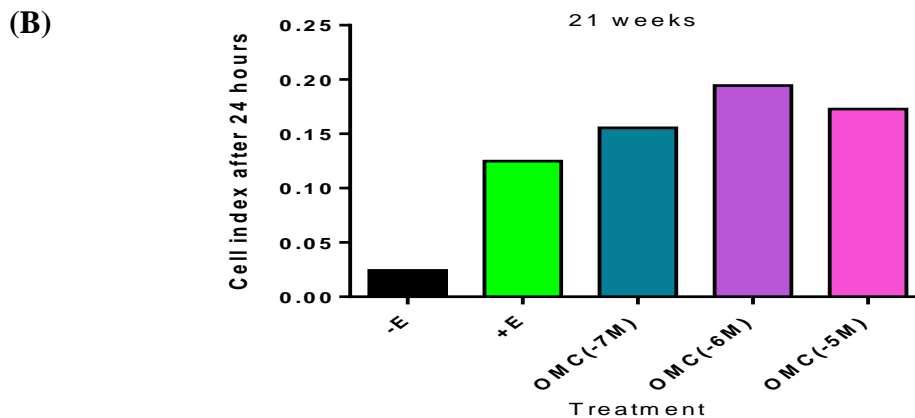
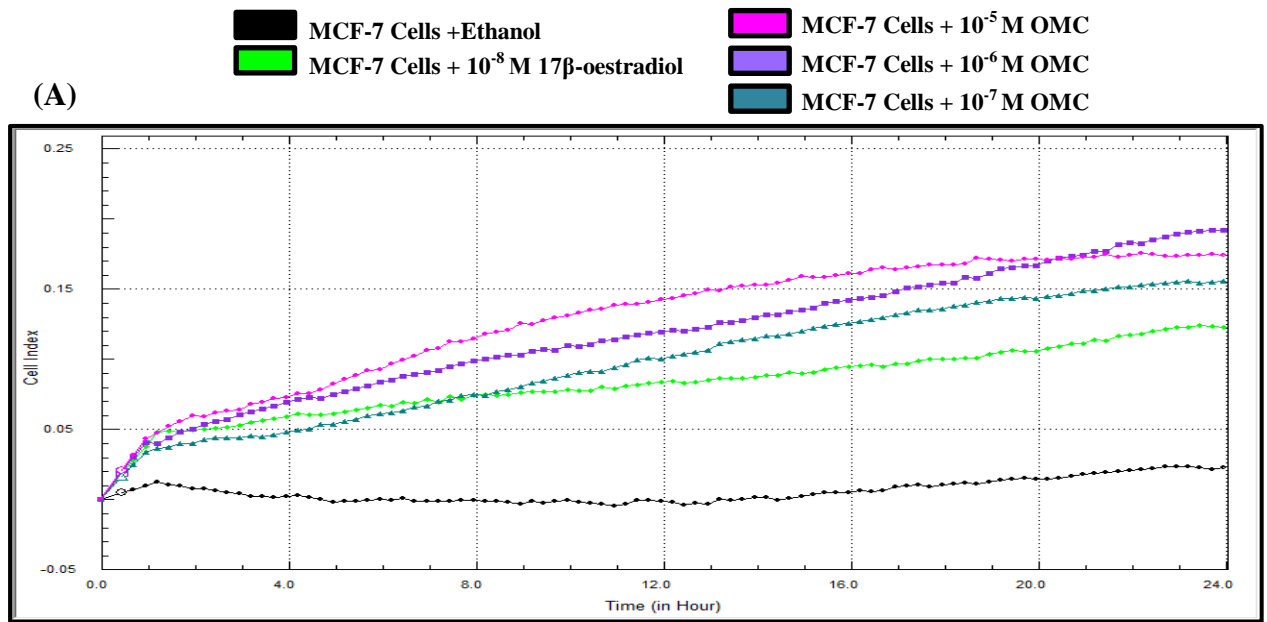


**Figure 4.24 Long-term effect of OMC or  $17\beta$ -oestradiol on migration of MCF-7 human breast cancer cells using chemotaxis stimulus as determined by xCELLigence technology.**

Cells were grown in phenol-red-free-DMEM containing 5% DCFCS with ethanol control only (-E),  $10^{-8}$  M  $17\beta$ -oestradiol (+E),  $10^{-7}$  M OMC (OMC (-7M)),  $10^{-6}$  M OMC (OMC (-6M)) or  $10^{-5}$  M OMC (OMC (-5M)) for 21 weeks. Media were replenished and cells were split every 3-4 days. (A) The relative change in cell index of duplicate wells as indicated by the changes in impedance caused by cell migration from upper chambers to lower ones through the pores of the polycarbonate membrane. Cell index was recorded every 5 minutes and monitored for 24 hours. (B) Bar graph represents the average of the end point measurements (Cell index) of cell migration of duplicate independent wells at 24 hours.

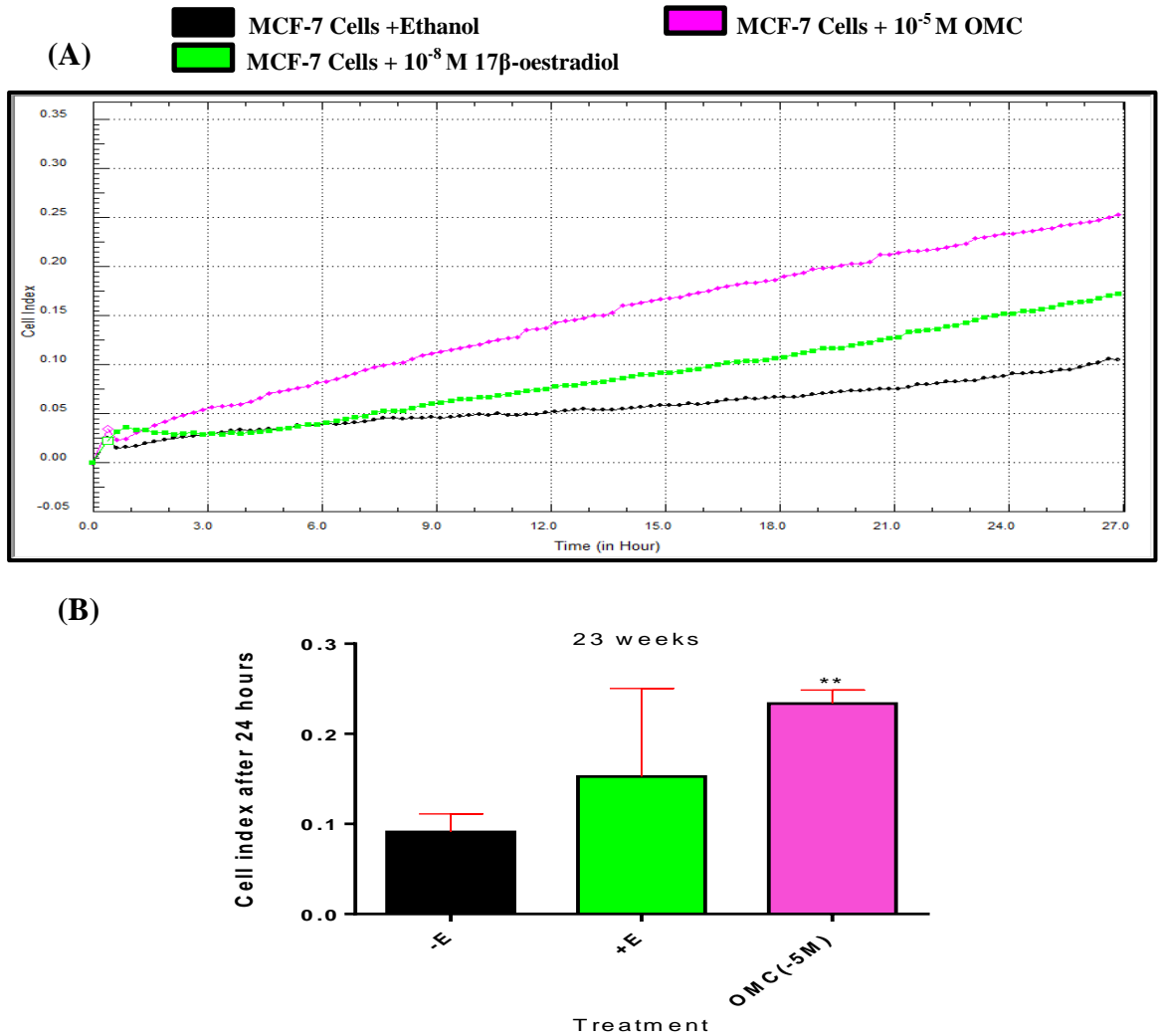


**Figure 4.25 Long-term effect of OMC or  $17\beta$ -oestradiol on migration of MCF-7 human breast cancer cells using chemotaxis stimulus as determined by xCELLigence technology.**

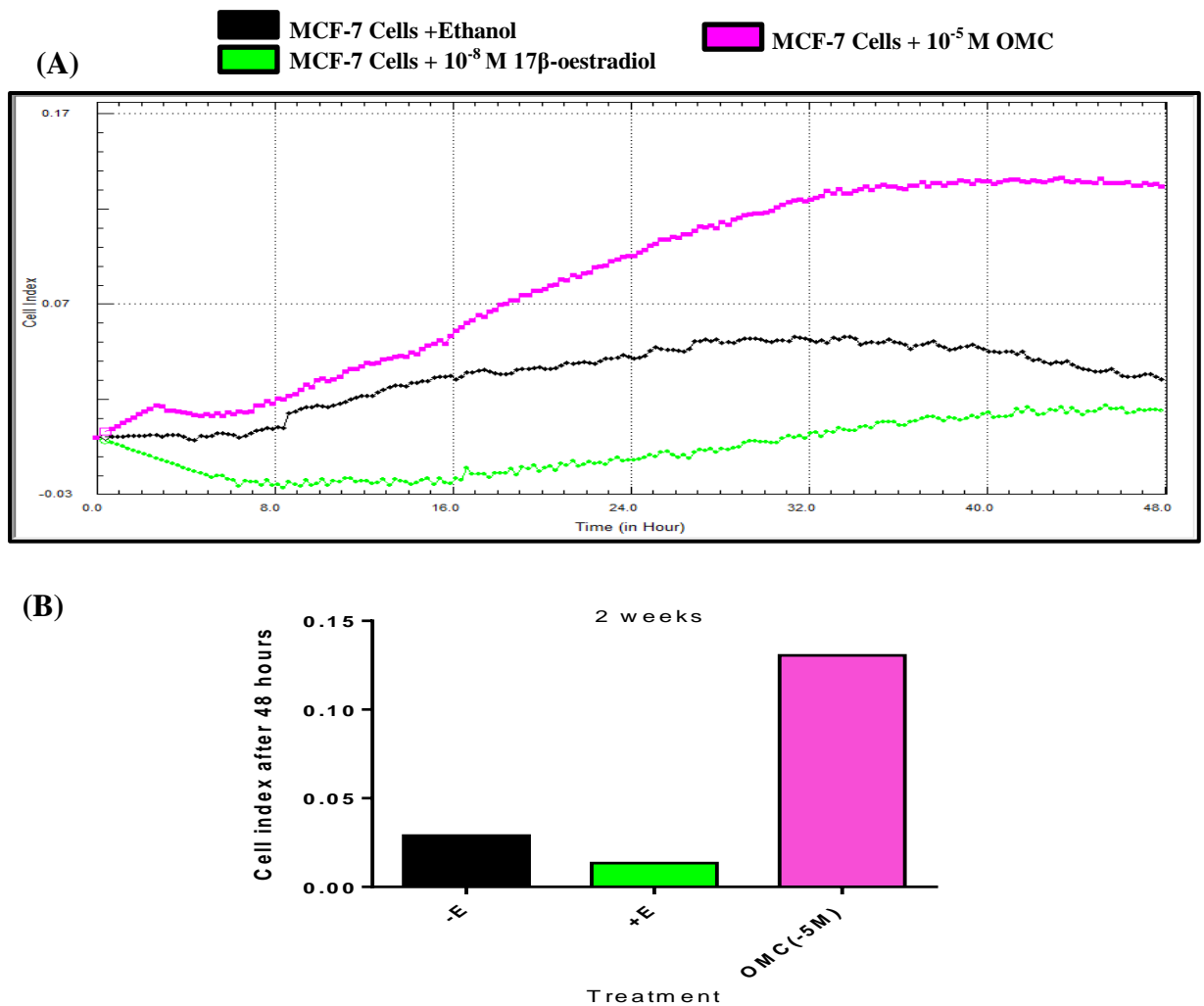
Cells were grown in phenol-red-free-DMEM containing 5% DCFCS with ethanol control only (-E),  $10^{-8}$  M  $17\beta$ -oestradiol (+E) or  $10^{-5}$  M OMC (OMC (-5M)) for 23 weeks. Media were replenished and cells were split every 3-4 days. (A) The relative change in cell index of triplicate wells as indicated by the changes in impedance caused by cell migration from upper chambers to lower ones through the pores of the polycarbonate membrane. Cell index was recorded every 5 minutes and monitored for 24 hours. (B) Bar graph represents the average of the end point measurements (Cell index) of cell migration of triplicate wells at 24 hours. Values are the average  $\pm$ SE of triplicate independent wells. \*\* *p*-value  $\leq 0.01$  versus no addition by one-way ANOVA Dunnett's test.

#### **4.3.4.4 Effects of OMC on invasion of MCF-7 human breast cancer cells as determined by xCELLigence technology**

Further investigation was carried out to observe the effect of OMC on the invasive activity of MCF-7 cells (as described in section 2.5). MCF-7 cells showed an increase in the invasive activity through matrigel after 2 weeks of exposure to  $10^{-5}$  M OMC (cell index 0.13) compared to the activity shown by the negative control cells (cell index 0.03) (Figure 4.26) and kept a similar increase with a cell index 0.21 after 10 weeks of exposure in comparison to the no addition cells (cell index 0.01) (Figure 4.27) and further exposure to  $10^{-5}$  M OMC for 31 weeks significantly increased the cell index ( $0.18 \pm 0.03$ ) of MCF-7 cells compared to the no addition cells ( $-0.08 \pm 0.02$ ) (Figure 4.28) ( $p$ -value  $\leq 0.01$ ). Lower cell index (negative signals) refers to lower dynamic range of cell invasion (ACEA application note no.6, 2013 ; Eisenberg et al., 2011). In figure 4.28, negative chemotactic cell index of the control cells and  $17\beta$ -oestradiol reflects the lower invasion through matrigel.

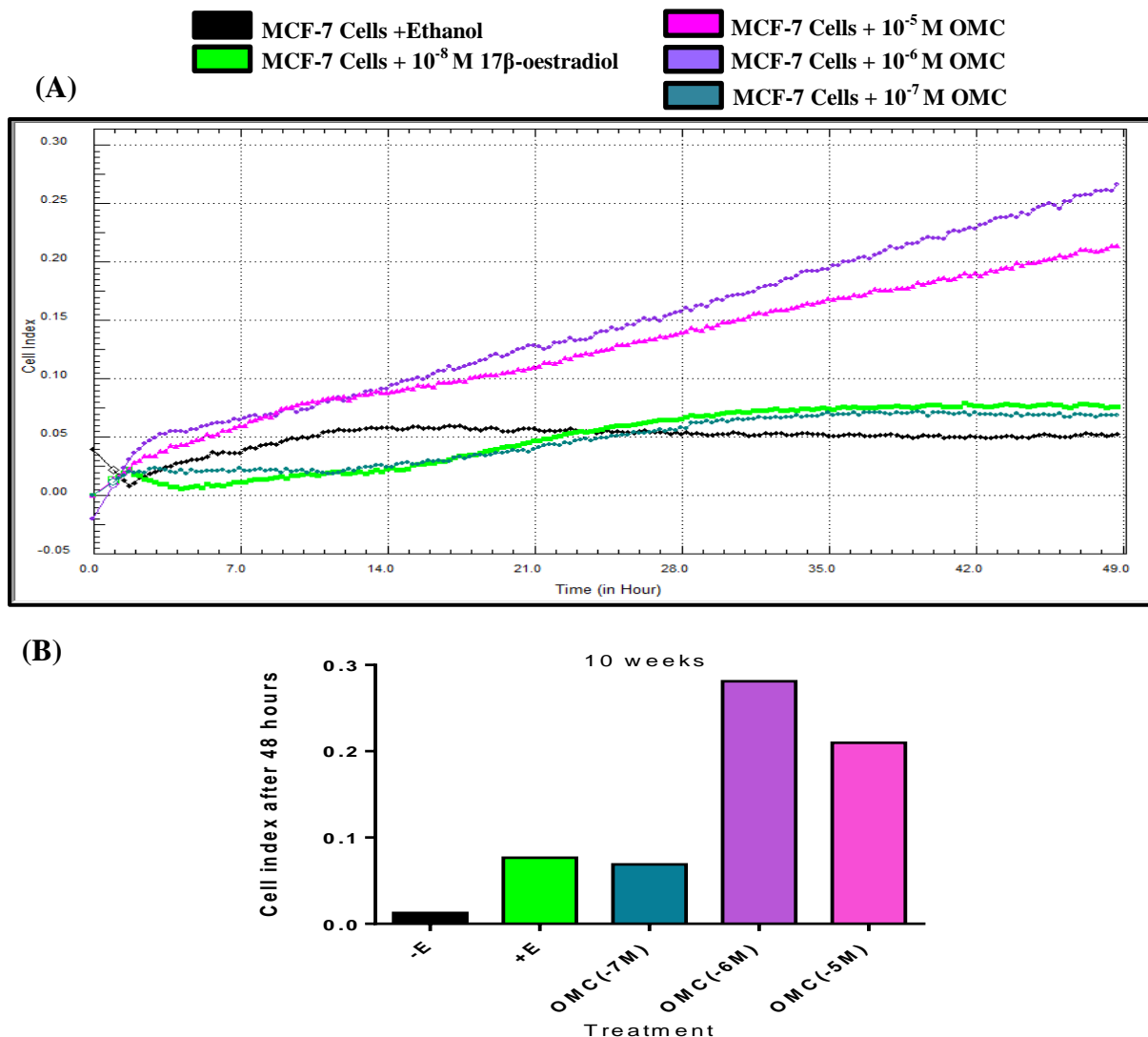
#### **4.3.4.5 Summary of effects with OMC**

Table 4.2 summarises all the results in section 4.3.4. The results are shown as determined by wound healing, time-lapse microscopy and the xCELLigence technology after 2 weeks and longer time points of exposure to concentrations of  $10^{-7}$  M and  $10^{-5}$  M OMC.



**Figure 4.26 Short-term effect of OMC or  $17\beta$ -oestradiol on invasion of MCF-7 human breast cancer cells through matrigel using chemotaxis stimulus as determined by xCELLigence technology.**

Cells were grown in phenol-red-free-DMEM containing 5% DCFCS with ethanol control only (-E),  $10^{-8}$  M  $17\beta$ -oestradiol (+E) or  $10^{-5}$  M OMC (OMC (-5M)) for 2 weeks. Media were replenished every 3-4 days. Cells were analysed for their invasive activity through matrigel (1:40) coated CIM-plate 16 in a real time invasion assay (xCELLigence RTCA device) (A) The relative change in cell index of duplicate wells as indicated by the changes in impedance caused by cell migration from upper chambers to lower ones through the pores of the polycarbonate membrane coated with matrigel. Cell index was recorded every 5 minutes and monitored for 48 hours. (B) Bar graph represents the average of the end point measurements (Cell index) of cell invasion of duplicate independent wells at 48 hours.



**Figure 4.27 Long-term effect of OMC or  $17\beta$ -oestradiol on invasion of MCF-7 human breast cancer cells through matrigel using chemotaxis stimulus as determined by xCELLigence technology.**

Cells were grown in phenol-red-free-DMEM containing 5% DCFCS with ethanol control only (-E),  $10^{-8}$  M  $17\beta$ -oestradiol (+E),  $10^{-7}$  M OMC (OMC (-7M)),  $10^{-6}$  M OMC (OMC (-6M)) or  $10^{-5}$  M OMC (OMC (-5M)) for 10 weeks. Media were replenished and cells were split every 3-4 days. Cells were analysed for their invasive activity through matrigel (1:40) coated CIM-plate 16 in a real time invasion assay (xCELLigence RTCA device) (A) The relative change in cell index of duplicate wells as indicated by the changes in impedance caused by cell migration from upper chambers to lower ones through the pores of the polycarbonate membrane coated with matrigel. Cell index was recorded every 5 minutes and monitored for 48 hours. (B) Bar graph represents the average of the end point measurements (Cell index) of cell invasion of duplicate independent wells at 48 hours.

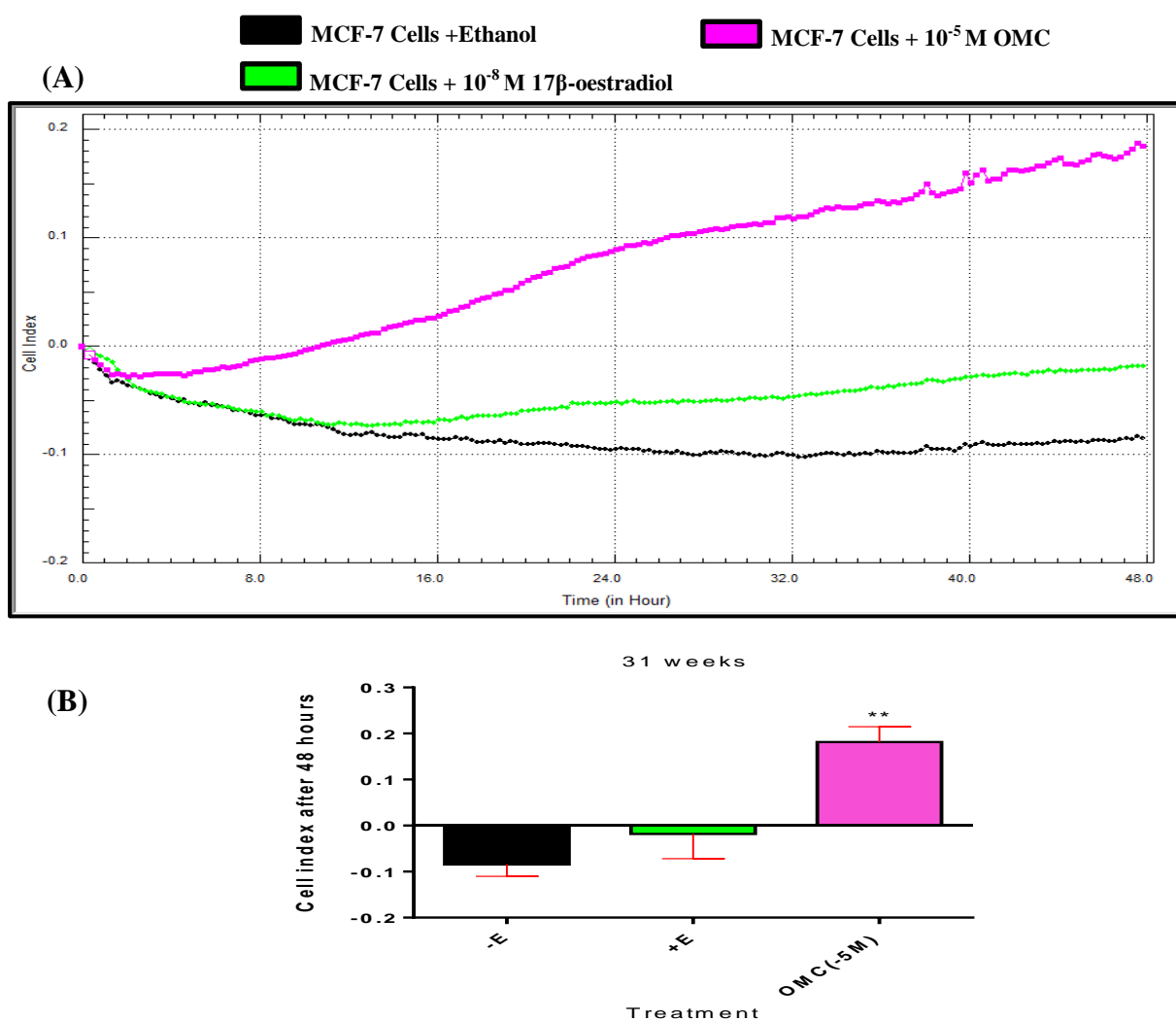


**Figure 4.28 Long-term effect of OMC or  $17\beta$ -oestradiol on invasion of MCF-7 human breast cancer cells through matrigel using chemotaxis stimulus as determined by xCELLigence technology.**

Cells were grown in phenol-red-free-DMEM containing 5% DCFCS with ethanol control only (-E),  $10^{-8}$  M  $17\beta$ -oestradiol (+E) or  $10^{-5}$  M OMC (OMC (-5M)) for 31 weeks. Media were replenished and cells were split every 3-4 days. Cells were analysed for their invasive activity through matrigel (1:40) coated CIM-plate 16 in a real time invasion assay (xCELLigence RTCA device) (A) The relative change in cell index of triplicate wells as indicated by the changes in impedance caused by cell migration from upper chambers to lower ones through the pores of the polycarbonate membrane coated with matrigel. Cell index was recorded every 5 minutes and monitored for 48 hours. (B) Bar graph represents the average of the end point measurements (Cell index) of cell invasion of triplicate wells at 48 hours. Values are the average  $\pm$  SE of triplicate independent wells. \*\*  $p$ -value  $\leq 0.01$  versus no addition by one-way ANOVA Dunnett's test.

**Table 4.4 Effects of OMC on motility and invasion of MCF-7 human breast cancer cells**

Experiment	Molar concentration		Incubation time prior to the experiment
	10 <sup>-7</sup> M	10 <sup>-5</sup> M	
Wound healing	--	(***)	7 weeks
	(####)	(####)	13 weeks
	(***)	n.s.	21 weeks
Time-lapse	n.s.	(*) in percentage of motile cells	2 weeks
	n.s.	--	21 weeks
Real-time monitoring of cell motility (xCELLigence)	n.o.	O.	2 weeks
	n.o.	n.o.	10 weeks
	O.	O.	21 weeks
	--	(**)	23 weeks
Real-time monitoring of cell invasion through matrigel (xCELLigence)	n.o.	O.	2 and 10 weeks
	--	(**)	31 weeks

(--) experiment was not conducted; \*  $p$ -value  $\leq 0.05$  increase versus no addition; \*\*  $p$ -value  $\leq 0.01$  increase versus no addition; \*\*\*  $p$ -value  $\leq 0.001$  increase versus no addition; ####  $p$ -value  $\leq 0.0001$  decrease versus no addition; (n.s.)  $p$ -value  $> 0.05$  not significant; (O.) effect observed using duplicates only-no statistical analysis possible for duplicates; (n.o.) no effects observed using duplicates.

### **4.3.5 Effects of 4MBC on migration of MCF-7 human breast cancer cells**

#### **4.3.5.1 Effects of 4MBC on collective migration of MCF-7 human breast cancer cells as measured by wound healing**

The wound healing assay was used to determine the effect of long term exposure to 4MBC on motility of MCF-7 human breast cancer cells. Although 4MBC increased the wound closure to  $47.02 \pm 3.11$  % significantly compared to no addition ( $19.80 \pm 0.65$  %) after 8 weeks of exposure (Figure 4.29 (A)) ( $p$ -value  $\leq 0.001$ ), results showed that 13 weeks of exposure to  $10^{-5}$  M 4MBC or  $10^{-7}$  M 4MBC did not have the same effect on the wound healing in MCF-7 cells (Figure 4.29 (B)). On the other hand, a longer exposure time showed that after 21 weeks of exposure to the same concentrations the wound healing in MCF-7 cells increased. The wound healing closure of MCF-7 cells exposed to  $10^{-5}$  M 4MBC was increased significantly to  $47.66 \pm 4.98$  % ( $p$ -value  $\leq 0.001$ ), while  $10^{-7}$  M 4MBC had increased the wound healing closure to  $42.61 \pm 2.22$  % in comparison to the negative control ( $24.75 \pm 0.68$  %) (Figure 4.29 (C)) ( $p$ -value  $\leq 0.01$ ).

#### **4.3.5.2 Effects of 4MBC on migration of individual MCF-7 human breast cancer cells as measured by time-lapse microscopy**

MCF-7 human breast cancer cells were exposed for 2 weeks and 21 weeks to 4MBC or no addition. 48 hours prior the experiment, cells were re-seeded in 12-well plates and cell migration was analysed using time-lapse microscopy. 10 cells were tracked in 5 fields per well for 24 hours and the number of motile cells and cumulative length moved were measured for each treatment. Although statistics did not show any significant increase in the percentage of motile cells after 2 weeks of exposure to  $10^{-5}$  M 4MBC (Figure 4.30 (A)), there was an indicated increase in the cumulative length moved by MCF-7 cells to  $78.85 \pm 22.10$  microns in comparison to  $19.51 \pm 12.25$  microns in the negative control (Figure 4.30 (B)) ( $p$ -value  $\leq 0.05$ ). After a longer exposure time (21 weeks),  $10^{-7}$  M 4MBC significantly increased the percentage of motile cells to  $13.33 \pm 2.91$  % almost double the percentage of that indicated in the negative control ( $6.00 \pm 2.91$  %) (Figure 4.30 (C)) ( $p$ -value  $\leq 0.01$ ), but no change in cumulative length was found in the same experiment (Figure 4.30 (D)).

#### **4.3.5.3 Effects of 4MBC on migration of MCF-7 human breast cancer cells as determined by xCELLigence technology**

MCF-7 cells were exposed to  $10^{-7}$  M 4MBC,  $10^{-6}$  M 4MBC,  $10^{-5}$  M 4MBC,  $10^{-8}$  M  $17\beta$ -oestradiol or no addition for 2, 10, 20 and 23 weeks prior to the experiment. Results of 2 and 10 weeks of exposure to 4MBC suggested only a minor effect of  $10^{-5}$  M 4MBC on MCF-7 cell motility in comparison with the negative control (Figures 4.31 and 4.32). Results also showed a reduction of cell motility after 2 and 10 weeks of exposure to  $10^{-7}$  M 4MBC and  $10^{-6}$  M 4MBC in comparison with no addition (Figures 4.31 and 4.32). However, longer exposure (20 weeks) showed an increase in cell motility for cells exposed to  $10^{-6}$  M 4MBC and  $10^{-5}$  M 4MBC (Figure 4.33) and after 23 weeks of exposure to  $10^{-5}$  M 4MBC the increase in cell index  $0.22 \pm 0.06$  was found to be significantly greater than the cell index of no addition ( $0.091 \pm 0.02$ ) (Figure 4.34) ( $p$ -value  $\leq 0.05$ ). Lower cell index (negative signals) of the negative control in Figure 4.33 refers to lower dynamic range of cell motility as described by (ACEA application note no.6, 2013 ; Eisenberg et al., 2011).

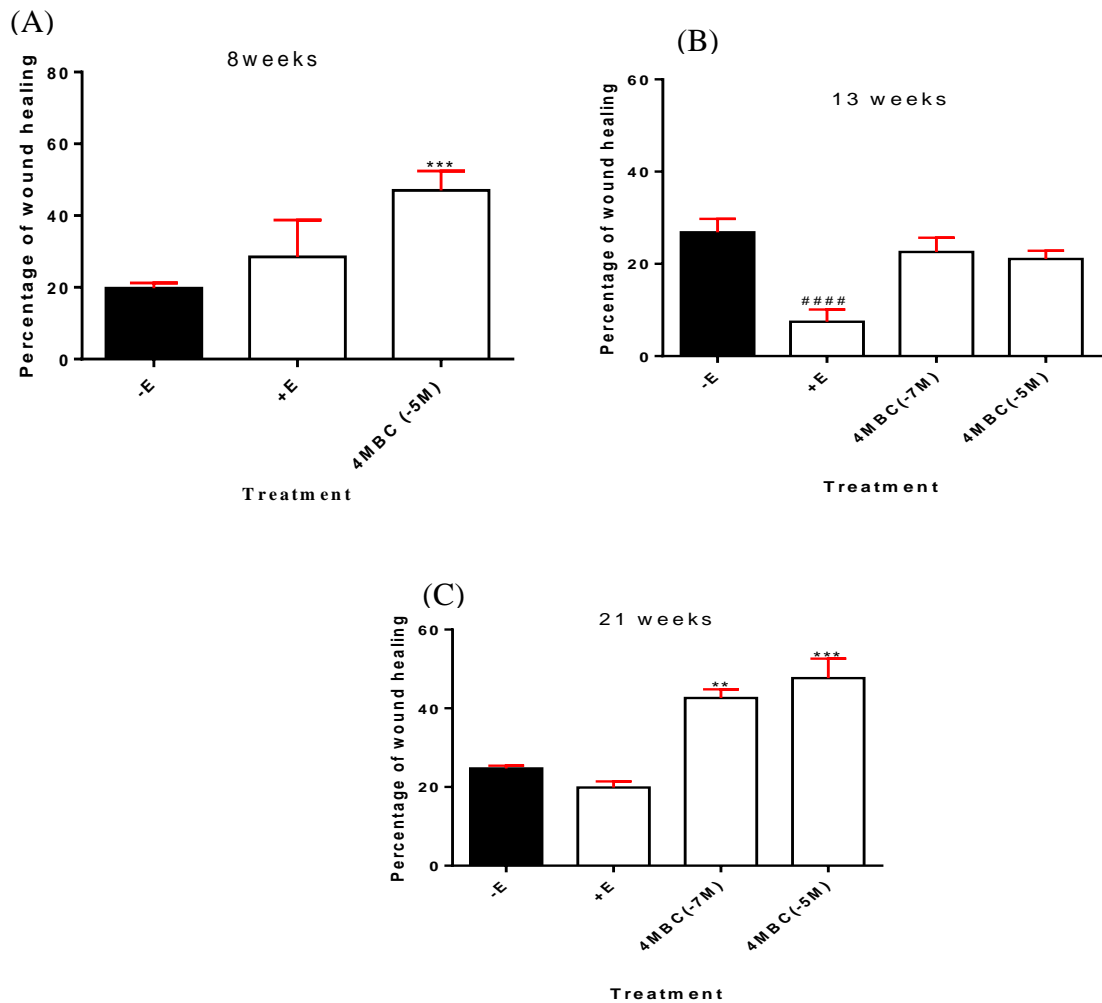


**Figure 4.29 Effect of exposure to 4MBC or 17 $\beta$ -oestradiol on collective motility of MCF-7 human breast cancer cells as measured by wound healing assay.**

Cells were grown in phenol-red-free-DMEM containing 5% DCFCS with ethanol control (-E) only, 10<sup>-8</sup> M 17 $\beta$ -oestradiol (+E), with 10<sup>-7</sup> M 4MBC (4MBC (-7M)) or with 10<sup>-5</sup> M 4MBC (4MBC (-5M)) for 8 weeks (A) 13 weeks (B) and 21 weeks (C). Media were replenished and cells were split every 3-4 days. Cells were then reseeded in 12-well plates and once the cells became  $\geq$  95% confluent, wound was made and mitomycin c (0.5  $\mu$ g/ml) was added. Images were captured at 0 hour and 24 hours. Cell migration was quantified by analysing minimum 5 images from each well. (A) Values are the average  $\pm$  SE of triplicate wells of three independent experiments (n=3). (B and C) Values are the average  $\pm$  SE of triplicate independent wells. \*\* *p*-value  $\leq$  0.01 and \*\*\* *p*-value  $\leq$  0.001 increase versus no addition. #### *p*-value  $\leq$  0.0001 decrease versus no addition by one-way ANOVA Dunnett's test.

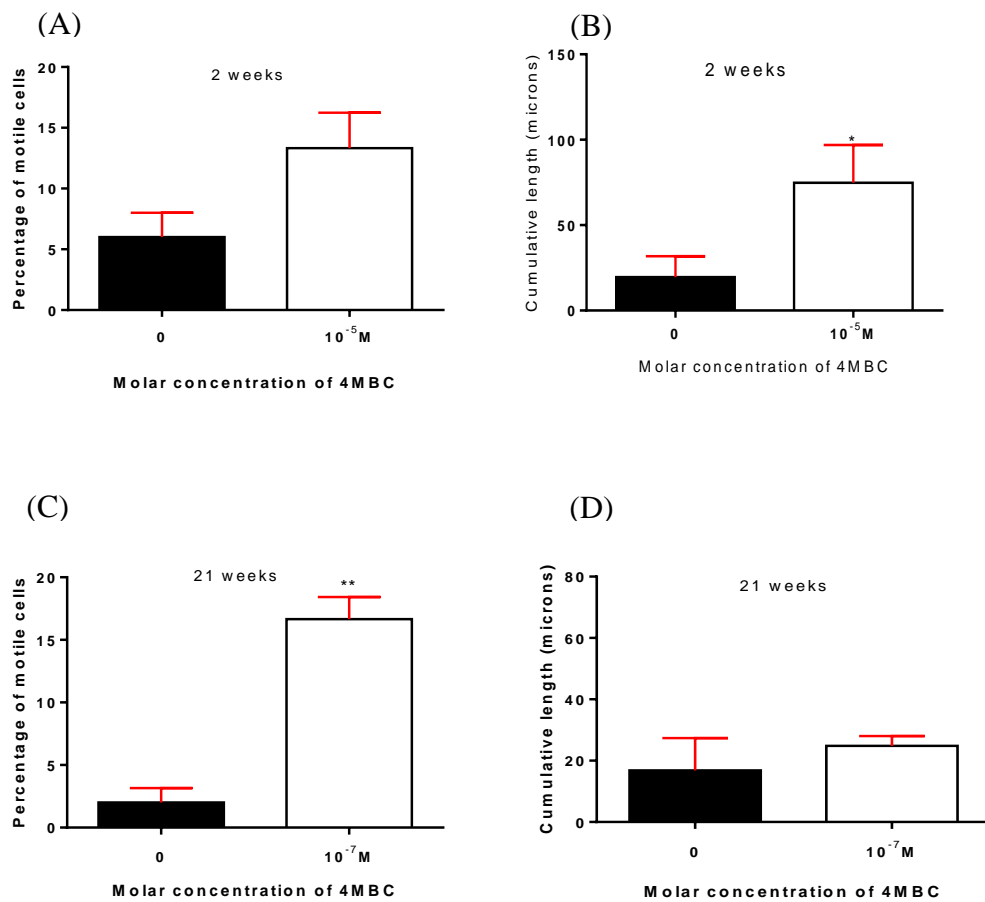


**Figure 4.30 Effect of exposure to 4MBC on motility of individual MCF-7 human breast cancer cells as determined by time-lapse microscopy.**

Cells were grown in phenol-red-free-DMEM containing 5% DCFCS with ethanol control (0) only or with 4MBC at indicated concentrations for 2 (A, B) and 21 weeks (C, D). Media were replenished and cells were split every 3-4 days. 2 days prior to the experiment, cells were reseeded in 12-well plates at  $0.2 \times 10^5$  cells/well. Time-lapse images of 5 fields per well were recorded. Results represent the percentage of motile cells (A, C) and cumulative length moved (B, D). Values are the average  $\pm$ SE of triplicate independent wells. \* *p-value*  $\leq 0.05$  and \*\* *p-value*  $\leq 0.01$  versus no addition by t-Test.

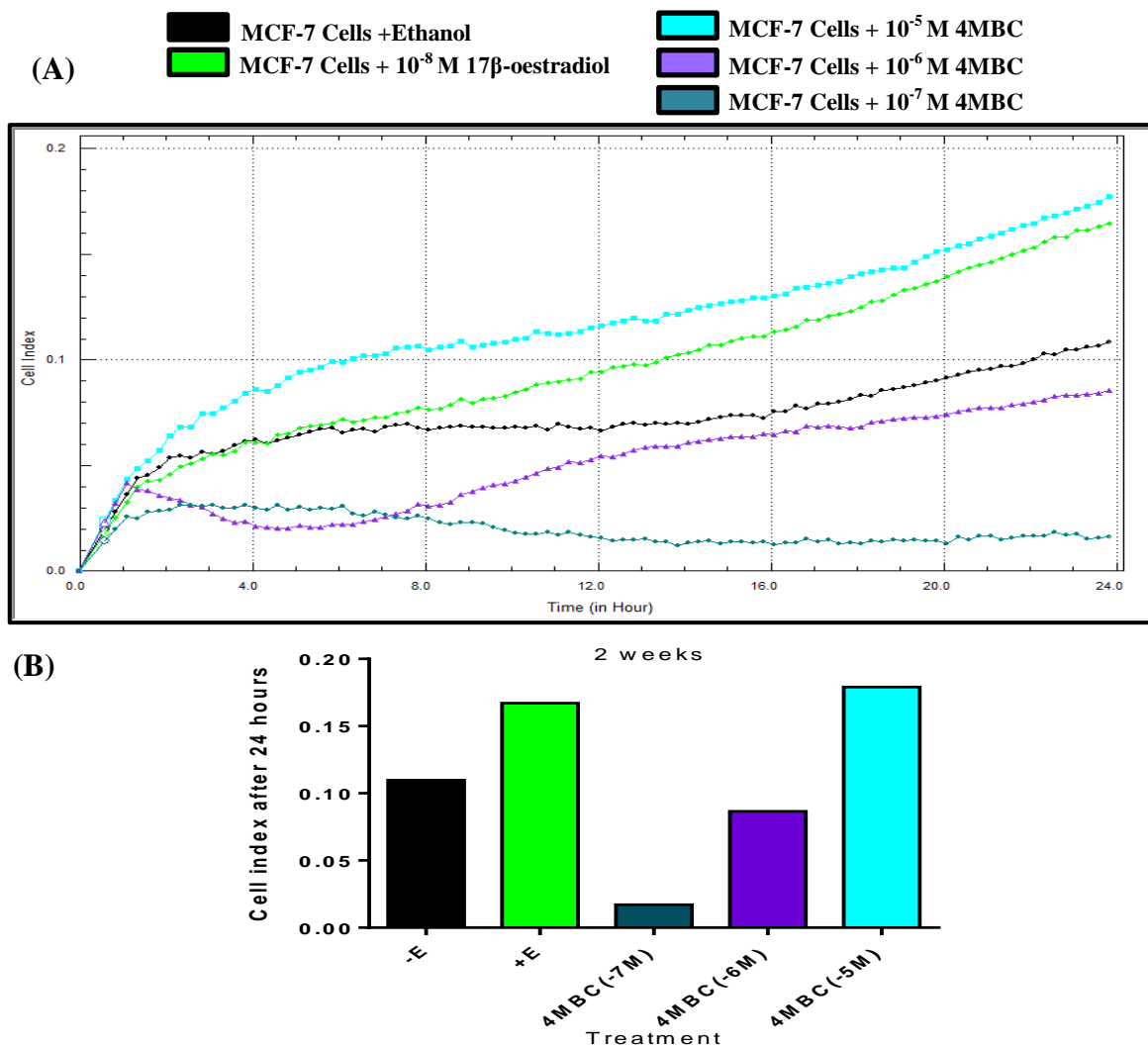


**Figure 4.31 Short-term effect of 4MBC or 17β-oestradiol on migration of MCF-7 human breast cancer cells using chemotaxis stimulus as determined by xCELLigence technology.**

Cells were grown in phenol-red-free-DMEM containing 5% DCFCS with ethanol control only (-E), 10<sup>-8</sup> M 17β-oestradiol (+E), 10<sup>-7</sup> M 4MBC (4MBC (-7M)), 10<sup>-6</sup> M 4MBC (4MBC (-6M)) or 10<sup>-5</sup> M 4MBC (4MBC (-5M)) for 2 weeks. Media were replenished and cells were split every 3-4 days. (A) The relative change in cell index of duplicate wells as indicated by the changes in impedance caused by cell migration from upper chambers to lower ones through the pores of the polycarbonate membrane. Cell index was recorded every 5 minutes and monitored for 24 hours. (B) Bar graph represents the average of the end point measurements (Cell index) of cell migration of duplicate independent wells at 24 hours.

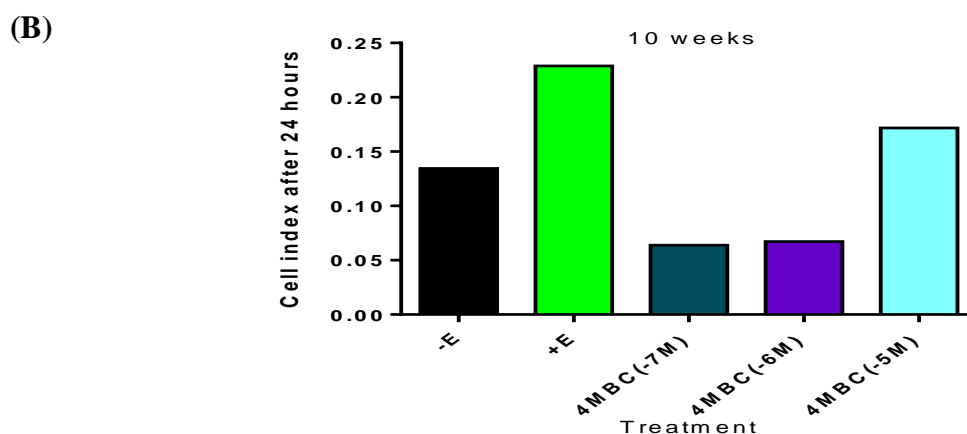
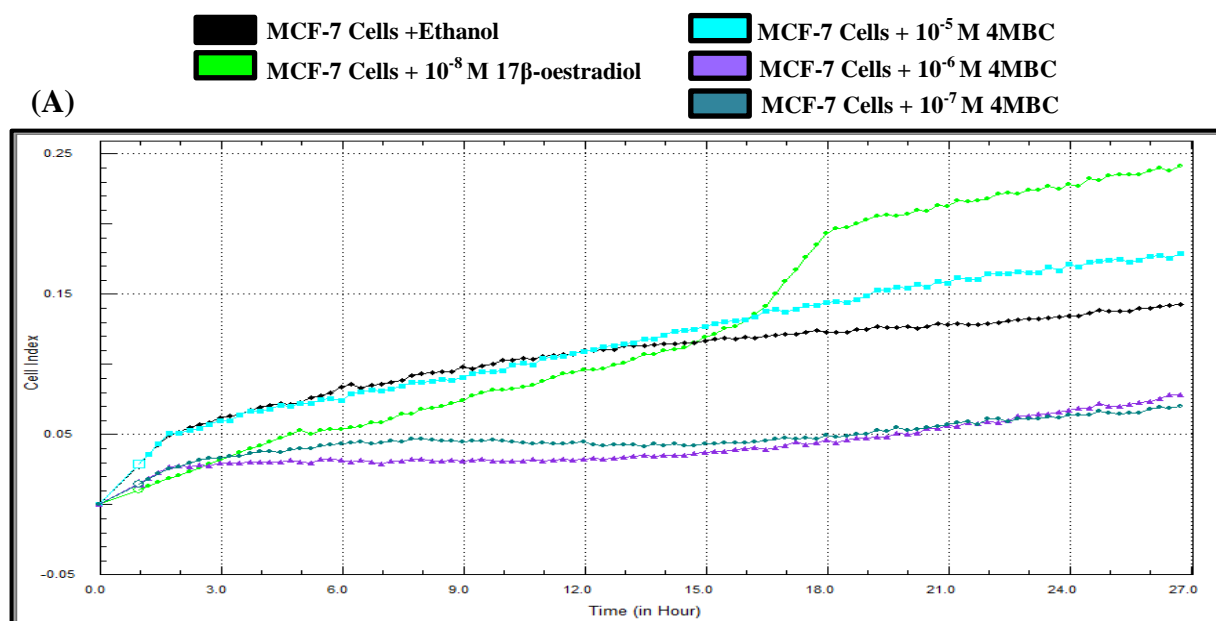


**Figure 4.32 Long-term effect of 4MBC or 17 $\beta$ -oestradiol on migration of MCF-7 human breast cancer cells using chemotaxis stimulus as determined by xCELLigence technology.**

Cells were grown in phenol-red-free-DMEM containing 5% DCFCS with ethanol control only (-E), 10<sup>-8</sup> M 17 $\beta$ -oestradiol (+E), 10<sup>-7</sup> M 4MBC (4MBC (-7M)), 10<sup>-6</sup> M 4MBC (4MBC (-6M)) or 10<sup>-5</sup> M 4MBC (4MBC (-5M)) for 10 weeks. Media were replenished and cells were split every 3-4 days. (A) The relative change in cell index of duplicate wells as indicated by the changes in impedance caused by cell migration from upper chambers to lower ones through the pores of the polycarbonate membrane. Cell index was recorded every 5 minutes and monitored for 24 hours. (B) Bar graph represents the average of the end point measurements (Cell index) of cell migration of duplicate wells at 24 hours.

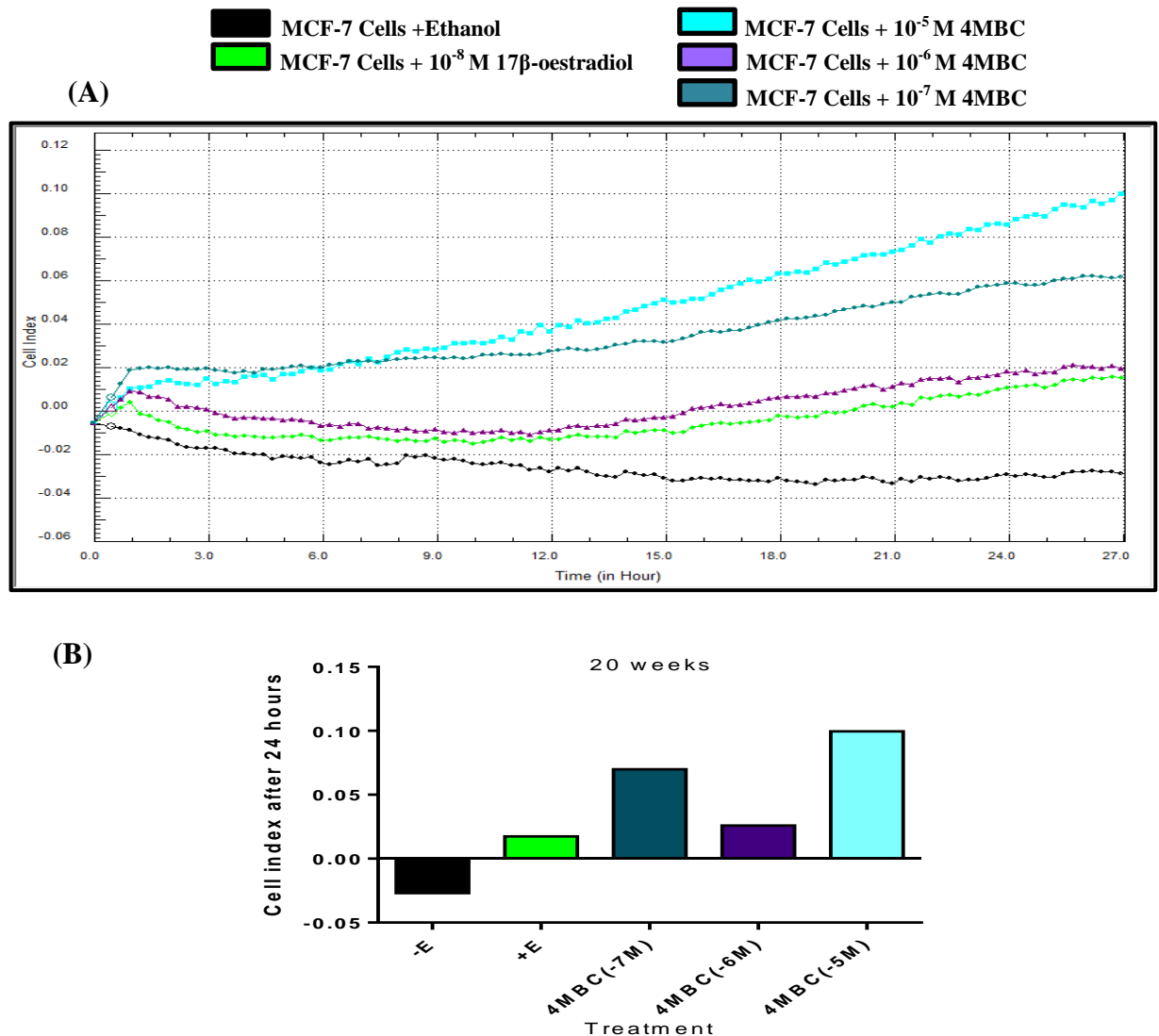


**Figure 4.33 Long-term effect of 4MBC or 17 $\beta$ -oestradiol on migration of MCF-7 human breast cancer cells using chemotaxis stimulus as determined by xCELLigence technology.**

Cells were grown in phenol-red-free-DMEM containing 5% DCFCS with ethanol control only (-E), 10<sup>-8</sup> M 17 $\beta$ -oestradiol (+E), 10<sup>-7</sup> M 4MBC (4MBC (-7M)), 10<sup>-6</sup> M 4MBC (4MBC (-6M)) or 10<sup>-5</sup> M 4MBC (4MBC (-5M)) for 20 weeks. Media were replenished and cells were split every 3-4 days. (A) The relative change in cell index of duplicate wells as indicated by the changes in impedance caused by cell migration from upper chambers to lower ones through the pores of the polycarbonate membrane. Cell index was recorded every 5 minutes and monitored for 24 hours. (B) Bar graph represents the average of the end point measurements (Cell index) of cell migration of duplicate wells at 24 hours.

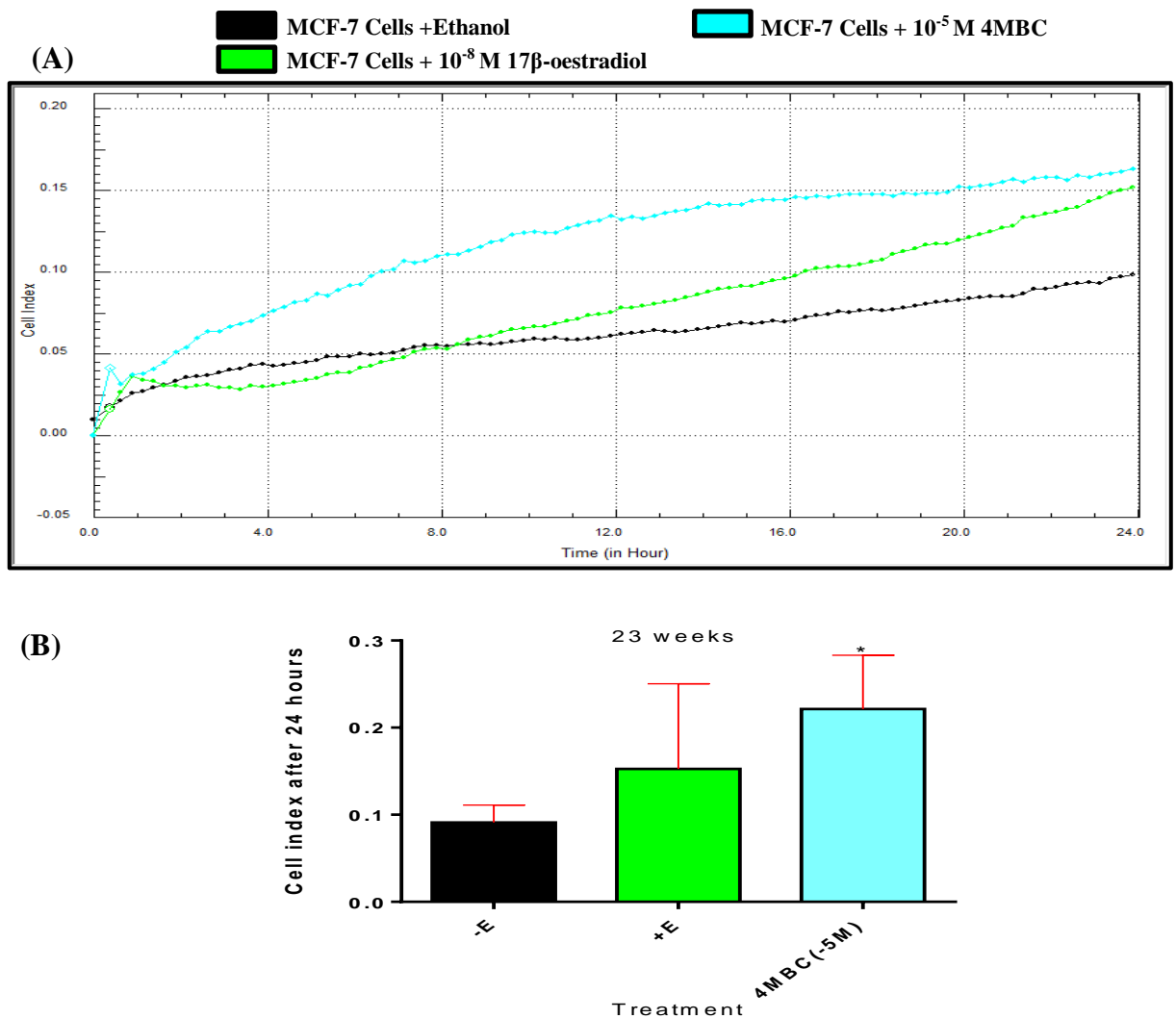


**Figure 4.34 Long-term effect of 4MBC or  $17\beta$ -oestradiol on migration of MCF-7 human breast cancer cells using chemotaxis stimulus as determined by xCELLigence technology.**

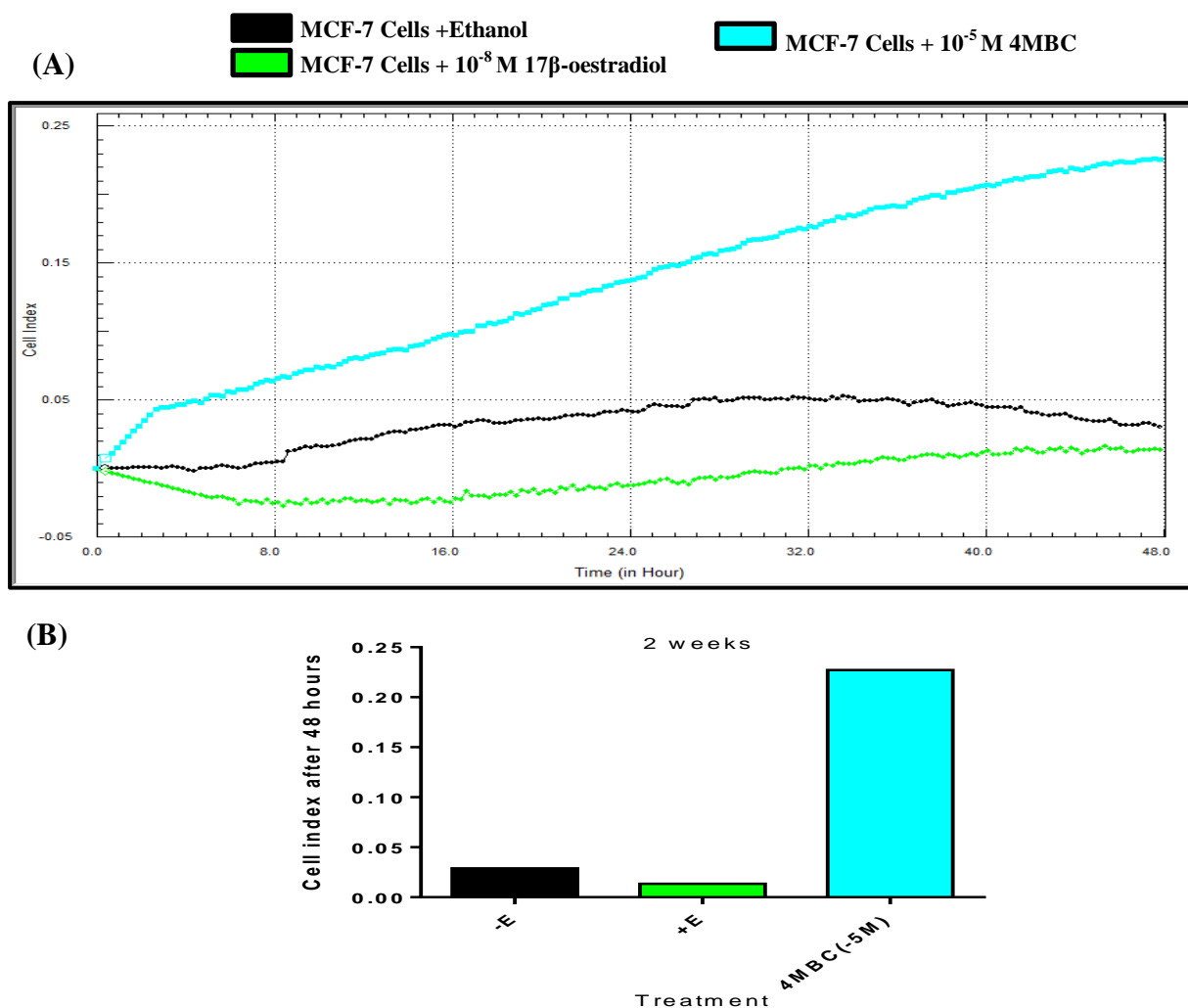
Cells were grown in phenol-red-free-DMEM containing 5% DCFCS with ethanol control only (-E),  $10^{-8}$  M  $17\beta$ -oestradiol (+E) or  $10^{-5}$  M 4MBC (4MBC (-5M)) for 23 weeks. Media were replenished and cells were split every 3-4 days. (A) The relative change in cell index of triplicate wells as indicated by the changes in impedance caused by cell migration from upper chambers to lower ones through the pores of the polycarbonate membrane. Cell index was recorded every 5 minutes and monitored for 24 hours. (B) Bar graph represents the average of the end point measurements (Cell index) of cell migration of triplicate wells at 24 hours. Values are the average  $\pm$ SE of triplicate independent wells. \*  $p$ -value  $\leq 0.05$  versus no addition by one-way ANOVA Dunnett's test.

#### **4.3.5.4 Effects of 4MBC on invasion of MCF-7 human breast cancer cells as determined by xCELLigence technology**

MCF-7 cells were exposed to  $10^{-7}$  M 4MBC,  $10^{-6}$  M 4MBC,  $10^{-5}$  M 4MBC,  $10^{-8}$  M  $17\beta$ -oestradiol or no addition for different exposure times prior to the experiment. The invasive activity of MCF-7 cells following the exposure to these concentrations was observed using the xCELLigence technology (as described in section 2.5).  $10^{-5}$  M 4MBC increased the invasive activity after 2 weeks (Figure 4.35), 10 weeks (Figure 4.36) and significantly after 31 weeks of exposure (Figure 4.37) ( $p$ -value  $\leq 0.05$ ). Lower cell index of the control cells and  $17\beta$ -oestradiol (negative signals) (Figure 4.37) refers to lower dynamic range of cell invasion according to (ACEA application note no.6, 2013; Eisenberg et al., 2011).

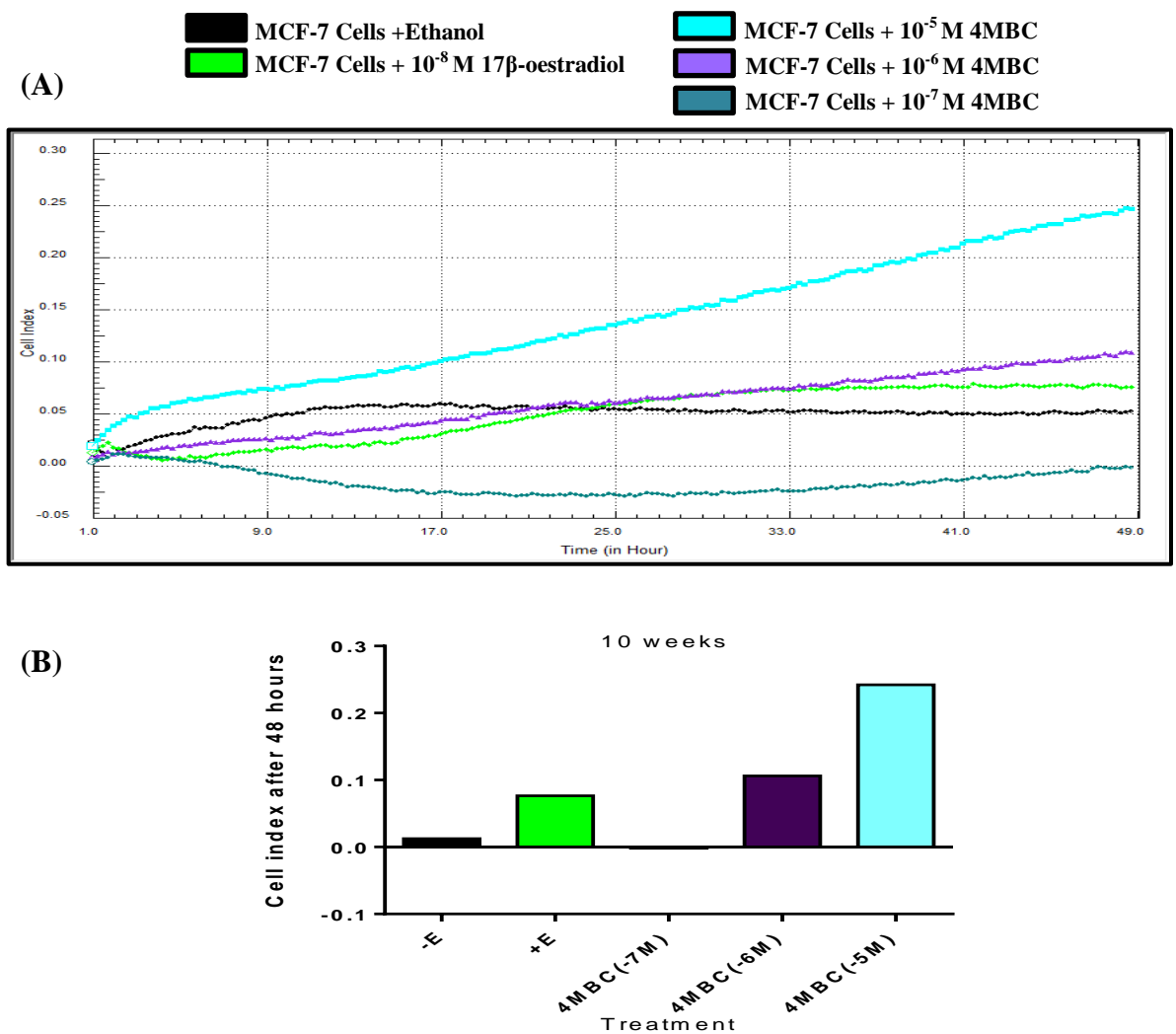
#### **4.3.5.5 Summary of effects with 4MBC**

Table 4.5 summarises all the results in section 4.3.5. The results are shown as determined by wound healing, time-lapse microscopy and the xCELLigence technology after 2 weeks and longer time points of exposure to concentrations of  $10^{-7}$  M and  $10^{-5}$  M 4MBC.



**Figure 4.35 Short-term effect of 4MBC or  $17\beta$ -oestradiol on invasion of MCF-7 human breast cancer cells through matrigel using chemotaxis stimulus as determined by xCELLigence technology.**

Cells were grown in phenol-red-free-DMEM containing 5% DCFCS with ethanol control only (-E),  $10^{-8}$  M  $17\beta$ -oestradiol (+E) or  $10^{-5}$  M 4MBC (4MBC (-5M)) for 2 weeks. Media were replenished and cells were split every 3-4 days. Cells were analysed for their invasive activity through matrigel (1:40) coated CIM-plate 16 in a real time invasion assay (xCELLigence RTCA device) (A) The relative change in cell index of duplicate wells as indicated by the changes in impedance caused by cell migration from upper chambers to lower ones through the pores of the polycarbonate membrane coated with matrigel. Cell index was recorded every 5 minutes and monitored for 48 hours. (B) Bar graph represents the average of the end point measurements (Cell index) of cell invasion of duplicate wells at 48 hours.



**Figure 4.36 Long-term effect of 4MBC or  $17\beta$ -oestradiol on invasion of MCF-7 human breast cancer cells through matrigel using chemotaxis stimulus as determined by xCELLigence technology.**

Cells were grown in phenol-red-free-DMEM containing 5% DCFCS with ethanol control only (-E),  $10^{-8}$  M  $17\beta$ -oestradiol (+E),  $10^{-5}$  M 4MBC (4MBC (-5M)),  $10^{-6}$  M 4MBC (4MBC (-6M)) or  $10^{-7}$  M 4MBC (4MBC (-7M)) for 10 weeks. Media were replenished and cells were split every 3-4 days. Cells were analysed for their invasive activity through matrigel (1:40) coated CIM-plate 16 in a real time invasion assay (xCELLigence RTCA device) (A) The relative change in cell index of duplicate wells as indicated by the changes in impedance caused by cell migration from upper chambers to lower ones through the pores of the polycarbonate membrane. Cell index was recorded every 5 minutes and monitored for 48 hours. (B) Bar graph represents the average of the end point measurements (Cell index) of cell invasion of duplicate wells at 48 hours.

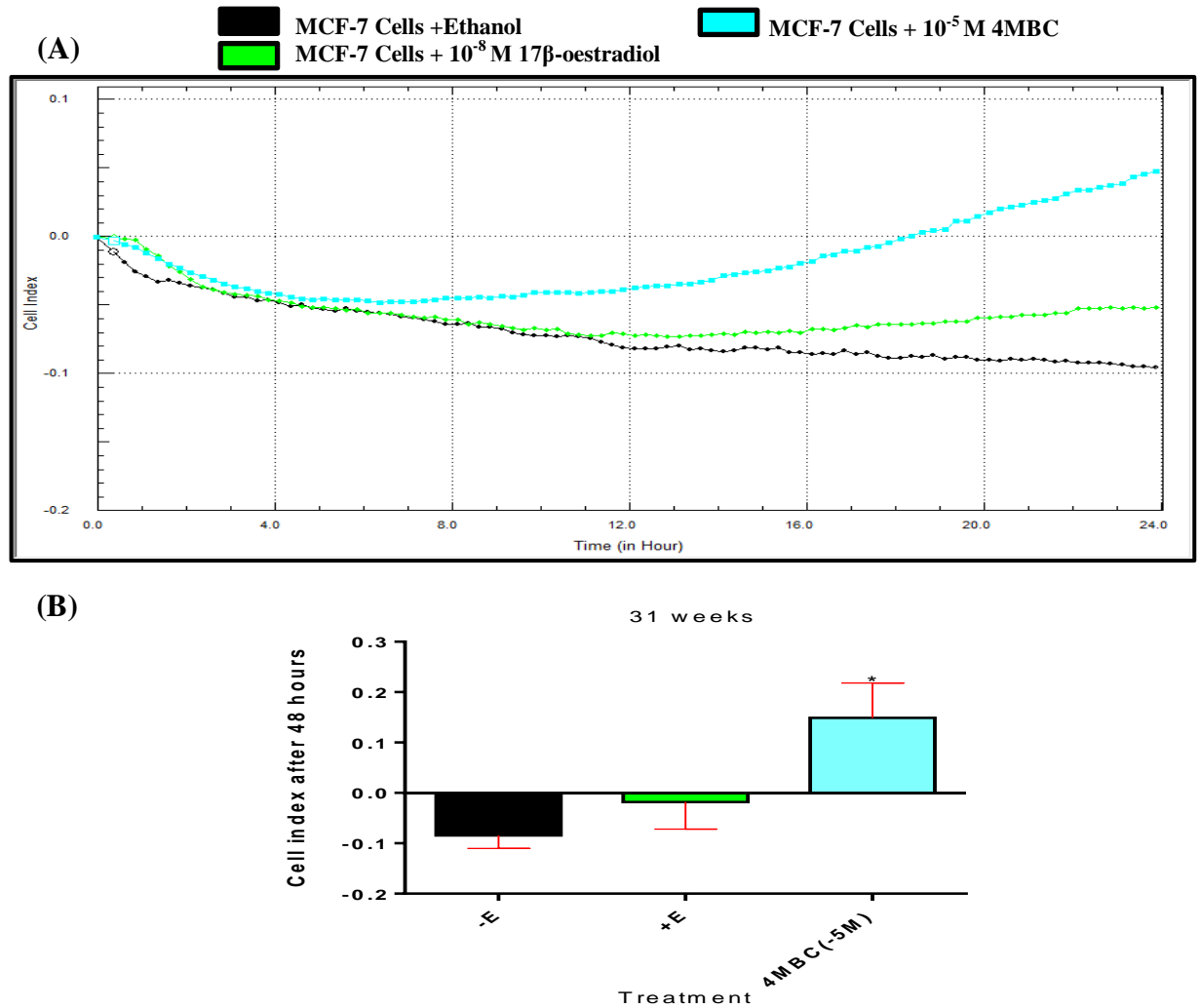


**Figure 4.37 Long-term effect of 4MBC or  $17\beta$ -oestradiol on invasion of MCF-7 human breast cancer cells through matrigel using chemotaxis stimulus as determined by xCELLigence technology.**

Cells were grown in phenol-red-free-DMEM containing 5% DCFCS with ethanol control only (-E),  $10^{-8}$  M  $17\beta$ -oestradiol (+E) or  $10^{-5}$  M 4MBC (4MBC (-5M)) for 31 weeks. Media were replenished and cells were split every 3-4 days. Cells were analysed for their invasive activity through matrigel (1:40) coated CIM-plate 16 in a real time invasion assay (xCELLigence RTCA device) (A) The relative change in cell index of triplicate wells as indicated by the changes in impedance caused by cell migration from upper chambers to lower ones through the pores of the polycarbonate membrane. Cell index was recorded every 5 minutes and monitored for 48 hours. (B) Bar graph represents the average of the end point measurements (Cell index) of cell invasion of triplicate wells at 48 hours. Values are the average  $\pm$ SE of triplicate independent wells. \*  $p$ -value  $\leq 0.05$  versus no addition by one-way ANOVA Dunnett's test.

**Table 4.5 Effects of 4MBC on motility and invasion of MCF-7 human breast cancer cells**

Experiment	Molar concentration		Incubation time prior to the experiment
	10 <sup>-7</sup> M	10 <sup>-5</sup> M	
Wound healing	--	(**)	8 weeks
	n.s.	n.s.	13 weeks
	(**)	(**)	21 weeks
Time-lapse	--	(*) in cumulative length moved by the cells	2 weeks
	**↑ in percentage of motile cells	--	21 weeks
Real-time monitoring of cell motility (xCELLigence)	n.o.	O.	2 weeks
	n.o.	O.	10 weeks
	O.	O.	21 weeks
	--	(*)	23 weeks
Real-time monitoring of cell invasion through matrigel (xCELLigence)	n.o.	O.	2 and 10 weeks
	--	(*)	31 weeks

(--) experiment was not conducted; \*  $p$ -value  $\leq 0.05$  versus no addition; \*\*  $p$ -value  $\leq 0.01$  versus no addition; (n.s.)  $p$ -value  $> 0.05$  not significant; (O.) effect observed using duplicates only-no statistical analysis possible for duplicates; (n.o.) no effects observed using duplicates.

### **4.3.6 Effects of HS on migration of MCF-7 human breast cancer cells**

#### **4.3.6.1 Effects of HS on collective migration of MCF-7 human breast cancer cells as measured by wound healing**

The wound healing assay was used to determine the effect of long term exposure to HS on motility of MCF-7 human breast cancer cells. Results showed that after 8 weeks of exposure to  $10^{-5}$  M HS the wound healing of MCF-7 cells was increased significantly to  $37.11 \pm 4.74$  % compared to  $19.8 \pm 0.66$  % in the negative control (Figure 4.38 (A)) ( $p$ -value  $\leq 0.01$ ). After 13 weeks of exposure to  $10^{-6}$  M HS or  $10^{-7}$  M HS did not increase the wound healing closure in MCF-7 cells (Figure 4.38 (B)). In contrast, after longer exposure time (21 weeks) the wound healing closure in MCF-7 cells exposed to  $10^{-6}$  M HS was increased significantly to  $44.72 \pm 6.91$  % and to  $10^{-7}$  M HS was increased to  $52.00 \pm 1.11$  % in comparison to the negative control ( $24.75 \pm 0.68$  %) (Figure 4.38 (C)) ( $p$ -value  $\leq 0.05$  and  $p$ -value  $\leq 0.01$ ).

#### **4.3.6.2 Effects of HS on migration of individual MCF-7 human breast cancer cells as measured by time-lapse microscopy**

MCF-7 human breast cancer cells were exposed for 2 weeks and 21 weeks to HS or no addition. 48 hours prior the experiment, cells were re-seeded in 12-well plates and cell migration was analysed using time-lapse microscopy. 10 cells were tracked in 5 fields per well for 24 hours and the number of motile cells and cumulative length moved were measured for each treatment. No significant increase in percentage of cell motility or cumulative length moved was indicated after 2 weeks of exposure to  $10^{-5}$  M HS (Figure 4.39 (A and B)). However, after 21 weeks of exposure to  $10^{-7}$  M HS results have shown a significant increase in the percentage of motile cells ( $27.33 \pm 2.40$  %) in comparison to the negative control ( $12.00 \pm 4.16$  %) (Figure 4.39 (C)) ( $p$ -value  $\leq 0.05$ ). In the same experiment the cumulative length moved was not increased significantly in comparison to the negative control (Figure 4.39 (D)).

#### **4.3.6.3 Effects of HS on migration of MCF-7 human breast cancer cells as determined by xCELLigence technology**

The movement of MCF-7 cells through  $8\mu\text{m}$  pores of a membrane towards a chemotaxis stimulus of FCS was observed following the exposure to  $10^{-5}$  M HS,  $10^{-6}$  M HS,  $10^{-7}$  M HS,

$10^{-8}$  M  $17\beta$ -oestradiol or no addition for 3, 11, 21 and 23 weeks prior to the experiment. Short-term exposure to  $10^{-5}$  M HS showed no increase in cell index (0.051) in comparison to the negative control (cell index 0.050) (Figure 4.40). However, 23 weeks of exposure increased the motility of MCF-7 cells significantly (cell index  $0.18 \pm 0.03$ ) in comparison to the negative control (cell index  $0.09 \pm 0.02$ ) (Figure 4.41) ( $p$ -value  $\leq 0.05$ ).

Observing the effects of the exposure to lower concentrations of HS ( $10^{-6}$  M HS and  $10^{-7}$  M HS) was conducted at 11 and 20 weeks of exposure. Cells exposed to  $10^{-6}$  M HS showed a minor increase in cell index in comparison to the negative control and no effect of exposure to  $10^{-7}$  M HS was observed in both experiments (Figures 4.42 and 4.43).

Although the effects of  $10^{-8}$  M  $17\beta$ -oestradiol at 10 weeks from independent experiments has shown irregular pattern of MCF-7 cells motility compared to no addition as indicated by chemotaxis (Figures 4.5, 4.11, 4.15, 4.23, 4.32 and 4.42), further statistical analysis using tow-way ANOVA Bonferroni's test showed no significant difference in the pattern of MCF-7 cells motility exposed to  $10^{-8}$  M  $17\beta$ -oestradiol in comparison to no addition.

#### **4.3.6.4 Effects of HS on invasion of MCF-7 human breast cancer cells as determined by xCELLigence technology**

MCF-7 Cells were grown in phenol-red-free-DMEM containing 5% DCFCS with ethanol control only,  $10^{-8}$  M  $17\beta$ -oestradiol or  $10^{-5}$  M HS for 2, 11 and 31 weeks. Cells were analysed for their invasive activity through matrigel (1:40) coated CIM-plate 16 in a real time invasion assay using the xCELLigence technology. No effect on MCF-7 cell invasive activity was observed after 11 weeks of exposure to  $10^{-7}$  M HS or  $10^{-6}$  M HS (data not shown). However, short-term exposure to  $10^{-5}$  M HS induced the cell index to 0.092 in comparison to the negative control (cell index 0.03) (Figure 4.44) and long-term (31 weeks) exposure of MCF-7 cells to  $10^{-5}$  M HS significantly induced the cell index to  $0.16 \pm 0.08$  in comparison to the control cells (cell index  $-0.08 \pm 0.02$ ) (Figure 4.45) ( $p$ -value  $\leq 0.05$ ). Lower cell index (negative signals) of the control cells and  $17\beta$ -oestradiol reflects lower dynamic range of cell invasion through matrigel (ACEA application note no.6, 2013; Eisenberg et al., 2011).

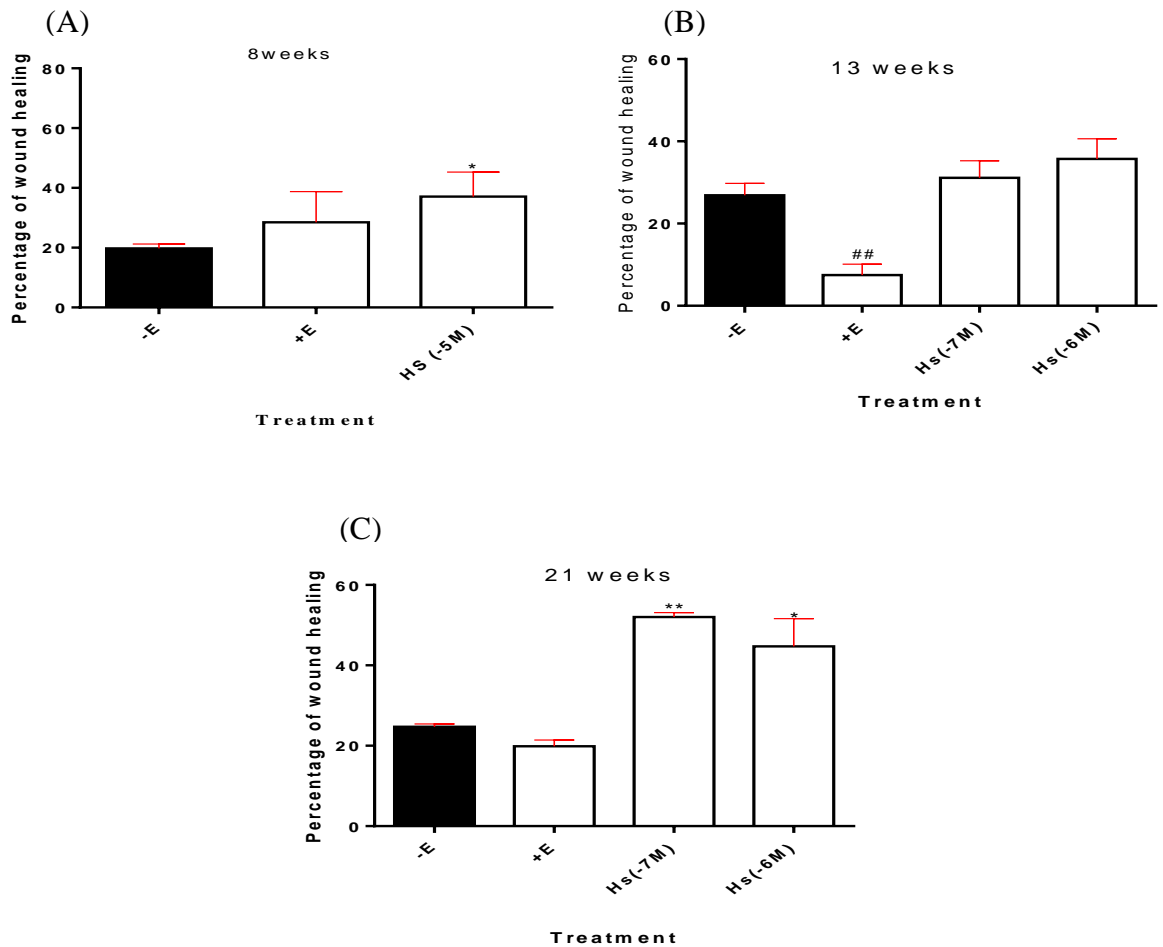


**Figure 4.38 Effect of exposure to HS or 17 $\beta$ -oestradiol on collective motility of MCF-7 human breast cancer cells as measured by wound healing assay.**

Cells were grown in phenol-red-free-DMEM containing 5% DCFCs with ethanol control (-E) only, 10<sup>-8</sup> M 17 $\beta$ -oestradiol (+E), with 10<sup>-7</sup> M HS (HS (-7M)), 10<sup>-6</sup> M HS (Hs (-6M)) or 10<sup>-5</sup> M HS (Hs (-5M)) for 8 weeks (A), 13 weeks (B) and 21 weeks (C). Media were replenished and cells were split every 3-4 days. Cells were then reseeded in 12-well plates and once the cells became  $\geq 95\%$  confluent, wound was made and mitomycin c (0.5  $\mu\text{g/ml}$ ) was added. Images were captured at 0 hour and 24 hours. Cell migration was quantified by analysing minimum 5 images from each well. (A) Values are the average  $\pm$  SE of triplicate wells of three independent experiments (n=3). (B and C) Values are the average  $\pm$  SE of triplicate independent wells. \* *p-value*  $\leq 0.05$  and \*\* *p-value*  $\leq 0.01$  increase versus no addition. ## *p-value*  $\leq 0.01$  decrease versus no addition by one-way ANOVA Dunnett's test.

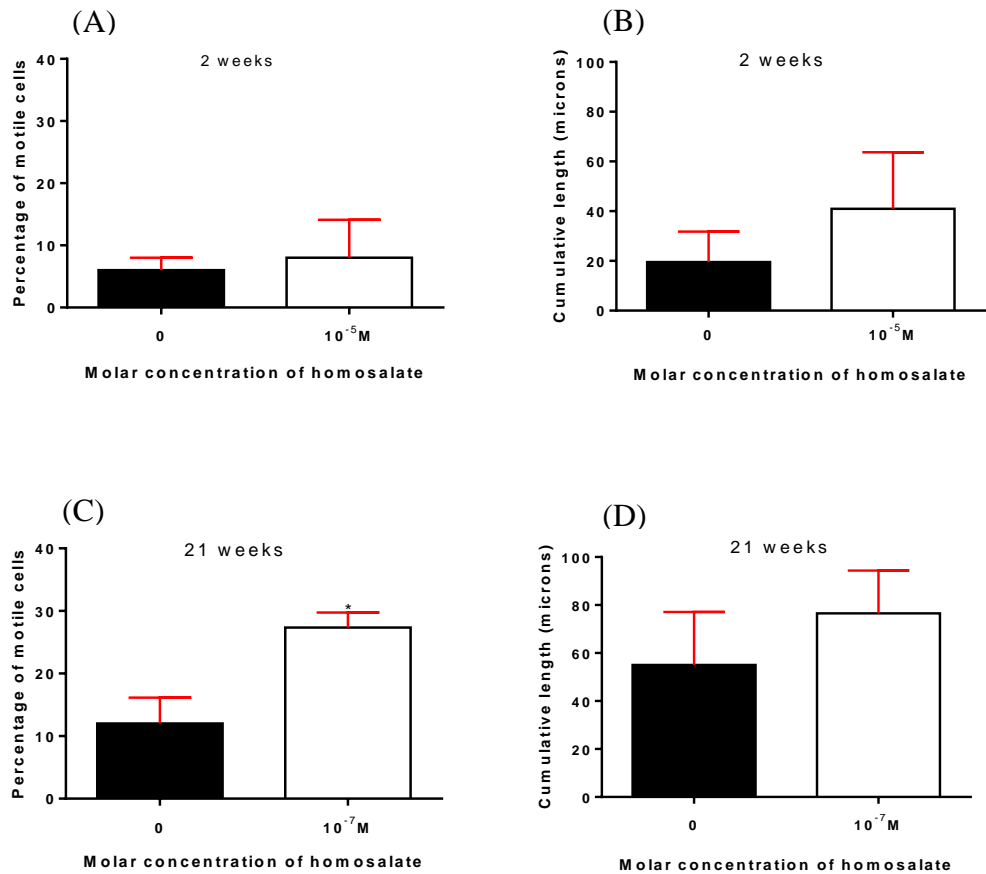


**Figure 4.39 Effect of exposure to HS on motility of individual MCF-7 human breast cancer cells as determined by time-lapse microscopy.**

Cells were grown in phenol-red-free-DMEM containing 5% DCFCS with ethanol control (0) only or with HS at indicated concentrations for 2 (A, B) and 21 weeks (C, D). Media were replenished and cells were split every 3-4 days. 2 days prior to the experiment, cells were reseeded in 12-well plates at  $0.2 \times 10^5$  cells/well. Time-lapse images of 5 fields per well were recorded. Results represent the percentage of motile cells (A, C) and cumulative length moved (B, D). Values are the average  $\pm$ SE of triplicate independent wells. \*  $p$ -value  $\leq 0.05$  versus no addition by t-Test.

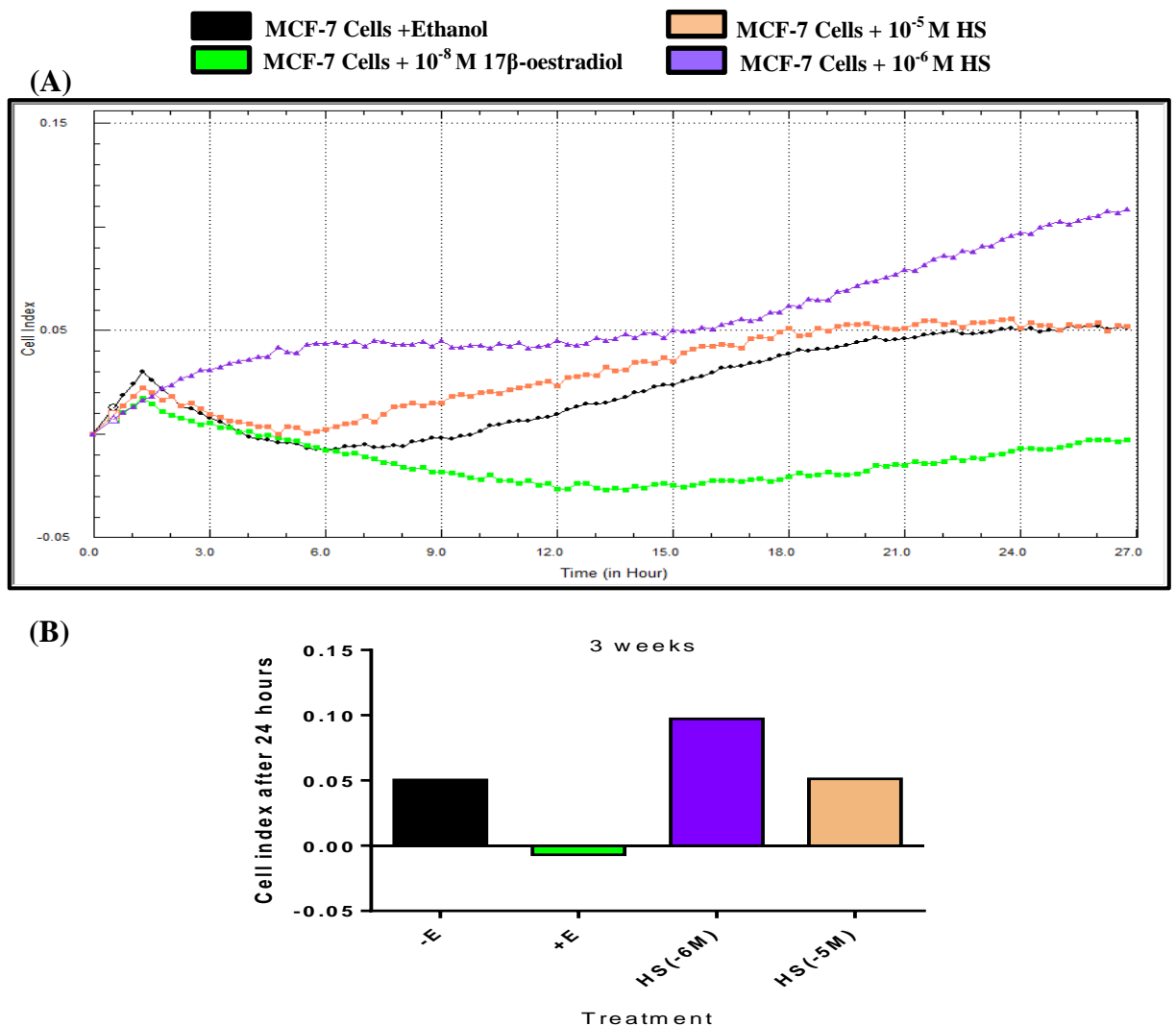


**Figure 4.40 Short-term effect of HS or  $17\beta$ -oestradiol on migration of MCF-7 human breast cancer cells using chemotaxis stimulus as determined by xCELLigence technology.**

Cells were grown in phenol-red-free-DMEM containing 5% DCFCS with ethanol control only (-E),  $10^{-8}$  M  $17\beta$ -oestradiol (+E),  $10^{-7}$  M HS (HS (-7M)) or  $10^{-6}$  M HS (HS (-6M)) for 3 weeks. Media were replenished and cells were split every 3-4 days. (A) The relative change in cell index of duplicate wells as indicated by the changes in impedance caused by cell migration from upper chambers to lower ones through the pores of the polycarbonate membrane. Cell index was recorded every 5 minutes and monitored for 24 hours. (B) Bar graph represents the average of the end point measurements (Cell index) of cell migration of duplicate independent wells at 24 hours.

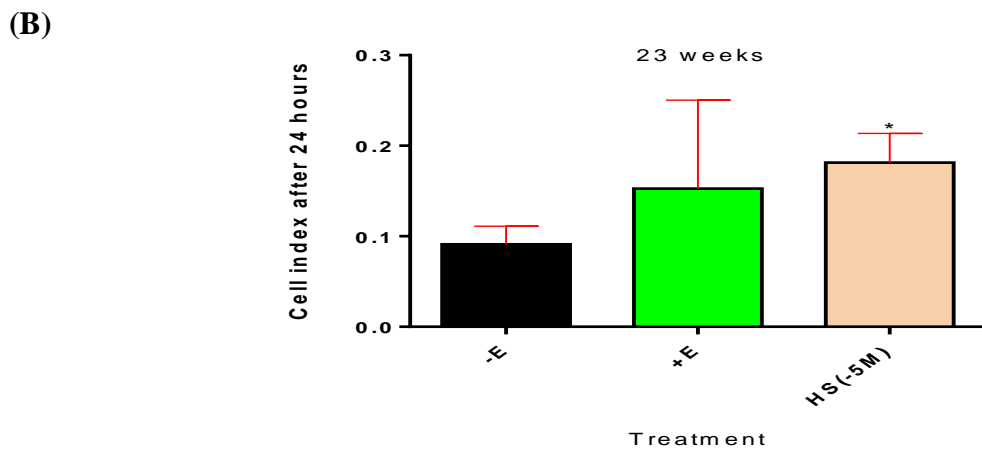
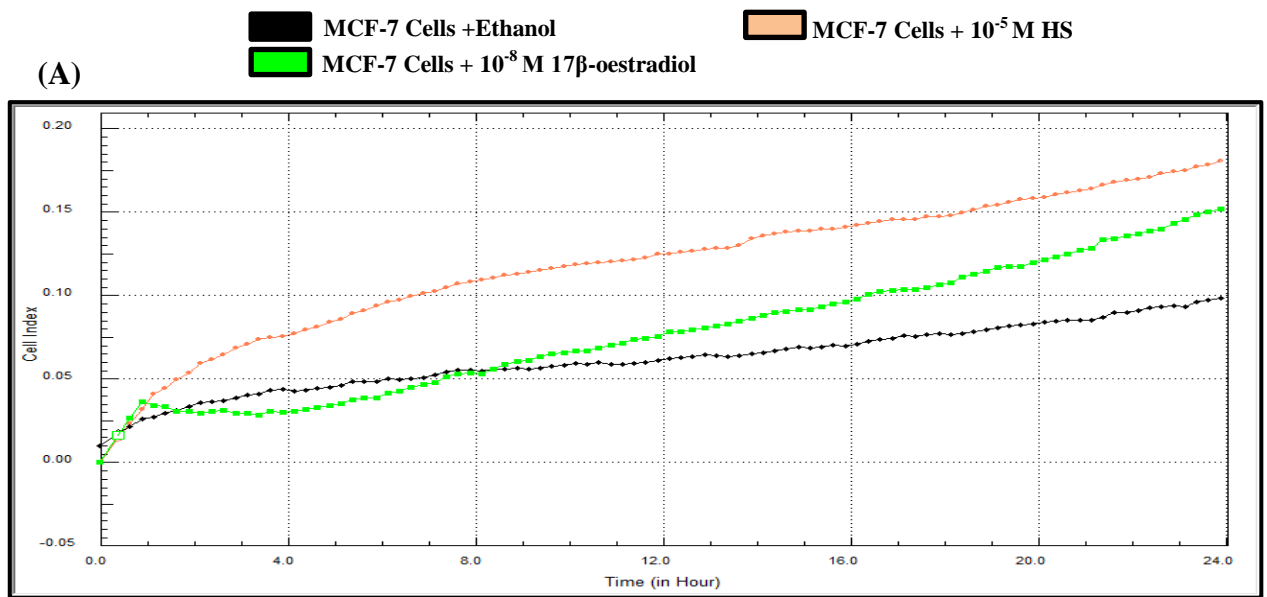
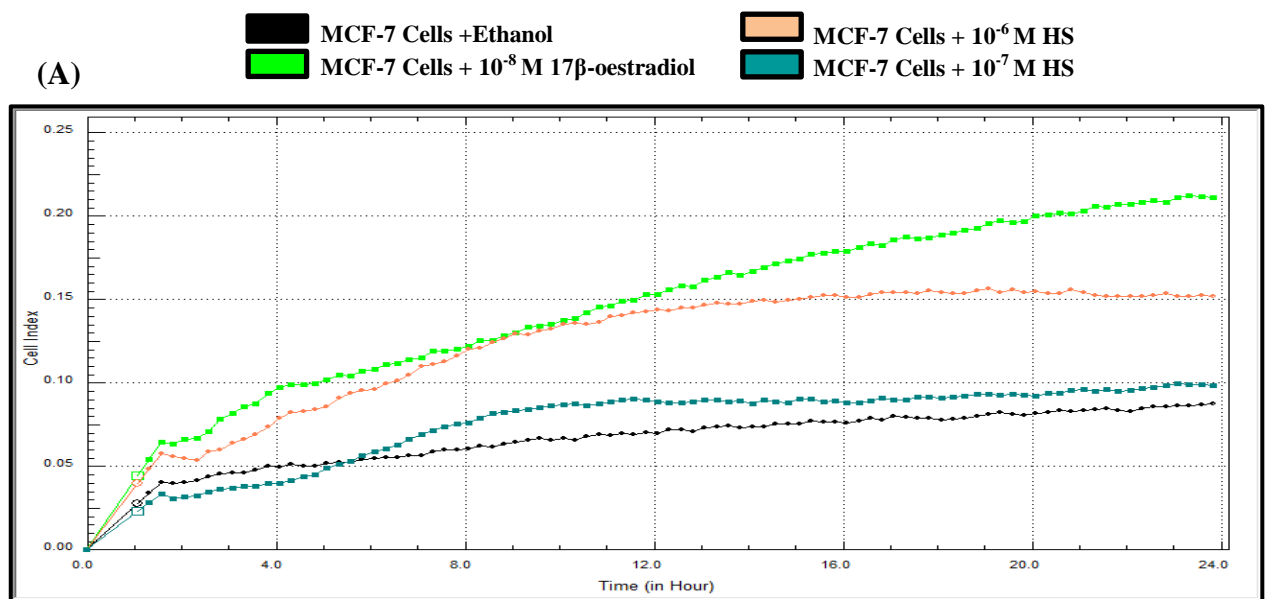


**Figure 4.41 Long-term effect of HS or  $17\beta$ -oestradiol on migration of MCF-7 human breast cancer cells using chemotaxis stimulus as determined by xCELLigence technology.**

Cells were grown in phenol-red-free-DMEM containing 5% DCFCS with ethanol control only (-E),  $10^{-8}$  M  $17\beta$ -oestradiol (+E) or  $10^{-5}$  M HS (HS (-5M)). Media were replenished and cells were split every 3-4 days. (A) The relative change in cell index of triplicate wells as indicated by the changes in impedance caused by cell migration from upper chambers to lower ones through the pores of the polycarbonate membrane. Cell index was recorded every 5 minutes and monitored for 24 hours. (B) Bar graph represents the average of the end point measurements (Cell index) of cell migration of triplicate independent wells at 24 hours. \*  $p$ -value  $\leq 0.05$  versus no addition by one-way ANOVA Dunnett's test.



(B)

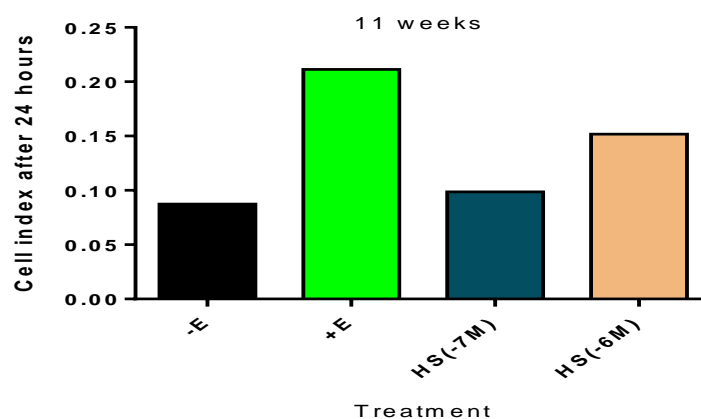


**Figure 4.42 Long-term effect of HS or  $17\beta$ -oestradiol on migration of MCF-7 human breast cancer cells using chemotaxis stimulus as determined by xCELLigence technology.**

Cells were grown in phenol-red-free-DMEM containing 5% DCFCS with ethanol control only (-E),  $10^{-8}$  M  $17\beta$ -oestradiol (+E),  $10^{-7}$  M HS (HS (-7M)) or  $10^{-6}$  M HS (HS (-6M)) for 11 weeks. Media were replenished and cells were split every 3-4 days. (A) The relative change in cell index of duplicate wells as indicated by the changes in impedance caused by cell migration from upper chambers to lower ones through the pores of the polycarbonate membrane. Cell index was recorded every 5 minutes and monitored for 24 hours. (B) Bar graph represents the average of the end point measurements (Cell index) of cell migration of duplicate independent wells at 24 hours.

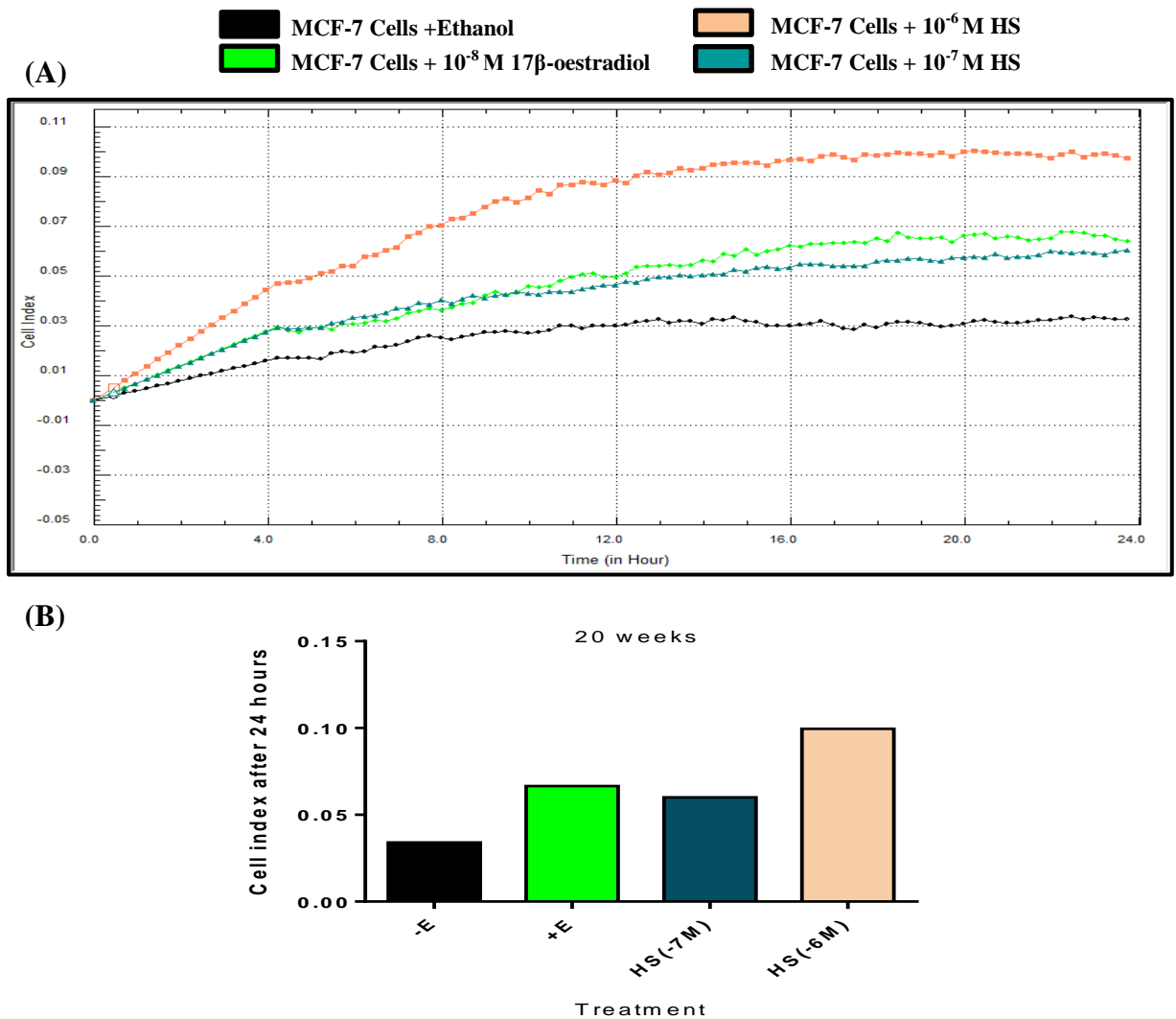


**Figure 4.43 Long-term effect of HS or 17 $\beta$ -oestradiol on migration of MCF-7 human breast cancer cells using chemotaxis stimulus as determined by xCELLigence technology.**

Cells were grown in phenol-red-free-DMEM containing 5% DCFCS with ethanol control only (-E), 10<sup>-8</sup> M 17 $\beta$ -oestradiol (+E), 10<sup>-7</sup> M HS (HS (-7M)) or 10<sup>-6</sup> M HS (HS (-6M)) for 20 weeks. Media were replenished and cells were split every 3-4 days. (A) The relative change in cell index of duplicate wells as indicated by the changes in impedance caused by cell migration from upper chambers to lower ones through the pores of the polycarbonate membrane. Cell index was recorded every 5 minutes and monitored for 24 hours. (B) Bar graph represents the average of the end point measurements (Cell index) of cell migration of duplicate independent wells at 24 hours.

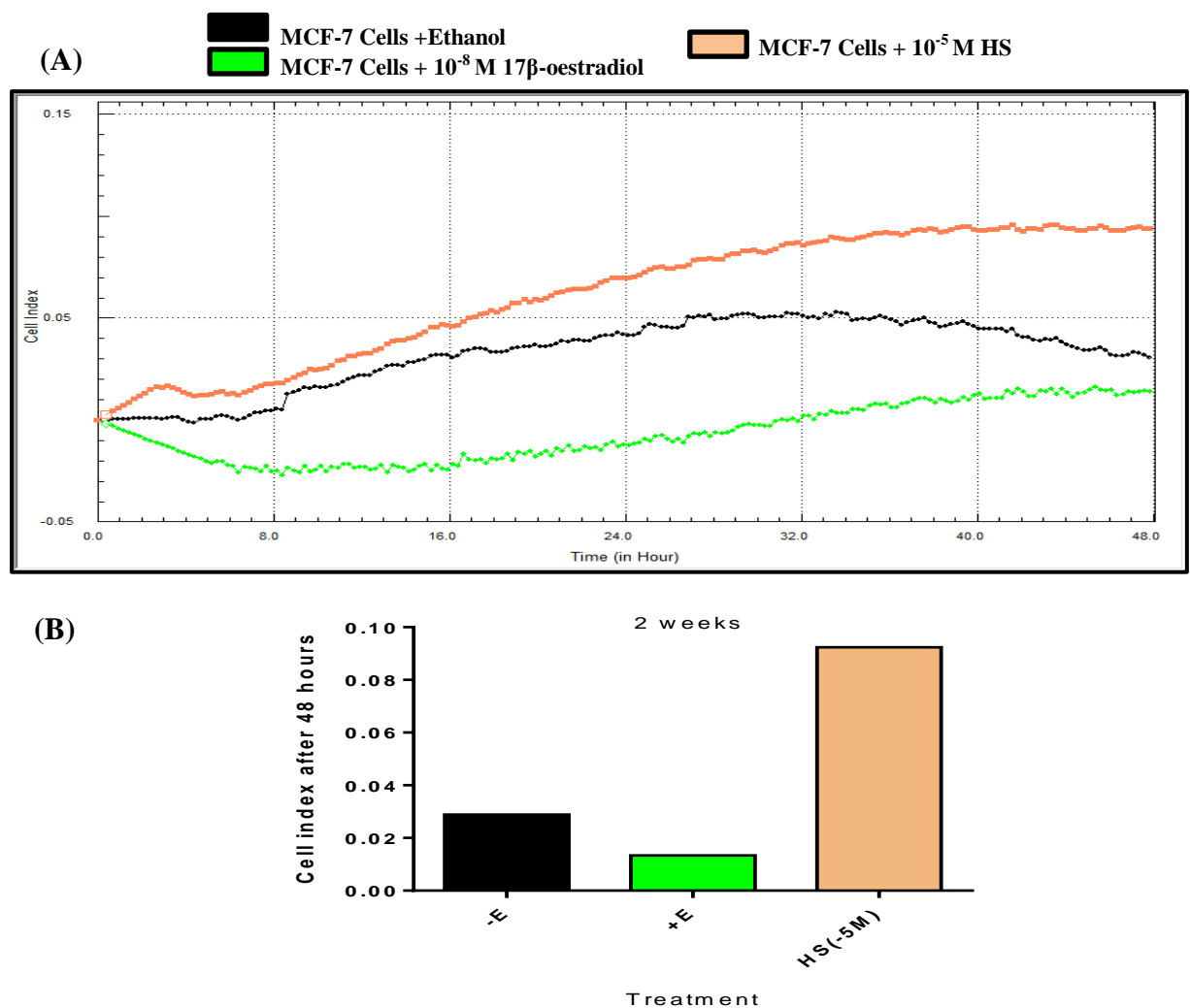


**Figure 4.44 Short-term effect of HS or 17β-oestradiol on invasion of MCF-7 human breast cancer cells through matrigel using chemotaxis stimulus as determined by xCELLigence technology.**

Cells were grown in phenol-red-free-DMEM containing 5% DCFCS with ethanol control only (-E), 10<sup>-8</sup> M 17β-oestradiol (+E) or 10<sup>-5</sup> M HS (HS (-5M)) for 2 weeks. Media were replenished and cells were split every 3-4 days. Cells were analysed for their invasive activity through matrigel (1:40) coated CIM-plate 16 in a real time invasion assay (xCELLigence RTCA device) (A) The relative change in cell index of duplicate wells as indicated by the changes in impedance caused by cell migration from upper chambers to lower ones through the pores of the polycarbonate membrane coated with matrigel. Cell index was recorded every 5 minutes and monitored for 48 hours. (B) Bar graph represents the average of the end point measurements (Cell index) of cell invasion of duplicate independent wells at 48 hours.

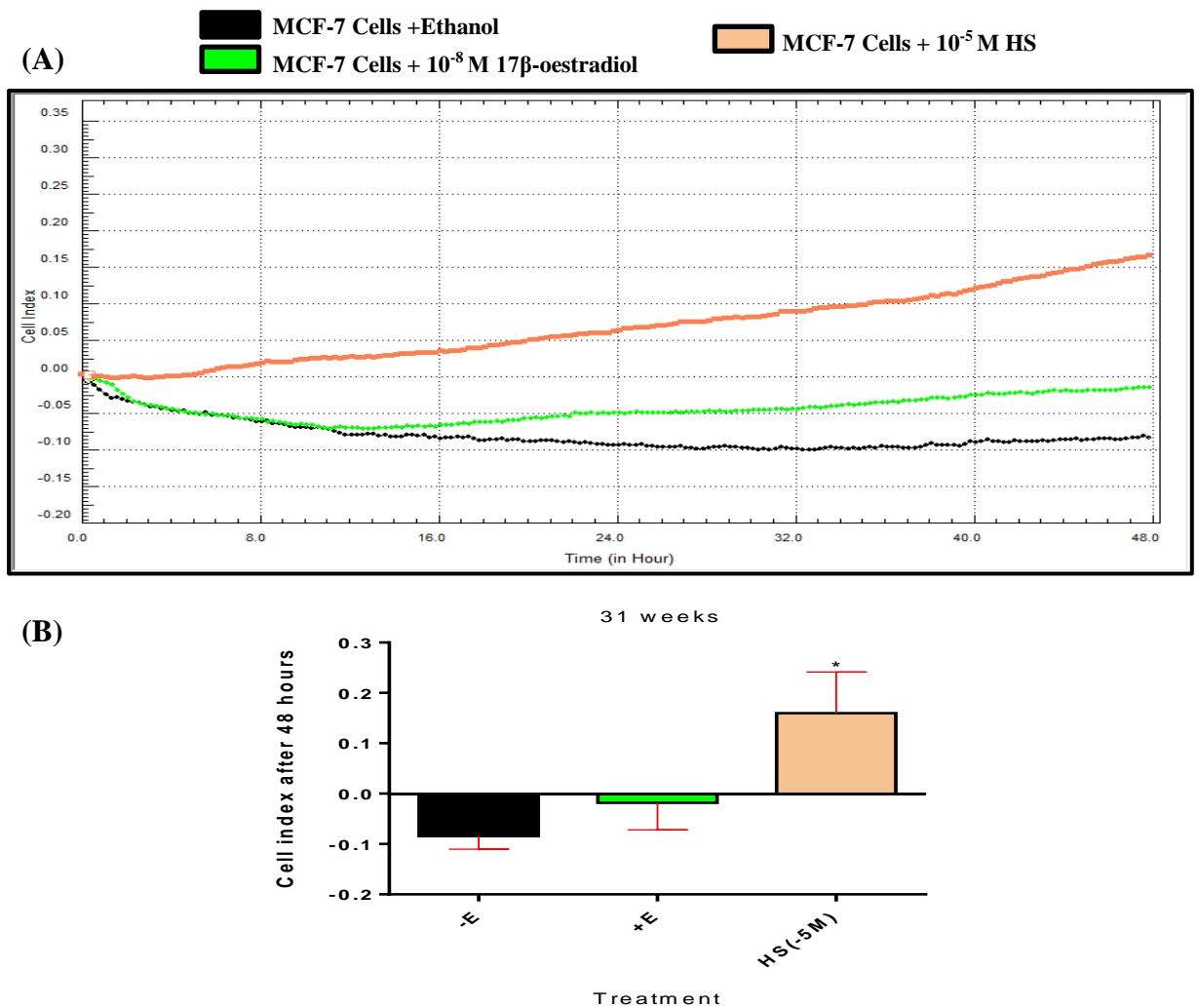


**Figure 4.45 Long-term effect of HS or  $17\beta$ -oestradiol on invasion of MCF-7 human breast cancer cells through matrigel using chemotaxis stimulus as determined by xCELLigence technology.**

Cells were grown in phenol-red-free-DMEM containing 5% DCFCS with ethanol control only (-E),  $10^{-8}$  M  $17\beta$ -oestradiol (+E) or  $10^{-5}$  M homosalate (HS (-5M)) for 31 weeks. Media were replenished and cells were split every 3-4 days. Cells were analysed for their invasive activity through matrigel (1:40) coated CIM-plate 16 in a real time invasion assay (xCELLigence RTCA device) (A) The relative change in cell index of triplicate wells as indicated by the changes in impedance caused by cell migration from upper chambers to lower ones through the pores of the polycarbonate membrane coated with matrigel. Cell index was recorded every 5 minutes and monitored for 48 hours. (B) Bar graph represents the average of the end point measurements (Cell index) of cell invasion of triplicate wells at 48 hours. Values are the average  $\pm$ SE of triplicate independent wells. \* *p*-value  $\leq 0.05$  versus no addition by one-way ANOVA Dunnett's test.

#### 4.3.6.5 Summary of effects with HS

Table 4.6 summarises all the results in section 4.3.6. The results are shown as determined by wound healing, time-lapse microscopy and the xCELLigence technology after 2 weeks and longer time points of exposure to concentrations of  $10^{-7}$  M and  $10^{-5}$  M HS.

**Table 4.6 Effects of HS on motility and invasion of MCF-7 human breast cancer cells**

Experiment	Molar concentration		Incubation time prior to the experiment
	$10^{-7}$ M	$10^{-5}$ M	
Wound healing	--	(**)	8 weeks
	n.s.	n.s.	13 weeks
	(**)	--	21 weeks
Time-lapse	--	n.s.	2 weeks
	(*)in percentage of motile cells	--	21 weeks
Real-time monitoring of cell motility (xCELLigence)	--	n.o.	2 weeks
	n.o.	--	10 weeks
	n.o.	--	20 weeks
	--	(*)	23 weeks
Real-time monitoring of cell invasion through matrigel ( xCELLigence)	n.o.	O.	2 and 10 weeks
	--	(*)	31 weeks

(-- ) experiment was not conducted; \*  $p$ -value  $\leq 0.05$  versus no addition; \*\*  $p$ -value  $\leq 0.01$  versus no addition; (n.s.)  $p$ -value  $> 0.05$  not significant; (O.) effect observed using duplicates only-no statistical analysis possible for duplicates; (n.o.) no effects observed using duplicates.

#### 4.3.7 Comparisons of effects among different UV screen and different exposure time points:

In order to compare the effect of different UV screens on MCF-7 cells motility, collected data from the wound healing assays were statistically compared using one-way ANOVA Tukey's test. Data from 7 weeks of exposure to  $10^{-5}$  M UV screens has shown no significant different in the effects caused by exposure to these chemicals but an increase in MCF-7 cells motility was indicated after exposure to  $10^{-5}$  M Bp2 and  $10^{-5}$  M 4MBC compared to  $10^{-8}$  M 17 $\beta$ -oestradiol (Figure 4.46 (A)). However, after 21 weeks of exposure to  $10^{-5}$  M UV screens Bp3 has shown a significant increase in MCF-7 cells motility compared to no addition,  $10^{-8}$  M 17 $\beta$ -oestradiol and  $10^{-5}$  M Bp1 (Figure 4.46 (B)). While 4MBC and HS has caused significant increase in MCF-7 cells motility compared to  $10^{-8}$  M 17 $\beta$ -oestradiol ( $p$ -value  $\leq 0.05$ ) (Figure 4.46 (B)).

No different between the effects of  $10^{-7}$  M of the UV screens was indicated following 13 weeks of exposure (data not shown). However, 21 weeks of exposure to  $10^{-7}$  M Bp1 has caused a significant increase in wound healing compared to  $10^{-7}$  M Bp3 and  $10^{-7}$  M OMC ( $p$ -value  $\leq 0.05$ ). Although no different was indicated after comparing the effects of  $10^{-7}$  M Bp1 and  $10^{-7}$  M Bp2, the effects of Bp2 on wound healing was significant compared to three UV screens ( $10^{-7}$  M Bp3,  $10^{-7}$  M OMC and  $10^{-7}$  M 4MBC) ( $p$ -value  $\leq 0.01$ ) (Figure 4.46 (C)).

In order to address whether the indicated affects of the UV screens on MCF-7 cells motility as indicated by wound healing assays or the xCELLigence technology have varied through the different time points of exposure, another statistical analysis was conducted using two-way ANOVA Bonferroni post-hoc test. The results of the motility of MCF-7 cells that were exposed to  $10^{-5}$  M of the UV screens for 7-8 and 21 weeks of exposure have shown that only effects of exposure to  $10^{-5}$  M Bp3 has increased significantly through the time line of the experiment as indicated by wound healing assay (Figure 4.47 (A)). However, the effects of the exposure to lower dose of the UV screens have shown a significant increase in MCF-7 cells motility after 21 weeks of exposure compared to 13 weeks of exposure to  $10^{-7}$  M Bp1 ( $p$ -value  $\leq 0.0001$ ),  $10^{-7}$  M Bp2 ( $p$ -value  $\leq 0.0001$ ),  $10^{-7}$  M Bp3 ( $p$ -value  $\leq 0.01$ ),  $10^{-7}$  M OMC,  $10^{-7}$  M 4MBC and  $10^{-7}$  M HS ( $p$ -value  $\leq 0.05$ ) as indicated by wound healing assay (Figure 4.47 (B)).

Results obtained of the chemotactic driven motility of MCF-7 cells by the xCELLigence have shown that the effect of exposure to  $10^{-7}$  M,  $10^{-6}$  M and  $10^{-5}$  M Bp3 has increased through the

time line (Figurer 4.48 (A)), and  $10^{-6}$  M OMC,  $10^{-7}$  M OMC and  $10^{-6}$  M 4MBC had shown a significant increase in motility after 21 weeks of exposure compared to 2 and 10 weeks of exposure (Figures 4.49 and 4.50).

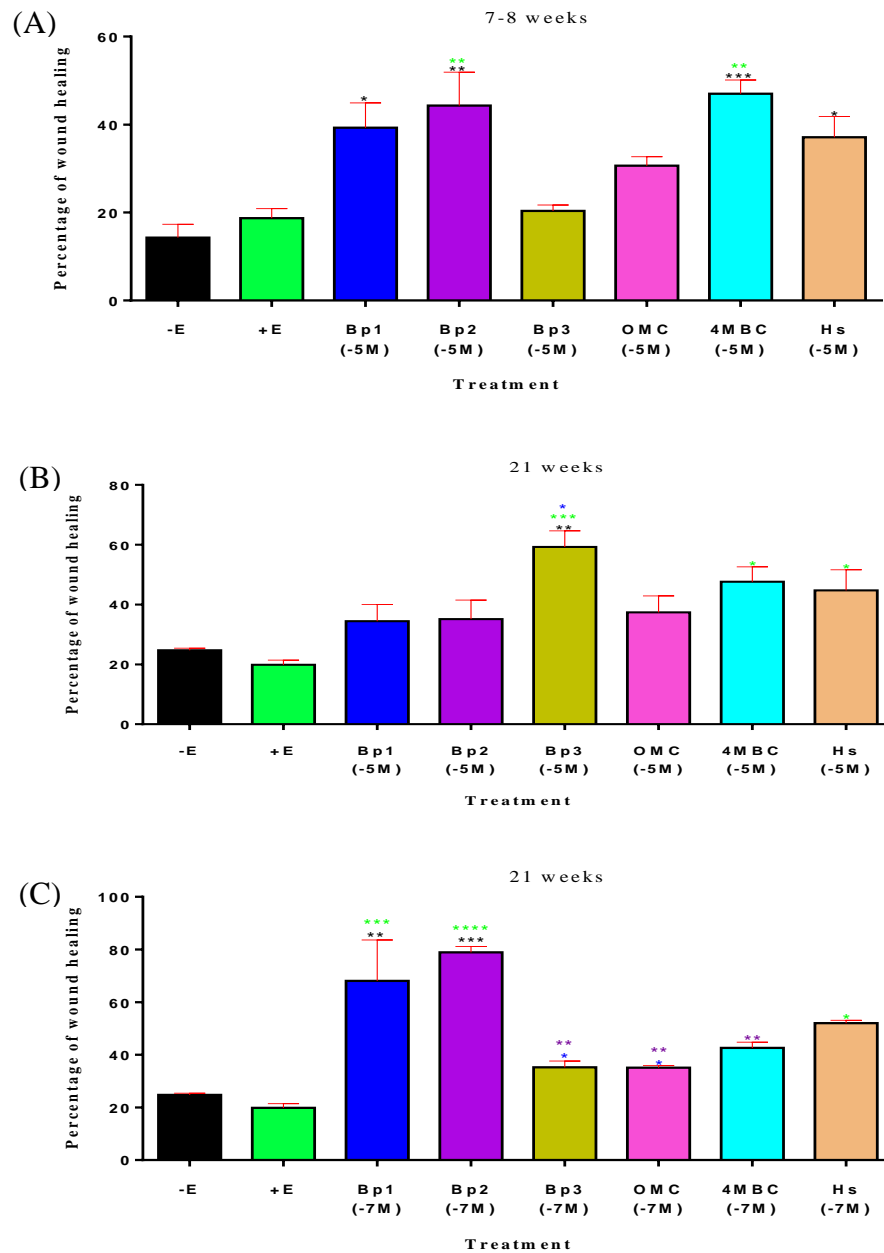


**Figure 4.46** Statistical comparison of the varying effect of the UV screens on MCF-7 human breast cancer cells collective motility as indicated by the wound healing assay.

Cells were grown in phenol-red-free-DMEM containing 5% DCFCS with ethanol control (-E) only,  $10^{-8}$  M  $17\beta$ -oestradiol (+E), with  $10^{-5}$  M of the UV screens for 7-8 weeks (A), 21 weeks (B) and to  $10^{-7}$  M UV screens for 21 weeks (C) respectively. Media were replenished and cells were split every 3-4 days. Cells were then reseeded in 12-well plates and once the cells became  $\geq 95\%$  confluent, wound was made and mitomycin c ( $0.5\mu\text{g/ml}$ ) was added. Images were captured at 0 hour and 24 hours. Cell migration was quantified by analysing 5 images from each well by using Image J software. Values are the average  $\pm$ SE of 3 independent wells ( $n=3$ ). \*  $p$ -value  $\leq 0.05$ , \*\*  $p$ -value  $\leq 0.01$  and \*\*\*\*  $p$ -value  $\leq 0.0001$  versus no addition (black asterisks),  $17\beta$ -oestradiol (green asterisks), Bp1 (blue asterisks) and Bp2 (purple asterisks) by one-way ANOVA Tukey's test.

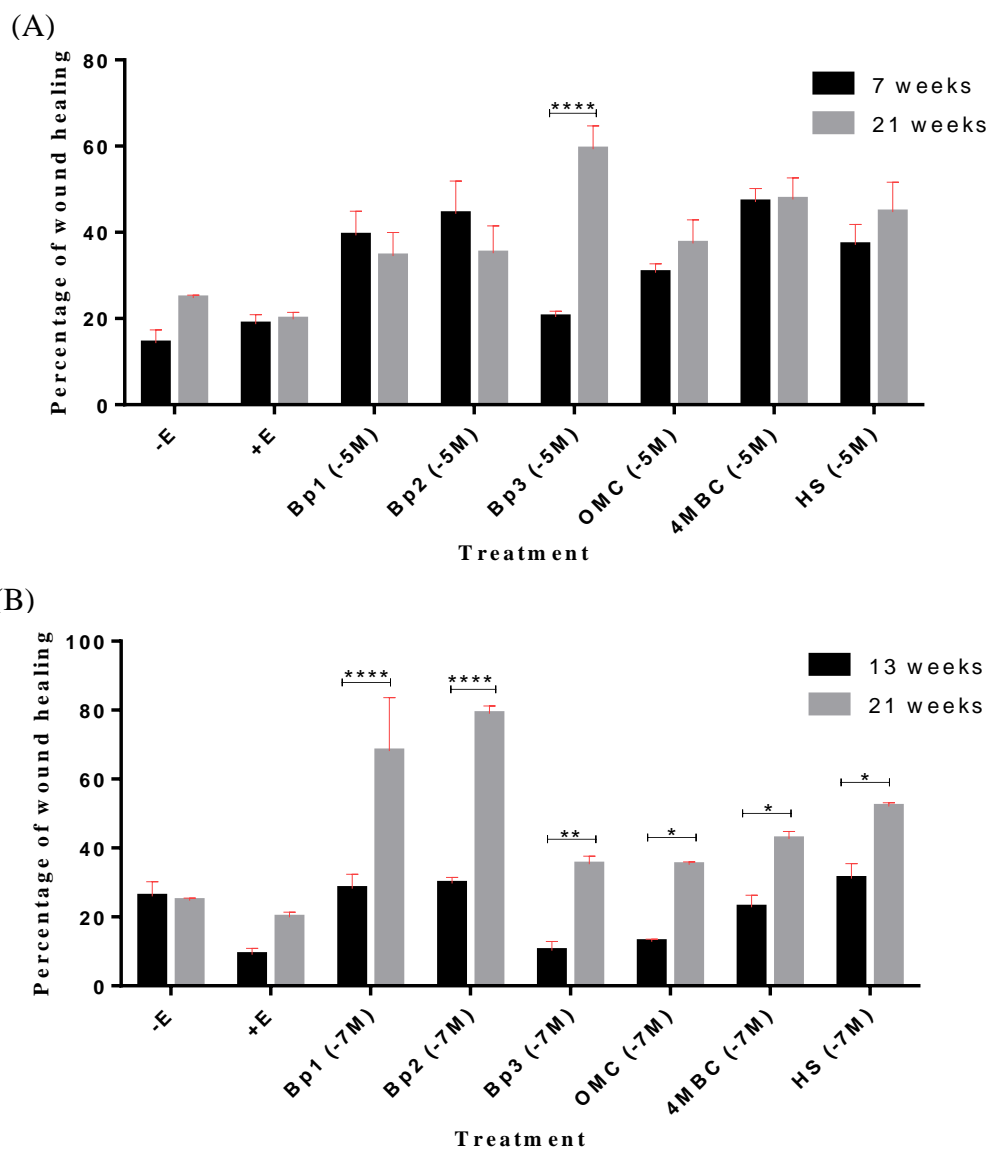


**Figure 4.47 Statistical comparison of the effects of different times of exposure of MCF-7 human breast cancer cells to the UV screens as indicated by the wound healing assay.**

Cells were grown in phenol-red-free-DMEM containing 5% DCFCS with ethanol control (-E) only,  $10^{-8}$  M  $17\beta$ -oestradiol (+E), with  $10^{-5}$  M of the UV screens for 7-8 and 21 weeks (A) and to  $10^{-7}$  M UV screens for 13 and 21 weeks (B) respectively. Media were replenished and cells were split every 3-4 days. Cells were then reseeded in 12-well plates and once the cells became  $\geq 95\%$  confluent, wound was made and mitomycin c ( $0.5\mu\text{g/ml}$ ) was added. Images were captured at 0 hour and 24 hours. Cell migration was quantified by analysing 5 images from each well by using Image J software. Values are the average  $\pm$ SE of 3 independent wells ( $n=3$ ). \*  $p$ -value  $\leq 0.05$ , \*\*  $p$ -value  $\leq 0.01$  and \*\*\*\*  $p$ -value  $\leq 0.0001$  versus the different time point for the same chemical by two-way ANOVA Bonferroni test.

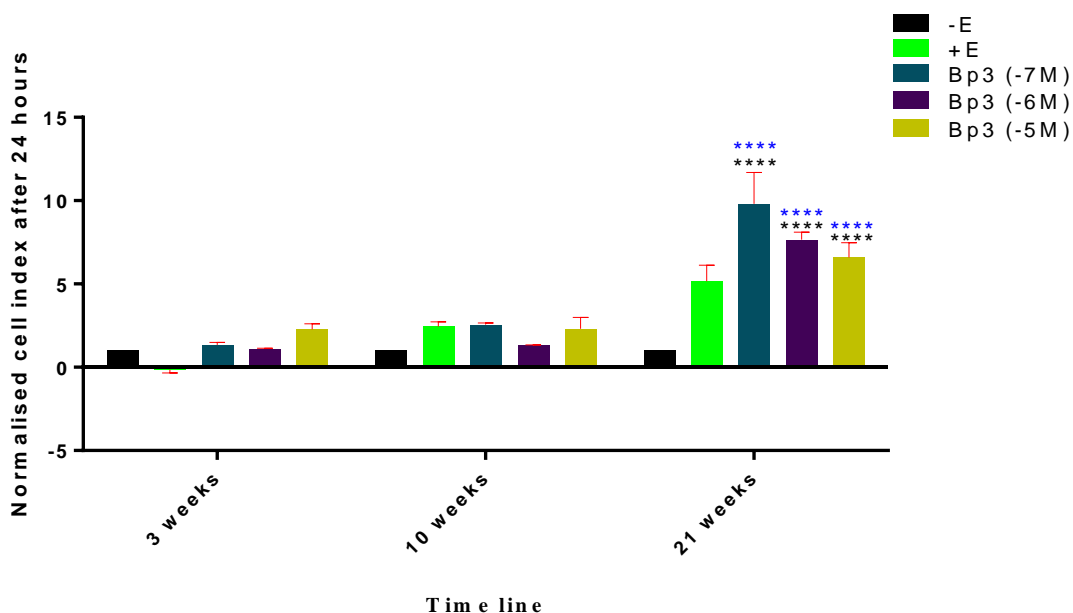


**Figure 4.48 Effect of different exposure times to Bp3 or 17 $\beta$ -oestradiol on migration of MCF-7 human breast cancer cells using chemotaxis stimulus as determined by xCELLigence technology.**

Cells were grown in phenol-red-free-DMEM containing 5% DCFCS with ethanol control only (-E),  $10^{-8}$  M 17 $\beta$ -oestradiol (+E),  $10^{-7}$  M Bp3 (Bp3 (-7M)),  $10^{-6}$  M Bp3 (Bp3 (-6M)) or  $10^{-5}$  M Bp3 (Bp3 (-5M)) for 3, 10 and 21 weeks. Media were replenished and cells were split every 3-4 days. The relative change in cell index of duplicate wells as indicated by the changes in impedance caused by cell migration from upper chambers to lower ones through the pores of the polycarbonate membrane was recorded every 5 minutes and monitored for 24 hours. The bar graph represents the normalised cell index values to the negative control at the end point of cell migration of duplicate independent wells at 24 hours. \*\*\*\*  $p$ -value  $\leq 0.0001$  versus the same concentration at 3 weeks (black asterisks) or 10 weeks (blue asterisks) by two-way ANOVA Bonferroni test.

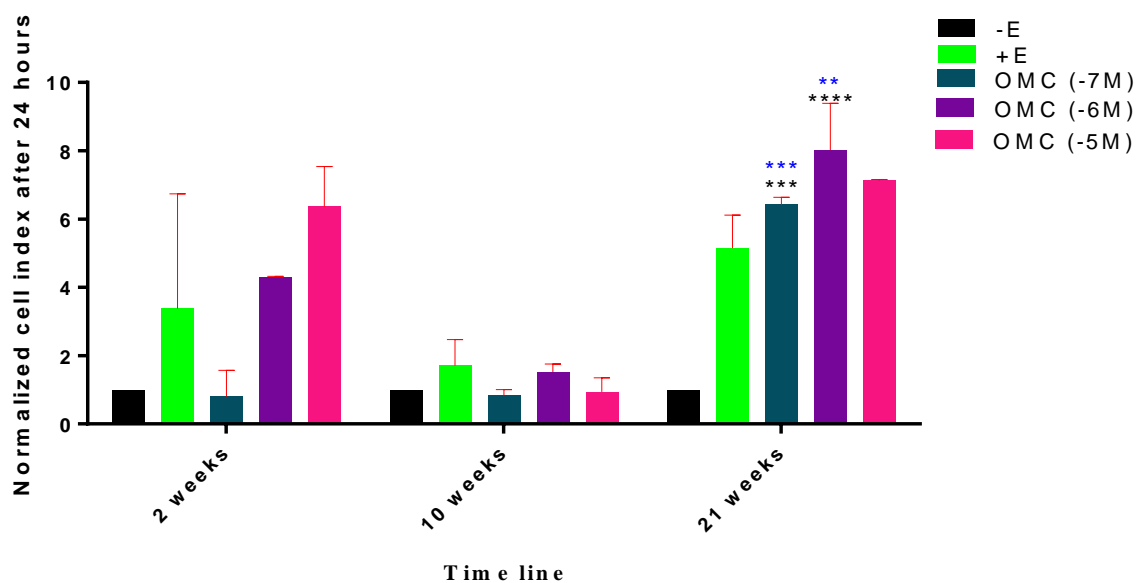


**Figure 4.49 Effect of different exposure times to OMC or 17 $\beta$ -oestradiol on migration of MCF-7 human breast cancer cells using chemotaxis stimulus as determined by xCELLigence technology.**

Cells were grown in phenol-red-free-DMEM containing 5% DCFCs with ethanol control only (-E), 10<sup>-8</sup> M 17 $\beta$ -oestradiol (+E), 10<sup>-7</sup> M OMC (OMC (-7M)), 10<sup>-6</sup> M OMC (OMC (-6M)) or 10<sup>-5</sup> M OMC (OMC (-5M)) for 2, 10 and 21 weeks. Media were replenished and cells were split every 3-4 days. The relative change in cell index of duplicate wells as indicated by the changes in impedance caused by cell migration from upper chambers to lower ones through the pores of the polycarbonate membrane was recorded every 5 minutes and monitored for 24 hours. The bar graph represents the normalised cell index values to the negative control at the end point of cell migration of duplicate independent wells at 24 hours. \*\* *p-value*  $\leq$  0.01, \*\*\* *p-value*  $\leq$  0.001 and \*\*\*\* *p-value*  $\leq$  0.0001 versus the same concentration at 2 weeks (black asterisks) or 10 weeks (blue asterisks) by two-way ANOVA Bonferroni test.

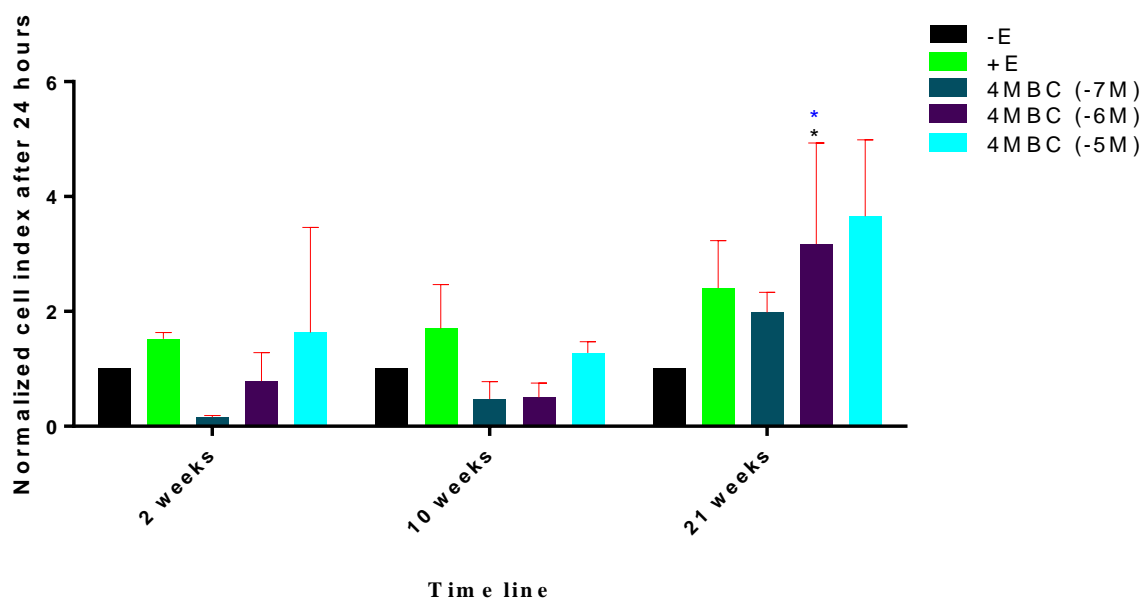


**Figure 4.50 Effect of different exposure times to 4MBC or  $17\beta$ -oestradiol on migration of MCF-7 human breast cancer cells using chemotaxis stimulus as determined by xCELLigence technology.**

Cells were grown in phenol-red-free-DMEM containing 5% DCFCS with ethanol control only (-E),  $10^{-8}$  M  $17\beta$ -oestradiol (+E),  $10^{-7}$  M 4MBC (OMC (-7M)),  $10^{-6}$  M 4MBC (OMC (-6M)) or  $10^{-5}$  M 4MBC (OMC (-5M)) for 2, 10 and 21 weeks. Media were replenished and cells were split every 3-4 days. The relative change in cell index of duplicate wells as indicated by the changes in impedance caused by cell migration from upper chambers to lower ones through the pores of the polycarbonate membrane was recorded every 5 minutes and monitored for 24 hours. The bar graph represents the normalised cell index values to the negative control at the end point of cell migration of duplicate independent wells at 24 hours.\*  $p$ -value  $\leq 0.05$  versus the same concentration at 2 weeks (black asterisks) or 10 weeks (blue asterisks) by two-way ANOVA Bonferroni test.

### **4.3.8 Effects of the UV screens on molecular markers related to motility and invasion of MCF-7 human breast cancer cells**

Alterations in MCF-7 cell epithelial morphology including the production of protrusions and lamellipodia were noticed after 23 weeks of exposure to the UV screens (Figures 4.51 and 4.52). Red arrows show cells which have changed to a more mesenchymal morphology by showing two morphological features; transiting to individual elongated cells or forming motility compartments including lamellipodial or filopodial protrusions. These morphological changes combined with changes in cell motility as described earlier, led to investigation of potential molecular mechanisms. The expression levels of two of the molecular markers involved in EMT (E-cadherin and  $\beta$ -catenin) were assessed using RT-PCR (as described in section 2.6) and western immunoblotting (as described in section 2.7). Also, the mRNA levels of Twist1 and Snail were assessed using RT-PCR. Further investigation also covered the effects of UV screens on the activity of MMP-2 and MMP-9 using zymography (as described in section 2.8). Moreover, this work examined the effects of UV screens on mRNA levels of two other genes (PIK3R1 and BMP7), which were found to be allied in both the metastable phenotype of MCF-7 cells and the mesenchymal breast cancer cell line MDA-MB-231 as described by Uchino et al. (2010).

#### **4.3.8.1 Effects of the UV screens on levels of E-cadherin in MCF-7 human breast cancer cells**

Effects of UV screens on levels of E-cadherin mRNA and protein levels were investigated after 1 week and 20 weeks+ of exposure. In order to measure the levels of E-cadherin mRNA using RT-PCR,  $\beta$ -actin was selected to be used as an endogenous control. Levels of E-cadherin mRNA were found to be significantly reduced in MCF-7 cells after 1 week of exposure to  $10^{-5}$  M 4MBC and  $10^{-5}$  M HS (Figure 4.53 (A)) ( $p$ -value  $\leq 0.001$ ). Also, longer exposure (24-25 weeks) to  $10^{-5}$  M Bp1,  $10^{-5}$  M Bp3,  $10^{-5}$  M OMC,  $10^{-5}$  M 4MBC or  $10^{-5}$  M HS were found to reduce E-cadherin mRNA levels (Figure 4.53 (B)).

E-cadherin was identified as 135 kDa band on western immunoblotting using molecular weight markers. After 1 week of exposure to  $10^{-5}$  M of the UV screens, no change in E-cadherin levels was indicated by western immunoblotting (data not shown). However, longer exposure time (24-25 weeks) to  $10^{-5}$  M Bp1 and  $10^{-5}$  M HS decreased the E-cadherin protein levels in comparison with the negative control (Figures 4.54 and 4.55) ( $p$ -value  $\leq 0.05$ ).

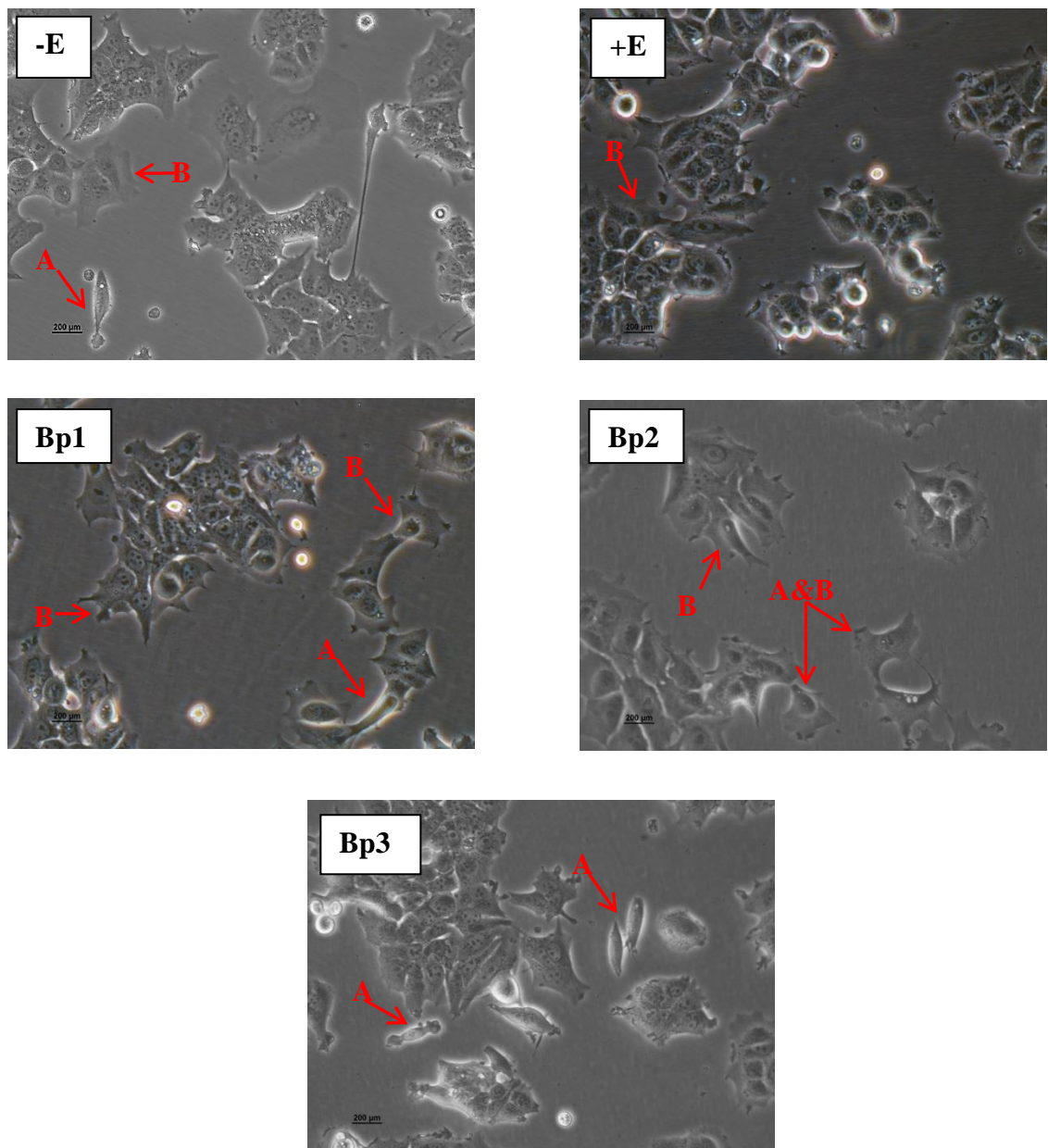


**Figure 4.51 Representative images of the long-term effect of UV screens on morphology of MCF-7 human breast cancer cells.**

Phase contrast images of MCF-7 cells grown in phenol-red-free-DMEM containing 5% DCFCS with ethanol control (-E) only, with  $10^{-5}$  M Bp1 (Bp1),  $10^{-5}$  M Bp2 (Bp2) or with  $10^{-5}$  M Bp3 (Bp3) or with  $10^{-8}$  M  $17\beta$ -oestradiol (+E) for 23 weeks. Red arrows show cells which have changed to a more mesenchymal morphology by becoming elongated individual cells (A) or showing the formation of motility compartments including lamellipodial or filopodial protrusions (B).

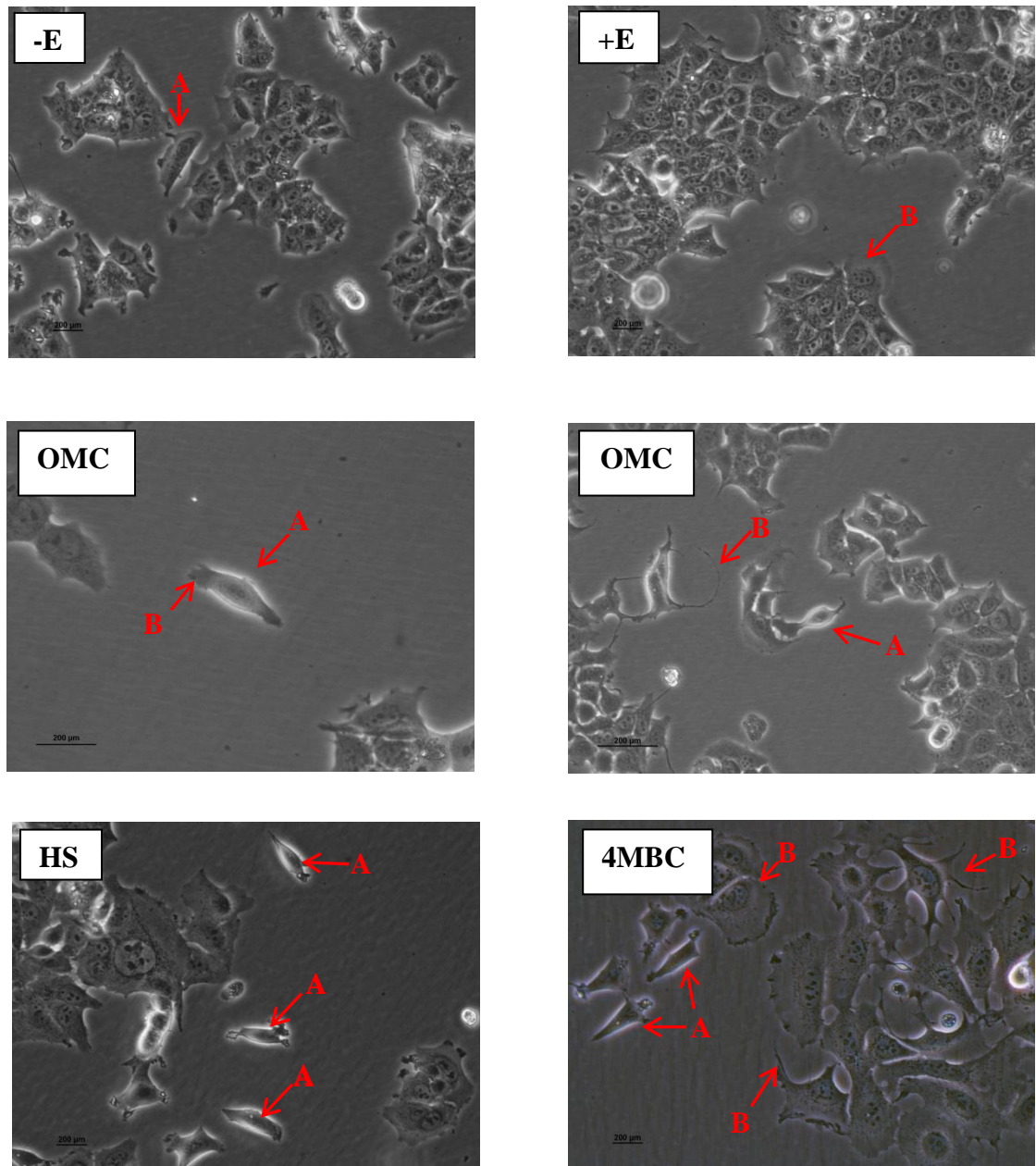


**Figure 4.52 Representative images of the long-term effect of UV screens on morphology of MCF-7 human breast cancer cells.**

Cells were grown in phenol-red-free-DMEM containing 5% DCFCS with ethanol control (-E) only, with  $10^{-5}$  M OMC (OMC),  $10^{-5}$  M 4MBC (4MBC) or with  $10^{-5}$  M homosalate (HS) or with  $10^{-8}$  M  $17\beta$ -oestradiol (+E) for 23 weeks. Red arrows show cells which have changed to a more mesenchymal morphology by becoming separated elongated individual cells (A) or showing the formation of motility compartments including lamellipodial or filopodial protrusions (B).

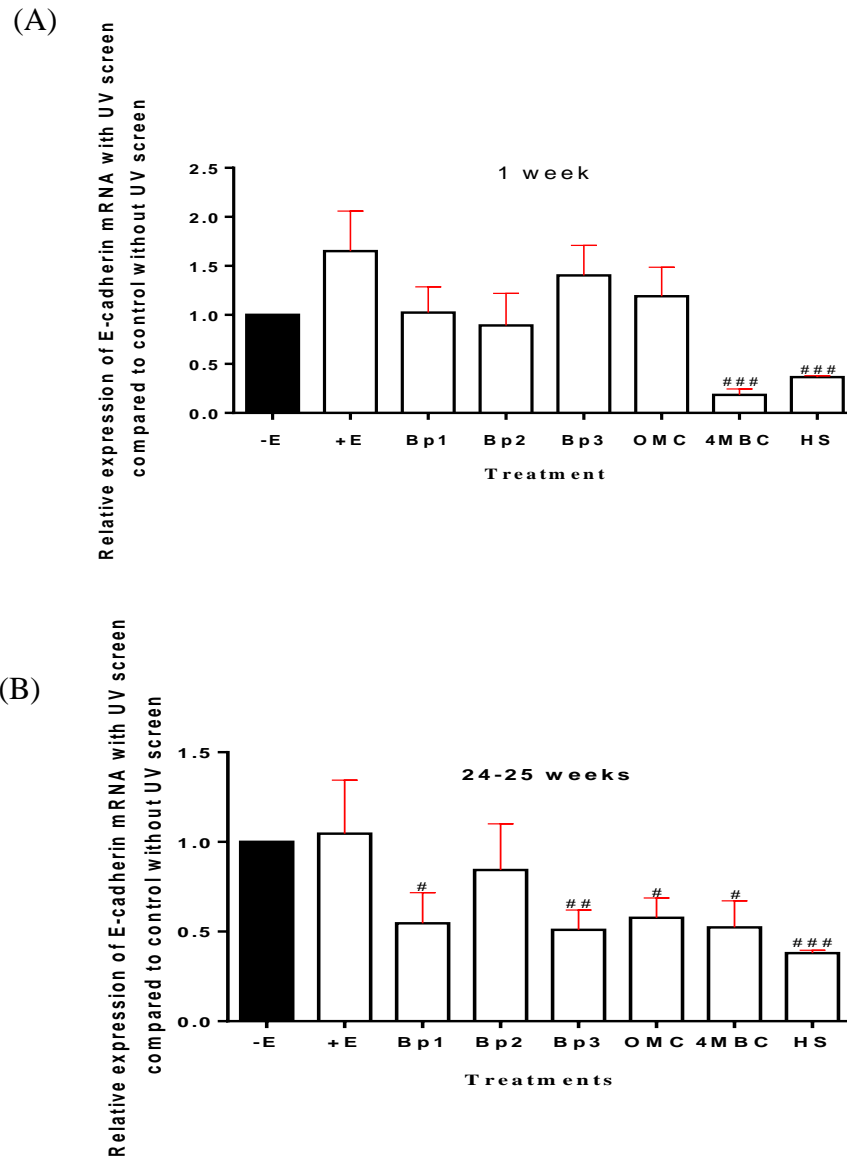


**Figure 4.53 Effect of exposure to the UV screens on levels of E-cadherin mRNA in MCF-7 cells as determined using real-time RT-PCR.**

Cells were assayed after 1 week (media were replenished two times)(A) or 24-25 weeks (media were changed and cells were split each 3-4 days) (B), with ethanol control (-E), with  $10^{-8}$  M  $17\beta$ -oestradiol (+E), with  $10^{-5}$  M Bp1 (Bp1), with  $10^{-5}$  M Bp2 (Bp2), with  $10^{-5}$  M Bp3 (Bp3), with  $10^{-5}$  M OMC (OMC), with  $10^{-5}$  M 4MBC (4MBC) or with  $10^{-5}$  M HS (HS). For each RT-PCR assay, E-cadherin values were normalised to  $\beta$ -actin values, expressed as fold change from control cells grown without the UV screens by  $2^{-\Delta\Delta C_T}$  method and the average SE of three independent experiment (n=3) taken from cells grown for 1 week or 24-25 weeks from independent cultures. Fold change for cell grown with  $17\beta$ -oestradiol or UV screens are shown in the bar graph compared to the negative control. # *p*-value  $\leq 0.05$ , ## *p*-value  $\leq 0.01$  and ### *p*-value  $\leq 0.001$  decrease versus no addition (-E) by t-Test.

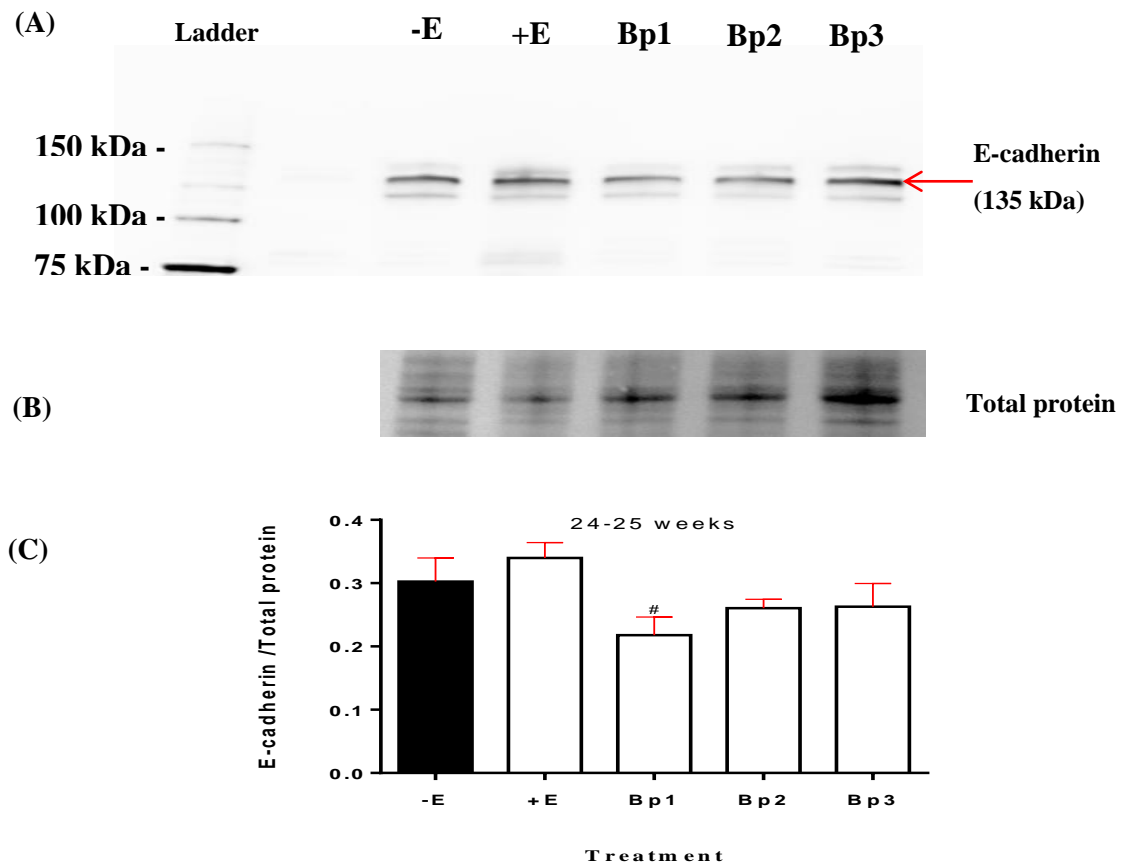


**Figure 4.54 Effect of long-term exposure to UV screens on the level of E-cadherin.**

MCF-7 human breast cancer cells were grown for 24-25 weeks in phenol-red-free-DMEM supplemented with 5% DCFCS, with or without  $10^{-8}$  M  $17\beta$ -oestradiol or with  $10^{-5}$  M Bp1 (Bp1 (-5M)), with  $10^{-5}$  M Bp2 (Bp2 (-5M)) or with  $10^{-5}$  M Bp3 (Bp3 (-5M)). Media were replenished and cells were split every 3-4 days. (A) Total cellular protein was loaded at 25  $\mu$ g per track and immunoblotted with antibody against E-cadherin. (B) Total protein was measured by the z-imager (Bio-RAD) prior to the immunoblotting steps. (C) The bar graph shows the level of E-cadherin relative to total protein from three independent experiments (n=3). # *p*-value  $\leq 0.05$  decreased versus no addition by t-Test.

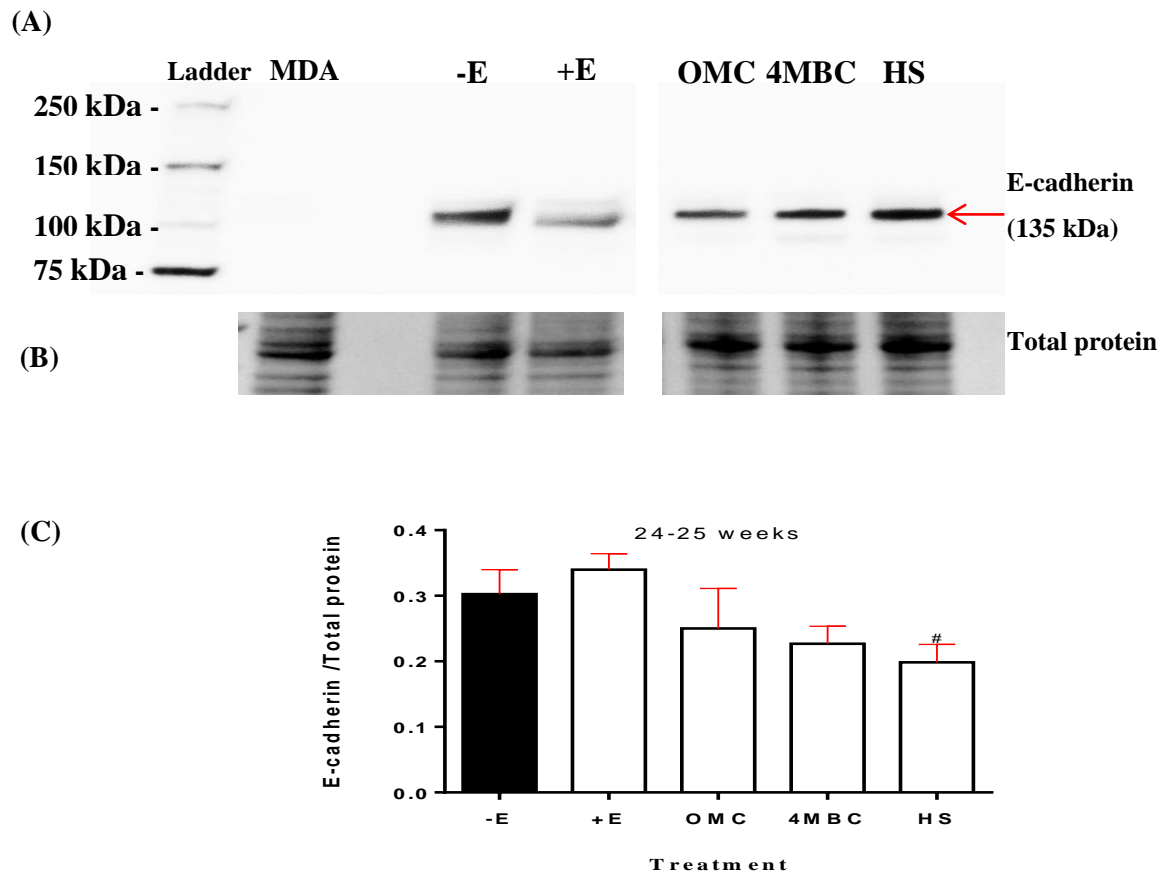


**Figure 4.55 Effect of long-term exposure to UV screens on the level of E-cadherin.**

MCF-7 human breast cancer cells were grown for 24-25 weeks in phenol-red-free-DMEM supplemented with 5% DCFCS, with or without  $10^{-8}$  M  $17\beta$ -oestradiol or with  $10^{-5}$  M OMC (OMC), with  $10^{-5}$  M 4MBC (4MBC) or with  $10^{-5}$  M HS (HS). Media were replenished and cells were split every 3-4 days. (A) MDA-MB-231 cell lysate was used as a negative control. Total cellular protein was loaded at 25  $\mu$ g per track and immunoblotted with antibody against E-cadherin. (B) Total protein was measured by the z-imager (Bio-RAD) prior to the immunoblotting steps. (C) The bar graph shows the level of E-cadherin relative to total protein for three independent experiments ( $n=3$ ). #  $p$ -value  $\leq 0.05$  decrease versus no addition by t-Test.

#### **4.3.8.2 Effects of the UV screens on levels of $\beta$ -catenin in MCF-7 human breast cancer cells**

Effects of UV screens on levels of  $\beta$ -catenin mRNA and protein levels were investigated after 1 week and 24-25 weeks of exposure. Levels of  $\beta$ -catenin mRNA were found to be significantly reduced in MCF-7 cells after 1 week of exposure to  $10^{-5}$  M HS (Figure 4.56 (A)) ( $p$ -value  $\leq 0.05$ ). Longer exposure (24-25 weeks) to  $10^{-5}$  M Bp2 or  $10^{-5}$  M Bp3 was found to reduce  $\beta$ -catenin mRNA levels in MCF-7 cells (Figure 4.56 (B)).

$\beta$ -catenin was identified as a 92 kDa band on western immunoblotting using molecular weight markers. After 1 week of exposure, MCF-7 cells exposed to  $10^{-5}$  M OMC or  $10^{-5}$  M HS showed lower levels of  $\beta$ -catenin in comparison to the negative control (Figure 4.58) ( $p$ -value  $\leq 0.05$ ) but no significant effects were found following exposure to the benzophenones or the other UV screens (Figures 4.57 and 4.58).

Significant reduction was found on  $\beta$ -catenin protein levels in MCF-7 cells following longer-term exposure (24-25 weeks) to  $10^{-5}$  M OMC (Figure 4.59) ( $p$ -value  $\leq 0.05$ ).

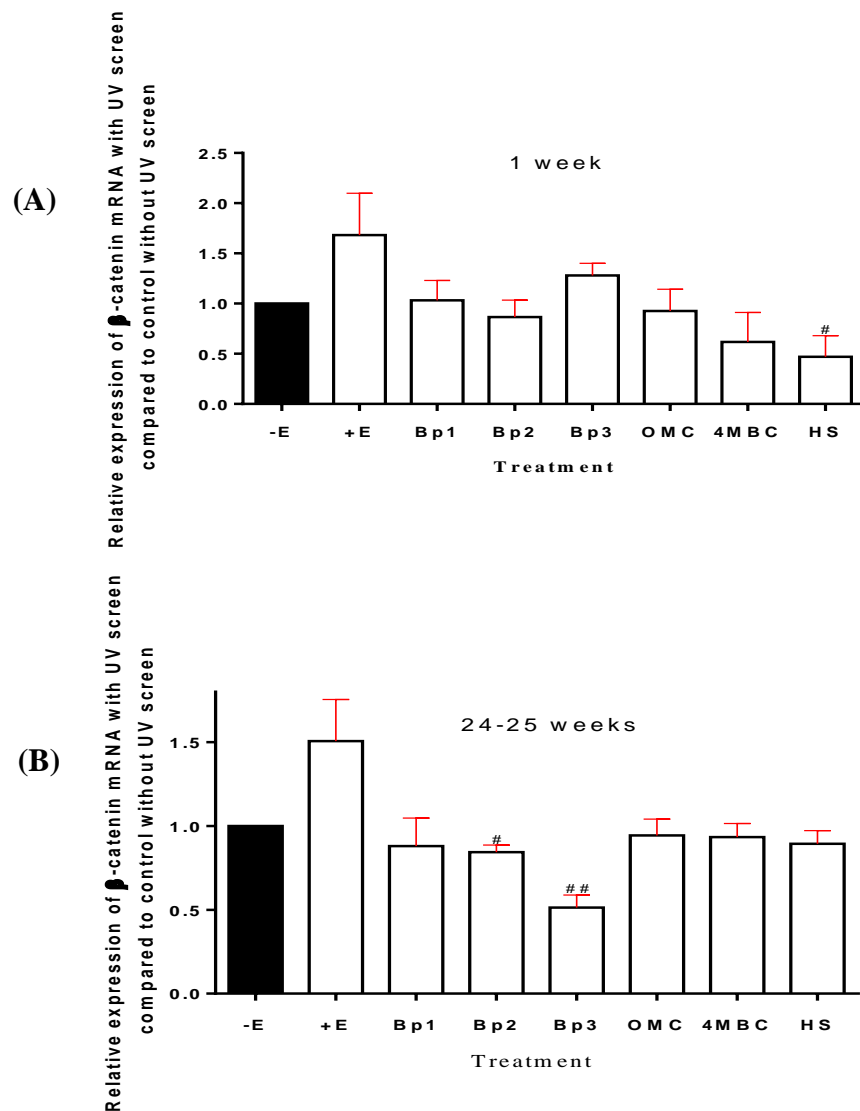


**Figure 4.56 Effect of exposure to the UV screens on levels of  $\beta$ -catenin mRNA in MCF-7 cells as determined using real-time RT-PCR.**

Cells were assayed after 1 week (media were replenished two times)(A) or 24-25 weeks (media were changed and cells were split each 3-4 days) (B) with ethanol, with  $10^{-8}$  M  $17\beta$ -oestradiol, with  $10^{-5}$  M Bp1 (Bp1), with  $10^{-5}$  M Bp2 (Bp2), with  $10^{-5}$  M Bp3 (Bp3), with  $10^{-5}$  M OMC (OMC), with  $10^{-5}$  M 4MBC (4MBC) or with  $10^{-5}$  M HS (HS). For each RT-PCR assay,  $\beta$ -catenin values were normalised to  $\beta$ -actin values, expressed as fold change from control cells grown without the UV screens by  $2^{-\Delta\Delta C_T}$  method and the average SE of three independent experiments (n=3) taken from cells grown for 1 weeks or 24-25 weeks of culture. Fold change for cell grown with  $17\beta$ -oestradiol or UV screens are shown in the bar graph compared to the negative control. # *p*-value  $\leq 0.05$  and ## *p*-value  $\leq 0.01$  versus no addition (-E) by t-Test.

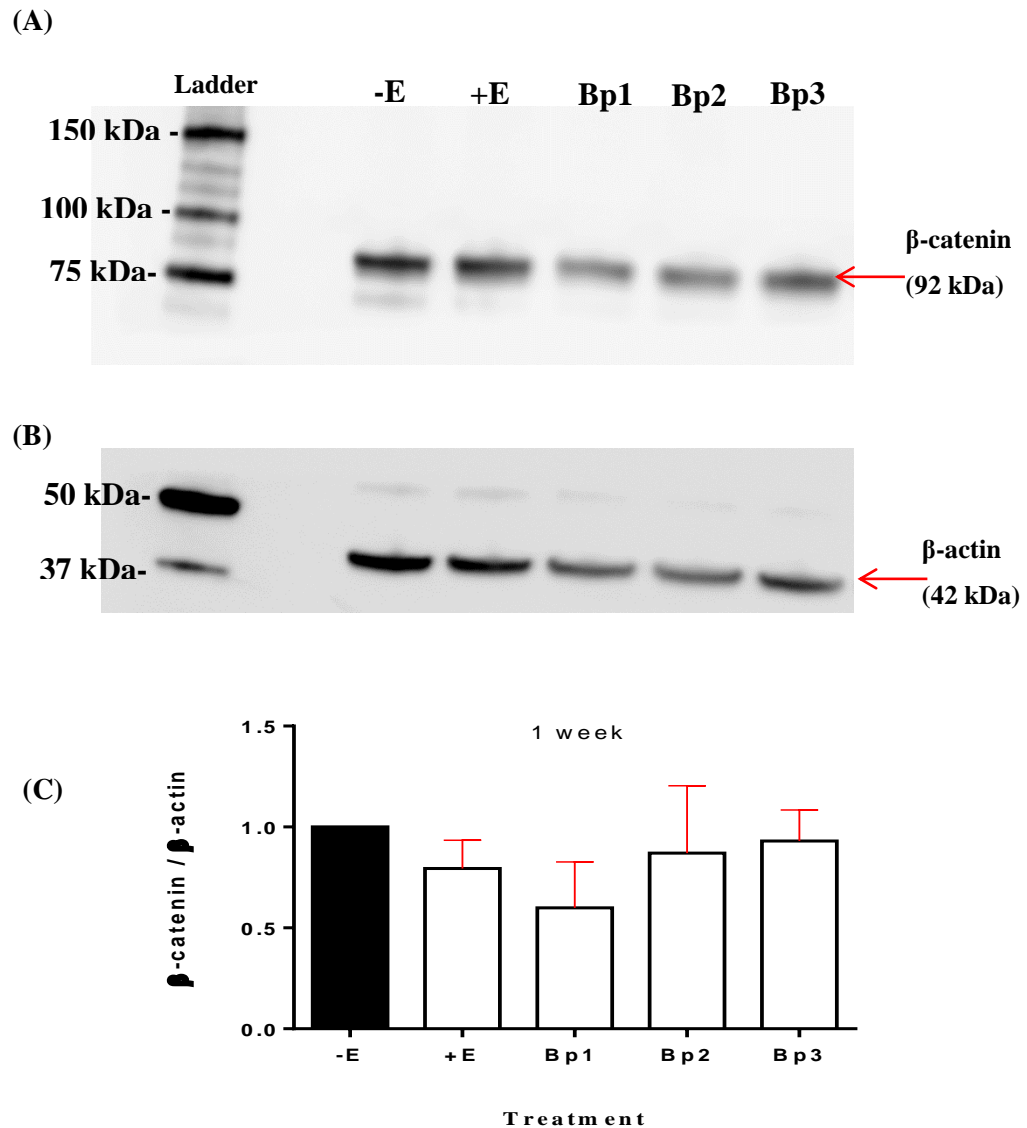


**Figure 4.57 Effect of short-term exposure to UV screens on the level of  $\beta$ -catenin.**

MCF-7 human breast cancer cells were grown for 1 week in phenol-red-free-DMEM supplemented with 5% DCFCS, with or without  $10^{-8}$  M  $17\beta$ -oestradiol or with  $10^{-5}$  M Bp1 (Bp1), with  $10^{-5}$  M Bp2 (Bp2) or  $10^{-5}$  M Bp3 (Bp3). Media were replenished twice. (A) Total cellular protein was loaded at 25  $\mu$ g per track and immunoblotted with antibody against  $\beta$ -catenin. (B) The loading control  $\beta$ -actin. (C) The bar graph shows the level of  $\beta$ -catenin relative to  $\beta$ -actin. Values are means and bars indicate SEM ( $n=3$  independent experiments) by t-Test.

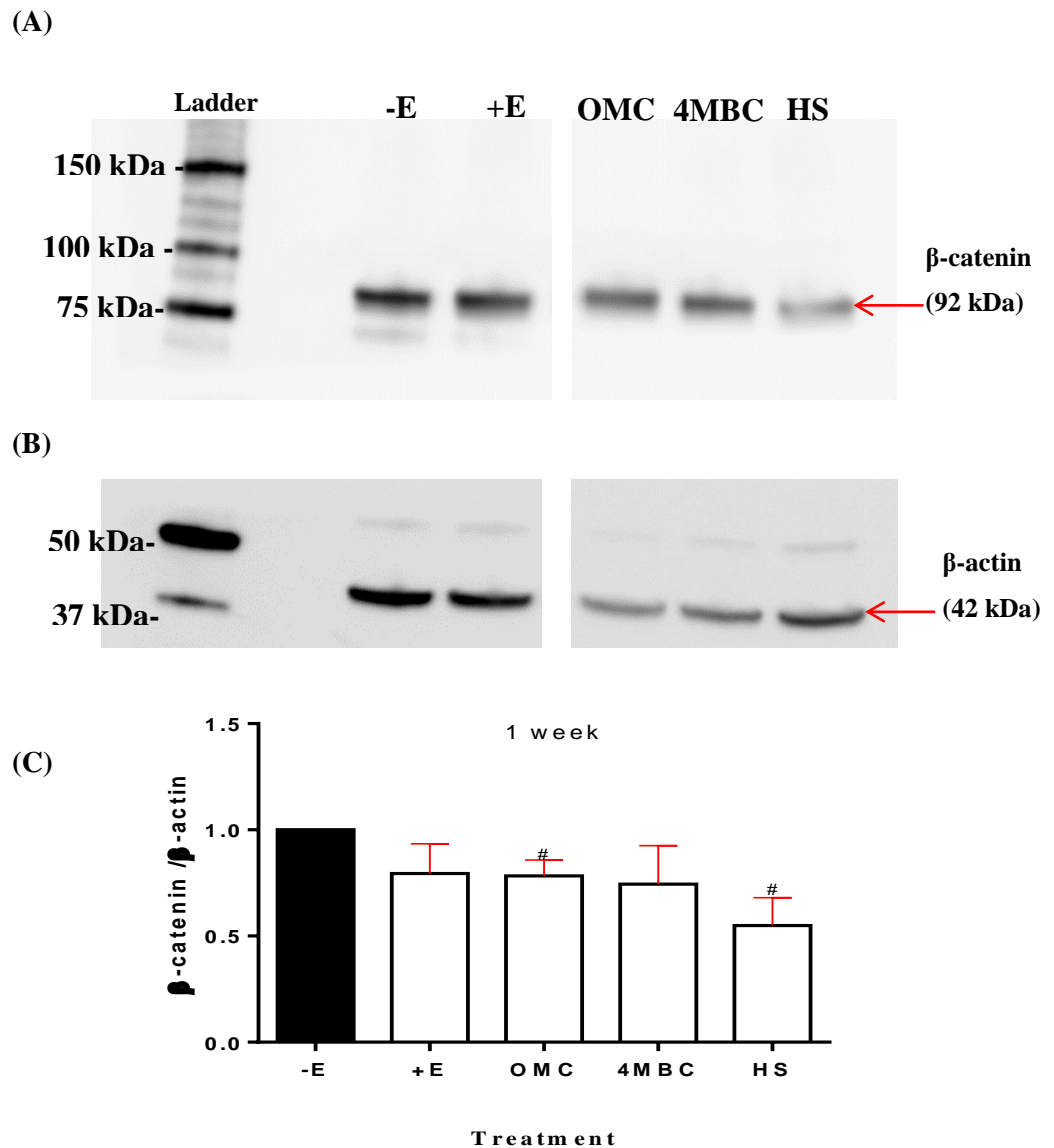


**Figure 4.58 Effect of short-term exposure to UV screens on the level of  $\beta$ -catenin.**

MCF-7 human breast cancer cells were grown for 1 week in phenol-red-free-DMEM supplemented with 5% DCFCS, with or without  $10^{-8}$  M  $17\beta$ -oestradiol or with  $10^{-5}$  M OMC (OMC), with  $10^{-5}$  M 4MBC (4MBC) or with  $10^{-5}$  M HS (HS). Media were replenished twice. (A) Total cellular protein was loaded at  $25 \mu\text{g}$  per track and immunoblotted with antibody against  $\beta$ -catenin. (B)  $\beta$ -actin the loading control. (C) The bar graph shows the level of  $\beta$ -catenin to  $\beta$ -actin. Values are means and bars indicate SEM ( $n=3$  independent experiments). #  $p$ -value  $\leq 0.05$  decrease versus no addition by t-Test.

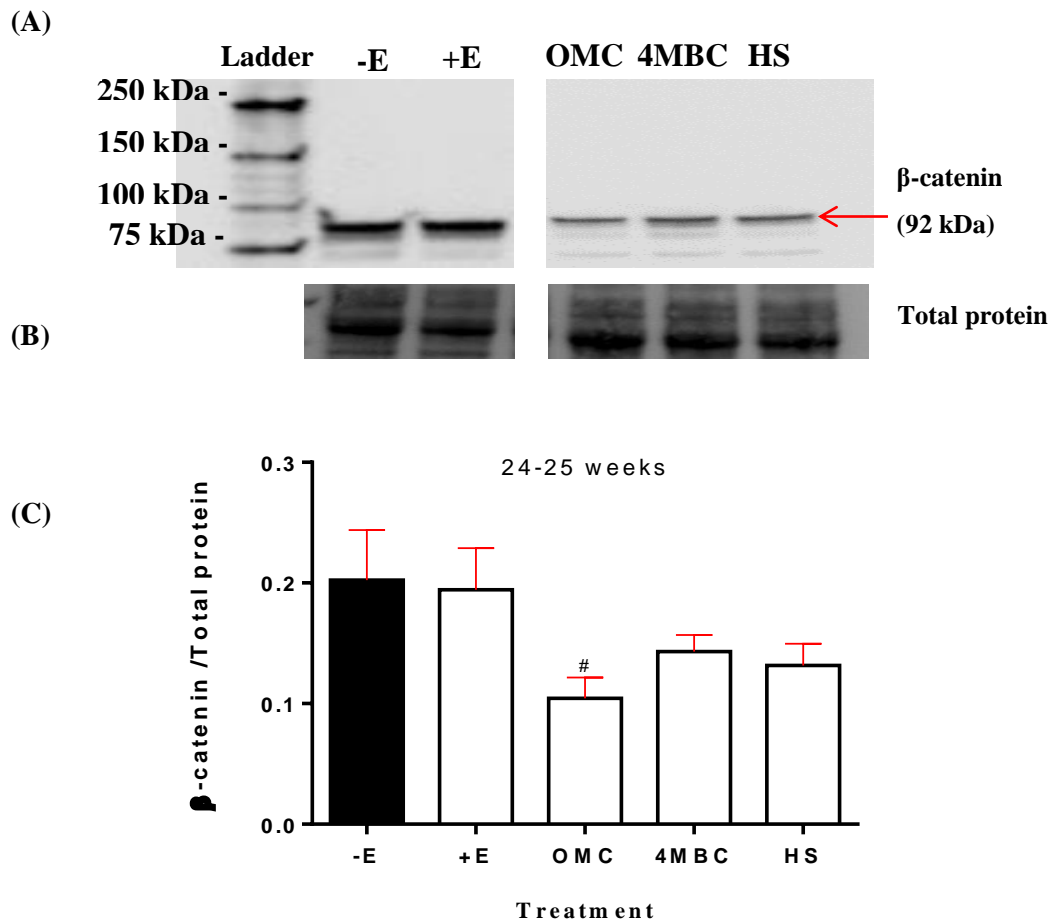


**Figure 4.59 Effect of long-term exposure to UV screens on the level of  $\beta$ -catenin.**

MCF-7 human breast cancer cells were grown for 24-25 weeks in phenol-red-free-DMEM supplemented with 5% DCFCS, with or without  $10^{-8}$  M  $17\beta$ -oestradiol or with  $10^{-5}$  M OMC (OMC), with  $10^{-5}$  M 4MBC (4MBC) or with  $10^{-5}$  M HS (HS). Media were replenished and cells were split every 3-4 days. (A) Total cellular protein was loaded at 25  $\mu$ g per track and immunoblotted with antibody against  $\beta$ -catenin. (B) Total protein was measured by the z-imager (Bio-RAD) prior to the immunoblotting steps. (C) The bar graph shows the level of  $\beta$ -catenin relative to total protein from three independent experiments ( $n=3$ ). #  $p$ -value  $\leq 0.05$  decrease versus no addition (-E) by t-Test.

### **4.3.8.3 Effects of the UV screens on MMPs in MCF-7 human breast cancer cells.**

Three MMPs were selected to be investigated after long-term exposure (35-37 weeks) of MCF-7 cells to the UV screens. Secreted MMP-2 and MMP-9 were measured in the conditioned media (serum free media) via zymography (as described in section 2.8). In the case of the intracellular MMP-14 protein levels, the effects were measured using western immunoblotting (as described in section 2.7).

#### **4.3.8.3.1 Effects of the UV screens on MMP-2 and MMP-9 activity of MCF-7 human breast cancer cells as determined by zymography**

After 36-38 weeks of exposure to  $10^{-5}$  M Bp1,  $10^{-5}$  M Bp2,  $10^{-5}$  M Bp3,  $10^{-5}$  M OMC,  $10^{-5}$  M 4MBC or  $10^{-5}$  M HS, conditioned media (serum free) which contained relevant concentration of each UV screen was added for 24 hours prior to collection. Then the collected media were concentrated using ultra-4 centrifugal-filter units (10,000 NMWL) (Milipore, USA). Samples were run on 10% gelatin gel and the zymogram was developed at 37°C for 24 hours. Gels were stained and de-stained. Images of the gels were captured using BioRad Gel Doc imager and the peak area of each band was quantified using Image J software. Results showed a significant increase in MMP-9 activity following long-term exposure to  $10^{-5}$  M Bp1 (Figure 4.60 (A and B)) ( $p$ -value  $\leq 0.001$ ) but no other benzophenones had an effect of either MMP-9 or MMP-2 (Figure 4.60 (B and C)). Also, no significant effect on MMP-2 or MMP-9 activities were detected following the long-term exposure to  $10^{-5}$  M OMC,  $10^{-5}$  M 4MBC or  $10^{-5}$  M HS (date not shown).

#### **4.3.8.3.2 Effects of the UV screens on levels of MMP-14 in MCF-7 human breast cancer cells as determined by western blotting**

The Pro form of MMP-14 was identified as a 62 kDa band on western immunoblotting using molecular weight markers, while the active form of MMP-14 was identified as a 50 kDa band. The cell lysates were prepared (as described in section 2.7.2.1) from the same dishes prepared for conditioned media collection (section 2.8.1). No significant difference was found between the levels of pro and active forms of MMP-14. However, levels of pro-MMP-14

were found significantly elevated after 36-38 weeks of exposure to  $10^{-5}$  M Bp1 compared to no addition (Figure 4.61) ( $p$ -value  $\leq 0.05$ ).

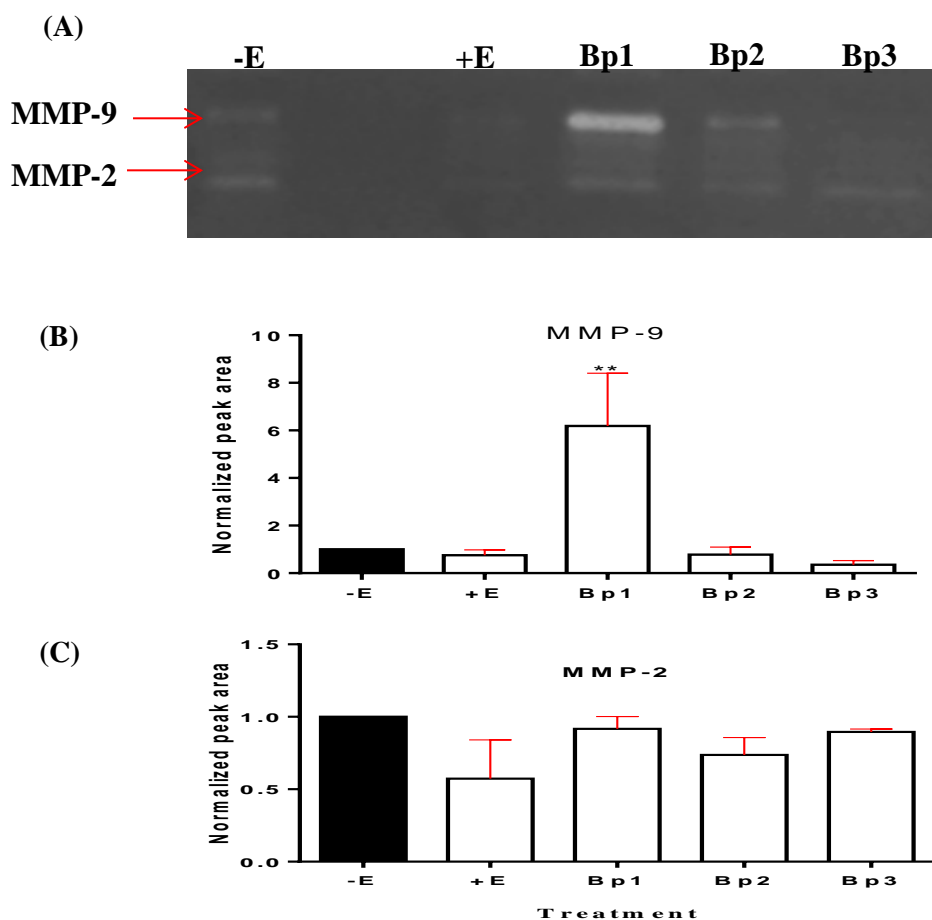


**Figure 4.60 Effect of benzophenones on secreted MMP-9 activity of MCF-7 human breast cancer cells as measured by gelatin zymography.**

MCF-7 Cells were grown in phenol-red-free-DMEM containing 5% DCFCS with ethanol control only (-E),  $10^{-8}$  M  $17\beta$ -oestradiol (+E),  $10^{-5}$  M Bp5 (Bp5),  $10^{-5}$  M Bp2 (Bp2) or  $10^{-5}$  M Bp3 (Bp3) for 35-37 weeks. Media were replenished and cells were split every 3-4 days. Cells were exposed to serum free media plus the relative chemicals for 24 hours prior collection. Collected media were concentrated using Amicon ultra centrifugal filters prior to gelatin gel zymography. (A) Representative scanned image showing the effect of the conditioned media on the activity of MMP-9 and MMP-2 on a 10% gelatin gel. (B) Bar graph represents the bands densities of MMP-9 and error bars are the standard error of triplicate independent experiments. (C) Bar graph represents the band densities of MMP-2 and error bars are the standard error of triplicate independent experiments ( $n=3$ ). \*\*  $p$ -value  $\leq 0.01$  versus no addition (-E) by t-Test.

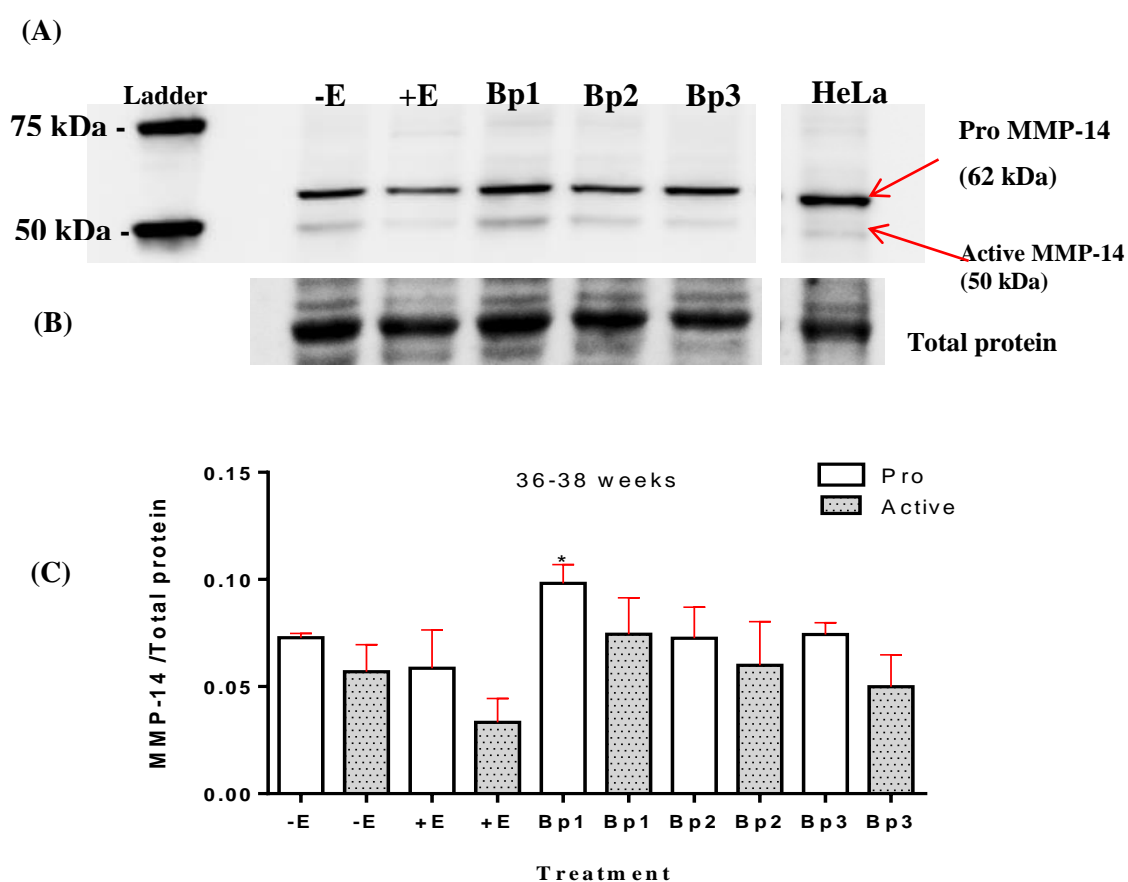


**Figure 4.61 Effect of long-term exposure to UV screens on the intracellular level of MMP-14 in MCF-7 cells.**

MCF-7 human breast cancer cells were grown for 35, 36 and 37 weeks in phenol-red-free-DMEM supplemented with 5% DCFCS, with or without  $10^{-8}$  M  $17\beta$ -oestradiol or with  $10^{-5}$  M Bp1 (Bp1), with  $10^{-5}$  M Bp2 (Bp2) or  $10^{-5}$  M Bp3 (Bp3) and HeLa human cervical carcinoma (HeLa) cells lysate was used as a positive control. Media were replenished and cells were split every 3-4 days. Cells were exposed to serum free media plus the relative chemicals for 24 hours prior to the cell lysate collection. (A) Total cellular protein was loaded at 25  $\mu$ g per track and immunoblotted with antibody against pro-MMP-14 (62 kDa) and activated-MMP-14 (50 kDa). (B) Total protein was measured by the z-imager (Bio-RAD) prior to the immunoblotting steps. (C) The bar graph shows the level of pro and active MMP-14 relative to total protein. Values are means and bars indicate SEM (n=3 independent experiments). \* *p*-value  $\leq 0.05$  versus no addition (-E) by t-Test.

#### 4.3.8.4 Effect of the UV screens on molecular markers of EMT in MCF-7 human breast cancer cells

Further investigation was carried out in order to observe the effect of UV screens on mRNA expression levels of two markers related to EMT; (Snail and Twist-1) and two markers related to cell motility (PIK3R1 and BMP7). mRNA levels were measured using RT-PCR (as described in section 2.6). MCF-7 human breast cancer cells in phenol-red-free-DMEM (Invitrogen) containing 5% DCFCS, 2mM L-glutamine, 100µg/ml streptomycin, 100U/ml penicillin (Invitrogen) were exposed to  $10^{-8}$  M  $17\beta$ -oestradiol,  $10^{-5}$  M of the UV screens or to ethanol for short-term (1 week) and long-term (24-25 weeks) prior to total RNA extraction, cDNA preparation and subsequent steps of RT-PCR assay. Results were normalised to  $\beta$ -actin values, expressed as fold change from control cells grown without the UV screens by the  $2^{-\Delta\Delta C_T}$  method and the results are shown as average  $\pm$ SE of 3 biological independent assays.

Although Snail mRNA levels were increased after exposure to  $10^{-8}$  M  $17\beta$ -oestradiol for 24-25 weeks (Figure 4.62 (B)) ( $p$ -value $\leq 0.05$ ), similar increases were not found in samples exposed to  $10^{-5}$  M of the UV screens for the same time of exposure. However, 1 week exposure to  $10^{-5}$  M Bp3 was found to increase Snail mRNA levels in MCF-7 cells (Figure 4.62 (A)) ( $p$ -value  $\leq 0.05$ ).

Short-term and long-term exposures to the UV screens have not shown an effect on Twist-1 mRNA levels in MCF-7 cells (Figure 4.63 (A and B)).

Levels of PIK3R1 mRNA were significantly reduced after 1 week of exposure to  $10^{-5}$  M Bp2 ( $p$ -value  $\leq 0.05$ ),  $10^{-5}$  M OMC ( $p$ -value  $\leq 0.01$ ) and  $10^{-5}$  M HS ( $p$ -value  $\leq 0.01$ ) in comparison with the negative control (Figure 4.64 (A)) and only to  $10^{-5}$  M Bp2 and  $10^{-5}$  M OMC after longer-term exposure (24-25 weeks) (Figure 4.64 (B)) ( $p$ -value  $\leq 0.05$ ).

Short-term exposure (1 week) to  $10^{-5}$  M 4MBC was found to decrease BMP7 mRNA levels (Figure 4.65 (A)) ( $p$ -value  $\leq 0.01$ ). On the contrary, 24-25 weeks of exposure to  $10^{-5}$  M 4MBC increased BMP7 mRNA levels (Figure 4.65 (B)) ( $p$ -value  $\leq 0.01$ ) and to  $10^{-5}$  M Bp3 and  $10^{-5}$  M OMC decreased BMP7 mRNA levels in comparison with the negative control (Figure 4.65 (B)) ( $p$ -value  $\leq 0.01$  and  $p$ -value  $\leq 0.05$  respectively).

#### **4.3.8.5 Summary of the effects of UV screens on selected molecular markers**

In order to illustrate the effects of the UV screens on the targeted markers in MCF-7 cells after 1 week and 24-25 weeks of exposure, a summary table showing the significant effects of each of the UV screens on each marker was generated (see Table 4.7).

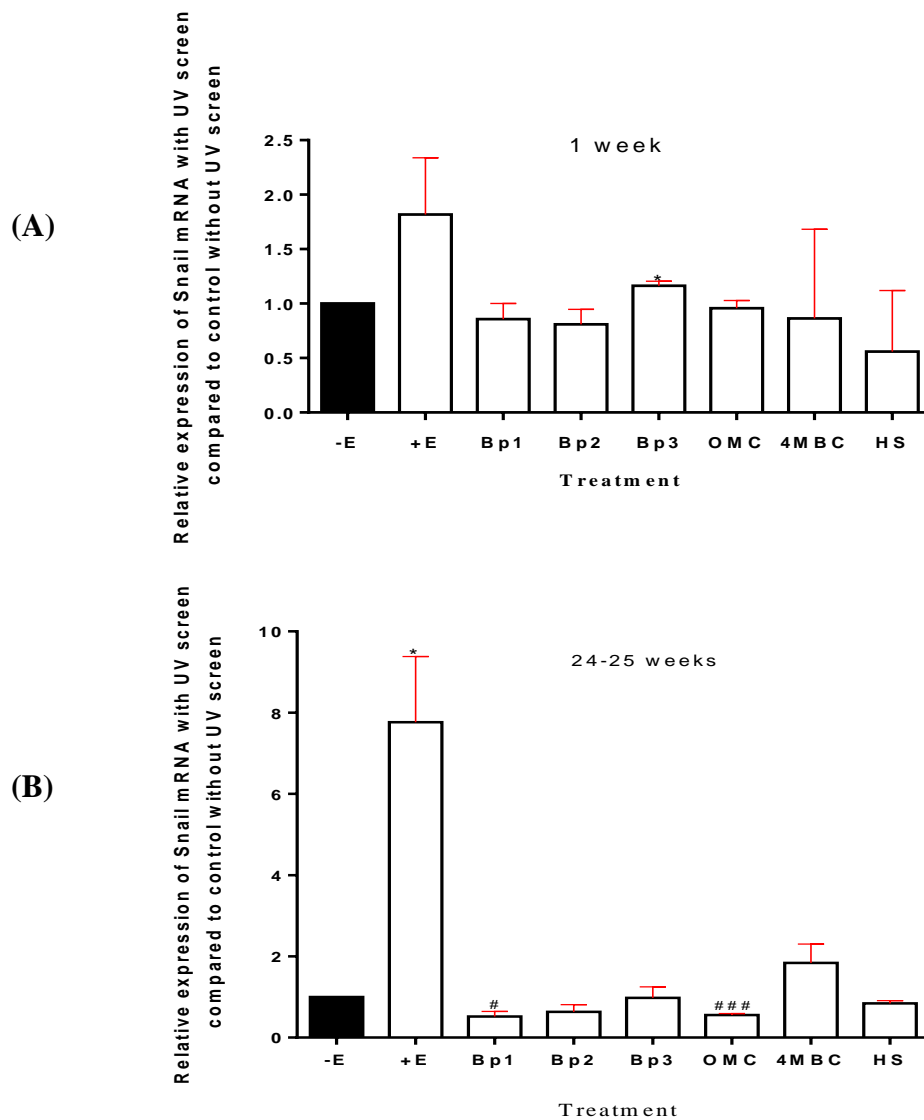


**Figure 4.62 Effect of exposure to the UV screens on levels of Snail mRNA in MCF-7 cells as determined using real-time RT-PCR.**

Cells were assayed after 1 (media were replenished two times)(A) or 24-25 weeks (media were changed and cells were split each 3-4 days) (B) with ethanol, with  $10^{-8}$  M  $17\beta$ -oestradiol, with  $10^{-5}$  M Bp1 (Bp1), with  $10^{-5}$  M Bp2 (Bp2), with  $10^{-5}$  M Bp3 (Bp3), with  $10^{-5}$  M OMC (OMC), with  $10^{-5}$  M 4MBC (4MBC) or with  $10^{-5}$  M HS (HS). For each RT-PCR assay, Snail values were normalised to  $\beta$ -actin values, expressed as fold change from control cells grown without the UV screens by  $2^{-\Delta\Delta C_T}$  method and the average SE of biological independent experiments assay (n=3) taken from cells grown for 1 week or 24-25 weeks of culture. Fold change for cell grown with  $17\beta$ -oestradiol or UV screens are shown in the bar graph compared to the negative control. \*  $p$ -value  $\leq 0.05$  and \*\*  $p$ -value  $\leq 0.01$  increase versus no addition (-E) by t-Test. #  $p$ -value  $\leq 0.01$  and ###  $p$ -value  $\leq 0.01$  decrease versus no addition (-E) by t-Test.

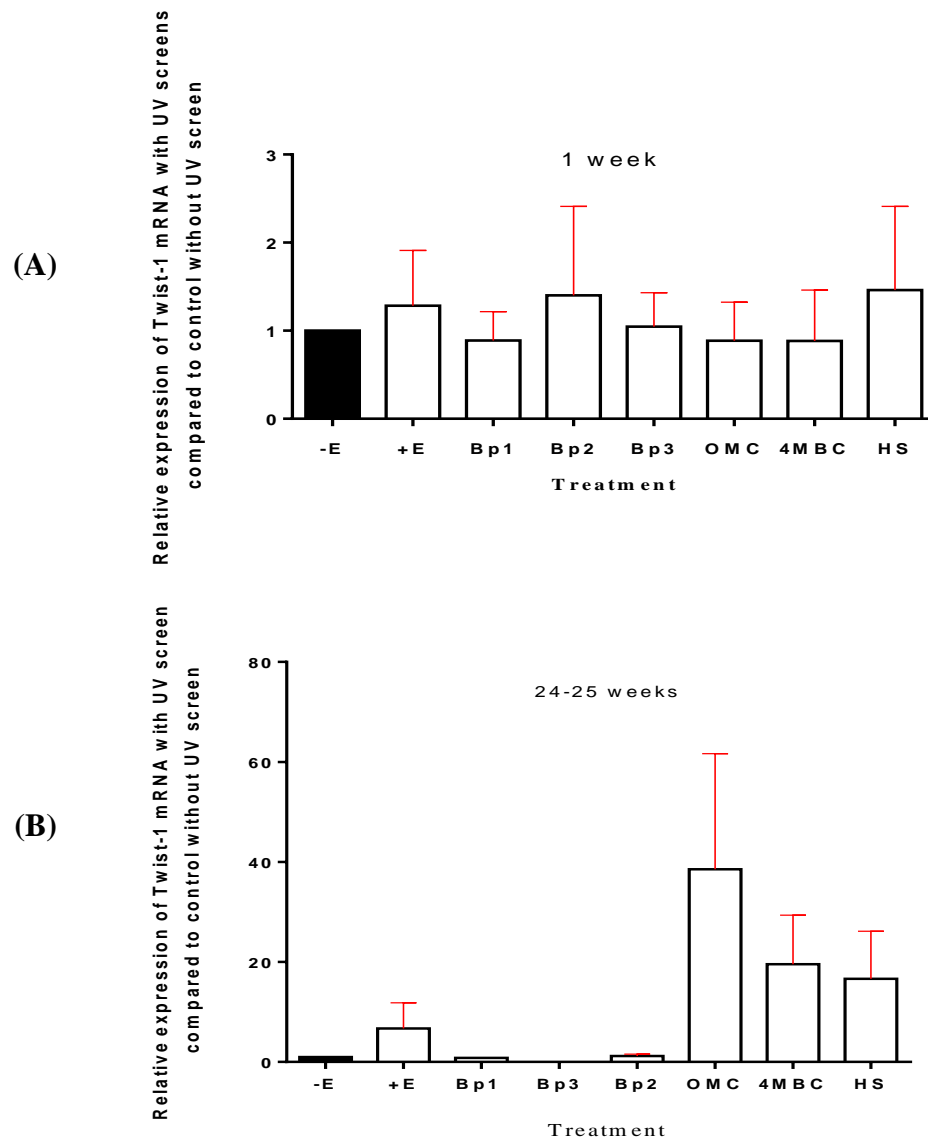


**Figure 4.63 Effect of exposure to the UV screens on levels of Twist-1 mRNA in MCF-7 cells as determined using real-time RT-PCR.**

Cells were assayed after 1 week (media were replenished two times)(A) or 24-25 weeks (media were changed and cells were split each 3-4 days) (B) with ethanol, with  $10^{-8}$  M  $17\beta$ -oestradiol, with  $10^{-5}$  M Bp1 (Bp1), with  $10^{-5}$  M Bp2 (Bp2), with  $10^{-5}$  M Bp3 (Bp3), with  $10^{-5}$  M OMC (OMC), with  $10^{-5}$  M 4MBC (4MBC) or with  $10^{-5}$  M HS (HS). For each RT-PCR assay, Twist-1 values were normalised to  $\beta$ -actin values, expressed as fold change from control cells grown without the UV screens by  $2^{-\Delta\Delta C_T}$  method and the average SE of biological independent experiments (n=3) taken from cells grown for 1 week or 24-25 weeks of culture. Fold change for cell grown with  $17\beta$ -oestradiol or UV screens are shown in the bar graph compared to the negative control (-E) by t-Test.

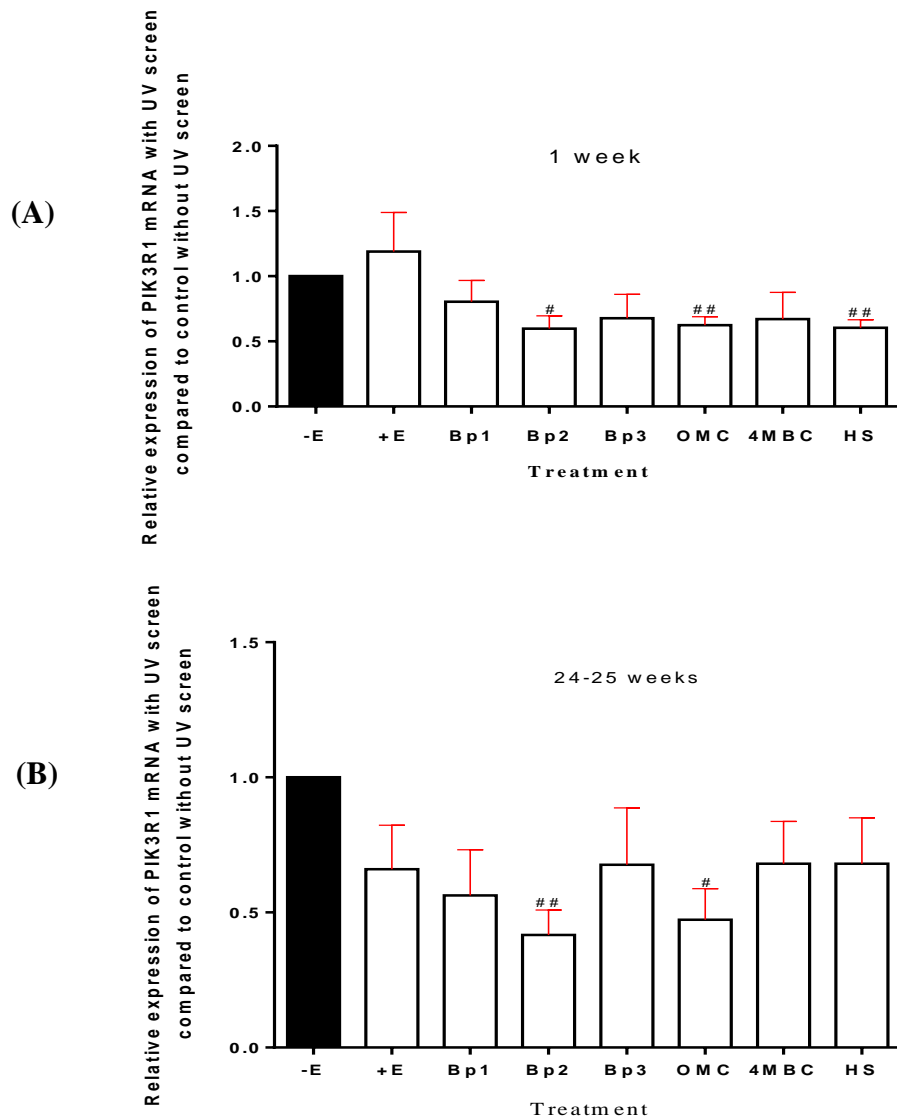


**Figure 4.64 Effect of exposure to the UV screens on levels of PIK3R1 mRNA in MCF-7 cells as determined using real-time RT-PCR.**

Cells were assayed after 1 week (media were replenished two times)(A) or 24-25 weeks (media were changed and cells were split each 3-4 days) (B) with ethanol, with  $10^{-8}$  M  $17\beta$ -oestradiol, with  $10^{-5}$  M Bp1 (Bp1), with  $10^{-5}$  M Bp2 (Bp2), with  $10^{-5}$  M Bp3 (Bp3), with  $10^{-5}$  M OMC (OMC), with  $10^{-5}$  M 4MBC (4MBC) or with  $10^{-5}$  M HS (HS). For each RT-PCR assay, PIK3R1 values were normalised to  $\beta$ -actin values, expressed as fold change from control cells grown without the UV screens by  $2^{-\Delta\Delta C_T}$  method and the average SE of biological independent experiments ( $n=3$ ) taken from cells grown for 1 week or 24-25 weeks of culture. Fold change for cell grown with  $17\beta$ -oestradiol or UV screens are shown in the bar graph compared to the negative control. #  $p$ -value  $\leq 0.05$  and ##  $p$ -value  $\leq 0.01$  decrease versus no addition (-E) by t-Test.

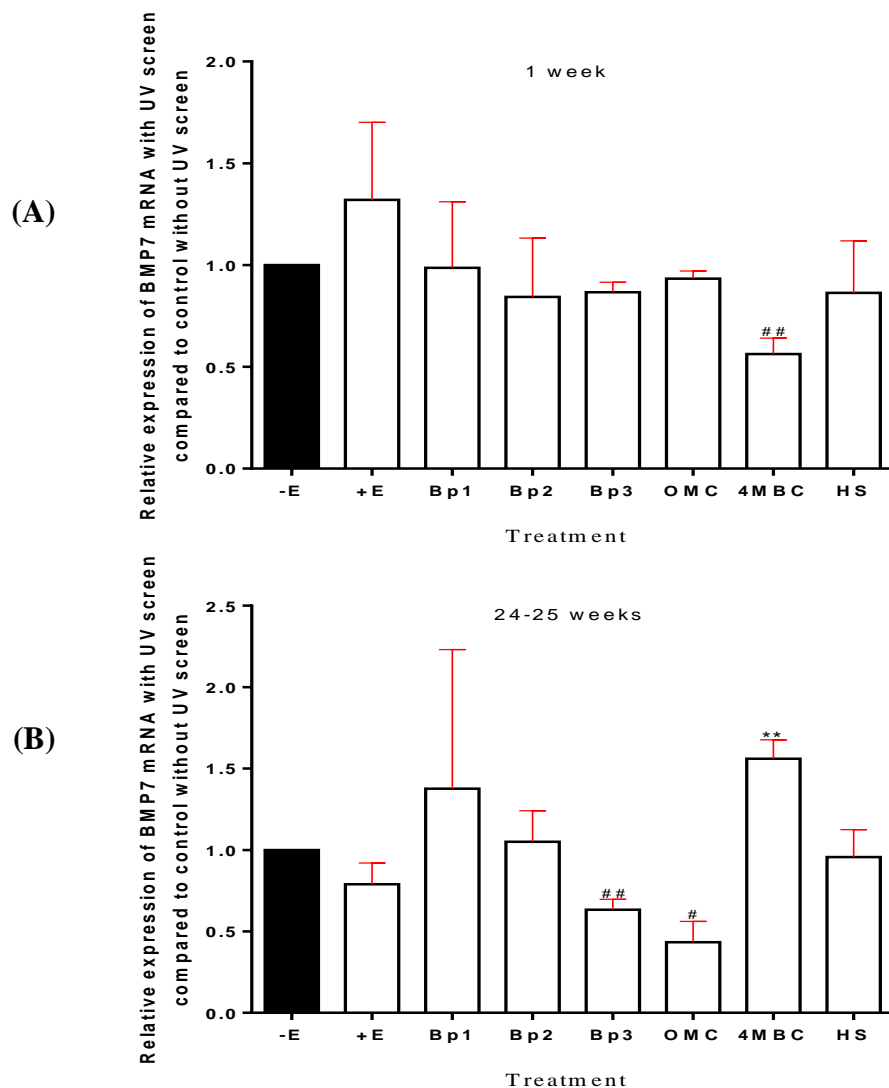


**Figure 4.65 Effect of exposure to the UV screens on levels of BMP7 mRNA in MCF-7 cells as determined using real-time RT-PCR.**

Cells were assayed after 1 week (media were replenished two times)(A) or 24-25 weeks (media were changed and cells were split each 3-4 days) (B) with ethanol, with  $10^{-8}$  M  $17\beta$ -oestradiol, with  $10^{-5}$  M Bp1 (Bp1), with  $10^{-5}$  M Bp2 (Bp2), with  $10^{-5}$  M Bp3 (Bp3), with  $10^{-5}$  M OMC (OMC), with  $10^{-5}$  M 4MBC (4MBC) or with  $10^{-5}$  M HS (HS). For each RT-PCR assay, BMP7 values were normalised to  $\beta$ -actin values, expressed as fold change from control cells grown without the UV screens by  $2^{-\Delta\Delta C_T}$  method and the average SE of biological independent experiments (n=3) taken from cells grown for 1 week or 24-25 weeks of culture. Fold change for cell grown with  $17\beta$ -oestradiol or UV screens are shown in the bar graph compared to the negative control. \* *p*-value  $\leq 0.05$  increase versus no addition. # *p*-value  $\leq 0.05$  and ## *p*-value  $\leq 0.01$  decrease versus no addition (-E) by t-Test.

**Table 4.7 Summary table of the effects of UV screens on selected molecular markers.**

This table summarises the effects of exposure to UV screens on molecular markers in MCF-7 cells. Fold numbers compared to control without UV screen. Purple shades represent decrease levels and green shades illustrate significant increase compared to control.

UV screen		E-cadherin		β- catenin		Snail	Twist-1	PIK3R1	BMP7
		mRNA levels	Protein levels	mRNA levels	Protein levels	mRNA levels	mRNA levels	mRNA levels	mRNA levels
<b>17β-oestradiol</b>	1 week	--	--	--	--	--	--	--	--
	24-25 weeks	--	--	--	--	7.76 ± 1.62	--	--	--
<b>Bp1</b>	1 week	--	--	--	--	--	--	--	--
	24-25 weeks	0.54 ± 0.17	0.74 ± 0.12	--	--	0.52 ± 0.12	--	--	--
<b>Bp2</b>	1 week	--	--	--	--	--	--	0.59 ± 0.09	--
	24-25 weeks	--	--	0.84 ± 0.04	--	--	--	0.42 ± 0.09	--
<b>Bp3</b>	1 week	--	--	--	--	1.16 ± 0.04	--	--	--
	24-25 weeks	0.51 ± 0.11	--	0.51 ± 0.07	--	--	--	--	0.58 ± 0.03
<b>OMC</b>	1 week	--	--	--	0.73 ± .07	--	--	0.57 ± 0.03	--
	24-25 weeks	0.60 ± 0.12	--	--	0.61 ± 0.17	0.55 ± 0.04	--	0.47 ± 0.11	0.43 ± 0.13
<b>4MBC</b>	1 week	0.18 ± 0.06	--	--	--	--	--	--	0.56 ± 0.07
	24-25 weeks	0.52 ± 0.15	--	--	--	--	--	--	1.55 ± 0.12
<b>HS</b>	1 week	0.36 ± 0.01	--	0.47 ± 0.21	0.54 ± 0.13	--	--	0.51 ± 0.08	--
	24-25 weeks	0.55 ± 0.17	0.79 ± 0.12	--	--	--	--	--	--

(--) represent no significant effect.

## 4.4 Discussion

The acquisition of migratory and invasive activity by epithelial cells is one of the hallmarks of cancer (Hanahan and Weinberg, 2011). The role of UV screens in influencing breast cancer cell migration has not been investigated previously. Results in this study, report for the first time that UV screens increase the motility of MCF-7 human breast cancer cells as shown in Tables 4.1- 4.6.

***Strength of this study by using different methods.*** The use of three techniques strengthened the evaluation of the influence of UV screens on the motility of MCF-7 cells but there were variations in results obtained from each technique due to the different perspective that each technique provides in the context of cell motility. The wound healing assay measures collective cell migration in a monolayer for cells that expresses cell-cell adhesion and cohesion (Friedl et al., 2004) and this technique facilitates the quantitation of cell motility in one direction (Hulkower and Herber, 2011). Time-lapse microscopy helps to observe the motility of individual cells in any direction (Jain et al., 2012). The xCELLigence technology monitors the motility of individual cells through pores of a membrane in real time towards the chemotactic effect of the serum (Limame et al., 2012).

***UV screens at  $10^{-5}$ M concentration increased cell migration.*** The evaluation of the effect of the UV screens using different techniques revealed that MCF-7 cells showed different types of motility in response to the different UV screens in this work. All of the six UV screens at  $10^{-5}$  M concentrations have increased MCF-7 cell collective motility after 7-8 weeks as determined by the wound healing. In the same time, increased MCF-7 cell motility towards chemotactic stimulus as determined by the xCELLigence technology was found for all the UV screens after 2 weeks of exposure except for HS. However, longer exposure times gave varied effects for the different chemicals.

$10^{-5}$  M Bp1 was found to increase MCF-7 cell motility towards the chemotactic effect with similar magnitude after 2 weeks and 21 $\geq$ weeks of exposure by the xCELLigence technology. In addition, even with the absence of the chemotaxis stimulus of FCS in time-lapse microscopy, an increase in the percentage of motile MCF-7 cells was found after short-term exposure (2 weeks) to  $10^{-5}$  M Bp1. While the collective migration of MCF-7 cells exposed to this chemical was only found after 7 weeks of exposure and not found after 21 weeks of exposure as assessed by the wound healing. Similar findings were found in MCF-7 cells exposed to  $10^{-5}$  M Bp2 where 2 weeks of exposure showed increased MCF-7 cell motility

towards the chemotactic effect, while 21 weeks of exposure to  $10^{-5}$  M Bp2 showed no effect on MCF-7 cell motility, which might be linked to the preservation of the oestrogenic properties by these chemicals compared to the more motile oestrogenic deprived cultures (Lewis-Wambi et al., 2008; Nguyen et al., 2015).

While the increase in MCF-7 cell motility was observed after the exposure to  $10^{-5}$  M Bp3 (2 weeks and 21 weeks) as determined by xCELLigence, the increase in wound closure of MCF-7 cells following exposure to  $10^{-5}$  M Bp3 was not found after 7 weeks and 13 weeks of exposure and increased significantly after 21 weeks of exposure, which was significantly increased through the time line of the experiment, suggesting that the increase in collective motility of MCF-7 cells after long-term exposure to  $10^{-5}$  M Bp3 is accumulative.

Concentrations of  $10^{-5}$  M OMC and  $10^{-5}$  M 4MBC were found to increase MCF-7 cell motility towards the chemotactic effect with similar magnitude after 2 weeks and 21 weeks of exposure as determined by the xCELLigence technology. In addition, an increase in the percentage of motile MCF-7 cells was found after 2 weeks of exposure to  $10^{-5}$  M OMC, and in cumulative length moved by cells exposed for 2 weeks to  $10^{-5}$  M 4MBC as determined by the time-lapse. These findings of the effects of 21 weeks of exposure to  $10^{-5}$  M 4MBC were supported by significant wound closure in the wound healing assay but not for OMC. Compared to the other chemicals,  $10^{-5}$  M HS was the only chemical that showed no influence on MCF-7 cell motility after 2 weeks but increased cell motility after 23 weeks of exposure as determined by the xCELLigence. Previous reports regarding the effect of UV screens on breast cancer cells *in vitro* have only focused on the proliferative response of MCF-7 cells towards the UV screens (Schlumpf et al., 2001; Nakagawa and Suzuki, 2002; Jimenez-Diaz et al., 2013; Kerdivel et al., 2013) and cell motility was never investigated until 2015. As data for this work were collected, Sol-Ji In and his colleagues have indicated the influence of  $10^{-5}$  M Bp1 in increasing the motility of MCF-7 human breast cancer cells after three days of exposure as assessed by the wound healing assay (In et al., 2015). Despite the differences in methodologies used by Sol-Ji In group and in this work, their finding is in line with the results obtained in this research after short-term (2 weeks) exposure to  $10^{-5}$  M Bp1 by the xCELLigence technology. Nevertheless, they have decreased this induced motility by using the ER $\alpha$  antagonist fulvestrant, suggesting that the increase of MCF-7 cell motility is ER mediated (In et al., 2015). In a more recent study, Shin and his colleagues have found that Bp1 increased the motility of BG-1 ovarian cancer cells and in agreement with the work by

Sol-Ji In on MCF-7 cells, the influence of Bp1 on BG-1 cells motility was decreased by fulvestrant (Shin et al., 2016).

***UV screens at  $10^{-7}$  M concentration increased cell migration.***  $10^{-7}$  M of the UV screens did not increase MCF-7 cell motility after 2 weeks of exposure, but did increase their motility after 21 weeks of exposure as measured by the wound healing assay. This increase in collective motility was statistically linked to the effect of the long-time of exposure. A similar pattern of increase in MCF-7 cell motility towards chemotactic stimulus was observed after 21 weeks of exposure to  $10^{-7}$  M Bp1,  $10^{-7}$  M Bp3,  $10^{-7}$  M OMC and  $10^{-7}$  M 4MBC as determined by the xCELLigence experiments. In addition, time-lapse analysis supported the influence of  $10^{-7}$  M Bp1,  $10^{-7}$  M Bp2,  $10^{-7}$  M Bp3,  $10^{-7}$  M 4MBC and  $10^{-7}$  M HS in increasing MCF-7 cell motility after 21 weeks of exposure, where  $10^{-7}$  M Bp2 and  $10^{-7}$  M Bp3 increased the cumulative length moved by MCF-7 cells and increased the percentage in motile cells following the long-term exposure to  $10^{-7}$  M Bp1,  $10^{-7}$  M Bp2,  $10^{-7}$  M 4MBC and  $10^{-7}$  M HS. The effect of long-term exposure to environmental oestrogens at low concentration is a rising concern because it reflects the reality of the exposure to environmental oestrogens in daily life (Darbre and Fernandez, 2013) and the effects of the long-term, low-dose model represented by this work support these rising concerns.

***Effect of  $17\beta$ -oestradiol and long-term oestrogen deprivation on cell migration.*** In line with previous reports regarding the influence of  $10^{-8}$  M  $17\beta$ -oestradiol in increasing MCF-7 cell motility (Saji et al., 2005; Malek et al., 2006; Planas-Silva and Waltz, 2007; Jimenez-Salazar et al., 2014),  $10^{-8}$  M  $17\beta$ -oestradiol in this work also increased MCF-7 cell motility in comparison with control cells after 2 weeks of exposure as measured using xCELLigence technology. However, longer term growth of cells with and without  $17\beta$ -oestradiol (starting from 7 weeks) showed a reduced difference between MCF-7 cells treated with  $10^{-8}$  M  $17\beta$ -oestradiol and the non-treated oestrogen deprived cells. Relevant data from the results section are summarised in Figures 4.66 and 4.67. Long-term oestrogen deprivation is known to result in loss of proliferative response to  $17\beta$ -oestradiol (Darbre, 2014) and recent work reported increased motility of long-term oestrogen-deprived MCF-7 cells (Lewis-Wambi et al., 2008; Nguyen et al., 2015). Long-term deprived cells are characterized by hypersensitivity to low concentrations of  $17\beta$ -oestradiol for the proliferative response (Masamura et al., 1995; Song et al., 2002a; Santen et al., 2005) and it is possible that there may similarly increase sensitivity towards the addition of  $17\beta$ -oestradiol and UV screens towards cell motility. Our

results indicated that  $10^{-7}$  M concentrations of the UV screens gave effects on MCF-7 cell motility in the longer term. However, whether this effect built up through the long-term exposure or was caused by the increased hypersensitivity of MCF-7 cells due to  $17\beta$ -oestradiol deprivation, there is no doubt that MCF-7 cell motility increased in comparison to the negative control. It is noteworthy that the increase in MCF-7 cell motility after short-term exposure to  $10^{-5}$  M Bp2, which was lost during the long-term exposure, might be due to the preserved oestrogenic action caused by this chemical in comparison with the other UV screens which gave weaker oestrogenic responses. The long-term oestrogen deprived model mimics the post-menopausal scenario in women when oestrogen drops to low levels (Faupel-Badger et al., 2010) and the risk of breast cancer increases (Ghiasvand et al., 2014). Thus, breast cancer cells might become more sensitive toward low oestrogen levels or towards the environmental oestrogenic activity of the UV screens.

***Effects of UV screens on MCF-7 cell invasive activity.*** Results showed that there is an increase in the invasive activities of MCF-7 cells after 2 weeks of exposure to  $10^{-5}$  M Bp3,  $10^{-5}$  M OMC,  $10^{-5}$  M 4MBC and  $10^{-5}$  M HS. Moreover, 31 weeks exposure to  $10^{-5}$  M Bp1,  $10^{-5}$  M OMC,  $10^{-5}$  M 4MBC and  $10^{-5}$  M HS had significantly increased the invasion of MCF-7 cells through matrigel in comparison to the control as determined by the xCELLigence technology. Not all of the UV screens tested increased the invasive activity of MCF-7 cells. Neither the concentrations tested of Bp2 in the different time points nor Bp3 after 31 weeks of exposure showed any effect on MCF-7 cell invasive capability. Invading the surrounding tissues is one of the first steps of cancer cells in the process of metastasis (Nguyen et al., 2009; Hanahan and Weinberg, 2011) and the ability of the UV screens to increase MCF-7 cells invasive ability might contribute to possible effects of UV screens on breast cancer progression.

The limited effect of some of the UV screens on MCF-7 cell motility and invasion does not negate the potential for them to act within different mixtures after long-term exposure. The effect of long-term exposure to mixtures of environmental oestrogens at low concentration is a rising concern because it reflects the reality of the exposure to environmental oestrogens in daily life (Darbre and Fernandez, 2013) and mixtures of UV screens at low concentrations have previously been reported to induce expression of the oestrogen responsive TFF1 gene (Heneweer et al., 2005). Thus studying the effect of mixtures of the UV screens must be considered in future research. Furthermore, the effect of metabolites of the UV screens should not be neglected. In this chapter Bp3 has only increased MCF-7 cell motility after long-term

exposure and had no influence on cell invasion after 31 weeks of exposure. On the other hand, Bp1 at different concentrations induced both the motility and invasive activity of MCF-7 cells and Bp1 has been reported to be one of the metabolites of Bp3 (Jeon et al., 2008).

It is worth noting that long-term exposure to UV screens caused morphological changes in MCF-7 cells including the presence of spindle shaped cells and the formation of protrusions of pseudopodia and such extensions are known to be related to higher metastatic potential in cancer cells (Partin et al., 1989). Change in motility of MCF-7 cells following exposure to the UV screens raises the questions of underlying molecular mechanisms. Among the different theories that can underly development of motility of epithelial cells, the epithelial–mesenchymal transition (EMT) was chosen to be investigated.

***Exposure to UV screens reduced levels of E-cadherin and  $\beta$ -catenin.*** Results showed that two of the six UV screens decreased E-cadherin protein and mRNA levels ( $10^{-5}$  M Bp1 and  $10^{-5}$  M HS).  $10^{-5}$  M Bp1 reduced E-cadherin mRNA expression and protein levels in MCF-7 cells after 24-25 weeks of exposure with no effect on  $\beta$ -catenin. However,  $10^{-5}$  M HS reduced E-cadherin mRNA expression after 1 week and 24-25 weeks of exposure, but decreased E-cadherin protein levels only after 24 weeks of exposure. It is noteworthy that  $10^{-5}$  M HS also reduced  $\beta$ -catenin mRNA expression at both time points but only reduced  $\beta$ -catenin protein levels in MCF-7 cells after 1 week of exposure. It was reported by Shin and colleagues that Bp1 reduces the E-cadherin protein levels in BG-1 ovarian cancer cells after 4 days of exposure (Shin et al., 2016), suggesting that the influence of Bp1 on cell motility might be via a similar mechanism. In another study of the effects of parabens, Khanna and colleagues reported down regulation in protein levels of E-cadherin and  $\beta$ -catenin in MCF-7 cells that showed increased motility after more than 20 weeks of exposure (Khanna et al., 2014). Repressed E-cadherin is one of the most critical molecular markers of EMT. Further, loss of cell-cell adhesion via disturbing the E-cadherin/ $\beta$ -catenin complex is linked to cancer progression (Heimann et al., 2000), poor prognosis of breast cancer (Gamallo et al., 1993; Hunt et al., 1997) and found to be associated with increase in metastases and invasiveness of breast cancer in clinical studies (Oka et al., 1993; Moll et al., 1993; Siitonen et al., 1996; Heimann et al., 2000). Experimentally repressing E-cadherin was also linked to an increase in MCF-7 cell invasive capacity (Hiscox et al., 2006). Others of the chemicals caused reduced mRNA levels but not the protein. E-cadherin mRNA expression was down-regulated by exposure to  $10^{-5}$  M Bp3,  $10^{-5}$  M OMC and  $10^{-5}$  M 4MBC after 24-25 weeks of exposure, but

no significant decrease in a protein level was indicated after exposure to these UV screens. E-cadherin is part of the cell-cell adherens junction (Bazzoun et al., 2013; Martin et al., 2013), which functions not only in maintaining the apical shape of the epithelial cells but also as a mediator in downstream signalling through its binding to  $\beta$ -catenin (Beavon, 2000; Wijnhoven et al., 2000; Vestweber, 2015). The contradictory results of the mRNA levels and the protein levels of E-cadherin, might be linked to the lower sensitivity of the western blotting technique in detecting small changes compared to other protein detections methods, while RT-PCR is a sensitive technique that efficiently amplifies changes of the targeted mRNA (Nicholas and Nelson, 2013). In addition, mRNA levels might not reflect protein levels (Schwanhausser et al., 2011).

Levels of  $\beta$ -catenin protein in MCF-7 cells were reduced only by  $10^{-5}$  M OMC and not by any other UV screens after 24-25 weeks of exposure. This UV screen has increased MCF-7 cell motility and invasive activity while retaining E-cadherin protein levels which suggests other possible pathways in the mechanism of inducing MCF-7 cell motility by  $10^{-5}$  M OMC. It was reported that a motile and invasive MCF-7 cell sub-clone expresses E-cadherin at similar levels compared to the wildtype cells (Uchino et al., 2010) but the report did not show results of levels of  $\beta$ -catenin protein. However,  $\beta$ -catenin down-regulation was reported to be linked to increased motility of another breast cancer cell line (MDA-MB-231) (Cai et al., 2014) as was observed here in. Down-regulation of  $\beta$ -catenin was also associated with invasion in breast cancer (De Leeuw et al., 1997) and more motility and invasion of MCF-7 cells (Yang and Kim, 2014).

Although repressed E-cadherin is an EMT marker and linked to cell motility, retaining E-cadherin expression and the epithelial morphology can be maintained during cancer cells motility (Liu et al., 2014; Shamir et al., 2014) and that might explain the increased MCF-7 cells motility following exposure to Bp3, OMC and 4MBC without reduction in E-cadherin protein levels. Other molecular markers were only studied using RT-PCR and levels of protein need to be considered in future work.

***UV screens caused no effect on Snail and Twist-1 mRNA levels.*** Results showed that  $10^{-5}$  M Bp3 induced Snail mRNA levels after 1 week of exposure using RT-PCR and no effects were observed after 24-25 weeks of exposure to this chemical or for any of the other UV screens tested but it increased by  $10^{-8}$  M  $17\beta$ -oestradiol. No effect on Twist-1 mRNA level was observed. Thus the mechanism of repressing E-cadherin by Bp1 and HS was not found and

more research on other transcriptional regulators that suppress E-cadherin such as Snail2 (Slug) (Hajra et al., 2002) and the Smad interacting protein ZEB2 (SIP1) (Comijn et al., 2001) might reveal the pathway. Nevertheless, slug and snail protein levels were reported to be increased in BG-1 ovarian cancer cells following 96 hours of exposure to  $10^{-6}$  M Bp1 (Shin et al., 2016). This difference between the findings of Shin and this work might be caused by the difference in the chemical concentration, the different cell line used or the endpoint measured by each experiment.

***UV screens reduced the levels of PIK3R1 and BMP7.*** The underlying molecular pathway seems to vary among these chemicals. The search for other molecular markers was conducted in order to explain the change in MCF-7 cells to a more motile phenotype. The investigation was driven toward two reported motility markers (PIK3R1 and BMP7) that were found in MCF-7 sub-cloned motile cells, which retained the expression of E-cadherin (Uchino et al., 2010). Results from this work showed that  $10^{-5}$  M OMC reduced the mRNA levels of PIK3R1 after 1 week of exposure and reduced the mRNA levels of both PIK3R1 and BMP7 after 24-25 weeks of exposure in comparison to un-treated cells, and that is in line with the reduction in PIK3R1 and BMP7 mRNA in motile sub-clone of MCF-7 cells as reported by Uchino *et al.* (2010). Moreover, results showed that BMP7 mRNA levels were also reduced in MCF-7 cells following 24-25 weeks of exposure to  $10^{-5}$  M Bp3 and  $10^{-5}$  M 4MBC, suggesting a possible mechanism underlying their action on MCF-7 cell motility.

PIK3R1 is a (p86) regulatory subunit of phosphoinositide 3-kinase (PI3K) and the loss of control of PI3K signalling by PIK3R1 reduction causes an increase in cancer cell proliferation, survival and motility (Luo and Cantley, 2005) and it has been reported to be reduced in human invasive breast cancer tissue (Cizkova et al., 2013). BMP7 is a member of the 20 bone morphogenetic proteins identified in the human body (Alarmo et al., 2009) and it negatively regulates transforming growth factor  $\beta$  (TGF- $\beta$ ) signalling, which when activated is found to be involved in breast cancer cell metastasis (Welch et al., 1990; Massague, 2008). In motile MDA-MB-231 breast cancer cells PI3KR1 mRNA levels were found to be reduced in comparison with levels in epithelial T-47-D cells (Buijs et al., 2007) and MCF-7 cells (Uchino et al., 2010). Moreover, BMP7 mRNA is found at greater levels in MCF-7 cells than in motile MDA-MB-231 cells (Alarmo et al., 2007). Both markers are reduced in the motile MCF-7 cell sub-clone (Uchino et al., 2010). Moreover, overexpressing PIK3R1 by transfection was found to reduce the motility and invasion of MDA-MB-231 and BT-474

breast cancer cells (Yan et al., 2016). Thus the ability of  $10^{-5}$ M OMC to reduce the mRNA levels of PIK3R1 and the reduced levels of BMP7 mRNA caused by the exposure of MCF-7 cells to  $10^{-5}$  M Bp3 and  $10^{-5}$  M 4MBC might be a possible explanation of the increase in MCF-7 cell motility after the exposure to these chemicals.

***UV screens affect the secretion of MMP-9 but not MMP-2.*** Among the six tested UV screens in this research, only  $10^{-5}$  M Bp1 increased MMP-9 secretion as determined by the zymogram and increased protein levels of pro-MMP-14 as measured by western immunoblotting. The investigation covered the effect of UV screens on MMP-2, MMP-9 and MMP-14 all of which are involved in cancer cells metastasis and invasion (Cockett et al., 1998; Forsyth et al., 1999; Seiki, 2002; Gupta et al., 2007; Yu and Stamenkovic, 2000; Zarrabi et al., 2011) and are known to be expressed by MCF-7 human breast cancer cells (Das et al., 2008). Reduction of MMP-2 and MMP-9 activity by  $17\beta$ -oestradiol was documented previously in oestrogen responsive breast cancer cells, while tamoxifen increased MMP-2 and MMP-9 activity (Nilsson et al., 2007) and increased individual MCF-7 cell migration (Lymperatou et al., 2013). Thus increasing the expression of MMP-9 by  $10^{-5}$ M Bp1 might be another pathway involved in increased motility of cells exposed to this chemical. It was recently reported that MMPs can also be modulated by environmental chemicals. MDA-MB-231 cells have shown more migration and invasion after long-term exposure to aluminium. This shift in motility activity was linked to the increase of MMP-9 activity as measured by gelatin zymography and the increase of MMP-14 RNA expression as measured by real time RT-PCR assay (Bakir and Darbre, 2015). Whether the effect of the UV screens on MMPs activity can be influenced by the presence of ECM material remains to be investigated in the future in order to explain the indicated MCF-7 cell invasive activity following exposure to  $10^{-5}$ M OMC,  $10^{-5}$ M 4MBC and  $10^{-5}$ M HS.

***To conclude,*** UV screens can change the MCF-7 cell phenotype *in vitro*. The effect of the UV screens on breast cancer cells is not therefore limited to the effect on proliferation but can be considered to influence another hallmark of cancer, cell motility and invasion. Until now, few studies have investigated the effect of environmental chemicals on cancer cell motility. Studies have reported increased motility following exposure to phthalates (Hsieh et al., 2012; Yao et al., 2012) and to parabens (Khanna et al., 2014), and the results here show effects of the UV screens as well. The variation between the effects of  $17\beta$ -oestradiol and the UV screens after long-term exposure on motility and on the molecular targets raises questions

regarding the involvement of the oestrogenic pathways in the increased MCF-7 cell motility following exposure to the UV screens. 24-25 weeks of exposure to the UV screen increased the motility of MCF-7 cells compared to both the negative control and cells exposed to 17 $\beta$ -oestradiol. Nevertheless, the effect of the UV screens on the different chosen molecular markers in this study did not match with the effects of 17 $\beta$ -oestradiol. Further studies must include the use of antioestrogen fulvestrant to confirm the involvement of the oestrogenic genomic pathway or the risen sensitivity to those chemicals especially with the recorded effect of long-term exposure to 10<sup>-5</sup> M 4MBC and HS in increasing TFF1 mRNA levels (see chapter 3), a gene that is linked to increased MCF-7 cell motility (Prest et al., 2002). Further research on the mechanism of action of the UV screens on breast cancer cell motility is needed including studies on the non-genomic pathway of the oestrogenic action.

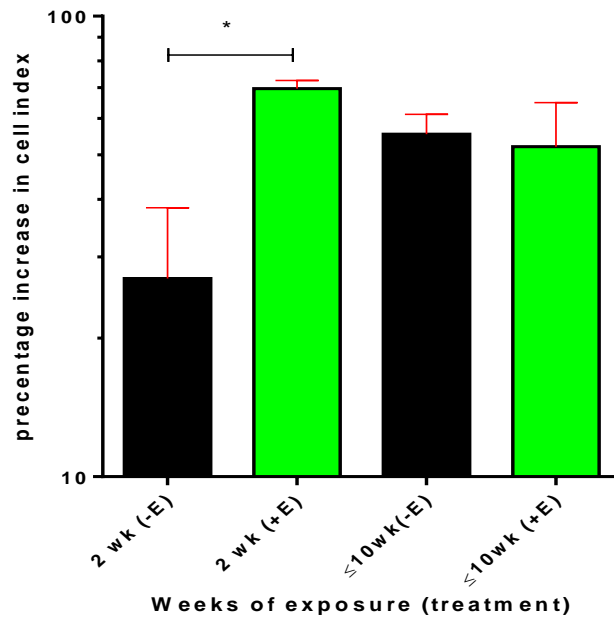


**Figure 4.66 The effect of 17 $\beta$ -oestradiol on MCF-7 human breast cells as determined by the xCELLigence technology.**

Cells were grown in phenol-red-free-DMEM containing 5% DCFCS with ethanol control only (-E) or with  $10^{-8}$  M 17 $\beta$ -oestradiol (+E) for 2 weeks and 10-13 weeks. Media were replenished and cells were split each 3-4 days. Cells were analysed for their motility activity on CIM-plate 16 (xCELLigence RTCA device). Bar graph represents the percentage increase in cell index calculated from the different between 1 hour and 24 hours time points. Values are the average  $\pm$ SE of triplicate biological independent replicates (n=3). \* *p-value*  $\leq$  0.05 versus no addition by one-way ANOVA Tukey's test.

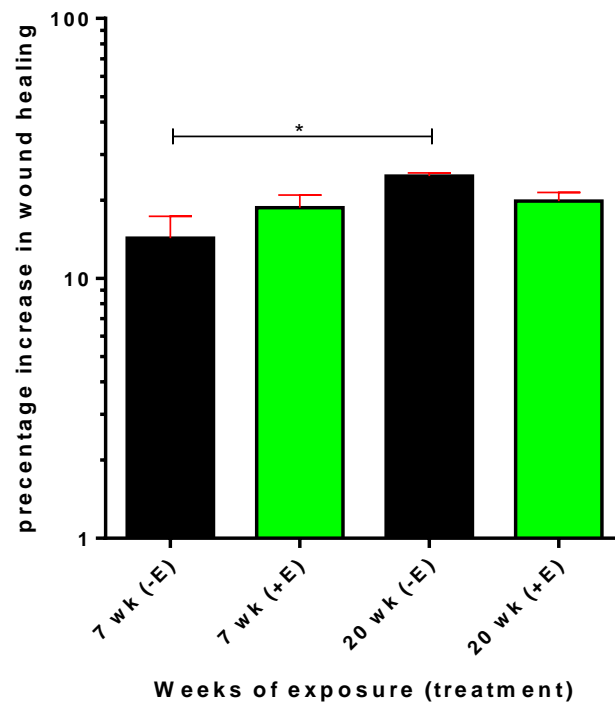


**Figure 4.67** The effect of 17 $\beta$ -oestradiol on MCF-7 human breast cells as determined by the wound healing assay.

Cells were grown in phenol-red-free-DMEM containing 5% DCFCS with ethanol control only (-E) or 10<sup>-8</sup> M 17 $\beta$ -oestradiol (+E) for 7 weeks and 20 weeks prior to the experiment. Media were replenished and cells were split each 3-4 days. Cells were then reseeded in 12-well plates and once the cells became  $\geq$  95% confluent, wound was made and mitomycin c (0.5  $\mu$ g/ml) was added. Images were captured at 0 hour and 24 hours. Cell migration was quantified by analysing minimum 5 images from each well. Values are the average  $\pm$ SE of triplicate wells. Bar graph represents the percentage increase in wound healing obtained from 0-24 hours. Values are the average  $\pm$ SE of triplicate biological independent experiments (n=3). \* *p-value*  $\leq$  0.05 versus no addition one-way ANOVA Tukey's test.

## Chapter 5 Effect of UV screens on T-47-D human breast cancer cells

### 5.1 Introduction

There is variation between breast cancer cell line responses toward anticancer drug therapies (Torbett et al., 2008; Heiser et al., 2012; Risinger et al., 2015; Stapf et al., 2016), toward growth factors (Ryde et al., 1992; Niepel et al., 2014) and in expressing different molecular biomarkers related to cell adhesion and motility (Chekhun et al., 2013). This necessitates the use of a panel of breast cancer cell lines to study also potential variation in the effect of environmental oestrogens.

The effect of UV screens on MCF-7 human breast cancer cell proliferation and motility were discussed in the previous chapters (chapters 3 and 4). The same cell line has been used as an *in vitro* model by several researchers to estimate the influence of the UV screens on breast cancer cell biology (Schlumpf et al., 2001; Heneweer et al., 2005; Kerdivel et al., 2013; Jimenez-Diaz et al., 2013; In et al., 2015). Therefore, the effect of the UV screens on proliferation and motility was investigated in this chapter using another oestrogen responsive cell line which shares some characteristics with MCF-7 cells.

T-47-D human breast cancer cells (Keydar et al., 1979) were chosen to carry out further investigation. Growth of T-47-D cells is not dependent on  $17\beta$ -oestradiol but responsive to it and shows an increase in cell proliferation following exposure to oestrogen (Darbre and Daly, 1989). Both T-47-D and MCF-7 cells are luminal, epithelial cell lines and express ER (Neve et al., 2006; Ford et al., 2011; Holliday and Speirs, 2011). To the best of my knowledge, the effect of the UV screens has never been studied on T-47-D human breast cancer cells.

## 5.2 Experimental aim

The overall aim of this chapter is to study the effect of six UV screens (Bp1, Bp2, Bp3, OMC, 4MBC and HS) on T-47-D human breast cancer cell proliferation and motility. To achieve this aim, the effect of different concentrations of each UV screen on T-47-D cell proliferation was determined following 1 week of exposure using the ZBI Coulter counter (as described in 2.2.1). The wound healing assay (described in 2.4.1) and xCELLigence (described in 2.4.3) were used to determine the effect of these chemicals on motility of T-47-D cells investigating both collective and individual chemotactic-derived motility following short-term (2 and 3 weeks) and long-term (13, 21 and 30 weeks) of exposure.

## 5.3 Results

### 5.3.1 Effects of UV screens on proliferation of T-47-D human breast cancer cells

17 $\beta$ -oestradiol increases the proliferation of T-47-D human breast cancer cells in a dose-dependent manner. Doses of 10<sup>-12</sup> M 17 $\beta$ -oestradiol and above simulated the proliferation of T-47-D cells with maximum stimulation between 10<sup>-11</sup> M and 10<sup>-8</sup> M after 7 days (Figure 5.1). In this section, the effect of UV screens (Table 2.1) on the proliferation of T-47-D human breast cancer cells was investigated after 1 week of exposure.

T-47-D human breast cancer cells were grown in phenol-red-free-DMEM containing 5% DCFCS with 10<sup>-8</sup> M 17 $\beta$ -oestradiol or with increasing concentrations of UV screens (from 10<sup>-8</sup> M to 10<sup>-5</sup> M for 7 days. Cell count experiments were conducted using ZIB Coulter counter (as described in section 2.2.1). Cell growth experiments showed that among the tested UV screens, 10<sup>-5</sup>M Bp1 (Figure 5.2) ( $p$ -value  $\leq$  0.0001) and 10<sup>-5</sup> M Bp2 (Figure 5.3) ( $p$ -value  $\leq$  0.0001) had the highest stimulation effect on the proliferation of T-47-D cells and the proliferation was stimulated significantly by 10<sup>-8</sup>M Bp1 (Figure 5.2) ( $p$ -value  $\leq$  0.05) and 10<sup>-6</sup> M Bp2 (Figure 5.3) ( $p$ -value  $\leq$  0.001). A lower significant response was found on the proliferation of T-47-D cells after short-term exposure to 10<sup>-5</sup> M Bp3 (Figure 5.4) ( $p$ -value  $\leq$  0.001). Concentrations of 10<sup>-8</sup> M to 10<sup>-5</sup> M OMC did not stimulate the proliferation of T-47-D cells (Figure 5.5). Proliferation of T-47-D cells was stimulated significantly by 10<sup>-5</sup> M 4MBC (Figure 5.6) ( $p$ -value  $\leq$  0.001) and 10<sup>-5</sup> M HS (Figure 5.7) ( $p$ -value  $\leq$  0.001).

Comparisons of the effects of  $10^{-5}$  M benzophenones (Bp1, Bp2 and Bp3) on T-47-D cell proliferation with  $17\beta$ -oestradiol revealed no significant difference. However, the effect of the benzophenones and  $17\beta$ -oestradiol on T-47-D cell proliferation was found significantly greater than the effects of concentrations of  $10^{-5}$  M OMC, 4MBC and HS (Figure 5.9).

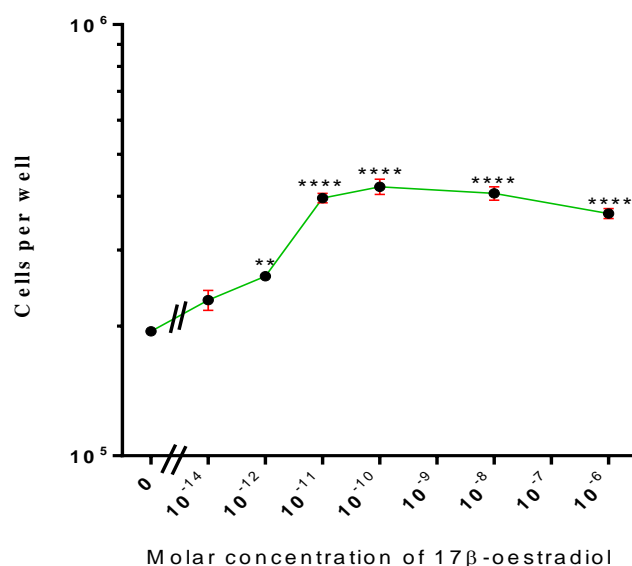


**Figure 5.1 Effect of  $17\beta$ -oestradiol on proliferation of T-47-D human breast cancer cells in monolayer culture.**

T-47-D Cells were grown for 7 days in phenol-red-free-DMEM containing 5% DCFCS with ethanol control only (0) or with indicated molecular concentrations of  $17\beta$ -oestradiol after short-term exposure (7 days). Media were replinshed on day 1 and day 4 of the experiment. Values are the average  $\pm$ SE of triplicate independent wells. \*\* *p-value*  $\leq 0.01$  and \*\*\*\* *p-value*  $\leq 0.0001$  versus no addition (0) by one-way ANOVA Dunnett's test.

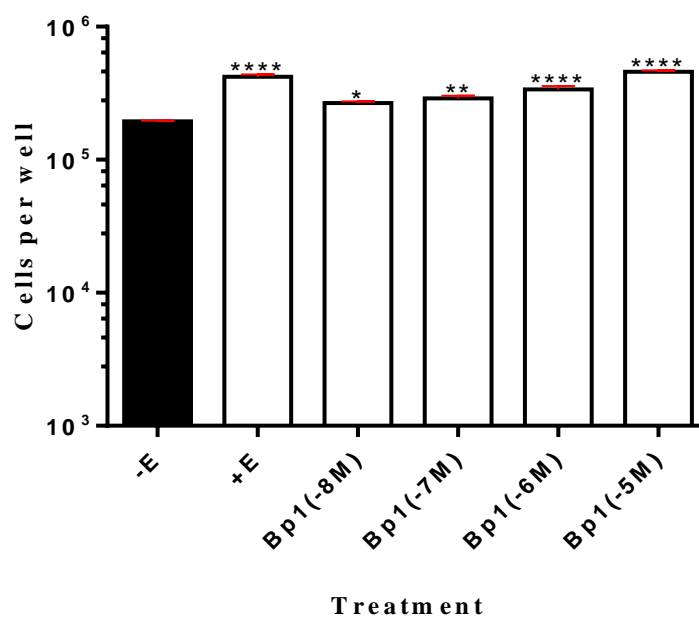


**Figure 5.2 Effect of Bp1 on proliferation of T-47-D human breast cancer cells in monolayer culture.**

Cells were grown in phenol-red-free-DMEM containing 5% DCFCS with ethanol control only (-E),  $10^{-8}$  M  $17\beta$ -oestradiol (+E), with  $10^{-8}$  M Bp1 (Bp1 (-8M)),  $10^{-7}$  M Bp1 (Bp1 (-7M)),  $10^{-6}$  M Bp1 (Bp1 (-6M)) or  $10^{-5}$  M Bp1 (Bp1 (-5M)) for 7 days. Media were replenished on day 1 and day 4 of the experiment. Values are the average  $\pm$ SE of triplicate independent wells. Where no bars are seen, error was too small to be visualized. \* *p*-value  $\leq 0.05$ , \*\* *p*-value  $\leq 0.01$  and \*\*\*\* *p*-value  $\leq 0.0001$  versus no addition (-E) by one-way ANOVA Dunnett's test. Two replicate experiments showed similar results (n=2).

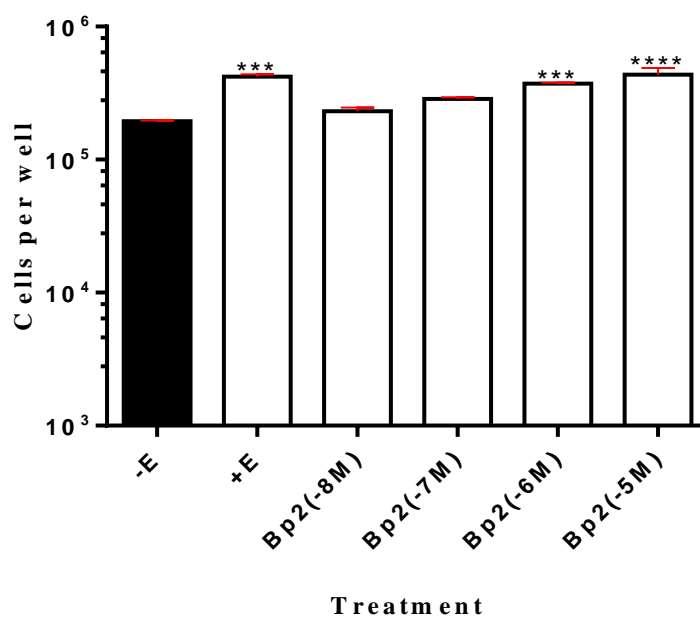


**Figure 5.3 Effect of Bp2 on proliferation of T-47-D human breast cancer cells in monolayer culture.**

Cells were grown in phenol-red-free-DMEM containing 5% DCFCS with ethanol control only (-E),  $10^{-8}$  M  $17\beta$ -oestradiol (+E), with  $10^{-8}$  M Bp2 (Bp2 (-8M)),  $10^{-7}$  M Bp2 (Bp2 (-7M)),  $10^{-6}$  M Bp2 (Bp2 (-6M)) or  $10^{-5}$  M Bp2 (Bp2 (-5M)) for 7 days. Media were replenished on day 1 and day 4 of the experiment. Values are the average  $\pm$ SE of triplicate independent wells. Where no bars are seen, error was too small to be visualized. \*\*\* *p*-value  $\leq 0.001$  and \*\*\*\* *p*-value  $\leq 0.0001$  versus no addition (-E) by one-way ANOVA Dunnett's test. Two replicate experiments showed similar results (n=2).

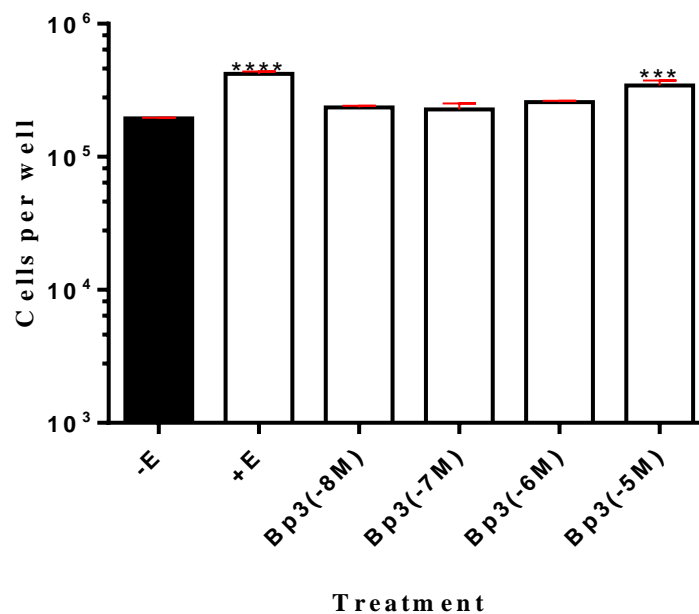


**Figure 5.4 Effect of Bp3 on proliferation of T-47-D human breast cancer cells in monolayer culture.**

Cells were grown in phenol-red-free-DMEM containing 5% DCFCS with ethanol control only (-E),  $10^{-8}$  M  $17\beta$ -oestradiol (+E), with  $10^{-8}$  M Bp3 (Bp3 (-8M)),  $10^{-7}$  M Bp3 (Bp3 (-7M)),  $10^{-6}$  M Bp3 (Bp3 (-6M)) or  $10^{-5}$  M Bp3 (Bp3 (-5M)) for 7 days. Media were replenished on day 1 and day 4 of the experiment. Values are the average  $\pm$ SE of triplicate independent wells. Where no bars are seen, error was too small to be visualized. \*\*\* *p*-value  $\leq 0.001$  and \*\*\*\* *p*-value  $\leq 0.0001$  versus no addition (-E) by one-way ANOVA Dunnett's test. Two replicate experiments showed similar results (n=2).

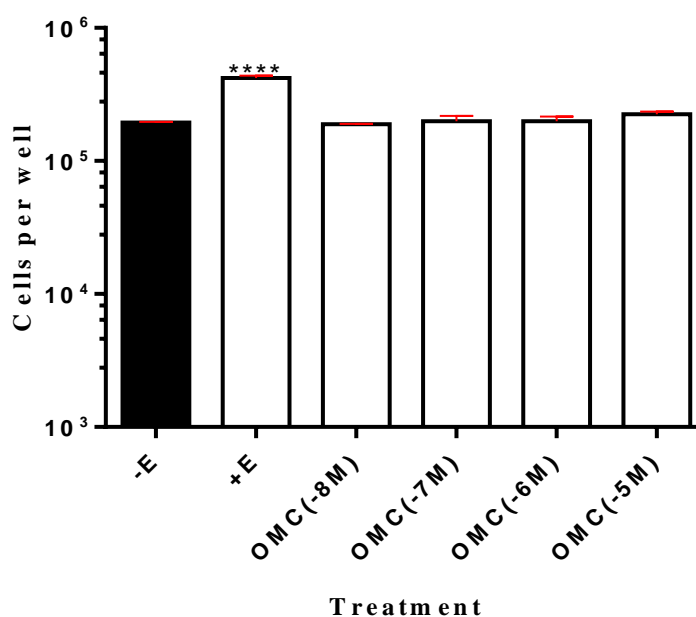


**Figure 5.5 Effect of OMC on proliferation of T-47-D human breast cancer cells in monolayer culture.**

Cells were grown in phenol-red-free-DMEM containing 5% DCFCS with ethanol control only (-E),  $10^{-8}$  M  $17\beta$ -oestradiol (+E), with  $10^{-8}$  M OMC (OMC (-8M)),  $10^{-7}$  M OMC (OMC (-7M)),  $10^{-6}$  M OMC (OMC (-6M)) or  $10^{-5}$  M OMC (OMC (-5M)) for 7 days. Media were replenished on day 1 and day 4 of the experiment. Values are the average  $\pm$ SE of triplicate independent wells. Where no bars are seen, error was too small to be visualized. \*\*\*\*  $p$ -value  $\leq 0.0001$  versus no addition (-E) by one-way ANOVA Dunnett's test. Two replicate experiments showed similar results (n=2).

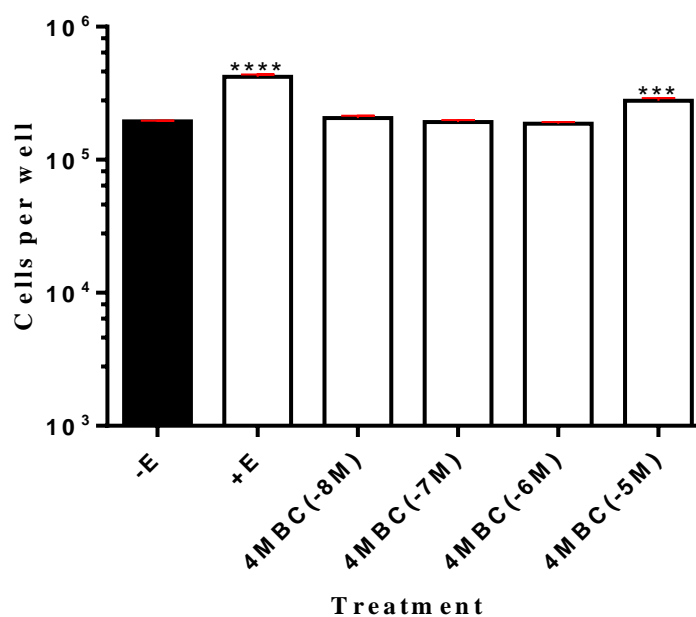


**Figure 5.6 Effect of 4MBC on proliferation of T-47-D human breast cancer cells in monolayer culture.**

Cells were grown in phenol-red-free-DMEM containing 5% DCFCS with ethanol control only (-E),  $10^{-8}$  M  $17\beta$ -oestradiol (+E), with  $10^{-8}$  M 4MBC (4MBC (-8M)),  $10^{-7}$  M 4MBC (4MBC (-7M)),  $10^{-6}$  M 4MBC (4MBC (-6M)) or  $10^{-5}$  M 4MBC (4MBC (-5M)) for 7 days. Media were replenished on day 1 and day 4 of the experiment. Values are the average  $\pm$ SE of triplicate independent wells. Where no bars are seen, error was too small to be visualized. \*\*\*  $p$ -value  $\leq 0.001$  and \*\*\*\*  $p$ -value  $\leq 0.0001$  versus no addition (-E) by one-way ANOVA Dunnett's test. Two replicate experiments showed similar results (n=2).

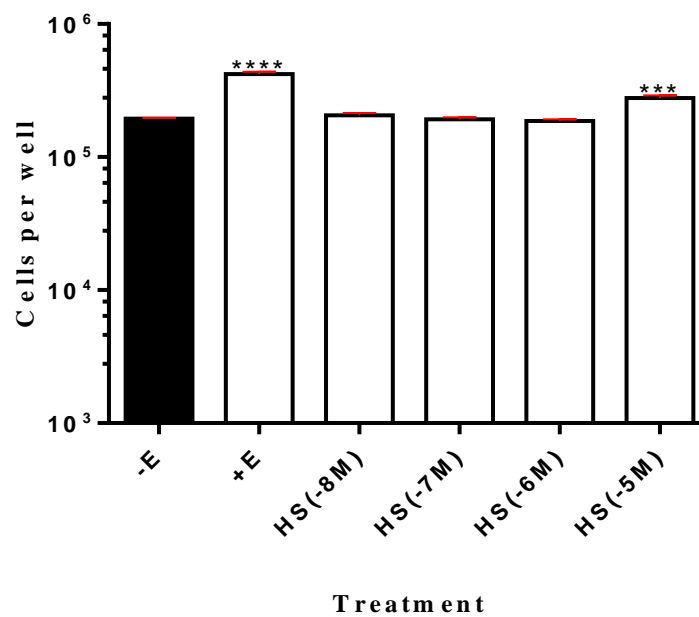


**Figure 5.7 Effect of HS on proliferation of T-47-D human breast cancer cells in monolayer culture.**

Cells were grown in phenol-red-free-DMEM containing 5% DCFCS with ethanol control only (-E),  $10^{-8}$  M  $17\beta$ -oestradiol (+E), with  $10^{-8}$  M homosalate (HS (-8M)),  $10^{-7}$  M homosalate (HS (-7M)),  $10^{-6}$  M homosalate (HS (-6M)) or  $10^{-5}$  M homosalate (HS (-5M)) for 7 days. Media were replenished on day 1 and day 4 of the experiment. Values are the average  $\pm$ SE of triplicate independent wells. Where no bars are seen, error was too small to be visualized. \*\*\*  $p$ -value  $\leq 0.001$  and \*\*\*\*  $p$ -value  $\leq 0.0001$  versus no addition (-E) by one-way ANOVA Dunnett's test. Two replicate experiments showed similar results (n=2).

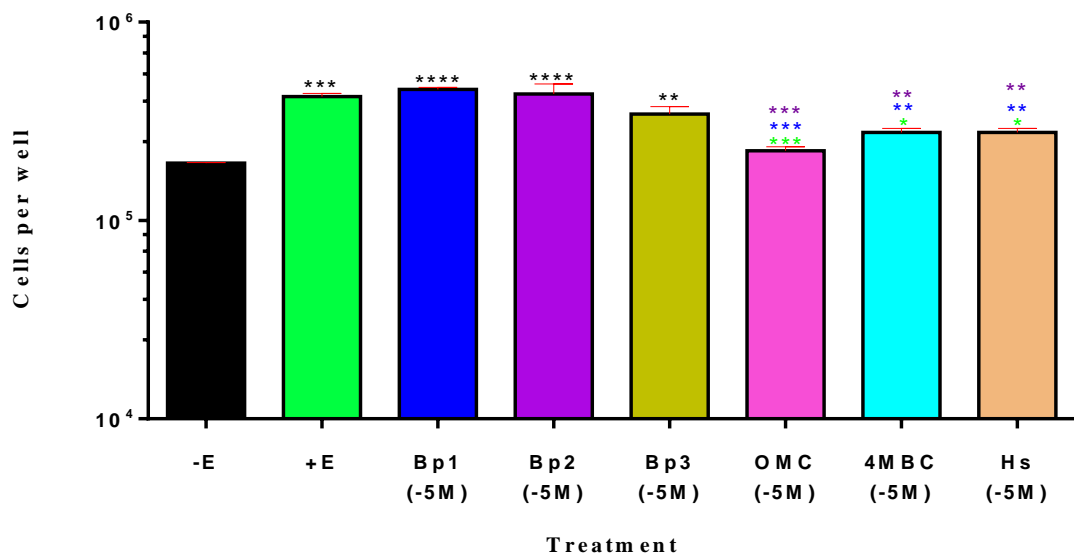


**Figure 5.8 Comparison and summary of the varying effect of the UV screens on proliferation of T-47-D human breast cancer cells in monolayer culture (B).** Monolayers of T-47-D cells ( $0.2 \times 10^5$  cells/well) were exposed to  $10^{-8}$  M  $17\beta$ -oestradiol (+E),  $10^{-5}$  M Bp1 (Bp1(-5M)),  $10^{-5}$  M Bp2 (Bp2(-5M)),  $10^{-5}$  M Bp3 (Bp3(-5M)),  $10^{-5}$  M OMC (OMC(-5M)),  $10^{-5}$  M 4MBC (4MBC(-5M)) or  $10^{-5}$  M HS (HS(-5M)) or ethanol control (-E) in phenol-red-free DMEM and 5% DCFS for 14 days (B). Values are the average  $\pm$ SE of 3 independent wells (n=3). \*  $p$ -value  $\leq 0.05$ , \*\*  $p$ -value  $\leq 0.01$  and \*\*\*\*  $p$ -value  $\leq 0.0001$  versus no addition (black asterisks),  $17\beta$ -oestradiol (green asterisks), Bp1 (blue asterisks), Bp2 (purple asterisks), Bp3 (lime asterisks) by one-way ANOVA Tukey's test.

## **5.3.2 Effects of UV screens on motility of T-47-D human breast cancer cells**

### **5.3.2.1 Effects of UV screens on motility of T-47-D human breast cancer cells as measured by wound healing**

The wound healing assay (Liang et al., 2007) was used to determine the effect of short-term (3 weeks) and long-term (13 and 30 weeks) exposure to the UV screens on motility of T-47-D human breast cancer cells (as described in section 2.4.1). Results showed that after 3 weeks of exposure to  $10^{-5}$  M Bp1 or  $10^{-5}$  M OMC the wound healing was higher than the negative control.  $10^{-5}$  M Bp1 closed  $44.63 \pm 2.27\%$  and  $10^{-5}$  M OMC closed  $39.09 \pm 3.56\%$  of the wound, while the closure percentage was  $23.35 \pm 5.28\%$  in the negative control wells (Figures 5.9 - 5.11) ( $p$ -value  $\leq 0.05$ ). Longer exposure times have shown that after 13 weeks of exposure neither  $10^{-5}$  M Bp1 nor  $10^{-5}$  M OMC increased T-47-D cell motility compared to the negative control (Figure 5.12). However, after 30 weeks of exposure to  $10^{-5}$  M Bp1 the wound healing was significantly higher ( $33.99 \pm 1.95\%$ ) than the negative control ( $23.09 \pm 0.59\%$ ) (Figures 5.13 and 5.14) ( $p$ -value  $\leq 0.05$ ) but with no indicated increase in the wound healing percentage in comparison with the results obtained after 3 weeks of exposure to  $10^{-5}$  M Bp1 (Figure 5.9).

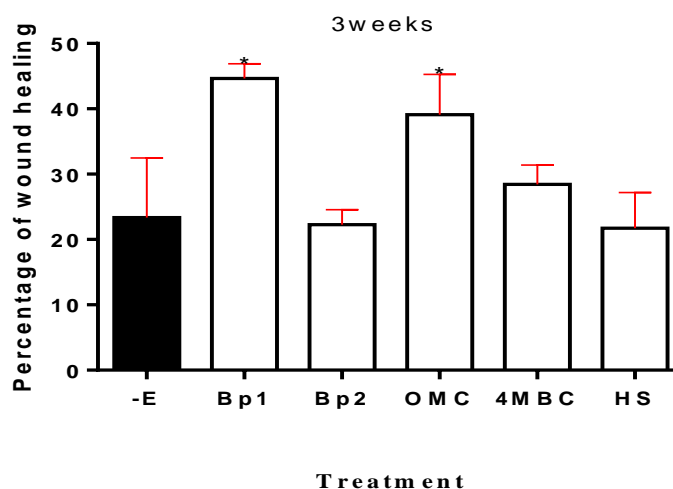


**Figure 5.9 Effect of 3 weeks of exposure to UV screens on motility of T-47-D human breast cancer cells as determined by wound healing assay.**

Cells were grown in phenol-red-free-DMEM containing 5% DCFCS with ethanol control (-E) only, with  $10^{-5}$  M Bp1 (Bp1), with  $10^{-5}$  M Bp2 (Bp2),  $10^{-5}$  M OMC (OMC), with  $10^{-5}$  M 4MBC (4MBC) or with  $10^{-5}$  M HS (HS) for 3 weeks. Media were replenished and cells were split every 3-4 days. Cells were then reseeded in 12-well plates and once the cells became  $\geq 95\%$  confluent, wound was made and mitomycin c ( $0.5 \mu\text{g/ml}$ ) was added. Images were captured at 0 hour and 24 hours. Cell migration was quantified by calculating the percentage of wound healing for minimum 3 images of each well using Image J software. Values are the average  $\pm$ SE of triplicate independent wells. \*  $p$ -value  $\leq 0.05$  versus no addition (-E) by t-Test.

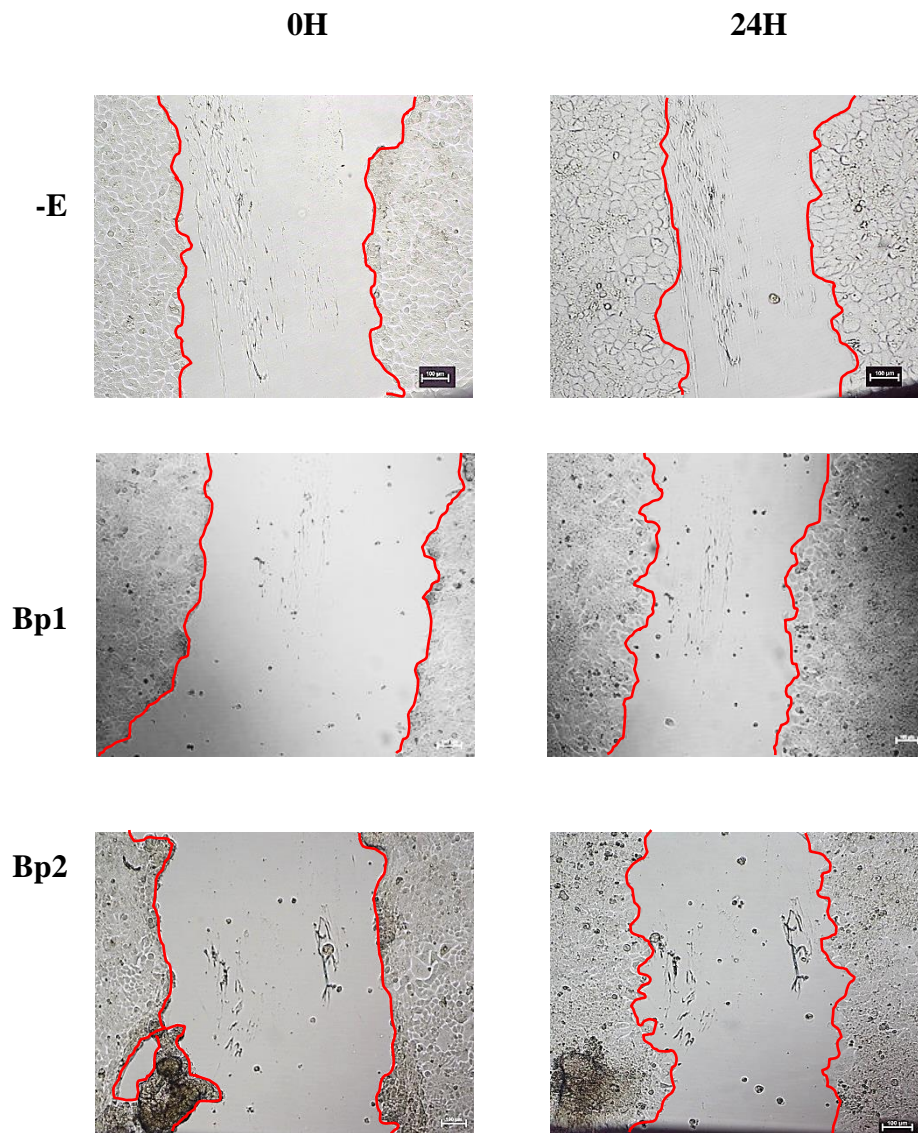


**Figure 5.10 Representative images of the effect of 3 weeks of exposure to UV screens on motility of T-47-D human breast cancer cells as determined by wound healing assay.**

Cells were grown in phenol-red-free-DMEM containing 5% DCFCS with ethanol control (-E) only, with  $10^{-5}$  M Bp1 (Bp1) or with  $10^{-5}$  M Bp2 (Bp2) 3 weeks. Cells were then reseeded in 12-well plates and once the cells became  $\geq 95\%$  confluent, wound was made and mitomycin c ( $0.5 \mu\text{g/ml}$ ) was added. Images were captured at 0 hour and 24 hours.

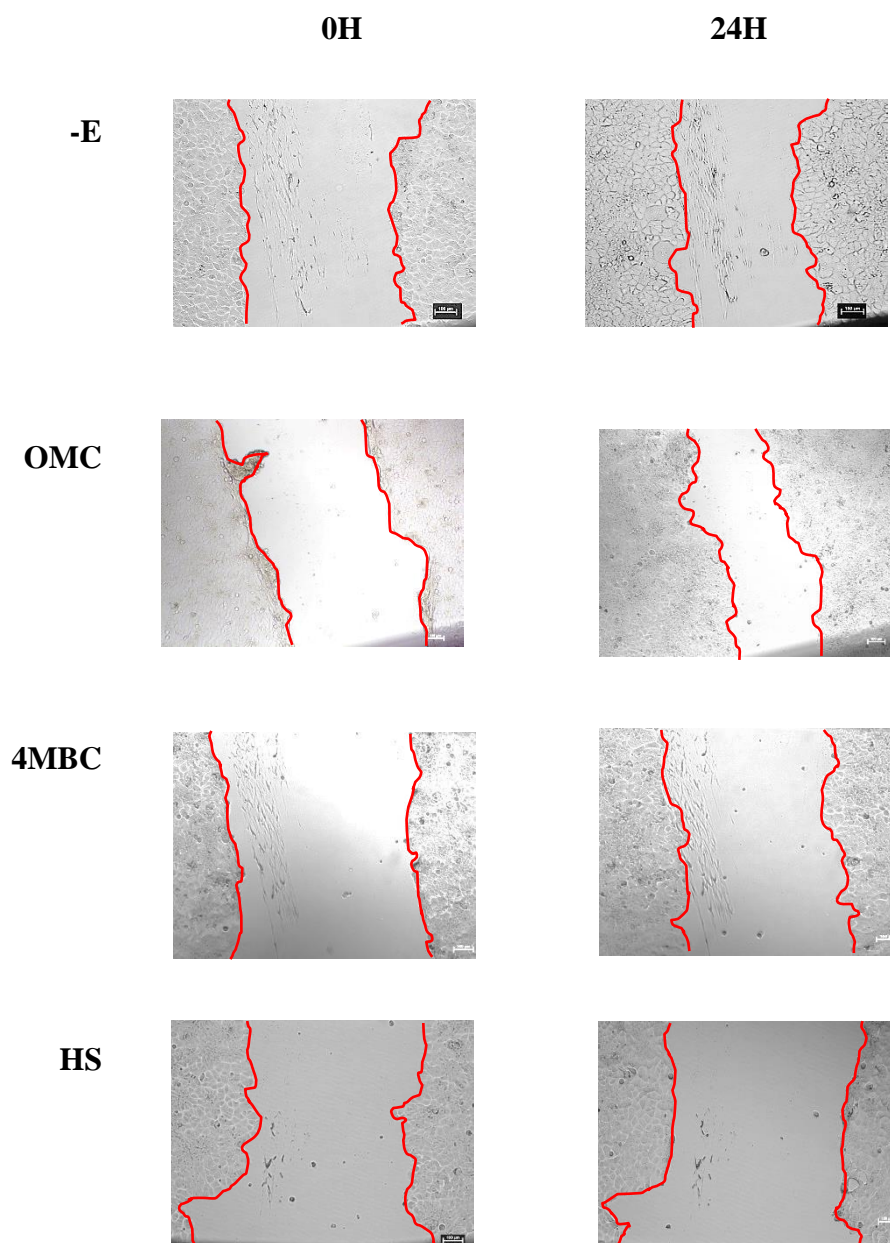


**Figure 5.11 Representative images of the effect of 3 weeks of exposure to UV screens on motility of T-47-D human breast cancer cells as determined by wound healing assay.**

Cells were grown in phenol-red-free-DMEM containing 5% DCFCS with ethanol control (-E) only, with  $10^{-5}$  M OMC (OMC), with  $10^{-5}$  M 4MBC (4MBC) or with  $10^{-5}$  M HS (HS) for 3 weeks. Cells were then reseeded in 12-well plates and once the cells became  $\geq 95\%$  confluent, wound was made and mitomycin c ( $0.5 \mu\text{g/ml}$ ) was added. Images were captured at 0 hour and 24 hours.

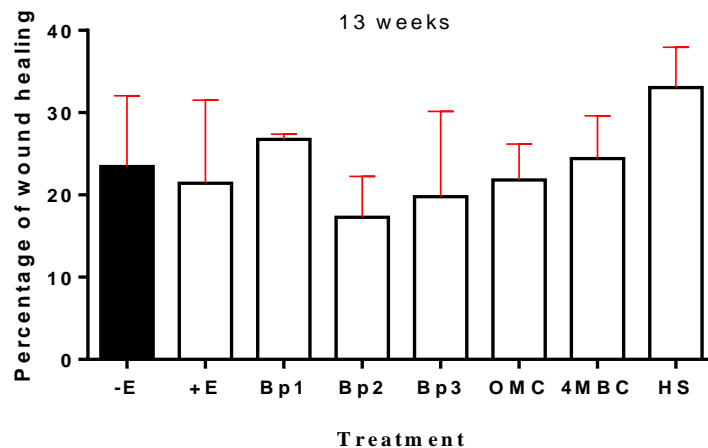


**Figure 5.12 Effect of 13 weeks of exposure to UV screens on motility of T-47-D human breast cancer cells as determined by wound healing assay.**

Cells were grown in phenol-red-free-DMEM containing 5% DCFCS with ethanol control (-E) only,  $10^{-8}$  M  $17\beta$ -oestradiol (+E), with  $10^{-5}$  M Bp1 (Bp1), with  $10^{-5}$  M Bp2 (Bp2), with  $10^{-5}$  M Bp3 (Bp3),  $10^{-5}$  M OMC (OMC), with  $10^{-5}$  M 4MBC (4MBC) or with  $10^{-5}$  M homosalate (HS) for 13 weeks. Media were replenished and cells were split every 3-4 days. Cells were then reseeded in 12-well plates and once the cells became  $\geq 95\%$  confluent, wound was made and mitomycin c ( $0.5 \mu\text{g/ml}$ ) was added. Images were captured at 0 hour and 24 hours. Cell migration was quantified by calculating the percentage of wound healing for minimum 3 images of each well using Image J software. Values are the average  $\pm$ SE of triplicate independent wells.

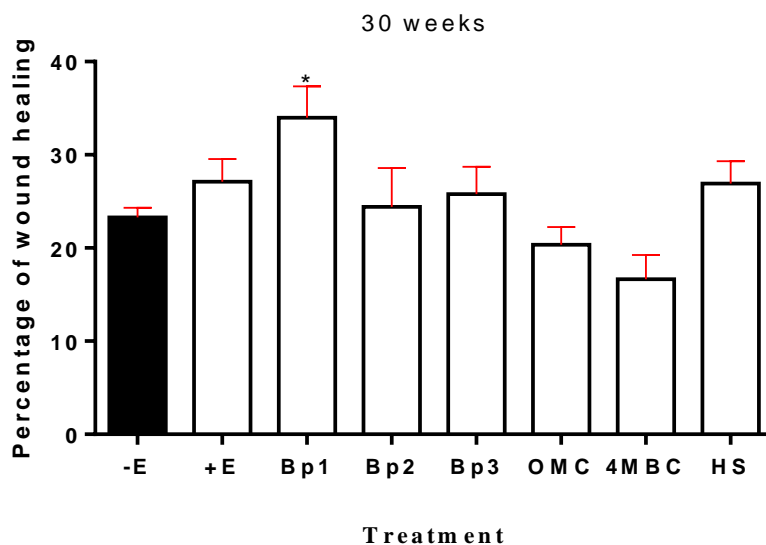


**Figure 5.13 Effect of 30 weeks of exposure to UV screens on motility of T-47-D human breast cancer cells as determined by wound healing assay.**

Cells were grown in phenol-red-free-DMEM containing 5% DCFCS with ethanol control (-E) only,  $10^{-8}$  M  $17\beta$ -oestradiol (+E), with  $10^{-5}$  M Bp1 (Bp1), with  $10^{-5}$  M Bp2 (Bp2), with  $10^{-5}$  M Bp3 (Bp3),  $10^{-5}$  M OMC (OMC), with  $10^{-5}$  M 4MBC (4MBC) or with  $10^{-5}$  M HS (HS) for 30 weeks. Media were replenished and cells were split every 3-4 days. Cells were then reseeded in 12-well plates and once the cells became  $\geq 95\%$  confluent, wound was made and mitomycin c ( $0.5 \mu\text{g/ml}$ ) was added. Images were captured at 0 hour and 24 hours. Cell migration was quantified by calculating the percentage of wound healing for minimum 3 images of each well using Image J software. Values are the average  $\pm$ SE of triplicate independent wells. \* *p-value*  $\leq 0.05$  versus no addition by t-Test.

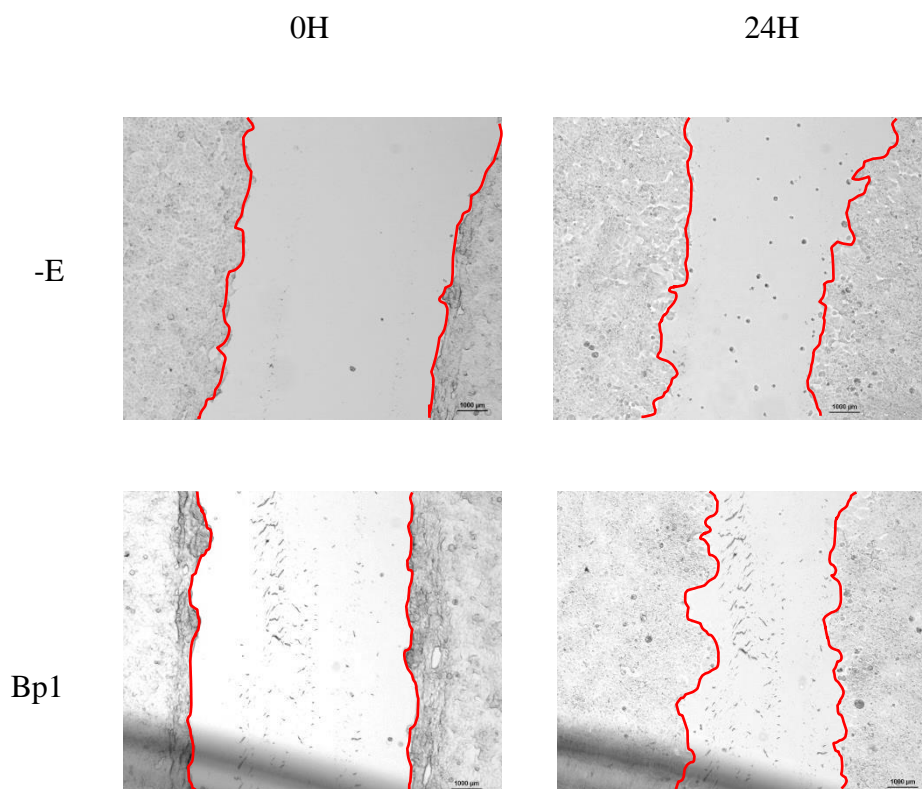


**Figure 5.14 Representative images of the effect of UV screens after 30 weeks on motility of T-47-D human breast cancer cells as determined by wound healing assay.**

Cells were grown in phenol-red-free-DMEM containing 5% DCFCS with ethanol control (-E) only or with  $10^{-5}$  M Bp1 (Bp1) for 30 weeks. Cells were then reseeded in 12-well plates and once the cells became  $\geq 95\%$  confluent, wound was made and mitomycin c ( $0.5 \mu\text{g/ml}$ ) was added. Images were captured at 0 hour and 24 hours.

### 5.3.2.2 Effects of UV screens on motility of T-47-D human breast cancer cells as determined by xCELLigence technology

The movement of T-47-D cells through 8µm pores of a membrane towards a chemotaxis stimulus of FCS was observed following the exposure to 10<sup>-8</sup> M 17β-oestradiol or the UV screens or no addition for 2, 7 and 21 weeks prior to the experiment which was conducted as described previously (in section 2.4.3).

2 weeks of exposure to 10<sup>-5</sup> M of the UV screens showed no increase in cell index in comparison to the negative control (Figures 5.15 and 5.16). However, 7 weeks of exposure increased the individual motility of T-47-D cells after exposure to 10<sup>-5</sup> M OMC (cell index 0.27 ± 0.05) (*p*-value ≤ 0.05) and 10<sup>-5</sup> M 4MBC (cell index 0.57 ± 0.05) (*p*-value ≤ 0.001) in comparison to the negative control (cell index 0.04 ± 0.02) (Figure 5.18) and no effect of benzophenones was recorded at the same time point (Figure 5.17).

Longer exposure up to 13 weeks gave no significant increase in T-47-D cell motility (Figure 5.19), but 21 weeks of exposure increased T-47-D cell motility after exposure to 10<sup>-5</sup> M Bp2 (cell index 0.16 ± 0.02) (*p*-value ≤ 0.05), 10<sup>-5</sup> M Bp3 (cell index 0.16 ± 0.01) (*p*-value ≤ 0.01), 10<sup>-5</sup> M OMC (cell index 0.19 ± 0.02) (*p*-value ≤ 0.01), 10<sup>-5</sup> M 4MBC (cell index 0.16 ± 0.03) (*p*-value ≤ 0.05) or 10<sup>-5</sup> M HS (cell index 0.21 ± 0.04) (*p*-value ≤ 0.05) in comparison with untreated cells (cell index 0.21 ± 0.04) (Figure 5.20).

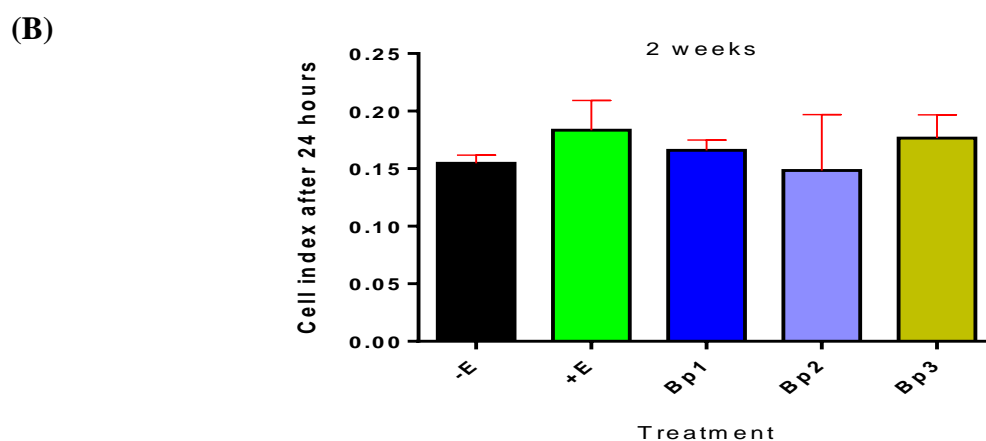
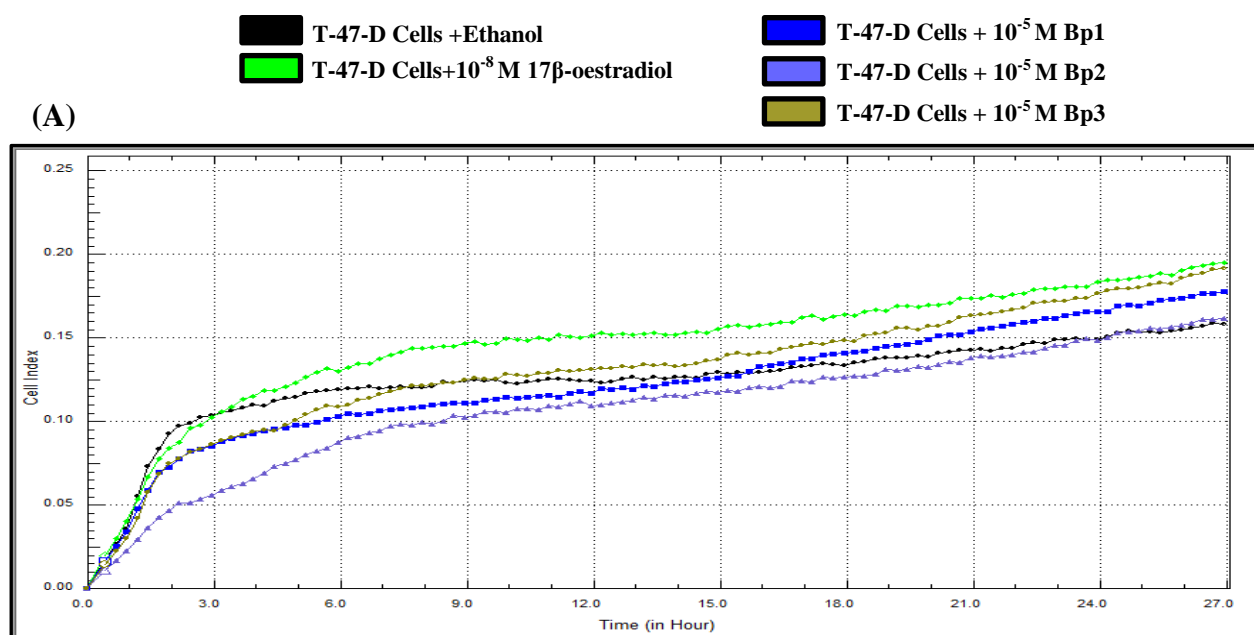


**Figure 5.15 Effect of 2 weeks of exposure to UV screens on T-47-D breast cancer cell migration towards chemotaxis stimulus on an uncoated surface.**

Cells were grown in phenol-red-free-DMEM containing 5% DCFCS with ethanol control only (-E),  $10^{-8}$  M  $17\beta$ -oestradiol (+E)  $10^{-5}$  M benzophenone-1 (Bp1),  $10^{-5}$  M benzophenone-2 (Bp2),  $10^{-5}$  M benzophenone-3 (Bp3) or ethanol (-E) for 2 weeks in phenol-red-free DMEM supplemented with 5% DCFCS. Media were replenished and cells were split every 3-4 days. (A) The relative change in cell index of triplicate wells as indicated by the changes in impedance caused by cell migration from upper chambers to lower ones through the pores of polycarbonate membrane. Cell index was recorded every 5 minutes and monitored for 24 hours. (B) Bar graph represents the average of the end point measurements (Cell index) of cell migration of triplicate wells at 24 hours. Values are the average  $\pm$ SE of triplicate independent wells.

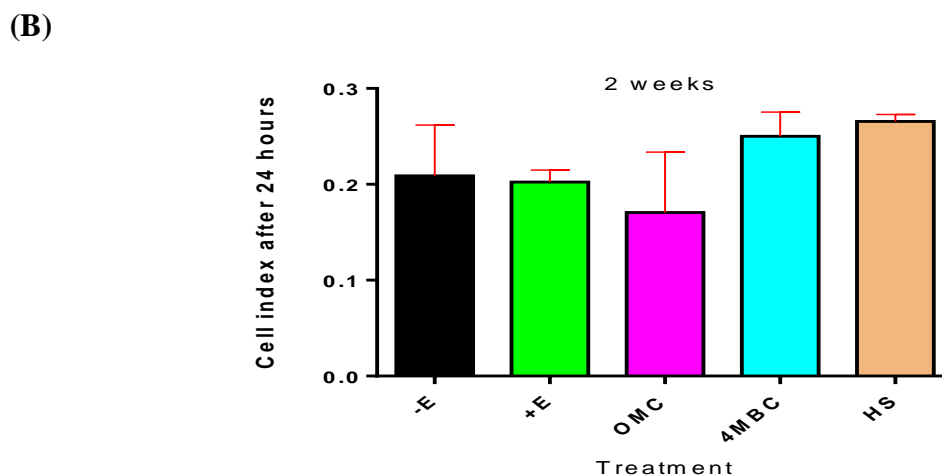
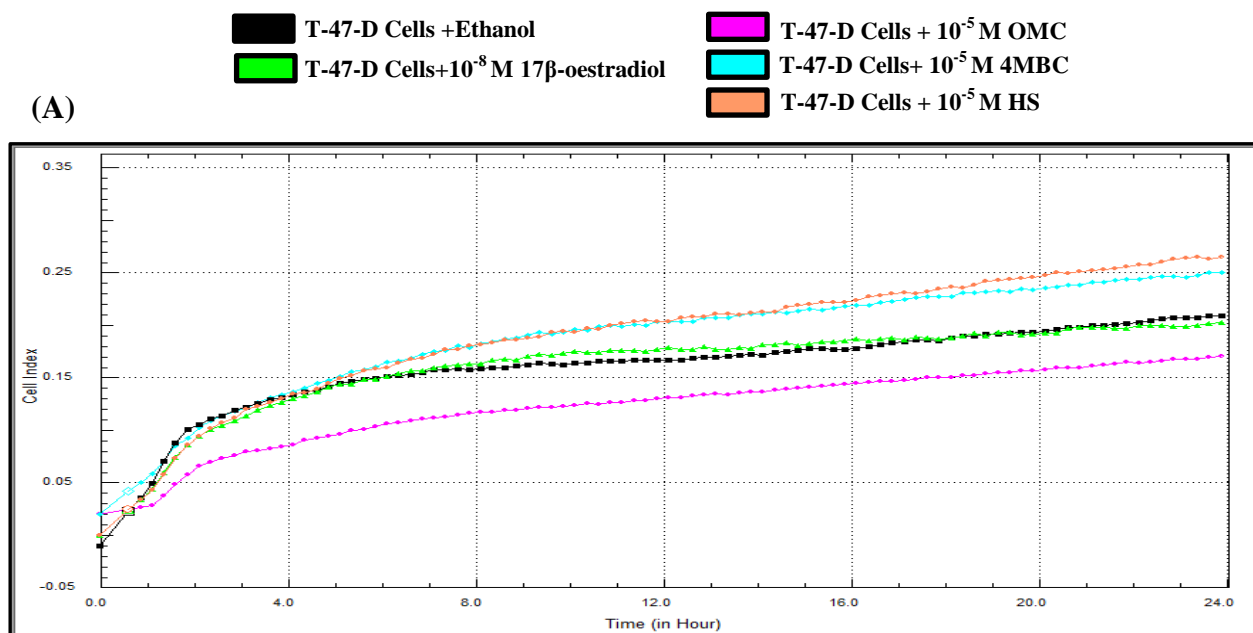


**Figure 5.16 Effect of 2 weeks of exposure to UV screens on T-47-D breast cancer cell migration towards chemotaxis stimulus on an uncoated surface.**

Cells were grown in phenol-red-free-DMEM containing 5% DCFCS with ethanol control only (-E),  $10^{-8}$  M  $17\beta$ -oestradiol (+E),  $10^{-5}$  M OMC (OMC),  $10^{-5}$  M 4MBC (4MBC),  $10^{-5}$  M HS (HS) or ethanol (-E) for 2 weeks in phenol-red-free DMEM supplemented with 5% DCFCS. Media were replenished and cells were split every 3-4 days. (A) The relative change in cell index of triplicate wells as indicated by the changes in impedance caused by cell migration from upper chambers to lower ones through the pores of polycarbonate membrane. Cell index was recorded every 5 minutes and monitored for 24 hours. (B) Bar graph represents the average of the end point measurements (Cell index) of cell migration of triplicate wells at 24 hours. Values are the average  $\pm$ SE of triplicate independent wells.

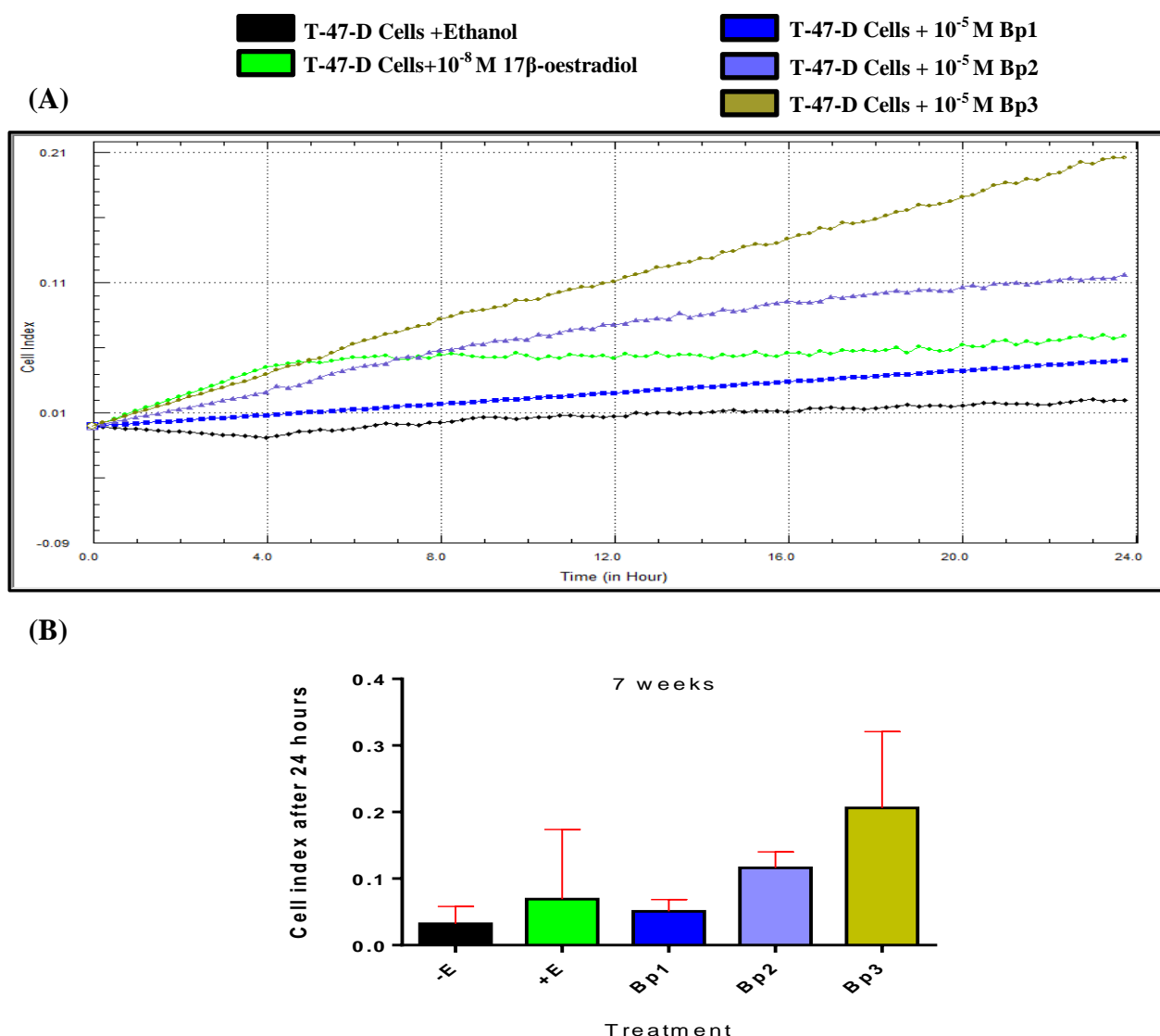


**Figure 5.17 Effect of 7 weeks of exposure to UV screens on T-47-D breast cancer cell migration towards chemotaxis stimulus on an uncoated surface.**

Cells were grown in phenol-red-free-DMEM containing 5% DCFCS with ethanol control only (-E),  $10^{-8}$  M  $17\beta$ -oestradiol (+E),  $10^{-5}$  M benzophenone-1 (Bp1),  $10^{-5}$  M benzophenone-2 (Bp2),  $10^{-5}$  M benzophenone-3 (Bp3) or ethanol (-E) for 7 weeks in phenol-red-free DMEM supplemented with 5% DCFCS. Media were replenished on day 1 and day 4. (A) The relative change in cell index of triplicate wells as indicated by the changes in impedance caused by cell migration from upper chambers to lower ones through the pores of polycarbonate membrane. Cell index was recorded every 5 minutes and monitored for 24 hours. (B) Bar graph represents the average of the end point measurements (Cell index) of cell migration of triplicate wells at 24 hours. Values are the average  $\pm$ SE of triplicate independent wells.

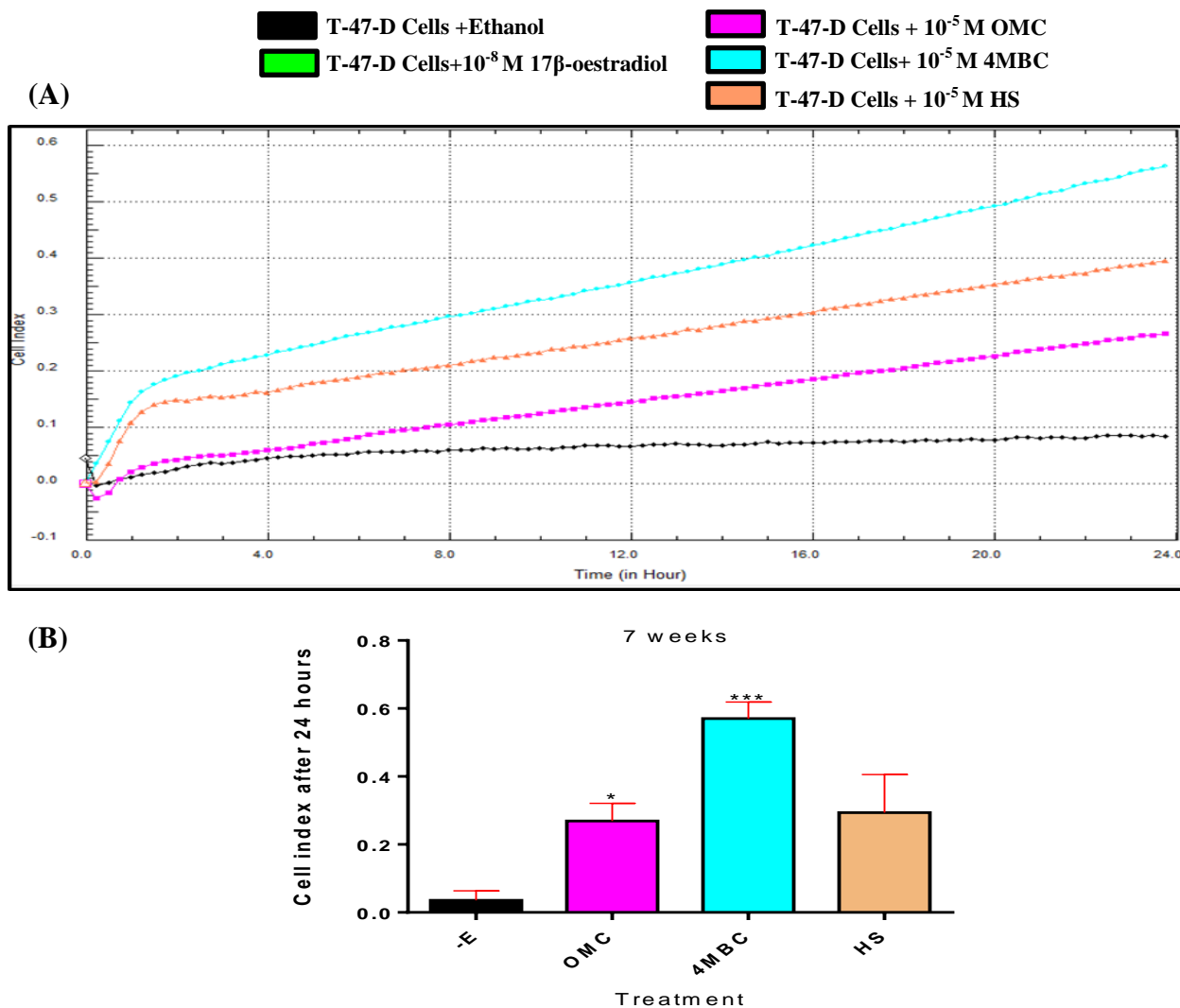


**Figure 5.18 Effect of 7 weeks of exposure to UV screens on T-47-D breast cancer cell migration towards chemotaxis stimulus on an uncoated surface.**

Cells were grown in phenol-red-free-DMEM containing 5% DCFCS with ethanol control only (-E),  $10^{-8}$  M  $17\beta$ -oestradiol (+E),  $10^{-5}$  M OMC (OMC),  $10^{-5}$  M 4MBC (4MBC),  $10^{-5}$  M HS (HS) or ethanol (-E) for 7 weeks in phenol-red-free DMEM supplemented with 5% DCFCS. Media were replenished on day 1 and day 4. (A) The relative change in cell index of triplicate wells as indicated by the changes in impedance caused by cell migration from upper chambers to lower ones through the pores of polycarbonate membrane. Cell index was recorded every 5 minutes and monitored for 24 hours. (B) Bar graph represents the average of the end point measurements (Cell index) of cell migration of triplicate wells at 24 hours. Values are the average  $\pm$ SE of triplicate independent wells. \*  $p$ -value  $\leq 0.05$  and \*\*\*  $p$ -value  $\leq 0.001$  versus no addition by t-Test.

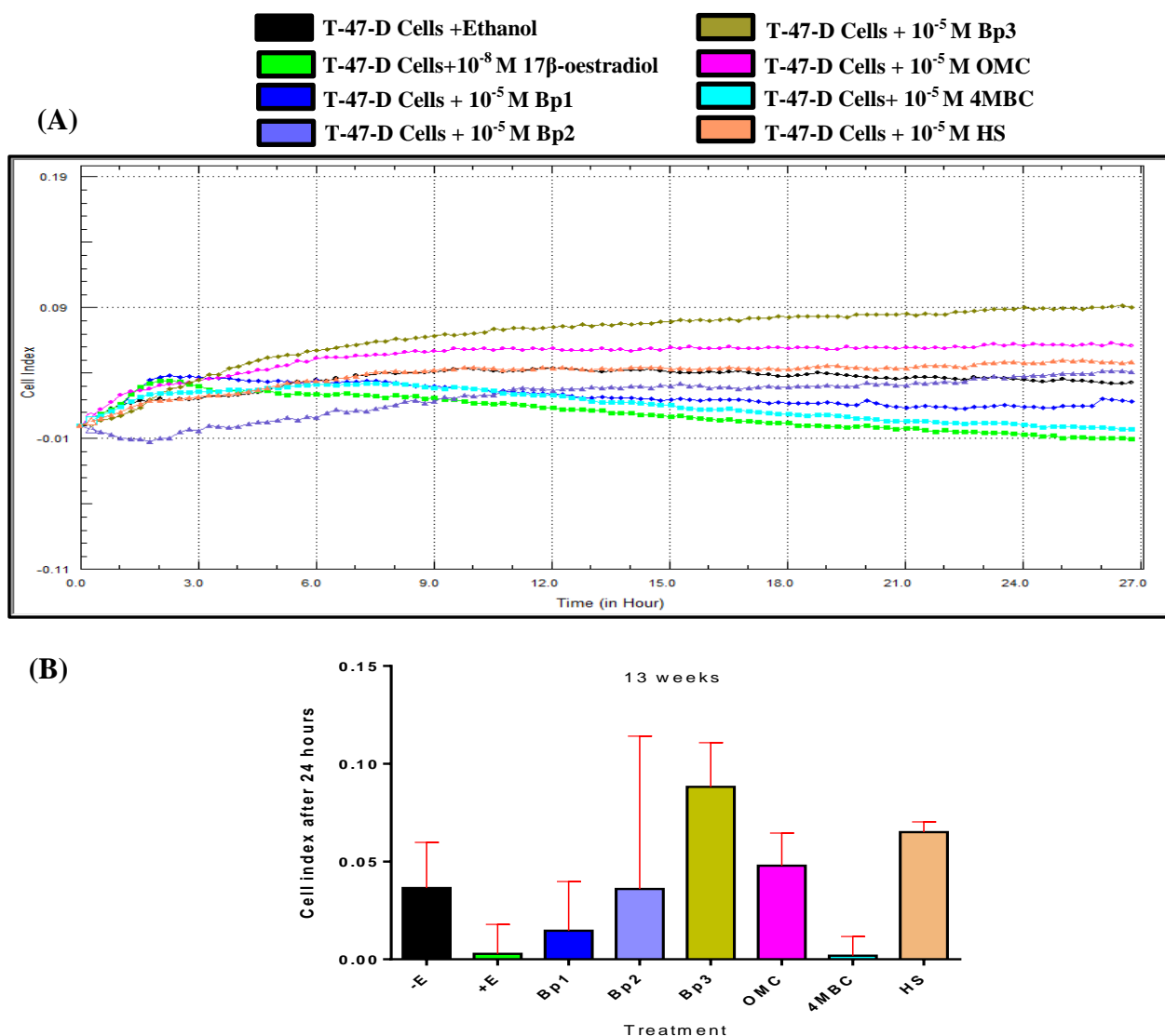


**Figure 5.19 Effect of 13 weeks of exposure to UV screens on T-47-D breast cancer cell migration towards chemotaxis stimulus on an uncoated surface.**

Cells were grown in phenol-red-free-DMEM containing 5% DCFCS with ethanol control only (-E),  $10^{-8}$  M  $17\beta$ -oestradiol (+E),  $10^{-5}$  M benzophenone-1 (Bp1),  $10^{-5}$  M benzophenone-2 (Bp2),  $10^{-5}$  M benzophenone-3 (Bp3),  $10^{-5}$  M OMC (OMC),  $10^{-5}$  M 4MBC (4MBC),  $10^{-5}$  M HS (HS) or ethanol (-E) for 13 weeks in phenol-red-free DMEM supplemented with 5% DCFCS. Media were replenished every 3-4 days. (A) The relative change in cell index of triplicate wells as indicated by the changes in impedance caused by cell migration from upper chambers to lower ones through the pores of polycarbonate membrane. Cell index was recorded every 5 minutes and monitored for 24 hours. (B) Bar graph represents the average of the end point measurements (Cell index) of cell migration of triplicate wells at 24 hours. Values are the average  $\pm$ SE of triplicate independent wells.

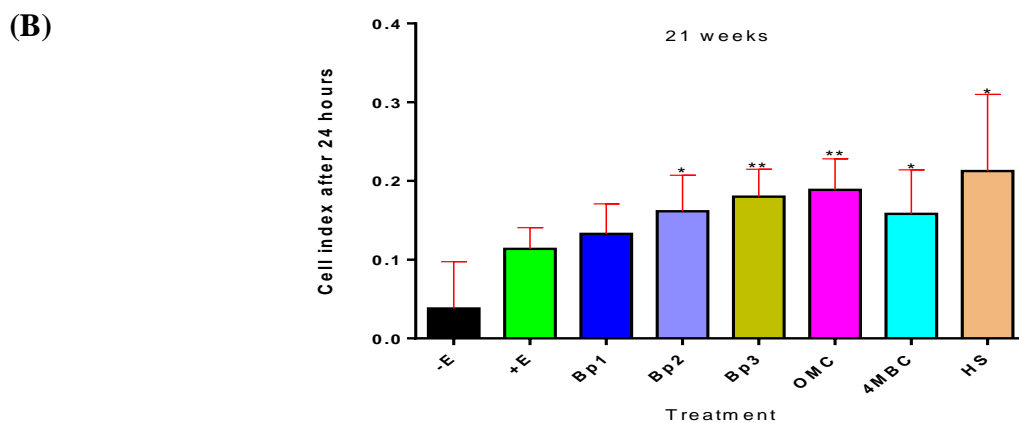
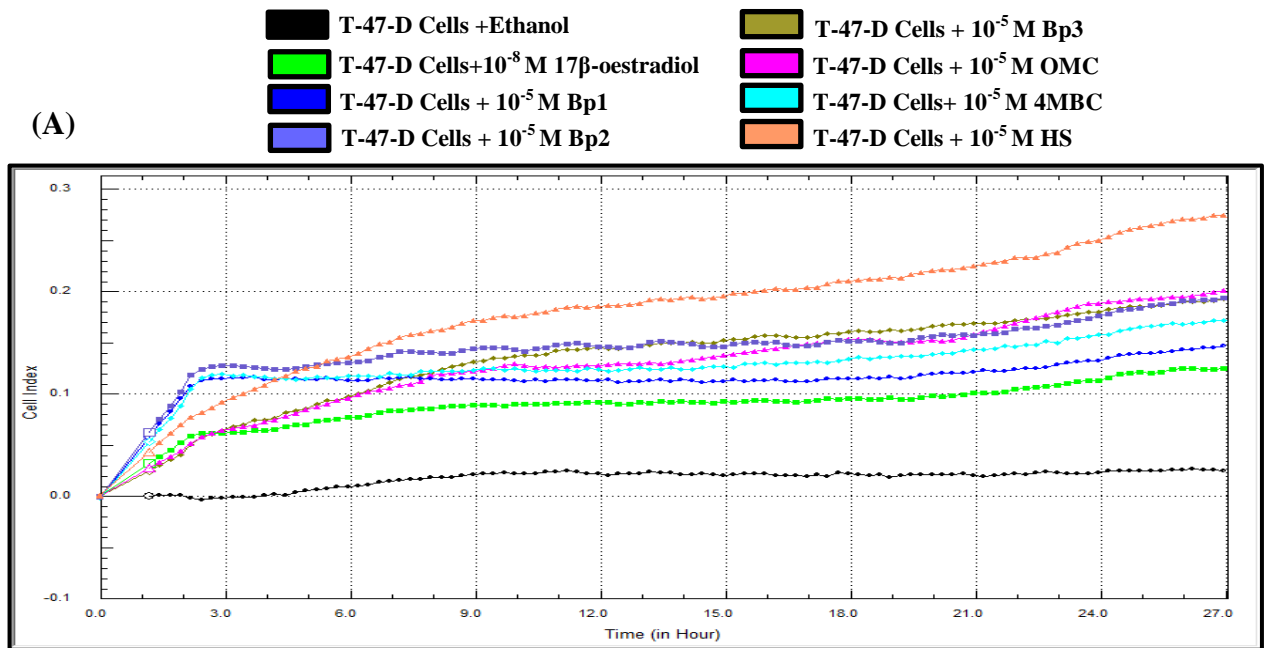


**Figure 5.20 Effect of 21 weeks of exposure to UV screens on T-47-D breast cancer cell migration towards chemotaxis stimulus on an uncoated surface.**

Cells were grown in phenol-red-free-DMEM containing 5% DCFCS with ethanol control only (-E),  $10^{-8}$  M  $17\beta$ -oestradiol (+E),  $10^{-5}$  M benzophenone-1 (Bp1),  $10^{-5}$  M benzophenone-2 (Bp2),  $10^{-5}$  M benzophenone-3 (Bp3),  $10^{-5}$  M OMC (OMC),  $10^{-5}$  M 4MBC (4MBC),  $10^{-5}$  M HS (HS) or ethanol (-E) for 21 weeks in phenol-red-free DMEM supplemented with 5% DCFCS. Media were replenished every 3-4 days. (A) The relative change in cell index of triplicate wells as indicated by the changes in impedance caused by cell migration from upper chambers to lower ones through the pores of polycarbonate membrane. Cell index was recorded every 5 minutes and monitored for 24 hours. (B) Bar graph represents the average of the end point measurements (Cell index) of cell migration of triplicate wells at 24 hours. Values are the average  $\pm$ SE of triplicate independent wells. \*  $p$ -value  $\leq 0.05$  and \*\* $p$ -value  $\leq 0.01$  versus no addition (-E) by t-Test.

## 5.4 Discussion

This study demonstrated effects of 6 UV screens on proliferation and motility of T-47-D cells which demonstrates the effects in MCF-7 cells described in chapter 4 can also be found in a second independent breast cell line. Two techniques were used to measure the effects on T-47-D cell motility following the exposure to the concentrations of the UV screens, which caused the highest proliferative response. The first assay used was the wound healing assay (Liang et al., 2007) that addresses the collective migration of cells (Friedl et al., 2004) but the second assay estimated individual cell motility through 8 $\mu$ m pores of a membrane towards a chemotaxis stimulus of FCS using the xCELLigence technology (RTCA DP, ACEA Biosciences Inc.).

***UV screens increased cell proliferation.*** This study demonstrated that exposure to UV screens can increase the proliferation of the T-47-D human breast cancer cell line. It also confirmed that T-47-D cell is responsive to 17 $\beta$ -oestradiol but not dependent on it (Darbre and Daly, 1989), whereas MCF-7 cell depends on 17 $\beta$ -oestradiol (see chapter 3). Compared to MCF-7 cells (see chapter 3), the maximal proliferation of T-47-D cell was caused by 10<sup>-5</sup> M Bp1 and 10<sup>-5</sup> M Bp2. Also, 10<sup>-5</sup> M 4MBC and 10<sup>-5</sup> M HS increased T-47-D cell proliferation. However, 10<sup>-5</sup> M Bp3 increased T-47-D cell proliferation and that was not found in the MCF-7 cell line. It is noteworthy that lower concentrations of Bp1(10<sup>-8</sup> M) caused an increase in T-47-D cell proliferation while lower concentrations of 4MBC and HS did not increase the proliferation of T-47-D cells and these findings differed from MCF-7 cell responses. The benzophenones increased T-47-D cell proliferation to a similar extent of 17 $\beta$ -oestradiol, which might be linked to their structure and their ligand binding to the ER $\alpha$  pocket (as discussed in chapter 3).

The proliferative response and sensitivity of T-47-D cells toward the UV screens is different from MCF-7 cells, and that may be explained by their different sensitivity to 17 $\beta$ -oestradiol (Karey and Sirbasku, 1988). Responses to drugs are also known to vary between these cell lines which may also be influenced by differences in the experimental conditions (Ryde et al., 1992; Schafer et al., 2000; Mooney et al., 2002; Radde et al., 2015; Risinger et al., 2015) which would be reflected in the response to environmental oestrogens including the UV screens. Each cell line possesses unique genomic and proteomic features (Shadeo and Lam, 2006; Aka and Lin, 2012) and that might not only influence the effect on proliferative response of these cells but also the motility response. Further study should be conducted to

confirm that the effects of UV screens on T-47-D cell proliferation are via oestrogenic pathway including the using of fulvestrant.

***UV screens increased the collective motility of cells.*** As discussed in the previous chapters, breast cancer metastasis is the main cause of mortality of breast cancer patients (Solomayer et al., 2000; Schairer et al., 2004; Manders et al., 2006). Thus, the effect of the UV screens on the motility of breast cancer cells was investigated using T-47-D cells as well as the MCF-7 cells. Results have shown that after only 3 weeks of T-47-D cell exposure to  $10^{-5}$  M Bp1 and  $10^{-5}$  M OMC, collective migration activity was increased. Longer-term exposure (30 weeks) caused only a significant increase in wound healing activity following the exposure to  $10^{-5}$  M Bp1.

***UV screens increased the motility of individual cells.*** In contrast to the results with MCF-7 cells (Chapter 4), the individual motility of T-47-D cells as determined by the xCELLigence was not found to be induced following 2 weeks of exposure to the UV screens using the same concentrations of the UV screens. However, the effect of OMC and 4MBC on individual cell motility was found to be started after 7 weeks of exposure and continued with the similar effect after 21 weeks of exposure. Similar to the findings with MCF-7 cells, Bp3 and HS induced T-47-D cell motility in the longer term. In contrast to MCF-7 cells, Bp2 induced T-47-D cell motility after 21 weeks of exposure, while the same chemical had no effect on individual MCF-7 cell motility on the longer run. This variation in between the results of both cells might be due to their different sensitivity to the UV screens as indicated by their different proliferative response to the different concentrations of the UV screens. Another possibility is the difference in their biology as MCF-7 cells and T-47-D cells were found to express 164 proteins differently including 3% of motility related proteins (Aka and Lin, 2012). This variation might also be justified by the finding of clinical studies that have suggested variation in metastatic potential among oestrogen receptor positive human breast cancers (Dai et al., 2005; Lower et al., 2005).

***To conclude***, effects of UV screens were observed on both motility of individual and collective cell motility. T-47-D human breast cancer cell motility has also been previously documented following long-term exposure to parabens (Khanna et al., 2014). In that study, the molecular mechanism underlying the motility of MCF-7 cells (loss of E-cadherin) was not found in T-47-D cells and that suggested that the induced motility had a different molecular mechanism. In this chapter the molecular mechanisms underlying the effect of the UV

screens on T-47-D cell motility were not investigated and whether the molecular mechanisms are similar or differ between MCF-7 cells and T-47-D cells remains to be determined.

Since breast cancer is a complex disease, to achieve a total understanding of the effects of UV screens on breast cancer progression, different models such as the *in vivo* model or xenograft model are needed to support the *in vitro* models findings described here (Vargo-Gogola and Rosen, 2007).

## Chapter 6 Effects of UV screens on MDA-MB-231 human breast cancer cells

### 6.1 Introduction

The MDA-MB-231 human breast cancer cell line is widely used as an *in vitro* model for cell invasion and metastasis (Holliday and Speirs, 2011). MDA-MB-231 cells are mesenchymal motile cells (Rajah et al., 1998) that express low levels of E-cadherin and high levels of vimentin (Uchino et al., 2010; Nieva et al., 2012; Zeng et al., 2012; Lin et al., 2014). This cell line is described as triple negative for not expressing the oestrogen receptor (ER), progesterone receptor (PR) or human epidermal growth factor receptor 2 (HER2) (Holliday and Speirs, 2011). However, MDA-MB-231 cells are ER $\alpha$  negative (Lu et al., 2005) but they express both ER $\beta$  mRNA variant (Vladusic et al., 1998; Kleuser et al., 2008), ER $\beta$  protein (Hamilton et al., 2015) and ER $\beta$  protein variant (Fuqua et al., 1999; AL-Bader et al., 2011) so an effect of 17 $\beta$ -oestradiol is still possible on this cell line. Although 17 $\beta$ -oestradiol does not alter the proliferation of MDA-MB-231 cells (Cestari et al., 2009; Girgert et al., 2014; Mints and Souchelnytskyi, 2014), it increases MDA-MB-231 cell motility (Azios and Dharmawardhane, 2005; Zhou et al., 2016), suggesting that environmental oestrogens could also influence motility of these cells.

The influence of environmental oestrogens on breast cancer cell migration is not limited to oestrogen responsive cell lines. Phthalates have been reported to increase MDA-MB-231 cell migration and invasive activity (Hsieh et al., 2012), Aluminium was found to increase the motility of MDA-MB-231 cells (Bakir and Darbre, 2015) and bisphenol A increased the migration and invasive capability of MDA-MB-231 and BT-549 triple negative human breast cancer cells (Zhang et al., 2016). Therefore the effect of the six UV screens was investigated on motility of the MDA-MB-231 cells.

MMPs are known to be involved in breast cancer cell migration and invasion (Cockett et al., 1998; Balduyck et al., 2000) (see section 1.3.3.3). The motile and invasive MDA-MB-231 cell expresses different MMPs. However, silencing MMP-2 or MMP-9 transcription (Mehner et al., 2014) or inhibiting their secretion (Kim et al., 2011) decreases both motility and invasion of MDA-MB-231 cells. It was previously reported that aluminium salts increase the secretion of MMP-9 along with the motility of the MDA-MB-231 cell line (Bakir and Darbre,

2015). Thus the effect of the six UV screens on the secretion of MMP-2 and MMP-9 by MDA-MB-231 cells was further investigated.

## **6.2 Experimental aims**

The overall aim of this chapter is to study the effect of six UV screens (Bp1, Bp2, Bp3, OMC, 4MBC and HS) on the proliferation and motility of the MDA-MB-231 human breast cancer cell line. The experiments of this chapter were not designed to address the oestrogenic activity of these chemicals as all the experiment were done using media with phenol-red and 10% FCS. To achieve this aim, the effect of UV screens on MDA-MB-231 cells proliferation was monitored on the xCELLigence machine each hour for 1 week.

In order to investigate the effect of the six UV screens on MDA-MB-231 cell motility, the individual chemotactic derived motility was determined by xCELLigence following 2 weeks and 8 weeks of exposure. In addition, live imaging by time-lapse microscopy was used to measure the effects on the cumulative length moved by the individual cells following 2 weeks and 15 weeks of exposure. Also, the effect of the exposure to these chemicals on cell invasion through matrigel coated plates was monitored using the xCELLigence technology after 4 weeks of exposure.

Further investigation of molecular mechanisms focused on changes in MMP-2 and MMP-9 secretion into the media using gelatin zymography and on measuring the levels of the intracellular MMP-14 using western immunoblotting.

## **6.3 Results**

### **6.3.1 Effects of UV screens on proliferation of MDA-MB-231 human breast cancer cells**

Electrical impedance (cell index) was used to monitor proliferation of MDA-MB-231 cells in response to exposure to the UV screens by xCELLigence technology (RTCA-DP, Cambridge Biosciences). As described previously (in section 2.2.2), stock MDA-MB-231 human breast cancer cells were grown in DMEM containing 10% FCS without or with  $10^{-5}$  M Bp1, with  $10^{-5}$  M Bp2, with  $10^{-5}$  M Bp3, with  $10^{-5}$  M OMC, with  $10^{-5}$  M 4MBC or with  $10^{-5}$  M HS for 7 days. Cell index was monitored every hour for one week. Results showed no difference in cell index between cells exposed to the UV screens and control cells without exposure to UV screens (Figure 6.1).

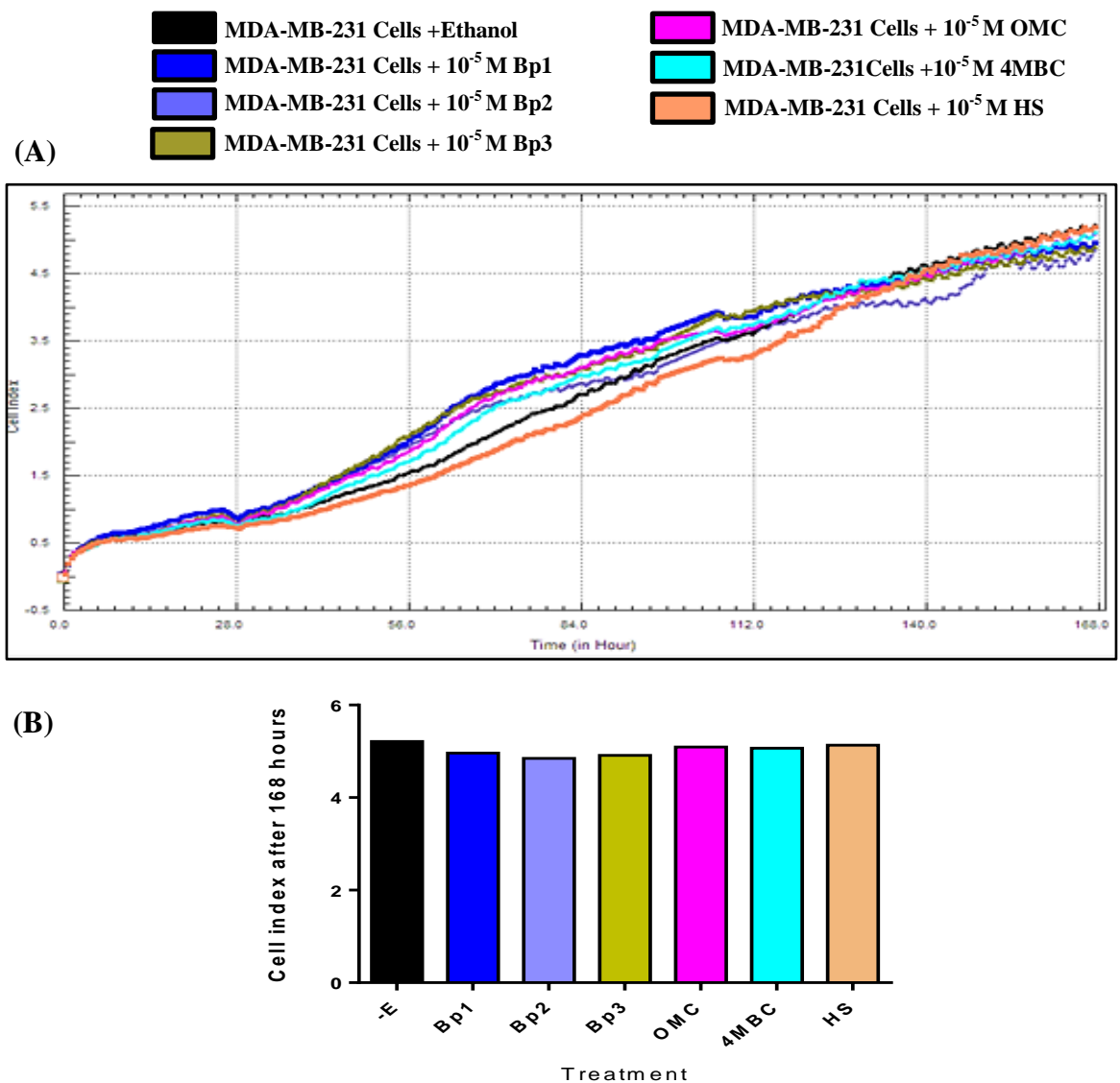


**Figure 6.1 Effect of UV screens on MDA-MB-231 breast cancer cell proliferation as determined by xCELLigence technology.**

Stock MDA-MB-231 cells were grown for up to 7 days in DMEM containing 10% FCS, with  $10^{-5}$ M benzophenone-1 (Bp1), with  $10^{-5}$ M benzophenone-2 (Bp2), with  $10^{-5}$ M benzophenone-3 (Bp3), with  $10^{-5}$ M octyl methoxycinnamate (OMC), with  $10^{-5}$ M 4-methylbenzylidene camphor (4MBC), with  $10^{-5}$ M homosalate (HS) or no addition ethanol control (-E). Media were replenished on day 1 and day 4. Cell proliferation was assessed by seeding 2000 cells in an E-plate 16 and cell index was monitored every 30 minutes over the period of 7 days. Each curve shows the average cell index of duplicate wells (A). Bar graph shows the average cell index after 7 days (168 hours) (B).

### **6.3.2 Effect of UV screens on motility of MDA-MB-231 human breast cancer cells**

The motility of MDA-MB-231 cells was assessed by measuring the movement of cells through 8µm pores of a membrane towards a chemotaxis stimulus of FCS as determined by the xCELLigence technology and by using live imaging by time-lapse microscopy.

#### **6.3.2.1 Effects of UV screens on motility of MDA-MB-231 human breast cancer cells as measured by xCELLigence technology**

Cells were exposed for 2 weeks to  $10^{-5}$  M of the 6 UV screens or no addition and to  $10^{-7}$  M and  $10^{-5}$  M of the 6 UV screens for 8 weeks prior to the experiments. Then the experiments were carried out according to the manufacturer's instructions (as described in section 2.4.3). Results showed no alteration to MDA-MB-231 cell chemotaxis driven motility after 2 weeks of exposure to  $10^{-5}$  M Bp1,  $10^{-5}$  M Bp3,  $10^{-5}$  M OMC,  $10^{-5}$  M 4MBC or  $10^{-5}$  M HS but reduced motility of cells exposed to  $10^{-5}$  M Bp2 (Figure 6.2). Long-term exposure of 8 weeks increased the cell motility following the exposure to  $10^{-5}$  M Bp2 (cell index  $1.04 \pm 0.03$  with  $p$ -value  $\leq 0.01$ ),  $10^{-5}$  M Bp3 (cell index  $1.15 \pm 0.05$  with  $p$ -value  $\leq 0.01$ ),  $10^{-5}$  M 4MBC (cell index  $1.22 \pm 0.13$  with  $p$ -value  $\leq 0.05$ ) or  $10^{-5}$  M HS (cell index  $1.63 \pm 0.21$  with  $p$ -value  $\leq 0.01$ ) in comparison with the no addition (cell index  $0.92 \pm 0.02$ ) (Figure 6.3). In contrast,  $10^{-5}$  M Bp1 reduced the MDA-MB-231 cells index ( $0.27 \pm 0.03$  with  $p$ -value  $\leq 0.001$ ) in comparison with no addition (Figure 6.3).

Results obtained by exposing MDA-MB-231 cells to  $10^{-7}$  M concentrations of Bp1, Bp2, Bp3, OMC, 4MBC or HS for 8 weeks showed similar findings to these after exposure to  $10^{-5}$  M concentrations with no reduction effect of  $10^{-7}$  M Bp1 on MDA-MB-231 cells motility (Figure 6.4). Thus  $10^{-7}$  M concentration was chosen to examine the effect of longer exposure time in the following experiments using time-lapse microscopy.

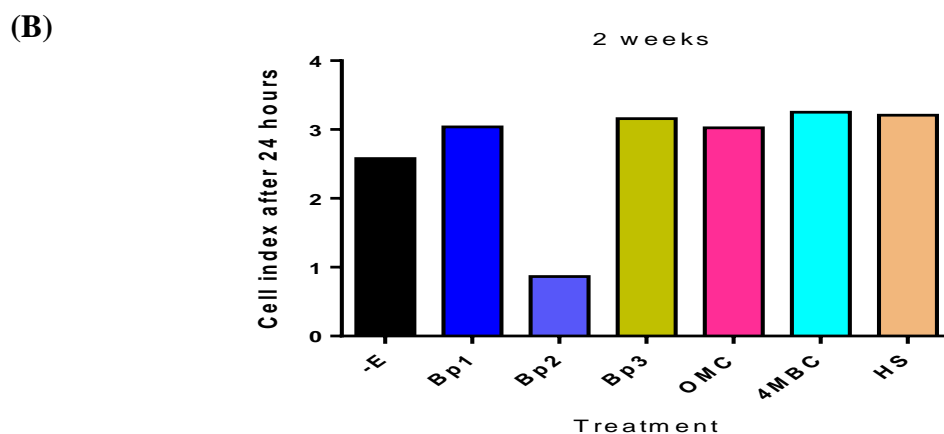
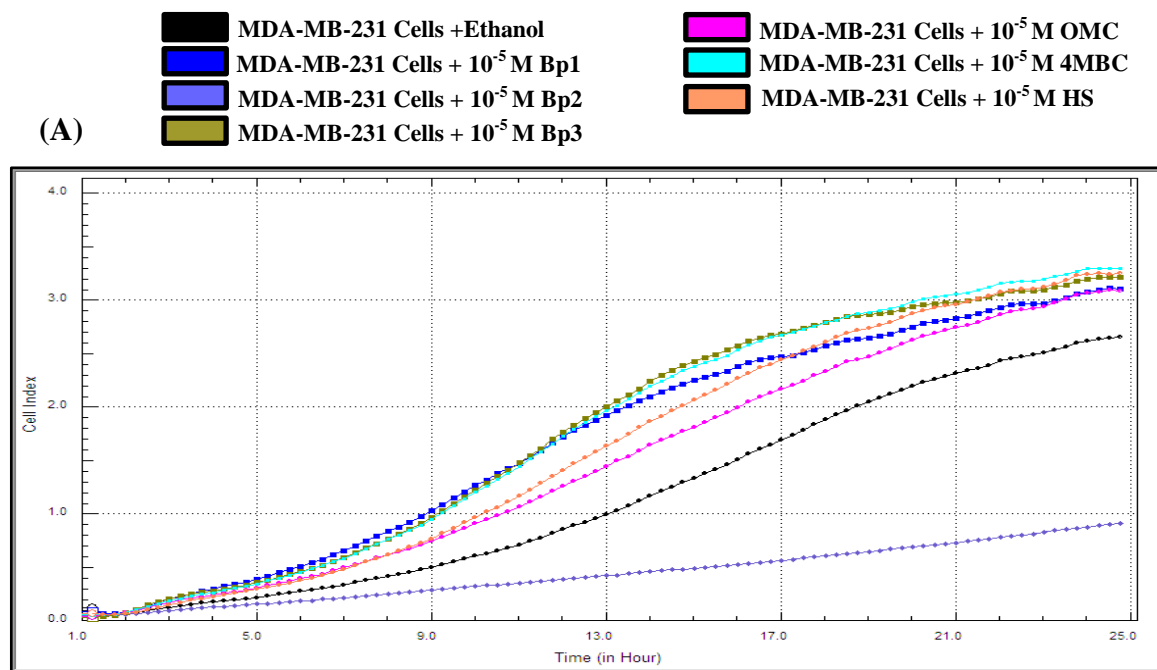


**Figure 6.2 Effect of 2 weeks of exposure to  $10^{-5}$  M of UV screens on MDA-MB-231 breast cancer cell migration towards chemotaxis on an uncoated surface.**

MDA-MB-231 cells were exposed to  $10^{-5}$  M benzophenone-1 (Bp1),  $10^{-5}$  M benzophenone-2 (Bp2),  $10^{-5}$  M Bp3 (Bp3),  $10^{-5}$  M OMC (OMC),  $10^{-5}$  M 4MBC (4MBC),  $10^{-5}$  M HS (HS) or ethanol (-E) for 2 weeks in DMEM supplemented with 10% FCS. Media were replenished and cells were split every 3-4 days. Cells were analysed for their migratory response to chemotaxis in a real time cell migration assay by using xCELLigence technology. (A) Curves represent the relative change in cell index of duplicate wells as indicated by the changes in impedance caused by cell migration from upper chambers to lower ones through the pores of a polycarbonate membrane. Cell index was recorded every 5 minutes and monitored for 24 hours. (B) Bar graph represents the average cell index of duplicate wells after 24 hours as indicated by the xCELLigence RTCA software.

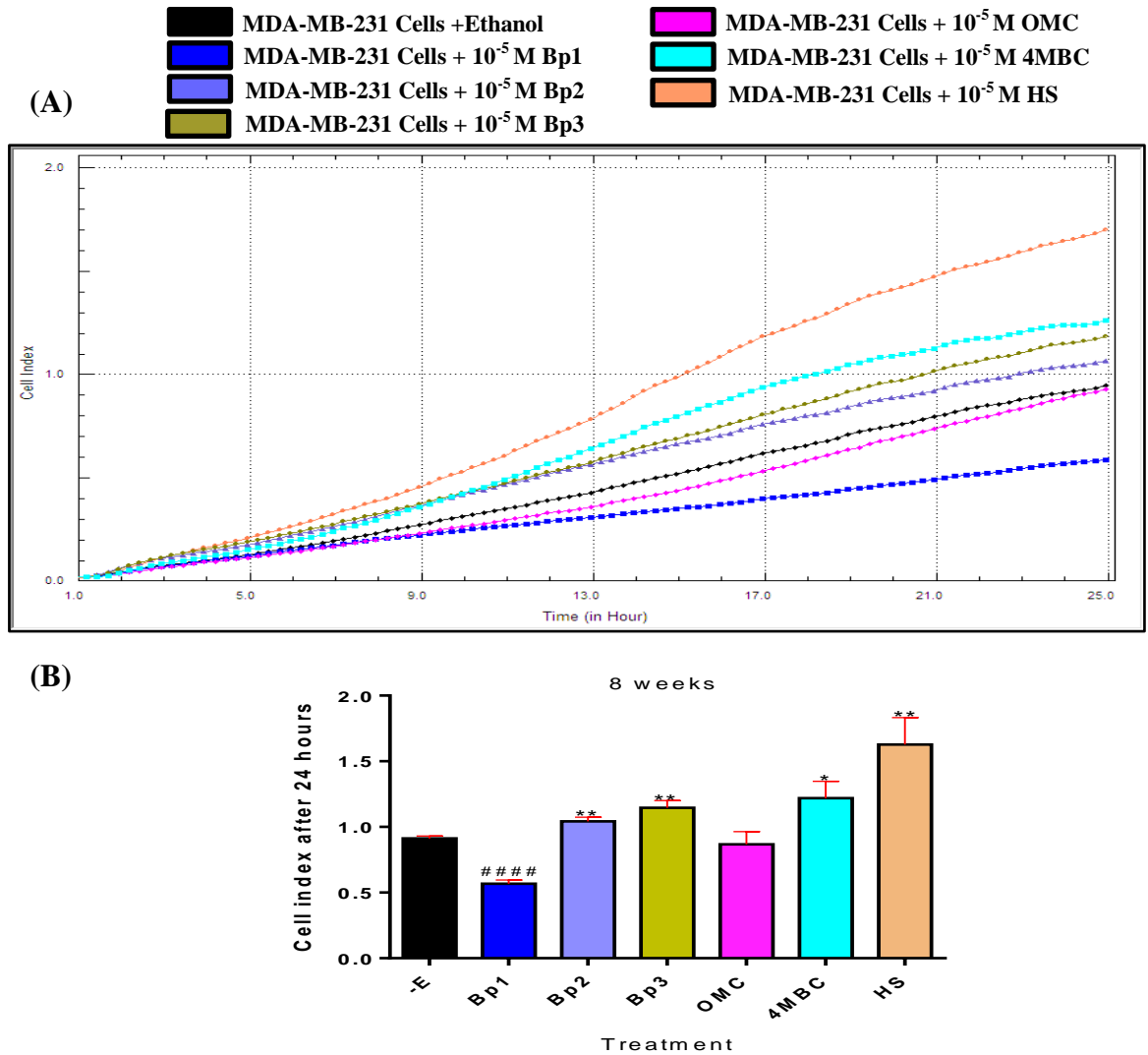


**Figure 6.3 Effect of 8 weeks of exposure to  $10^{-5}$  M concentrations of UV screens on MDA-MB-231 breast cancer cell migration towards chemotaxis on an uncoated surface.**

MDA-MB-231 cells were exposed to  $10^{-5}$  M Bp1 (Bp1),  $10^{-5}$  M Bp2 (Bp2),  $10^{-5}$  M Bp3 (Bp3),  $10^{-5}$  M OMC (OMC),  $10^{-5}$  M 4MBC (4MBC),  $10^{-5}$  M HS (HS) or ethanol (-E) for 8 weeks in DMEM supplemented with 5% FCS. Cells were analysed for their migratory response to chemotaxis in a real time cell migration assay by using xCELLigence technology. Media were replenished and cells were split every 3-4 days. (A) Curves represent the relative change in cell index of triplicate wells as indicated by the changes in impedance caused by cell migration from upper chambers to lower ones through the pores of polycarbonate membrane. Cell index was recorded every 5 minutes and monitored for 24 hours. (B) Bar graph represents the cell index at 48 hours as calculated by the xCELLigence RTCA software. Values are the average  $\pm$ SE of triplicate independent wells. \* *p*-value  $\leq 0.05$  and \*\* *p*-value  $\leq 0.01$  increase versus (-E). #### *p*-value  $\leq 0.0001$  decrease versus (-E) by t-Test.

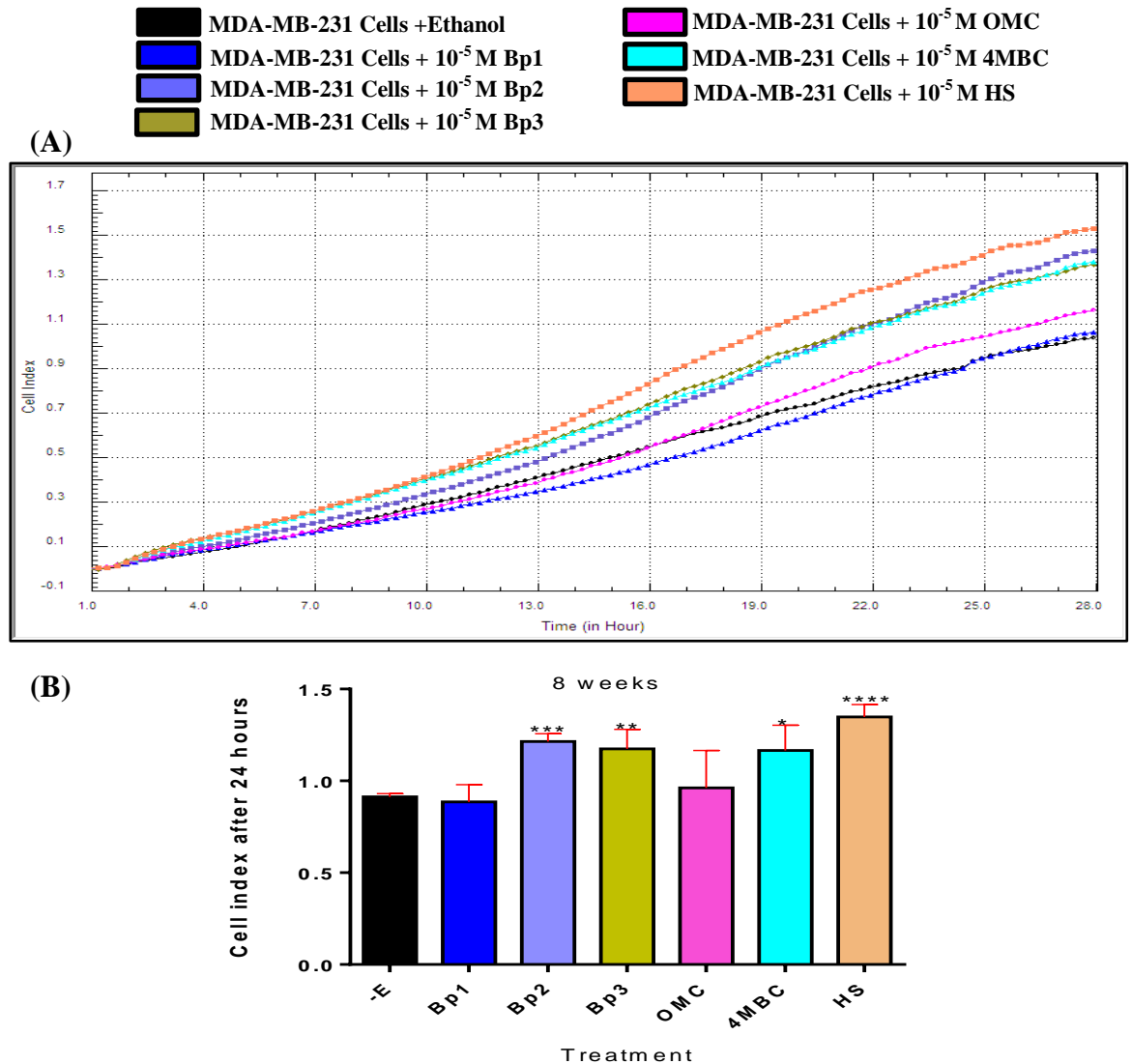


**Figure 6.4** Effect of 8 weeks of exposure to  $10^{-7}$  M concentrations of UV screens on MDA-MB-231 breast cancer cell migration towards chemotaxis on an uncoated surface.

MDA-MB-231 cells were exposed to  $10^{-7}$  M Bp1 (Bp1),  $10^{-7}$  M Bp2 (Bp2),  $10^{-7}$  M Bp3 (Bp3),  $10^{-7}$  M OMC (OMC),  $10^{-7}$  M 4MBC (4MBC),  $10^{-7}$  M HS (HS) or ethanol (-E) for 8 weeks in DMEM supplemented with 10% FCS. Media were replenished and cells were split every 3-4 days. Cells were analysed for their migratory response to chemotaxis in a real time cell migration assay by using xCELLigence technology. (A) Curves represent the relative change in cell index of triplicate wells as indicated by the changes in impedance caused by cell migration from upper chambers to lower ones through the pores of polycarbonate membrane. Cell index was recorded every 5 minutes and monitored for 24 hours. (B) Bar graph represents the cell index at 48 hours as calculated by the xCELLigence RTCA software. Values are the average  $\pm$ SE of triplicate independent wells. \* *p*-value  $\leq 0.05$ , \*\* *p*-value  $\leq 0.01$ , \*\*\* *p*-value  $\leq 0.001$  and \*\*\*\* *p*-value  $\leq 0.0001$  versus the control (-E) by t-Test.

### **6.3.2.2 Effects of UV screens on motility of MDA-MB-231 human breast cancer cells as measured by time-lapse microscopy**

Prior to the experiment MDA-MB-231 human breast cancer cells were exposed for 2 weeks or 15 weeks to  $10^{-7}$  M concentrations of Bp1, Bp2, Bp3, OMC, 4MBC, HS or no addition. 48 hours prior the experiment, cells were re-seeded in 12-well plates and cell migration was analysed using live cell imaging (time-lapse microscopy) (as described in section 2.4.2). 10 cells were tracked in 3 fields of view per well for 6 hours and the average cumulative length moved (total travelled length of cell) was measured for each treatment.

Results showed no effect of 2 weeks of exposure to the UV screens on the cumulative length moved by MDA-MB-231 cells exposed to  $10^{-7}$  M concentrations of Bp1, Bp3, OMC, 4MBC or HS (Figure 6.5). However, 15 weeks of exposure caused an increase in cumulative length moved by individual MDA-MB-231 cells following exposure to  $10^{-7}$  M Bp1 ( $135.60 \pm 3.57$  microns with  $p$ -value  $\leq 0.05$ ),  $10^{-7}$  M Bp2 ( $169 \pm 4.91$  microns with  $p$ -value  $\leq 0.001$ ),  $10^{-7}$  M Bp3 ( $161.4 \pm 4.87$  microns with  $p$ -value  $\leq 0.001$ ) compared to no addition ( $111.3 \pm 3.01$  microns) (Figure 6.6 (A)). There was also an increase in cumulative length moved by individual MDA-MB-231 cells following the exposure to  $10^{-7}$  M OMC ( $162.30 \pm 8.38$  microns with  $p$ -value  $\leq 0.01$ ),  $10^{-7}$  M 4MBC ( $139.30 \pm 4.85$  microns with  $p$ -value  $\leq 0.05$ ) or  $10^{-7}$  M HS ( $160 \pm 9.57$  microns with  $p$ -value  $\leq 0.01$ ) in comparison with no addition ( $106.90 \pm 3.09$  microns) (Figure 6.6 (B)).

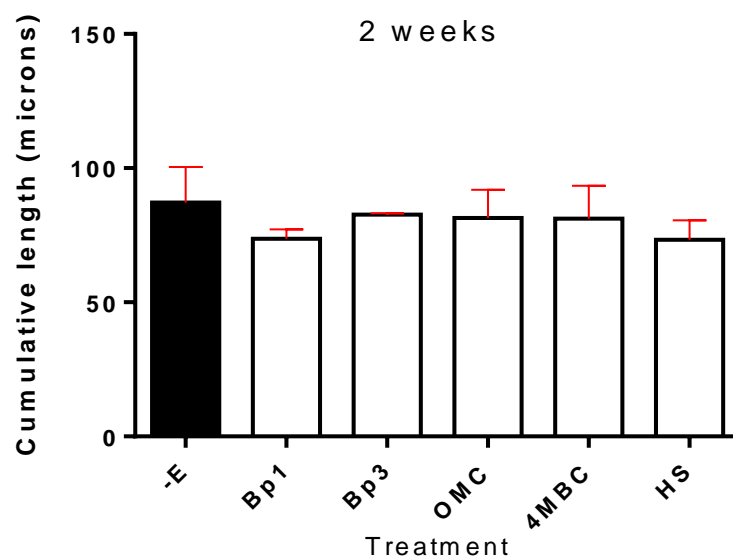


**Figure 6.5 Effect of 2 weeks of exposure to UV screens on MDA-MB-231 breast cancer cell motility as measured by time-lapse microscopy.**

Effect of exposure to UV screens on MDA-MB-231 human breast cancer cells motility as determined by time-lapse microscopy. Cells were exposed to  $10^{-7}$  M Bp1 (Bp1),  $10^{-7}$  M Bp3 (Bp3),  $10^{-7}$  M OMC (OMC),  $10^{-7}$  M 4MBC (4MBC),  $10^{-7}$  M HS (HS) or ethanol (-E) for 2 weeks in DMEM supplemented with 10% FCS. Media were replenished and cells were split every 3-4 days. Cells were seeded in 12-well plate at  $0.5 \times 10^5$  cells/well. Time-lapse images of 3 fields of view per well were recorded every 5 minutes for 6 hours. Results represent the cumulative length moved. Values are the average of 10 tracked cells per field of view from 3 fields of view per well and 2 independent duplicate wells. Error bars show mean with range of duplicate wells.

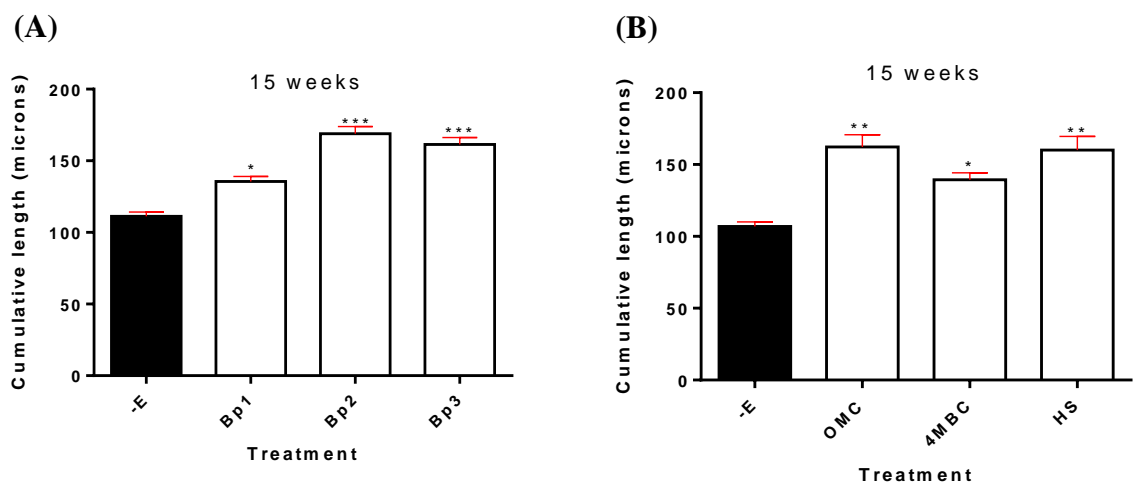


**Figure 6.6 Effect of 15 week of exposure to UV screens on MDA-MB-231 breast cancer cell motility as measured by time-lapse microscopy.**

(A) Cells were exposed to  $10^{-7}$  M Bp1 (Bp1),  $10^{-7}$  M Bp2 (Bp2),  $10^{-7}$  M Bp3 (Bp3), (B)  $10^{-7}$  M OMC (OMC),  $10^{-7}$  M 4MBC (4MBC),  $10^{-7}$  M HS (HS) or ethanol (-E) for 15 weeks in DMEM supplemented with 10% FCS. Media were replenished and cells were split every 3-4 days. Cells were seeded in 12-well plate at  $0.5 \times 10^5$  cells/well. Time-lapse images of 3 fields of view per well were recorded every 5 minutes for 6 hours. Results represent the cumulative length moved. Values are the average of 10 tracked cells per field of view for independent triplicate independent wells  $\pm$ SE. \* *p*-value  $\leq 0.05$ , \*\* *p*-value  $\leq 0.01$  and \*\*\* *p*-value  $\leq 0.001$  versus no addition (-E) by t-Test.

### **6.3.3 Effect of UV screens on invasion of MDA-MB-231 human breast cancer cells as determined by xCELLigence technology**

MDA-MB-231 cells exposed to the UV screens for 4 weeks were monitored for their invasive activity in real time using xCELLigence technology. According to the manufacturer's instructions (ACEA Biosciences, USA), cells were seeded on matrigel (1:40 dilution) in the upper chamber of a CIM-plate 16 (as described in section 2.5). The lower chamber of the plate was filled with DMEM without or with  $10^{-5}$  M Bp1,  $10^{-5}$  M Bp2,  $10^{-5}$  M Bp3,  $10^{-5}$  M OMC,  $10^{-5}$  M 4MBC or  $10^{-5}$  M HS supplemented with 10% FCS, while the upper chamber was filled with the same media without the serum. Invasion was monitored every 5 minutes for 48 hours as cells moved through matrigel coated membrane into the lower chamber by chemotaxis.

The experiment showed that only  $10^{-5}$  M Bp2 increased the cell index ( $1.845 \pm 0.017$ ) in comparison with no addition ( $1.238 \pm 0.029$ ) (Figure 6.7) ( $p$ -value  $\leq 0.0001$ ). Investigation of the other concentrations and the other different time points was not achieved due to technical problems with the xCELLigence machine during the period of MDA-MB-231 cell culture.

### **6.3.4 Effect of UV screens on matrix metalloproteinase activity of MDA-MB-231 human breast cancer cells as measured by zymography**

MMP-2, MMP-9 and MMP-14 were selected for investigating the effect of long-term exposure (14-15 weeks) to the UV screens on MDA-MB-231 cells. Secreted MMP-2 and MMP-9 were measured in the conditioned media (serum free media) via zymography (as described in section 2.8) and the intracellular MMP-14 protein levels were estimated using western immunoblotting (as described in section 2.7).

Results showed a significant increase in MMP-2 secretion following the exposure to  $10^{-7}$  M OMC and  $10^{-7}$  M 4MBC but no effect on MMP-2 was indicated following exposure to the other the UV screens (Figure 6.8) ( $p$ -value  $\leq 0.05$ ). MMP-9 secretion was not altered by the exposure to the UV screens (data not shown). Also, the UV screens had no significant effect on pro and activated MMP-14 levels (Figure 6.9).

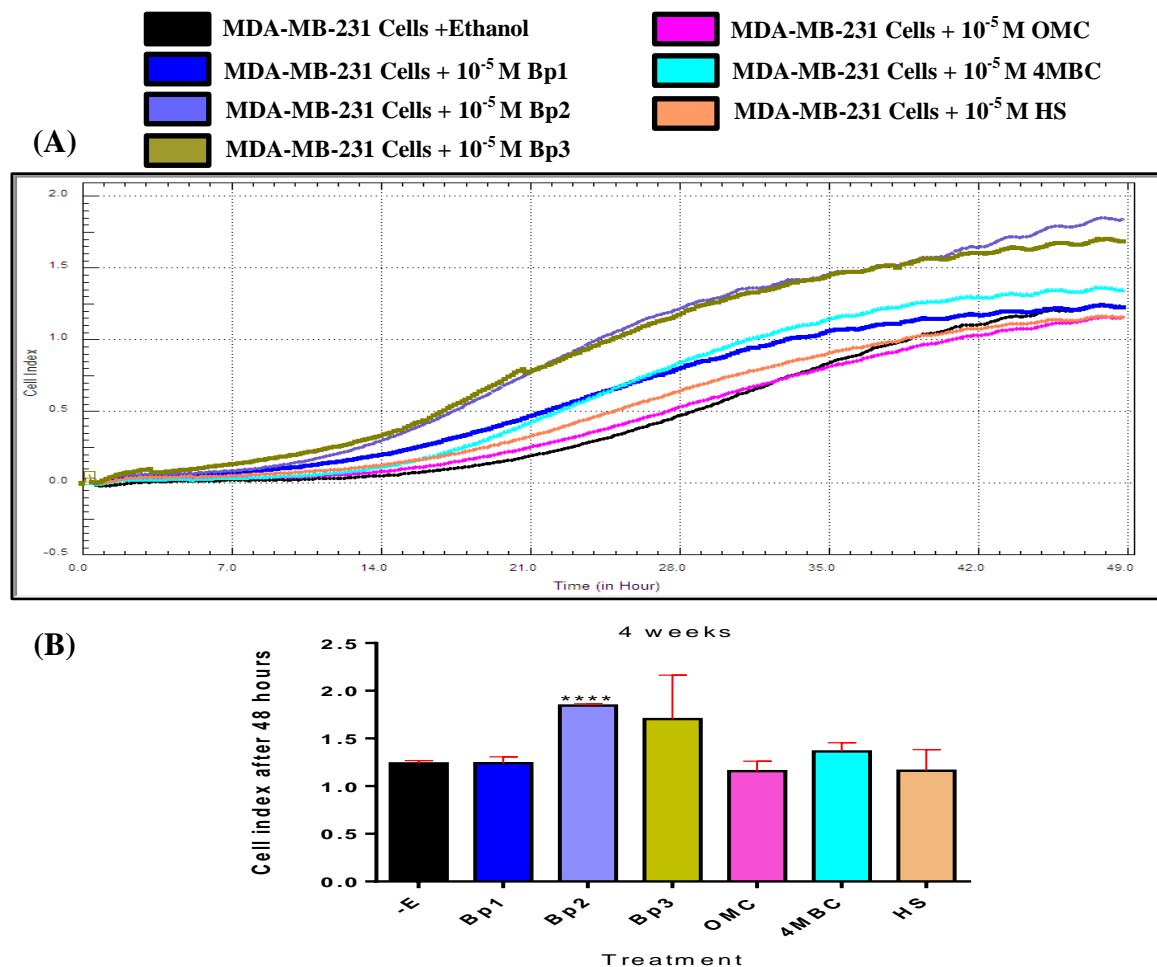


**Figure 6.7 Effects of UV screens on MDA-MB-231 human breast cancer cells invasion through matrigel coated surfaces.**

MDA-MB-231 cells were exposed to  $10^{-5}$  M Bp1 (Bp1),  $10^{-5}$  M Bp2 (Bp2),  $10^{-5}$  M Bp3 (Bp3),  $10^{-5}$  M OMC (OMC),  $10^{-5}$  M 4MBC (4MBC),  $10^{-5}$  M HS (HS) or ethanol (-E) for 4 weeks in DMEM supplemented with 10% FCS. Cells were analysed for their migratory response to chemotaxis stimulus towards FCS in a real time cell migration assay by using xCELLigence technology. Media were replenished and cells were split every 3-4 days. Cells were analysed for their invasive activation through matrigel (1:40) coated CIM-plate 16 in a real time cell invasion assay by using the xCELLigence technology. (A) Curves represent the relative change in cell index of triplicate wells as indicated by the changes in impedance caused by cell migration from upper chambers to lower ones through the matrigel coated pores of polycarbonate membrane. Cell index was recorded every 5 minutes and monitored for 48hrs hours. (B) Bar graph represents the cell index at 48 hours as calculated by the xCELLigence RTCA software. Values are the average  $\pm$ SE of triplicate independent wells. \*\*\*\*  $p$ -value  $\leq 0.0001$  versus ethanol control (-E) by t-Test.

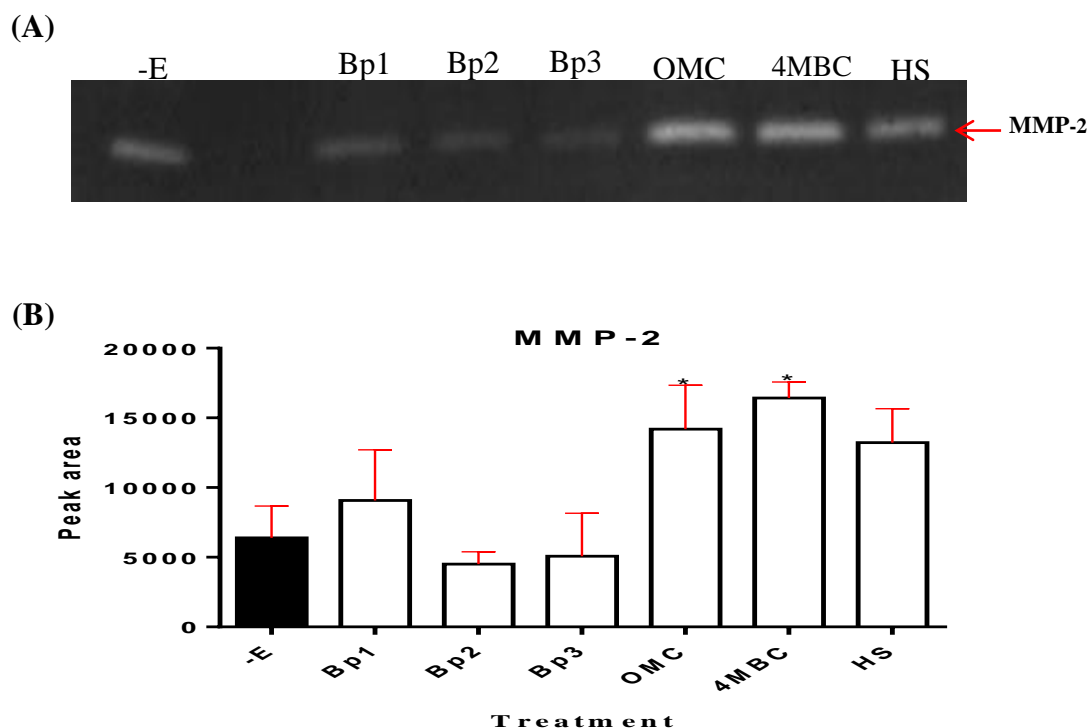


**Figure 6.8 Effects of UV screens on secreted MMP-2 of MDA-MB-231 breast cancer cells as measured by gelatin zymography.**

MDA-MB-231 cells were exposed to  $10^{-7}$  M Bp1 (Bp1),  $10^{-7}$  M Bp2 (Bp2),  $10^{-7}$  M Bp3 (Bp3),  $10^{-7}$  M OMC (OMC),  $10^{-7}$  M 4MBC (4MBC),  $10^{-7}$  M HS (HS) or ethanol (-E) for 14-15 weeks in DMEM supplemented with 10% FCS. Media were replenished and cells were split every 3-4 days. Cells were exposed to serum free media plus the relative chemicals for 24 hours prior collection. Collected media were concentrated using Amicon ultra centrifugal filters prior to gelatin gel zymography. (A) Representative scanned image showing the effect of the conditioned media on the activity of MMP-2 on a 10% gelatin gel. (B) Bar graph represents the band densities of MMP-2 and error bars the standard error of triplicate independent experiments (n=3). \* *p-value*  $\leq 0.05$  versus ethanol control (-E) by t-Test.

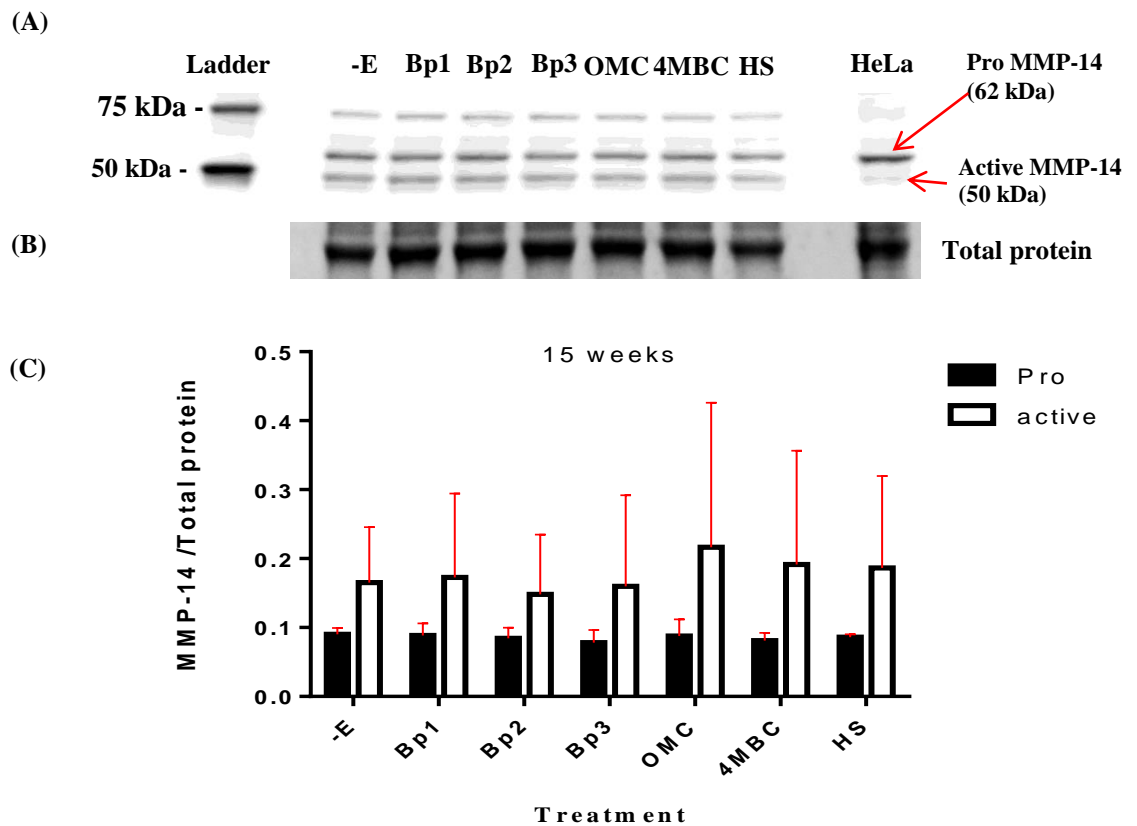


**Figure 6.9 Effect of long-term exposure to UV screens on the protein level of MMP-14 in MDA-MB-231 breast cancer cells as determined by western immunoblotting.**

MDA-MB-231 human breast cancer cells were grown for 14-15 weeks in DMEM supplemented with 10% FCS, with  $10^{-7}$  M Bp1 (Bp1), with  $10^{-7}$  M Bp2 (Bp2) or  $10^{-7}$  M Bp3 (Bp3), with  $10^{-7}$  M OMC (OMC), with  $10^{-7}$  M 4MBC (4MBC) or with  $10^{-7}$  M HS (HS) and HeLa human cervical carcinoma (HeLa) cells lysate was used as a positive control. Media were replenished and cells were split every 3-4 days. Cells were exposed to serum free media plus the relative chemicals for 24 hours prior to the cell lysate collection. (A) Total cellular protein was loaded at  $25\mu\text{g}$  per track and immunoblotted with antibody against pro-MMP-14 (62 kDa) and activated-MMP-14 (50 kDa). (B) Total protein. (C) The bar graph shows the level of pro and active MMP-14 relative to total protein. Values are means and bars indicate SEM ( $n=3$  independent experiments).

## 6.4 Discussion

It has been documented that the 6 UV screens studied here interact with the human ER and many studies have described oestrogenic action of the UV screens on the oestrogen responsive MCF-7 human breast cancer cell line (Schreurs et al., 2002; Gomez et al., 2005; Miller et al., 2001; Kunz and Fent, 2006; Schlumpf et al., 2004). To the best of my knowledge, the effects of the six UV screens are documented for the first time in this chapter in an ER $\alpha$  negative cell line.

***UV screens increase motility but not proliferation of MDA-MB-231 cells.*** Results showed no effect of the UV screens on MDA-MB-231 cell proliferation which is in line with their previously reported oestrogen insensitivity (Berthois et al., 1986; Charlier et al., 1995; Jones et al., 1998). However, an increase in cell motility was recorded following long-term exposure to  $10^{-7}$  M Bp2,  $10^{-5}$  M Bp2,  $10^{-7}$  M Bp3,  $10^{-5}$  M Bp3,  $10^{-7}$  M 4MBC,  $10^{-5}$  M 4MBC,  $10^{-7}$  M HS and  $10^{-5}$  M HS as measured by the xCELLigence technology and from cumulative length moved by MDA-MB-231 cells following 15 weeks of exposure to  $10^{-7}$  M of all of the tested UV screens. It is noteworthy that  $10^{-5}$  M Bp1 reduced the motility of MDA-MB-231 cells and the lower concentration of  $10^{-7}$  M Bp1 had no effect on MDA-MB-231 cell motility as indicated by xCELLigence, while this chemical was found to induce the motility of MCF-7 cells (see chapter 4). In another comparison,  $10^{-5}$  M Bp2 showed no effect on MCF-7 cell invasion after long-term of exposure but was the only chemical found to increase the MDA-MB-231 cells invasion following 4 weeks of exposure. This shows that motility can be influenced in ER $\alpha$ -negative cells as well as ER $\alpha$ + positive cells and suggests that mechanisms are not always ER mediated.

Previous studies have suggested that oestrogens and the environmental oestrogens can increase MDA-MB-231 cell motility via non-ER mediated molecular mechanisms. Zhou and his colleagues have recently shown that 17 $\beta$ -oestradiol induces the motility of MDA-MB-231 cells via the ER $\beta$ /AKT signalling pathway through increasing the phosphorylation of ezrin a member of the actin-binding protein family ERM (ezrin/radixin/moesin) that is involved in cytoskeletal rearrangement (Zhou et al., 2016). Another group has reported that phthalates can increase MDA-MB-231 cell motility via stimulating the cell surface aryl hydrocarbon receptor (AhR), which leads to an increase in the expression of HDAC6 (histone deacetylase 6) and then facilitate the nuclear assembly of the  $\beta$ -catenin-LEF1/TCF4 transcriptional complex and subsequently transactivates the c-Myc gene (Hsieh et al., 2012). It is noteworthy

that Bp3 and HS were found to interact with ER $\beta$  (Schreurs et al., 2002). Moreover, 4MBC was found to bind with high affinity to ER $\beta$  in the ER binding assay (Mueller et al., 2003) and *in vitro* to compete with  $16\alpha^{125}\text{I}$ -oestradiol to bind with human oestrogen receptor  $\beta$  (Schlumpf et al., 2004), which might suggest an ER- $\beta$  mechanism of Bp3, 4MBC and HS in the MDA-MB-231 cells as they express ER $\beta$  (Fuqua et al., 1999; AL-Bader et al., 2011; Hamilton et al., 2015). In order to confirm this assumption, knocking down ER $\beta$  by using the RNA interference (siRNA) or the oestrogen receptor antagonist fulvestrant, combined with using phenol-red-free media and DCFCS should be considered in future studies.

***UV screens increase the secretion of MMP-2 but not MMP-9.*** The investigation of the effect of exposure to UV screens on MMP secretion and expression in MDA-MB-231 cells was carried out in this chapter. As described previously (see chapter 4) MMPs have an important role modulating the ECM during cancer cell invasion.  $10^{-7}$  M OMC and  $10^{-7}$  M 4MBC increased the secretion of MMP-2 by MDA-MB-231 cells after 14-15 weeks of exposure and no effect on MMP-14 protein was detected. Both chemicals were found to induce the individual cumulative length moved by MDA-MB-231 cells after 15 weeks of exposure. MMP-2 is linked to increased invasion, angiogenesis and proliferation of cancer cells (Kessenbrock et al., 2010). It is also measured at higher levels in sera of breast cancer patients by zymogram (La Rocca et al., 2004).

Moreover, Zhang and his colleagues have linked the increase in migration and invasive capability of MDA-MB-231 and BT-549 triple negative human breast cancer cells after treatment with bisphenol A to increases in MMP-2 and MMP-9 expression via oestrogen related receptor gamma with the involvement of ERK1/2 and Akt signalling pathways (Zhang et al., 2016). Further, MDA-MB-231 cell motility caused by long-term exposure to aluminium was linked to an increase of MMP-9 activity as measured by gelatin zymography and an increase of MMP-14 mRNA expression as measured by real time RT-PCR assay (Bakir and Darbre, 2015). In this work, MDA-MB-231 cell secretion of MMP-9 was not altered by the exposure to UV screens. However, MMP-9 secretion from MDA-MB-231 cells is believed to be stimulated by the presence of matrigel (Balduyck et al., 2000) which was not used in our assays.

***To conclude***, UV screens increase the motility of MDA-MB-231 cells but whether the mechanism underlying this effect is non-ER mediated or through ER $\beta$  remains to be clarified in future research.

## Chapter 7 General discussion

In this work, the effect of UV screens on proliferation and motility of human breast cancer cells was explored. The ability of these chemicals to mimic oestrogen action was assessed in terms of oestrogen regulated gene expression and cell proliferation. The chemicals were able to induce expression of an ERE-Luciferase reporter gene and to increase the proliferation of oestrogen responsive cells. These results are in line with previous reports (Miller et al., 2001; Nakagawa and Suzuki, 2002; Schlumpf et al., 2001; Schreurs et al., 2002; Schlumpf et al., 2004; Gomez et al., 2005; Heneweer et al., 2005; Kunz and Fent, 2006; Kerdivel et al., 2013; Jimenez-Diaz et al., 2013) (see chapter 3).

One strength of this study was the use of three breast cancer cell lines. The MCF-7 cell line was used because it possesses ER $\alpha$ , it proliferates in response to oestrogen (Brooks et al., 1973; Berthois et al., 1986; Darbre and Daly, 1989) and has been used as the basis for the E-screen used to identify oestrogenic activity of endocrine disrupting chemicals (Soto et al., 1995). The second cell line is another oestrogen responsive cell line; the luminal epithelial T-47-D human breast cancer cell line (Keydar et al., 1979; Darbre and Daly, 1989) for which no previous work on UV screens has been reported. The third was the ER $\alpha$  negative MDA-MB-231 human breast cancer cell line (Lu et al., 2005), which was used to investigate any non-ER $\alpha$  mediated mechanisms of the UV screens.

Effects of the UV screens in increasing breast cancer cell proliferation were assessed in two oestrogen responsive MCF-7 and T-47-D cell lines. MCF-7 and T-47-D cells showed an increase in cell proliferation after exposure to Bp1, Bp2, 4MBC and HS but only T-47-D cell proliferation increased in response to Bp3 with cell doubling number in 7 days of  $2.77 \pm 0.081$  compared to MCF-7 cells doubling number of  $0.33 \pm 0.07$  in response to Bp3. The highest effects in increasing MCF-7 cell proliferation by Bp1 and Bp2 was decreased by the use of the antioestrogen fulvestrant, suggesting that the effect of these chemicals on proliferation of breast cancer cells is ER $\alpha$  mediated. The effect of Bp1 and Bp2 is related to their structure; both chemicals possess phenolic-rings that are capable of activating ER conformation, which is in line with previous studies of docking analysis of Bp2 (Kerdivel et al., 2013) and binding affinity of Bp1 (Blair et al., 1999). Although MDA-MB-231 cell proliferation was not altered by the exposure to the UV screens, the presence of 10% FCS and

the phenol-red in the media would have masked any possible oestrogenic action effects of these chemicals on this cell line.

The effects of long-term chemical exposure are as important to determine short-term effects, and might provide different results than the one provided by the acute effect of the short-term model. Long-term tissue culture models have been previously used to develop the oestrogen deprivation model, which compares proliferation of breast cancer cells in the presence or absence of  $17\beta$ -oestradiol after 6-12 months (Katzenellenbogen et al., 1987; Daly and Darbre, 1990; Stephen et al., 2001; Shaw et al., 2006). Long-term exposure models have also been used to develop the model of antioestrogen resistance by exposing MCF-7 cells for long periods in excess of 1 year to tamoxifen or fulvestrant (Lykkesfeldt et al., 1995; McClelland et al., 2001; Knowlden et al., 2003; Shaw et al., 2006). The use of the long-term model in studying the effect of the exposure to environmental oestrogens was first reported by Khanna and co-workers where they have exposed oestrogen responsive MCF-7 cells, T-47-D cells and ZR-75 human breast cancer cells to parabens for up to 20 weeks (Khanna et al., 2014). This thesis reports the effect of UV screens on breast cancer cells in the long-term model which reflects the real-life scenario where effects are in the long-term at low dose levels.

One of the main findings of this work is that the UV screens caused an increase in breast cancer cell motility although with variation between the cell lines used. Motility was assessed using three techniques; the wound healing assay, time-lapse microscopy and the xCELLigence technology. These methodologies determine different types of motility. During this study, different cell lines showed a distinguished type of motility based on the cell line biology, and that could explain the contradicting results generated from applying different techniques to determine the motility of MCF-7 cell line. The wound healing measures the collective cell migration, a type of motility much related to epithelial cells such as MCF-7, while the time-lapse is preferred to determined mesenchymal individual cells motility such as MDA-MB-231 cells but not suitable for MCF-7 cells. The effects of the UV screens on the increased motility of MCF-7 cells started after 2 weeks of exposure as indicated by the xCELLigence, while no increases in motility of T-47-D cells or MDA-MB-231 cells were indicated using the same technique following the same exposure time. T-47-D cells showed less sensitivity to the short-term influence of UV screens in increasing cell motility and it needed a longer time of exposure to show an increase in cell motility in comparison to the MCF-7 cells. This could be explained given the differences between these cell lines at the

genomic and the proteomic levels (Shadeo and Lam, 2006; Aka and Lin, 2012) and their variance in response to oestrogen, drugs and experimental conditions (Ryde et al., 1992; Schafer et al., 2000; Mooney et al., 2002; Radde et al., 2015; Risinger et al., 2015). Moreover, T-47-D cells needed a longer time to lose the proliferative response to oestrogen in oestrogen deprived conditions in comparison with MCF-7 cells (Daly and Darbre, 1990). This variation in motility observed here might be important in considering the ability of the cells to metastasise and might also relate to the finding of clinical studies that have suggested a variation in metastatic potential between oestrogen receptor positive human breast cancers (Dai et al., 2005; Lower et al., 2005). In parallel with previous reports, the only UV screen that has been previously documented to increase the motility of oestrogen responsive cells is Bp1, which was reported to increase the motility of MCF-7 cells (In et al., 2015) and the BG-1 ovarian cancer cell line (Shin et al., 2016).

Another important point is that the results showed lower concentrations took longer time to give a measurable effect. The effect of  $10^{-7}$  M UV screens on motility of MCF-7 cells and MDA-MB-231 cells was not observed after 2 weeks of exposure but a longer period of exposure (15 weeks for MDA-MB-231 cells and 21 weeks for MCF-7 cells) increased the motility of both breast cancer cell lines. This is in line with previous suggestions of the ability of low doses of environmental chemicals to cause effects after long-term exposure (Darbre and Fernandez, 2013; Goodson et al., 2015).

The variation in increase in motility among the three breast cancer cell lines following exposure to different UV screens can reflect the variation in susceptibility among human individuals. The effect on motility of the oestrogen unresponsive MDA-MB-231 cells following exposure to the UV screens or the effect caused by weaker oestrogenic chemicals such as OMC and 4MBC on MCF-7 oestrogen responsive cells suggest a possible mechanism of action other than through ER $\alpha$ .

Molecular mechanisms underlying the increase in motility of breast cancer cells following exposure to the UV screens were further investigated using MCF-7 cells (chapter 4). Bp1 and HS reduced the protein levels of E-cadherin suggesting an increase in cell motility through phenotypic changing by EMT. A similar finding was linked to the increase of MCF-7 cell motility following exposure to parabens (Khanna et al., 2014). OMC reduced the protein levels of  $\beta$ -catenin and the mRNA levels of other motility markers of breast cancer cells including PIK3R1 and BMP7. Bp2 also reduced the levels of PIK3R1 mRNA while 4MBC

and HS have reduced BMP7 mRNA levels. Although the reduction of PIK3R1 and BMP7 was only studied on mRNA levels, reduction of both markers at an mRNA level is linked to increased motility of breast cancer cells (Luo and Cantley, 2005; Uchino et al., 2010). Further studies are needed to be conducted on protein levels and further exploration might reveal more pathways involved in increasing the motility of MCF-7 cells and the other cell lines (see Table 4.7). Another pathway is the increase in the secretion of MMPs as indicated by zymography. The increase of the secretion of MMP-9 by MCF-7 cells following the exposure to Bp1 and of MMP-2 following the exposure to OMC and 4MBC by MDA-MB-231 cells suggests another mechanism of action of these chemicals in increasing motility of these cell lines and this mechanism was suggested to be the route of aluminium salts to influence the motility of MDA-MB-231 cells (Bakir and Darbre, 2015).

In this study, the effects of the UV screens on breast cancer cell proliferation have been conducted using a range of UV screen concentrations ( $10^{-8}$  M to  $10^{-5}$  M) and the concentrations used in motility experiments were  $10^{-7}$  M and  $10^{-5}$  M which poses the question of whether these concentrations can occur in human samples. Previous work has not measured the concentrations of UV screens in human breast tissue. However, when this work was started the measurement of the UV screens in human urine, serum (Zhang et al., 2013; Janjua et al., 2008), placenta (Vela-Soria et al., 2011; Jimenez-Diaz et al., 2013; Valle-Sistac et al., 2016) and milk (Schlumpf et al., 2010; Rodriguez-Gomez et al., 2015) were published by others (see Table 1.4). The range of the UV screens found in human milk (Schlumpf et al., 2010) were calculated in molarity as the following Bp3 ( $1.14 \times 10^{-9}$  M to  $2 \times 10^{-8}$  M), OMC ( $3 \times 10^{-10}$  M to  $1 \times 10^{-8}$  M), 4MBC ( $1 \times 10^{-9}$  M to  $7.6 \times 10^{-9}$  M) and HS ( $1.7 \times 10^{-9}$  M to  $9.33 \times 10^{-9}$  M). Although the lowest concentration used for motility work ( $10^{-7}$  M) is 10 fold higher than the highest concentration found in the human milk, these results provide an indication of the potential for these chemicals to have adverse effects on breast cancer cell biology but for final conclusions measurements of these chemicals are now needed in human breast tissue.

In breast milk more than one UV screen was measured (Schlumpf et al., 2010) and therefore the effect of mixtures of UV screens needs to be considered. The exposure to low concentrations of mixtures of endocrine disruptors for a long period is a current health concern (Darbre and Fernandez, 2013). A previous study has shown that mixtures of parabens in concentrations found in the human breast tissue at the no effect concentration levels

increased MCF-7 cell proliferation (Charles and Darbre, 2013). In another study, mixtures of four UV screens (Bp1, Bp3, OMC and 4MBC) at their mid effect concentration induced the oestrogen responsive TFF1 gene mRNA levels in MCF-7 cells similar to levels induced by 17 $\beta$ -oestradiol (Heneweer et al., 2005). Knowing the levels and concentrations of these chemicals in human breast tissue in the future besides the levels measured in human samples might inform the exploration of the effect of these chemicals in mixtures especially in designing long-term experiments.

Most reported studies have been carried out using cells grown on plastic culture dishes. However, this is not a physiological surface and it is known that cell proliferation and cell responses to drugs can vary on different ECM surfaces (Schwartz et al., 1995; Longhurst and Jennings, 1998; Sonohara et al., 1998; Woodward et al., 2000; Korah et al., 2004; Ohbayashi et al., 2008; Pontiggia et al., 2012). The effect of the ECM materials on the action of the UV screens on the proliferation of MCF-7 cells was also explored in this research. To the best of my knowledge, this is the first study to explore the effect of ECM materials on the proliferation of breast cancer cells in response to any environmental oestrogen (see chapter 3). A laminin coating increased the proliferation of MCF-7 cells following the exposure to OMC which was not observed for MCF-7 cells or for T-47-D cells exposed to OMC on plastic. This demonstrates that the effect of these chemicals needs to be studied within the context of the complex microenvironment of cancer cells, rather than just using an *in vitro* model on plastic. The ECM components interact with various molecular pathways (Schwartz et al., 1995; Burrige and Chrzanowska-Wodnicka, 1996; Longhurst and Jennings, 1998) and studying the influence of the presence of different ECM components in combination with environmental oestrogens might aid in obtaining closer data to the possible effect of these chemicals *in vivo*. In this work the invasion assays were conducted on matrigel, which is an extract driven from the basement membrane of EHS-mouse tumour (Kleinman and Martin, 2005) but coating with other components of the ECM might provide different invasion results and should be used in future research.

Because UV screens are mainly used to protect the skin from exposure to UV rays, research in this area has been directed towards the role of UV screens in preventing melanoma caused by the UV rays (Wolf et al., 1994) rather than the effect of UV screens in terms of causing the hallmarks of cancer. Results reported here demonstrate that the UV screens can cause the development in human breast cancer epithelial cells of at least 2 of the hallmarks of cancer,

namely sustained proliferation and invasion and metastasis. Further studies are now needed to investigate whether the UV screens can influence development of any other hallmarks of cancer in breast cells. However, in view of the application of UV screens to skin, it would also be interesting to investigate any potential for development of hallmarks of cancer in keratinocytes.

## References

- Adolfsson-Erici, M., Pettersson, M., Parkkonen, J. and Sturve, J. (2002). Triclosan, a commonly used bactericide found in human milk and in the aquatic environment in Sweden. *Chemosphere*. **46**(9-10):1485–1489.
- ACEA, B. (2013). From Classical to Online Monitoring of G-ProteinCoupled Receptor Stimulation in Living Cells. *Application Note No.6*. : 2–14.
- Aka, J.A. and Lin, S.-X. (2012). Comparison of functional proteomic analyses of human breast cancer cell lines T47D and MCF7. *PloS one*. **7**(2): e31532.
- Alarmo, E.-L., Kuukasjarvi, T., Karhu, R. and Kallioniemi, A. (2007). A comprehensive expression survey of bone morphogenetic proteins in breast cancer highlights the importance of BMP4 and BMP7. *Breast Cancer Research and Treatment*. **103**(2): 239–246.
- Alarmo, E.-L., Parssinen, J., Ketolainen, J.M., Savinainen, K., Karhu, R. and Kallioniemi, A. (2009). BMP7 influences proliferation, migration, and invasion of breast cancer cells. *Cancer Letters*. **275**(1): 35–43.
- Alarmo, E.-L., Rauta, J., Kauraniemi, P., Karhu, R., Kuukasjarvi, T. and Kallioniemi, A. (2006). Bone morphogenetic protein 7 is widely overexpressed in primary breast cancer. *Genes, Chromosomes & Cancer*. **45**(4): 411–419.
- AL-Bader, M., Ford, C., Al-Ayadhy, B. and Francis, I. (2011). Analysis of estrogen receptor isoforms and variants in breast cancer cell lines. *Experimental and Therapeutic Medicine*. **2**(3): 537–544.
- Al-Eid, H.S., Areth, S.O., Bazarbashi, S. and Al-Zahrani, A. (2004). *Cancer Incidence Report Saudi Arabia 2004*. 1-100.
- Al-Kuraya, K., Schraml, P., Sheikh, S., Amr, S., Torhorst, J., Tapia, C., Novotny, H., Spichtin, H., Maurer, R., Mirlacher, M., Simon, R. and Sauter, G. (2005). Predominance of high-grade pathway in breast cancer development of Middle East women. *Modern pathology : an official journal of the United States and Canadian Academy of Pathology, Inc*. **18**(7): 891–897.

- Allred, D.C., Mohsin, S.K. and Fuqua, S.A.W. (2001). Histological and biological evolution of human premalignant breast disease. *Endocrine-Related Cancer*. **8**(1): 47–61.
- Alonso, L.C. and Rosenfield, R.L. (2002). Oestrogens and puberty. *Best Practice & Research. Clinical Endocrinology & Metabolism*. **16**(1): 13–30.
- Altucci, L., Addeo, R., Cicatiello, L., Dauvois, S., Parker, M.G., Truss, M., Beato, M., Sica, V., Bresciani, F. and Weisz, A. (1996). 17beta-Estradiol induces cyclin D1 gene transcription, p36D1-p34cdk4 complex activation and p105Rb phosphorylation during mitogenic stimulation of G(1)-arrested human breast cancer cells. *Oncogene*. **12**(11): 2315–2324.
- Anand, P., Kunnumakara, A.B., Sundaram, C., Harikumar, K.B., Tharakan, S.T., Lai, O.S., Sung, B. and Aggarwal, B.B. (2008). Cancer is a Preventable Disease that Requires Major Lifestyle Changes. *Pharmaceutical Research*. **25**(9): 2097–2116.
- Andre, F. and Puztai, L. (2006). Molecular classification of breast cancer: implications for selection of adjuvant chemotherapy. *Nature Clinical Practice Oncology*. **3**(11): 621–632.
- Arevalo, M.-A., Azcoitia, I. and Garcia-Segura, L.M. (2015). The neuroprotective actions of oestradiol and oestrogen receptors. *Nature reviews. Neuroscience*. **16**(1): 17–29.
- Artym, V. V, Zhang, Y., Seillier-Moiseiwitsch, F., Yamada, K.M. and Mueller, S.C. (2006). Dynamic interactions of cortactin and membrane type 1 matrix metalloproteinase at invadopodia: defining the stages of invadopodia formation and function. *Cancer Research*. **66**(6): 3034–3043.
- Ascenzi, P., Bocedi, A. and Marino, M. (2006). Structure-function relationship of estrogen receptor alpha and beta: impact on human health. *Molecular Aspects of Medicine*. **27**(4): 299–402.
- Atkinson, S.J., Crabbe, T., Cowell, S., Ward, R. V, Butler, M.J., Sato, H., Seiki, M., Reynolds, J.J. and Murphy, G. (1995). Intermolecular autolytic cleavage can contribute to the activation of progelatinase A by cell membranes. *The Journal of Biological Chemistry*. **270**(51): 30479–30485.
- Azios, N.G. and Dharmawardhane, S.F. (2005). Resveratrol and estradiol exert disparate effects on cell migration, cell surface actin structures, and focal adhesion assembly in MDA-MB-231 human breast cancer cells. *Neoplasia (New York, N.Y.)*. **7**(2): 128–140.

- Bafico, A. and Aaronson, S. (2003). Classification of Growth Factors and Their Receptors. In: Kufe D., Pollock R., Weichselbaum R. and Et.al., editors. *Holland-Frei Cancer Medicine*. 6<sup>th</sup> edition. Hamelton: *BC Decker publisher*.
- Bakir, A. and Darbre, P.D. (2015). Effect of aluminium on migration of oestrogen unresponsive MDA-MB-231 human breast cancer cells in culture. *Journal of Inorganic Biochemistry*. **152**: 180–185.
- Balduyck, M., Zerimech, F., Gouyer, V., Lemaire, R., Hemon, B., Grard, G., Thiebaut, C., Lemaire, V Dacquembronne, E Duhem, T., Lebrun, A., Dejonghe, M. and Huet, G. (2000). Specific expression of matrix metalloproteinases 1, 3, 9 and 13 associated with invasiveness of breast cancer cells in vitro. *Clinical and Experimental Metastasis*. **18**(2): 171–178.
- Balmer, M.E., Buser, H.-R., Muller, M.D. and Poiger, T. (2005). Occurrence of some organic UV filters in wastewater, in surface waters, and in fish from Swiss Lakes. *Environmental Science & Technology*. **39**(4): 953–962.
- Bradner, W.T. (2001). Mitomycin C: a clinical update. *Cancer Treatment Reviews*. **27**(1): 35–50.
- Barr, L., Metaxas, G., Harbach, C.A.J., Savoy, L.A. and Darbre, P.D. (2012). Measurement of paraben concentrations in human breast tissue at serial locations across the breast from axilla to sternum. *Journal of Applied Toxicology*. **32**(3): 219–232.
- Batlle, E., Sancho, E., Franci, C., Dominguez, D., Monfar, M., Baulida, J. and Garcia De Herreros, A. (2000). The transcription factor snail is a repressor of E-cadherin gene expression in epithelial tumour cells. *Nature Cell Biology*. **2**(2): 84–89.
- Bazzoun, D., Lelievre, S. and Talhouk, R. (2013). Polarity proteins as regulators of cell junction complexes: implications for breast cancer. *Pharmacology & Therapeutics*. **138**(3): 418–427.
- Beato, M. and Klug, J. (2000). Steroid hormone receptors: an update. *Human Reproduction Update*. **6**(3): 225–236.
- Beatson, G. (1896). On the treatment of inoperable cases of carcinoma of the mamma: suggestions for a new method of treatment, with illustrative cases.1. *The Lancet*. **148**(3802): 104–107.

- Beavon, I.R. (2000). The E-cadherin-catenin complex in tumour metastasis: structure, function and regulation. *European Journal of Cancer*. **36**(13 Spec No): 1607–1620.
- Behrens, J., von Kries, J.P., Kuhl, M., Bruhn, L., Wedlich, D., Grosschedl, R. and Birchmeier, W. (1996). Functional interaction of beta-catenin with the transcription factor LEF-1. *Nature*. **382**(6592): 638–642.
- Beral, V. (2003). Breast cancer and hormone-replacement therapy in the Million Women Study. *The Lancet*. **362**(9382): 419–427.
- Berthois, Y., Katzenellenbogen, J.A. and Katzenellenbogen, B.S. (1986). Phenol red in tissue culture media is a weak estrogen: implications concerning the study of estrogen-responsive cells in culture. *Proceedings of the National Academy of Sciences of the United States of America*. **83**(8): 2496–2500.
- Berx, G., Staes, K., van Hengel, J., Molemans, F., Bussemakers, M.J., van Bokhoven, A. and van Roy, F. (1995). Cloning and characterization of the human invasion suppressor gene E-cadherin (CDH1). *Genomics*. **26**(2): 281–289.
- Blair, R.M., Fang, H., Branham, W.S., Hass, B.S., Dial, S.L., Moland, C.L., Tong, W., Shi, L., Perkins, R. and Sheehan, D.M. (2000). The estrogen receptor relative binding affinities of 188 natural and xenochemicals: structural diversity of ligands. *Toxicological Sciences : an official journal of the Society of Toxicology*. **54**(1):138–153.
- Borras, M., Hardy, L., Lempereur, F., el Khissiin, A.H., Legros, N., Gol-Winkler, R. and Leclercq, G. (1994). Estradiol-induced down-regulation of estrogen receptor. Effect of various modulators of protein synthesis and expression. *The Journal of Steroid Biochemistry and Molecular Biology*. **48**(4): 325–336.
- Boyer, B., Dufour, S. and Thiery, J.P. (1992). E-cadherin expression during the acidic FGF-induced dispersion of a rat bladder carcinoma cell line. *Experimental Cell Research*. **201**(2): 347–357.
- Boyle, P. (2005). Breast cancer control: signs of progress, but more work required. *Breast (Edinburgh, Scotland)*. **14**(6): 429–38.
- Brooke, D.N., Burns, J.S. and Crookes, M.J. (2008). UV-filters in cosmetics – prioritisation for environmental assessment. *Bristol: Environment Agency*. Available from:

[https://www.gov.uk/government/uploads/system/uploads/attachment\\_data/file/291007/sch\\_o1008bpay-e-e.pdf](https://www.gov.uk/government/uploads/system/uploads/attachment_data/file/291007/sch_o1008bpay-e-e.pdf).

- Brooks, S.C., Locke, E.R. and Soule, H.D. (1973). Estrogen Receptor in human cell line (MCF-7) from breast carcinoma. *The Journal of Biological Chemistry*. **248**(17): 6251–6253.
- Brown, A.M., Jeltsch, J.M., Roberts, M. and Chambon, P. (1984). Activation of pS2 gene transcription is a primary response to estrogen in the human breast cancer cell line MCF-7. *Proceedings of the National Academy of Sciences of the United States of America*. **81**(20): 6344–6348.
- Brzozowski, A.M., Pike, A.C., Dauter, Z., Hubbard, R.E., Bonn, T., Engstrom, O., Ohman, L., Greene, G.L., Gustafsson, J.A. and Carlquist, M. (1997). Molecular basis of agonism and antagonism in the oestrogen receptor. *Nature*. **389**(6652): 753–758.
- Buijs, J.T., Henriquez, N. V, van Overveld, P.G.M., van der Horst, G., Que, I., Schwaninger, R., Rentsch, C., Ten Dijke, P., Cleton-Jansen, A.-M., Driouch, K., Lidereau, R., Bachelier, R., Vukicevic, S., Clezardin, P., Papapoulos, S.E., Cecchini, M.G., Lowik, C.W.G.M. and van der Pluijm, G. (2007). Bone morphogenetic protein 7 in the development and treatment of bone metastases from breast cancer. *Cancer Research*. **67**(18): 8742–8751.
- Bukholm, I.K., Nesland, J.M. and Borresen-Dale, A.L. (2000). Re-expression of E-cadherin, alpha-catenin and beta-catenin, but not of gamma-catenin, in metastatic tissue from breast cancer patients [see comments]. *The Journal of Pathology*. **190**(1): 15–19.
- Bunone, G., Briand, P.A., Miksicek, R.J. and Picard, D. (1996). Activation of the unliganded estrogen receptor by EGF involves the MAP kinase pathway and direct phosphorylation. *The EMBO Journal*. **15**(9): 2174–2183.
- Burdall, S.E., Hanby, A.M., Lansdown, M.R.J. and Speirs, V. (2003). Breast cancer cell lines: friend or foe?. *Breast Cancer Research*. **5**(2): 89–95.
- Burridge, K. and Chrzanowska-Wodnicka, M. (1996). Focal adhesions, contractility, and signaling. *Annual Review of Cell and Developmental Biology*. **12**: 463–518.

- Burridge, K., Fath, K., Kelly, T., Nuckolls, G. and Turner, C. (1988). Focal adhesions: transmembrane junctions between the extracellular matrix and the cytoskeleton. *Annual Review of Cell Biology*. **4**: 487–525.
- Buser, H.-R., Balmer, M.E., Schmid, P. and Kohler, M. (2006). Occurrence of UV filters 4-methylbenzylidene camphor and octocrylene in fish from various Swiss rivers with inputs from wastewater treatment plants. *Environmental Science & Technology*. **40**(5): 1427–1431.
- Byford, J., Shaw, L., Drew, M.G., Pope, G., Sauer, M. and Darbre, P. (2002). Oestrogenic activity of parabens in MCF7 human breast cancer cells. *The Journal of Steroid Biochemistry and Molecular Biology*. **80**(1): 49–60.
- Cai, K., Jiang, L., Wang, J., Zhang, H., Wang, X., Cheng, D. and Dou, J. (2014). Downregulation of beta-catenin decreases the tumorigenicity, but promotes epithelial-mesenchymal transition in breast cancer cells. *Journal of Cancer Research and Therapeutics*. **10**(4): 1063–1070.
- Calderwood, D.A., Shattil, S.J. and Ginsberg, M.H. (2000). Integrins and actin filaments: reciprocal regulation of cell adhesion and signaling. *The Journal of Biological Chemistry*. **275**(30): 22607–22610.
- Coldham, N.G., Dave, M., Sivapathasundaram, S., McDonnell, D.P., Connor, C. and Sauer, M.J. (1997). Evaluation of a recombinant yeast cell estrogen screening assay. *Environmental Health Perspectives*. **105**(7): 734–742.
- Collaborative Group on Hormonal Factors in Breast Cancer (1996). Breast cancer and hormonal contraceptives: collaborative reanalysis of individual data on 53 297 women with breast cancer and 100 239 women without breast cancer from 54 epidemiological studies. *Lancet (London, England)*. **347**(9017): 1713–1727.
- Careghini, A., Mastorgio, A.F., Saponaro, S. and Sezenna, E. (2015). Bisphenol A, nonylphenols, benzophenones, and benzotriazoles in soils, groundwater, surface water, sediments, and food: a review. *Environmental Science and Pollution Research International*. **22**(8): 5711–5741.
- Cestari, S.H., Figueiredo, N.B., Conde, S.J., Clara, S., Katayama, M.L.H., Padovani, C.R., Brentani, M.M. and Nogueira, C.R. (2009). Influence of estradiol and triiodothyronine on

- breast cancer cell lines proliferation and expression of estrogen and thyroid hormone receptors. *Arquivos Brasileiros de Endocrinologia e Metabologia*. **53**(7): 859–864.
- Chakravarty, D., Nair, S.S., Santhamma, B., Nair, B.C., Wang, L., Bandyopadhyay, A., Agyin, J.K., Brann, D., Sun, L.-Z., Yeh, I.-T., Lee, F.Y., Tekmal, R.R., Kumar, R. and Vadlamudi, R.K. (2010). Extranuclear functions of ER impact invasive migration and metastasis by breast cancer cells. *Cancer Research*. **70**(10): 4092–4101.
- Chao, H.-R., Wang, S.-L., Lee, W.-J., Wang, Y.-F. and Papke, O. (2007). Levels of polybrominated diphenyl ethers (PBDEs) in breast milk from central Taiwan and their relation to infant birth outcome and maternal menstruation effects. *Environment International*. **33**(2): 239–245.
- Charles, A.K. and Darbre, P.D. (2013). Combinations of parabens at concentrations measured in human breast tissue can increase proliferation of MCF-7 human breast cancer cells. *Journal of applied toxicology*. **33**(5): 390–398.
- Charlier, C., Chariot, A., Antoine, N., Merville, M.P., Gielen, J. and Castronovo, V. (1995). Tamoxifen and its active metabolite inhibit growth of estrogen receptor-negative MDA-MB-435 cells. *Biochemical Pharmacology*. **49**(3): 351–358.
- Chatelain, E., Gabard, B. and Surber, C. (2003). Skin penetration and sun protection factor of five UV filters: effect of the vehicle. *Skin Pharmacology and Applied Skin Physiology*. **16**(1): 28–35.
- Chaudhri, R.A., Olivares-Navarrete, R., Cuenca, N., Hadadi, A., Boyan, B.D. and Schwartz, Z. (2012). Membrane Estrogen Signaling Enhances Tumorigenesis and Metastatic Potential of Breast Cancer Cells via Estrogen Receptor- $\alpha$ 36 (ER $\alpha$ 36). *The Journal of Biological Chemistry*. **287**(10): 7169–7181.
- Chekhun, S., Bezdenezhnykh, N., Shvets, J. and Lukianova, N. (2013). Expression of biomarkers related to cell adhesion, metastasis and invasion of breast cancer cell lines of different molecular subtype. *Experimental Oncology*. **35**(3): 174–179.
- Chen, C.-S., Hong, S., Indra, I., Sergeeva, A.P., Troyanovsky, R.B., Shapiro, L., Honig, B. and Troyanovsky, S.M. (2015).  $\alpha$ -Catenin-mediated cadherin clustering couples cadherin and actin dynamics. *The Journal of Cell Biology*. **210**(4): 647–661.

- Chen, Y.-C., Allen, S.G., Ingram, P.N., Buckanovich, R., Merajver, S.D. and Yoon, E. (2015). Single-cell Migration Chip for Chemotaxis-based Microfluidic Selection of Heterogeneous Cell Populations. *Scientific Reports. Nature*. **5**(9980): 1-15.
- Cheng, Z.N., Shu, Y., Liu, Z.Q., Wang, L.S., Ou-Yang, D.S. and Zhou, H.H. (2001). Role of cytochrome P450 in estradiol metabolism in vitro. *Acta pharmacologica Sinica*. **22**(2): 148–154.
- Cheskis, B.J., Greger, J.G., Nagpal, S. and Freedman, L.P. (2007). Signaling by estrogens. *Journal of Cellular Physiology*. **213**(3): 610–617.
- Cheung, K.J., Gabrielson, E., Werb, Z. and Ewald, A.J. (2013). Collective invasion in breast cancer requires a conserved basal epithelial program. *Cell*. **155**(7): 1639–51.
- Christiansen, J.J. and Rajasekaran, A.K. (2006). Reassessing epithelial to mesenchymal transition as a prerequisite for carcinoma invasion and metastasis. *Cancer Research*. **66**(17): 8319–8326.
- Cichon, M.A., Degnim, A.C., Visscher, D.W. and Radisky, D.C. (2010). Microenvironmental influences that drive progression from benign breast disease to invasive breast cancer. *Journal of Mammary Gland Biology and Neoplasia*. **15**(4): 389–397.
- Ciobanaru, C., Faivre, B. and Le Clainche, C. (2013). Integrating actin dynamics, mechanotransduction and integrin activation: the multiple functions of actin binding proteins in focal adhesions. *European Journal of Cell Biology*. **92**(10-11): 339–348.
- Cizkova, M., Vacher, S., Meseure, D., Trassard, M., Susini, A., Mlcuchova, D., Callens, C., Rouleau, E., Spyrtos, F., Lidereau, R. and Bieche, I. (2013). PIK3R1 underexpression is an independent prognostic marker in breast cancer. *BMC Cancer*. **13**:545.
- Clark, A.G. and Vignjevic, D.M. (2015). Modes of cancer cell invasion and the role of the microenvironment. *Current Opinion in Cell Biology*. **36**: 13–22.
- Claus, E.B., Schildkraut, J., Iversen, E.S.J., Berry, D. and Parmigiani, G. (1998). Effect of BRCA1 and BRCA2 on the association between breast cancer risk and family history. *Journal of the National Cancer Institute*. **90**(23): 1824–1829.
- Cockett, M.I., Murphy, G., Birch, M.L., O’Connell, J.P., Crabbe, T., Millican, A.T., Hart, I.R. and Docherty, A.J. (1998). Matrix metalloproteinases and metastatic cancer. *Biochemical Society Symposium*. **63**: 295–313.

- Colognato, H. and Yurchenco, P.D. (2000). Form and function: the laminin family of heterotrimers. *Developmental Dynamics: an official publication of the American Association of Anatomists*. **218**(2): 213–234.
- Comijn, J., Berx, G., Vermassen, P., Verschueren, K., van Grunsven, L., Bruyneel, E., Mareel, M., Huylebroeck, D. and van Roy, F. (2001). The two-handed E box binding zinc finger protein SIP1 downregulates E-cadherin and induces invasion. *Molecular Cell*. **7**(6): 1267–1278.
- Contrò, J.R., Proia, P. and Valentina, B. (2015). Sex steroid hormone receptors, their ligands, and nuclear and non-nuclear pathways. *AIMS Molecular Science*. **2**(3): 294–310.
- Dai, H., van't Veer, L., Lamb, J., He, Y.D., Mao, M., Fine, B.M., Bernards, R., van de Vijver, M., Deutsch, P., Sachs, A., Stoughton, R. and Friend, S. (2005). A cell proliferation signature is a marker of extremely poor outcome in a subpopulation of breast cancer patients. *Cancer Research*. **65**(10): 4059–4066.
- Daly, R.J. and Darbre, P.D. (1990). Cellular and molecular events in loss of estrogen sensitivity in ZR-75-1 and T-47-D human breast cancer cells. *Cancer Research*. **50**(18): 5868–5875.
- Darbre, P., Yates, J., Curtis, S. and King, R.J. (1983). Effect of estradiol on human breast cancer cells in culture. *Cancer Research*. **43**(1): 349–354.
- Darbre, P.D. (2006). Environmental oestrogens, cosmetics and breast cancer. Best Practice & Research. *Clinical Endocrinology & Metabolism*. **20**(1): 121–143.
- Darbre, P.D. (2012). Molecular mechanisms of oestrogen action on growth of human breast cancer cells in culture. *Hormone Molecular Biology and Clinical Investigation*. **9**(1): 65–85.
- Darbre, P.D. (2014). Hypersensitivity and growth adaptation of oestrogen-deprived MCF-7 human breast cancer cells. *Anticancer Research*. **34**(1): 99–105.
- Darbre, P.D. (Editor) (2015). Endocrine disruption and human health. 1st ed. London: *Elsevier*.
- Darbre, P.D., Aljarrah, A., Miller, W.R., Coldham, N.G., Sauer, M.J. and Pope, G.S. (2004). Concentrations of parabens in human breast tumours. *Journal of Applied Toxicology*. **24**(1): 5–13.

- Darbre, P.D. and Charles, A.K. (2010). Environmental oestrogens and breast cancer: evidence for combined involvement of dietary, household and cosmetic xenoestrogens. *Anticancer Research*. **30** (3): 815–827.
- Darbre, P.D. and Daly, R.J. (1989). Effects of oestrogen on human breast cancer cells in culture. *Proceeding of the Royal Society of Edinburgh*. **95**: 119–132.
- Darbre, P.D., Bakir, A. and Iskakova, E. (2013). Effect of aluminium on migratory and invasive properties of MCF-7 human breast cancer cells in culture. *Journal of Inorganic Biochemistry*. **128**: 245–249.
- Darbre, P.D. and Fernandez, M.F. (2013). Environmental oestrogens and breast cancer: long-term low-dose effects of mixtures of various chemical combinations. *Journal of Epidemiology and Community Health*. **67**(3): 203–205.
- Das, S. Banerji, A., Feri, E. and Chatterjee, A. (2008). Rapid expression and activation of MMP-2 and MMP-9 upon exposure of human breast cancer cells (MCF-7) to fibronectin in serum free medium. *Life Sciences*. **82**(9-10): 467–476.
- Delemarre, E.M., Felijs, B. and Delemarre-van de Waal, H.A. (2008). Inducing puberty. *European Journal of Endocrinology*. **159** (Suppl): S9–15.
- DePasquale, J.A. (1999). Rearrangement of the F-actin cytoskeleton in estradiol-treated MCF-7 breast carcinoma cells. *Histochemistry and Cell Biology*. **112**(5): 341–350.
- Deryugina, E.I., Luo, G.X., Reisfeld, R.A., Bourdon, M.A. and Strongin, A. (1997). Tumor cell invasion through matrigel is regulated by activated matrix metalloproteinase-2. *Anticancer Research*. **17**(5A): 3201–3210.
- Deryugina, E.I., Ratnikov, B., Monosov, E., Postnova, T.I., DiScipio, R., Smith, J.W. and Strongin, A.Y. (2001). MT1-MMP initiates activation of pro-MMP-2 and integrin  $\alpha$ v $\beta$ 3 promotes maturation of MMP-2 in breast carcinoma cells. *Experimental Cell Research*. **263**(2): 209–223.
- Devy, L., Huang, L., Naa, L., Yanamandra, N., Pieters, H., Frans, N., Chang, E., Tao, Q., Vanhove, M., Lejeune, A., van Gool, R., Sexton, D.J., Kuang, G., Rank, D., Hogan, S., Pazmany, C., Ma, Y.L., Schoonbroodt, S., Nixon, A.E., Ladner, R.C., Hoet, R., Henderikx, P., Tenhoor, C., Rabbani, S.A., Valentino, M.L., Wood, C.R. and Dransfield,

- D.T. (2009). Selective inhibition of matrix metalloproteinase-14 blocks tumor growth, invasion, and angiogenesis. *Cancer Research*. **69**(4): 1517–1526.
- Doisneau-Sixou, S.F., Sergio, C.M., Carroll, J.S., Hui, R., Musgrove, E.A. and Sutherland, R.L. (2003). Estrogen and antiestrogen regulation of cell cycle progression in breast cancer cells. *Endocrine-Related Cancer*. **10**(2): 179–186.
- Drasin, D.J., Robin, T.P. and Ford, H.L. (2011). Breast cancer epithelial-to-mesenchymal transition: examining the functional consequences of plasticity. *Breast Cancer Research*. **13**(6): 226.
- Dubik, D., Dembinski, T.C. and Shiu, R.P. (1987). Stimulation of c-myc oncogene expression associated with estrogen-induced proliferation of human breast cancer cells. *Cancer Research*. **47**(24 Pt 1): 6517–6521.
- Dufourny, B., Alblas, J., van Teeffelen, H.A., van Schaik, F.M., van der Burg, B., Steenbergh, P.H. and Sussenbach, J.S. (1997). Mitogenic signaling of insulin-like growth factor I in MCF-7 human breast cancer cells requires phosphatidylinositol 3-kinase and is independent of mitogen-activated protein kinase. *The Journal of Biological Chemistry*. **272**(49): 31163–31171.
- Dupont, J. and Le Roith, D. (2001). Insulin-like growth factor 1 and oestradiol promote cell proliferation of MCF-7 breast cancer cells: new insights into their synergistic effects. *Molecular Pathology*. **54**(3): 149–154.
- Eastman, Q. and Grosschedl, R. (1999). Regulation of LEF-1/TCF transcription factors by Wnt and other signals. *Current Opinion in Cell Biology*. **11**(2): 233–240.
- Eisenberg, M.C., Kim, Y., Li, R., Ackerman, W.E., Kniss, D.A. and Friedman, A. (2011). Mechanistic modeling of the effects of myoferlin on tumor cell invasion. *Proceedings of the National Academy of Sciences of the United States of America*. **108**(50): 20078–20083.
- Enmark, E., Peltö-Huikko, M., Grandien, K., Lagercrantz, S., Lagercrantz, J., Fried, G., Nordenskjöld, M. and Gustafsson, J.A. (1997). Human estrogen receptor beta-gene structure, chromosomal localization, and expression pattern. *The Journal of Clinical Endocrinology and Metabolism*. **82**(12): 4258–4265.

- Eroles, P., Bosch, A., Alejandro Pérez-Fidalgo, J. and Lluch, A. (2012). Molecular biology in breast cancer: Intrinsic subtypes and signaling pathways. *Cancer Treatment Reviews*. **38**(6): 698–707.
- Exley, C., Charles, L.M., Barr, L., Martin, C., Polwart, A. and Darbre, P.D. (2007). Aluminium in human breast tissue. *Journal of Inorganic Biochemistry*. **101**(9): 1344–1346.
- Fan, Y. and Guo, Y. (2015). Knockdown of eIF3D inhibits breast cancer cell proliferation and invasion through suppressing the Wnt/ $\beta$ -catenin signaling pathway. *International Journal of Clinical and Experimental Pathology*. **8**(9): 10420–10427.
- Fang, H., Tong, W., Shi, L.M., Blair, R., Perkins, R., Branham, W., Hass, B.S., Xie, Q., Dial, S.L., Moland, C.L. and Sheehan, D.M. (2001). Structure-activity relationships for a large diverse set of natural, synthetic, and environmental estrogens. *Chemical Research in Toxicology*. **14**(3): 280–294.
- Farmer, P., Bonnefoi, H., Becette, V., Tubiana-Hulin, M., Fumoleau, P., Larsimont, D., Macgrogan, G., Bergh, J., Cameron, D., Goldstein, D., Duss, S., Nicoulaz, A.-L., Brisken, C., Fiche, M., Delorenzi, M. and Iggo, R. (2005). Identification of molecular apocrine breast tumours by microarray analysis. *Oncogene*. **24**(29): 4660–4671.
- Faupel-Badger, J.M., Fuhrman, B.J., Xu, X., Falk, R.T., Keefer, L.K., Veenstra, T.D., Hoover, R.N. and Ziegler, R.G. (2010). Comparison of liquid chromatography-mass spectrometry, radioimmunoassay, and enzyme-linked immunosorbent assay methods for measurement of urinary estrogens. *Cancer Epidemiology, Biomarkers & Prevention: a publication of the American Association for Cancer Research, cosponsored by the American Society of Preventive Oncology*. **19**(1): 292–300.
- Felix, T., Hall, B.J. and S. Brodbelt, J. (1998). Determination of benzophenone-3 and metabolites in water and human urine by solid-phase microextraction and quadrupole ion trap GC–MS. *Analytica Chimica Acta*. **371**(2-3): 195–203.
- Filardo, E.J., Quinn, J.A., Bland, K.I. and Frackelton, A.R.J. (2000). Estrogen-induced activation of Erk-1 and Erk-2 requires the G protein-coupled receptor homolog, GPR30, and occurs via trans-activation of the epidermal growth factor receptor through release of HB-EGF. *Molecular Endocrinology (Baltimore, Md.)*. **14**(10): 1649–1660.

- Filardo, E.J., Quinn, J.A., Frackelton, A.R.J. and Bland, K.I. (2002). Estrogen action via the G protein-coupled receptor, GPR30: stimulation of adenylyl cyclase and cAMP-mediated attenuation of the epidermal growth factor receptor-to-MAPK signaling axis. *Molecular Endocrinology*. **16**(1): 70–84.
- Ford, C.H.J., Al-Bader, M., Al-Ayadhi, B. and Francis, I. (2011). Reassessment of estrogen receptor expression in human breast cancer cell lines. *Anticancer Research*. **31**(2): 521–527.
- Forsyth, P.A., Wong, H., Laing, T.D., Rewcastle, N.B., Morris, D.G., Muzik, H., Leco, K.J., Johnston, R.N., Brasher, P.M.A., Sutherland, G. and Edwards, D.R. (1999). Gelatinase-A (MMP-2), gelatinase-B (MMP-9) and membrane type matrix metalloproteinase-1 (MT1-MMP) are involved in different aspects of the pathophysiology of malignant gliomas. *British Journal of Cancer*. **79**(11-12): 1828–1835.
- Frasor, J., Danes, J.M., Komm, B., Chang, K.C.N., Lyttle, C.R. and Katzenellenbogen, B.S. (2003). Profiling of estrogen up- and down-regulated gene expression in human breast cancer cells: insights into gene networks and pathways underlying estrogenic control of proliferation and cell phenotype. *Endocrinology*. **144**(10): 4562–4574.
- Friedl, P. and Alexander, S. (2011). Cancer invasion and the microenvironment: plasticity and reciprocity. *Cell*. **147**(5): 992–1009.
- Friedl, P. and Gilmour, D. (2009). Collective cell migration in morphogenesis, regeneration and cancer. *Nature Reviews. Molecular Cell Biology*. **10**(7): 445–457.
- Friedl, P., Hegerfeldt, Y. and Tusch, M. (2004). Collective cell migration in morphogenesis and cancer. *The International Journal of Developmental Biology*. **48**(5-6): 441–449.
- Friedl, P., Locker, J., Sahai, E. and Segall, J.E. (2012). Classifying collective cancer cell invasion. *Nature Cell Biology*. **14**(8): 777–783.
- Friedl, P. and Wolf, K. (2003). Tumour-cell invasion and migration: diversity and escape mechanisms. *Nature Reviews. Cancer*. **3**(5): 362–374.
- Fuqua, S.A., Schiff, R., Parra, I., Friedrichs, W.E., Su, J.L., McKee, D.D., Slentz-Kesler, K., Moore, L.B., Willson, T.M. and Moore, J.T. (1999). Expression of wild-type estrogen receptor beta and variant isoforms in human breast cancer. *Cancer Research*. **59**(21): 5425–5428.

- Gago-Ferrero, P., Díaz-Cruz, M.S. and Barceló, D. (2015). UV filters bioaccumulation in fish from Iberian river basins. *The Science of the Total Environment*. **518-519**:518–525.
- Gamallo, C., Palacios, J., Suarez, A., Pizarro, A., Navarro, P., Quintanilla, M. and Cano, A. (1993). Correlation of E-cadherin expression with differentiation grade and histological type in breast carcinoma. *The American Journal of Pathology*. **142**(4): 987–993.
- Ganapathy, V., Banach-Petrosky, W., Xie, W., Kareddula, A., Nienhuis, H., Miles, G. and Reiss, M. (2012). Luminal breast cancer metastasis is dependent on estrogen signaling. *Clinical & Experimental Metastasis*. **29**(5): 7-14.
- Gao, J., Zhu, Y., Nilsson, M. and Sundfeldt, K. (2014). TGF- $\beta$  isoforms induce EMT independent migration of ovarian cancer cells. *Cancer Cell International*. **14**: 72.
- Garbett, E.A., Reed, M.W.R., Stephenson, T.J. and Brown, N.J. (2000). Proteolysis in human breast cancer. *Molecular Pathology*. **53**(2): 99–106.
- Ghiasvand, R., Adami, H.-O., Harirchi, I., Akrami, R. and Zendehdel, K. (2014). Higher incidence of premenopausal breast cancer in less developed countries; myth or truth?. *BMC Cancer*. **14**: 343.
- Giretti, M.S., Fu, X.-D., De Rosa, G., Sarotto, I., Baldacci, C., Garibaldi, S., Mannella, P., Biglia, N., Sismondi, P., Genazzani, A.R. and Simoncini, T. (2008). Extra-nuclear signalling of estrogen receptor to breast cancer cytoskeletal remodelling, migration and invasion. *PloS one*. **3**(5): e2238.
- Girgert, R., Emons, G. and Grundker, C. (2014). Inhibition of GPR30 by estriol prevents growth stimulation of triple-negative breast cancer cells by 17 $\beta$ -estradiol. *BMC Cancer*. **14**: 935.
- Gomez, D.E., Alonso, D.F., Yoshiji, H. and Thorgeirsson, U.P. (1997). Tissue inhibitors of metalloproteinases: structure, regulation and biological functions. *European Journal of Cell Biology*. **74**(2): 111–122.
- Gomez, E., Pillon, A., Fenet, H., Rosain, D., Duchesne, M.J., Nicolas, J.C., Balaguer, P. and Casellas, C. (2005). Estrogenic activity of cosmetic components in reporter cell lines: parabens, UV screens, and musks. *Journal of Toxicology and Environmental Health*. Part A. **68**(4): 239–251.

Goodson, W.H. 3rd, Lowe, L., Carpenter, D.O., Gilbertson, M., Manaf Ali, A., Lopez de Cerain Salsamendi, A., Lasfar, A., Carnero, A., Azqueta, A., Amedei, A., Charles, A.K., Collins, A.R., Ward, A., Salzberg, A.C., Colacci, A., Olsen, A.-K., Berg, A., Barclay, B.J., Zhou, B.P., Blanco-Aparicio, C., Baglolle, C.J., Dong, C., Mondello, C., Hsu, C.-W., Naus, C.C., Yedjou, C., Curran, C.S., Laird, D.W., Koch, D.C., Carlin, D.J., Felsher, D.W., Roy, D., Brown, D.G., Ratovitski, E., Ryan, E.P., Corsini, E., Rojas, E., Moon, E.-Y., Laconi, E., Marongiu, F., Al-Mulla, F., Chiaradonna, F., Darroudi, F., Martin, F.L., Van Schooten, F.J., Goldberg, G.S., Wagemaker, G., Nangami, G.N., Calaf, G.M., Williams, G., Wolf, G.T., Koppen, G., Brunborg, G., Lyerly, H.K., Krishnan, H., Ab Hamid, H., Yasaei, H., Sone, H., Kondoh, H., Salem, H.K., Hsu, H.-Y., Park, H.H., Koturbash, I., Miousse, I.R., Scovassi, A.I., Klaunig, J.E., Vondracek, J., Raju, J., Roman, J., Wise, J.P.S., Whitfield, J.R., Woodrick, J., Christopher, J.A., Ochieng, J., Martinez-Leal, J.F., Weisz, J., Kravchenko, J., Sun, J., Prudhomme, K.R., Narayanan, K.B., Cohen-Solal, K.A., Moorwood, K., Gonzalez, L., Soucek, L., Jian, L., D'Abronzio, L.S., Lin, L.-T., Li, L., Gulliver, L., McCawley, L.J., Memeo, L., Vermeulen, L., Leyns, L., Zhang, L., Valverde, M., Khatami, M., Romano, M.F., Chapellier, M., Williams, M.A., Wade, M., Manjili, M.H., Leonart, M.E., Xia, M., Gonzalez, M.J., Karamouzis, M. V, Kirsch-Volders, M., Vaccari, M., Kuemmerle, N.B., Singh, N., Cruickshanks, N., Kleinstreuer, N., van Larebeke, N., Ahmed, N., Ogunkua, O., Krishnakumar, P.K., Vadgama, P., Marignani, P.A., Ghosh, P.M., Ostrosky-Wegman, P., Thompson, P.A., Dent, P., Heneberg, P., Darbre, P., Sing Leung, P., Nangia-Makker, P., Cheng, Q.S., Robey, R.B., Al-Temaimi, R., Roy, R., Andrade-Vieira, R., Sinha, R.K., Mehta, R., Vento, R., Di Fiore, R., Ponce-Cusi, R., Dornetshuber-Fleiss, R., Nahta, R., Castellino, R.C., Palorini, R., Abd Hamid, R., Langie, S.A.S., Eltom, S.E., Brooks, S.A., Ryeom, S., Wise, S.S., Bay, S.N., Harris, S.A., Papagerakis, S., Romano, S., Pavanello, S., Eriksson, S., Forte, S., Casey, S.C., Luanpitpong, S., Lee, T.-J., Otsuki, T., Chen, T., Massfelder, T., Sanderson, T., Guarnieri, T., Hultman, T., Dormoy, V., Otero-Marah, V., Sabbisetti, V., Maguer-Satta, V., Rathmell, W.K., Engstrom, W., Decker, W.K., Bisson, W.H., Rojanasakul, Y., Luqmani, Y., Chen, Z. and Hu, Z. (2015). Assessing the carcinogenic potential of low-dose exposures to chemical mixtures in the environment: the challenge ahead. *Carcinogenesis*. **36** (Suppl-1): 254–296.

- Gosden, J.R., Middleton, P.G. and Rout, D. (1986). Localization of the human oestrogen receptor gene to chromosome 6q24---q27 by in situ hybridization. *Cytogenetics and Cell Genetics*. **43**(3-4): 218–220.
- Gruber, C.J., Gruber, D.M., Gruber, I.M.L., Wieser, F. and Huber, J.C. (2004). Anatomy of the estrogen response element. *Trends in Endocrinology & Metabolism*. **15**(2): 73–78.
- Guarino, M., Rubino, B. and Ballabio, G. (2007). The role of epithelial-mesenchymal transition in cancer pathology. *Pathology*. **39**(3): 305–318.
- Gupta, G.P., Nguyen, D.X., Chiang, A.C., Bos, P.D., Kim, J.Y., Nadal, C., Gomis, R.R., Manova-Todorova, K. and Massague, J. (2007). Mediators of vascular remodelling co-opted for sequential steps in lung metastasis. *Nature*. **446**(7137): 765–770.
- Gustafsson, J.-A. (2003). What pharmacologists can learn from recent advances in estrogen signalling. *Trends in Pharmacological Sciences*. **24**(9): 479–485.
- Hajra, K.M., Chen, D.Y.-S. and Fearon, E.R. (2002). The SLUG zinc-finger protein represses E-cadherin in breast cancer. *Cancer Research*. **62**(6): 1613–1618.
- Hall, J.M., Lee, M.K., Newman, B., Morrow, J.E., Anderson, L.A., Huey, B. and King, M.C. (1990). Linkage of early-onset familial breast cancer to chromosome 17q21. *Science*. **250**(4988): 1684–1689.
- Hamelers, I.H.L., van Schaik, R.F.M.A., Sussenbach, J.S. and Steenbergh, P.H. (2003). 17 $\beta$ -Estradiol responsiveness of MCF-7 laboratory strains is dependent on an autocrine signal activating the IGF type I receptor. *Cancer Cell International*. **3**:10.
- Hamilton, N., Marquez-Garban, D., Mah, V., Fernando, G., Elshimali, Y., Garban, H., Elashoff, D., Vadgama, J., Goodglick, L. and Pietras, R. (2015). Biologic roles of estrogen receptor-beta and insulin-like growth factor-2 in triple-negative breast cancer. *BioMed Research International*. **2015**: 925703.
- Hanahan, D. and Weinberg, R.A. (2000). The hallmarks of cancer. *Cell*. **100**(1): 57–70.
- Hanahan, D. and Weinberg, R.A. (2011). Hallmarks of cancer: The next generation. *Cell*. **144**(5): 646–674.
- Hartman, J., Strom, A. and Gustafsson, J.-A. (2009). Estrogen receptor beta in breast cancer-diagnostic and therapeutic implications. *Steroids*. **74**(8): 635–641.

- Harvell, D.M.E., Strecker, T.E., Tochacek, M., Xie, B., Pennington, K.L., McComb, R.D., Roy, S.K. and Shull, J.D. (2000). Rat strain-specific actions of 17 $\beta$ -estradiol in the mammary gland: Correlation between estrogen-induced lobuloalveolar hyperplasia and susceptibility to estrogen-induced mammary cancers. *Proceedings of the National Academy of Sciences of the United States of America*. **97**(6): 2779–2784.
- Hayden, C.G., Roberts, M.S. and Benson, H.A. (1997). Systemic absorption of sunscreen after topical application. *Lancet (London, England)*. **350**(9081): 863–4.
- Haynes, M.P., Sinha, D., Russell, K.S., Collinge, M., Fulton, D., Morales-Ruiz, M., Sessa, W.C. and Bender, J.R. (2000). Membrane estrogen receptor engagement activates endothelial nitric oxide synthase via the PI3-kinase-Akt pathway in human endothelial cells. *Circulation Research*. **87**(8): 677–682.
- He, T.C., Sparks, A.B., Rago, C., Hermeking, H., Zawel, L., da Costa, L.T., Morin, P.J., Vogelstein, B. and Kinzler, K.W. (1998). Identification of c-MYC as a target of the APC pathway. *Science (New York, N.Y.)*. **281**(5382): 1509–1512.
- Heerboth, S., Housman, G., Leary, M., Longacre, M., Byler, S., Lapinska, K., Willbanks, A. and Sarkar, S. (2015). EMT and tumor metastasis. *Clinical and Translational Medicine*. **4**:6.
- Heimann, R., Lan, F., McBride, R. and Hellman, S. (2000). Separating favorable from unfavorable prognostic markers in breast cancer: the role of E-cadherin. *Cancer Research*. **60**(2): 298–304.
- Heiser, L.M., Sadanandam, A., Kuo, W.-L., Benz, S.C., Goldstein, T.C., Ng, S., Gibb, W.J., Wang, N.J., Ziyad, S., Tong, F., Bayani, N., Hu, Z., Billig, J.I., Dueregger, A., Lewis, S., Jakkula, L., Korkola, J.E., Durinck, S., Pepin, F., Guan, Y., Purdom, E., Neuvial, P., Bengtsson, H., Wood, K.W., Smith, P.G., Vassilev, L.T., Hennessy, B.T., Greshock, J., Bachman, K.E., Hardwicke, M.A., Park, J.W., Marton, L.J., Wolf, D.M., Collisson, E.A., Neve, R.M., Mills, G.B., Speed, T.P., Feiler, H.S., Wooster, R.F., Haussler, D., Stuart, J.M., Gray, J.W. and Spellman, P.T. (2012). Subtype and pathway specific responses to anticancer compounds in breast cancer. *Proceedings of the National Academy of Sciences of the United States of America*. **109**(8): 2724–2729.

- Heldring, N., Pike, A., Andersson, S., Matthews, J., Cheng, G., Hartman, J., Tujague, M., Strom, A., Treuter, E., Warner, M. and Gustafsson, J.-A. (2007). Estrogen receptors: how do they signal and what are their targets. *Physiological Reviews*. **87**(3): 905–931.
- Heneweer, M., Muusse, M., van den Berg, M. and Sanderson, J.T. (2005). Additive estrogenic effects of mixtures of frequently used UV filters on pS2-gene transcription in MCF-7 cells. *Toxicology and Applied Pharmacology*. **208**(2): 170–177.
- Herschkowitz, J.I., Simin, K., Weigman, V.J., Mikaelian, I., Usary, J., Hu, Z., Rasmussen, K.E., Jones, L.P., Assefnia, S., Chandrasekharan, S., Backlund, M.G., Yin, Y., Khramtsov, A.I., Bastein, R., Quackenbush, J., Glazer, R.I., Brown, P.H., Green, J.E., Kopelovich, L., Furth, P.A., Palazzo, J.P., Olopade, O.I., Bernard, P.S., Churchill, G.A., Van Dyke, T. and Perou, C.M. (2007). Identification of conserved gene expression features between murine mammary carcinoma models and human breast tumors. *Genome Biology*. **8**(5): R76–R76.
- Hu, Z., Fan, C., Oh, D.S., Marron, J.S., He, X., Qaqish, B.F., Livasy, C., Carey, L.A., Reynolds, E., Dressler, L., Nobel, A., Parker, J., Ewend, M.G., Sawyer, L.R., Wu, J., Liu, Y., Nanda, R., Tretiakova, M., Ruiz Orrico, A., Dreher, D., Palazzo, J.P., Perreard, L., Nelson, E., Mone, M., Hansen, H., Mullins, M., Quackenbush, J.F., Ellis, M.J., Olopade, O.I., Bernard, P.S. and Perou, C.M. (2006). The molecular portraits of breast tumors are conserved across microarray platforms. *BMC Genomics*. **7**: 96
- van Hengel, J., Nollet, F., Berx, G., van Roy, N., Speleman, F. and van Roy, F. (1995). Assignment of the human beta-catenin gene (CTNNB1) to 3p22-->p21.3 by fluorescence in situ hybridization. *Cytogenetics and Cell Genetics*. **70**(1-2): 68–70.
- de Herreros, A.G., Peiro, S., Nassour, M. and Savagner, P. (2010). Snail family regulation and epithelial mesenchymal transitions in breast cancer progression. *Journal of Mammary Gland Biology and Neoplasia*. **15**(2): 135–147.
- Hiscox, S., Jiang, W.G., Obermeier, K., Taylor, K., Morgan, L., Burmi, R., Barrow, D. and Nicholson, R.I. (2006). Tamoxifen resistance in MCF7 cells promotes EMT-like behaviour and involves modulation of beta-catenin phosphorylation. *International Journal of Cancer*. **118**(2): 290–301.
- Ho, J.-Y., Chang, F.-W., Huang, F.S., Liu, J.-M., Liu, Y.-P., Chen, S.-P., Liu, Y.-L., Cheng, K.-C., Yu, C.-P. and Hsu, R.-J. (2016). Estrogen Enhances the Cell Viability and Motility

- of Breast Cancer Cells through the ERalpha-DeltaNp63-Integrin beta4 Signaling Pathway. *PloS one*. **11**(2): e0148301.
- Hoffmann, K., Laperre, J., Avermaete, A., Altmeyer, P. and Gambichler, T. (2001). Defined UV protection by apparel textiles. *Archives of Dermatology*. **137**(8): 1089–1094.
- Holbeck, S., Chang, J., Best, A.M., Bookout, A.L., Mangelsdorf, D.J. and Martinez, E.D. (2010). Expression Profiling of Nuclear Receptors in the NCI60 Cancer Cell Panel Reveals Receptor-Drug and Receptor-Gene Interactions. *Molecular Endocrinology*. **24**(6): 1287–1296.
- Holliday, D.L. and Speirs, V. (2011). Choosing the right cell line for breast cancer research. *Breast Cancer Research*. **13**(4): 215.
- Hortobagyi, G.N., de la Garza Salazar, J., Pritchard, K., Amadori, D., Haidinger, R., Hudis, C.A., Khaled, H., Liu, M.-C., Martin, M., Namer, M., O’Shaughnessy, J.A., Shen, Z.Z. and Albain, K.S. (2005). The global breast cancer burden: variations in epidemiology and survival. *Clinical Breast Cancer*. **6**(5): 391–401.
- Hsieh, T.-H., Tsai, C.-F., Hsu, C.-Y., Kuo, P.-L., Lee, J.-N., Chai, C.-Y., Wang, S.-C. and Tsai, E.-M. (2012). Phthalates induce proliferation and invasiveness of estrogen receptor-negative breast cancer through the AhR/HDAC6/c-Myc signaling pathway. *FASEB journal : official publication of the Federation of American Societies for Experimental Biology*. **26**(2): 778–787.
- Hsu, S.C., Galceran, J. and Grosschedl, R. (1998). Modulation of transcriptional regulation by LEF-1 in response to Wnt-1 signaling and association with beta-catenin. *Molecular and Cellular Biology*. **18**(8): 4807–4818.
- Hu, X. and Beeton, C. (2010). Detection of functional matrix metalloproteinases by zymography. *Journal of Visualized Experiments*. (45): 2445.
- Hu, Z. and Xie, L. (2015). LHX6 inhibits breast cancer cell proliferation and invasion via repression of the Wnt/beta-catenin signaling pathway. *Molecular Medicine Reports*. **12**(3): 4634–4639.
- Huang, H., Du, G., Zhang, W., Hu, J., Wu, D., Song, L., Xia, Y. and Wang, X. (2014). The in vitro estrogenic activities of triclosan and triclocarban. *Journal of Applied Toxicology*. **34**(9): 1060–1067.

- Hulka, B.S. and Moorman, P.G. (2001). Breast cancer: hormones and other risk factors. *Maturitas*. **38**(1): 103–106.
- Hulkower, K.I. and Herber, R.L. (2011). Cell Migration and Invasion Assays as Tools for Drug Discovery. *Pharmaceutics*. **3**(1): 107–124.
- Hunt, N.C., Douglas-Jones, A.G., Jasani, B., Morgan, J.M. and Pignatelli, M. (1997). Loss of E-cadherin expression associated with lymph node metastases in small breast carcinomas. *Virchows Archiv : an international journal of pathology*. **430**(4): 285–289.
- Hwang, S., Zimmerman, N.P., Agle, K.A., Turner, J.R., Kumar, S.N. and Dwinell, M.B. (2012). E-cadherin Is Critical for Collective Sheet Migration and Is Regulated by the Chemokine CXCL12 Protein During Restitution. *The Journal of Biological Chemistry*. **287**(26): 22227–22240.
- In, S.-J., Kim, S.-H., Go, R.-E., Hwang, K.-A. and Choi, K.-C. (2015). Benzophenone-1 and nonylphenol stimulated MCF-7 breast cancer growth by regulating cell cycle and metastasis-related genes via an estrogen receptor alpha-dependent pathway. *Journal of Toxicology and Environmental Health. Part A*. **78**(8): 492–505.
- Inui, M., Adachi, T., Takenaka, S., Inui, H., Nakazawa, M., Ueda, M., Watanabe, H., Mori, C., Iguchi, T. and Miyatake, K. (2003). Effect of UV screens and preservatives on vitellogenin and choriogenin production in male medaka (*Oryzias latipes*). *Toxicology*. **194**(1-2): 43–50.
- Ioachim, E., Kamina, S., Kontostolis, M. and Agnantis, N.J. (1997). Immunohistochemical expression of cathepsin D in correlation with extracellular matrix component, steroid receptor status and proliferative indices in breast cancer. *Virchows Archiv: An International Journal of Pathology*. **431**(5): 311–316.
- Jain, P., Worthylake, R.A. and Alahari, S.K. (2012). Quantitative Analysis of Random Migration of Cells Using Time-lapse Video Microscopy. *Journal of Visualized Experiments*. (63): 3585.
- Jakowlew, S.B., Breathnach, R., Jeltsch, J.M., Masiakowski, P. and Chambon, P. (1984). Sequence of the pS2 mRNA induced by estrogen in the human breast cancer cell line MCF-7. *Nucleic Acids Research*. **12**(6): 2861–2878.

- Janjua, N.R., Kongshoj, B., Andersson, A.-M. and Wulf, H.C. (2008). Sunscreens in human plasma and urine after repeated whole-body topical application. *Journal of the European Academy of Dermatology and Venereology*. **22**(4): 456–461.
- Janjua, N.R., Mogensen, B., Andersson, A.-M., Petersen, J.H., Henriksen, M., Skakkebaek, N.E. and Wulf, H.C. (2004). Systemic absorption of the sunscreens benzophenone-3, octyl-methoxycinnamate, and 3-(4-methyl-benzylidene) camphor after whole-body topical application and reproductive hormone levels in humans. *The Journal of Investigative Dermatology*. **123**(1): 57–61.
- Janjua, N.R., Mortensen, G.K., Andersson, A.-M., Kongshoj, B., Skakkebaek, N.E. and Wulf, H.C. (2007). Systemic uptake of diethyl phthalate, dibutyl phthalate, and butyl paraben following whole-body topical application and reproductive and thyroid hormone levels in humans. *Environmental Science & Technology*. **41**(15): 5564–5570.
- Jarry, H., Christoffel, J., Rimoldi, G., Koch, L. and Wuttke, W. (2004). Multi-organic endocrine disrupting activity of the UV screen benzophenone 2 (BP2) in ovariectomized adult rats after 5 days treatment. *Toxicology*. **205**(1-2): 87–93.
- Jarvinen, T.A., Pelto-Huikko, M., Holli, K. and Isola, J. (2000). Estrogen receptor beta is coexpressed with ERalpha and PR and associated with nodal status, grade, and proliferation rate in breast cancer. *The American Journal of Pathology*. **156**(1): 29–35.
- Jeon, H.-K., Sarma, S.N., Kim, Y.-J. and Ryu, J.-C. (2008). Toxicokinetics and metabolisms of benzophenone-type UV filters in rats. *Toxicology*. **248**(2-3): 89–95.
- Jeschke, U., Mylonas, I., Kuhn, C., Shabani, N., Kunert-Keil, C., Schindlbeck, C., Gerber, B. and Friese, K. (2007). Expression of E-cadherin in human ductal breast cancer carcinoma in situ, invasive carcinomas, their lymph node metastases, their distant metastases, carcinomas with recurrence and in recurrence. *Anticancer Research*. **27**(4A): 1969–1974.
- Jiang, R., Roberts, M.S., Collins, D.M. and Benson, H.A. (1999). Absorption of sunscreens across human skin: an evaluation of commercial products for children and adults. *British Journal of Clinical Pharmacology*. **48**(4): 635–637.
- Jimenez-Diaz, I., Molina-Molina, J.M., Zafra-Gomez, A., Ballesteros, O., Navalon, A., Real, M., Saenz, J.M., Fernandez, M.F. and Olea, N. (2013). Simultaneous determination of the UV-filters benzyl salicylate, phenyl salicylate, octyl salicylate, homosalate, 3-(4-methylbenzylidene) camphor and 3-benzylidene camphor in human placental tissue by

- LC-MS/MS. Assessment of their in vitro endocrine activity. *Journal of Chromatography B, Analytical Technologies in the Biomedical and Life Sciences*. **936**: 80–87.
- Jimenez-Salazar, J.E., Posadas-Rodriguez, P., Lazzarini-Lechuga, R.C., Luna-Lopez, A., Zentella-Dehesa, A., Gomez-Quiroz, L.E., Konigsberg, M., Dominguez-Gomez, G. and Damian-Matsumura, P. (2014). Membrane-initiated estradiol signaling of epithelial-mesenchymal transition-associated mechanisms through regulation of tight junctions in human breast cancer cells. *Hormones & Cancer*. **5**(3): 161–173.
- Jones, P.A., Baker, V.A., Irwin, A.J. and Earl, L.K. (1998). Interpretation of the in vitro proliferation response of MCF-7 cells to potential oestrogens and non-oestrogenic substances. *Toxicology in vitro: an international journal published in association with BIBRA*. **12**(4): 373–382.
- Jordan, V.C. (2006). Tamoxifen (ICI46,474) as a targeted therapy to treat and prevent breast cancer. *British Journal of Pharmacology*. **147**(Suppl-1): S269–276.
- Jordan, V.C., Mittal, S., Gosden, B., Koch, R. and Lieberman, M.E. (1985). Structure-activity relationships of estrogens. *Environmental Health Perspectives*. **61**: 97–110.
- Jørgensen, M., Vendelbo, B., Skakkebaek, N.E. and Leffers, H. (2000). Assaying estrogenicity by quantitating the expression levels of endogenous estrogen-regulated genes. *Environmental Health Perspectives*. **108**(5): 403–412.
- Jung, E.-M., An, B.-S., Yang, H., Choi, K.-C. and Jeung, E.-B. (2012). Biomarker genes for detecting estrogenic activity of endocrine disruptors via estrogen receptors. *International Journal of Environmental Research and Public Health*. **9**(3): 698–711.
- Jurado, A., Gago-Ferrero, P., Vázquez-Suñé, E., Carrera, J., Pujades, E., Díaz-Cruz, M.S. and Barceló, D. (2014). Urban groundwater contamination by residues of UV filters. *Journal of Hazardous Materials*. **271**: 141–149.
- Kahlert, U.D., Maciaczyk, D., Doostkam, S., Orr, B.A., Simons, B., Bogiel, T., Reithmeier, T., Prinz, M., Schubert, J., Niedermann, G., Brabletz, T., Eberhart, C.G., Nikkhah, G. and Maciaczyk, J. (2012). Activation of canonical WNT/ $\beta$ -catenin signaling enhances in vitro motility of glioblastoma cells by activation of ZEB1 and other activators of epithelial-to-mesenchymal transition. *Cancer Letters*. **325**(1): 42–53.

- Kalluri, R. and Weinberg, R.A. (2009). The basics of epithelial-mesenchymal transition. *The Journal of Clinical Investigation*. **119**(6): 1420–1428.
- Karey, K.P. and Sirbasku, D.A. (1988). Differential responsiveness of human breast cancer cell lines MCF-7 and T47D to growth factors and 17beta-estradiol. *Cancer Research*. **48**(14): 4083–4092.
- Katzenellenbogen, B.S., Choi, I., Delage-Mourroux, R., Ediger, T.R., Martini, P.G., Montano, M., Sun, J., Weis, K. and Katzenellenbogen, J.A. (2000). Molecular mechanisms of estrogen action: selective ligands and receptor pharmacology. *The Journal of Steroid Biochemistry and Molecular Biology*. **74**(5): 279–285.
- Katzenellenbogen, B.S., Kendra, K.L., Norman, M.J. and Berthois, Y. (1987). Proliferation, hormonal responsiveness, and estrogen receptor content of MCF-7 human breast cancer cells grown in the short-term and long-term absence of estrogens. *Cancer Research*. **47**(16): 4355–4360.
- Katzenellenbogen, J.A. (1995). The structural pervasiveness of estrogenic activity. *Environmental Health Perspectives*. **103** (Suppl-7): 99–101.
- Katzenellenbogen, J.A., O'Malley, B.W. and Katzenellenbogen, B.S. (1996). Tripartite steroid hormone receptor pharmacology: interaction with multiple effector sites as a basis for the cell- and promoter-specific action of these hormones. *Molecular Endocrinology*. **10**(2): 119–131.
- Kemler, R. (1993). From cadherins to catenins: cytoplasmic protein interactions and regulation of cell adhesion. *Trends in Genetics*. **9**(9): 317–321.
- Kenny, P.A., Lee, G.Y., Myers, C.A., Neve, R.M., Semeiks, J.R., Spellman, P.T., Lorenz, K., Lee, E.H., Barcellos-Hoff, M.H., Petersen, O.W., Gray, J.W. and Bissell, M.J. (2007). The morphologies of breast cancer cell lines in three-dimensional assays correlate with their profiles of gene expression. *Molecular Oncology*. **1**(1): 84–96.
- Kerdivel, G., Le Guevel, R., Habauzit, D., Brion, F., Ait-Aissa, S. and Pakdel, F. (2013). Estrogenic potency of benzophenone UV filters in breast cancer cells: proliferative and transcriptional activity substantiated by docking analysis. *PloS one*. **8**(4): e60567.
- Kessenbrock, K., Plaks, V. and Werb, Z. (2010). Matrix Metalloproteinases: Regulators of the Tumor Microenvironment. *Cell*. **141**(1): 52–67.

- Key, T.J., Verkasalo, P.K. and Banks, E. (2001). Epidemiology of breast cancer. *The Lancet. Oncology*. **2**(3): 133–140.
- Keydar, I., Chen, L., Karby, S., Weiss, F.R., Delarea, J., Radu, M., Chaitcik, S. and Brenner, H.J. (1979). Establishment and characterization of a cell line of human breast carcinoma origin. *European Journal of Cancer*. **15**(5): 659–670.
- Khanna, S., Dash, P.R. and Darbre, P.D. (2014). Exposure to parabens at the concentration of maximal proliferative response increases migratory and invasive activity of human breast cancer cells in vitro. *Journal of Applied Toxicology*. **34**(9): 1051–1059.
- Kida, N., Yoshimura, T., Mori, K. and Hayashi, K. (1989). Hormonal regulation of synthesis and secretion of pS2 protein relevant to growth of human breast cancer cells (MCF-7). *Cancer Research*. **49**(13): 3494–3498.
- Kim, J.J., Ha, A.W., Kim, H.S. and Kim, W.K. (2011). Inorganic sulfur reduces the motility and invasion of MDA-MB-231 human breast cancer cells. *Nutrition Research and Practice*. **5**(5): 375–380.
- Kim, T.H., Shin, B.S., Kim, K.-B., Shin, S.W., Seok, S.H., Kim, M.K., Kim, E.J., Kim, D., Kim, M.G., Park, E.-S., Kim, J.-Y. and Yoo, S.D. (2014). Percutaneous absorption, disposition, and exposure assessment of homosalate, a UV filtering agent, in rats. *Journal of Toxicology and Environmental Health. Part A*. **77**(4): 202–213.
- Kiyama, R. and Wada-Kiyama, Y. (2015). Estrogenic endocrine disruptors: Molecular mechanisms of action. *Environment International*. **83**: 11–40.
- Klammer, H., Schlecht, C., Wuttke, W. and Jarry, H. (2005). Multi-organic risk assessment of estrogenic properties of octyl-methoxycinnamate in vivo A 5-day sub-acute pharmacodynamic study with ovariectomized rats. *Toxicology*. **215**(1-2): 90–6.
- Klammer, H., Schlecht, C., Wuttke, W., Schmutzler, C., Gotthardt, I., Kohrle, J. and Jarry, H. (2007). Effects of a 5-day treatment with the UV-filter octyl-methoxycinnamate (OMC) on the function of the hypothalamo-pituitary-thyroid function in rats. *Toxicology*. **238**(2-3): 192–199.
- Klein-Hitpass, L., Schorpp, M., Wagner, U. and Ryffel, G.U. (1986). An estrogen-responsive element derived from the 5' flanking region of the *Xenopus vitellogenin A2* gene functions in transfected human cells. *Cell*. **46**(7): 1053–1061.

- Kleinman, H.K. and Martin, G.R. (2005). Matrigel: basement membrane matrix with biological activity. *Seminars in Cancer Biology*. **15**(5): 378–386.
- Kleuser, B., Malek, D., Gust, R., Pertz, H.H. and Potteck, H. (2008). 17Beta-estradiol inhibits transforming growth factor-beta signaling and function in breast cancer cells via activation of extracellular signal-regulated kinase through the G protein-coupled receptor 30. *Molecular Pharmacology*. **74**(6): 1533–1543.
- Klinge, C.M., Brolly, C.L., Bambara, R.A. and Hilf, R. (1997). hsp70 is not required for high affinity binding of purified calf uterine estrogen receptor to estrogen response element DNA in vitro. *The Journal of Steroid Biochemistry and Molecular Biology*. **63**(4-6): 283–301.
- Klymkowsky, M.W. and Savagner, P. (2009). Epithelial-mesenchymal transition: a cancer researcher's conceptual friend and foe. *The American Journal of Pathology*. **174**(5): 1588–1593.
- Knowlden, J.M., Hutcheson, I.R., Jones, H.E., Madden, T., Gee, J.M.W., Harper, M.E., Barrow, D., Wakeling, A.E. and Nicholson, R.I. (2003). Elevated levels of epidermal growth factor receptor/c-erbB2 heterodimers mediate an autocrine growth regulatory pathway in tamoxifen-resistant MCF-7 cells. *Endocrinology*. **144**(3): 1032–1044.
- Ko, A., Kang, H.-S., Park, J.-H., Kwon, J.-E., Moon, G.I., Hwang, M.-S. and Hwang, I.G. (2016). The Association Between Urinary Benzophenone Concentrations and Personal Care Product Use in Korean Adults. *Archives of Environmental Contamination and Toxicology*. **70**(4): 640–646.
- Kohrmann, A., Kammerer, U., Kapp, M., Dietl, J. and Anacker, J. (2009). Expression of matrix metalloproteinases (MMPs) in primary human breast cancer and breast cancer cell lines: New findings and review of the literature. *BMC Cancer*. **9**: 188.
- Korah, R., Boots, M. and Wieder, R. (2004). Integrin alpha5beta1 promotes survival of growth-arrested breast cancer cells: an in vitro paradigm for breast cancer dormancy in bone marrow. *Cancer Research*. **64**(13): 4514–4522.
- Kortenkamp, A. (2007). Ten years of mixing cocktails: a review of combination effects of endocrine-disrupting chemicals. *Environmental Health Perspectives*. **115**: 98–105.

- Kousidou, O.C., Berdiaki, A., Kletsas, D., Zafiropoulos, A., Theocharis, A.D., Tzanakakis, G.N. and Karamanos, N.K. (2008). Estradiol-estrogen receptor: a key interplay of the expression of syndecan-2 and metalloproteinase-9 in breast cancer cells. *Molecular Oncology*. **2**(3): 223–232.
- Kow, L.-M. and Pfaff, D.W. (2016). Rapid estrogen actions on ion channels: A survey in search for mechanisms. *Steroids*. **111**: 46–53.
- Krause, M., Klit, A., Blomberg Jensen, M., Soeborg, T., Frederiksen, H., Schlumpf, M., Lichtensteiger, W., Skakkebaek, N.E. and Drzewiecki, K.T. (2012). Sunscreens: are they beneficial for health? An overview of endocrine disrupting properties of UV-filters. *International Journal of Andrology*. **35**(3): 424–436.
- Kunz, P.Y. and Fent, K. (2006). Estrogenic activity of UV filter mixtures. *Toxicology and Applied Pharmacology*. **217**(1): 86–99.
- Kunz, P.Y., Galicia, H.F. and Fent, K. (2006). Comparison of in vitro and in vivo estrogenic activity of UV filters in fish. *Toxicological Sciences : an official journal of the Society of Toxicology*. **90**(2): 349–361.
- Lai, A., Sarcevic, B., Prall, O.W. and Sutherland, R.L. (2001). Insulin/insulin-like growth factor-I and estrogen cooperate to stimulate cyclin E-Cdk2 activation and cell Cycle progression in MCF-7 breast cancer cells through differential regulation of cyclin E and p21(WAF1/Cip1). *The Journal of Biological Chemistry*. **276**(28): 25823–25833.
- Lamouille, S., Xu, J. and Derynck, R. (2014). Molecular mechanisms of epithelial-mesenchymal transition. *Nature Reviews. Molecular Cell Biology*. **15**(3): 178–196.
- Landau-Ossondo, M., Rabia, N., Jos-Pelage, J., Marquet, L.M., Isidore, Y., Saint-Aime, C., Martin, M., Irigaray, P. and Belpomme, D. (2009). Why pesticides could be a common cause of prostate and breast cancers in the French Caribbean Island, Martinique. An overview on key mechanisms of pesticide-induced cancer. *Biomedicine & Pharmacotherapy*. **63**(6): 383–395.
- Larsen, M., Artym, V. V, Green, J.A. and Yamada, K.M. (2006). The matrix reorganized: extracellular matrix remodeling and integrin signaling. *Current Opinion in Cell Biology*. **18**(5): 463–471.

- Latha, M.S., Martis, J., Shobha, V., Sham Shinde, R., Bangera, S., Krishnankutty, B., Bellary, S., Varughese, S., Rao, P. and Naveen Kumar, B.R. (2013). Sunscreening Agents: A Review. *The Journal of Clinical and Aesthetic Dermatology*. **6**(1): 16–26.
- Lee, A. V, Jackson, J.G., Gooch, J.L., Hilsenbeck, S.G., Coronado-Heinsohn, E., Osborne, C.K. and Yee, D. (1999). Enhancement of insulin-like growth factor signaling in human breast cancer: estrogen regulation of insulin receptor substrate-1 expression in vitro and in vivo. *Molecular Endocrinology*. **13**(5): 787–796.
- Lee, J.M., Dedhar, S., Kalluri, R. and Thompson, E.W. (2006). The epithelial–mesenchymal transition: new insights in signaling, development, and disease. *The Journal of Cell Biology*. **172**(7): 973–981.
- De Leeuw, W.J., Berx, G., Vos, C.B., Peterse, J.L., Van de Vijver, M.J., Litvinov, S., Van Roy, F., Cornelisse, C.J. and Cleton-Jansen, A.M. (1997). Simultaneous loss of E-cadherin and catenins in invasive lobular breast cancer and lobular carcinoma in situ. *The Journal of Pathology*. **183**(4): 404–411.
- Lewis-Wambi, J.S., Cunliffe, H.E., Kim, H.R., Willis, A.L. and Jordan, V.C. (2008). Overexpression of CEACAM6 promotes migration and invasion of oestrogen deprived breast cancer cells. *European Journal of Cancer*. **44**(12): 1770–1779.
- Li, C., Yanqun, T., Juhui, Q., Yiming, Z., Xiangdong, L., Linlin, Z. and Guixue, W. (2014). Effects of Type I Collagen and Fibronectin on Regulation of Breast Cancer Cell Biological and Biomechanical Characteristics. *Journal of Medical and Biological Engineering*. **34**(1): 62-68.
- Li, Y., Wang, J.-P., Santen, R.J., Kim, T.-H., Park, H., Fan, P. and Yue, W. (2010). Estrogen stimulation of cell migration involves multiple signaling pathway interactions. *Endocrinology*. **151**(11): 5146–5156.
- Liang, C.-C., Park, A.Y. and Guan, J.-L. (2007). In vitro scratch assay: a convenient and inexpensive method for analysis of cell migration in vitro. *Nature Protocols*. **2**(2): 329–333.
- Liao, X.-H., Lu, D.-L., Wang, N., Liu, L.-Y., Wang, Y., Li, Y.-Q., Yan, T.-B., Sun, X.-G., Hu, P. and Zhang, T.-C. (2014). Estrogen receptor alpha mediates proliferation of breast cancer MCF-7 cells via a p21/PCNA/E2F1-dependent pathway. *The FEBS Journal*. **281**(3): 927–942.

- Limame, R., Wouters, A., Pauwels, B., Franssen, E., Peeters, M., Lardon, F., De Wever, O. and Pauwels, P. (2012). Comparative Analysis of Dynamic Cell Viability, Migration and Invasion Assessments by Novel Real-Time Technology and Classic Endpoint Assays. *PLoS ONE*. **7**(10): e46536.
- Lin, S.Y., Xia, W., Wang, J.C., Kwong, K.Y., Spohn, B., Wen, Y., Pestell, R.G. and Hung, M.C. (2000). Beta-catenin, a novel prognostic marker for breast cancer: its roles in cyclin D1 expression and cancer progression. *Proceedings of the National Academy of Sciences of the United States of America*. **97**(8): 4262–4266.
- Lin, Y., Yang, Z., Xu, A., Dong, P., Huang, Y., Liu, H., Li, F., Wang, H., Xu, Q., Wang, Y., Sun, D., Zou, Y., Zou, X., Wang, Y., Zhang, D., Liu, H., Wu, X., Zhang, M., Fu, Y., Cai, Z., Liu, C. and Wu, S. (2015). PIK3R1 negatively regulates the epithelial-mesenchymal transition and stem-like phenotype of renal cancer cells through the AKT/GSK3beta/CTNNB1 signaling pathway. *Scientific Reports*. **5**: 8997.
- Lin, Y.-C., Lee, Y.-C., Li, L.-H., Cheng, C.-J. and Yang, R.-B. (2014). Tumour suppressor SCUBE2 inhibits breast-cancer cell migration and invasion through the reversal of epithelial-mesenchymal transition. *Journal of Cell Science*. **127**(Pt 1): 85–100.
- Lippman, M., Monaco, M.E. and Bolan, G. (1977). Effects of estrone, estradiol, and estriol on hormone-responsive human breast cancer in long-term tissue culture. *Cancer Research*. **37**(6): 1901–1907.
- Lippman, M.E. and Dickson, R.B. (1989). Mitogenic regulation of normal and malignant breast epithelium. *The Yale Journal of Biology and Medicine*. **62**(5): 459–480.
- Lippman, M.E., Dickson, R.B., Gelmann, E.P., Rosen, N., Knabbe, C., Bates, S., Bronzert, D., Huff, K. and Kasid, A. (1987). Growth regulation of human breast carcinoma occurs through regulated growth factor secretion. *Journal of Cellular Biochemistry*. **35**(1): 1–16.
- Liu, J.S. and Gartner, Z.J. (2012). Directing the assembly of spatially organized multicomponent tissues from the bottom up. *Trends in Cell Biology*. **22**(12): 683–91.
- Liu, X., Huang, H., Remmers, N. and Hollingsworth, M.A. (2014). Loss of E-cadherin and epithelial to mesenchymal transition is not required for cell motility in tissues or for metastasis. *Tissue Barriers*. **2**(4): e969112.

- Livak, K.J. and Schmittgen, T.D. (2001). Analysis of relative gene expression data using real-time quantitative PCR and the  $2^{-\Delta\Delta CT}$  method. *Methods*. **25**(4): 402–408.
- Longhurst, C.M. and Jennings, L.K. (1998). Integrin-mediated signal transduction. *Cellular and Molecular Life Sciences*. **54**(6): 514–526.
- Lower, E.E., Glass, E.L., Bradley, D.A., Blau, R. and Heffelfinger, S. (2005). Impact of metastatic estrogen receptor and progesterone receptor status on survival. *Breast Cancer Research and Treatment*. **90**(1): 65–70.
- Lu, M., Mira-y-Lopez, R., Nakajo, S., Nakaya, K. and Jing, Y. (2005). Expression of estrogen receptor alpha, retinoic acid receptor alpha and cellular retinoic acid binding protein II genes is coordinately regulated in human breast cancer cells. *Oncogene*. **24**(27): 4362–4369.
- Luo, J. and Cantley, L.C. (2005). The negative regulation of phosphoinositide 3-kinase signaling by p85 and its implication in cancer. *Cell Cycle*. **4**(10): 1309–1312.
- Lykkesfeldt, A.E., Larsen, S.S. and Briand, P. (1995). Human breast cancer cell lines resistant to pure anti-estrogens are sensitive to tamoxifen treatment. *International Journal of Cancer*. **61**(4): 529–534.
- Lymperatou, D., Giannopoulou, E., Koutras, A.K. and Kalofonos, H.P. (2013). The exposure of breast cancer cells to fulvestrant and tamoxifen modulates cell migration differently. *BioMed Research International*. **2013**: 147514.
- Ma, H. and Gollahon, L.S. (2016). ERalpha Mediates Estrogen-Induced Expression of the Breast Cancer Metastasis Suppressor Gene BRMS1. *International Journal of Molecular Sciences*. **17**(2): 158.
- Malek, D., Gust, R. and Kleuser, B. (2006). 17- $\beta$ -estradiol inhibits transforming-growth-factor- $\beta$ -induced MCF-7 cell migration by Smad3-repression. *European Journal of Pharmacology*. **534**(1): 39–47.
- Malhotra, G.K., Zhao, X., Band, H. and Band, V. (2010). Histological, molecular and functional subtypes of breast cancers. *Cancer Biology & Therapy*. **10**(10): 955–960.
- Manders, J.B. and Gradishar, W.J. (2005). The evolving role of endocrine therapy for early stage breast cancer. *Breast Cancer*. **12**(2): 62–72.

- Manders, K., van de Poll-Franse, L. V, Creemers, G.-J., Vreugdenhil, G., van der Sangen, M.J.C., Nieuwenhuijzen, G.A.P., Roumen, R.M.H. and Voogd, A.C. (2006). Clinical management of women with metastatic breast cancer: a descriptive study according to age group. *BMC Cancer*. **6**: 179.
- Manová, E., von Goetz, N., Hauri, U., Bogdal, C. and Hungerbühler, K. (2013). Organic UV filters in personal care products in Switzerland: a survey of occurrence and concentrations. *International Journal of Hygiene and Environmental Health*. **216**(4): 508–514.
- Maor, S., Mayer, D., Yarden, R.I., Lee, A. V, Sarfstein, R., Werner, H. and Papa, M.Z. (2006). Estrogen receptor regulates insulin-like growth factor-I receptor gene expression in breast tumour cells: involvement of transcription factor Sp1. *The Journal of Endocrinology*. **191**(3): 605–612.
- Marchbank, T., Westley, B.R., May, F.E., Calnan, D.P. and Playford, R.J. (1998). Dimerization of human pS2 (TFF1) plays a key role in its protective/healing effects. *The Journal of Pathology*. **185**(2): 153–158.
- Martin, T.A., Ye, L., Sanders, A.J., Lane, J. and Jiang, W.G. (2013). Cancer Invasion and Metastasis: Molecular and Cellular Perspective In: R. Jandial, ed. *Metastatic Cancer: Clinical and Biological Perspectives*. Cardiff: *Landes Bioscience*.
- Masamura, S. Santer, S.J., Heitjan, D.F. and Santen, R.J. (1995). Estrogen deprivation causes estradiol hypersensitivity in human breast cancer cells. *The Journal of Clinical Endocrinology and Metabolism*. **80**(10): 2918–2925.
- Masiakowski, P., Breathnach, R., Bloch, J., Gannon, F., Krust, A. and Chambon, P. (1982). Cloning of cDNA sequences of hormone-regulated genes from the MCF-7 human breast cancer cell line. *Nucleic Acids Research*. **10**(24): 7895–7903.
- Massague, J. (2008). TGFbeta in Cancer. *Cell*. **134**(2): 215–230.
- Matsuda, T., Yamamoto, T., Muraguchi, A. and Saaticioglu, F. (2001). Cross-talk between transforming growth factor-beta and estrogen receptor signaling through Smad3. *The Journal of Biological Chemistry*. **276**(46): 42908–42914.
- Mawson, A., Lai, A., Carroll, J.S., Sergio, C.M., Mitchell, C.J. and Sarcevic, B. (2005). Estrogen and insulin/IGF-1 cooperatively stimulate cell cycle progression in MCF-7

- breast cancer cells through differential regulation of c-Myc and cyclin D1. *Molecular and Cellular Endocrinology*. **229**(1-2): 161–73.
- May, C.D., Sphyris, N., Evans, K.W., Werden, S.J., Guo, W. and Mani, S.A. (2011). Epithelial-mesenchymal transition and cancer stem cells: a dangerously dynamic duo in breast cancer progression. *Breast Cancer Research*. **13**(1): 202.
- May, F.E. and Westley, B.R. (1986). Cloning of estrogen-regulated messenger RNA sequences from human breast cancer cells. *Cancer Research*. **46**(12 Pt 1): 6034–6040.
- May, F.E. and Westley, B.R. (1997). Trefoil proteins: their role in normal and malignant cells. *The Journal of Pathology*. **183**(1): 4–7.
- McClelland, R.A., Barrow, D., Madden, T.A., Dutkowski, C.M., Pamment, J., Knowlden, J.M., Gee, J.M. and Nicholson, R.I. (2001). Enhanced epidermal growth factor receptor signaling in MCF7 breast cancer cells after long-term culture in the presence of the pure antiestrogen ICI 182,780 (Faslodex). *Endocrinology*. **142**(7): 2776–2788.
- McDevitt, M.A., Glidewell-Kenney, C., Jimenez, M.A., Ahearn, P.C., Weiss, J., Jameson, J.L. and Levine, J.E. (2008). New insights into the classical and non-classical actions of estrogen: evidence from estrogen receptor knock-out and knock-in mice. *Molecular and Cellular Endocrinology*. **290**(1-2): 24–30.
- McPherson, K., Steel, C.M. and Dixon, J.M. (2000). ABC of breast diseases. Breast cancer-epidemiology, risk factors, and genetics. *British Medical Journal*. **321**(7261): 624–628.
- Mehner, C., Hockla, A., Miller, E., Ran, S., Radisky, D.C. and Radisky, E.S. (2014). Tumor cell-produced matrix metalloproteinase 9 (MMP-9) drives malignant progression and metastasis of basal-like triple negative breast cancer. *Oncotarget*. **5**(9): 2736–2749.
- Mense, S.M., Remotti, F., Bhan, A., Singh, B., El-Tamer, M., Hei, T.K. and Bhat, H.K. (2008). Estrogen-induced breast cancer: alterations in breast morphology and oxidative stress as a function of estrogen exposure. *Toxicology and Applied Pharmacology*. **232**(1): 78–85.
- Micalizzi, D.S., Farabaugh, S.M. and Ford, H.L. (2010). Epithelial-mesenchymal transition in cancer: parallels between normal development and tumor progression. *Journal of Mammary Gland Biology and Neoplasia*. **15**(2): 117–134.

- Miller, D., Wheals, B.B., Beresford, N. and Sumpter, J.P. (2001). Estrogenic activity of phenolic additives determined by an in vitro yeast bioassay. *Environmental Health Perspectives*. **109**(2): 133–138.
- Mints, M. and Souchelnytskyi, S. (2014). Impact of combinations of EGF, TGFbeta, 17beta-oestradiol, and inhibitors of corresponding pathways on proliferation of breast cancer cell lines. *Experimental Oncology*. **36**(2): 67–71.
- Missmer, S.A., Eliassen, A.H., Barbieri, R.L. and Hankinson, S.E. (2004). Endogenous estrogen, androgen, and progesterone concentrations and breast cancer risk among postmenopausal women. *Journal of the National Cancer Institute*. **96**(24): 1856–1865.
- Miyoshi, Y., Murase, K., Saito, M., Imamura, M. and Oh, K. (2010). Mechanisms of estrogen receptor-alpha upregulation in breast cancers. *Medical Molecular Morphology*. **43**(4): 193–196.
- Mohan, A.K., Hauptmann, M., Linet, M.S., Ron, E., Lubin, J.H., Freedman, D.M., Alexander, B.H., Boice, J.D.J., Doody, M.M. and Matanoski, G.M. (2002). Breast cancer mortality among female radiologic technologists in the United States. *Journal of the National Cancer Institute*. **94**(12): 943–948.
- Moll, R., Mitze, M., Frixen, U.H. and Birchmeier, W. (1993). Differential loss of E-cadherin expression in infiltrating ductal and lobular breast carcinomas. *The American Journal of Pathology*. **143**(6): 1731–1742.
- Mooney, L.M., Al-Sakkaf, K.A., Brown, B.L. and Dobson, P.R.M. (2002). Apoptotic mechanisms in T47D and MCF-7 human breast cancer cells. *British Journal of Cancer*. **87**(8): 909–917.
- Morohoshi, K., Yamamoto, H., Kamata, R., Shiraishi, F., Koda, T. and Morita, M. (2005). Estrogenic activity of 37 components of commercial sunscreen lotions evaluated by in vitro assays. *Toxicology in Vitro*. **19**(4): 457–469.
- Morton, P.E. and Parsons, M. (2011). Dissecting cell adhesion architecture using advanced imaging techniques. *Cell Adhesion & Migration*. **5**(4): 351–359.
- Mosselman, S., Polman, J. and Dijkema, R. (1996). ER beta: identification and characterization of a novel human estrogen receptor. *FEBS Letters*. **392**(1): 49–53.

- Mueller, S.O., Kling, M., Arifin Firzani, P., Mecky, A., Duranti, E., Shields-Botella, J., Delansorne, R., Broschard, T. and Kramer, P.-J. (2003). Activation of estrogen receptor alpha and ERbeta by 4-methylbenzylidene-camphor in human and rat cells: comparison with phyto- and xenoestrogens. *Toxicology Letters*. **142**(1-2): 89–101.
- Muscat, J.E., Britton, J.A., Djordjevic, M. V, Citron, M.L., Kemeny, M., Busch-Devereaux, E., Pittman, B. and Stellman, S.D. (2003). Adipose concentrations of organochlorine compounds and breast cancer recurrence in Long Island, New York. *Cancer Epidemiology, Biomarkers & Prevention*. **12**(12): 1474–1478.
- Musgrove, E.A., Lee, C.S., Buckley, M.F. and Sutherland, R.L. (1994). Cyclin D1 induction in breast cancer cells shortens G1 and is sufficient for cells arrested in G1 to complete the cell cycle. *Proceedings of the National Academy of Sciences of the United States of America*. **91**(17): 8022–8026.
- Nadal-Serrano, M., Sastre-Serra, J., Pons, D.G., Miro, A.M., Oliver, J. and Roca, P. (2012). The ERalpha/ERbeta ratio determines oxidative stress in breast cancer cell lines in response to 17beta-estradiol. *Journal of Cellular Biochemistry*. **113**(10): 3178–3185.
- Nagafuchi, A. and Takeichi, M. (1989). Transmembrane control of cadherin-mediated cell adhesion: a 94 kDa protein functionally associated with a specific region of the cytoplasmic domain of E-cadherin. *Cell Regulation*. **1**(1): 37–44.
- Nagase, H. and Woessner, J.F.J. (1999). Matrix metalloproteinases. *The Journal of Biological Chemistry*. **274**(31): 21491–21494.
- Nakagawa, Y. and Suzuki, T. (2002). Metabolism of 2-hydroxy-4-methoxybenzophenone in isolated rat hepatocytes and xenoestrogenic effects of its metabolites on MCF-7 human breast cancer cells. *Chemico-Biological Interactions*. **139**(2): 115–128.
- Nandi, S., Guzman, R.C. and Yang, J. (1995). Hormones and mammary carcinogenesis in mice, rats, and humans: a unifying hypothesis. *Proceedings of the National Academy of Sciences of the United States of America*. **92**(9): 3650–3657.
- Nelson, L.R. and Bulun, S.E. (2001). Estrogen production and action. *Journal of the American Academy of Dermatology*. **45**(3 Suppl): S116–124.
- Neve, R.M., Chin, K., Fridlyand, J., Yeh, J., Baehner, F.L., Fevr, T., Clark, L., Bayani, N., Coppe, J.-P., Tong, F., Speed, T., Spellman, P.T., DeVries, S., Lapuk, A., Wang, N.J.,

- Kuo, W.-L., Stilwell, J.L., Pinkel, D., Albertson, D.G., Waldman, F.M., McCormick, F., Dickson, R.B., Johnson, M.D., Lippman, M., Ethier, S., Gazdar, A. and Gray, J.W. (2006). A collection of breast cancer cell lines for the study of functionally distinct cancer subtypes. *Cancer Cell*. **10**(6): 515–527.
- Nguyen, D.X., Bos, P.D. and Massague, J. (2009). Metastasis: from dissemination to organ-specific colonization. *Nature Reviews. Cancer*. **9**(4): 274–284.
- Nguyen, V.T.M., Barozzi, I., Faronato, M., Lombardo, Y., Steel, J.H., Patel, N., Darbre, P., Castellano, L., Gyorffy, B., Woodley, L., Meira, A., Patten, D.K., Viricillo, V., Periyasamy, M., Ali, S., Frige, G., Minucci, S., Coombes, R.C. and Magnani, L. (2015). Differential epigenetic reprogramming in response to specific endocrine therapies promotes cholesterol biosynthesis and cellular invasion. *Nature Communications*. **6**: 10044.
- Niepel, M., Hafner, M., Pace, E.A., Chung, M., Chai, D.H., Zhou, L., Muhlich, J.L., Schoeberl, B. and Sorger, P.K. (2014). Analysis of growth factor signaling in genetically diverse breast cancer lines. *BMC Biology*. **12**: 20.
- Nieva, C., Marro, M., Santana-Codina, N., Rao, S., Petrov, D. and Sierra, A. (2012). The lipid phenotype of breast cancer cells characterized by Raman microspectroscopy: towards a stratification of malignancy. *PloS one*. **7**(10): e46456.
- Nicholas, M.W. and Nelson, K. (2013). North, South, or East? Blotting Techniques. *Journal of Investigative Dermatology*. **133**(7): 1–3.
- Nilsson, S., Makela, S., Treuter, E., Tujague, M., Thomsen, J., Andersson, G., Enmark, E., Pettersson, K., Warner, M. and Gustafsson, J.A. (2001). Mechanisms of estrogen action. *Physiological Reviews*. **81**(4): 1535–1565.
- Nilsson, U.W., Garvin, S. and Dabrosin, C. (2007). MMP-2 and MMP-9 activity is regulated by estradiol and tamoxifen in cultured human breast cancer cells. *Breast Cancer Research and Treatment*. **102**(3): 253–261.
- Nista, A., Leonetti, C., Bernardini, G., Mattioni, M. and Santoni, A. (1997). Functional role of alpha4beta1 and alpha5beta1 integrin fibronectin receptors expressed on adriamycin-resistant MCF-7 human mammary carcinoma cells. *International Journal of Cancer*. **72**(1): 133–141.

- Niu, D., Wang, G. and Wang, X. (2015). Up-regulation of cyclin E in breast cancer via estrogen receptor pathway. *International journal of clinical and experimental medicine*. **8**(1): 910–915.
- Novak, A. and Dedhar, S. (1999). Signaling through beta-catenin and Lef/Tcf. *Cellular and Molecular Life Sciences*. **56**(5-6): 523–537.
- Oesterreich, S., Deng, W., Jiang, S., Cui, X., Ivanova, M., Schiff, R., Kang, K., Hadsell, D.L., Behrens, J. and Lee, A. V (2003). Estrogen-mediated down-regulation of E-cadherin in breast cancer cells. *Cancer Research*. **63**(17): 5203–5208.
- Office for National Statistics (2016). Statistical bulletin: Cancer Registration Statistics, England: 2014. Available from:  
<http://www.ons.gov.uk/peoplepopulationandcommunity/healthandsocialcare/conditionsanddiseases/bulletins/cancerregistrationstatisticsengland/2014>.
- Ogba, N., Manning, N.G., Bliesner, B.S., Ambler, S.K., Haughian, J.M., Pinto, M.P., Jedlicka, P., Joensuu, K., Heikkilä, P. and Horwitz, K.B. (2014). Luminal breast cancer metastases and tumor arousal from dormancy are promoted by direct actions of estradiol and progesterone on the malignant cells. *Breast Cancer Research*. **16**(6): 489.
- Ohbayashi, M., Yasuda, M., Kawakami, I., Kohyama, N., Kobayashi, Y. and Yamamoto, T. (2008). Effect of interleukins response to ECM-induced acquisition of drug resistance in MCF-7 cells. *Experimental Oncology*. **30**(4): 276–282.
- Oka, H., Shiozaki, H., Kobayashi, K., Inoue, M., Tahara, H., Kobayashi, T., Takatsuka, Y., Matsuyoshi, N., Hirano, S. and Takeichi, M. (1993). Expression of E-cadherin cell adhesion molecules in human breast cancer tissues and its relationship to metastasis. *Cancer Research*. **53**(7): 1696–1701.
- Olea, N. and Fernandez, M. (2007). Endocrine disruption. *Journal of Epidemiology and Community Health*. **61**(5): 372–373.
- Olsen, C.M., Meussen-Elholm, E.T.M., Samuelsen, M., Holme, J.A. and Hongslo, J.K. (2003). Effects of the environmental oestrogens bisphenol A, tetrachlorobisphenol A, tetrabromobisphenol A, 4-hydroxybiphenyl and 4,4'-dihydroxybiphenyl on oestrogen receptor binding, cell proliferation and regulation of oestrogen sensitive proteins in the human. *Pharmacology & Toxicology*. **92**(4): 180–188.

- Oostenbrink, B.C., Pitera, J.W., MM, van L., Meerman, J.H. and WF, van G. (2000). Simulations of the estrogen receptor ligand-binding domain: affinity of natural ligands and xenoestrogens. *Journal of Medicinal Chemistry*. **43**(24): 4594–4605.
- Osborne, C.K., Hobbs, K. and Trent, J.M. (1987). Biological differences among MCF-7 human breast cancer cell lines from different laboratories. *Breast Cancer Research and Treatment*. **9**(2): 111–121.
- Osborne, C.K., Schiff, R., Fuqua, S.A. and Shou, J. (2001). Estrogen receptor: current understanding of its activation and modulation. *Clinical Cancer Research*. **7**(12 Suppl): 4338s–4342s; discussion 4411s–4412s.
- Oskarsson, T. (2013). Extracellular matrix components in breast cancer progression and metastasis. *The Breast*. **22**: S66–S72.
- Ozawa, M., Baribault, H. and Kemler, R. (1989). The cytoplasmic domain of the cell adhesion molecule uvomorulin associates with three independent proteins structurally related in different species. *The EMBO Journal*. **8**(6): 1711–1717.
- Papkoff, J., Rubinfeld, B., Schryver, B. and Polakis, P. (1996). Wnt-1 regulates free pools of catenins and stabilizes APC-catenin complexes. *Molecular and Cellular Biology*. **16**(5): 2128–2134.
- Parisini, E., Higgins, J.M.G., Liu, J., Brenner, M.B. and Wang, J. (2007). The crystal structure of human E-cadherin domains 1 and 2, and comparison with other cadherins in the context of adhesion mechanism. *Journal of Molecular Biology*. **373**(2): 401–411.
- Partin, A.W., Schoeniger, J.S., Mohler, J.L. and Coffey, D.S. (1989). Fourier analysis of cell motility: correlation of motility with metastatic potential. *Proceedings of the National Academy of Sciences of the United States of America*. **86**(4):1254–1258.
- Paruthiyil, S., Parmar, H., Kerekatte, V., Cunha, G.R., Firestone, G.L. and Leitman, D.C. (2004). Estrogen receptor beta inhibits human breast cancer cell proliferation and tumor formation by causing a G2 cell cycle arrest. *Cancer Research*. **64**(1): 423–428.
- Patel, S.D., Chen, C.P., Bahna, F., Honig, B. and Shapiro, L. (2003). Cadherin-mediated cell-cell adhesion: sticking together as a family. *Current Opinion in Structural Biology*. **13**(6): 690–698.

- Payne, J., Scholze, M. and Kortenkamp, A. (2001). Mixtures of four organochlorines enhance human breast cancer cell proliferation. *Environmental Health Perspectives*. **109**(4): 391–397.
- Pearce, S.T. and Jordan, V.C. (2004). The biological role of estrogen receptors alpha and beta in cancer. *Critical Reviews in Oncology/Hematology*. **50**(1): 3–22.
- Pecina-Slaus, N. (2003). Tumor suppressor gene E-cadherin and its role in normal and malignant cells. *Cancer Cell International*. **3**(1): 17.
- Perou, C.M. and Network, T.C.G.A. (2012). Comprehensive molecular portraits of human breast tumors. *Nature*. **490**(7418): 61–70.
- Perou, C.M., Sorlie, T., Eisen, M.B., van de Rijn, M., Jeffrey, S.S., Rees, C.A., Pollack, J.R., Ross, D.T., Johnsen, H., Akslen, L.A., Fluge, O., Pergamenschikov, A., Williams, C., Zhu, S.X., Lonning, P.E., Borresen-Dale, A.L., Brown, P.O. and Botstein, D. (2000). Molecular portraits of human breast tumours. *Nature*. **406**(6797): 747–752.
- Pharoah, P.D., Day, N.E., Duffy, S., Easton, D.F. and Ponder, B.A. (1997). Family history and the risk of breast cancer: a systematic review and meta-analysis. *International Journal of Cancer*. **71**(5): 800–809.
- Picotto, G., Vazquez, G. and Boland, R. (1999). 17beta-oestradiol increases intracellular Ca<sup>2+</sup> concentration in rat enterocytes. Potential role of phospholipase C-dependent store-operated Ca<sup>2+</sup> influx. *The Biochemical Journal*. **339** (Pt 1): 71–77.
- Pinkas, J. and Leder, P. (2002). MEK1 signaling mediates transformation and metastasis of EpH4 mammary epithelial cells independent of an epithelial to mesenchymal transition. *Cancer Research*. **62**(16): 4781–4790.
- Planas-Silva, M.D. and Waltz, P.K. (2007). Estrogen promotes reversible epithelial-to-mesenchymal-like transition and collective motility in MCF-7 breast cancer cells. *The Journal of Steroid Biochemistry and Molecular Biology*. **104**(1-2): 11–21.
- Planas-Silva, M.D. and Weinberg, R.A. (1997). Estrogen-dependent cyclin E-cdk2 activation through p21 redistribution. *Molecular and Cellular Biology*. **17**(7): 4059–4069.
- Poiger, T., Buser, H.-R., Balmer, M.E., Bergqvist, P.-A. and Muller, M.D. (2004). Occurrence of UV filter compounds from sunscreens in surface waters: regional mass balance in two Swiss lakes. *Chemosphere*. **55**(7): 951–963.

- Pontiggia, O., Sampayo, R., Raffo, D., Motter, A., Xu, R., Bissell, M.J., Joffé, E.B. de K. and Simian, M. (2012). The tumor microenvironment modulates tamoxifen resistance in breast cancer: a role for soluble stromal factors and fibronectin through  $\beta$ 1 integrin. *Breast Cancer Research and Treatment*. **133**(2): 459–471.
- Prall, O.W., Rogan, E.M. and Sutherland, R.L. (1998). Estrogen regulation of cell cycle progression in breast cancer cells. *The Journal of Steroid Biochemistry and Molecular Biology*. **65**(1-6): 169–174.
- Prasad, C.P., Mirza, S., Sharma, G., Prashad, R., DattaGupta, S., Rath, G. and Ralhan, R. (2008). Epigenetic alterations of CDH1 and APC genes: relationship with activation of Wnt/beta-catenin pathway in invasive ductal carcinoma of breast. *Life Sciences*. [Online]. **83**(9-10): 318–25.
- Pratt, W.B. (1992). Control of steroid receptor function and cytoplasmic-nuclear transport by heat shock proteins. *BioEssays: News and Reviews in Molecular, Cellular and Developmental Biology*. **14**(12): 841–848.
- Prest, S.J., May, F.E.B. and Westley, B.R. (2002). The estrogen-regulated protein, TFF1, stimulates migration of human breast cancer cells. *FASEB journal: official publication of the Federation of American Societies for Experimental Biology*. **16**(6): 592–594.
- Price, A.R.G. (1993). The Gulf: Human impacts and management initiatives. *Marine Pollution Bulletin*. **27**: 17–27.
- Radde, B.N., Ivanova, M.M., Mai, H.X., Salabei, J.K., Hill, B.G. and Klinge, C.M. (2015). Bioenergetic differences between MCF-7 and T47D breast cancer cells and their regulation by oestradiol and tamoxifen. *The Biochemical Journal*. **465**(1): 49–61.
- Radisky, E.S. and Radisky, D.C. (2010). Matrix metalloproteinase-induced epithelial-mesenchymal transition in breast cancer. *Journal of Mammary Gland Biology and Neoplasia*. **15**(2): 201–212.
- Rai, R., Shanmuga, S.C. and Srinivas, C.R. (2012). Update on Photoprotection. *Indian Journal of Dermatology*. **57**(5): 335–342.
- Rajah, T.T., Abidi, S.M., Rambo, D.J., Dmytryk, J.J. and Pentto, J.T. (1998). The motile behaviour of human breast cancer cells characterized by time-lapse video microscopy. *In vitro Cellular & Developmental Biology*. **34**(8): 626–628.

- Ratheesh, A. and Yap, A.S. (2012). A bigger picture: classical cadherins and the dynamic actin cytoskeleton. *Nature Reviews. Molecular Cell Biology*. **13**(10): 673–679.
- Razandi, M., Oh, P., Pedram, A., Schnitzer, J. and Levin, E.R. (2002). ERs associate with and regulate the production of caveolin: implications for signaling and cellular actions. *Molecular Endocrinology*. **16**(1): 100–115.
- Redig, A.J. and McAllister, S.S. (2013). Breast cancer as a systemic disease: a view of metastasis. *Journal of Internal Medicine*. **274**(2): 113–126.
- Ridley, A.J., Schwartz, M.A., Burridge, K., Firtel, R.A., Ginsberg, M.H., Borisy, G., Parsons, J.T. and Horwitz, A.R. (2003). Cell migration: integrating signals from front to back. *Science (New York, N.Y.)*. **302**(5651): 1704–1709.
- Rimm, D.L., Koslov, E.R., Kebriaei, P., Cianci, C.D. and Morrow, J.S. (1995). Alpha 1(E)-catenin is an actin-binding and -bundling protein mediating the attachment of F-actin to the membrane adhesion complex. *Proceedings of the National Academy of Sciences of the United States of America*. **92**(19): 8813–8817.
- Rio, M.C., Bellocq, J.P., Daniel, J.Y., Tomasetto, C., Lathe, R., Chenard, M.P., Batzenschlager, A. and Chambon, P. (1988). Breast cancer-associated pS2 protein: synthesis and secretion by normal stomach mucosa. *Science (New York, N.Y.)*. **241**(4866):705–708.
- Risinger, A.L., Dybdal-Hargreaves, N.F. and Mooberry, S.L. (2015). Breast Cancer Cell Lines Exhibit Differential Sensitivities to Microtubule-targeting Drugs Independent of Doubling Time. *Anticancer Research*. **35**(11): 5845–5850.
- La Rocca, G., Pucci-Minafra, I., Marrazzo, A., Taormina, P. and Minafra, S. (2004). Zymographic detection and clinical correlations of MMP-2 and MMP-9 in breast cancer sera. *British Journal of Cancer*. **90**(7): 1414–1421.
- Rochefort, H., Platet, N., Hayashido, Y., Derocq, D., Lucas, A., Cunat, S. and Garcia, M. (1998). Estrogen receptor mediated inhibition of cancer cell invasion and motility: an overview. *The Journal of Steroid Biochemistry and Molecular Biology*. **65**(1-6): 163–168.
- Rodriguez-Boulan, E. and Nelson, W.J. (1989). Morphogenesis of the polarized epithelial cell phenotype. *Science (New York, N.Y.)*. **245**(4919): 718–725.

- Rodriguez-Gomez, R., Zafra-Gomez, A., Dorival-Garcia, N., Ballesteros, O. and Navalon, A. (2015). Determination of benzophenone-UV filters in human milk samples using ultrasound-assisted extraction and clean-up with dispersive sorbents followed by UHPLC-MS/MS analysis. *Talanta*. **134**: 657–664.
- Roy, R., Yang, J. and Moses, M.A. (2009). Matrix metalloproteinases as novel biomarkers and potential therapeutic targets in human cancer. *Journal of Clinical Oncology : official journal of the American Society of Clinical Oncology*. **27**(31): 5287–5297.
- Russo, J., Hu, Y.-F., Yang, X. and Russo, I.H. (2000). Chapter 1: Developmental, Cellular, and Molecular Basis of Human Breast Cancer. *Journal of the National Cancer Institute Monographs*. **2000**(27): 17–37.
- Russo, J. and Russo, I.H. (2014). Histological Evaluation of the Normal Breast In: Techniques and Methodological Approaches in Breast Cancer Research. *Springer*. P. 301.
- Russo, J. and Russo, I.H. 2006. The role of estrogen in the initiation of breast cancer. *The Journal of Steroid Biochemistry and Molecular Biology*. **102**(1-5): 89–96.
- Russo, J. and Russo, I.H. (1994). Toward a Physiological Approach to Breast Cancer prevention. *Cancer Epidemiology, Biomarkers & Prevention*. **3**: 353–364.
- Ryde, C.M., Nicholls, J.E. and Dowsett, M. (1992). Steroid and growth factor modulation of aromatase activity in MCF7 and T47D breast carcinoma cell lines. *Cancer Research*. **52**(6): 1411–1415.
- Saceda, M., Lippman, M.E., Chambon, P., Lindsey, R.L., Ponglikitmongkol, M., Puente, M. and Martin, M.B. (1988). Regulation of the estrogen receptor in MCF-7 cells by estradiol. *Molecular Endocrinology (Baltimore, Md.)*. **2**(12): 1157–1162.
- Saha Roy, S. and Vadlamudi, R.K. (2012). Role of estrogen receptor signaling in breast cancer metastasis. *International Journal of Breast Cancer*. **2012**: 654698.
- Saji, S., Kawakami, M., Hayashi, S.-I., Yoshida, N., Hirose, M., Horiguchi, S.-I., Itoh, A., Funata, N., Schreiber, S.L., Yoshida, M. and Toi, M. (2005). Significance of HDAC6 regulation via estrogen signaling for cell motility and prognosis in estrogen receptor-positive breast cancer. *Oncogene*. **24**(28): 4531–4539.
- Sanchez-Tillo, E., Liu, Y., de Barrios, O., Siles, L., Fanlo, L., Cuatrecasas, M., Darling, D.S., Dean, D.C., Castells, A. and Postigo, A. (2012). EMT-activating transcription factors in

- cancer: beyond EMT and tumor invasiveness. *Cellular and Molecular Life Sciences*. **69**(20): 3429–3456.
- Santen, R.J., Song, R.X., Zhang, Z., Kumar, R., Jeng, M.-H., Masamura, A., Lawrence, J.J., Berstein, L. and Yue, W. (2005). Long-term estradiol deprivation in breast cancer cells up-regulates growth factor signaling and enhances estrogen sensitivity. *Endocrine-Related Cancer*. **12** (Suppl-1): S61–73.
- Sapino, A., Pietribiasi, F., Bussolati, G. and Marchisio, P.C. (1986). Estrogen- and tamoxifen-induced rearrangement of cytoskeletal and adhesion structures in breast cancer MCF-7 cells. *Cancer Research*. **46**(5): 2526–2531.
- Sato, H., Takino, T., Okada, Y., Cao, J., Shinagawa, A., Yamamoto, E. and Seiki, M. (1994). A matrix metalloproteinase expressed on the surface of invasive tumour cells. *Nature*. **370**(6484): 61–65.
- Sbardella, D., Fasciglione, G.F., Gioia, M., Ciaccio, C., Tundo, G.R., Marini, S. and Coletta, M. (2012). Human matrix metalloproteinases: an ubiquitous class of enzymes involved in several pathological processes. *Molecular Aspects of Medicine*. **33**(2): 119–208.
- Schafer, J.M., Lee, E.S., O'Regan, R.M., Yao, K. and Jordan, V.C. (2000). Rapid development of tamoxifen-stimulated mutant p53 breast tumors (T47D) in athymic mice. *Clinical Cancer Research: an official journal of the American Association for Cancer Research*. **6**(11): 4373–4380.
- Schairer, C., Mink, P.J., Carroll, L. and Devesa, S.S. (2004). Probabilities of death from breast cancer and other causes among female breast cancer patients. *Journal of the National Cancer Institute*. **96**(17): 1311–1321.
- Schlecht, C., Klammer, H., Frauendorf, H., Wuttke, W. and Jarry, H. (2008). Pharmacokinetics and metabolism of benzophenone 2 in the rat. *Toxicology*. **245**(1-2): 11–17.
- Schlumpf, M., Cotton, B., Conscience, M., Haller, V., Steinmann, B. and Lichtensteiger, W. (2001). In vitro and in vivo estrogenicity of UV screens. *Environmental Health Perspectives*. **109**(3): 239–244.
- Schlumpf, M., Kypke, K., Wittassek, M., Angerer, J., Mascher, H., Mascher, D., Vokt, C., Birchler, M. and Lichtensteiger, W. (2010). Exposure patterns of UV filters, fragrances,

- parabens, phthalates, organochlor pesticides, PBDEs, and PCBs in human milk: correlation of UV filters with use of cosmetics. *Chemosphere*. **81**(10): 1171–1183.
- Schlumpf, M., Schmid, P., Durrer, S., Conscience, M., Maerkel, K., Henseler, M., Gruetter, M., Herzog, I., Reolon, S., Ceccatelli, R., Faass, O., Stutz, E., Jarry, H., Wuttke, W. and Lichtensteiger, W. (2004). Endocrine activity and developmental toxicity of cosmetic UV filters-an update. *Toxicology*. **205**(1-2): 113–122.
- Schlumpf, M., Jarry, H., Wuttke, W., Ma, R. and Lichtensteiger, W. (2004a). Estrogenic activity and estrogen receptor beta binding of the UV filter 3-benzylidene camphor. Comparison with 4-methylbenzylidene camphor. *Toxicology*. **199**(2-3):109–120.
- Schmutzler, C., Bacinski, A., Gotthardt, I., Huhne, K., Ambrugger, P., Klammer, H., Schlecht, C., Hoang-Vu, C., Gruters, A., Wuttke, W., Jarry, H. and Kohrle, J. (2007). The ultraviolet filter benzophenone 2 interferes with the thyroid hormone axis in rats and is a potent in vitro inhibitor of human recombinant thyroid peroxidase. *Endocrinology*. **148**(6): 2835–2844.
- Schreurs, R., Lanser, P., Seinen, W. and van der Burg, B. (2002). Estrogenic activity of UV filters determined by an in vitro reporter gene assay and an in vivo transgenic zebrafish assay. *Archives of Toxicology*. **76**(5-6): 257–261.
- Schreurs, R.H.M.M., Sonneveld, E., Jansen, J.H.J., Seinen, W. and van der Burg, B. (2005). Interaction of polycyclic musks and UV filters with the estrogen receptor (ER), androgen receptor (AR), and progesterone receptor (PR) in reporter gene bioassays. *Toxicological Sciences*. **83**(2): 264–272.
- Schwalbe, M., Sanger, J., Eggers, R., Naumann, A., Schmidt, A., Hoffken, K. and Clement, J.H. (2003). Differential expression and regulation of bone morphogenetic protein 7 in breast cancer. *International Journal of Oncology*. **23**(1): 89–95.
- Schwanhausser, B., Busse, D., Li, N., Dittmar, G., Schuchhardt, J., Wolf, J., Chen, W. and Selbach, M. (2011). Global quantification of mammalian gene expression control. *Nature*. **473**(7347): 337–342.
- Schwartz, M.A., Schaller, M.D. and Ginsberg, M.H. (1995). Integrins: emerging paradigms of signal transduction. *Annual Review of Cell and Developmental Biology*. **11**: 549–599.

- Seidlová-Wuttke, D., Christoffel, J., Rimoldi, G., Jarry, H. and Wuttke, W. (2006). Comparison of effects of estradiol with those of octylmethoxycinnamate and 4-methylbenzylidene camphor on fat tissue, lipids and pituitary hormones. *Toxicology and Applied Pharmacology*. **214**(1): 1–7.
- Seiki, M. (2002). The cell surface: the stage for matrix metalloproteinase regulation of migration. *Current Opinion in Cell Biology*. **14**(5): 624–632.
- Serpone, N., Dondi, D. and Albini, A. (2007). Inorganic and organic UV filters: Their role and efficacy in sunscreens and suncare products. *Inorganic Chimica Acta*. **360**: 794–802.
- Shaath, N.A. (2010). Ultraviolet filters. *Photochemical & Photobiological Sciences : Official Journal of the European Photochemistry Association and the European Society for Photobiology*. **9**(4): 464–469.
- Shadeo, A. and Lam, W.L. (2006). Comprehensive copy number profiles of breast cancer cell model genomes. *Breast Cancer Research*. **8**(1): R9.
- Shamir, E.R., Pappalardo, E., Jorgens, D.M., Coutinho, K., Tsai, W.-T., Aziz, K., Auer, M., Tran, P.T., Bader, J.S. and Ewald, A.J. (2014). Twist1-induced dissemination preserves epithelial identity and requires E-cadherin. *The Journal of Cell Biology*. **204**(5): 839–856.
- Shaw, L.E., Sadler, A.J., Pugazhendhi, D. and Darbre, P.D. (2006). Changes in oestrogen receptor-a and -b during progression to acquired resistance to tamoxifen and fulvestrant (Faslodex, ICI 182,780) in MCF7 human breast cancer cells. *Journal of Steroid Biochemistry and Molecular Biology*. **99**(1): 19–32.
- Shin, S., Go, R.-E., Kim, C.-W., Hwang, K.-A., Nam, K.-H. and Choi, K.-C. (2016). Effect of benzophenone-1 and octylphenol on the regulation of epithelial-mesenchymal transition via an estrogen receptor-dependent pathway in estrogen receptor expressing ovarian cancer cells. *Food and chemical toxicology : an international journal published for the British Industrial Biological Research Association*. **93**: 58–65.
- Shtutman, M., Zhurinsky, J., Simcha, I., Albanese, C., D'Amico, M., Pestell, R. and Ben-Ze'ev, A. (1999). The cyclin D1 gene is a target of the beta-catenin/LEF-1 pathway. *Proceedings of the National Academy of Sciences of the United States of America*. **96**(10): 5522–5527.

- Siitonen, S.M., Kononen, J.T., Helin, H.J., Rantala, I.S., Holli, K.A. and Isola, J.J. (1996). Reduced E-cadherin expression is associated with invasiveness and unfavorable prognosis in breast cancer. *American Journal of Clinical Pathology*. **105**(4): 394–402.
- Sisci, D., Aquila, S., Middea, E., Gentile, M., Maggiolini, M., Mastroianni, F., Montanaro, D. and Ando, S. (2004). Fibronectin and type IV collagen activate ERalpha AF-1 by c-Src pathway: effect on breast cancer cell motility. *Oncogene*. **23**(55): 8920–8930.
- Snedeker, S.M. and Diaugustine, R.P. (1996). Hormonal and environmental factors affecting cell proliferation and neoplasia in the mammary gland. *Progress in Clinical and Biological Research*. **394**: 211–253.
- Solomayer, E.F., Diel, I.J., Meyberg, G.C., Gollan, C. and Bastert, G. (2000). Metastatic breast cancer: clinical course, prognosis and therapy related to the first site of metastasis. *Breast Cancer Research and Treatment*. **59**(3): 271–278.
- Song, R., Santen, R., Kumar, R., Adam, L., Jeng, M.-H., Masamura, S. and Yue, W. (2002a). Adaptive mechanisms induced by long-term estrogen deprivation in breast cancer cells. *Molecular and Cellular Endocrinology*. **193**(1): 29–42.
- Song, R.X.-D, McPherson, R.A., Adam, L., Bao, Y., Shupnik, M., Kumar, R. and Santen, R.J. (2002b). Linkage of rapid estrogen action to MAPK activation by ERalpha-Shc association and Shc pathway activation. *Molecular Endocrinology (Baltimore, Md.)*. **16**(1): 116–127.
- Song, R.X.-D., Zhang, Z., Chen, Y., Bao, Y. and Santen, R.J. (2007). Estrogen signaling via a linear pathway involving insulin-like growth factor I receptor, matrix metalloproteinases, and epidermal growth factor receptor to activate mitogen-activated protein kinase in MCF-7 breast cancer cells. *Endocrinology*. **148**(8): 4091–4101.
- Sonohara, S., Mira-y-Lopez, R. and Brentani, M.M. (1998). Laminin and estradiol regulation of the plasminogen-activator system in MCF-7 breast-carcinoma cells. *International Journal of Cancer*. **76**(1): 77–85.
- Sorlie, T., Perou, C.M., Tibshirani, R., Aas, T., Geisler, S., Johnsen, H., Hastie, T., Eisen, M.B., van de Rijn, M., Jeffrey, S.S., Thorsen, T., Quist, H., Matese, J.C., Brown, P.O., Botstein, D., Lonning, P.E. and Borresen-Dale, A.L. (2001). Gene expression patterns of breast carcinomas distinguish tumor subclasses with clinical implications. *Proceedings of the National Academy of Sciences of the United States of America*. **98**(19):10869–10874.

- Soto, A.M., Chung, K.L. and Sonnenschein, C. (1994). The pesticides endosulfan, toxaphene, and dieldrin have estrogenic effects on human estrogen-sensitive cells. *Environmental Health Perspectives*. **102**(4): 380–383.
- Soto, A.M., Sonnenschein, C., Chung, K.L., Fernandez, M.F., Olea, N. and Serrano, F.O. (1995). The E-SCREEN assay as a tool to identify estrogens: an update on estrogenic environmental pollutants. *Environmental Health Perspectives*. **103**(Suppl 7): 113–122.
- Stamenkovic, I. (2000). Matrix metalloproteinases in tumor invasion and metastasis. *Seminars in Cancer Biology*. **10**(6): 415–433.
- Stapf, M., Pompner, N., Teichgraber, U. and Hilger, I. (2016). Heterogeneous response of different tumor cell lines to methotrexate-coupled nanoparticles in presence of hyperthermia. *International Journal of Nanomedicine*. **11**: 485–500.
- Steeg, P.S. (2006). Tumor metastasis: mechanistic insights and clinical challenges. *Nature Medicine*. **12**(8): 895–904.
- Stellman, S.D., Djordjevic, M. V, Britton, J.A., Muscat, J.E., Citron, M.L., Kemeny, M., Busch, E. and Gong, L. (2000). Breast cancer risk in relation to adipose concentrations of organochlorine pesticides and polychlorinated biphenyls in Long Island, New York. *Cancer Epidemiology, Biomarkers & Prevention*. **9**(11): 1241–1249.
- Stephen, R.L., Shaw, L.E., Larsen, C., Corcoran, D. and Darbre, P.D. (2001). Insulin-like growth factor receptor levels are regulated by cell density and by long term estrogen deprivation in MCF7 human breast cancer cells. *The Journal of Biological Chemistry*. **276**(43): 40080–40086.
- Stewart, A.J., Johnson, M.D., May, F.E. and Westley, B.R. (1990). Role of insulin-like growth factors and the type I insulin-like growth factor receptor in the estrogen-stimulated proliferation of human breast cancer cells. *The Journal of Biological Chemistry*. **265**(34): 21172–21178.
- Strom, A., Hartman, J., Foster, J.S., Kietz, S., Wimalasena, J. and Gustafsson, J.-A. (2004). Estrogen receptor beta inhibits 17beta-estradiol-stimulated proliferation of the breast cancer cell line T47D. *Proceedings of the National Academy of Sciences of the United States of America*. **101**(6): 1566–1571.

- Sutherland, R.L., Prall, O.W., Watts, C.K. and Musgrove, E.A. (1998). Estrogen and progestin regulation of cell cycle progression. *Journal of Mammary Gland Biology and Neoplasia*. **3**(1): 63–72.
- Suzuki, T., Ide, K. and Ishida, M. (2001). Response of MCF-7 human breast cancer cells to some binary mixtures of oestrogenic compounds in-vitro. *The Journal of Pharmacy and Pharmacology*. **53**(11): 1549–1554.
- SZYBALSKI, W. and IYER, V.N. (1964). Crosslinking of DNA by enzymatically or chemically activated mytomycins and porfiromycins, bifunctionally ‘ALKYLATING’ antibiotics. *Federation Proceedings*. **23**: 946–957.
- Takeichi, M. (1991). Cadherin cell adhesion receptors as a morphogenetic regulator. *Science (New York, N.Y.)*. **251**(5000): 1451–1455.
- Takino, T., Sato, H., Shinagawa, A. and Seiki, M. (1995). Identification of the second membrane-type matrix metalloproteinase (MT-MMP-2) gene from a human placenta cDNA library. MT-MMPs form a unique membrane-type subclass in the MMP family. *The Journal of Biological Chemistry*. **270**(39): 23013–23020.
- Tan, Z., Zheng, H., Liu, X., Zhang, W., Zhu, J., Wu, G., Cao, L., Song, J., Wu, S., Song, L. and Li, J. (2016). MicroRNA-1229 overexpression promotes cell proliferation and tumorigenicity and activates Wnt/beta-catenin signaling in breast cancer. *Oncotarget*. **7**(17): 24076–24087.
- Thiery, J.P. (2002). Epithelial-mesenchymal transitions in tumour progression. *Nature Reviews. Cancer*. **2**(6): 442–454.
- Thomas, M.P. and Potter, B.V.L. (2013). The structural biology of oestrogen metabolism. *The Journal of Steroid Biochemistry and Molecular Biology*. **137**: 27–49.
- Tilghman, R.W. and Parsons, J.T. (2008). Focal adhesion kinase as a regulator of cell tension in the progression of cancer. *Seminars in Cancer Biology*. **18**(1): 45–52.
- Timar, J., Csuka, O., Orosz, Z., Jeney, A. and Kopper, L. (2001). Molecular pathology of tumor metastasis. I. Predictive pathology. *Pathology Oncology Research*. **7**(3): 217–230.
- Tinwell, H., Lefevre, P.A., Moffat, G.J., Burns, A., Odum, J., Spurway, T.D., Orphanides, G. and Ashby, J. (2002). Confirmation of uterotrophic activity of 3-(4-methylbenzylidene) camphor in the immature rat. *Environmental Health Perspectives*. **110**(5): 533–536.

- Toft, D. and Gorski, J. (1966). A receptor molecule for estrogens: isolation from the rat uterus and preliminary characterization. *Proceedings of the National Academy of Sciences of the United States of America*. **55**(6): 1574–1581.
- Tokunaga, M., Norman, J.E.J., Asano, M., Tokuoka, S., Ezaki, H., Nishimori, I. and Tsuji, Y. (1979). Malignant breast tumors among atomic bomb survivors, Hiroshima and Nagasaki, 1950-74. *Journal of the National Cancer Institute*. **62**(6): 1347–1359.
- Toms, L.-M.L., Allmyr, M., Mueller, J.F., Adolfsson-Erici, M., McLachlan, M., Murby, J. and Harden, F.A. (2011). Triclosan in individual human milk samples from Australia. *Chemosphere*. **85**(11): 1682–1686.
- Torbett, N.E., Luna-Moran, A., Knight, Z.A., Houk, A., Moasser, M., Weiss, W., Shokat, K.M. and Stokoe, D. (2008). A chemical screen in diverse breast cancer cell lines reveals genetic enhancers and suppressors of sensitivity to PI3K isoform-selective inhibition. *The Biochemical Journal*. **415**(1): 97–110.
- Trehan, A.S., Arora, M.K., Seth, S. and Chauhan, A. (2012). Endogenous hormones in postmenopausal females with breast cancer--before and after treatment. *Clinical Laboratory*. **58**(7-8): 771–777.
- Tsai, J.-H., Hsu, L.-S., Lin, C.-L., Hong, H.-M., Pan, M.-H., Way, T.-D. and Chen, W.-J. (2013). 3,5,4'-Trimethoxystilbene, a natural methoxylated analog of resveratrol, inhibits breast cancer cell invasiveness by downregulation of PI3K/Akt and Wnt/ $\beta$ -catenin signaling cascades and reversal of epithelial-mesenchymal transition. *Toxicology and Applied Pharmacology*. **272**(3): 746–56.
- Uchino, M., Kojima, H., Wada, K., Imada, M., Onoda, F., Satofuka, H., Utsugi, T. and Murakami, Y. (2010). Nuclear beta-catenin and CD44 upregulation characterize invasive cell populations in non-aggressive MCF-7 breast cancer cells. *BMC Cancer*. **10**: 414.
- Umayahara, Y., Kawamori, R., Watada, H., Imano, E., Iwama, N., Morishima, T., Yamasaki, Y., Kajimoto, Y. and Kamada, T. (1994). Estrogen regulation of the insulin-like growth factor I gene transcription involves an AP-1 enhancer. *The Journal of Biological Chemistry*. **269**(23): 16433–16442.
- Valle-Sistac, J., Molins-Delgado, D., Díaz, M., Ibáñez, L., Barceló, D. and Silvia Díaz-Cruz, M. (2016). Determination of parabens and benzophenone-type UV filters in human

- placenta. First description of the existence of benzyl paraben and benzophenone-4. *Environment international*. **88**: 243–249.
- Vargo-Gogola, T. and Rosen, J.M. (2007). Modelling breast cancer: one size does not fit all. *Nature Reviews. Cancer*. **7**(9): 659–672.
- Vela-Soria, F., Jimenez-Diaz, I., Rodriguez-Gomez, R., Zafra-Gomez, A., Ballesteros, O., Navalon, A., Vilchez, J.L., Fernandez, M.F. and Olea, N. (2011). Determination of benzophenones in human placental tissue samples by liquid chromatography-tandem mass spectrometry. *Talanta*. **85**(4): 1848–1855.
- Venkitaraman, A.R. (2002). Cancer susceptibility and the functions of BRCA1 and BRCA2. *Cell*. **108**(2): 171–182.
- Vestweber, D. (2015). Cadherins in tissue architecture and disease. *Journal of Molecular Medicine (Berlin, Germany)*. **93**(1): 5–11.
- Vestweber, D. and Kemler, R. (1984). Rabbit antiserum against a purified surface glycoprotein decompacts mouse preimplantation embryos and reacts with specific adult tissues. *Experimental Cell Research*. **152**(1): 169–178.
- Vesuna, F., van Diest, P., Chen, J.H. and Raman, V. (2008). Twist is a transcriptional repressor of E-cadherin gene expression in breast cancer. *Biochemical and Biophysical Research Communications*. **367**(2): 235–241.
- Villalobos, M., Olea, N., Brotons, J.A., Olea-Serrano, M.F., Ruiz de Almodovar, J.M. and Pedraza, V. (1995). The E-screen assay: a comparison of different MCF7 cell stocks. *Environmental Health Perspectives*. **103**(9): 844–850.
- Vizoso, F.J., González, L.O., Corte, M.D., Rodríguez, J.C., Vázquez, J., Lamelas, M.L., Junquera, S., Merino, A.M. and García-Muñiz, J.L. (2007). Study of matrix metalloproteinases and their inhibitors in breast cancer. *British Journal of Cancer*. **96**(6): 903–911.
- Vladusic, E.A., Hornby, A.E., Guerra-Vladusic, F.K. and Lupu, R. (1998). Expression of estrogen receptor beta messenger RNA variant in breast cancer. *Cancer Research*. **58**(2): 210–214.
- Wakeling, A.E. (1995). Use of pure antioestrogens to elucidate the mode of action of oestrogens. *Biochemical Pharmacology*. **49**(11): 1545–1549.

- Wakeling, A.E., Dukes, M. and Bowler, J. (1991). A potent specific pure antiestrogen with clinical potential. *Cancer Research*. **51**(15): 3867–3873.
- Waliszewski, S.M., Bermudez, M.T., Infanzon, R.M., Silva, C.S., Carvajal, O., Trujillo, P., Gomez Arroyo, S., Villalobos Pietrini, R., Saldana, V.A., Melo, G., Esquivel, S., Castro, F., Ocampo, H., Torres, J. and Hayward-Jones, P.M. (2005). Persistent organochlorine pesticide levels in breast adipose tissue in women with malignant and benign breast tumors. *Bulletin of Environmental Contamination and Toxicology*. **75**(4): 752–759.
- Walter, P., Green, S., Greene, G., Krust, A., Bornert, J.M., Jeltsch, J.M., Staub, A., Jensen, E., Scrace, G. and Waterfield, M. (1985). Cloning of the human estrogen receptor cDNA. *Proceedings of the National Academy of Sciences of the United States of America*. **82**(23): 7889–7893.
- Wang, M., Liu, Y.E., Greene, J., Sheng, S., Fuchs, A., Rosen, E.M. and Shi, Y.E. (1997). Inhibition of tumor growth and metastasis of human breast cancer cells transfected with tissue inhibitor of metalloproteinase 4. *Oncogene*. **14**(23): 2767–2774.
- Watson, P.H., Pon, R.T. and Shiu, R.P. (1991). Inhibition of c-myc expression by phosphorothioate antisense oligonucleotide identifies a critical role for c-myc in the growth of human breast cancer. *Cancer Research*. **51**(15): 3996–4000.
- Webb, P., Nguyen, P., Valentine, C., Lopez, G.N., Kwok, G.R., McInerney, E., Katzenellenbogen, B.S., Enmark, E., Gustafsson, J.A., Nilsson, S. and Kushner, P.J. (1999). The estrogen receptor enhances AP-1 activity by two distinct mechanisms with different requirements for receptor transactivation functions. *Molecular Endocrinology (Baltimore, Md.)*. **13**(10): 1672–1685.
- Weigelt, B., Glas, A.M., Wessels, L.F.A., Witteveen, A.T., Peterse, J.L. and van't Veer, L.J. (2003). Gene expression profiles of primary breast tumors maintained in distant metastases. *Proceedings of the National Academy of Sciences of the United States of America*. **100**(26): 15901–15905.
- Weisbrod, C.J., Kunz, P.Y., Zenker, A.K. and Fent, K. (2007). Effects of the UV filter benzophenone-2 on reproduction in fish. *Toxicology and Applied Pharmacology*. **225**(3): 255–266.

- Welch, D.R., Fabra, A. and Nakajima, M. (1990). Transforming growth factor beta stimulates mammary adenocarcinoma cell invasion and metastatic potential. *Proceedings of the National Academy of Sciences of the United States of America*. **87**(19): 7678–7682.
- Wheelock, M.J., Shintani, Y., Maeda, M., Fukumoto, Y. and Johnson, K.R. (2008). Cadherin switching. *Journal of Cell Science*. **121**(Pt 6): 727–735.
- Wijnhoven, B.P., Dinjens, W.N. and Pignatelli, M. (2000). E-cadherin-catenin cell-cell adhesion complex and human cancer. *The British Journal of Surgery*. **87**(8): 992–1005.
- Wolf, P., Donawho, C.K. and Kripke, M.L. (1994). Effect of sunscreens on UV radiation-induced enhancement of melanoma growth in mice. *Journal of the National Cancer Institute*. **86**(2): 99–105.
- Woodhouse, E.C., Chuaqui, R.F. and Liotta, L.A. (1997). General mechanisms of metastasis. *Cancer*. **80**(8 Suppl): 1529–1537.
- Woodward, T.L., Lu, H. and Haslam, S.Z. (2000). Laminin inhibits estrogen action in human breast cancer cells. *Endocrinology*. **141**(8): 2814–2821.
- Wooster, R., Neuhausen, S.L., Mangion, J., Quirk, Y., Ford, D., Collins, N., Nguyen, K., Seal, S., Tran, T. and Averill, D. (1994). Localization of a breast cancer susceptibility gene, BRCA2, to chromosome 13q12-13. *Science*. **265**(5181): 2088–2090.
- World Health Organization, N. (2008). The Global Burden of Disease: 2004 update. *WHO Library Cataloguing-in-Publication Data*. [Online], p.146. Available from: [http://www.who.int/healthinfo/global\\_burden\\_disease/2004\\_report\\_update/en/index.html](http://www.who.int/healthinfo/global_burden_disease/2004_report_update/en/index.html).
- Wright, J. V, Schliesman, B. and Robinson, L. (1999). Comparative measurements of serum estriol, estradiol, and estrone in non-pregnant, premenopausal women; a preliminary investigation. *Alternative Medicine Review: a journal of clinical therapeutic*. **4**(4): 266–270.
- Wypych, G. (2015). Handbook of UV Degradation and Stabilization. Elsevier.
- Xie, J.-W. and Haslam, S.Z. (2008). Extracellular matrix, Rac1 signaling, and estrogen-induced proliferation in MCF-7 breast cancer cells. *Breast Cancer Research and Treatment*. **110**(2): 257–268.

- Xu, J., Prosperi, J.R., Choudhury, N., Olopade, O.I. and Goss, K.H. (2015).  $\beta$ -Catenin Is Required for the Tumorigenic Behavior of Triple-Negative Breast Cancer Cells. O. Williams, ed. *PLoS ONE*. **10**(2): e0117097.
- Xue, C., Plieth, D., Venkov, C., Xu, C. and Neilson, E.G. (2003). The gatekeeper effect of epithelial-mesenchymal transition regulates the frequency of breast cancer metastasis. *Cancer Research*. **63**(12): 3386–3394.
- Yan, L.-X., Liu, Y.-H., Xiang, J.-W., Wu, Q.-N., Xu, L.-B., Luo, X.-L., Zhu, X.-L., Liu, C., Xu, F.-P., Luo, D.-L., Mei, P., Xu, J., Zhang, K.-P. and Chen, J. (2016). PIK3R1 targeting by miR-21 suppresses tumor cell migration and invasion by reducing PI3K/AKT signaling and reversing EMT, and predicts clinical outcome of breast cancer. *International Journal of Oncology*. **48**(2): 471–484.
- Yang, J., Mani, S.A., Donaher, J.L., Ramaswamy, S., Itzykson, R.A., Come, C., Savagner, P., Gitelman, I., Richardson, A. and Weinberg, R.A. (2004). Twist, a master regulator of morphogenesis, plays an essential role in tumor metastasis. *Cell*. **117**(7): 927–939.
- Yang, S. and Kim, H.-M. 2014. ROCK inhibition activates MCF-7 cells. *PloS one*. **9**(2): e88489.
- Yang, S., Zhong, C., Frenkel, B., Reddi, A.H. and Roy-Burman, P. (2005). Diverse biological effect and Smad signaling of bone morphogenetic protein 7 in prostate tumor cells. *Cancer Research*. **65**(13): 5769–5777.
- Yao, D., Dai, C. and Peng, S. (2011). Mechanism of the mesenchymal-epithelial transition and its relationship with metastatic tumor formation. *Molecular Cancer Research*. **9**(12): 1608–1620.
- Yao, P.-L., Lin, Y.-C. and Richburg, J.H. (2012). Mono-(2-ethylhexyl) phthalate (MEHP) promotes invasion and migration of human testicular embryonal carcinoma cells. *Biology of Reproduction*. **86**(5): 1–10,160.
- Yap, A.S., Niessen, C.M. and Gumbiner, B.M. (1998). The Juxtamembrane Region of the Cadherin Cytoplasmic Tail Supports Lateral Clustering, Adhesive Strengthening, and Interaction with p120(ctn) . *The Journal of Cell Biology*. **141**(3): 779–789.
- Ye, L. and Jiang, W.G. (2015). Bone morphogenetic proteins in tumour associated angiogenesis and implication in cancer therapies. *Cancer Letters*. **380**(2): 586–597.

- Yoneda, T., Sasaki, A., Dunstan, C., Williams, P.J., Bauss, F., De Clerck, Y.A. and Mundy, G.R. (1997). Inhibition of osteolytic bone metastasis of breast cancer by combined treatment with the bisphosphonate ibandronate and tissue inhibitor of the matrix metalloproteinase-2. *The Journal of Clinical Investigation*. **99**(10): 2509–2517.
- Yonemura, S. (2011). Cadherin-actin interactions at adherens junctions. *Current Opinion in Cell Biology*. **23**(5): 515–22.
- Yook, J.I., Li, X.-Y., Ota, I., Hu, C., Kim, H.S., Kim, N.H., Cha, S.Y., Ryu, J.K., Choi, Y.J., Kim, J., Fearon, E.R. and Weiss, S.J. (2006). A Wnt-Axin2-GSK3beta cascade regulates Snail1 activity in breast cancer cells. *Nature Cell Biology*. **8**(12): 1398–1406.
- Youliden, D.R., Cramb, S.M., Dunn, N.A.M., Muller, J.M., Pyke, C.M. and Baade, P.D. (2012). The descriptive epidemiology of female breast cancer: an international comparison of screening, incidence, survival and mortality. *Cancer Epidemiology*. **36**(3): 237–248.
- Yousif, E. and Hasan, A. (2015). Photostabilization of poly (vinyl chloride) – Still on the run. *Journal of Taibah University for Science*. **9**(4): 421–448.
- Yu, Q. and Stamenkovic, I. (2000). Cell surface-localized matrix metalloproteinase-9 proteolytically activates TGF- $\beta$  and promotes tumor invasion and angiogenesis. *Genes & Development*. **14**(2): 163–176.
- Yue, W., Wang, J.-P., Li, Y., Fan, P., Liu, G., Zhang, N., Conaway, M., Wang, H., Korach, K.S., Bocchinfuso, W. and Santen, R. (2010). Effects of estrogen on breast cancer development: role of estrogen receptor independent mechanisms. *International Journal of Cancer*. **127**(8).1748–1757.
- Yurchenco, P.D., Amenta, P.S. and Patton, B.L. (2004). Basement membrane assembly, stability and activities observed through a developmental lens. *Matrix Biology*. **22**(7): 521–538.
- Zarrabi, K., Dufour, A., Li, J., Kuscu, C., Pulkoski-Gross, A., Zhi, J., Hu, Y., Sampson, N.S., Zucker, S. and Cao, J. (2011). Inhibition of matrix metalloproteinase 14 (MMP-14)-mediated cancer cell migration. *The Journal of Biological Chemistry*. **286**(38): 33167–33177.

- Zeng, Q., Li, W., Lu, D., Wu, Z., Duan, H., Luo, Y., Feng, J., Yang, D., Fu, L. and Yan, X. (2012). CD146, an epithelial-mesenchymal transition inducer, is associated with triple-negative breast cancer. *Proceedings of the National Academy of Sciences of the United States of America*. **109**(4): 1127–1132.
- Zhang, T., Sun, H., Qin, X., Wu, Q., Zhang, Y., Ma, J. and Kannan, K. (2013). Benzophenone-type UV filters in urine and blood from children, adults, and pregnant women in China: partitioning between blood and urine as well as maternal and fetal cord blood. *The Science of the Total Environment*. **461-462**: 49–55.
- Zhang, X.-L., Liu, N., Weng, S.-F. and Wang, H.-S. (2016). Bisphenol A Increases the Migration and Invasion of Triple Negative Breast Cancer Cells via Oestrogen-related Receptor Gamma. *Basic & Clinical Pharmacology & Toxicology*. **119**(4): 389-395.
- Zhang, Z., Ren, N., Li, Y.-F., Kunisue, T., Gao, D. and Kannan, K. (2011). Determination of benzotriazole and benzophenone UV filters in sediment and sewage sludge. *Environmental Science & Technology*. **45**(9): 3909–3916.
- Zhou, K., Sun, P., Zhang, Y., You, X., Li, P. and Wang, T. (2016). Estrogen stimulated migration and invasion of estrogen receptor-negative breast cancer cells involves an ezrin-dependent crosstalk between G protein-coupled receptor 30 and estrogen receptor beta signaling. *Steroids*. **111**: 113-121.
- Zhu, B.T., Han, G.-Z., Shim, J.-Y., Wen, Y. and Jiang, X.-R. (2006). Quantitative structure-activity relationship of various endogenous estrogen metabolites for human estrogen receptor alpha and beta subtypes: Insights into the structural determinants favoring a differential subtype binding. *Endocrinology*. **147**(9): 4132–4150.
- Zhu, W. and Nelson, C.M. (2013). Adipose and mammary epithelial tissue engineering. *Biomatter*. **3**(3): 1–6.
- Zhurinsky, J., Shtutman, M. and Ben-Ze'ev, A. (2000). Plakoglobin and beta-catenin: protein interactions, regulation and biological roles. *Journal of Cell Science*. **113** (Pt 1): 3127–3139.
- Ziegler, R.G., Hoover, R.N., Pike, M.C., Hildesheim, A., Nomura, A.M., West, D.W., Wu-Williams, A.H., Kolonel, L.N., Horn-Ross, P.L., Rosenthal, J.F. and Hyer, M.B. (1993). Migration patterns and breast cancer risk in Asian-American women. *Journal of the National Cancer Institute*. **85**(22): 1819–1827.

van Zijl, F., Krupitza, G. and Mikulits, W. (2011). Initial steps of metastasis: cell invasion and endothelial transmigration. *Mutation Research*. **728**(1-2): 23–34.